Elucidating the role of EP300/CBP mediated FOXO3 acetylation in tumorigenesis and cancer drug resistance

Thesis submitted by

Zimam Mahmud

To

Imperial College London

For the degree of Doctor of Philosophy

Department of Surgery and Cancer
1st floor, Imperial Center for Translational and Experimental Medicine
Imperial College London
Hammersmith Hospital
Du Cane Road
London W12 0NN

2019-2020

DECLARATION OF ORIGINALITY

This thesis is the result of my own experimental works, unless stated in the ‘‘List of contributions’’ or any collaborative work mentioned in the text with references.

COPYRIGHT DECLARATION

The copyright of this thesis rests with the author and is made available under a Creative Commons Attribution Non-Commercial No Derivatives licence. Researchers are free to copy, distribute or transmit the thesis on the condition that they attribute it, that they do not use it for commercial purposes and that they do not alter, transform or build upon it. For any reuse or redistribution, researchers must make clear to others the licence terms of this work.

LIST OF CONTRIBUTIONS

All the experiments described in this thesis were performed and analysed by me, with the following exceptions.

1. Chapter 3

- Lapatinib resistant BT474 Lap^R and SKBR3 Lap^R cells were generated by Dr. Ana Rita Gomes.
- Anti-AcFOXO3 antibody was generated by Professor Eric Lam.
- In figure 3.2A, ChIP experiments were performed and analysed by Dr. Ana Rita Gomes.
- In figure 3.17, immunohistochemistry experiment was performed and analysed by Dr. Hee Jin Lee and Dr. Gyungyub Gong.
- In appendix figure A3.3, one set of clonogenic assay was performed and analysed by Dr. Ana Rita Gomes.

2. Chapter 5

- SIRT2 inhibitor scAB8A44 was designed and synthesized in Professor Matthew Fuchter's lab.
- In figure 5.14C, 5.15, 5.17, 5.21, 5.22 and 5.23, all the experiments were performed and analysed together with Sathid Aimjongjun (Equal contributions were mentioned in the published article). These experiments are considered as a collaborative works.

3. Chapter 6

- Stably overexpressed Hs578T cell lines were generated by Dr. Muhammad Asaduzzaman. Drug resistant Hs578T cell lines were generated by Dr. Ernesto Yagüe.
- For Immunohistochemistry, breast cancer sample screening, scoring and analysis were performed by Dr. Muhammad Asaduzzaman and Dr. Ernesto Yagüe.
- Microarray data was analysed by Dr. Yunhui Hu.
- Dr. Nahal Masrour performed methylation experiments and analysis.

ABSTRACT

Forkhead Box O3 (FOXO3) is a tumour suppressor whose functional activity is predominantly regulated by post-translational modifications (PTMs). Of all PTMs, the best-studied PTM of FOXO proteins is phosphorylation, however, acetylation by EP300 or the CREB-binding protein (CBP) has been increasingly recognised as a novel axis regulating FOXO proteins. Herein, using the BT474 breast cancer cells and its lapatinib resistant derivative BT474 Lap^R cells, I observed that higher FOXO3 and acetylated Ac-FOXO3 levels correlate with lapatinib sensitivity. Subsequent ectopic expression of EP300, as well as CBP, led to an increase in acetylated-FOXO3 in sensitive, but not in resistant BT474 cells. Moreover, lapatinib sensitive BT474 cells exhibited enhanced lapatinib cytotoxicity upon over-expression of wild-type but not acetylation-deficient EP300 or CBP as revealed by drug sensitivity assays. Besides, using SIRT1/6 specific siRNAs and chemical inhibitor, I also found that SIRT1 and SIRT6 play a part in fine-tuning FOXO3 acetylation and lapatinib sensitivity. Notably, we next explored that not only SIRT1/6 but also SIRT2 plays a significant role in regulating FOXO3 acetylation and lapatinib sensitivity of BT474 and nasopharyngeal cancers. Taken together, these results suggest the involvement of acetyltransferases EP300/CBP and nuclear sirtuins in regulating FOXO3 acetylation and lapatinib sensitivity of breast cancers.

Despite having a tumour-suppressive role, some reports suggested the oncogenic role of EP300 in the development and progression of cancers. To uncover this, I used Hs578T cells which have E-cadherin promoter hypermethylated. Interestingly, overexpression of EP300 led to the up-regulation of mesenchymal and stemness markers, increases in cell migration, invasion, anchorage-independent growth, and drug resistance. Moreover, genome-wide expression profiling identified Aldo-keto reductases AKR1C1-3 as positive modulators of cancer stemness and drug resistance, since their pharmacological inhibition with flufenamic acid restored both doxorubicin and paclitaxel sensitivity and reduced mammosphere formation. Thus, EP300 functions as an oncogene via the up-regulation of AKR1Cs in cells where the E-cadherin promoter is hypermethylated. This important finding offers the rationale of using current AKR1Cs inhibitors in the treatment of triple-negative breast cancers.

PUBLICATIONS

Mahmud Z, Gomes AR, Lee HJ, Aimjongjun S, Jiramongkol Y, Yao S, Zona S, Alasiri G, Gong G, Yagüe E, Lam EW-F. EP300 and SIRT1/6 Co-Regulate Lapatinib Sensitivity Via Modulating FOXO3-Acetylation and Activity in Breast Cancer. *Cancers*. 2019; 11(8):1067.

Mahmud Z, Asaduzzaman M, Kumar U, Masrour N, Jugov R, Coombes RC, Shousha S, Hu Y, Lam EW-F, Yagüe E. Oncogenic EP300 can be targeted with inhibitors of aldo-keto reductases, *Biochemical Pharmacology*, 2019; Vol:163, ISSN:0006-2952, Pages:391-403.

Aimjongjun S[#], **Mahmud Z**[#], Jiramongkol Y, Alasiri G, Yao S, Yagüe E, Lam E. Lapatinib sensitivity in nasopharyngeal carcinoma is modulated by SIRT2-mediated FOXO3 deacetylation, *BMC Cancer 19*, 1106 (2019) doi:10.1186/s12885-019-6308-7.([#]Contributed equally and should be recongised as co-first authors)

Sundriyal S[#], Moniot S[#], **Mahmud Z**, Yao S, Di Fruscia P, Reynolds CR, Dexter DT, Sternberg MJE, Lam EW, Steegborn C, and Fuchter MJ. Thienopyrimidinone Based Sirtuin-2 (SIRT2)-Selective Inhibitors Bind in the Ligand Induced Selectivity Pocket.*Journal of Medicinal Chemistry,* 2017; 60 (5), 1928-1945 ([#]These authors contributed equally)

Yao S, **Mahmud Z,** Sachini N, Aimjongjun S, Saavedra-García P, Lam EW-F. Characterization of FOXO acetylation, *Methods in Molecular Biology*, 2019; Vol: 1890, Pages: 77-90, ISSN: 1940-6029

Alasiri G, Jiramongkol Y, Zona S, Fan L, **Mahmud Z**, Gong G, Lee HJ, Lam EW. Regulation of PERK expression by FOXO3: a vulnerability of drug-resistant cancer cells, *Oncogene*, 2019; ISSN: 0950-9232

Saavedra-García P, Nichols K, **Mahmud Z,** Fan LY, Lam EW. Unravelling the role of fatty acid metabolism in cancer through the FOXO3-FOXM1 axis. *Molecular and Cellular Endocrinology*, 2017; ISSN: 1872-8057

ACKNOWLEDGEMENTS

Firstly, I would like to thank my supervisor Professor Eric Lam for allowing me to pursue my PhD in his lab at Imperial College London. I am extremely grateful to him for his continuous support in every aspect of my PhD. Thanks a lot, Eric!

A massive thanks to my co-supervisor Dr. Ernesto Yagüe. Your support and kindness are amazing. Thank you for your all types of supervision.

I would also like to thank my lab supervisor Dr. Ana Rita Gomes who has taught me most of the techniques from the beginning. I am grateful to her for her patience while teaching me. I am also grateful to all the members of the Lam's lab, past, and present. Special thanks to Dr. Stefania Zona, Dr. Paula Saavedra García, Dr. Shang Yao and Mr. Glowi Alasiri for your continuous help and supports in the lab works. I would also like to thank all other lab members Sathid Aimjongjun, Jaysze Young, Lavender Fan, Yannasitha Jiramongkol and Sasanan Trakansuebkul.I've had a good time with all of you. I would also like to thank Mr. Roman Jugov and Mr. Uttom Kumar from Dr. Ernesto's Lab for your kind helps during experimental works.

I would like to thank my father Mr. Nasir Uddin Mahmud, my mother Dil Afroz Khanam, my brothers and sisters for their continued support. Especially thanks to my brother Dr. Zobaer Al Mahmud, your presence during my surgery times helped me a lot to pass those hardships. A special mention goes to my neighbours here in London Dr. Ali Ashek Polok and his family, Dr. Mursalin Billah (Sir!), Mrs. Farah Sabrin, Dr. A. M. Mahedi Hasan, and Dr. Nurun Nahar Fancy. I have had a lot of good memories with all of you.

A big thank you goes to my wife Israt Dilruba Mishu (and her family). Without your support, I could not pass those tough times of PhD tenure. I am indebted to you for your endurance during my stay over here in London. Your affection, inspiration, encouragement and fabulous support helped me a lot throughout the entire period of the study. Thank you so much, Mishtyy!

Lastly, thanks to the Commonwealth Scholarship Commission, UK for funding my PhD work at Imperial College London. I would also like to acknowledge all the funding bodies contributed to Prof. Eric Lam and Dr. Ernesto Yagües' projects.

Funding sources for Prof. Eric Lam's projects:
Eric W.-F. Lam's work is supported by MRC (MR/N012097/1), CRUK (C37/A12011), Breast Cancer Now (2012 May PR070; 2012 Nov PhD 016; 2014 Nov PhD 326), the Cancer Research UK Imperial Centre, Imperial ECMC and NIHR Imperial BRC.

Funding sources for Dr. Ernesto Yagüe's project:
The National Institute for Health Research Imperial Biomedical Research Centre, the Imperial Experimental Cancer Medicine Centre and the Cancer Research UK Imperial Centre at Imperial College London provided infrastructure support. Some tissue samples were provided by Breast Cancer Now Tissue Bank and the Imperial College Healthcare NHS Trust Tissue Bank, which is funded by the National Institute for Health Research (NIHR) Biomedical Research Centre based at Imperial College Healthcare NHS Trust and Imperial College London.

LIST OF ABBREVIATIONS

Ac-FOXO3	Acetylated FOXO3
ABC	ATP-binding cassette
AL	Autoregulatory Loop
APS	Ammonium persulphate
ATCC	American Type Culture Collection
ABCB1	ATP-binding cassette, sub-family B, member 1
ATM	Ataxia-telangiectasia mutated
BAD	Bcl-2-associated death promoter
Bcl-2	B-cell lymphoma 2
BCRP	Breast cancer resistant protein
BRCA1	Breast cancer associated gene 1
BRCA2	Breast cancer associated gene 2
BSA	Bovine serum albumin
CREB	Cyclic-AMP response element binding protein
CBP	CREB binding protein
CKI	Cyclin- dependent kinase inhibitor
ChIP	Chromatin immunoprecipitation
Co-IP	Co-immunoprecipitation
c-Myc	C-myelocytomatosis
CDK	Cyclin-dependent kinase
CDKI	Cyclin-dependent kinase inhibitor
cDNA	complementary DNA
DNA	Deoxyribonucleic acid
DBD	DNA binding domain
DMEM	Dulbecco's Modified Eagle Medium
DTT	Dithiothreitol
DMSO	Dimethyl Sulphoxide
EP300	E1A binding protein p300
E1	Ubiquitin-activating enzyme
ECL	Enhanced Chemi-Luminescence
EDTA	Ethylenediaminetetraacetic acid
EGFR	Epidermal growth factor receptor

ER	Estrogen receptor
ERK	Extracellular signal-regulated kinase
EMT	Epithelial-mesenchymal transition
FOXO	Forkhead box, subgroup O, transcription factor
FHRE	Forkhead responsive element
FOXM1	Forkhead box M1
GADD45	Growth arrest and DNA damage 45
GFP	Green fluorescent protein
g	gravitational
h	hour
HAT	Histone acetyltransferase
HDAC	Histone deacetylase
HER	Human Epidermal growth factor Receptor
HIF-1α	Hypoxia-inducible factor-1 α
H3	Histone 3
H3K9	Histone 3 lysine 9
H3K56	Histone 3 lysine 56
H4	Histone 4
H4K16	Histone 4 lysine 16
HDACi	Histone deacetylase inhibitors
HRP	Horseradish peroxidase
IHC	Immunohistochemistry
IKK	I-kappa-B kinase
JNK	c-Jun N-terminal kinase
KO	Knockout
L19	Ribosomal protein L19
Lap^R	Lapatinib resistant
MDR1	Multi-drug resistance gene 1
MCF-7	Michigan Cancer Foundation-7
m	Milli
M	Molar
MAPK	Mitogen activated protein kinase
MEFs	Mouse embryonic fibroblasts
Min	minutes

MnSOD	Manganese superoxide dismutase
MEK	MAPK/ERK kinase
miR	Micro-RNA
MMP	Matrix metalloproteinase
MRP	Multidrug resistant associated protein
mTOR	Mammalian target of rapamycin
mut	Mutant
NES	Nuclear export sequence
NLS	Nuclear localisation signal
NSC	Non-specific control
n	nano
NAM	Nicotinamide
NAD+	Nicotinamide adenine dinucleotide
NaF	Sodium fluoride
Na3VO4	Sodium orthovanadate
NER	Nucleotide excision repair
PAGE	Polyacrylamide gel electrophoresis
PARP1	Poly ADP-ribose polymerase1
PBS	Phosphate buffered saline
PDK1	Phosphoinositide–dependent kinase 1
P-gp	P-glycoprotein
PI3K	Phosphatidylinositol-3 kinase
PIK3CA	Phosphoinositide-3-kinase, catalytic, alpha polypeptide
PIP2	Phosphatidylinositol 4,5-bisphosphate
PIP3	Phosphatidylinositol 3,4,5-triphosphate
PMSF	Phenylmethylsulfonyl fluorid
PR	Progesterone Receptor
PTEN	Phosphatase and tensin homolog
P-FOXO3	Phosphorylated FOXO3
PTM	Post translational Modification
PKB (AKT)	Protein kinase B
PCR	Polymerase chain reaction
ROS	Reactive oxygen species
RT	Room temperature

RTK	Receptor tyrosine kinase
RT-qPCR	Reverse transcription quantitative polymerase chain reaction
Rb	Retinoblastoma
RPM	Revolutions per minute
SDS	Sodium dodecyl sulphate
sec	second
SGK	Serum and glucocorticoid kinase
siRNA	Small interfering RNA
SKP2	S-phase kinase-associated protein 2
SRB	Sulphorhodamine B
Sir2	Silent Information Regulator 2
SIRTs	Sirtuins
TAD	Transactivation domain
TBP	TATA-binding protein
TCA	Trichloroacetic acid
TGFβ	Transforming growth factor β
TKI	Tyrosine kinase inhibitor
TNBC	Triple negative breast cancer
TNF	Tumour necrosis factor
TRADD	TNF-receptor-associated death domain
TRAIL	TNF-related apoptosis inducing ligand
TSA	Tricostatin A
TBST	Tris buffered saline-Tween 20
TEMED	N,N,N,‟N-tetramethylethylenediamine
Tris	Tris (hydroxymethyl)aminomethane
Tween 20	polyoxyethylene-sorbitan monolaurate
µ	Micro
VEGF	Vascular endothelial growth factor

TABLE OF CONTENTS

DECLARATION OF ORIGINALITY	**2**
COPYRIGHT DECLARATION	**2**
LIST OF CONTRIBUTIONS	**3**
ABSTRACT	**4**
PUBLICATIONS	**5**
ACKNOWEDGEMENTS	**6**
ABBREVIATIONS	**8**

CHAPTER 1 INTRODUCTION		**27**
1.1	Cancer	**28**
1.2	Breast cancer	**28**
1.3	Classification of breast cancer based on molecular subtyping	**29**
1.4	HER2 overexpressed breast cancer	**30**
1.5	Adjuvant therapies for breast cancer treatment	**32**
1.6	Nasopharyngeal carcinoma	**34**
1.7	Treatment options for nasopharyngeal carcinoma	**34**
1.8	Chemotherapeutic drug resistance	**35**
1.9	Aldo-keto-reductases family (AKR1C) and breast cancer drug resistance	**38**
1.10	Epithelial to mesenchymal transitions as a hallmark of aggressive cancers	**38**
1.11	EMT in breast cancer	**42**
1.12	Histone acetylation and de-acetylation	**46**
1.13	Histone acetyl-transferases (HATs)	**48**
1.14	HDACs and breast cancer	**48**
1.15	EP300 and CBP as lysine acetyl-transferases	**50**
1.15.1	Structural description of EP300 and CBP proteins	**50**
1.15.2	Functional role of EP300 and CBP	**54**
1.15.3	EP300/CBP as classic tumor suppressors	**54**
1.15.4	EP300/CBP as positive modulators of tumour development	**55**
1.16	FOXO transcription factors	**56**

1.16.1	Structural insights of FOXO proteins	**57**
1.16.2	FOXO3-FOXM1 axis	**58**
1.16.3	FOXOs in cellular senescence and autophagy	**59**
1.17	Post translational modifications of FOXO	**61**
1.17.1	Phosphorylation of FOXO	**62**
1.17.2	Acetylation and deacetylation of FOXO proteins	**66**
1.18	Sirtuins in the regulation of FOXO acetylation	**67**
1.18.1	SIRT1 in FOXO regulation	**68**
1.18.2	SIRT2 in FOXO regulation	**69**
1.18.3	SIRT6 in FOXO regulation	**70**
1.18.4	The role of SIRT3 and SIRT7	**71**
1.18.5	Sirtuin inhibitors	**72**
1.19	Aims and objectives of the project	**75**
CHAPTER 2: Materials and Methods		**76**
2.1	Cell lines, cell culture and treatments	**77**
2.2	Plasmids and their isolation	**78**
2.3	Breast cancer cell transfections	**78**
2.4	Generation of stable cell lines	**79**
2.5	Generation of drug resistant Hs578T cell lines	**80**
2.6	Duolink in situ proximity ligation assay (PLA)	**80**
2.7	Protein extraction and quantification	**83**
2.8	Western blotting	**83**
2.9	Real-time quantitative PCR	**85**
2.10	Co-immunoprecipitation assay	**91**
2.11	Chromatin Immunoprecipitation (ChIP)	**91**
2.12	Sub-cellular fractionation	**92**
2.13	Sulphorhodamine B (SRB) colourimetric assay	**93**
2.14	Clonogenic assay	**94**
2.15	Patients and tissue specimens (For chapter 3)	**94**
2.16	Clinical samples (For chapter 6)	**95**
2.17	Wound healing migration assay (Scratch assay)	**95**
2.18	Transwell cell migration and invasion assay	**96**

2.19	Senescence-associated β-galactosidase activity assay	**96**
2.20	Caspase-Glo assay	**97**
2.21	Anchorage independent soft agar growth assay	**98**
2.22	Mammosphere formation assay	**98**
2.23	Immunofluorescence	**98**
2.24	Flow cytometry	**99**
2.25	Affymetrix whole transcriptome (WT) array	**99**
2.26	Microarray data processing and analysis	**103**
2.27	Pyrosequencing	**104**
2.28	Statistical Analysis	**105**
CHAPTER 3: EP300 and SIRT1/6 co-regulate lapatinib sensitivity via modulating FOXO3 acetylation and activity in breast cancer		**106**
3.1	Introduction	**107**
3.2	Results	**109**
3.2.1	Lapatinib treatment increases FOXO3 acetylation and its activity in sensitive BT474 cells	**109**
3.2.2	Lapatinib induces FOXO3 recruitment to its target gene promoters in sensitive but not in lapatinib-resistant cells	**112**
3.2.3	Triple foxo1/3/4 knock-out mouse embryonic fibroblasts are resistant to lapatinib	**112**
3.2.4	FOXO3 plays a key role in regulating lapatinib sensitivity in BT474 LapR and triple foxo1/3/4 knock-out MEFs	**114**
3.2.5	EP300-FOXO3 interaction is induced by lapatinib treatment in BT474 cells	**117**
3.2.6	EP300 acetylates FOXO3 and induces lapatinib sensitivity	**118**
3.2.7	EP300 regulates long-term lapatinib sensitivity in wild-type BT474 but not in BT474-Lap^R cells	**122**
3.2.8	SIRT1 and SIRT6 regulate the acetylation status, expression and activity of FOXO3 in MEFs	**124**
3.2.9	Lapatinib treatment increases acetylated FOXO3 levels as well as its activity in MEFs	**126**
3.2.10	Silencing of SIRT1 and SIRT6 correlates with increased FOXO3 acetylation and its transcriptional activity in HER2 overexpressed breast	**129**

	cancer	
3.2.11	Knockdown of SIRT6 increases lapatinib cytotoxicity in sensitive cells	**133**
3.2.12	Inhibition of sirtuins by sirtinol induces FOXO3 acetylation and lapatinib sensitivity	**134**
3.2.13	FOXO3 expression correlates with SIRT6 and SIRT1 levels in different breast cancer subtypes	**136**
3.3	Discussion	**138**
CHAPTER 4: CBP mediated FOXO3 acetylation increases lapatinib sensitivity via inducing cell senescence and apoptotic cell death of breast cancer		**143**
4.1	Introduction	**144**
4.2	Results	**146**
4.2.1	Lapatinib treatment enhances CBP expression which in turn induces FOXO3 acetylation and autophagic protein expression	**146**
4.2.2	CBP overexpression caused an increase of FOXO3 acetylation which sequentially upregulates the expression of cell senescence and autophagic markers	**147**
4.2.3	CBP downregulates breast cancer drug resistance genes ABCG2, ABCC1, ABCC4 and ABCC5 in BT474 Lap^R cells	**151**
4.2.4	Co-immunoprecipitation assay confirms CBP mediated FOXO3 acetylation and shows the interaction between CBP and FOXO3	**153**
4.2.5	Ectopic overexpression of CBP enhances short-term and long-term lapatinib sensitivity	**156**
4.2.6	Ectopic CBP overexpression reduces mammosphere forming capacity of BT474 and Lap^R cells	**158**
4.2.7	Overexpression of CBP can be combined with lapatinib to promote FOXO3 acetylation and activity	**160**
4.2.8	CBP overexpression augments senescent phenotype in both BT474 and SKBR3 upon lapatinib treatment	**162**
4.2.9	CBP overexpression facilitates caspase mediated apoptosis in BT474 cells	**163**
4.2.10	CBP overexpressing cells gain motility and invasion	**164**
4.2.11	siRNA mediated knockdown of CBP suppresses the expression of Bim, $p27^{Kip1}$, $p16^{INK4a}$ and LC3BII	**168**

4.2.12	CBP deficient BT474 cells are resistant to lapatinib	**170**
4.2.13	Knockdown of CBP enhances cell migration of both BT474 and BT474 Lap^R	**172**
4.2.14	Silencing of CBP favours mammosphere formation in BT474 and BT474 Lap^R cells	**173**
4.2.15	CBP inhibitors C646 and PFCB1 reduces FOXO3 acetylation and downstream transcriptional activity	**175**
4.2.16	CBP inhibitors C646 and PFCB1 increases clonogenic potentiality of BT474 cells	**179**
4.3	Discussion	**182**
CHAPTER 5: Elucidating the role of SIRT2 in regulating FOXO3 acetylation as well as lapatinib sensitivity of breast and nasopharyngeal cancer		**186**
5.1	Introduction	**187**
5.2	Results	**190**
5.2.1	Duolink proximity ligation assay indicates upregulation of acetylation of FOXO3 after silencing SIRT2	**190**
5.2.2	Silencing of SIRT2 combined with lapatinib treatment upregulates FOXO3 acetylation and its transcriptional activity	**191**
5.2.3	Knockdown of SIRT2 increases lapatinib cytotoxicity in sensitive cells	**195**
5.2.4	Newly designed SIRT2 inhibitor exhibited potential cellular activity by increasing acetylated tubulin levels	**197**
5.2.5	SIRT2 inhibitors maintain FOXO3 levels but reduces FOXM1 and c-Myc expression in MCF-7 cells	**200**
5.2.6	SIRT2 inhibitor scAB8A44 induces FOXO3 acetylation and its transcriptional activity in BT474 cells	**202**
5.2.7	Inhibition of SIRT2 facilitates FOXO3 acetylation which results in a reduced cell proliferation and increased lapatinib sensitivity	**206**
5.2.8	Effects of lapatinib on cell viability of different nasopharyngeal carcinoma (NPC) cell lines	**209**
5.2.9	Effects of lapatinib on the expression and activity of proteins involved in EGFR/ERBB2 signalling in the 5-8F and 6-10B NPC cells	**211**
5.2.10	FOXOs mediate the cytotoxic function of lapatinib	**214**

5.2.11	The clonogenic survival of NPC cells is sensitive to chemical inhibitors of SIRTs	**216**
5.2.12	SIRT2 inhibitors AK1 and AGK2 function cooperatively with lapatinib in NPC cells	**218**
5.2.13	Silencing of SIRT2 enhances lapatinib sensitivity of NPC cells	**223**
5.2.14	Inhibition and silencing of SIRT2 can combine with lapatinib to promote FOXO3 acetylation	**225**
5.3	Discussion	**227**
CHAPTER 6: Oncogenic EP300 can be targeted with inhibitors of aldo-keto reductases (AKR1C) in triple negative breast cancer Hs578T		**232**
6.1	Introduction	**233**
6.2	Preliminary Results	**235**
6.2.1	Correlation of EP300 and E-cadherin in breast tissue	**235**
6.2.2	Loss of EP300 and E-cadherin expression correlates with metastatic lymph node invasion in breast cancer	**237**
6.3	Results	**238**
6.3.1	A cell model to study EP300 function independently of E-cadherin	**238**
6.3.2	EP300 overexpression upregulates the expression of epithelial to mesenchymal transition (EMT) markers in Hs578T cells	**239**
6.3.3	EP300 cannot induce FOXO3 acetylation but acetylates snail and zeb1 in Hs578T cells	**243**
6.3.4	Subcellular fractionation confirmed nuclear localisation of EMT inducing transcription factors	**245**
6.3.5	5-Aza-dC treatment restores E-cadherin expression in EP300 overexpressed Hs578T cells	**246**
6.3.6	High level of ALDH activity identifies involvement of EP300 in producing cancer stem cells	**248**
6.3.7	EP300 overexpressing Hs578T cells are enriched in a $CD44^{high}CD24^{low}$ cell sub-population	**250**
6.3.8	EP300 overexpressing Hs578T cells gain migration and invasion capacity	**251**
6.3.9	EP300 overexpression enhances mammosphere forming efficiency and anchorage independence soft agar cell growth of Hs578T cells	**253**

6.3.10	EP300 increases long-term doxorubicin and paclitaxel resistance in Hs578T cells	**256**
6.3.11	Molecular signature of oncogenic EP300 indicates a major role of aldo-keto reductases	**258**
6.3.12	Validation of up/down-regulated genes by RT qPCR	**260**
6.3.13	Drug resistant Hs578T cells show upregulated AKR1C as well as EMT markers	**262**
6.3.14	Bioinformatic analyses of ChIP-seq data indicate the binding of EP300 to AKR1C genes promoter	**264**
6.3.15	Oncogenic EP300 can be targeted with FFA	**266**
6.3.16	FFA reduces the expression of some EMT markers andAKR1Cs in drug resistant Hs578T cells	**268**
6.3.17	FFA inhibits sphere forming efficiency of both EP300 overexpressed and drug resistant Hs578T cells	**269**
6.4	Discussion	**272**
CHAPTER 7: Final discussions		**276**
7.1	EP300 and SIRT1/6 co-regulate lapatinib sensitivity via modulating FOXO3 acetylation	**277**
7.2	CBP mediated FOXO3 acetylation suppresses cell proliferation via inducing cellular senescence and apoptosis	**281**
7.3	SIRT2 mediated FOXO3 deacetylation modulates lapatinib sensitivity both in BT474 and nasopharyngeal carcinoma	**284**
7.4	Oncogenic EP300 can be targeted with inhibitors of AKR1C	**286**
References		**291**
Appendices		**317**

List of figures

Figure 1.1	Molecular subtyping of breast cancer	**29**
Figure 1.2	HER2 Signalling pathway and the targeted therapies for HER2 overexpressed breast cancers	**31**
Figure 1.3	The chemical structure of lapatinib	**33**
Figure 1.4	Major mechanisms of cancer drug resistances	**37**
Figure 1.5	Primary signalling pathways regulating EMT	**40**
Figure 1.6	Opposite roles of HATs and HDACs in normal and cancer cells in terms of gene regulation.	**47**
Figure 1.7	Domain architecture of EP300	**52**
Figure 1.8	Schematic representation of the domain architecture of CBP	**53**
Figure 1.9	Domain structure of FOXO proteins	**57**
Figure 1.10	Cellular roles of FOXO3-FOXM1 axis in cancer	**61**
Figure 1.11	Signalling pathways regulating FOXO3 phosphorylation	**64**
Figure 1.12	Regulation of FOXO phosphorylation by 14-3-3 scaffolding protein	**65**
Figure 1.13	Downstream targets and cellular functions of SIRT1	**69**
Figure 1.14	Schematic representation of the possible regulation of FOXO3 acetylation by SIRT1, SIRT2 and SIRT6	**71**
Figure 2.1	Schematic representation of generation of stable cell lines using lentivirus	**79**
Figure 2.2	Schematic representation of in situ Proximity Ligation Assay (PLA)	**82**
Figure 2.3	Schematic representation of WT Plus amplification and labelling processes	**101**
Figure 3.1	Lapatinib treatment increases acetylation of FOXO3 as well as its expression and transcriptional activity in BT474 sensitive cells but not in resistant cells	**111**
Figure 3.2	FOXO3 regulates lapatinib sensitivity in BT4T4 and MEFs	**113**
Figure 3.3	Overexpression of FOXO3 in BT474 Lap^R cells reuces cell viability	**115**
Figure 3.4	Overexpression of FOXO3 in MEFscells inhibits cell growth	**116**

Figure 3.5	Duolink proximity ligation assay (PLA) for detecting the protein-protein interactions between EP300 and FOXO3 in BT474 and BT474 Lap^R cells	**117**
Figure 3.6	EP300 overexpression upregulates FOXO3 acetylation and its transcriptional activity	**120**
Figure 3.7	EP300 overexpression upregulates FOXO3 acetylation and increases lapatinib sensitivity	**121**
Figure 3.8	EP300 expression correlates with increased long-term lapatinib cytotoxicity in sensitive but not BT474 Lap^R cells	**123**
Figure 3.9	SIRT1 and SIRT6 regulates the acetylation status, expression levels and activity of FOXO3	**125**
Figure 3.10	Assessing the role of SIRT1 in regulating acetylation of FOXO3 upon lapatinib treatment	**127**
Figure 3.11	Assessing the role of SIRT6 in regulating acetylation of FOXO3 upon lapatinib treatment	**128**
Figure 3.12	Silencing of SIRT1 and SIRT6 with or without Lapatinib treatment correlates with increased FOXO3 acetylation and its transcriptional activity	**130**
Figure 3.13	Silencing of SIRT1 and SIRT6 with or without Lapatinib treatment correlates with increased FOXO3 transcriptional activity	**131**
Figure 3.14	Silencing of SIRT1 and SIRT6 positively correlates with increased FOXO3 acetylation	**132**
Figure 3.15	Silencing of SIRT6 increases long-term lapatinib cytotoxicity in BT474 cells	**133**
Figure 3.16	Sirtinol treatment increases FOXO3 acetylation and inhibits long-term cell growth in BT474 cells	**135**
Figure 3.17	FOXO3 expression correlates with SIRT6 and SIRT1 levels in different breast cancer subtypes	**137**
Figure 3.18	Schematic model showing the regulation of FOXO3 acetylation by EP300 and SIRT1/6 and its subsequent outcome on Lapatinib sensitivity and resistance in breast cancer cells	**142**
Figure 4.1	Lapatinib treatment enhances CBP expression which in turn induces FOXO3 acetylation and autophagic gene expression	**147**

Figure 4.2	CBP overexpression upregulates FOXO3 acetylation and its downstream transcriptional activity	**149**
Figure 4.3	CBP overexpression upregulates FOXO3 acetylation and its downstream transcriptional activity	**150**
Figure 4.4	CBP downregulates breast cancer drug resistant genes ABCG2, ABCC1, ABCC4 and ABCC5	**152**
Figure 4.5	CBP acetylates FOXO3 in BT474 cells	**154**
Figure 4.6	CBP interacts with FOXO3 in naïve and FOXO3 overexpressed cells	**155**
Figure 4.7	CBP overexpression increases short and long-term lapatinib sensitivity	**157**
Figure 4.8	CBP regulates mammosphere forming capacity in both sensitive and resistant BT474 cells	**159**
Figure 4.9	CBP overexpression combined with lapatinib upregulates FOXO3 acetylation and its activity	**161**
Figure 4.10	CBP overexpression with lapatinib treatment increases SA-β-Gal expression in BT474 and SKBR3 cells	**162**
Figure 4.11	CBP overexpressed cells undergo apoptosis via caspase pathway. BT474 cells were transfected with, pLVX, CBP and CBP dHAT	**163**
Figure 4.12	CBP impairs BT474 cell motility	**164**
Figure 4.13	CBP impairs BT474 Lap^R cell motility	**165**
Figure 4.14	CBP overexpression reduces cell migration capabilities	**166**
Figure 4.15	CBP overexpression reduces cell invasion capabilities	**167**
Figure 4.16	Knockdown of CBP inhibits FOXO3 acetylation and its transcriptipnal activity	**169**
Figure 4.17	CBP deficient cells are resistant to lapatinib compared to non-silenced control	**171**
Figure 4.18	Knockdown of CBP enhances BT474 cell motility	**172**
Figure 4.19	Knockdown of CBP enhances BT474 LapR cell motility	**173**
Figure 4.20	Silencing CBP increases sphere forming capacity	**174**
Figure 4.21	Determination of IC50 of C646 and PFCBP1 in BT474 and BT474 Lap^R cells	**176**

Figure 4.22	CBP inhibitors reduces FOXO3 acetylation and activity	**177**
Figure 4.23	CBP inhibitors reduces FOXO3 acetylation and its transcriptional activity	**178**
Figure 4.24	CBP inhibition increases clonogenic potential in BT474 cells	**180**
Figure 4.25	CBP inhibition reduces lapatinib resistance in BT474 LapR	**181**
Figure 5.1	Duolink proximity ligation assay (PLA) for detecting the acetylation level of FOXO3 by silencing of SIRT2 in BT474 WT and BT474 Lap^R cell lines	**190**
Figure 5.2	Silencing of SIRT2 with lapatinib treatment correlates with increased FOXO3 acetylation and its transcriptional activity	**192**
Figure 5.3	Silencing of SIRT2 with or without lapatinib induces caspase mediated apoptosis	**193**
Figure 5.4	Knockdown of SIRT2 with lapatinib increases FOXO3 expression and activity at mRNA level	**194**
Figure 5.5	Knocking down of SIRT2 correlates with increased long-term lapatinib cytotoxicity in sensitive and resistant BT474 cells	**196**
Figure 5.6	Effect of SIRT2 inhibitors on tubulin acetylation	**198**
Figure 5.7	Protein quantification analysis by using ImageJ	**199**
Figure 5.8	Effect of ScA-B8A44, DK-029, AGK2 and ScA-A13B7 in the regulation of expression of FOXO3, Ac-FOXO3 and FOXM1	**201**
Figure 5.9	Effect of SIRT2 inhibitor ScAB8A44 on FOXO3 acetylation and activity in BT474	**203**
Figure 5.10	Effect of SIRT2 inhibitor ScAB8A44 on FOXO3 acetylation and activity in BT474	**204**
Figure 5.11	ScAB8A44 induces cell death via caspase activation pathway	**205**
Figure 5.12	ScAB8A44 induced FOXO3 acetylation increases lapatinib sensitivity in BT474 cells	**207**
Figure 5.13	AGK2 induced FOXO3 acetylation inhibits cell proliferation	**208**
Figure 5.14	Effect of Lapatinib on cell growth and proliferation of NPC cells	**210**
Figure 5.15	Effect of lapatinib on the expression and activation of proteins involved in ERBB1 and ERBB2 signaling pathways in high -low metastatic NPC cell lines	**213**
Figure 5.16	FOXO3 regulates EGFR and ERBB2 expression and increases	**215**

	lapatinib sensitivity in mouse embryonic fibroblast cells	
Figure 5.17	Inhibition of SIRT2 by AGK2, AK1 and EX527 inhibits long-term cell growth and colony formation of high and low metastatic NPC cells	**217**
Figure 5.18	Determination of IC50 of SIRT inhibitors from SRB assay	**219**
Figure 5.19	High and low metastatic NPC cells show increased Lapatinib sensitivity upon combination treatment with AGK2 and AK1 but not with Sirtinol or EX527	**220**
Figure 5.20	High and low metastatic NPC cells show increased Lapatinib sensitivity upon combination treatment with AGK2 and AK1 but not with Sirtinol or EX527	**221**
Figure 5.21	Lapatinib in combination with AGK2/AK1 increase long term cell sensitivity compared to lapatinib alone	**222**
Figure 5.22	Silencing of SIRT2 increases long-term lapatinib cytotoxicity in NPC cells	**224**
Figure 5.23	Inhibition of SIRT2 by AGK2 as well as silencing of SIRT2 in combination with Lapatinib upregulates acetylated FOXO3 levels in 5-8F and 6-10B cells	**226**
Figure 6.1	EP300 and E-cadherin expression in breast tissue	**236**
Figure 6.2	E-cadherin promoter is methylated in EP300^{high}/E-cadherin^{low} tumours	**239**
Figure 6.3	EP300 overexpression upregulates expression of epithelial to mesenchymal transition (EMT) markers in Hs578T cells	**241**
Figure 6.4	Immunofluorescence experiment confirms EP300 mediated EMT induction (^{low}E-cadherin/^{High}Vimentin)	**242**
Figure 6.5	EP300 cannot increase acetylation of FOXO3 but induces acetylation of snail and zeb1 in Hs578T cells	**244**
Figure 6.6	Subcellular fractionation confirms nuclear localization of EMT inducing transcription factors	**245**
Figure 6.7	5´-Aza-dC treatment restores E-cadherin expression in EP300 overexpressed Hs578T cells	**247**
Figure 6.8	High level of aldehyde dehydrogenase (ALDH) activity identifies involvement of EP300 in producing cancer stem cells	**249**

Figure 6.9	EP300 overexpressed cells are enriched in $CD44^{high}CD24^{low}$ cell population	**251**
Figure 6.10	EP300 overexpression correlates with increased cell migration and invasion of Hs578T	**252**
Figure 6.11	EP300 enhances anchorage independent growth of Hs578T	**254**
Figure 6.12	EP300 enhances mammosphere formation efficiency of Hs578T	**255**
Figure 6.13	Overexpressing EP300 increases long-term doxorubicin and paclitaxel resistance in Hs578T cells	**257**
Figure 6.14	Overexpressing EP300 increases long-term doxorubicin and paclitaxel resistance in Hs578T cells	**258**
Figure 6.15	Validation of up-regulated genes from micro-array analysis	**260**
Figure 6.16	Validation of down--regulated genes from micro-array analysis	**261**
Figure 6.17	Up-regulation of aldo-keto reductases and EMT markers in Hs578T drug resistant cells	**263**
Figure 6.18	Bioinformatic analyses of chromatin immunoprecipitation-sequencing (ChIP-seq) data from The Encyclopedia of DNA Elements (ENCODE)	**265**
Figure 6.19	Pharmacological inhibition of aldo-keto reductases reverts drug resistance	**267**
Figure 6.20	FFA reduces the expression of some EMT markers	**268**
Figure 6.21	FFA reduces anchorage independent growth	**270**
Figure 6.22	FFA reduces mammosphere formation of drug resistant Hs578T cells	**271**
Figure 6.23	Schematic model representing the oncogenic role of EP300 that can be targeted with inhibitor of AKR1C	**275**

List of Appendix figures

Appendix figure A3.1	Validation of Lapatinib resistance in BT474 Lap^R cells	**317**
Appendix figure A3.2	Overexpression of EP300 or EP300 ΔHAT does not affect Lapatinib resistance in BT474 cells	**317**
Appendix figure A3.3	Overexpression of EP300 in BT474 and Lap^R	**318**
Appendix figure A3.4	Lapatinib treatment in SKBR3 cells	**319**
Appendix figure A3.5	Overexpression of EP300 in SKBR3 cells	**320**
Appendix figure A3.6	Knockdown of SIRT6 increases lapatinib cytotoxicity in sensitive BT474 cells but not in resistant cells	**320**
Appendix figure A4.1	Subcellular fractionation confirms nuclear localization ofCBP and FOXO3	**321**
Appendix figure A4.2	Overexpression of CBP increases FOXO3 acetylation and its transcriptipnal activity in SKBR3 cells	**322**
Appendix figure A4.3	CBP overexpressed SKBR3 cells are sensitive to lapatinib compared to control and HAT mutant	**323**

List of Tables

Table 1.1	List of EMT regulators in breast cancer progression and metastasis.	**45**
Table 1.2	General classification of Human HDACs	**49**
Table 1.3	Genes targeted by FOXO3 and their respective cellular functions in regulating tumorigenesis	**59**
Table 2.1	Human primers used for RT-qPCR	**87**
Table 2.2	Mouse primers used for RT-qPCR	**90**
Table 2.3	Human primers used for ChIP	**92**
Table 6.1	Expression of E-cadherin correlates with that of its transcriptional activator EP300 in both non-malignant and breast cancer	**237**
Table 6.2	Correlation between EP300 and E-cadherin expression is a good predictor of lymph node metastasis	**238**
Table 6.3	Selection of most up-and down-regulated genes in Hs-EP300 cells.	**259**

CHAPTER 1

INTRODUCTION

1.1 Cancer

Cancer is a type of condition where abnormal cells continue to grow and proceed to uncontrolled cell divisions. Some cancers may ultimately migrate throughout the body that is defined as metastasis. Approximately 18.1 million new cancer cases and 9.6 million cancer deaths were estimated in 2018 worldwide [1]. According to GLOBOCAN 2018, lung cancer has been described as the most frequently detected cancer. Therefore, lung cancer is considered as the principal cause of cancer-associated death followed by female breast cancer, prostate cancer, and colorectal cancer [2]. However, the frequency of cancer incidence and mortality vary from country to country. In the UK, around 363,000 new cancer cases and about 164,000 cancer deaths recognised every year (2014-2016) (Statistics obtained from the Cancer Research UK website, 2016).

1.2 Breast cancer

Breast cancer is a common cancer in women and one of the leading causes of cancer-related mortality [3]. About 627,000 female death occurred from breast cancer in 2018 that is approximately 15% of all cancer deaths among women (World Health Organisation report 2019). According to GLOBOCAN 2018 report breast cancer is the most commonly reported cancer in most of the countries (154 of 185). To date, breast cancer cases were found to be maximum in Australia/New Zealand, Northern Europe (e.g., the United Kingdom, Sweden, Finland, and Denmark), Western Europe (Belgium, Netherlands, and France), Southern Europe (Italy), and Northern America [1]. However, in recent years breast cancer death rates declined significantly due to increased awareness, early detection, and improved treatment options available [3].

There are various environmental and genetic factors responsible for causing breast cancer. Obesity, alcohol intake and exposure to radiation are the three major reasons contributing to the growth and progression of breast cancer [4]. However, about 5% to 10% of breast cancer deaths are thought to be genetic [3] and mainly triggered by the inheritance of multiple genes harbouring mutations. For example, the two most studied genes that gain and harbour mutations are Breast cancer type 1 susceptibility protein (BRCA1) and breast cancer type 2 susceptibility protein (BRCA2). It is also known that mutations in *BRCA1* are responsible for breast and

ovarian cancer in women, while male breast cancers are triggered by mutations in the *BRCA2* gene as these mutations were found to be associated with aggressive breast cancer in men [5]. Active BRCA1 and BRCA2 both act as tumour suppressors and regulate different biological processes especially DNA damage and repair functions.

1.3 Classification of breast cancer based on molecular subtyping

Breast cancer is classified into three basic groups based on clinical studies. The estrogen receptor (ER) positive class is associated with breast, colon, ovarian and endometrial cancers [6]. For example, an increased level of ERα expression was observed in 70% of breast cancer cases, therefore termed as ERα positive tumours. Another important group of breast cancer is the human epidermal growth factor receptor 2, *HER2* (also called *ERBB2*) amplified group as it occurs in 20–30% of breast cancers and ovarian cancers [7]. Moreover, triple-negative breast cancers (TNBC) lack expression of ER, progesterone receptor (PR) and HER2, which is also termed as basal-like breast cancer [8]. The only therapeutic option for TNBCs is radio and chemotherapy while ER-positive and HER2-positive patients depend fully on targeted therapies. Recent studies using genome-wide expression technologies identified several inherent molecular subtypes of breast cancers. These cancer types are classified as basal-like, HER2-overexpressed, normal breast-like, luminal subtype A and luminal subtype B (Figure 1.1) [8-10].

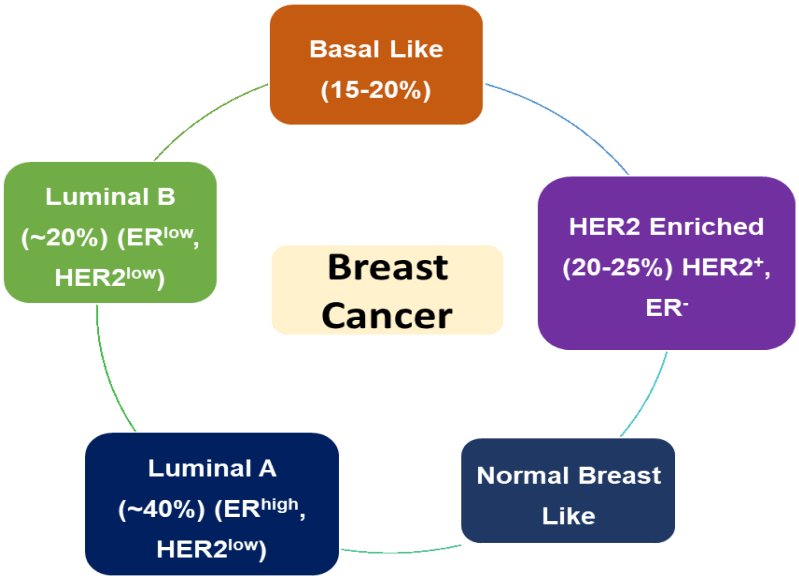


Figure 1.1 Molecular subtyping of breast cancer [adapted from [11]

1.4 HER2 overexpressed breast cancer

The HER receptors play a key role in the development and progression of various human cancers [12]. The HER family is comprised of four members, e.g. HER1 (human epidermal growth factor receptor, EGFR), HER2, HER3, and HER4 [13]. The HER2 receptor is a transmembrane glycoprotein with a size of 185 KDa containing 1255 amino acids and is positioned at the long arm of human chromosome 17 (17q12) [14]. HER proteins transduce multiple signalling programmes to show their biological functions. To do this, these proteins undergo dimerization upon ligand binding to their extracellular domains. Apart from EGFR, HER3 and HER4, HER2 proteins were found to undergo ligand-independent spontaneous dimerization upon HER2 overexpression (Figure 1.2) [15]. Concomitant auto-phosphorylation of their intracellular domains further activates multiple signalling pathways including the mitogen-activated protein kinase (MAPK) and phosphatidyl-inositol-3-kinase (PI3K) pathways (Figure 1.2) [13, 16]. These activated signal transduction pathways promote cell survival, differentiation, DNA damage repair and angiogenesis. Moreover, dimerization of HER2 induces the cytoplasmic sequestration and proteosomal degradation of cell-cycle inhibitor protein which in turn activate cell cycle progression [17]. However, HER2 can also be activated after forming complexes with other membrane receptors. For example, it has been found from a scientific study that HER2 can form complexes with insulin-like growth factor receptor 1 to induce downstream signalling pathways, contributing to trastuzumab resistance of breast cancer [18].

Twenty percent of breast cancers were found to express an alternatively spliced version of HER2 that is responsible for the expression of the juxtamembrane domain. Importantly, this spliced form of HER2 can form homodimers and thus constitutively active [19]. In addition, genetic overexpression of this shortened form of HER2 in mice induces the growth and progression of aggressive cancer [20]. Furthermore, less than 10% of ER+ cancers were found to express high level of HER2, suggesting that HER2 overexpression is negatively correlated with estrogen receptor (ER) expression [21]. Elevated HER expression was also found to be linked with ER-independent cell proliferation and reduced sensitivity to endocrine therapy [22]. In addition, mutations harboured in HER2 gene play a major role in causing aberrant HER2 expression. Approximately 20–30% of breast cancers over-express

HER2 due to genetic mutation [23]. Aberrant expression of the HER2 receptor significantly contributes to tumorigenesis and drug resistance of this type of breast cancer.

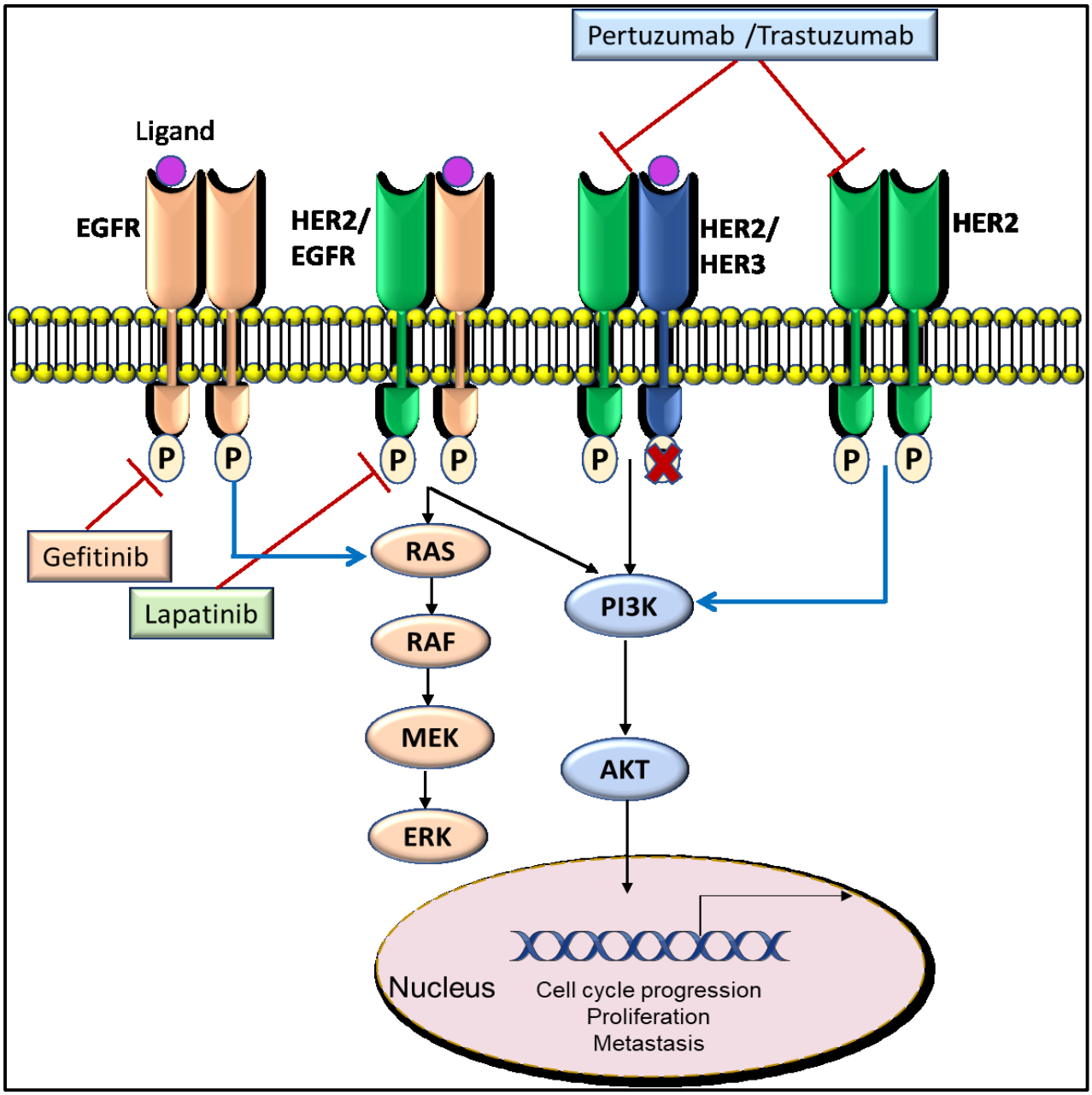


Figure 1.2 HER2 Signalling pathway and the targeted therapies for HER2 overexpressed breast cancers. The HER2 or EGFR receptors are activated by auto-phosphorylation upon ligand binding. HER2 does not need to be bound to a ligand for their activation. HER2 is the favoured dimerization partner among all the receptors. Dimerization and subsequent phosphorylation result in the activation of downstream pathways, including the PI3K/AKT and RAF/MEK/MAPK pathways. Chemotherapeutic drug Gefitinib selectively inhibits autophosphorylation of EGFR whereas lapatinib targets both EGFR and HER2. [Adapted from [24]]

1.5 Adjuvant therapies for breast cancer treatment

Adjuvant system therapies are applied to most women having early-stage breast cancer. Endocrine therapy, tissue-targeted therapies, and chemotherapeutic treatments substantially reduce tumour relapse and associated death. Taxanes (e.g. Paclitaxel and Docetaxel) and anthracyclines (e.g. Epirubicin and Doxorubicin) are the two most effective and broadly used chemotherapeutic drugs for treating triple-negative breast cancer patients [25, 26]. Anthracyclines act as DNA damaging agents via the inhibition of the activity of the topoisomerase II. Topoisomerases are ubiquitous enzymes which are crucial for DNA replication and transcription, as they regulate the winding and unwinding of the DNA structure to create transient single-stranded breaks (by Topoisomerase I) or double-stranded breaks (by Topoisomerase II) in the helix, for the insertion of new DNA strands [27]. Anthracycline particularly targets Topoisomerase II to accelerate the rate of insertion of double-stranded breaks, while refraining the enzyme from its re-sealing capacity. To enhance their disruptive activity, anthracyclines simultaneously intercalate within the DNA strands and stimulate the generation of reactive oxygen species (ROS), as well as activating ataxia telangiectasia mutated kinase (ATM) in response to DNA damage, inducing p53 nuclear translocation, and eventually leading to cell cycle inhibition and apoptotic induction [28, 29]. Unlike anthracyclines, paclitaxel plays its role as a microtubule stabilizer and acts primarily in the G2/M phase of the cell cycle process. These perform their cytotoxic function through impairment of the centrosome, induction of abnormal spindle morphology and disruption of normal spindle dynamics, eventually causing cell cycle arrest. However, patients with less sensitivity to drugs or those later becoming resistant to taxane or anthracyclines have limited therapeutic options and consequently, their survival rate is reduced [30].

As mentioned before, HER2-positive breast cancers usually show less responsiveness to hormonal therapy and chemotherapy. Therefore, chemotherapeutic approaches that unambiguously target HER2 receptors are most effective. To date, several pharmacological treatments were attempted to treat HER2 positive breast cancers. For example, an effective treatment strategy for HER2-overexpressing breast cancer patients is the treatment with a monoclonal antibody named as Trastuzumab (Herceptin) that is directed against the extracellular domain

of HER2/neu receptor and has been considered as one of the most important types of HER2 inhibitors that are currently in clinical use [31]. It is noteworthy that, as is the case with many targeted therapies, major number of patients with HER2 positive cancers develop resistance to trastuzumab, resulting in disease progression and thus restricts its clinical efficacy [32].

Lapatinib is a dual EGFR/HER2 tyrosine kinase inhibitor (TKI) that is originally designed and commercialized by Glaxo-Smith-Kline (GSK) to use as an orally active drug for treating HER2 positive breast cancer patients (Figure 1.3). It prevents both HER2 and EGFR signalling pathways and was permitted by the U.S. Food and Drug Administration (FDA) to be used as a combination therapy for the treatment of patients with breast cancers overexpressing HER2 and for those who are unresponsive to trastuzumab [33, 34]. Mechanistically, lapatinib action is induced by binding to the ATP-binding pocket of the EGFR/HER2 protein kinase domain and subsequently inhibiting HER2/EGFR receptor signalling processes [35]. Binding of lapatinib not only blocks the auto-phosphorylation of HER2 receptors but also the downstream signalling through inhibition of PI3K/AKT/mTOR pathway. Any interruption in any of the processes may result in uncontrolled cell growth, metastasis and angiogenesis [36]. In short, lapatinib action is accompanied by inhibition of HER2/ AKT/mTOR pathway via inhibiting tyrosine kinase mediated phosphorylation in HER2 overexpressed breast cancer. To date, lapatinib responsiveness in trastuzumab-resistant cancers was found to be less than 25% [37]. Therefore, understanding the molecular mechanisms that lead to lapatinib resistance may ultimately improve the clinical benefit that patients receive from lapatinib-based treatment.

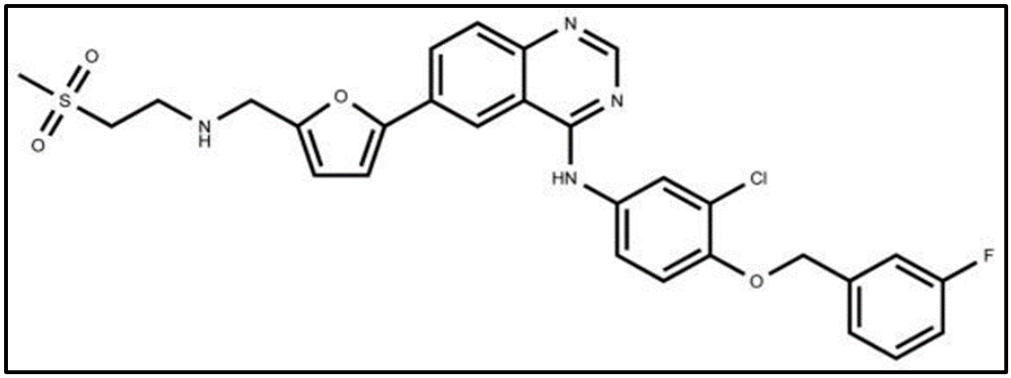


Figure 1.3 The chemical structure of lapatinib [38]

1.6 Nasopharyngeal cancers

Nasopharyngeal cancers (NPC) is one class of head and neck cancer, initiating from the epithelial cells that cover the surface and line on the nasopharyngeal cavity [39]. China, Taiwan, Thailand and Southeast Asia are the regions where NPC cancer is very common. Although NPC aetiology remains unclear, one of the unique features of NPC is its linkage with the Epstein-Barr virus (EBV) infection, which is possibly the most broadly studied contributing factor for NPC [40]. Most of the endemic cases of NPC possess EBV gene products or clonal EBV genomes and this linkage has been shown to be responsible for both the genesis and progression of cancer. Consistently, scientists observed a significant correlation between pre- and post-treatment EBV DNA levels and patient survival [41, 42]. Besides, an elevated level of EGFR expression was also found to be associated with the NPC cancer cell proliferation, survival as well as cell motility and thus EGFR/HER2 is considered as an important receptor target for the treatment of NPC cancer patients [43].

1.7 Treatment options for nasopharyngeal carcinoma

Although the precise mechanism of NPC progression is still unclear, substantial progress has been achieved in NPC management and treatment. Cisplatin and 5-fluorouracil-based chemoradiotherapy regimens are widely used as therapeutic treatment options with occasional surgical intervention. Recently, targeted molecular therapies and immunotherapy have shown promises in the treatment of NPC as these therapies are more effective with fewer side effects compared to the traditional treatment strategy. As mentioned, EGFR is a commonly overexpressed receptor in NPC. Therefore, EGFR-targeted therapies such as cetuximab and nimotuzumab have been trialled in NPC of which cetuximab is directed against the extracellular domain of the EGFR. Combination therapy including cetuximab with carboplatin has also been shown to be effective for those patients with relapsed or aggressive NPC and also to those who have less responsiveness to platinum therapy [44]. Alternatively, gefitinib was examined in a group of heavily pre-treated recurrent NPC patients to target EGFR family of proteins. Moreover, VEGF also plays a pivotal role in lymph node metastasis through the induction of angiogenesis. Therefore, the use of bevacizumab to block angiogenesis explored an improved treatment option via inhibiting VEGF mediated angiogenesis [45, 46]. Targeting recombinant adenovirus-

p53 (rAd-*p53*) gene transduction has also been explored for NPC treatment with the aim of restoring p*53* function, resulting in enhanced radio-sensitivity of NPC cells [47, 48]. Furthermore, a novel curcumin analogue FM807 has been reported to exhibit anticancer properties against both well-differentiated and poorly-differentiated NPC cell lines [49]. In fact, a newly identified Hsp90 inhibitor, AT13387, has been tested in several clinical trials, demonstrating anti-oncogenic effects in the EBV-positive NPC cell line C666 [50].

1.8 Chemotherapeutic drug resistance

Most of the failure of cancer drug treatments are caused by the acquisition and development of cancer drug resistance. There are several factors contributing to chemotherapeutic resistance. Inherent genetic differences in patients and somatic mutations in several tumour suppressor genes are the two main reasons for the drugs to be resistant to conventional therapies. From the scientific literatures, it has been identified that elevated expression of transporters inducing drug efflux, changes in drug metabolism, genetic or induced mutations of specific drug targets and the activation of proliferation pathways or inactivation of downstream apoptotic signalling pathways are major contributing factors for the acquisition of chemotherapeutic drug resistance (Figure 1.4) [51].

Multiple transporter proteins positioned within the cell membranes have been identified as the activator of drug efflux and thus associated with drug resistance. The ABC (ATP-binding cassette) transporters family are the major drivers of the drug transport through the cell membrane. Of all 49 members of ABC transporters, only three have been studied broadly, including multi-drug resistance protein 1 (MDR1), MDR-associated protein 1 (MRP1) and breast cancer resistance protein (BCRP) (Figure 1.4) [52]. Aberrant overexpression of MDR1 has been found to be linked with drug resistance in many cancers, including breast cancers, colon cancers, liver cancers, leukaemias and lymphomas [52]. In addition, the overexpression of MRP1/ABCC1 has been shown to be positively associated with drug ressiatnce in breast, prostate, and lung cancers [53], [54], [55]. The third major protein involved in drug efflux is BCRP/ABCG2 and involved for the chemoresistance of breast cancer and leukaemia [56, 57]. Importantly, HER2/EGFR targeted therapies including imatinib, erlotinib, sunitinib and nilotinib act as substrates for MDR1 and BCRP as

reported by previous study [58]. Moreover, cancer stem cells expressing high CD44 levels also exhibit enhanced levels of drug efflux induced by elevated transporter proteins which is positively associated with patient's death [59]. Indeed, cancer stem cells show high levels of MDRs, especially BCRP transporters [60].

Scientists have proposed various mechanisms to help understand the acquired resistance to endocrine therapies. Resistance to endocrine therapies is positively correlated with crosstalk between ER and HER2 signalling as reported by a previous study [61]. Furthermore, increased expression of EGFR and PI3K activity has also been associated with endocrine resistance [62]. Moreover, induction of EGF-mediated growth response and MAPK activation were also shown to compensate for the estrogen-deprivation in MCF-7 cells [63]. Conversely, in the presence of specific tyrosine kinase inhibitors, sensitivity to endocrine treatment was restored and reversed tamoxifen-resistant tumour growth [64].

Taxane (e.g. paclitaxel) resistance has been linked to mutations in its various targets, such as tubulin, Aurora-A, Bcl-2, and Tau. Overexpression of Bcl-2 elicits resistance to docetaxel whereas silencing of Tau can restore paclitaxel sensitivity [65, 66]. Moreover, chromosomal instability genes have been identified as another important mechanism behind taxane resistance [67]. Anthracycline resistance develops by a multitude of processes, including overexpression of MDR1/ABCB1 and the BCRP transporter proteins [68, 69]. In addition, topoisomerase II mutations, overexpression of DNA repair mechanism and deregulation in the apoptotic signalling (e.g. specific mutations in *p53* are associated with doxorubicin resistance and culminate in an early relapse in breast cancer) have been found to be responsible for anthracycline resistance [70, 71].

Apart from ER-positive breast cancer, HER-2 positive tumours also become resistant against targeted therapies. For example, acquisition of *PIK3CA* gene mutations [72], loss of tumour suppressor PTEN [73], and overexpression of insulin-like growth factor receptor (IGF-1R) have been suggested as major contributing factors for Herceptin resistance. On the other hand, the presence of truncated isoforms of the HER2 receptor (e.g. p95 HER-2 and HER2Δ16) lacking the extracellular trastuzumab-binding domain has been identified as a potential mechanism of

trastuzumab-mediated resistance. The p95 HER-2 mutant isoform is found in around 60% of all HER-2 positive tumours [74]. Lapatinib-acquired resistance has been shown to be mediated by enhanced estrogen receptor signalling as a consequence of FOXO3 activation [75]. However, it has been previously shown that activation of FOXO3 is induced upon lapatinib treatment [76], therefore, it seems contradictory that lapatinib resistance arises from its potent growth inhibitory effect.

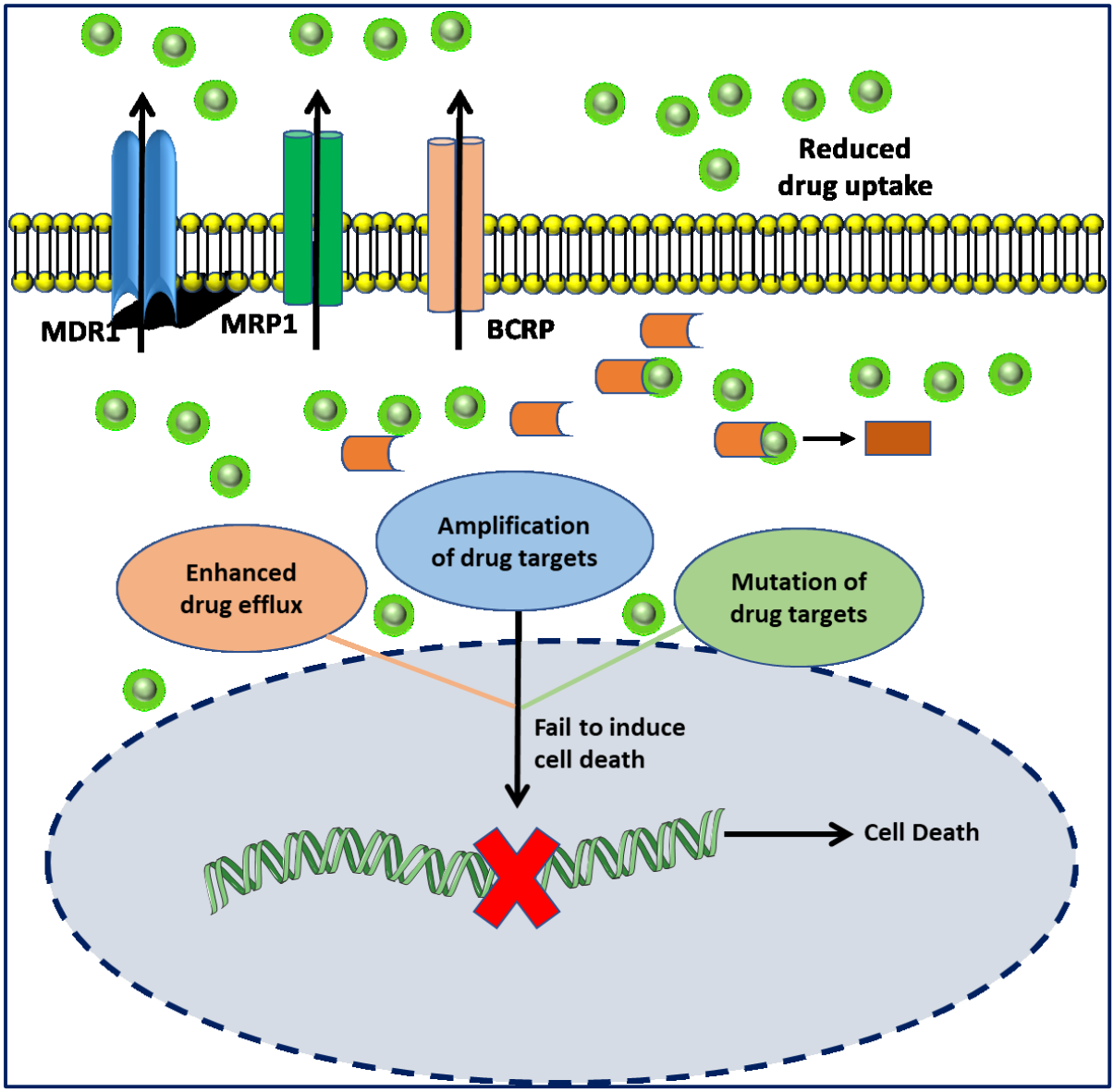


Figure 1.4 Major mechanisms of cancer drug resistances. Chemotherapeutic drug resistance can be evolved by enhanced drug efflux, reduced expression of drug target, mutation of receptor proteins, and a repression of apoptotic cell death. [Adapted from [51]]

1.9 Aldo-keto-reductases family (AKR1C) and breast cancer drug resistance

Aldo–keto reductases sub-family C (AKR1C) catalyse NADPH dependent reduction and comprise of four enzymes AKR1C1–AKR1C4. These enzymes show both catalytic and non-catalytic functions and involved in biosynthesis, intermediary metabolism, detoxification [77]. Recent studies have provided shreds of evidence of their role in regulating malignant transformation as well as the chemotherapeutic resistance [78]. Among the AKR1Cs, AKR1C1 and AKR1C2 are abundantly expressed in mammary glands whereas AKR1C3 and AKR1C4 almost exclusively function in liver and prostate [79, 80]. The role of AKR1C isoforms has been identified in drug metabolism and resistance in cancer. Previous studies explored that AKR1C1, AKR1C2, and AKR1C4 catalyse the carbonyl reduction of the anticancer drug oracin and thus produce its inactive metabolite DHO [81]. Interestingly, AKR1C3 is found to activate the anti-apoptotic PTEN/ AKT pathway, which ultimately causes doxorubicin resistance in human breast cancer [82]. Moreover, AKR1C3 catalyses the reduction of daunorubicin and idarubicin mediating anthracycline resistance of cancer cells [83]. In addition, cisplatin resistance of ovarian cancer cells has been reported to be due to upregulation of AKR1C1 and AKR1C3, as depletion of both enzymes in the resistant cells, or treatment with specific inhibitors of AKR1Cs, enhanced cisplatin sensitivity [84].

1.10 Epithelial to mesenchymal transitions as a hallmark of aggressive cancers

Epithelial-mesenchymal transition (EMT) is a biological process that undergo multiple biochemical changes enabling it to acquire a mesenchymal phenotype including increased migratory capacity, invasiveness and especially enhanced resistance to apoptosis [85]. Therefore, transformation of epithelial cells to mesenchymal cells with increased motile phenotype is one of the key characteristics of EMT process. Extracellular matrix (ECM) degrading protease enzymes, such as serine, cysteine, and metalloproteases play a vital role in the invasion of cancer cells by promoting the EMT-induction. Moreover, acquisition of an EMT phenotype renders tumour cells to gain a capacity to migrate and infiltrate neighbour tissues, allowing them to travel and invade to distant organs [86]. A

number of multiple molecular processes are involved in order to initiate an EMT. These include activation of transcription factors, expression of specific cell-surface proteins, reduced expression of epithelial markers, up-regulation of mesenchymal molecular markers, shifting from keratin to vimentin-type cytoskeleton, and changes in the expression of specific microRNAs. Besides, EMT has been described as a major effector of cancer stem cells as well as tumour [87]. EMT cells gain self-renewal capability, similar to those that are exhibited by the embryonic stem cells and hence, the acquisition of a “cancer stem cell-like” phenotype, known as “cancer stemness” [88, 89].

The EMT process can be activated via extracellular signalling from various growth factors including epidermal growth factor (EGF), fibroblast growth factor (FGF), the transforming growth factor-β (TGF-β), hepatocyte growth factor (HGF), bone morphogenic proteins (BMPs), Wnts and Notch (Figure 1.5). The TGF-β family is a vital factor for EMT due to its crucial control of embryonic processes, fibrotic diseases and tumour metastasis. Upon ligand binding, TGF-β stimulates EMT activation through phosphorylation of SMAD proteins. Consequently, the downstream cytoplasmic proteins regulating cell polarity are activated which in turn promote the development of tight junctions [90]. Other signalling pathways that are regulated by TGF-β are Notch, Wnt or integrin signaling which also involve in the progression of EMT. For example, Wnt signalling pathways can initiate EMT by inhibiting the kinase activity of glycogen synthase kinase-3β (GSK3β) which would otherwise induce cytoplasmic degradation of β-catenin (Figure 1.5). Activated β-catenin translocate from cytoplasm to nucleus, where it acts as a transcription factor and activate the transcription of multiple EMT inducing transcription factors including snail, slug, zeb1/2, twist (Figure 1.5).

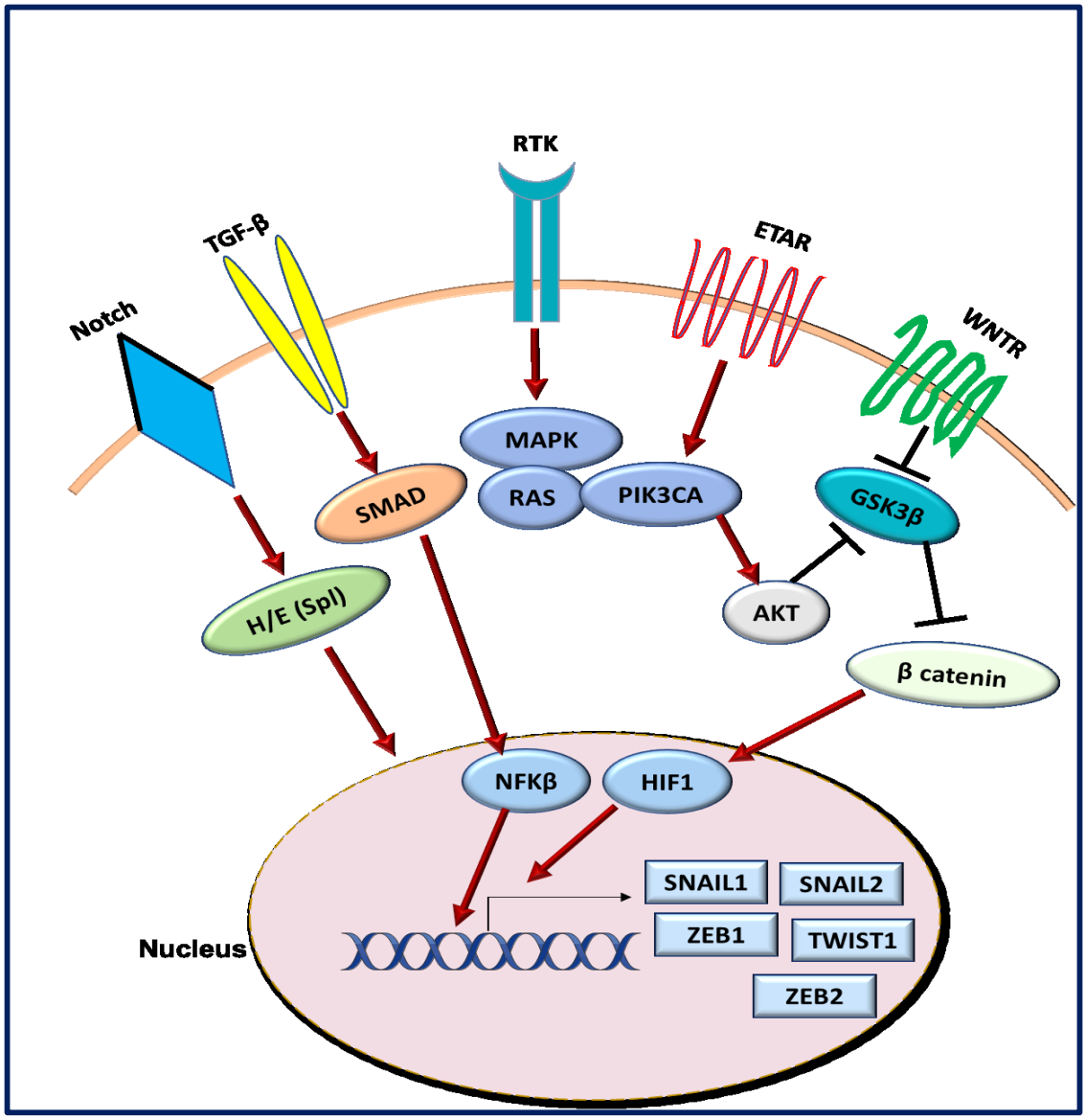


Figure 1.5 Primary signalling pathways regulating EMT. Notch, TGF-β, receptor tyrosine kinase (RTK), endothelin A receptor and Wnt can individually promote EMT through different signalling pathways as depicted in the image. Briefly, Notch induces activation of hairy and enhancer of split (H/E (Spl)), which can in turn activate transcription factors located in the nucleus. Alternatively, TGF-β can act through the Smad proteins to their nuclear effectors. Both RTK and ETAR can instead regulate a MAPK/Ras/PIK3CA protein complex, which can trigger transcription through AKT. Both the AKT, and WNT also act by impeding GSK3β, which would otherwise initiate transcription through activating β-catenin. Transcription factors such as nuclear factor NF-κβ, HIF1, Snail1 and 2, Zinc Finger E-Box Binding Homeobox 1 (ZEB1) and 2 (ZEB2), and the Twist Family (Twist1) are responsible for the initiation of EMT. [Adapted from [91]]

A critical part of the EMT programme is the loss of E-cadherin, a tight junction glycoprotein. Moreover, loss of E-cadherin expression has been recognised as a key marker of malignant tumour. Mechanistically, E-cadherin functions by creating haemophilic interactions with nearby E-cadherin molecules on surrounding cells in a calcium-dependent manner. On the cytoplasmic end, E-cadherin is linked with the

actin cytoskeleton via p120 catenin, α- and β-catenin. However, for functional activity, E-cadherin is linked with both β- and γ-catenin, which serve to link the carboxy-terminal cytoplasmic tail of E-cadherin to α-catenin. Alpha-catenin will then bind to the actin cytoskeleton, either directly or via alpha-actinin [92, 93]. A wide range of transcription factors including the zinc-finger proteins Snail, Slug, SIP1 and helix-loop-helix transcription factor E12/E47 regulate E-cadherin expression at the transcriptional level. For example, Snail is particularly known for its activity to repress E-cadherin, resistance to apoptosis, elevation of cell motility and thus concomitant development of the EMT process in metastatic cancer cells [94].

Expression of E-cadherin can be reduced by various ways, mainly by mutational or epigenetic inactivation. Hyper-methylation of E-cadherin is an important epigenetic silencing process by which E-cadherin transcriptional activity is repressed. Alternatively, matrix metalloproteases (MMPs) are the protease enzymes that catalyse proteolytic reactions to degrade all extracellular matrix (ECM) components. For example, MMP2, MMP9, MMP7 and MMP14, -mediated proteolytic degradation inhibits E-cadherin activity [95]. Nawrocki et al. showed the significant role of MMPs in regulating E-cadherin expression, as MMPs-mediated cleavage of E-cadherin results in the secretion of the cleaved/soluble E-cadherin fragments (sE-cadherin), up-regulating the expression of MMPs in lung cancer [96].

To date, it is not clear what is the main inducer that drive cancer cells to undergo EMT. Scientists have revealed that signals triggering EMT during embryogenesis may come from nearby tumour-associated stromal cells [97]. Metastatic cancers are also known to have an increased expression of markers typically expressed during embryogenesis. For instance, the expression of N-cadhernin is up-regulated in metastatic cancers. This transmembrane glycoprotein is also associated with migrating neurons and mesenchymal cells during organogenesis suggesting its possible role in EMT [98]. N-cadherin belongs to the calcium-dependent cell adhesion molecule family and encoded by the cluster of differentiation 325 gene, or CDH2. In healthy tissues, N-cadherin is indispensable for the normal function of the cardiac muscle, whereby it mediates adherents' junctions of intercalated discs, thus mechanically and electrically coupling adjacent cardiomyocytes. Originally named for its role in neurons, this protein is now under extensive studies for its contribution to

tumour progression and metastasis, where it has been shown to provide a mechanism for trans- endothelial migration. N-cadherin replaces E-cadherin during both developmental and pathogenic EMT, whereas Vimentin and fibronectin replace cytokeratins. Therefore, a polarised epithelial cell can undergo the interactions with its basement membrane and proceed to the morphological changes which enable it to display a mesenchymal phenotype. These mesenchymal cells show reduced sensitivity to apoptosis, higher production of extra-cellular matrix components, and the crucial ability to both migrate and invade. In addition, disassembly of the static actin structures occurs in migrating cells in order to gain motility, so as to obtain a fine actin network capable of being flexible to form membrane protrusions called lamellipodia [99, 100].

1.11 EMT in breast cancer

EMT in breast cancer is usually found to be linked with CSC like properties, self-renewal capabilities and resistance to traditional cancer therapies [89]. Studies suggest that acquisition and maintenance of stem cells can be promoted by EMT [101]. To date, multiple pathways have been discovered to lead to the EMT in breast cancer cell lines. For instance, TGF-β1, hepatocyte growth factors, and PDGF are some of the up-stream growth factors which activate a series of transcription factors such as Snail 1, Snail 2 (slug), Twist 1, FOXC1, and FOXC2, as well as the E-box binding zinc finger proteins Zinc1 and Zinc2 (Sip1) to regulate EMT programme [102, 103]. Previously, one study aimed to determine whether an 'EMT core signature' exists in breast cancer. In this study, each signalling pathway was activated individually to determine which activated genes are common to all pathways. Thus, a panel of 159 genes was found to be down-regulated in a breast mammary epithelial cell line (HMLE) while 87 genes were up-regulated. Importantly, from this study, E-cadherin was found to be down-regulated, and N-cadherin, Vimentin, and MMP2 were up-regulated. Another gene that usually switch EMT was Zeb1 that was also upregulated [102]. Another report compared several mutations in E-cadherin gene (*CDH1*) in breast cancers (namely, infiltrating lobular carcinomas, infiltrating ducto-lobular carcinomas and infiltrative ductal carcinomas), and concluded that 56% of infiltrating lobular breast carcinomas presented E-cadherin inactivation mutations,

while the other breast cancer subtypes presented none [104]. Further studies revealed that E-cadherin expression in lobular breast carcinomas presented mutational inactivations, which are also accompanied by loss of α- and β-catenin expression. In 50% of the cases, this is also accompanied by the loss of function of γ-catenin. This pattern indicates that simultaneous loss of E-cadherin, and related catenin's may not only be important for the formation of lobular breast carcinoma *in situ*, but also for the development of a mesenchymal phenotype. Importantly, the study has concluded that 84% of lobular breast carcinomas have a complete loss of E-cadherin protein expression. These reveal how all the components of the tight junctions are necessary for its proper function, and that a mutation in either could result in the loss of function of E-cadherin [92].

In a separate study, CDH1 mutations were found in 50% of the gastric cancer cases. Amongst these, there was a mutation in the wild-type allele, which was attributed to promoter hypermethylation in 83% of the cases [105, 106]. Similarly, in lobular breast carcinoma (LBC), E-cadherin expression has been found to be absent in 85% of sporadic invasive cases. Likewise, 56% of these sporadic LBC cases have CDH1 mutation. The LBC is distinctive for its infiltrative cancer cells, which are generally highly dispersive and isolated [107]. In contrast, in invasive ductal carcinoma (DGC) cases, somatic CDH1 mutations are not present, and the tumour is generally not characterised by a complete loss of E-cadherin expression [104]. Comparative analysis between sporadic LBC and DGC have noted that LBC generally presents nonsense or frameshift mutations, which lead to the formation of non-functional proteins but DGCs display splice-site or in frame mutations [108]. Furthermore, these two tumour types also differ in the localisation of their mutations, which tend to be scattered throughout the *CDH1* gene in LBC but clustered in DGCs [109].

E-cadherin can be inactivated in several manners: these include genetic mutations, chromosomal deletions, cleavage by proteolytic enzymes or silencing of the E-cadherin gene promoter. Silencing of CDH1 promoter can be induced by DNA hypermethylation or by transcription factor including Slug, Snail or Twist or by mutational inactivation of the gene. However, a thorough study on mammary cell lines, including aggressive breast cancer tumour cells, has shown that a precursor to

EMT is the hypermethylation of CDH1 gene at promoter region, and not the gene inactivation by mutations [93].

Depletion of E-cadherin has a diverse-range of implications. It does not only allow cells to lose their tight junctions, but also activates an extensive range of signalling pathways which initiate the EMT pathway. A study conducted on non-metastatic breast cell lines, revealed that E-cadherin silencing was sufficient to activate EMT, as well as to facilitate the progression towards the metastatic phenotype by increasing their migratory and invasive potential, and resistance to apoptosis. Amongst the 19 transcription factors, those were upregulated upon E-cadherin loss, Twist and ZEB-1 were marked as the suppressors of E-cadherin. Enhanced expression of Twist and ZEB-1 upon E-cadherin silencing causes a feed-forward signalling pathway, promoting the EMT, as well as the maintenance of the mesenchymal phenotype [110].

Table 1.1 EMT regulators in cancer invasion and metastasis. [Adapted from [111]]

EMT regulators	Biological functions	References
E-cadherin	Involves in assemble of epithelial cell sheets and maintain the positioning of the cells within these sheets	[98]
Snail	Reduces the expression of claudins, occludins, and mucin-1	[112]
Slug	Overexpressed in breast cancer and maintains cell migration, invasion, metastasis, cell cycle regulation and resistance to chemotherapeutic drugs	[113]
Zeb1	Promote invasion and distant metastasis in breast cancer	[114, 115]
RAE1	Stimulates the expression of *ZEB1*which in turninduces EMT in breast cancer	[115]
Zeb2	Promotes cell migration and invasion in ER+ breast cancer cells	[116]
Twist1	Twist overexpression enhances cell motility, mammosphere formation, and the expression of CSC markers.	[114, 117]
PKD1	Inhibits EMT induction vianuclear export of snail and show reduced expression in breast cancer	[118]
FOXC2	Transcriptional activators of EMT that are highly expressed in aggressive breast cancer	[119]
miR-9	Induces tumour formation and is highly expressed in breast cancer	[120]
miR-34	The tumor suppressor gene that is de-regulated in breast cancer	[121]
FGF2	Control a wide range of biological processes including Cellproliferation, survival, migration, invasion and differentiation	[122]
MMP3	Act as a modulator of the tumor progression in pancreatic, pulmonary, and mammary carcinoma	[123]
SMYD3	Favors TGFβ-induced epithelial–mesenchymal transition (EMT) in breast cancer by promoting mesenchymal and EMT transcription factors expression	[124]
FAD104	A novel repressor of TGF-β–mediated EMT in cervical cancers	[125]

1.12 Histone acetylation and de-acetylation

Both histone and non-histone proteins make the infrastructure of DNA into chromatin and form a compact chromatin structure in the nucleus. Nucleosome is the unit term of chromatin. In this genetic unit, DNA is enfolded around an octamer. The histone octamer is consists of four main histone proteins including H2A, H2B, H3 and H4 [126]. These four canonical histone proteins undergo multiple PTMs including acetylation, phosphorylation, methylation, ubiquitylation and sumoylation to both the globular and tail domains. Histone acetylation is crucial for epigenetic control of gene expression. A well-balanced action of lysine acetyltransferases (KATs) and lysine deacetylases (KDACs) is necessary to maintain and regulate histone acetylation [127]. HATs acetylate histones, leading to open chromatin where transcription factors can bind to their targeted DNA and thus a subsequent expression of target genes is induced. In contrast, HDACs mediated deacetylation results in a closed and compact chromatin structure, repressing gene transcription (Figure 1.6). However, this regulation is often deregulated in cancers as the imbalanced functional activity of HATs and HDACs has been described in the development of breast cancer [128].

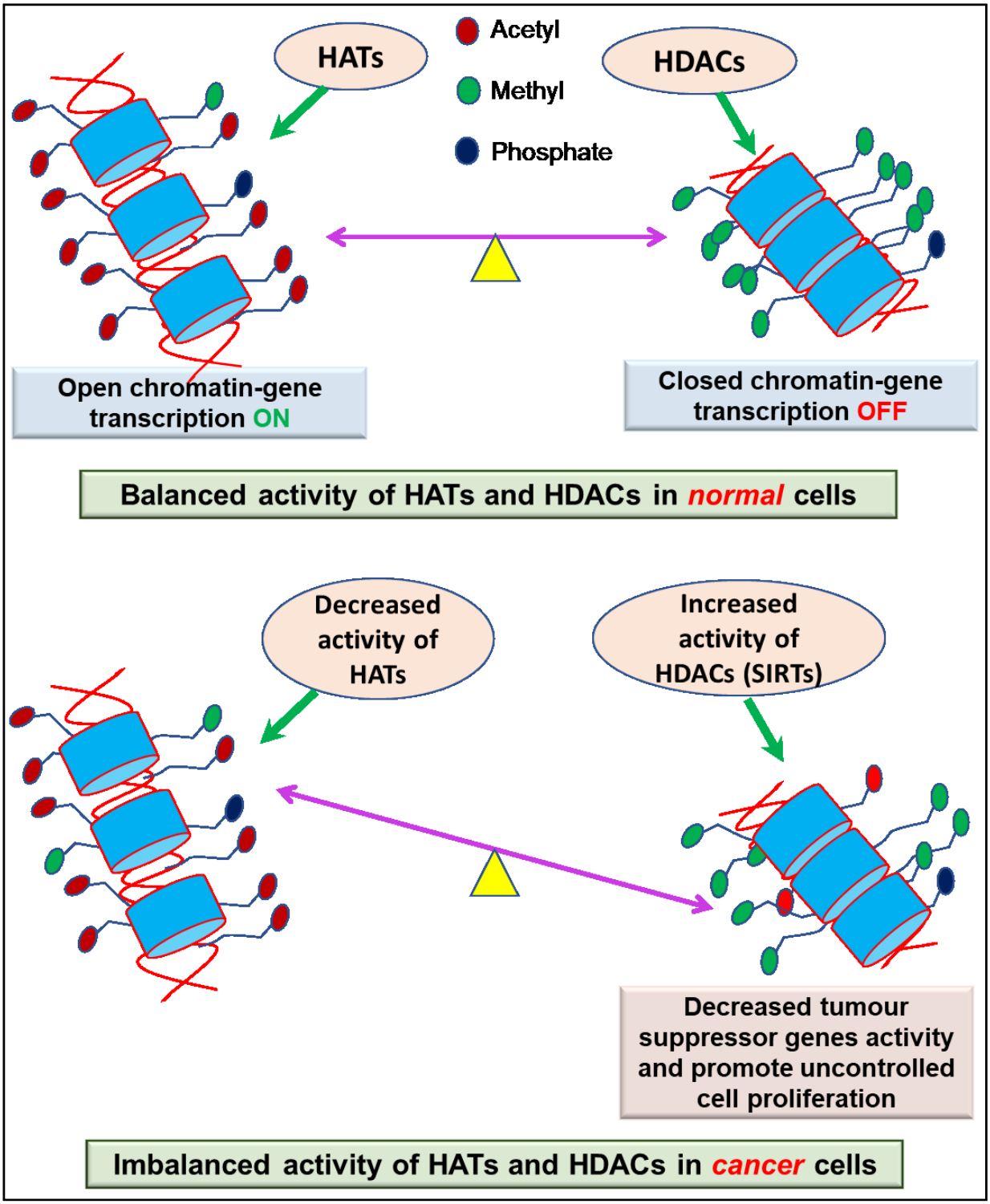


Figure 1.6. Opposite roles of HATs and HDACs in normal and cancer cells in terms of gene regulation. Adapted from [128].

1.13 Histone acetyl-transferases (HATs)

Histone acetylation is catalysed by HATs by transferring an acetyl group to lysine amino acids of histone proteins and thus induces gene transcription. In details, an acetyl group from the acetyl-coenzyme A (acetyl-coA) is transferred to the €-amino nitrogen group of lysine. The initial finding of a transcriptional co-activator protein localised in the nucleus, GCN5 as HAT directed to a flow in HAT-associated studies [129]. Based on their catalytic domains, HATs (recently named as KATs) are classified into three major groups: GCN5 N-acetyltransferases or GNATs (including Gcn5, PCAF, HAT1); EP300 and CREB-binding Protein (EP300/CBP) and MYST (e.g. MOZ/Morf, Ybf2, Sas2, and Tip60) [130]. However, transcription factor related KATs and nuclear receptor family of KATs have been described as two other KAT protein families. These enzymes have effective roles in signalling pathways, cell cycle, DNA damage repair, metastasis and apoptosis. To date, uncontrolled activation of HATs leads to irregular amplification of cells which results in cancer development and metastasis. Of all KATs, as my research focused on EP300/CBP protein families, these are discussed thoroughly in the later parts.

1.14 HDACs and breast cancer

Histone deacetylases (HDACs) are the deacetylase that catalyses removal of the acetyl group from histone or nonhistone signalling proteins. These enzymes are mainly localized in the nucleus, however, some HDACs shuttle between cytoplasm and nucleus in response to different stress or environmental cues. Based on their homology, HDACs are classified into four different families including class I, II, III and IV (Table 1.2) [131]. HDAC 1, 2, 3, and 8 belong to Class I HDACs which are exclusively present in the nucleus. Class II HDACs consists of HDAC 4, 5, 6 7, 9 and 10. The expression of class II HDACs can shift from cytoplasm to nucleus or from nucleus to cytoplasm. Class III HDACs are named as sirtuins (SIRTs) of which there are seven proteins including 1 to 7. To date, NAD^+ is essential as a co-factor for sirtuins deacetylation activity [131]. On the other hand, HDAC11 belongs to Class IV. Moreover, the Zn^{2+} ions are required for the enzymatic activity of Class I, II and IV HDACs [132].

It has been reported that disruption of acetylation of H4K16 plays a critical role in tumour development especially in breast, colon, lung and leukaemia cancers [133],

suggesting that increased HDAC activity or reduced HAT activity is a feature of oncogenesis. Consistently, in breast cancer, the altered expression of HDAC1, 2, 3, 4, and 6 have been observed. Suzuki *et.al*. confirmed that reduced expression of HDAC1, 2, and 6 occurs during tumour development which in turn changes histone acetylation status inducing the transformation of mammary epithelial cells to ductal carcinoma [134]. Specifically, H4 hypoacetylation is linked with breast cancer development and progression from normal epithelium to metastatic cancer. Moreover, Krusche *et al*. suggested a possible correlation between the expression level of HDAC1/3, PRs, ERs and HDAC1 [135]. Depletion of HDAC6 by siRNA has also shown to cause inhibition of cell motility and invasion in breast cancer cells [136]. Furthermore, previous study confirmed elevated expression of class I HDACs compared with class II HDACs in breast cancer tissues and is associated with cancer development. Conversely, those that possess increased expression of class II HDACs had a more favourable outcome [137, 138].

Table 1.2 General classification of Human HDACs. Adapted from [139].

Classification	Members	Subcellular localisation
HDAC Class I (yeast Rpd3 homologue, Zn^{2+} ion-dependent)	HDAC1 HDAC2 HDAC3 HDAC8	Nucleus Nucleus Nucleus/cytoplasm Nucleus
HDACClass II (yeast HDA1 homologue, Zn^{2+} ion-dependent)	HDAC4 HDAC5 HDAC6 HDAC7 HDAC9 HDAC10	Nucleus/cytoplasm Nucleus/cytoplasm Nucleus/cytoplasm Nucleus/cytoplasm Nucleus/cytoplasm Nucleus/cytoplasm
HDAC Class III (Sirtuins) (yeast Sir2 homologue, NAD+ dependent)	SIRT1 SIRT2 SIRT3 SIRT4 SIRT5 SIRT6 SIRT7	Nucleus/cytoplasm Cytoplasm/nucleus Nucleus/Mitochondria Mitochondria Mitochondria Nucleus Nucleolus
HDAC Class IV (Homologous to Class I and II, Zn^{2+} ion dependent)	HDAC11	Nucleus/cytoplasm

1.15 EP300 and CBP as lysine acetyl-transferases

EP300 is a transcriptional co-activator possessing inherent histone/lysine acetyl-transferase (HAT/KAT) activity. It was originally identified as an adenoviral E1A-binding protein with a molecular weight of ~300 KDa thus named as EP300. CBP (CREB-binding protein) is a paralog of EP300 that also acts as a co-activator of gene transcription and possesses HAT/KAT activity. EP300/CBP co-operate and interact physically or functionally with approximately 400 different proteins, of which most are the transcription factors [140]. EP300/CBP show a little sequence similarity to other KAT families except in the bromodomain [140]. This suggests that EP300 and CBP have unique functions that cannot be replaced by other acetyl-transferases. In agreement, EP300/CBP has been found to regulate the acetylation status of histone H3 lysine 18 (H3K18) *in vivo* [141]. Moreover, acetylation at a specific histone residue, histone H3 lysine 27 (H3K27) induced by EP300/CBP promotes transcriptional enhancer function [142], and deletion of EP300/CBP in mouse fibroblasts eliminates the vast majority of H3K27 acetylation [143]. EP300/CBP also acetylates nonhistone proteins, such as p53 and BCL6 [144, 145]. Notably, it has been found difficult to distinguish their specific involvements in various biological processes as well as in cancers because of the versatility of these proteins. For example, EP300 and CBP have been found to play overlapping functions to the same biological pathways especially in gene regulation suggesting the redundancy of these co-activators. However, despite having sequence homology and functional similarity, genetic and molecular pathway analyses suggest that both co-activators possess intrinsic unique functions [146].

1.15.1 Structural description of EP300 and CBP proteins

The HAT domain of EP300 and CBP has a potential role in the regulation of the acetyl-transferase activity and substrate specificity. Bromodomain (BRD), cysteine/histidine-rich region 2 (CH2), and cysteine/histidine-rich region 3 (CH3) are other three functional domain contributing to the functional role of EP300/CBP (Figure 1.7 and 1.8). The BRD domain of EP300/CBP contributes to the function of the HAT domain by binding to acetylated lysine's of H2A, H2B, H3, and H4 proteins [147-149]. The CH2 domain of EP300 and CBP has been shown to reduce the transcriptional activity of *in vitro* transfected reporter genes, although contradictory

results were described [147, 148]. Moreover, the CH2 region consists of a plant homeodomain (PHD) motif and an associated RING domain. Loss of RING domain or the mutation in E1242K found to interrupt into the interaction among the CH2 domain and the HAT domain. This proximity further enhanced the auto-acetylation of EP300 at position K1499 and acetylation of p53 at position K382 [148, 150]. However, reduced acetylation of histone H3 at position K9 or K14 was observed in cells lacking RING domain, deflecting the substrate specificity of this domain [150]. To date, an autoregulatory loop (AL) is located within the HAT domain of EP300 and CBP. This AL region competes with positively charged substrates for binding to the active site and thus blocks acetyl-transferase activity [151]. Notably, although HAT and flanking domains of EP300 and CBP possess 88% sequence homology, still they vary in their specificity and selectivity for substrate molecules [152, 153]. Further studies are necessary to increase our understanding of the role and regulation of the HAT activity of EP300/CBP family.

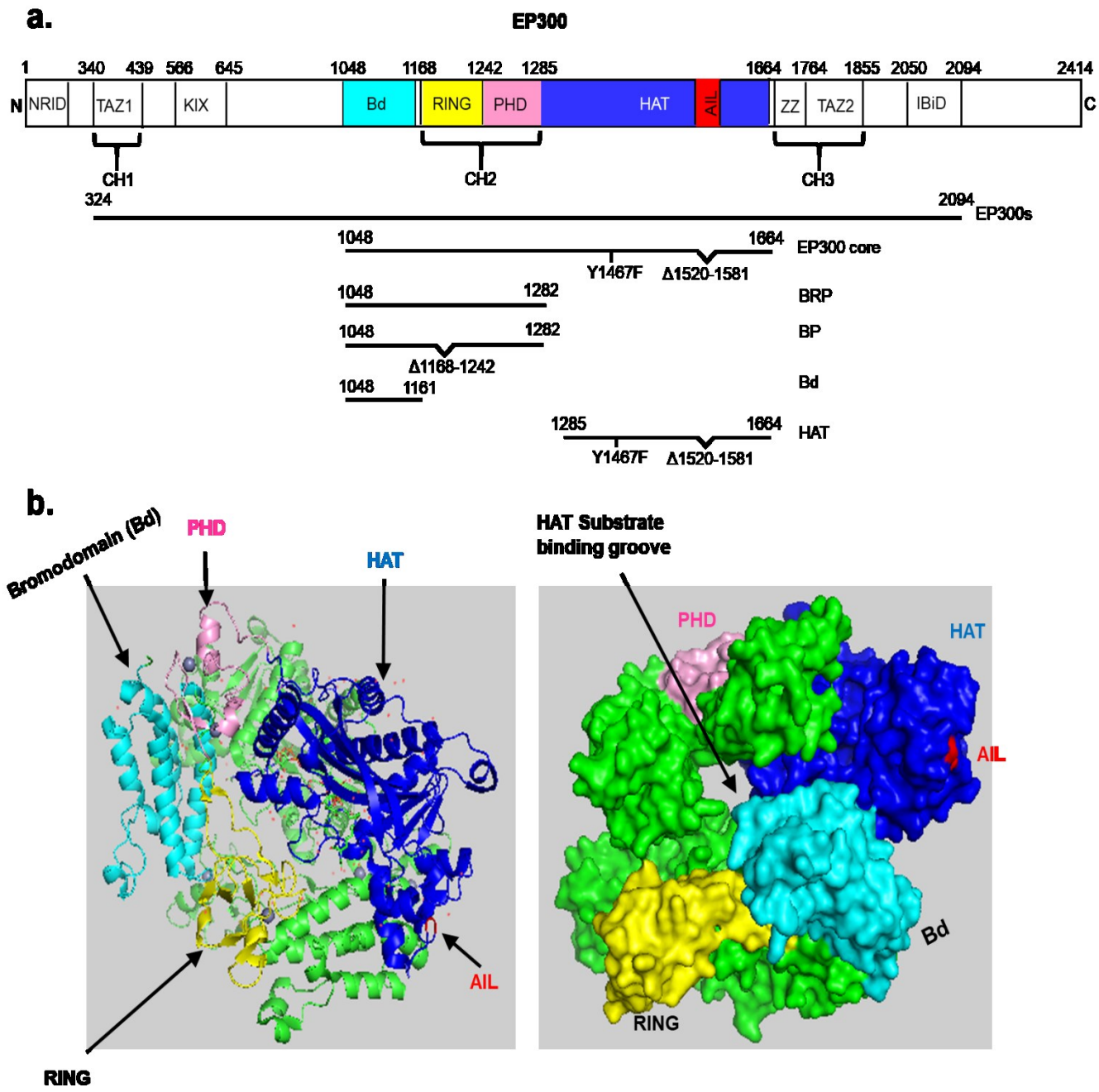


Figure 1.7 (a) Domain architecture of EP300. NRID, nuclear receptor interaction domain; TAZ1, transcriptional adaptor zinc-finger domain 1 (also known as cysteine-histidine–rich (CH) region 1 (CH1)); KIX, kinase-inducible domain of CREB-interacting domain; Bd, bromodomain; RING, really interesting new gene; PHD, plant homeodomain; HAT, histone acetyltransferase domain; ZZ, ZZ-type zinc-finger domain; TAZ2, transcriptional-adaptor zinc-finger domain 2; IBiD, IRF3-binding domain (also known as nuclear coactivator-binding domain (NCBD)); The RING-PHD segment is also known as the CH2 region and the ZZ-TAZ2 domains as the CH3 region. The crystallized construct, EP300 core, contains an Y1467F mutation and a deletion of the AIL (Δ1520–1581) in the HAT domain. **(b) Ribbon and surface representations of the EP300 core structure.** The bromodomain (Bd), RING and PHD domains are shown in cyan, yellow and pink, respectively. The HAT domain is shown in blue. The position of the deleted AIL is indicated with red. Adapted from [146].

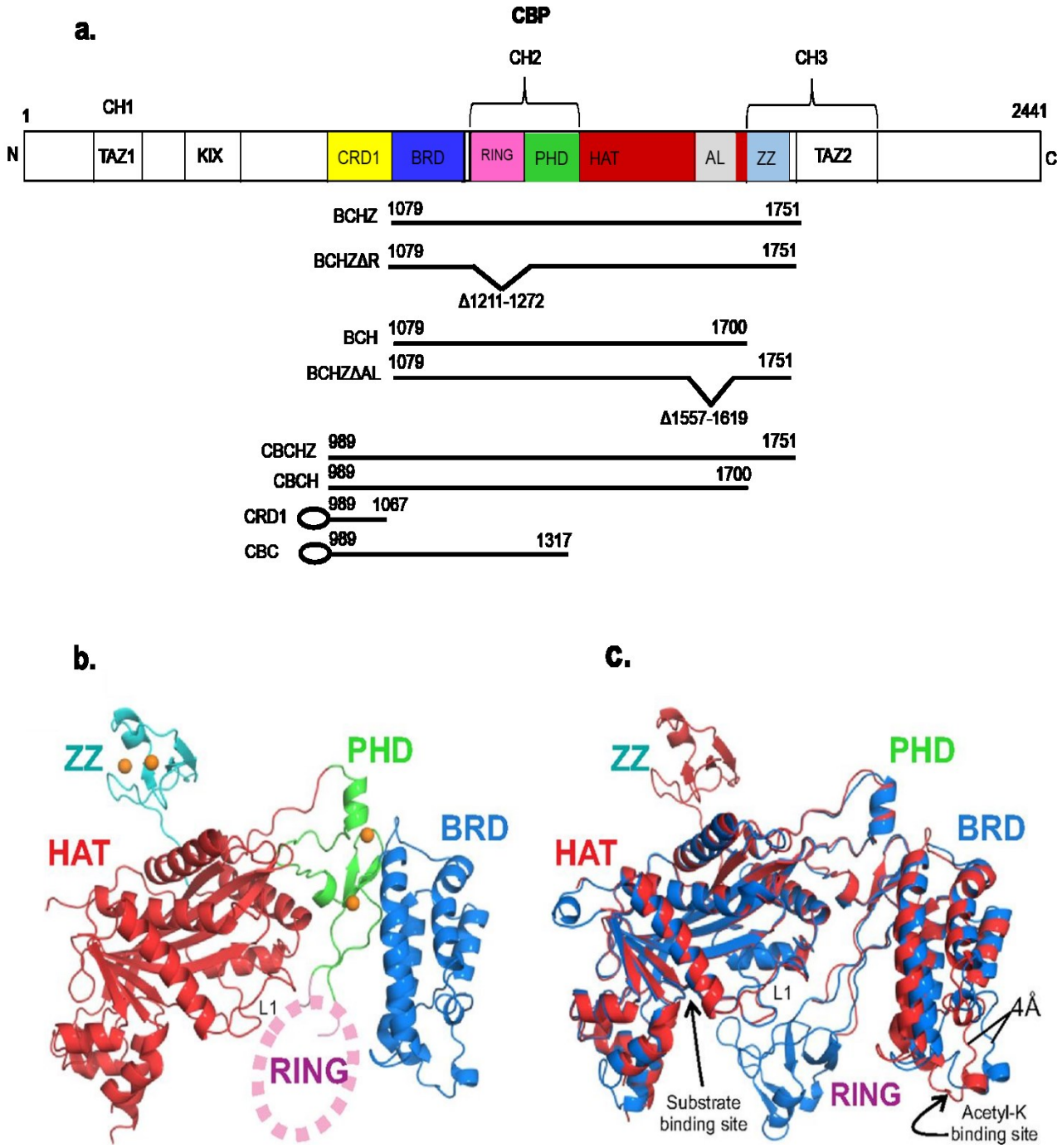


Figure 1.8 (a) Schematic representation of the domain architecture of CBP. (b) Crystal structure of CBP and (c) comparison with EP300. (a) The BRD, PHD, HAT, and ZZ domains are shown in blue, green, red, and cyan, respectively. Adapted from [154]. **(b)** Zinc atoms are shown as orange spheres. Electron density for the RING domain was largely absent, and its approximate location is indicated schematically by the pink oval. **(c)** Superposition of the CBP (red) and EP300 (PDB ID code 4BHW, blue) structures showing that the acetyl-lysine binding site of the BRD is ~4 Å closer to the HAT domain in CBP compared with EP300. The acetyl-lysine binding site of the BRD and the substrate binding site of the HAT domain are indicated by arrows. Taken and adapted from [154].

1.15.2 Functional role of EP300 and CBP

Both EP300 and CBP form a framework to assimilate multiple transcription factors, therefore regulating the expression of genes involved in biological processes. They also participate in non-transcriptional functions on regulatory pathways such as DNA replication and metabolism. These co-activator proteins also induce direct acetylation of specific lysine residues both within histone or non-histone transcription factors and even within themselves by auto-acetylation. Induced acetylation results in the modification of the activity of transcription factors and opening of the chromatin which in turn stimulate the gene transcriptional machinery [155, 156]. Subsequently, these proteins contribute to cell cycle regulation, differentiation, homeostasis, DNA damage repair and apoptosis [146, 157].

The exact role of EP300/CBP in cancer progression and metastasis is still elusive. The precise functions of each acetyl-transferase to the cancer phenotype have not been identified precisely. Therefore, it is noteworthy that the functional activities of EP300/CBP are diverse and more importantly they play both tumour-suppressive and pro-oncogenic role in response with different environmental stress. To date, scientists attempted to identify the effects of somatic mutations in EP300 and CBP, which have been identified in genomic studies from several types of cancers. Moreover, determining specific signalling pathways that are unambiguously affected by mutations in EP300 or CBP is crucial to define genetic or epigenetic alterations of these proteins. Notably, despite having substantial sequence identity, these proteins are involved in non-overlapping biological functions and can interact with a wide range of substrates [152, 153, 158].

1.15.3 EP300/CBP as classic tumour suppressors

Germline heterozygous mutations in CBP and less frequently in EP300 were observed in Rubinstein–Taybi syndrome (RTS), which was described as a reason for oncogenic processes. For example, RTS patients had an increased incidence of cancer with ~5% diagnosed with childhood tumours of neural crest origin [159]. Moreover, mutations in EP300/CBP have been found in several human cancers. For instance, gastric, colon and breast cancers were found to be predisposed with

bi-allelic somatic mutations in the EP300 gene. Some of these mutations have been found to cause non-functional or spliced protein products, suggesting their tumour repressive activities [160]. In addition, tumour-associated inactivating genetic lesions were observed in EP300 in breast and colorectal primary tumours which further support the tumour-suppressive role of EP300/CBP in humans [160].

EP300/CBP play a key role in regulating other genuine tumour suppressors, such as p53, RB1, BRCA1. They also show this type of function by inducing the activation of TGF-β and its downstream genes [146, 161-163]. Among these tumour suppressing proteins, p53-mediated gene regulation by EP300/CBP is widely studied. For example, EP300/CBP induce p53-dependent gene transcription that is vital to block cell cycle progression and to stimulate DNA damage repair function [163]. Moreover, it has been found that EP300 helps in p53 movement from cytoplasm to nucleus to stabilize p53 via nuclear accumulation. BRCA1, which is recurrently mutated in breast and ovarian cancers, also activated by EP300/CBP. Therefore, EP300/CBP show their tumour suppressive role by regulating cell-cycle checkpoint and DNA damage repair via activation of BRCA1 [162, 164-166]. EP300/CBP also found to act as transcriptional regulators of Smad3, thereby modulate the outcomes of TGF-β signalling [167, 168]. Furthermore, depletion of the EP300 has been found to inhibit cellular senescence suggesting its capacity to suppress tumour growth via inhibition of cell senescence [169]. More recently, Asaduzzaman et al. have been demonstrated that EP300 acts as a tumour repressor by upregulating the transcription of E-cadherin in epithelial breast cancers [170].

1.15.4 EP300/CBP as positive modulators of tumour development

Apart from their tumour-inhibitory roles of EP300/CBP, multiple investigations suggest that they can also play as a positive modulator of oncogenesis. There are several reasons behind their dual roles, however, the exact mechanism is still ambiguous. To date, it has been found that inhibitory mutations of EP300/CBP are the cause of multiple cancer phenotypes [171, 172]. Moreover, cancer may be developed from some other tumour-associated point mutations of EP300/CBP [173]. Mutations in the RING domain of EP300 were also observed which cause various cancers like melanoma, endometrial and colorectal carcinoma [174]. These

mutations further enhance the HAT functions of EP300 [148], although the role of elevated HAT activity to drive cancers is not clear.

It has been mentioned before that EP300/CBP promotes acetylation of H3K18 and H3K27. However, they also induce the acetylation of H3K56. The induced acetylation (H3K56) was found to induce nucleosome assembly in yeast and DNA replication and repair in mammals [175-177]. Multiple epithelial cancers were found to show enhanced cellular levels of histone H3K56ac and are related to tumour development and metastatic phenotypes [178]. All these results suggest a key role of increased EP300/CBP HAT activity in cancer development and progression.

1.16 FOXO transcription factors

Forkhead box (FOX) transcription factors play a vital role in the regulation of a myriad of biological processes such as cell cycle progression, differentiation, metabolism, apoptosis and the protection from oxidative stress [179]. An exclusive feature of FOX proteins is its “Forkhead” box that is a sequence of 100 amino acids. This sequence allows binding to specific DNA sequences of FOXO target genes. Due to its discrete butterfly-like appearance, the forkhead motif is also renowned as a “winged-helix” DNA binding domain (DBD). The first FOX member was discovered in *Drosophila Melanogaster* when mutation of the forkhead gene in these flies was found to result in fork-patterned embryo heads. Till now over 50 mammalian FOX proteins have been discovered, and further divided into 19 subclasses (FOXA to FOXS) based on their protein sequence homology [180].

Of all FOX proteins, forkhead box O (FOXO) proteins are a subgroup of transcription factors that are characterised by a conserved DNA-binding forkhead domain and were first identified in the nematode *Caenorhabditis elegans (C. elegans)* as Daf-16 [181, 182]. FOXO proteins regulate a plethora of physiological and pathological processes and thus recognised as major signalling regulators [183]. Notably, FOXOs are evolutionarily conserved from invertebrates to mammals as invertebrates possess one *FOXO* gene whereas mammals have four FOXO family members: FOXO1, FOXO3, FOXO4 and FOXO6 [184]. FOXO proteins show their tumour inhibitory role by suppressing cell growth and promoting apoptosis. After activation, FOXO proteins bind to the conserved sequence motif GTAAA(C/T)A to stimulate

transcription of their downstream target genes [76, 185], which results in the upregulation of genes involved in cell cycle arrest, DNA repair and apoptosis [185]. However, it is noteworthy that FOXOs are often deactivated in various cancers such as breast, prostate, glioblastoma and leukaemia [183].

1.16.1 Structural insights of FOXO proteins

FOXO transcription factors share a highly conserved DNA-binding domain, named as forkhead box domain (FH). The FH domain is flanked by large N- and C-terminal regions which are crucial for the regulation of FOXO function (Figure 1.9) [186]. 3D structures of FH domains of three FOXOs (FOXO1, 3 and 4) revealed an analogous mode of DNA recognition when analysed both free and in complex with DNA [187]. Moreover, the DNA recognition ability and the transcriptional activity of FOXOs are regulated by direct cooperation of DNA binding domain with other two consensus sequences e.g. the Daf-16 family binding element (DBE) with the consensus sequence of TT(G/A)TTTAC and the insulin-responsive sequence (IRE) with the consensus sequence of TT(G/A)TTTTG [188] [189]. It has been found that the C-terminal disordered region harbours the auto-inhibitory motif. This motif is also named as the FOXO transactivation domain (TA) because of its major role in interactions with transcriptional regulators, including p53 [190]. Further studies on the molecular and structural details of the regulatory domains of FOXOs will help us to understand their diverse cellular functions.

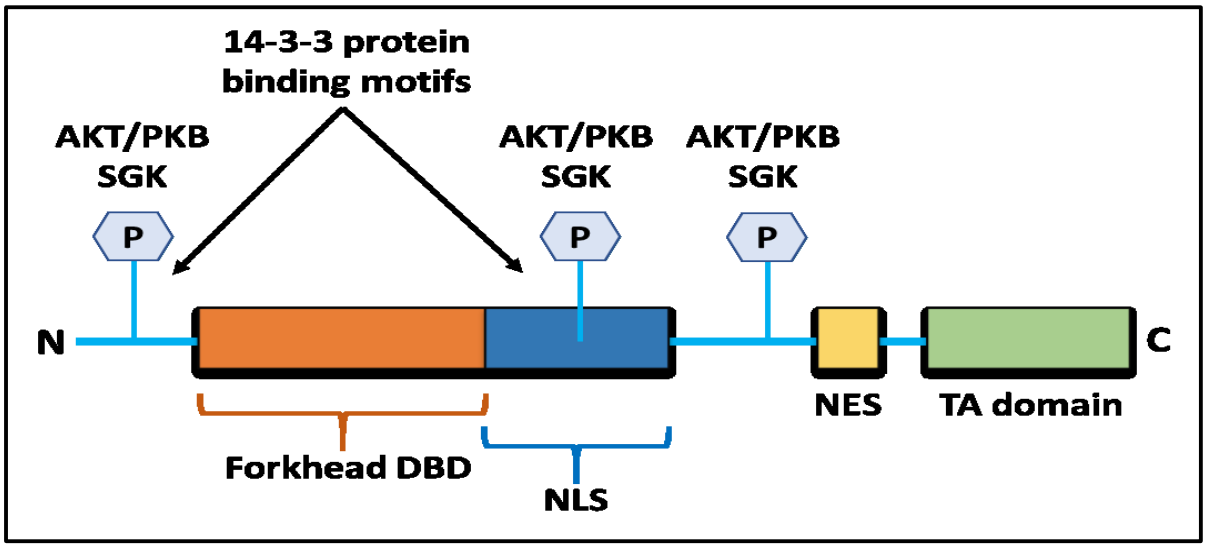


Figure 1.9 Domain structure of FOXO proteins. All FOXO proteins have a similar domain architecture which contains forkhead DNA-binding domain (DBD), nuclear localization signal (NLS), nuclear export sequence (NES) and a transactivation domain (TA). Only the AKT/PKB and SGK phosphorylation sites are shown. Adapted from [191]

1.16.2 FOXO3-FOXM1 axis

FOXO3 and FOXM1 are two forkhead box transcription factors with conflicting roles in breast cancer. FOXO3 usually acts as a tumour suppressor, whereas FOXM1 is considered as a dominat oncogene in cancer cells [180]. Various types of aggressive cancers including breast cancer show increased level of FOXM1. FOXM1 has been found to induce G1/S and G2/M transitions. It also upregulates the expression of M phase-associated genes e.g. *CDC25B*, cyclin B (*CCNB1*), Aurora A kinase (*AURKA*), polo-like kinase 1 (*PLK1*), survivin (*BIRC5*), and centromere protein A (*CENPA*) and thus promote cell cycle progression and proliferation of cancer growth. Furthermore, FOXM1 also found to regulate the transcription of genes involved in EMT, cellular senescence, DNA repair, angiogenesis and metastasis [192]. On the other hand, accumulated evidence shows that FOXO3 activates or represses cell proliferation, differentiation, cell cycle regulation, apoptosis, DNA damage repair, protection against oxidative stress, and metabolism [193]. It has been reported that FOXO3 directly binds to the *FOXM1* promoter to repress FOXM1 expression and inhibit the transcription of its downstream target genes [76]. Scientists also revealed that overexpression of FOXO3 *in vitro* hinders cell growth via inducing phosphorylation of AKT in drug sensitive cancer cells. On the other hand, FOXO3 inactivation was found to accelerate AKT phosphorylation but not growth arrest in drug resistant cancer cells. Therefore, drug resistant breast cancer cells usually show deregulation of FOXO3 activity [30]. In contrast to FOXO3, FOXM1 expresses widely in proliferating tissues and plays a pivotal role in tumorigenesis and cancer progression [179]. Recent studies also suggest the role of FOXM1 to protect cells from drug-induced senescence and cell death [194]. Interestingly, apart from its tumour suppressive roles, FOXO3 has been found to stabilize cancer cell proliferation which in turn promote drug resistance. Therefore, abnormal regulation of the FOXO3-FOXM1 axis may modify cellular conditions either to proliferation or to the induction of apoptosis [195, 196].

Table 1.3 Genes targeted by FOXO3 and their respective cellular functions in regulating tumorigenesis. Adapted from [196]

Gene Symbol	Cellular functions	Cancer types	References
Bim, FasL, TRAIL	Apoptosis	Breast cancer, colorectal cancer, hepatocellular carcinoma (HCC)	[197-199]
$p27^{Kip1}$, $p16^{INK4a}$, p130 (Rb2), GADD45	Cell cycle, proliferative arrest and cellular senescence	Breast cancer	[197, 198, 200]
VEGF	Angiogenesis, metastasis and tumour microenvironment	Breast cancer	[76]
FOXM1, miR-21, Fas-L, Survivin	DNA damage repair	Breast cancer	[201, 202]
ABCB1, TRAIL, SIRT1, SIRT2, SIRT6	Drug resistance	Breast cancer, colon cancer	[194, 199, 203, 204]
ABCB1, PIK3CA, β-catenin, c-Myc, MnSOD, SOD2	Cancer cell stemness	Brain glioblastoma, myeloid leukaemia	[205-209]
ATG, MAP1, LC3, BNIP3,	Autophagy	Breast cancer	[210, 211]

1.16.3 FOXOs in cellular senescence and autophagy

Senescence is defined as one of the stable conditions of growth arrest. In other words, it can be termed as the age-linked reduction of the self-renewal property of stem cells. Several studies have been implicated to identify the mechanism of FOXO regulated cell senescence. FOXO-induced growth arrest is regulated through the transcription of a multiple cell cycle kinase inhibitors (CKI) including $p27^{kip1}$ (*CDKN1B*) [196]. Besides, FOXOs have also been recognised as master regulators of $p21^{cip1}$, $p57^{kip2}$, $p16^{INK4a}$, $P18^{INK4c}$ and $p19^{INK4d}$ [212-214]. These CKI expressions, in turn, inhibit the formation of Cyclin/CDK complexes which further block the progression of different stages of the cell cycle. By this mechanism, FOXO induced CKI expression inhibits cell cycle arrest in G_0/G_1, G_2 phases. For example, a unique feature of p21 is its ability to associate with the proliferating cell nuclear

antigen (PCNA) and it had been suggested that p21 might inhibit cell cycle progression by inducing the suppression of PCNA function resulting in both G1 and G2 arrest [215]. Another protein named as the retinoblastoma family protein p130 (RB2) also found to be activated upon induction of FOXO3, inducing cellular senescence of dividing cells.

Autophagy is an evolutionarily conserved cellular 'self-digesting' process which transports cytoplasmic machinery to the lysosome for degradation. Autophagy can be grouped into three classes including macro-autophagy, micro-autophagy and chaperone mediated autophagy. It has been shown that FOXO1 and FOXO3 are directly associated with the regulation of autophagy, especially in response to oxidative stress [216]. Moreover, sirtuins are also described to be involved in the autophagy process as SIRT1-induced autophagy has been described to regulate cell proliferation, survival, and acquired resistance to stress [217]. To date, SIRT1 deacetylates histone H4 (at lysine residue 16; H4K16ac), FOXO1, FOXO3, E2F1, and NF-KB which in turn induce autophagy-related genes [218-221]. Moreover, in response to reduced nutrition, SIRT1 also found to deacetylate ATGs 5, 7, and 8, which results in the stimulation of autophagy [222].

It is noteworthy that FOXO3 and sirtuins co-regulate autophagic processes. Especially, SIRT2 has been found to deacetylate FOXO3 in response to oxidative stress. The deacetylated FOXO1, in turn, binds to ATG-7 inducing transcription-independent autophagy and promoting suppression of tumour development [223]. However, FOXO3 enhances autophagy by promoting the transcription of autophagy-related (ATG) genes or autophagy regulatory genes e.g. microtubules associated protein 1 light chain (MAP1LC3) and BCL2/adenovirus E1B19-kDa interacting protein 3 (BNIP3) [210, 224]. FOXO3 has also been found to upregulate the activity of PI3K/AKT signalling, which in turn phosphorylate and induce nuclear exportation of FOXO1, as a result inducing autophagy. Furthermore, FOXO3 binds to the FOXO1 promoter region, thus upregulating FOXO1 transcription to induce autophagy [225]. Therefore, pharmacological inhibition of autophagy in cancers by targeting FOXO3-FOXO1-SIRT1/2 axis could be a possible approach for developing new therapeutic strategy.

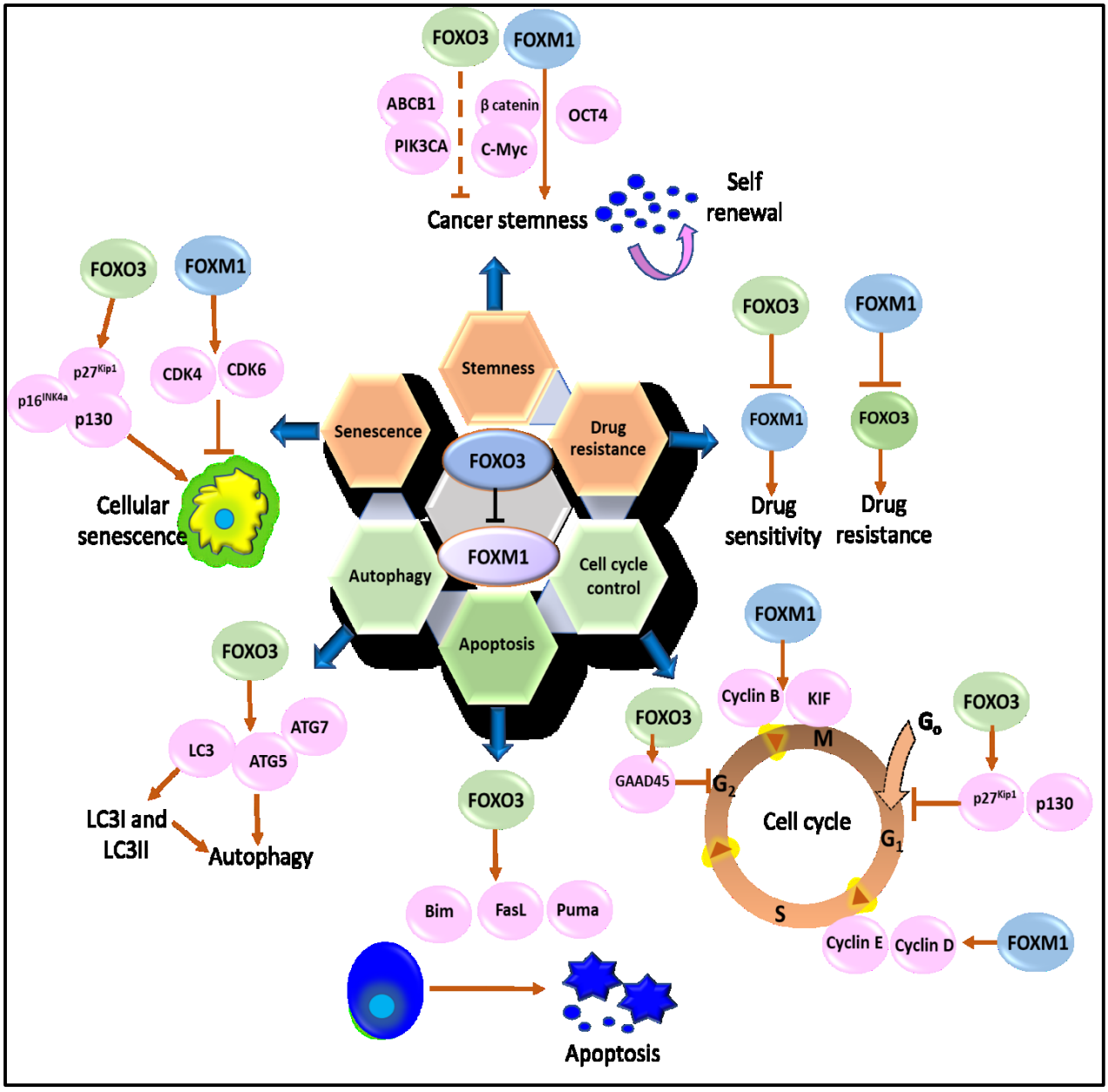


Figure 1.10 Cellular roles of FOXO3-FOXM1 axis in cancer. FOXO3 and FOXM1 employ opposing functions in the regulation of cancer-associated processes including cell cycle control, apoptosis, autophagy, cellular senescence, cancer stemness and drug resistances. Downstream gene targets of FOXO3 and FOXM1 are shown. Adapted from [196].

1.17 Post translational modifications of FOXO

The biological activities of FOXOs are mainly regulated by various post-translational modifications (PTMs) in response to different environmental stimuli [226]. These PTMs include phosphorylation, acetylation, sumoylation, methylation, ubiquitination, glycosylation, small ubiquitin-like modification and nitrosylation. Importantly, these modifications further change the target gene specificity of FOXO proteins, regulate

FOXO protein expression, their subcellular localisation, DNA binding ability, transcriptional activity and half-life of proteins via multiple enzymatic reactions [193], [226, 227]. To date, PTMs of FOXO proteins generate a 'FOXO code' that is read by protein binding partners directing the expression level and transcriptional activity of FOXOs. Consequently, FOXO PTMs may play their functions by both affecting protein conformation and creating docking sites for FOXO binding partners. This further modulates FOXO functions and in turn determine their downstream target gene specificity [228].

1.17.1 Phosphorylation of FOXO

FOXO proteins undergo phosphorylation by a panel of kinase enzymes at multiple serine or threonine sites. One of the first and potentially most important PTM of FOXO is its phosphorylation by the PI3K (phosphatidylinositol 3-kinase)/AKT (PKB) pathway [229], which subsequently regulate FOXOs protein stability and its DNA binding ability. Besides, this modification plays a vital role in a variety of cellular processes controlled by FOXOs, such as cellular differentiation, tumour suppression, metabolism, cell cycle arrest, cell death and protection from stress [230]. In response to growth and survival factors such as insulin and insulin-like growth factor 1, AKT and serum/glucocorticoid inducible kinase (SGK) promote phosphorylation of FOXO3 at three conserved sites (T32, S253, and S315). AKT is relatively more responsible for the phosphorylation of S253, while SGK catalyses phosphorylation at S315. Moreover, both kinases effectively phosphorylate the N-terminal T32 residue of FOXO3 [231]. Notably, the phosphorylation of these key sites enhances the binding of FOXO3 with 14-3-3 proteins (Figure 1.12) [183, 204, 232, 233]. This in turn results in its nuclear exclusion, cytoplasmic accumulation and subsequent proteosomal degradation [183, 229, 234], which is known to be associated with tumorigenesis and is linked with poor survival of the patients with breast tumours [235].

Moreover, FOXO3 de-phosphorylation and its cytoplasmic to nuclear translocation induce further activation of their target genes upon response to lack of growth factors. Amongst these target genes, $p27^{kip1}$, *Bim* and *FasL* are the most important which are also considered as the anti-proliferative and pro-apoptotic genes [76, 183,

202]. Notably, hyper-activation of the PI3K/AKT pathway occurs during cancer development suppressing FOXO3 and its tumour inhibitory activities [236, 237]. Interestingly, phosphorylation of FOXO can trigger the contradictory effects depending on the inducing environmental cues present. For example, in response to oxidative stress, JNK (c-Jun N-terminal kinase) or p38 mitogen-activated protein kinase (MAPK) is activated and results in increased phosphorylation of FOXO3 which in turn leads to the accumulation of FOXO protein in the nucleus (Figure 1.11) [238, 239]. Additionally, activation of JNK results in ERK and AKT inactivation, leading to FOXO3 nuclear translocation [240] and regulation of target genes. Another regulatory kinase e.g. ERK has been reported to phosphorylate FOXO3, resulting in its degradation through an MDM2-mediated ubiquitin-proteasome pathway [241]. In addition, the AMP-activated protein kinase (AMPK) plays a critical role in the regulation of FOXO3 localisation and activity which has been shown to phosphorylate FOXO3 at six different sites T179, S399, S413, S555, S588, and S626 [242]. AMPK mediated phosphorylation has been shown to increase FOXO3 transactivation, however, the intricate mechanism by which phosphorylation at these sites regulate FOXO's activation have not been well explored and thus remains unclear.

Consistent with scientific studies, chemotherapeutic drugs have been designed to prevent the phosphorylation of FOXO3 mediated by PI3K/AKT signalling [243]. For example, lapatinib is a dual tyrosine kinase inhibitor which is applied to patients with breast cancers overexpressing HER2 [76, 244]. Mechanistically, lapatinib inhibits AKT signalling initiated by the EGFR and HER2 to prevent the subsequent phosphorylation of FOXO3 [244, 245]. On the other hand, inhibitors that block the MAPK and PI3K cascades hinder cancer cell survival and proliferation by inactivating FOXO3 phosphorylation [76].

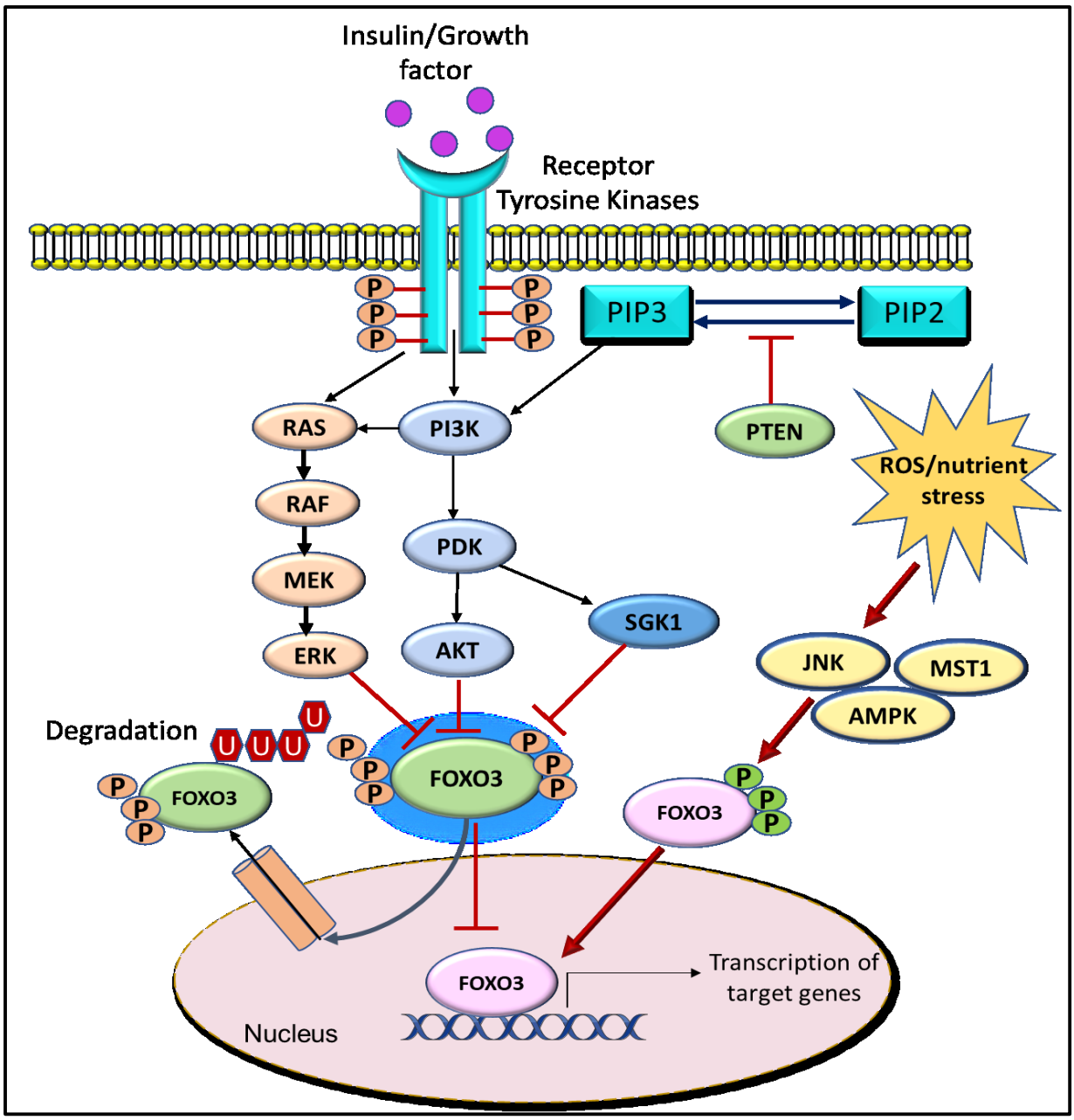


Figure 1.11 Signaling pathways regulating FOXO3 phosphorylation.
AKT mediated FOXO phosphorylation induces its cytoplasmic sequestration and/or proteosomal degradation. Phosphatase and tensin homolog (PTEN) promote FOXO activation and nuclear localisation by inhibiting the activation of PI3K. Reactive oxygen species (ROS) promote nuclear localisation and activation of FOXO by activating the c-Jun N-terminal kinase (JNK). JNK directly phosphorylates FOXOs, thereby inducing activation of transcriptional regulation. Adapted from [246].

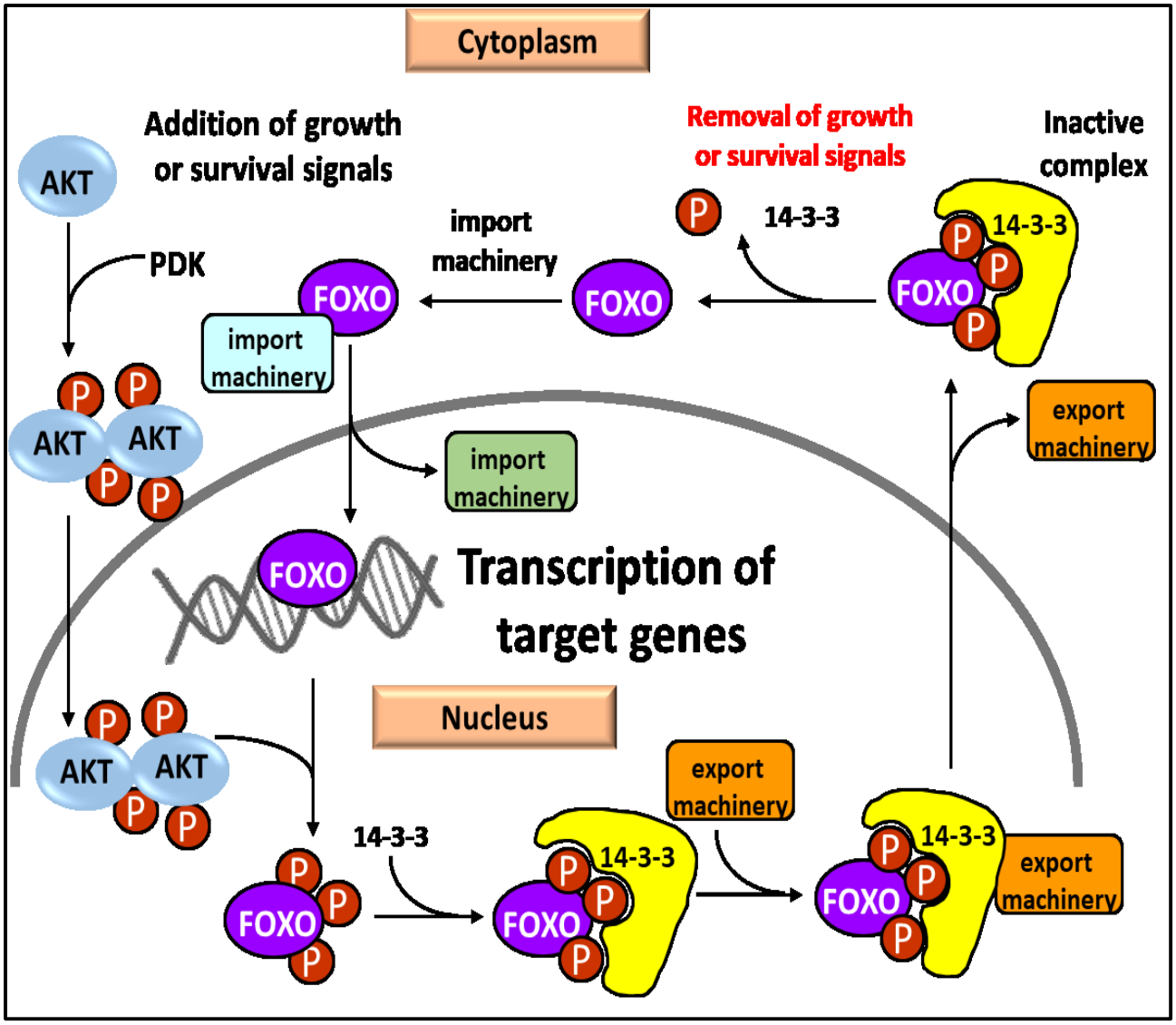


Figure 1.12 Regulation of FOXO phosphorylation by 14-3-3 scaffolding protein. In the presence of growth factors, AKT is recruited to the plasma membrane where it is phosphorylated on two specific sites. Activated AKT detaches from the plasma membrane and translocate to the nucleus, where it phosphorylates serine or threonine residues within an AKT phosphorylation motif of FOXO. When FOXO is phosphorylated at three highly conserved AKT phosphorylation sites, it binds to the 14-3-3 protein which provides a nuclear export sequence. The resulting complex is then translocated into the cytoplasm where the bound 14-3-3 protein prevents its re-entry into the nucleus. However, in absence of growth factors, AKT is being inactive and so FOXO can translocate into the nucleus and initiates the transcription of target genes. Adapted from [247]

1.17.2 Acetylation and deacetylation of FOXO proteins

Phosphorylation of FOXO transcription factors was considered to be the only FOXO regulatory pathway. However, several recent studies identified the acetylation of FOXOs as a novel regulatory mechanism. FOXO acetylation is regulated by the opposing actions of the acetyl-transferase's EP300 or CBP, and the deacetylases known as sirtuins (SIRTs) [181, 204, 248-250]. Oxidative stress and the formation of reactive oxygen species (ROS) have been found to induce FOXO3 acetylation on multiple lysine residues termed as K242, K245, K259 [232], which are located within the DNA binding domain of the FOXO3. Calnan and Brunet described six known acetylation sites each in human FOXO1 (K245, K248, K262, K274, K294, K559) and in human FOXO3 (K242, K245, K259, K271, K290, K569) as well as five acetylation sites each in human FOXO4 (K186, K189, K215, K237, K407) and in human FOXO6 (K173, K176, K190, K202, K229) [226]. Another previous research specified FOXO1 (K265) and FOXO3 (K203) as additional acetylation sites [191].

Scientific studies revealed that acetylation of FOXO3 affects the DNA binding ability and transcriptional activity of this protein. However, it is still under debate as to whether this modification causes an increase or a decrease in the protein's binding affinity for DNA [184, 228]. Besides, acetylation has also been reported to switch target gene expression from cell cycle arrest to apoptotic cell death and increase the nuclear accumulation of FOXO proteins [179, 184, 227]. On the other hand, FOXO3 deacetylation has been shown to promote expression of genes implicated in cell cycle arrest and stress resistance [204]. Therefore, the acetylation status of FOXO3 protein can determine target gene specificity and in turn define the nature of FOXO3-dependent effects. It is noteworthy that, EP300 mediated FOXO3 acetylation promotes preferential induction of apoptotic genes such as *Bim* and *FasL* over other genes involved in cell cycle arrest e.g. $p27^{Kip1}$ or $p16^{INK4a}$ [184, 251, 252].

As mentioned before, EP300/CBP interact and acetylate FOXO factors, however, the effects of FOXO acetylation and target-gene regulation are contradictory. According to some scientists, acetylation of FOXO factors inhibits FOXO activity [249, 250] and thus repressing their downstream target gene expression. However, some other suggested that acetylation enhances FOXO activity by increasing target gene transcription [184, 204, 249]. This inconsistency raised questions on our

understanding on the role of FOXO3 acetylation as well as its regulation. Furthermore, acetylation has been shown to induce FOXO target genes that induce apoptosis and attenuate target genes associated with cell-cycle arrest and protection against oxidative stress [204]. However, a major drawback of this study was that the difference between FOXO acetylation and histone acetylation is often not made.

Consistent with the previous writings, to elucidate the dual role of EP300/CBP in FOXO-mediated transcription, it is important to differentiate between acetylation of histone–DNA and acetylation of FOXO transcription factors. For example, the role of EP300/CBP in FOXO-mediated transcription was evaluated using mutation analysis and a chromosomal-integrated FOXO-reporter construct that was fused to luciferase. In this study, EP300/CBP has been shown to have a dual role as acetylation of FOXO inhibits their transcriptional activity on target genes, however, EP300/CBP was an indispensable co-activator for FOXO-mediated transcriptional activity [250]. In contrast with this finding, some other data suggested that the mechanism of FOXO acetylation by EP300/CBP shares similarities with that of p53 regulation by EP300/CBP and might accelerate FOXO DNA-binding properties [253].

1.18 Sirtuins in the regulation of FOXO acetylation

Sirtuins are a family of NAD^+ dependent deacetylases which play a key role in the regulation of acetylation status of FOXO3. Multiple SIRTs have been proposed to contribute to the development and progression of cancer as well as in chemotherapeutic drug resistance. In mammals seven different sirtuins have been identified till now and named as SIRT1-7. They are particularly involved in the control of a plethora of cellular processes including cell division, differentiation, metabolism, and cellular senescence [254]. Of all sirtuins, SIRT2 is mainly cytoplasmic, SIRT3, SIRT4 and SIRT5 are mitochondrial proteins, SIRT1 and SIRT6 are nuclear and SIRT7 is predominantly localized in nucleolus. However, SIRT2 can shuttle between cytoplasm and nucleus. Therefore, SIRT1, SIRT2 and SIRT6 play their major role in the regulation of chromatin structure and gene expression [255-257]. Accumulated evidence suggests that SIRT proteins interact and modulate the activity of tumour suppressor proteins e.g. p53, p73, E2F1, and FOXO3 determining their role in regulating chemotherapeutic resistance [258].

1.18.1 SIRT1 in FOXO regulation

SIRT1 is the most studied sirtuin which possesses the closest homology with yeast Sir2. SIRT1 is upregulated in various cancers including prostate, ovarian, breast cancer, neuroblastoma and osteosarcoma. It is also found to be involved in causing drug resistance of cancer cells when compared with their drug-sensitive counterparts [259, 260]. Besides, it has been shown that several transcription factors including p53, p73, E2F1, FOXOs, and NF-κB can be deacetylated by SIRT1 and results in induced drug resistance of cancer cells [258]. However, the complexity of SIRT1-FOXO axis made it difficult to elucidate their functional effects as they usually vary depending on the FOXO downstream target genes. In fact, the expression of multiple FOXO downstream target genes is regulated by SIRT1, although the exact mechanism is still unclear. For example, SIRT1 mediated deacetylation of FOXO prevents activation of apoptotic genes such as *Bim* and *Fas* ligand, while it promotes the expression of cell cycle related genes $p27^{Kip1}$ and *GADD45α* to induce cell-cycle arrest [181, 204, 261]. It has also been reported that ectopic overexpression of SIRT1 inhibits FOXO3 mediated apoptosis upon cellular stress. Furthermore, increased sensitivity to oxidative damage was observed in SIRT1 knockout fibroblast cells ($sirt1^{-/-}$ MEFs). Here, $sirt1^{-/-}$ MEFs showed reduced ability of FOXO3 to induce cell cycle arrest [204, 261]. Therefore, SIRT1 alters FOXO-mediated response away from apoptosis toward cell cycle arrest, suggesting that FOXO acetylation/deacetylation can be switched to regulate target genes specificity. Notably, these contradictory dual roles of SIRT1 may be attributed to the dual ability of SIRT1 to bind to FOXO and to deacetylate FOXO. Taken together, these results provide convincing evidence that SIRT1 plays a crucial role in the cancer progression as well as in the development of drug resistance via regulating FOXO acetylation.

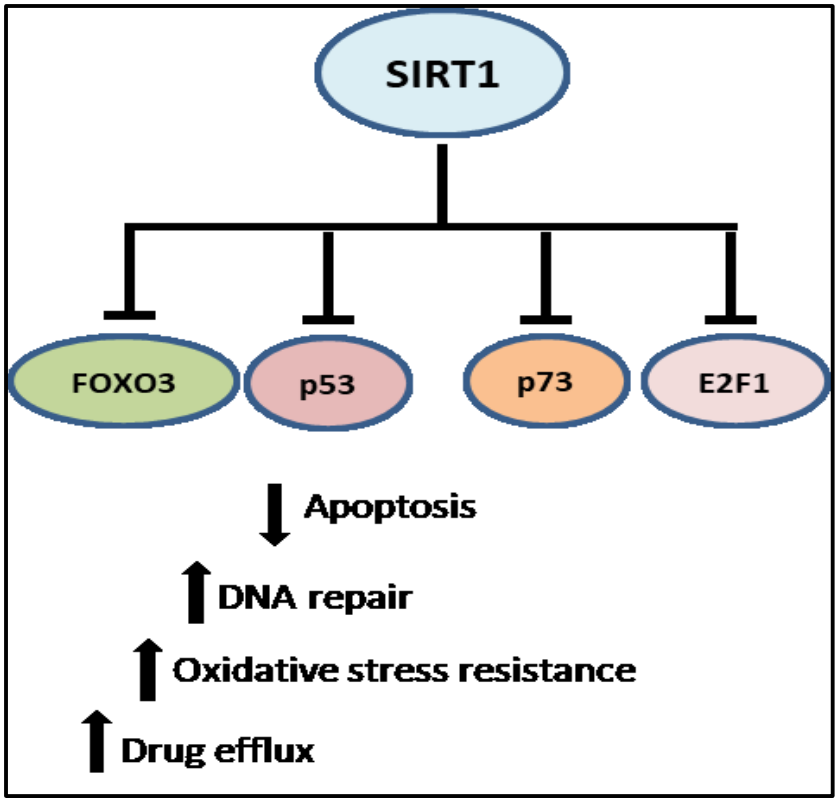


Figure 1.13 Downstream targets and cellular functions of SIRT1. Adapted from [262].

1.18.2 SIRT2 in FOXO regulation

SIRT2 is mostly a cytoplasmic protein that deacetylates cytoplasmic α-tubulin to control microtubule structure, assembly and dynamics [263]. However, SIRT2 has also been found to localise in the nucleus, where it can deacetylate various histone and non-histone proteins such as p53, FOXO1, and FOXO3 [264]. SIRT2 also shuttles from the cytoplasm to nucleus during the G2/M phase where it can deacetylate histone 4 on lysine 16 site (H4K16) [265-267]. As mentioned, SIRT2 binds and deacetylates FOXO3 and in turn enhances the expression of FOXO target genes $p27^{Kip1}$, *MnSOD*, and *Bim* [268]. Therefore, SIRT2 decreases cellular ROS levels by inducing the activation of mitochondrial antioxidant enzyme suggesting its role in the cellular defence against genotoxic agents and oxidative stress. However, in the presence of enhanced cellular stress, SIRT2 promotes apoptotic cell death by inducing Bim expression. Besides, SIRT2 mediated FOXO1 deacetylation has been shown to regulate the pathway of adipocyte differentiation [269].

Deregulation of SIRT2 has been found to be one of the significant causes of cancer metastasis and drug resistance [270-280]. However, the role of this protein in cancer is much more complex and likely context specific [274, 275, 281]. For example, inhibition of SIRT2 causes apoptosis via activation of p53 in cancer cell lines such as HeLa, but not in normal epithelial cells [282]. For this, SIRT2 inhibition has been considered as a potential approach to induce cancer cell apoptosis. Moreover, scientific study revealed that acetylation of FOXO1 in response to environmental stress is predominantly a cytoplasmic event in cancer cells since FOXO1 specifically interacts with Atg7 to induce autophagic cell death [223]. Therefore, SIRT2 plays a key role in restricting the tumour inhibitory functions of FOXO1 [223]. It has also been reported that SIRT2 interacts with RelA (p65, an NF-κB family member) in the cytoplasm and inhibits NF-kB dependent gene expression (e.g. IAPs) indicating its role as a tumour promoting factor [283]. Therefore, SIRT2 has been described to act as a tumour suppressor or tumour promoter dependent upon breast tumour grade [284].

1.18.3 SIRT6 in FOXO regulation

SIRT6 is another important nuclear deacetylase that is involved in modulating DNA repair. Besides, SIRT6 also regulates the acetylation and expression levels of some protein targets e.g. p53, FOXO3 that play a significant role in the regulation of cell proliferation, survival, and apoptosis. Previous studies reported that SIRT6 is involved in base excision repair [285] and in enabling efficient repair of DNA double-strand breaks (DSBs) through both non-homologous end joining and homologous recombination [286-288]. To date, it has been shown that knockout of SIRT6 in mouse cells made them to be oversensitive to certain types of DNA damage, especially those arisen from genotoxic drug treatments, and results in reduced genomic stability [285]. Therefore, SIRT6 promotes chemotherapeutic resistance by reducing cells protection to various environmental stress. Interestingly, this function of SIRT6 is facilitated by inhibiting NF-κB activity at least in some part. Here, SIRT6 binds to the RelA subunit of NF-κB and thus recruited to target gene promoters. After recruitment, SIRT6 deacetylates histone H3 lysine 9 (H3K9), preventing the binding and interaction of NF-κB to chromatin [289]. Collectively, by inhibiting the induction of NF-κB target genes essential for cell cycle arrest and apoptosis, SIRT6 act as a positive mediator of drug resistance. This role of SIRT6 is further supported by

another study that explored SIRT6 as a modulator of the effects of paclitaxel on cell cycle arrest and cell death in breast cancers [194].

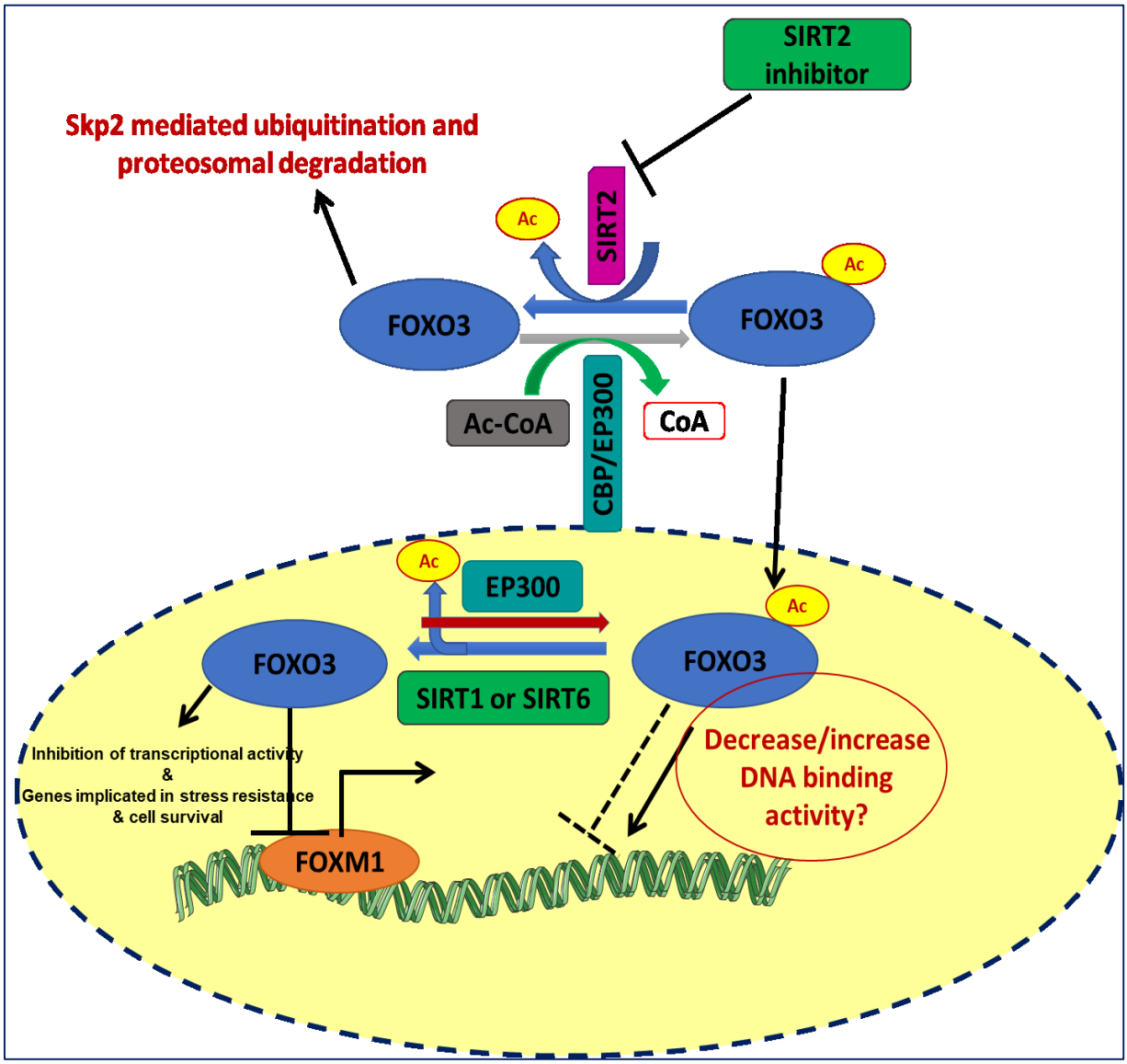


Figure 1.14 Schematic representation of the possible regulation of FOXO3 acetylation by SIRT1, SIRT2 and SIRT6.

1.18.4 The role of SIRT3 and SIRT7

Mitochondrial sirtuins are comprised of three groups named as SIRT3, SIRT4, and SIRT5. These deacetylases mainly act as oxidative sensors that modulate the functional activity of metabolic enzymes. However, they also play a vital role in regulating protein deacetylation and/or mono-ADP-ribosylation. For example, SIRT3 has been found to translocate from the nucleus to the mitochondria in response to different stress or stimuli, including ultraviolet (UV) irradiation and the drug etoposide

[290]. Nuclear SIRT3, has been shown to deacetylate and activate the double-stranded DNA break (DSB) repair protein Ku-70 which in turn protects cardiac muscle cells from stress-induced cell death [291].

SIRT7 is a positive modulator of the expression of DNA polymerase I (Pol I) and is localised predominantly in the nucleolus [285]. According to scientific reports, SIRT7 cooperates and interacts with the upstream binding factor (UBF) subunit of the RNA polymerase I complex which subsequently facilitates ribosomal gene (rDNA) transcription. Depletion of SIRT7 has been shown to induce cell cycle arrest and apoptosis [285]. In addition, SIRT7 also binds and deacetylates p53 *in vitro* to regulate p53 mediated functions [292]. In fact, knockout of SIRT7 in cardiac muscle cells exhibits elevated acetylation level of endogenous p53, although it remains unclear whether this effect is mediated by direct interaction of p53 and SIRT7. Therefore, SIRT7 is likely associated with drug resistance of cancer cells by inhibiting p53 functions as well as by inducing cell proliferation.

1.18.5 Sirtuin inhibitors

The dual role of SIRTs in modulating the deacetylation of histone and non-histone proteins makes them as an attractive therapeutic target for various neurological disorders, cancers and cardiovascular diseases [293]. It has been suggested that cancer cells and especially drug resistant cancer cells are relatively prone to high levels of SIRT activity, rendering them more susceptible to SIRT-inhibition. Potent and effective SIRT inhibitors include EX527 (6-Chloro-2, 3, 4, 9-tetrahydro-1H-carbazole-1-carboxamide) [294], Sirtinol (2-[(2-Hydroxynaphthalen-1-ylmethylene) amino]-N-(1-phenethyl) benzamide) [295] and Salermide, N-{3-[(2-hydroxynaphthalen-1-ylmethylene)-amino]-phenyl-2-phenyl-propionamide [296]. Some other commonly used sirtuin inhibitors are nicotinamide and its derivatives [297-299], cambinol [300, 301] and AGK2 [302].

Nicotinamide is one of the earliest sirtuin inhibitors identified which inhibits SIRT1, SIRT2, SIRT3, SIRT5 and SIRT6 with IC_{50} values varying from 50 to 184 μM [303]. It can inhibit cell growth and induce apoptosis in leukemic cells as well as blocking the growth and viability of human prostate cancer cells [304]. Sirtinol inhibits human

SIRT1 which is also reported to have antitumour activity. It induces cellular senescence with reduced activation of RAS-MAPK pathway in human breast cancer MCF7 cells and lung cancer H1299 cells [305]. Another study reported that sirtinol induces apoptosis in MCF-7 cells via p53 activation [264]. Moreover, sirtinol treatment combined with cisplatin showed a synergistic effect at inhibiting the growth of HeLa cell [306]. Salermide, a reversed amide based on the structure of sirtinol which induces apoptosis in various cancer cell lines through inhibition of SIRT1 in a p53-independent manner. It shows relatively more significant inhibition of leukaemia cell lines (MOLT4 and KG1A), colon cancer (SW480) and lymphoma (Raji) cells than the breast cancer cell line MDA-MB-231 [296]. Salermide also induces apoptosis in non-small cell lung cancer (NSCLC) cells through up-regulation of death receptor 5 (DR5) [307]. Another selective SIRT1 inhibitor is EX527 that has an IC_{50} value in the range of 60 nM to 100 nM in vitro. Inhibition of SIRT1 with EX527 leads to increased p53 acetylation after DNA damage in mammary epithelial cells and a wide range of cancer cell lines [308].

Sirtuin inhibitors are used as adjuvant treatments to combat drug resistance in cancer. However, little is known about the *in vivo* efficacy of these inhibitors or their specific mechanisms of action on cellular targets. Previous study showed that both Sirtinol and Salermide induce apoptosis in cancer cells whereas SIRT1 inhibitor EX527 is not able to activate the apoptotic pathway [264]. However, EX527 has been found to induce cell cycle arrest by inhibiting G1 phase transition [264]. Furthermore, enhanced apoptotic cell death was observed upon disruption of the *Sirt1* and *Sirt2* genes in a *p53*-deficient chicken cell line when treated with radiation, cisplatin and etoposide [309]. This experiment suggests that SIRT inhibitors can target p53-independent pathways to increase chemotherapy-induced apoptosis. Notably, the cellular targets of the SIRT inhibitors are likely to involve histones and other non-histone transcription factors in these p53-deficient metastatic tumours.

To date, other SIRT1 inhibitors have also been reported. One such inhibitor is JGB1741. In the p53-deficient MDA-MB-231 breast cancer cells JGB1741 treatment induces strong apoptotic effects [310], approving the efficacy and activity of SIRT inhibitors in p53-null cancers. Another active SIRT1 inhibitor is amurensin G and was extracted from Amur grapes (*Vitis amurensis*). Amurensin G has been shown to

inhibit the genetic expression of FOXO1 and MDR1 in the adriamycin-resistant (MCF-7/ADR) breast cancer cells [311].

Finally, it is noteworthy that SIRT inhibitors can also be used in combinatorial treatments with conventional chemotherapeutics to increase the activity of drugs and to overcome drug resistance. For example, a novel sirtuin inhibitor BZD9L has been used as a potential adjuvant to increase the sensitivity of colorectal cancer cells to 5-fluorouracil [312]. Therefore, detail understanding of the role and regulation of SIRTs, the functional outcomes on their targets and the possible use of the adjuvant therapy will lead us to generate a more effective pharmacological approach for the treatment of metastatic cancers.

1.19. Aims and objectives of the project

Because of the roles of FOXO3 acetylation in drug response [252], I aimed to better characterise the role of EP300/CBP mediated acetylation on the cancer cell proliferation and survival functions of FOXO3 in drug resistant HER2 overexpressed breast cancer cell lines. Importantly, cancers with hyper-active PI3K/AKT pathway have been found to be associated with enhanced AKT-dependent phosphorylation of FOXO3, which in turn inhibit proteins interaction with EP300 [183, 313, 314]. Therefore, FOXO3-EP300/CBP interaction and the resulting FOXO3 acetylation were thought to be induced upon lapatinib induced reduction of phosphorylation of FOXO3. This further suggest that EP300/CBP regulates FOXO3 activity either by altering the acetylation status of the FOXO3 or by affecting its transcriptional activity on target genes abd thus involve in modulating lapatinib sensitivity. Therefore, we think the study will increase our understanding of the functional role of PTMs, more specifically acetylation, on FOXO3 activity which is critical to better characterise the role of this tumour suppressor protein in lapatinib sensitivity and resistance of breast cancer. Furthermore, EP300 has been recently found to be associated with doxorubicin resistance in breast cancer cells and this is related to the acquisition of an EMT phenotype via down-regulation of E-cadherin [315-317]. Thus, elucidating the role of EP300-mediated acetylation of FOXO3 as well as its role in EMT, stemness and drug resistance will enable a more promising and cautious approach in the choice and combination of drugs used for treating breast cancer patients and can be used as reliable screening, diagnostic and prognostic biomarkers for early new and recurrent breast cancer detection and for monitoring treatment response.

Collectively, the major aims of this PhD thesis can be summarised by following ways:

(1) Investigate the functional outcome of EP300-mediated FOXO3's acetylation as well as the role ofmsirtuins and their inhibitors in regulating FOXO3 acetylation.
(2) Characterise the impact of CBP-mediated acetylation of FOXO3 in regulating lapatinib sensitivity and resistance.
(3) Elucidate the role of SIRT2 in regulating FOXO3 acetylation as well as lapatinib sensitivity of breast and nasopharyngeal cancer.
(4) Understand the role of EP300 in EMT, cancer stemness and drug resistance of breast cancer.

CHAPTER 3
MATERIALS AND METHODS

2.1 Cell lines, cell culture, and treatments

The BT474 cell line was obtained from the American Type Culture Collection (ATCC), whereas, human breast cancer cell line, MCF-7 (Michigan Cancer Foundation-7) was received from the Cell Culture Service of Cancer Research UK, where they were generated, tested and authenticated. Lapatinib resistant BT474 cells (BT474 Lap^R) were derived from wild-type BT474 cells by Dr. Ana Rita Gomes and were continuously treated with 1 μM lapatinib for more than 3 months. BT474 Lap^R cells were regularly maintained with 1 μM lapatinib in the growth medium. Wild type mouse embryonic fibroblasts (MEFs) and triple knock-out *foxo1/3/4*$^{-/-}$ MEFs cells received as a gift from Prof. Boudewijn Burgering, UMC, Utrecht, the Netherlands and have been described previously [318].

The NPC cell line TW01 is derived from moderately differentiated keratinising NPC tissues, and was kindly provided by Prof. Chin-Tarng Lin, National Taiwan University, Taipei [319]. TW01 cells were cultured with DMEM supplemented with 10% v/v foetal calf serum (FCS), 100 U/mL penicillin, and 100 μg/mL streptomycin. Poorly differentiated human NPC cell lines SUNE 5-8 F (highly tumorigenic and metastatic) and 6-10B (highly tumorigenic but poorly metastatic) derived from the parental line SUNE-1, were obtained from the Prof. Qingling Zhang, Southern Medical University, Guangzhou China [320, 321]. HK1 is a well-differentiated squamous carcinoma cell line and was obtained from the Queen Elizabeth Hospital, University of Hong Kong [322]. C666-1 is an undifferentiated NPC cell line obtained from Prof. Maria L. Lung, Center for Nasopharyngeal Carcinoma Research, and from Prof. George SW Tsao, University of Hong Kong [323]. These last four NPC cell lines were cultured in RPMI medium supplemented with 10% FBS, 100 U/mL penicillin, and 100 μg/mL streptomycin.

In general, all NPC cells (unless specific cells and media were mentioned) were cultured in Dulbecco's modified eagle's medium (DMEM) (Sigma Aldrich, Poole, UK) and supplemented with 10% (v/v) foetal calf serum (FCS) (First Link Ltd, Birmingham, UK), 100 Unit/ml penicillin/streptomycin (Sigma-Aldrich, UK) and 2 mM glutamine and maintained at 37°C in a humidified atmosphere containing 10% CO_2. Cultured cells were also maintained by serial passaging using 25 g/L trypsin solution

(Sigma Aldrich, Poole, UK) in 0.02% ethylene diamine tetra acetic acid (EDTA) (Sigma Aldrich, Poole, UK) when cell confluency reached to 70-80%.

2.2 Plasmids and their isolation

Plasmid pcDNA3.1-p300 (plasmid #23252), the acetyl-transferase mutant pcDNA3.1-p300 (HAT-) (plasmid #23254) and hE-cadherin-pcDNA3 (plasmid #45769) were obtained from Addgene (Addgene, MA, USA). Empty vector pcDNA3.1 was purchased from Invitrogen. Plasmid pLVX, pLVX-CREBBP WT and plVX-CREBBP HAT- were obtained as kind gift from Grace Liu, China. All plasmids were cloned into *E. coli* DH5α and the Purelink®HiPure Plasmid Maxiprep Kit (Thermo Fisher Scientific, Hemel Hampstead, UK) was used to isolate plasmid DNA as indicated in the manufacturer's instructions.

2.3 Breast cancer cell transfections

BT474 and BT474-Lap^R cell lines were seeded to achieve approximately 60-70% confluency in 75 cm^2 (T75) flasks before transfection. The plasmid-encoding human EP300, pcDNA3.1-EP300, the acetyl-transferase mutant, pcDNA3.1-p300 (HAT-), and the empty vector were transfected into cells using XtremeGene (Sigma-aldrich). Transfection was performed at a 3:1 (XtremeGene: DNA) ratio using 8 µg of plasmid following manufacturer's instruction. Briefly, Xtremegene was diluted in OPTIMEM serum free medium and left at room temperature for 5 min. The plasmid DNA was then slowly added into the mixture and incubated up to 20-30 min. Then, the mixtures were slowly transferred into the culture plates and left at least 24 to 48 h before further analysis. Transfected cells were counted and used for any subsequent assays 24 hours post-transfection. For gene silencing, cells were plated in at 60-70% densities. The following day, cells were transfected with ON-TARGET plus siRNAs (GE Dharmacon, Horizon Discovery LTD, UK) targeting EP300 (L-003486-00-0005), CREBBP (L-003477-00-0005), SIRT1 (L-003540-00-0005), SIRT2 (L-004826-00-0005) or SIRT6 (L-013306-00-0005) using oligofectamine (Invitrogen, Thermo Fisher Scientific, UK) according to the manufacturer's protocol. Non-Targeting siRNA pool (GE Dharmacon; D-001210-01-05) was used as transfection control.

2.4 Generation of stable cell lines

To obtain stable CBP overexpressed BT474 and BT474 Lap^R cell lines, lentiviral transduction experiment was performed. To produce lentivirus, HEK293T cells were co-transfected with pLVX, pLVX-CREBBP, pLVX CREBBP HAT-, psPAX2 and pCMV-VSV-G for packaging using Polyethyleneimine (PEI) Transfection Reagent (Figure). The plasmid psPAX2 (Addgene plasmid # 12260) and pCMV-VSV-G (Addgene plasmid # 8454) was a gift from Dr. Ernesto Yagüe. After 48 h, supernatant was filtered and added to BT474 and Lap^R cells with polybrene. All the transduced cells were selected in a medium containing 1 µg/mL puromycin (Invitrogen).

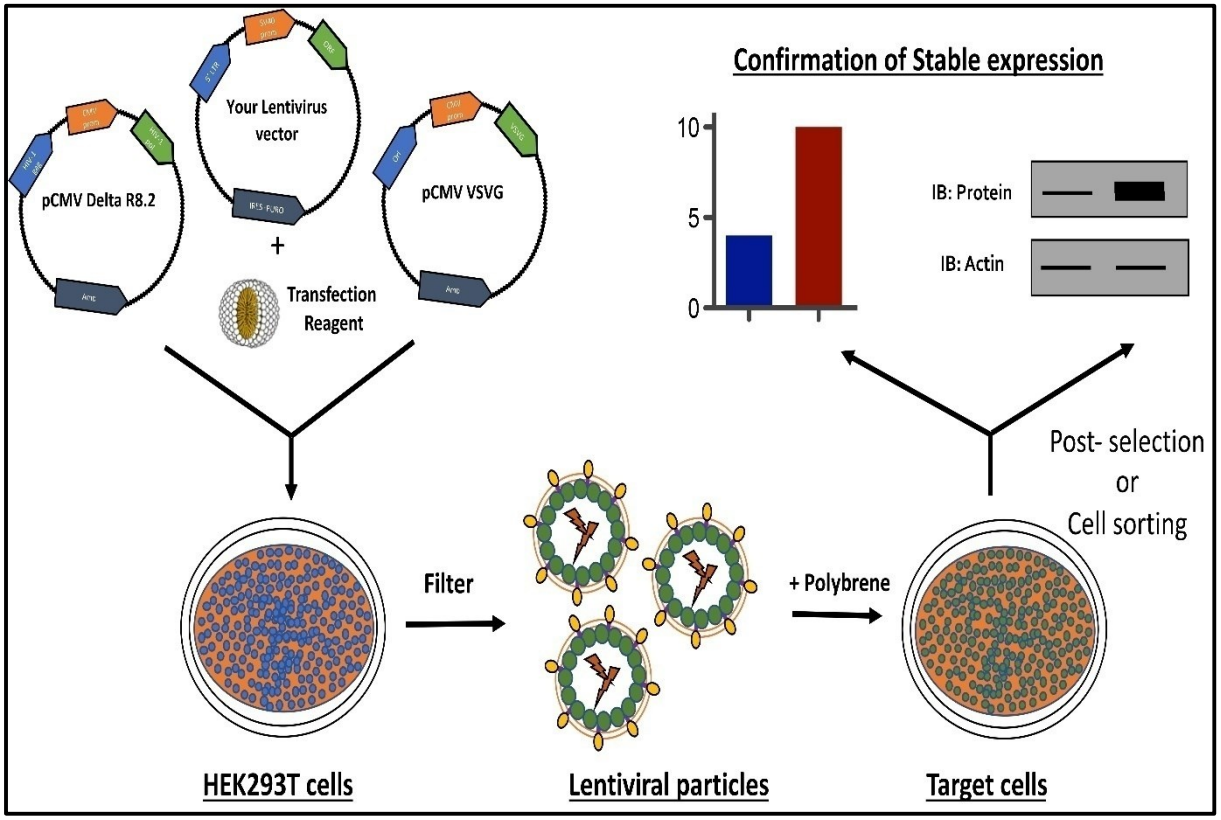


Figure 2.1 Schematic representation of generation of stable cell lines using lentivirus. [324]

Over-expression of EP300 and CDH1 in Hs578T was performed by Mr. Muhammad Asaduzzaman by stable expression of a pcDNA3.1-derived construct carrying the full-length EP300 and E-cadherin cDNA (pcDNA3.1-EP300, #23252, hE-cadherin-pcDNA3, #45769, Addgene, Watertown, MA, USA) [325]. Plasmid DNA was linearized by *Pvu*I and transfected into Hs578T cells using GenJet (SignaGen Laboratories, Rockville, MD, USA) following manufacturer's instructions and selected

and maintained with 1 mg/mL G418 (Sigma-Aldrich, St. Louis, MO, USA). Pools of at least 200 G418-resistant clones were used in all cases.

2.5 Generation of drug resistant Hs578T cell lines

Hs578T cells were obtained from Sigma-Aldrich (St. Louis, MO, USA). Medium for Hs578T cells contained DMEM, FCS, and 10 µg/ml recombinant human insulin (Sigma Aldrich, St. Louis, MO, USA). Where indicated, cells were treated with 5-Aza-2'-deoxycytidine (AzaC; Sigma Aldrich, St. Louis, MO, USA) daily in fresh medium for up to four days or with flufenamic acid (N-(α,α,α-Trifluoro-*m*-tolyl)-anthranilic acid; 2-[[3-(trifluoro-methyl) phenyl] amino]-Benzoic acid, FFA; Sigma Aldrich, St. Louis, MO, USA) as indicated. Drug resistant derivatives from Hs578T cells were generated by Dr. Ernesto Yagüe using drug pulses in an escalating manner essentially as described [315] until cells were able to proliferate after 3-day toxic pulses of paclitaxel (Hs TAX cells) and doxorubicin (Hs DOX cells). Drug resistant cells were routinely grown drug free with drug treatments (25 nM paclitaxel or 100 nM doxorubicin) every 5 passages to maintain the resistant phenotype. A sulphorhodamine B (Sigma Aldrich, St. Louis, MO, USA) assay was used to screen for drug cytotoxicity as described [315].

2.6 Duolink *in situ* proximity ligation assay (PLA)

The analysis was carried out according to the manufacturer's instructions [326]. This assay is used to detect, visualize and quantify protein expression, protein interactions, and specific post-translational protein modification [326]. To detect protein-protein interactions and post-translational modifications, two primary antibodies were used which are raised from different species. At first, samples were incubated with these two primary antibodies that bind to the proteins to be detected. Then, secondary antibodies called PLA probes was applied (PLA probe MINUS and PLA probe PLUS) where each one is conjugated with a unique oligonucleotide (Sigma-Aldrich, DUO92008 SIGMA; POOLE UK). After this, the ligation solution, consisting of two oligonucleotides and ligase, was added. When the two PLA probes are in close proximity (< 40 nm), the oligonucleotides will hybridize and join to a closed circle by adding enzymatic ligation solution. Then, the amplification solution, consisting of nucleotides, polymerase and fluorescently labelled oligonucleotides was added. The oligonucleotide arm of one of the PLA probes acts as a primer for

the rolling circle amplification using the ligated circle as a template, generating several hundred-fold concatemeric (repeated sequence) products subsequently. The replicated product can be easily visible as distinct fluorescent spot when viewed with a fluorescence microscopy. Here, I used Leica SP5 confocal microscope with 63x oil lenses for microscopy. Nuclear staining was performed by using Dapi solution.

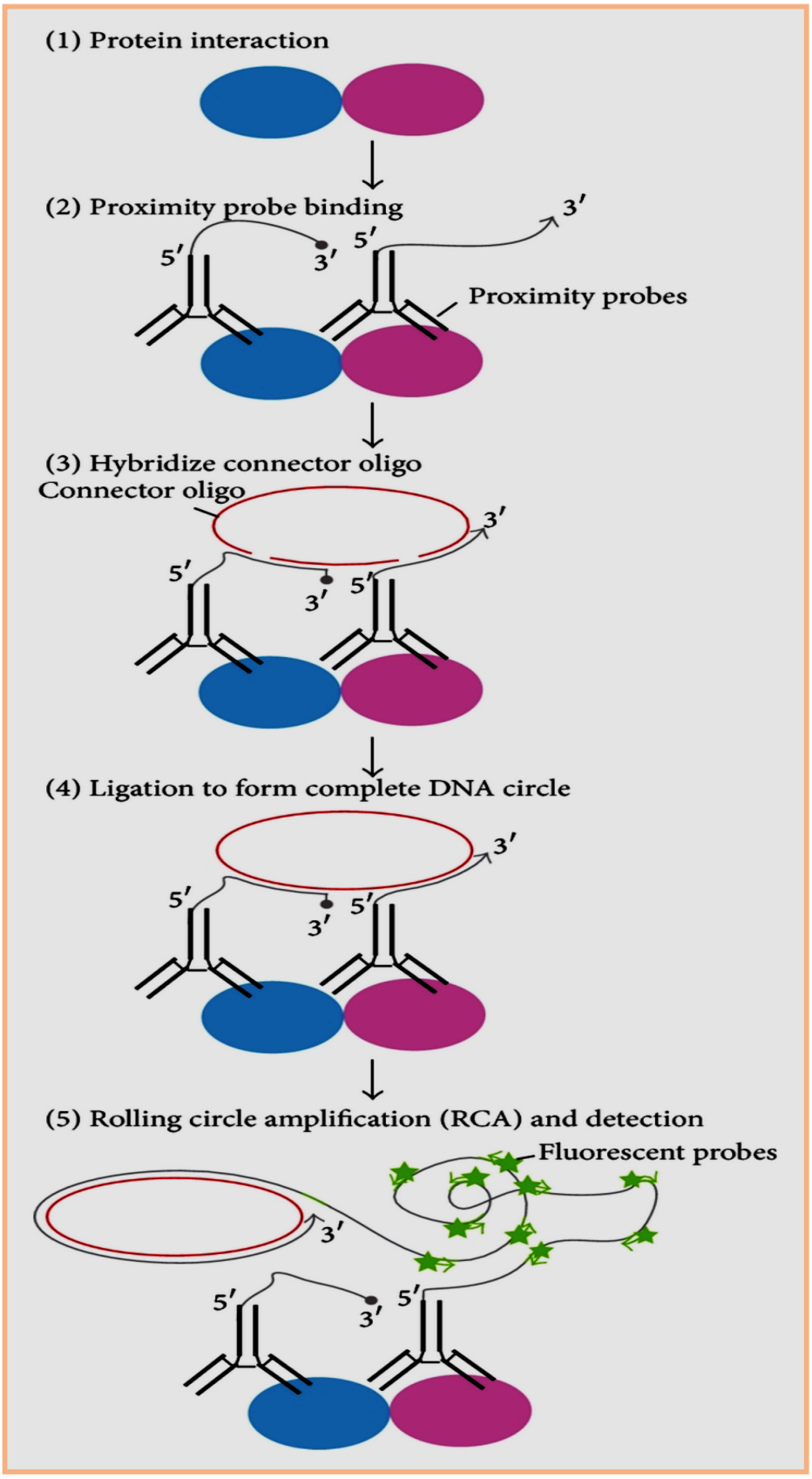


Figure 2.2 Schematic representation of in situ Proximity Ligation Assay (PLA) [327]

2.7 Protein extraction and quantification

Whole cell extracts were prepared by harvesting cells using 1× trypin-EDTA. Once the cells detached, medium was added into cell culture plates to inactivate the trypsin and samples were spun in 2000× rpm for 5 minutes. The supernatant was discarded, and cell pellets were washed in PBS and spun for an additional 5 minutes (1200 ×g). The supernatant was discarded, and the cell pellet was frozen at -80^{0}C until lysis was performed. Frozen pellets were lysed in lysis buffer (150 mM NaCl,50 mM Tris-HCl (pH 7.4), 5 mM EDTA, 5 mM Dithiothreitol (DTT), 1% NP-40 (or IGEPAL), and 1 tablet of protease inhibitors ("Complete" protease inhibitor mixture, as instructed by the manufacturer, Roche Applied Science; Burgess Hill, UK) supplemented with phosphatase inhibitors (1 mM sodium fluoride (NaF), 1 mM sodium orthovanadate (Na_3VO_4) and 1 mM PMSF as protease inhibitor. The samples were kept on ice for 10 minutes, vortex every 3 minutes to disrupt the cell membranes. The supernatants (protein extracts) were finally collected after centrifugation at 800 ×g for 10 minutes at 4^{0}C. Protein concentration was determined using the Pierce BCA Protein Assay Reagents A and B (Thermo Scientific) according to manufacturer's instruction. Absorbance was read at 562 nm using the Sunrise spectrophotometer (Tecan; Reading, UK). Protein concentrations were determined by the equation of absorbance x 25 = µg/µl.

2.8 Western blotting

SDS-PAGE gels are consisting of an upper stacking and a lower resolving gel. The resolving gel was made with varying amounts of poly-acrylamide solution, according to the molecular size of the protein being isolated with percentages of gels used varying from 7 to 14. Lower percentage gels allowed better separation of proteins of higher molecular weight (MW) and vice versa. The poly-acrylamide with 25% ammonium persulfate (APS) and tetra-methylethylenediamine (TEMED) were used as the catalysts for gel polymerization.

To separate proteins, 10-20 µg of protein lysate was added with 2 × SDS loading buffer (200 mM Tris-HCl pH 6.8, 6% sodium dodecyl sulfate (SDS), 2 mM EDTA, 10% 2-mercaptoethanol, 10% glycerol, 0.02% bromophenol blue) and boiled for 5

minutes at 100ºC. Samples were then spun at 800 ×g for 1 minute and the appropriate volume of sample was loaded into the stacking wells. SDS-PAGE gels were run in running buffer (25 mM Tris-Base, 250 mM glycine, 0.1 % (w/v) SDS) at 60V through the stacking gel and then 90-100V through the resolving gel.

Once the proteins had been separated by SDS-PAGE, proteins were electro-transferred on to 0.45 μm Protran nitrocellulose membranes (Schleicher and Schuell, Whatman, Brentford, UK) using a wet tank blotting system (Bio-Rad Laboratories Trans-Blot Cell) in transfer buffer (25 mM Tris, 190 mM glycine and 20% (v/v) ethanol) for 90 minutes at 90V. Tanks were packed in ice or if possible put in 4ºC to avoid overheating.

Membranes were then blocked in 5% (w/v) bovine serum albumin (BSA) in Tris-buffered solution with 0.05% Tween-20 (TBST, pH 7.5) for 1 hour at room temperature. Primary antibodies were diluted in a 5% BSA-TBST solution and membranes were incubated in primary antibodies overnight at 4°C. The membranes were washed three to four times with TBST, every 5 minutes with 50 ml TBST at room temperature. Membranes were then incubated in their respective secondary antibodies (anti-rabbit or anti-mouse; Santa-Cruz Biotechnologies; Santa Cruz, CA, USA) coupled with horseradish peroxidase (Dako, Ely, UK) at a 1:2000 dilution for 1 hour at room temperature. After that, membranes were washed for five times every 5 minutes with 50 ml TBST at room temperature to remove excess secondary antibodies. Proteins were then visualized using enhanced chemiluminescence detection system (GE Healthcare, UK).

Primary antibody against Ac-FOXO3 (K242/K245) was developed by Professor Eric Lam and produced by PickCell Laboratories. Other primary antibodies used were P-EGFR (Cell signalling, #2234), EGFR (Cell signalling, #4267), P-HER2 (Cell signalling, #2244), HER2 (Cell signalling, #2242), P- AKT (S473) (Cell signalling, #4060), AKT (Cell signalling, #4685), β-tubulin (Santa Cruz Biotechnology, #sc9104), EP300 (Abcam, ab10485), P-FOXO3 (T32) (Cell signalling, #9464), FOXO3 (cell signalling, #2497), Ac-p53 (K382) (Cell signalling, #2525), p53 (Santa Cruz Biotechnology, #sc98), FOXM1 (Santa Cruz Biotechnology, sc502), $p27^{Kip1}$

(Santa cruz biotechnology, sc-528), SIRT1 (Abcam, Ab32441), SIRT2 (Santa Cruz Biotechnology, sc20966), SIRT6 (Cell Signaling, 2590 and Abcam, ab62739), HER3 (Cell signalling #4754), H3K27Ac (Abcam, #ab4729), Bim (Cell signalling, #2933), p130 (BD Biosciences, #610272), $p16^{INK4a}$ (BD Biosciences, #554079), Acetylated lysine (Cell signalling, #9441), anti-acetyl α-tubulin (Lys40) (Cell signalling, D20G3, #5335),α-tubulin (Abcam, ab7291), β-actin antibody (Santa cruz, sc-1616), cleaved PARP (Asp214) (Cell signalling, #5625), PARP (Cell signalling, #9532) cleaved caspase 3 (Asp175) (Cell signalling, #9664), cleaved caspase 7 (Asp198) (Cell signalling, #8438), cleaved caspase 9 (Asp315) (Cell signalling, #9505), CBP (Cell signalling, #7389), p62/SQSTM1 (Thermo Scientific, #PA5-27247), LC3B (Cell signalling, #2775), Puma (Cell signalling, #4976), Bcl-xL (Cell signalling, #2764), Bax (Cell signalling, #2772BC), Lamin B (Santa Cruz, #sc6217), HER3 (Santa Cruz, #sc-285), P-HER3 (Cell signalling, #4791), JNK (Santa Cruz, #sc7345), P-JNK (Cell signalling, #9251), p38 (Cell signalling, #9212), P-p38 (Cell signalling, #9215), c-Myc (Santa Cruz, #sc-40), cyclin B1 (Santa Cruz, #sc752), EP300 (Santa Cruz, #sc585), EP300 (Santa Cruz, #sc48343), EP300 (EMD Millipore, #05-257), $p21^{Cip1}$ (Santa Cruz, #sc817), E-cadherin (Cell signalling, 24E10 #3195), N-cadherin (Cell signalling, #4061), Vimentin (Cell signalling, D21H3 #5741), Snail (Cell signalling, C15D3 #3897), Slug (Cell signalling, C19G7 #9585), β-catenin (BD Transduction, #610153), p120 (Abcam, #ab92514), Zeb1 (Cell signalling, #3396), P-NF-kB p65 (S536) (Cell signalling, #3033), NF-kB p65 (Cell signalling, #4764), Twist 2C1a (Santa Cruz, #sc81417)

2.9 Real-time quantitative PCR

Cells were harvested by centrifugation (1200 ×g) and cell pellets were stored at -80°C until RNA extraction. Total mRNA was extracted from frozen cell pellets using the RNeasy Mini Kit (Qiagen, UK) according to manufacturer's instructions. The purity and concentrations of obtained mRNA were determined by measuring the absorbance at 260 nm and 280 nm using NanoDrop ND-1000.

Two µg of extracted total mRNA was used as a template for first strand cDNA synthesis reaction and the resulting first-strand cDNA was used as template in the

real-time PCR. The initial reaction to reverse transcribe the total RNA contained random primers, 10 µM of each dNTP, and Superscript III reverse transcriptase (Invitrogen). The initial mixture was heated for 65 °C (5 min) for denaturation and cooled on ice. 5 x First-Strand Buffer, 0.1 M DTT and RNaseOUT RNase Inhibitor (40 units/µl) were added to the denatured samples and were returned to the PCR machine programmed to incubate at 25 °C (5 min) and 50 °C (60 min) for annealing and cDNA synthesis respectively. A final deactivation was performed by heating at 70 °C for (15 min). A cDNA standard solution was prepared by pooling equal amounts of all diluted cDNA samples. Four serial 1:4 dilutions (1/4, 1/16, 1/64, and 1/256) of the standard in DEPC (RNAase-free) water were used for the generation of standard curve.

To conduct the Real time quantitative PCR (RT-qPCR), 100 ng cDNA was added to SYBR-Green Master Mix (Applied BioSystems). The reaction mixture was prepared using 2 µl mRNA sample and 18 µl SYBR-Green Master Mix and primers to a final volume of 20 µl. All RT-qPCR assays were performed in 96-well plates in the ABI PRISM® 7900 HT Fast Real-time PCR System (Applied BioSystems) on a cycling program of 90°C for 10 min for enzyme activation followed by 40 cycles of denaturation and primer annealing/extension consisting of 95°C for 10s and 60°C for 30s respectively. The non-regulated ribosomal housekeeping gene *RPL19 or RPS14* was used as an internal control to normalize gene expression between samples. All amplifications and measurements were performed in triplicate. Efficiency of RT-qPCR was obtained from the slope of the standard curve. A comparative threshold cycle was used to determine relative gene expression with standard curves for each gene as previously described [315].

Table 2.1 Human primers used for RT-qPCR

Gene	Human Primer Sequences (5′-3′)
EP300 forward	AAAAATAAGAGCAGCCTGAG
EP300 reverse	AGACCTCTTTATGCTTCTTCC
FOXO3 forward	TCTACGAGTGGATGGTGCGTT
FOXO3 reverse	CGACTATGCAGTGACAGGTTGTG
$p27^{Kip1}$ forward	CATTTGGTGGACCCAAAGAC
$p27^{Kip1}$ reverse	CTTCTGAGGCCAGGCTTCTT
RPL19 forward	GCGGAAGGGTACAGCCAAT
RPL19 reverse	GCAGCCGGCGCAAA
RPS14 forward	TCACCGCCCTACACATCAAACT
RPS14 reverse	CTGCGAGTGCTGTCAGAGG
FOXM1 forward	TGCAGCTAGGGATGTGAATCTTC
FOXM1 reverse	GGAGCCCAGTCCATCAGAACT
CBP forward	AACATGTCACTCAGGACC
CBP reverse	AATATTCATCCCTGCTGTTG
Bim forward	TGAGAAGATCCTCCCTGCTG
Bim reverse	TCTTGGGCGATCCATATCTC
$p16^{INK4a}$ forward	AGCATGGAGCCTTCG
$p16^{INK4a}$ reverse	ATCATGACCTGGATCGG
p62 forward	CTGGGACTGAGAAGGCTCAC
p62 reverse	GCAGCTGATGGTTTGGAAAT
Nanog forward	CCAAATTCTCCTGCCAGTGAC
Nanog reverse	CACACGTCTTCAGGTTGCAT
Sox2 forward	TCAGGAGTTGTCAAGGCAGAG
Sox2 reverse	CGCCGCCGATGATTGTTATTA
Pou5F1/OCT4 forward	GAGAACCGAGTGAGAGGCAACC
Pou5F1/OCT4 reverse	CATAGTCGCTGCTTGATCGCTTG
ABCB1/MDR1 forward	GGGAGCTTAACACCCGACTT
ABCB1/MDR1 reverse	AGGGTTAGCTTCCAACCACG
ABCG2/BCRP forward	AGTGGCTTTCTACCTTGTCGA
ABCG2/BCRP reverse	ATGGCGTTGAGACCAGGTTT
ABCC1 forward	CTTCTGCAGCGCCGATGG
ABCC1 reverse	GTAGAAGGGGAAACAGGCCC

ABCC2 forward	CGCAGTCCAGGAATCATGCT
ABCC2 reverse	AGGAGCCATAGGTAGCCCAA
ABCC3 forward	CTCGCCTTCCTTGCAGCC
ABCC3 reverse	CAGGGAGTTCTGGAAGCAGG
ABCC4 forward	CTCTGCTCACGCGTGTTCTT
ABCC4 reverse	CCTCTCCAAGGTGCTGTGAG
ABCC5 forward	GTGAGGGAGAGAACCAGCAC
ABCC5 reverse	GCATCAAGAGAGAGGCCCTC
SIRT1 forward	AGGAGGAGGAAGAGGCGG
SIRT1 reverse	GAGCTTGCATGTGAGGCTCT
SIRT2 forward	CCTCGCCTGCTCATCAACA
SIRT2 reverse	CCCATAATCATCCCCAGGAA
SIRT6 forward	AGGAGCTGGAGCGGAAGGT
SIRT6 reverse	TGGAACACCACACTGGAAGACT
E-cadherin/CDH1 forward	GATTCTGCTGCTCTTGCT
E-cadherin/CDH1 reverse	GATTCTGCTGCTCTTGCT
Vimentin forward	AGTCCACTGAGTACCGGAGAC
Vimentin reverse	CATTTCACGCATCTGGCCGTTC
N-cadherin/CDH2 forward	GCGTCTGTAGAGGCTTCTGG
N-cadherin/CDH2 reverse	AAATCTGCAGGCTCACTGCT
Zeb1 forward	TTACACCTTTGCATACAGAACCC
Zeb1 reverse	TTTACGATTACACCCAGACTGC
Snail1 forward	AGGCCATGTCCGGACCCACA
Snail1 reverse	GTGGAGCAGGGACATTCGGGA
Snail2/slug forward	CAGTGATTATTTCCCCGTATC
Snail2/slug reverse	CCCCAAAGATGAGGAGTATC
AKR1C1 forward	AGGTGGAATGTCATCCTTAC
AKR1C1 reverse	CTATAGGCAACCAGAACAATG
AKR1C2 forward	CTCATGAGATCTGGTTGTTTG
AKR1C2 reverse	GTAACATCATGAAGGAAGGTG
AKR1C3 forward	AAAGCTTTGGTCCACTTTTC
AKR1C3 reverse	AAGATAGAGGTCAACATAGTCC
MEF2C forward	ATGCCATCAGTGAATCAAAG
MEF2C reverse	CTCGGTACCATATGTTGTTG

ALDH1 forward	GACAATGGAGTCAATGAATGG
ALDH1 reverse	ATCAATTGGTATTGTACGGC
CDH6 forward	CAAGTTACATTCAGACCAGG
CDH6 reverse	TCCCTGTCCTTCTGTTTATAG
ATP6 forward	AGCAGAAATTGTGAAGAAGG
ATP6 reverse	AACTTGGGAACTACTACCAG
ELF1 forward	TATTAGGACTATACAGGCTCC
ELF1 reverse	GTTACTGTATGCAACTGCTG
AVEN forward	CCTGAAATCCAAGGAAGATG
AVEN reverse	TTTTCTTCAGTCACAGATGG
TP53 forward	CGTACAATGACTCTTCTTGC
TP53 reverse	GCTGGATGTCTTTTATAGCTG
KCTD11 forward	CCTGGTTCATATCTGTGTTG
KCTD11 reverse	CTAATTGTCAACCACCTCAC
IGFBP3 forward	AATCATCATCAAGAAAGGGC
IGFBP3 reverse	GAACTTCAGGTGATTCAGTG
MXI forward	AGAGGAGATTGAAGTGGATG
MXI reverse	CTGGGTTCTATGAAGTGAATG
BIN3 forward	AGATATCCTTGGACTTACTCTC
BIN3 reverse	CACCTTTTCCTGATTGAAGG

Table 2.2. Mouse primers used for RT-qPCR

Gene	Mouse Primer Sequences (5′-3′)
Foxo1 forward	AAGAGCGTGCCCTACTTCAA
Foxo1 reverse	TCCTTCA-TTCTGCACTCGAA
Foxo3 forward	CCGGACAAACGGCTCACT
Foxo3 reverse	GGCACACAGCGCACCAT
Foxo4 forward	AGGACAAGGGTGACAGCAAC
Foxo4 reverse	GGTTCAGCATCCACCAAGAG
Erbb2 forward	GCTCTTTGAGGACAAGTATG
Erbb2 reverse	AAGATCTCTGTGAGACTTCG
Egfr forward	CTGTCGCAAAGTTTGTAATG
Egfr reverse	GAATTTCTAGTTCTCGTGGG
Ep300 forward	CAATAGAGCGGAATACTATCAC
Ep300 reverse	CAGTATTCATAGGAACTGGAC
SIRT1 forward	GCAGGTTGCAGGAATCCAAA
SIRT1 reverse	CCACGAACAGCTTCACAATCA
SIRT6 forward	CCCAACAGCCCTATACTCCA
SIRT6 reverse	GCCTGGGCTATAGCAGTGAG
$p27^{Kip1}$ forward	GGACCAAATGCCTGACTCGT
$p27^{Kip1}$ reverse	CGCTTCCTCATCCCTGGAC
Bim forward	CACCTGCTGTGTGCTTCCTA
Bim reverse	GCTGGCCTAAAGCAGTGAAC
$p21^{cip1}$ forward	GCCTTAGCCCTCACTCTGTG
$p21^{cip1}$ reverse	AGGGCCCTACCGTCCTACTA

2.10 Co-immunoprecipitation assay

Co-immunoprecipitation (Co-IP) was performed to detect protein-protein interactions. Cells were plated and treated according to the experimental procedure. BT474, BT474-Lap^R, Hs578T and its derivatives were harvested as already described for protein extraction. Cells were lysed and the proteins were extracted using the IP lysis buffer (1% Nonidet P-40, 150 mM NaCl, 50 mM Tris-HCl (pH 7.4), 5 mM EDTA) supplemented with fresh 1 mM PMSF, 1 mM NaF, 1 mM Na_3VO_4, 1 mM DTT and one EDTA-free protease inhibitor tablet (Complete protease inhibitor cocktail; Roche, Lewes, UK). At first, the samples were incubated for 20 min on ice and vortexed every 5 min to disrupt cell membrane. Samples were then centrifuged at 800 ×g for 10 min at 4°C to collect protein extract in a new eppendorf tube. Obtained protein was quantified using the BCA Protein Assay Kit (Pierce, Rockford, USA) and 5-10% of the total protein (25-50 µg) from each sample was kept as an input control. Protein lysates (250-500 µg) were then pre-cleaned by incubating with 20 µl of protein A/G magnetic beads (invitrogen) for 4 h at 4ºC to reduce non-specific binding. After the pre-clearing step, the lysates were transferred to new pre-chilled eppendorf tubes containing new beads that was previously washed three times with IP lysis buffer. Then, protein samples were incubated overnight with 0.25-0.5 µg of primary anti-FOXO3 (#2497, Cell-Signalling technology), Anti-acetyl lysine (#9441, Cell-Signalling technology), anti-EP300 (ab10485, Abcam) or IgG negative control (2729, Cell-Signalling technology) at 4^0C on a rotator. On the following day, the supernatant was removed, and beads were washed three to four times with IP lysis buffer. Proterin samples were then heated with 2 × SDS sample buffer at 100 °C for 5 minutes. Co-immunprecipitated protein samples were then analyzed by SDS-PAGE followed by immunoblotting with specific primary antibodies incubation.

2.11 Chromatin Immunoprecipitation (ChIP)

BT474 cells at 90% confluence in 100 mm culture dishes with or without drug treatment (1 µM Lapatinib for 2 and 4 h) were cross-linked for 10 min at room temperature with formaldehyde (Sigma). Untreated cells were used as control. Cells were then rinsed in ice-cold PBS and scraped off the dish in 1 mL of scraping buffer. After washing in PBS, Buffer I and Buffer II sequentially, the cell pellet was resuspended in 300 µl Lysis buffer and sonicated. After removing the insoluble fraction, the cell lysate was mixed with 300 µl buffer D and 100 µl was then taken as

the INPUT control. Dynabeads Protein A (Invitrogen Dynal A.S., Oslo, Norway) were first washed with TSE I buffer three times before binding with the primary antibody (1 µg) overnight at 4ºC, while dynabeads with IgG were used as negative control. A total of 500 µl sonicated lysate was then added to the dynabeads and rotated overnight at 4ºC. After washing the dynabeads five times with TSE I and twice with TE buffer, 100 µl of Elution buffer was added to the dynabeads and the mixture was rotated at RT for 1 h. The eluted supernatant was then transferred to a collection eppendorf while 100 µl fresh elution buffer was added to elute one more time at RT for 1 h. Finally, a total of 200 µl of the sample were de-crosslinked by incubation at 65ºC overnight. Qiagen PCR Purification Kit (QIAGEN, UK) was used to extract DNA from the de-crosslinked sample. Approximately 30 µl of DNA was eluted from each sample and 3 µl of each were used in one PCR reaction later. The 7900HT Fast Real-Time PCR System (Applied Biosystems, Carlsbad, USA) was used for RT-qPCR analysis. The first stage was performed at 95°C for 10 min. Then, the amplification was carried out by 40 cycles of the following three steps: 95 °C for 15 seconds, 60 °C for 30 seconds and 72 °C for 30 seconds. To test the primer specificity, a dissociation stage consisting of three steps (95°C, 60°C and 95°C for 15 seconds each) was used. Human ChIP primers that were used for ChIP experiments are mentioned below.

Table 2.3 Human primers used for ChIP

Gene	Human ChIP Primer Sequences (5′-3′)
Rictor forward	AAACAAACCCATCTCCACTGC
Rictor reverse	TTTCCCTTCTGCTTCCCTTT
$p27^{Kip1}$ forward	CCGTTTGGCTAGTTTGTTTGTCT
$p27^{Kip1}$ reverse	TGACTGCTGGAGGGGTACTG
RAD-51 forward	ATGCGAGTAGGAGGCTCAGA
RAD-51 reverse	AGCGCTCTTGTGGTTTGTTT

2.12 Sub-cellular fractionation

Subcellular fractionation assay was performed using the NE-PER Nuclear and Cytoplasmic Extraction Reagents (Perbio, Erembodegem, Belgium). Cells were harvested with trypsin-EDTA and then centrifuged at 1200 rpm for 5 minutes. After

washing the cell pellets with PBS they were transferred into 1.5 mL eppendorf tubes and pelleted by centrifugation at 5000 rpm for 2-3 min in a bench top centrifuge at 4 ºC. The obtained pellet was re-suspended in 200 µl ice-cold CER I buffer, protease inhibitors were added, and subjected to continuous vortexing for 15 sec. After incubation on ice for 10min, 11 µl ice-cold CER II solution was added to the sample tube. The tube was then vortexed for 5 sec and incubated on ice for 1 min. This mixture was further vortexed for 5 sec on the highest setting and then centrifuged at 13000 rpm on a desktop centrifuge for 5 min at 4°C. The obtained supernatant was then transferred to a clean, pre-chilled, labelled eppendorf as the cytoplasmic extract. The remaining insoluble fraction was then resuspended in 100 µl ice-cold NER solution, which had been pre-mixed with protease inhibitors. This mixture contains nuclear proteins and was subjected to vigorous vortexing to disrupt the nuclear membrane for 15 sec. Then, the mixture was left on ice for 10 min. The same procedure was repeated three times for a total of 40 min. Finally, the tube was centrifuged at maximum speed for 10 min and the supernatant was collected in a pre-chilled tube as the nuclear fraction.

2.13 Sulphorhodamine B (SRB) colourimetric assay

The SRB assay is used for the examination of cell proliferation/viability as the colorimetric measurement of the bound dye allows a measurement of cellular protein content. Lapatinib resistance and sensitivity of cell lines were examined using the SRB assay essentially as described [328]. Briefly, after 24 h post-transfection, 5000 cells/well of BT474 and 2000 cells/well of BT474 Lap^R were seeded in 96-well plates, respectively. Then, cells were allowed to attach for 24 h and treated with the different concentrations of Lapatinib drug or other sirtuin inhibitors depending on the assay. After culture, 100µL of trichloroacetic acid (TCA) was added to each well and incubated for 1 h at 4°C. The plates were then washed with deionized water three times before incubation at room temperature for one hour with 0.4% sulforhodamine B in 1% acetic acid. Then, 500 µL 1% (v/v) acetic acid was used to remove excess dye. The plates were then left to air-dry overnight and then 100 µL Tris (10 mmol/L) was added to each well to solubilize the bound sulforhodamine B dye and placed on a shaker for 30 minutes to evenly distribute the dye. Finally, absorbance of the SRB solution was read at 492 nm using a microplate reader (Sunrise Tecan, Männedorf, Switzerland).

2.14 Clonogenic assay

Clonogenic assay was performed to determine clonal survival and long-term sensitivity to Lapatinib and/or other inhibitors e.g sirtinol, FFA. At first, one day post-transfection, the cells were counted using a hemocytometer and plated into 6-well plates at a density of 2000 and 1000 cells per well for BT474 and BT474 Lap^R cells, respectively. Cells were incubated to form colonies for 28 and 14 days in sensitive and resistant BT474 cells, respectively. When significant colonies were formed, plates were removed from the incubator, culture medium was removed and washed three times with PBS. Then cell colonies were fixed with 4% Para-formaldehyde (PFA) in PBS, washed three times with PBS and then stained with 0.5% (w/v) crystal violet. Plates were then submerged in water to remove the excess of crystal violet and left air dried at room temperature for a 1-2 days. Pictures were taken and 33% (v/v) acetic acid was added to solubilize the bound crystal violet. The plates were then left on a shaker for 1-2 hours for evenly solubilisation. The optical density (OD) was then measured at 592 nm using a microplate reader (Sunrise, Tecan).

For Hs578T cells, 2-5 × 10^3 cells were seeded into 6-well plates, at least in duplicate. After 24 h, the cells were treated with paclitaxel or doxorubicin (Tocris Bioscience, Bristol, UK) for 3 days and 2 days, respectively. Cells were incubated in culture for 28 days with a replacement of drug-free medium every three days. At the end of this period, drug resistant clones were fixed with 1% formaldehyde in PBS, washed 3 times with PBS and stained with 0.5% (w/v) crystal violet. Pictures were taken and the stain was solubilised with 33% acetic acid for OD_{592} nm measurement.

2.15 Patients and tissue specimens (For chapter 3)

The patient tissue samples came from a study consisting of 688 breast cancer patients who underwent surgery for primary breast cancer between 1993 and 1998, at the Department of Pathology, Asan Medical Center, Seoul, Korea. Formalin-fixed, paraffin-embedded tissue samples from these preoperatively chemo- and radiotherapy naive patients were available for analysis as previously described [329]. The expression levels of standard biomarkers, including estrogen receptor (ER), progesterone receptor (PR), and HER2, were reviewed by immunohistochemical staining at the time of diagnosis, independently by two pathologists. HER2-overexpressing tumours were defined as those that score of 3+ by

immunohistochemistry (IHC) or by gene amplification using either fluorescence in situ hybridization or silver in situ hybridization [330]. Exemption from informed consent after the de-identification of information was approved by the Institutional Review Board of Asan Medical Center (2013-0641). Tissue microarray sections were evaluated with an automated immunohistochemical staining device (Benchmark XT; Ventana Medical Systems, Tucson, AZ, USA). Antibodies to FOXO3 (1:400 dilution; EMD Millipore, Billerica, MA, USA), SIRT1 (1:50 dilution; Abcam, Cambridge, MA, USA), SIRT6 (1:50 dilution; Cell Signaling Technology, Danvers, MA, USA) were used. Each case was evaluated by estimating the percentage and staining intensity (negative, 0; weak, 1; moderate, 2; and strong, 3) of tumour cells showing a cytoplasmic or nuclear staining pattern for FOXO3. We then classified the expression levels as high or low based on the mean staining intensity value obtained by the multiplication of each protein.

2.16 Clinical samples (For chapter 6)

Initially, 61 archival formalin fixed paraffin embedded breast tissues were collected by Dr E. Yagüe from Imperial College Healthcare Tissue Bank (R14086 and R17041) and Breast Cancer Now Tissue Bank (BCNTB-TR000054) after ethics approval by both institutions and complying with the 1964 Helsinki declaration and its later amendments or comparable ethical standards. For this type of study formal consent is not required. Samples comprised those from normal breast tissues as well as ductal and lobullar carcinoma, and were screened for EP300 and E-cadherin expression by immunohistochemistry by Mr. Muhammad Asaduzzaman as described [331], so that both E-cadherin^{high} and E-cadherin^{low} samples would be included.

2.17 Wound healing migration assay (Scratch assay)

In vitro wound healing was performed using a scratch assay. BT474 and BT474-Lap^{R} cells were first transfected with the relative overexpression or silencing protocol according to experiment and was performed twenty-four hours prior to seeding at a density of 500,000 and 250,000 cells respectively into 6 well plates to obtain 100% cell confluency. After 24 hours, the 6 well plates were then washed with PBS to remove cell debris or floating cells. The wounds were created by scratching in each confluent monolayer using a 200 µl pipette tips. The scratched plates were washed three times with 1xPBS to remove cell debris and the remaining cells were cultured

in serum-free medium in a humidified incubator at 37ºC with 10% CO_2 for the duration of the experiment. After 0, 6, 24 hours, the images were captured by phase contrast microscopy with a 4× objective lens. Serum-free media was replaced prior to each imaging procedure. To ensure images were taken of the same location, a permanent marker was used to mark the bottom of the plate at the beginning of the experiment. All images were taken, and the wound size was measured in each well per group. The wound enclosure areas were determined using imageJ analysis software to measure the distance travelled during the desired time frame.

2.18 Transwell cell migration and invasion assay

Migration and invasion assays were performed essentially as described [332] using Corning Boyden chambers (24-well insert, 8 μm, Corning, NY, USA). Approximately 20,000 cells were seeded with serum-free DMEM in the Transwell Permeable Support, 8.0 μm polycarbonate membrane, 6.5 mm inserts (Pittsburg Corning, UK). The bottom part of the well was covered with DMEM with 10% FCS in the lower chamber as the chemo-attractant. After 24 hours of seeding, cells migrated though the pores to the bottom surface of the transwell were fixed with 4% paraformaldehyde, washed three times with PBS and stained with 0.5% crystal violet for visualization. The stain was solubilised with 33% acetic acid for OD_{592} nm measurement. Six random microscopic fields were taken for each group for quantification. Cell invasion was assayed in transwell coated with Matrigel (BD Biosciences, San Jose, CA, USA). Cells crossed the Matrigel-coated filter were fixed as above and stained with DAPI (4′,6-diamidino-2-phenylindole, Sigma-Aldrich, St. Louis, MO, USA). The stained cell images were captured by a microscope (EVOS, Thermo Fisher Scientific, Whaltham, MA, USA) at five random fields using 10× magnification for quantification.

2.19 Senescence-associated β-galactosidase activity assay

BT474 and SKBR3 cells were seeded into 6 well plates at a density of 20,000 cells/well. After 24 hours, lapatinib (0.1 μM for SKBR3 and 1 μM for BT474) was added at various time points. Culture medium was then changed and left them to grow further for 7 days. Cells were then fixed and stained using a Senescence

associated β-Galactosidase Staining Kit (Cell Signaling Technology, Danvers, MA, USA, cat. no. 9860). The kit detects β-galactosidase activity at pH 6 in cultured cells and tissue sections. β-galactosidase activity at pH 6 is present only in senescent cells and is not found in pre-senescent, quiescent or immortal cells. Before staining the cells, the culture medium was removed, and the cells were fixed with 1x fixative solution for 15 min. The plates were then rinsed twice with 2 ml 1x PBS, stained for β-Galactosidase and incubated overnight at 37 °C in a dry incubator (no CO_2) for 18 hours. Blue staining was captured using a bright-field microscope. The percentage of SA β-gal-positive cells was compared between treated and untreated cells and the cells were quantified from five random fields.

2.20 Caspase-Glo assay

Caspase assay offers a direct measurement of different effector caspases (cysteine aspartic acid-specific proteases) such as caspase 3, 7, 8 and 9 that are involved in extrinsic and/or intrinsic apoptotic pathway. To determine caspase activity, I measured the activation of various caspases by using kits (Promega®). The Caspase-Glo® 3-7, Caspase-Glo® 8 and Caspase-Glo® 9 assays are homogeneous luminescent assays that measure caspase 3-7, caspase-8, and -9 activities, respectively. For this assay, cells (10,000/well) were seeded in 96-well plates and incubated overnight at 37°C with 5% CO_2. On the following day, cells were treated with a selected range of lapatinib concentrations (0, 0.1 and 1uM) for 24 hours in the same condition, i.e., incubating at 37°C with 5% CO_2. Cells were also treated with various concentrations of SIRT2 inhibitor scAB8A44. Next, the freshly prepared Caspase-Glo® (Promega) reagents were added and incubated at room temperature for 30 min to 1 hour (covering with foil, to protect from light) and the luminescent signals were read using a luminometer. The values obtained were normalized from the background and eventually the fold changes were compared with respect to the empty vector or untreated controls.

2.21 Anchorage independent soft agar growth assay

Hs578T cells (5×10^4) were mixed with DMEM medium containing 0.3% soft agar noble (Difco Laboratories, Detroit, MI, USA) on 6 well plates with a bottom layer of solidified 0.6% agar noble in the same medium. Cultures were prepared in triplicate for each cell type that were incubated and maintained for 8 weeks at 37 °C in an atmosphere of 5% CO_2 and 95% air. Also, 300 µL fresh DMEM medium was added twice a week to keep cells alive. After 8 weeks of incubation, cell colonies larger than 20 µm in diameter were counted under a simple Nikon® microscope (Model: Eclipse, TS100; Japan) and photographed using EVOS FL Cell Imaging System® (Life Technologies, Paisley, UK).

2.22 Mammosphere formation assay

For mammosphere formation assays, 3 x 10^3 cells/well were seeded, at least in duplicate, in ultra-low attachment 6-well plates (Corning, NY, USA) in DMEM/F12 medium supplemented with 20 ng/ml epidermal growth factor (EGF, Sino Biologicals, Wayne, PA, USA), 20 ng/ml basic fibroblast growth factor (bFGF, Thermo Fisher Scientific, Whaltham, MA, USA) and B27 (Thermo Fisher Scientific, Whaltham, MA, USA). Fresh medium (500 µl) was added every 3-5 days for two weeks after which the spherical clusters of cells were counted with naked eye. Clone or sphere forming efficiency was calculated relative to the total number of plated cells x100. Mammosphere volume was calculated according to the formula volume = 0.5 x width^2 x length. Images were captured using an EVOS FL Cell Imaging System® (Thermo Fisher Scientific, Whaltham, MA, USA).

2.23 Immunofluorescence

Hs578T and EP300/CDH1 overexpressing Hs578T cells were seeded at a density of 10,000 cells/well in Eight-well chamber culture slides (BD Falcon, Erembodegem, Belgium). On the following day, cells were washed twice with PBS and then fixed with 4% formaldehyde in PBS for 10 minutes at room temperature. The fixative was removed, and the cells were washed three times with PBS for 5 minutes on a slow shaker. The cells were then permeabilised with 0.1% Triton in PBS for 10 min, washed again three times with PBS, followed by blocking with 5% goat serum in 10% BSA for 30 minutes at room temperature. The primary anti-rabbit E-cadherin

(Cell signalling, 24E10 #3195), anti-rabbit Vimentin (Cell signalling, D21H3 #5741) antibodies were added at a dilution of 1:100 in 10% BSA blocking solution, incubated for 1 hour and then washed three times with PBS each for 5 minutes. The secondary antibody (Alexa-Fluor 594 anti-rabbit, Invitrogen) was then added (1:500 dilution in 10% BSA) and the cells were incubated in the dark for 45 minutes. The cells were washed again three times in PBS for 5 minutes each. Cells were then incubated in DAPI (Invitrogen) with mounting medium for nuclear staining (1:1000 dilution in 10% BSA) followed by covering with a glass coverslip and sealing with clear nail polish. The slides were put in dark for 30 minutes. The slides were analysed using a Leica confocal laser scanning microscope with the respective software (Leica).

2.24 Flow cytometry

For stem cell markers, anti-CD44 (APC) and anti-CD24 (PE), both from BD Biosciences (San Jose, CA, USA), were used essentially as described [333] . Briefly, 1 x 10^6 cells were resuspended in 100 µl FACS buffer and anti-CD44 or anti-CD24 antibodies added and incubated for 30 min at 4°C. Isotype APC or PE-labelled antibodies (BD Biosciences, San Jose, CA, USA) were used as control. The tubes were then covered with aluminium foil as the antibodies are light sensitive. An Aldefluor assay kit (StemCell Technologies, Vancouver, Canada) was used for the determination of aldehyde dehydrogenase (ALDH) activity by flow cytometry essentially as described [333]. Briefly, cells were resuspended in assay buffer (10^6 cells/ml). Activated Aldefluor substrate (5 µl) was added to samples and incubated at 37 °C for 45 min to allow substrate conversion. As a negative control for all experiments, an aliquot of Aldefluor-stained cells was immediately quenched with 1.5-mM diethylaminobenzaldehyde (DEAB), a specific ALDH inhibitor.

2.25 Affymetrix whole transcriptome (WT) array

Affymetrix whole transcriptome (WT) array was performed using GeneChip® WT PLUS Reagent Kit (WT PLUS Kit, catalog no. 902280). At first, Total RNA was prepared from three independent biological replicates of empty-vector and EP300 transfected Hs578T cells using an RNeasy Kit (Qiagen, Crawley, UK). RNA integrity was evaluated using an Agilent 2100 Bioanalyzer (Agilent Technologies, Santa Clara, CA, USA). cDNA synthesis and further processing was performed using

GeneChip WT PLUS Reagent kit (Thermo Fisher Scientific, Whaltham, MA, USA). Hybridization to Clariom S arrays (Thermo Fisher Scientific, Whaltham, MA, USA) followed manufacturer's protocol. These procedures are described below in details.

a) Preparation of total RNA/Poly-A RNA control mixture

RNA extractions from Hs578T and Hs578T-EP300 were performed using RNeasy Mini Kit® from QIAGEN (Manchester, UK). Following assessment of RNA integrity (as measured from the RNA integrity number, RIN), three independent biological repeats for each cell type were used for microarray analysis. After preparing a control RNA sample, poly-A RNA controls were also prepared for 100 ng of total RNA according to the protocol. The quality of all RNA samples was determined by measuring the A260/A280 ratio (RNA of acceptable quality was considered in the range of 1.7 to 2.1) followed by evaluating the integrity of the RNA sample by microfluidic analysis using the Agilent 2100 Bioanalyzer (DE24802458, ver. 2.6) with an RNA LabChip® Kit or equivalent instrument. Finally, total RNA/Poly-A RNA Control Mixture were prepared for 100 ng of total RNA according to the protocol.

b) Synthesis of first and second -strand cDNA

Total RNA (100 ng), for each sample, was primed with primers containing a T7 promoter sequence. The reaction synthesizes single-stranded cDNA with T7 promoter sequence at the 5' end. First-strand cDNAs were prepared according to the protocol which were then converted to double-stranded cDNA that acts as a template for in vitro transcription. The reaction uses DNA polymerase and RNase H to simultaneously degrade the RNA and synthesize second-strand cDNA. Second strand cDNAs were prepared by following the protocol outlined in the UserGuide on GeneChip® WT PLUS Reagent Kit provided by Affymetrix.

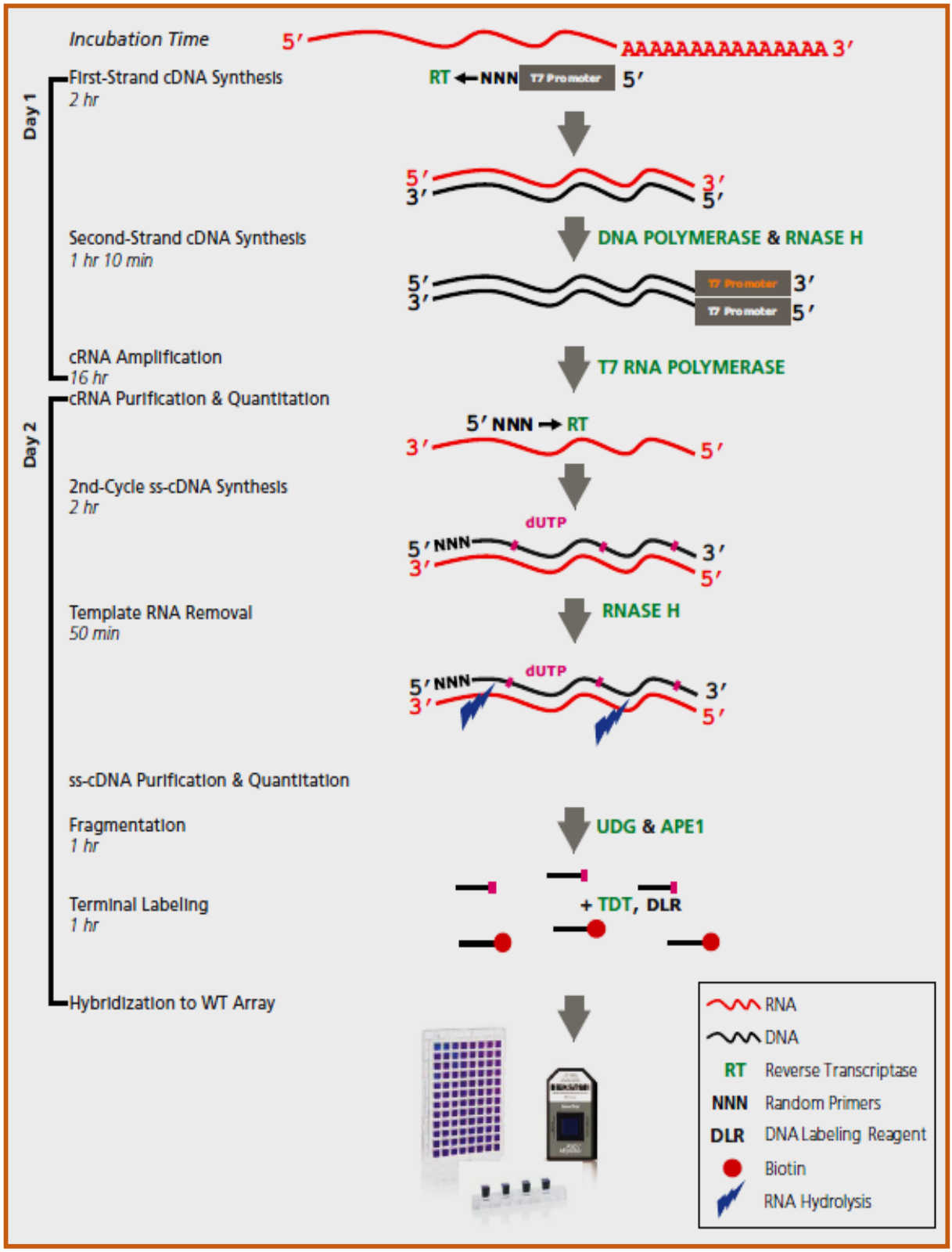


Figure 2.3 Schematic representation of WT Plus amplification and labelling processes (taken from UserGuide on GeneChip® WT PLUS Reagent Kit).

c) Synthesis and purification of cRNA by in vitro transcription

Antisense RNA (complimentary RNA or cRNA) was synthesized and amplified by in vitro transcription (IVT) of the second-stranded cDNA template using T7 RNA polymerase. In this step, all the cRNAs were prepared by following the stepwise protocol as outlined where all the reactions for cRNA preparation, including the preparation of the IVT master mix, were carried out at room temperature. Following synthesis, cRNAs were purified using the beads supplied and the concentration of a cRNAs were determined by measuring its absorbance at 260 nm using NanoDrop Spectrophotometer.

d) Synthesis and purification of 2nd-cycle single-stranded cDNA

In this procedure, sense-strand cDNA was synthesized by the reverse transcription of cRNA (anti-sense strand) using 2nd-Cycle Primers. The sense-strand cDNA contains dUTP at a fixed ratio relative to dTTP. 15 µg of cRNA is required for 2nd-cycle single-stranded cDNA synthesis. Next, the 2nd-Cycle ss-cDNA master mix was prepared (on ice) in a nuclease- free tube according to the protocol. Finally, 2nd-Cycle ss-cDNA master mix was added to 28 µL cRNA/2nd-Cycle primers samples, mixed thoroughly by gently vortexing the tube and incubated in a thermal cycler setting the program as mentioned in the protocol. Notably, RNase H was added to each 2nd-cycle ss-cDNA sample for hydrolysing the cRNA template in order to obtain single-stranded cDNA. After hydrolysis, the 2nd-cycle single-stranded cDNAs were purified to remove enzymes, salts, and unincorporated dNTPs according to the protocol. The yield of the purified 2nd-cycle single-stranded cDNAs were determined by measuring the absorbance of the ss-cDNA solutions (1.5 µL) at 260 nm.

e) Fragmentation and labelling of single-stranded cDNA

In this procedure, the purified, single-strand cDNA was fragmented by uracil-DNA glycosylase (UDG) and apurinic/apyrimidinic endonuclease 1 (APE 1) at the unnatural dUTP residues and thus breaking the DNA strand. The fragmented cDNA was labelled by terminal deoxynucleotidyl transferase (TdT) using the Affymetrix proprietary DNA Labelling Reagent that is covalently linked to biotin. Then, the fragmentation master mix was prepared by combining the components in a sequence as mentioned in the protocol. The fragmentation master mix was transferred to each of purified ss-cDNA sample which was then incubated in a

thermal cycler by following the program as prescribed in the protocol. A post-fragmentation analysis was then performed to confirm the size distribution of the fragmented ss-cDNA samples by using a Bioanalyzer. After confirming the ss-cDNA integrity, the labelling master mix was prepared on ice by combining the components mentioned in the protocol. The resulting mixture was then mixed thoroughly by gentle vertexing and incubated in a thermal cycler as per the program set in the protocol. The fragmented and labelled ss-cDNAs were then processed for WT array hybridization.

f) Microarray hybridization, washing, staining and scanning

After preparing the hybridization master mix and hybridization cocktail, the hybridization was performed according to the prescribed protocol. All the reactions for hybridizations were carried out using appropriate instruments as suggested in the protocol and using the facilities provided by the Genomics lab of Kings College London. All the subsequent washing, staining and scanning steps were performed by following the Affymetrix® GeneChip® Fluidics Station 450 User Guide AGCC (P/N 08-0295), the GeneChip® Expression Wash, Stain, and Scan User Guide for Cartridge Arrays (PN 702731), and the Affymetrix® GeneChip® Command Console® User Guide (P/N 702569).

2.26 Microarray data processing and analysis

Data were analysed with Robust Multichip Analysis (RMA) algorithm using default analysis settings and global scaling as a normalisation method by Dr Yunhui Hu. Values presented are log2 RMA signal intensity. RMA background correction (using RMA algorithm and filtering out the control probes), quantile normalization, log2 transformation, and probeset summarization were followed using Affymetrix Expression Console® Software (ver. 1.4.0.38). All the QC/QA analyses for signal intensity histogram, log probe cell intensity plot, and principle component analysis (PCA) were performed by using Partek Genomic Suits® (Partek, USA). Microarray data was deposited at the NCBI Gene Expression Omnibus (http://ncbi.nlm.nih.gov/geo/) under accession number **GSE116370**.

2.27 Pyrosequencing

The methylation status of well-characterized 21 cytosine residues in the *CDH1* gene promoter [334] was determined following bisulphite modification of DNA essentially as described [335] and performed by Ms Nahal Masrour. Briefly, genomic DNA was extracted from FFPE cancer samples using a QIAamp DNA FFPE Tissue Kit (Qiagen, Crawley, UK). Genomic DNA was bisulphite treated using EZ DNA Methylation kit (Zymo Research, Irvine, CA, USA) and PCR amplified with FastStart Taq DNA Polymerase (Roche, Basel, Switzerland) using annealing temperature of 58°C for *CDH1* and 53ºC for *LINE1* for 45 cycles. Primers were designed using PyroMark Assay Design 2.0 (Qiagen) to amplify 4 regions in the proximal *CDH1* promoter.

Primers were: Region 1 (Forward 5'-Biotin- TTTAGTAATTTTAGGTTAGAGGGTTA, Reverse 5'- TCACCTACCCACCACAACCAATCAACAA, Sequencing 5'-CAACAACCCCAACCCCTCCCCA), Region 2 (Forward 5'-ATTGGTTGTGGTAGGTAGGTGAATT, Reverse 5'-Biotin-AACTTCCCCAAACTCACAAATACTTTAC, Sequencing 5'-GTAGGTGAATTTTTAGTTAA), Region 3 (Forward 5'-GGAATTGTAAAGTATTTGTGAGTTTG, Reverse 5'-Biotin-AAAAACTACCACTCCAAAAACCCATA, Sequencing 5'-GTTTGAGGAAGTTAGTTTAGATTTT), Region 4 (Forward 5'- Biotin-TGTGAGTTTGAGGAAGTTAGTTTAGAT, Reverse 5'-AAAAACTACCACTCCAAAAACCCATAAC, Sequencing 5'-CAAAAACCCATAACTAACC).

LINE primers have been described [335]. The biotinylated strands of the amplicons were purified with streptavidin coated Sepharose beads (GE Healthcare, Chalfont St Giles, UK) and Vacuum Prep Tool (Qiagen, Crawley, UK) and subsequently annealed to the sequencing primer. Pyrosequencing was performed using PyroGold Reagent kit (Qiagen, Crawley, UK) with Pyromark Q96 MD instrument. The percentage methylation at individual CG sites was analysed using Pyro Q-CpG software (Qiagen, Crawley, UK). All runs contained an unmethylated DNA standard curve prepared with normal human female DNA (Promega, Madison, Wisconsin, USA) that was whole genome amplified (GE Healthcare Life Sciences, Little Chalfornt, UK). The methylated standard curve was prepared by diluting hypermethylated DNA (CpGenome Universal Methylated DNA, Millipore, Whatford,

UK) in the whole genome amplified DNA. Untreated normal female DNA was used as a control.

2.28 Statistical Analysis

GraphPad Prism was used for statistical analysis (version 5, San Diego, CA, USA), and two-tailed unpaired Student's t-test was used to compare the means between two variables. For comparisons between groups of more than two unpaired values, one-way analysis of variance (ANOVA) followed by post-hoc Dunnett's test was used. Two-way ANOVA was used between groups of 2 variables, and $*P < 0.05$, $**P < 0.01$, $***P < 0.001$ were considered as statistically significant. Chi-square statistical analysis were used to test the correlations between protein expression of breast cancer patients, respectively using SPSS 16.0 (Imperial College London, Software Shop, UK); $*p \leq 0.05$ and $**p \leq 0.01$ were considered as statistically significant and very significant, respectively. All results shown represent the average of three independent experiments unless otherwise stated, which were each performed in triplicate (presented as the mean ± SEM).

CHAPTER 3

EP300 and SIRT1/6 co-regulate lapatinib sensitivity via modulating FOXO3 acetylation and activity in breast cancer

3.1 Introduction

FOXO3 is one of the well-characterized members of the FOXO subclass of FOX (Forkhead Box) transcription factors that acts as a tumour suppressor and is often deregulated in various cancers, including glioblastoma, leukaemia, breast and prostate cancer [183]. FOXO3 plays a major role in suppressing tumour by restricting cell proliferation and promoting cell death. Besides, FOXO3 act as a core regulator of cellular homeostasis, stress response, and longevity since it can modulate a variety of stress responses upon nutrient shortage, hypoxia, heat shock, and DNA damage. Activated FOXO3 proteins bind to the conserved sequence motif GTAAA(C/T)A to induce transcription of their downstream target genes [76, 185].

The biological activity of FOXO3 is predominantly regulated by post-translational modifications (PTMs) in response to a wide range of environmental and intracellular stimuli including insulin, nutrients, and oxidative stress [226]. Moreover, PTMs of FOXO3 drive its shuttling between cytoplasm and nucleus, thereby determining its inactivation (cytoplasm) or activation (nucleus and mitochondria). Depending on the stress stimulus and subcellular localisation, activated FOXO3 can induce specific sets of nuclear genes, including cell cycle inhibitors, pro-apoptotic genes, autophagy effectors, and gluconeogenic enzymes. Phosphorylation, acetylation, methylation, ubiquitination and sumoylation are the major PTMs that are discovered till now. These modifications further control FOXO3 protein expression, subcellular localisation, DNA binding ability, transcriptional activity and the half-life of FOXO3 protein [226, 227]. Phosphorylation is the best-studied modification among all FOXO PTMs. FOXO3 becomes phosphorylated upon PI3K/AKT activation, and shuttled from the nucleus to the cytosol, leading to its functional inactivation. Thus, phosphorylation affects FOXO3 subcellular localization, leading to its association with the 14-3-3 scaffolding protein. In turn, this binding excludes FOXO3 from the nucleus, promoting its cytoplasmic accumulation and subsequent proteosomal degradation. Consequently, AKT-mediated FOXO3 phosphorylation inhibits FOXO3 transcriptional activity.

Protein acetylation is considered as another important PTM of FOXO3 but yet not well-studied. Acetylation is often regulated by the contrasting role of the acetyl-transferases [e.g. EP300 or CREB binding protein (CBP)] and the de-acetylases, such as sirtuins (SIRTs). CBP and EP300 are the close paralogs possessing histone acetyltransferase activity which modulate gene expression by inducing enzymatic catalysis of acetylation of the lysine residues. Contrarily, sirtuins catalyse deacetylation reactions of various histone and non-histone proteins which in turn regulate cellular metabolism and homeostasis. It has been reported that oxidative stress and the formation of reactive oxygen species (ROS) induce FOXO3 acetylation on lysine residues located within the DNA binding domain of the FOXO protein such as K242, K245, K259, K262 and K271 [232]. However, it is still under debate as to whether this modification causes an increase or a decrease in the affinity of FOXO3 for DNA [184, 228]. Furthermore, some other study reported that acetylation shifts target gene expression from cell cycle arrest to apoptosis and enhances the nuclear accumulation of FOXO proteins [194, 227]. Conversely, de-acetylation of FOXO3 by sirtuins stimulate expression of genes related with cell cycle arrest and cellular stress resistance, however, the effect of sirtuin on FOXO3 function varies depending on the target genes [204]. Therefore, the acetylation status of this transcription factor can potentially determine target gene specificity, DNA binding ability, stability and proteosomal degradation.

Lapatinib is a small molecule inhibitor administered to patients with metastatic breast cancer over-expressing the human epidermal growth factor receptor 1/2 (EGFR1/HER2*)* [244]. It acts as a dual tyrosine kinase inhibitor (TKI) that inhibits downstream signalling initiated by the epidermal growth factor (EGF) receptor (EGFR, also known as *HER1*) and HER2 [244, 245]. However, resistance to lapatinib often arises through various mechanisms, including increased drug efflux, enhanced pro-survival pathways and over-activation of PI3K/AKT signalling pathway [76].

To elucidate the association of FOXO3 expression and acetylation with lapatinib response, I aimed to better characterise the role of EP300 and nuclear sirtuins in FOXO3 acetylation on the anti-proliferative functions of FOXO3 in sensitive and drug resistant breast cancer cells. In this study, I used the *HER2* overexpressing breast cancer cell line, BT474, and a lapatinib resistant derivative (BT474 Lap^R) to investigate the functional outcome of FOXO3 acetylation as well as the role of FOXO3 acetylation in modulating lapatinib response.

3.2 Results

3.2.1 Lapatinib treatment increases FOXO3 acetylation and its activity in sensitive BT474 cells

To better characterise the role of EP300-mediated regulation of FOXO3 in mediating lapatinib response, I evaluated the effects of the dual tyrosine kinase inhibitor lapatinib on FOXO3 acetylation and activity in BT474 and BT474-Lap^R cells, a recently developed BT474 lapatinib-resistant derivative. Validation of lapatinib resistance are shown in appendix figure A3.1. Lapatinib activity was confirmed in both cells, since treatment with 1 μM lapatinib for 1 hour notably reduced EGFR phosphorylation without changing its expression (Figure 3.1A). Similar effects were observed with HER2 in BT474 cells, although HER2 expression was diminished in BT474-Lap^R cells, probably during the acquisition of resistance. Lapatinib was also found to inhibit AKT phosphorylation in BT474 cells, as AKT acts downstream from HER2, whereas it did not have any effect on resistant cells.

Lapatinib treatment also induced the expression of EP300 and FOXO3, an effect observed at both the mRNA and protein levels, and efficiently inhibited FOXO3 phosphorylation (T32), due to its inhibition of AKT, in BT474 cells, but not in BT474 Lap^R cells (Figure 3.1B, C). Importantly, both FOXO3 and p53 acetylation in BT474 cells followed similar trends as EP300 expression, indicating that they are good markers for EP300 acetyl-transferase activity [336]. As expected, there were no acetylation changes in BT474 Lap^R cells. Notably, high levels of acetylated FOXO3 after lapatinib treatment in BT474 cells positively correlated with the expression of its

downstream transcriptional target $p27^{Kip1}$ at both mRNA and protein levels (Figure 3.1B,C). Moreover, high levels of FOXM1 expression were found in resistant cells at both mRNA and protein levels (Figure 3.1B,C). To date, FOXM1 functions as an oncogene repressed by FOXO3 activity. It has also been reported that FOXM1 has significant role in inducing lapatinib resistance [337, 338]. Lower levels of EP300 and higher levels of the nuclear histone deacetylases, sirtuins (e.g. SIRT1 and SIRT6) were also detected in the BT474 Lap^R cells, which might also contribute to the reduced FOXO3 expression and activity in BT474 Lap^R cells, and therefore lapatinib resistance in HER2-positive breast cancer cells (Figure 3.1B). Thus, lapatinib induces EP300 expression and FOXO3 acetylation in BT474 cells.

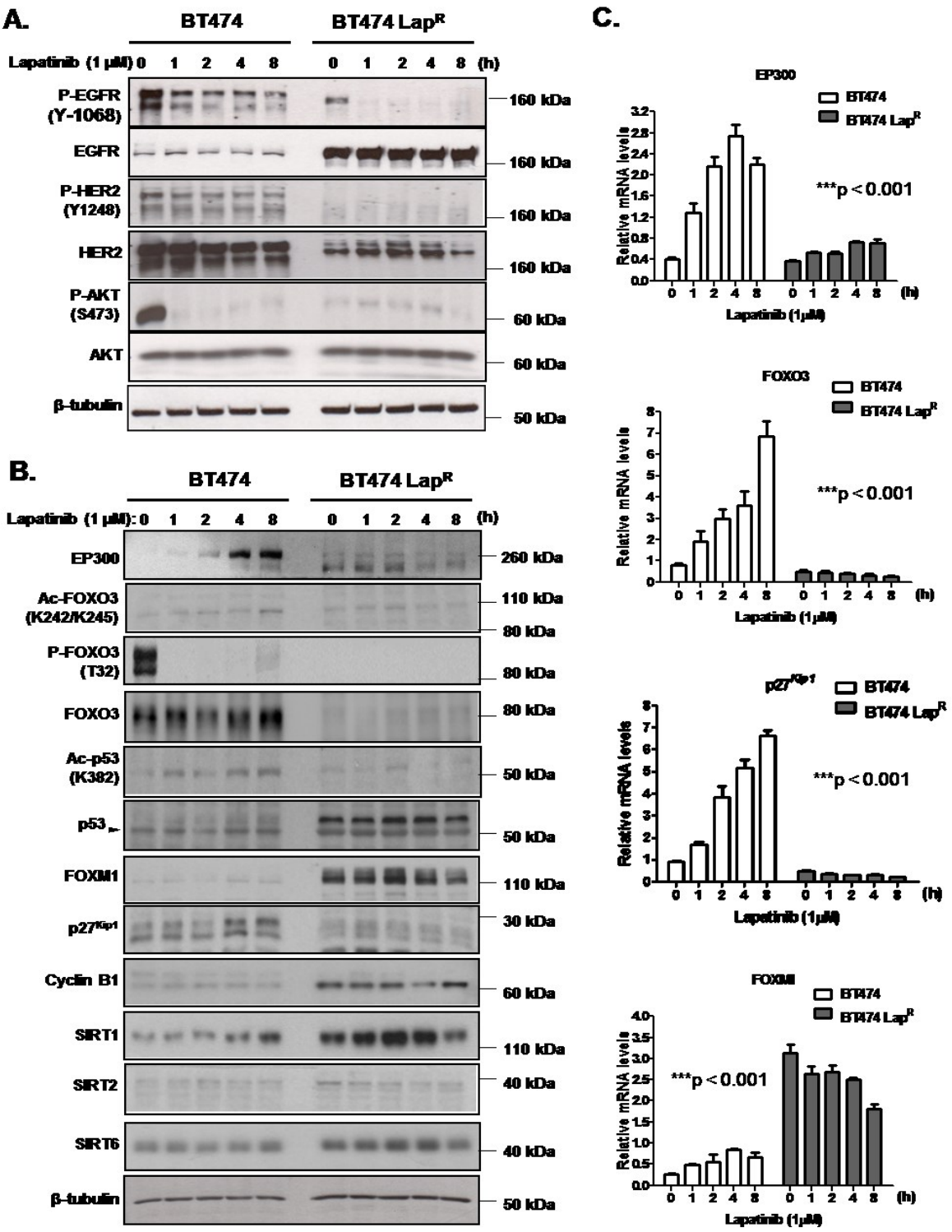


Figure 3.1 Lapatinib treatment increases acetylation of FOXO3 as well as its expression and transcriptional activity in BT474 sensitive cells but not in resistant cells. (A, B) The sensitive (BT474) and lapatinib resistant BT474 Lap^R cells were either left untreated or treated with 1 μM lapatinib for the mentioned time points. Protein lysates from whole-cell extracts were then analyzed by western blotting using the antibodies against the proteins indicated. **(C)** The mRNA levels of *EP300, FOXO3, p27^{kip1}* and *FOXM1* were assessed by real time RT qPCR. The RPL19 housekeeping gene was used as a control to normalise gene expression. The kinetics of *EP300, FOXO3, p27^{kip1}* and *FOXM1* mRNA expression were analyzed by two-way ANOVA and found to be significantly different between BT474 and BT474 Lap^R cells. Data are representative of at least 3 independent experiments. Data represent means ± SEM (***p < 0.001, for all mRNA species, respectively).

3.2.2 Lapatinib induces FOXO3 recruitment to its target gene promoters in sensitive but not in lapatinib-resistant cells

Previously our lab and others demonstrated that FOXO3 activates expression of downstream target genes which orchestrate a transcriptional programme leading to lapatinib sensitivity [75, 337-340]. Therefore, we aimed to determine whether FOXO3 is recruited to the promoters of its target genes in response to lapatinib treatment. To this end, we used chromatin immunoprecipitation (ChIP) to determine the recruitment of endogenous FOXO3 to its transcriptional targets *RICTOR*, *p27^{Kip1}*and *RAD51* [193, 233, 341]. FOXO3 displayed low binding to its target genes in untreated BT474 cells (Figure 3.2A), which increased upon lapatinib exposure. FOXO3 had the maximum binding at 4 hours post-lapatinib treatment, except for *RAD51* which was induced with faster kinetics 2 hours after drug treatment. In contrast, FOXO3 binding was very weak in untreated BT474-Lap^{R} cells and after lapatinib treatment. Collectively, these results suggest that lapatinib responses are mediated by FOXO3 binding and subsequent activation of its target genes in BT474 but not in lapatinib-resistant cells.

3.2.3 Triple *foxo1/3/4* knock-out mouse embryonic fibroblasts are resistant to lapatinib

Previous studies have shown that FOXO proteins are functionally redundant and can compensate for the loss of one another [342]. To ascertain the role of FOXO3 on lapatinib response, we studied the effects of lapatinib treatment on wild-type (WT) and *foxo1/3/4* $^{-/-}$ MEFs. Western blot analysis showed high levels of HER2 expression in *foxo1/3/4* $^{-/-}$ MEFs (Figure 3.2B), suggesting that they might be susceptible to the antiproliferative function of lapatinib. Interestingly, both EP300 and FOXO3 were practically absent upon *foxo1/3/4* knock-out and, as expected, the direct FOXO3 target p27^{Kip1} was down-regulated. As previously found in BT474 cells, when MEFs were treated with 1 μM lapatinib for 24 h, EP300 expression was up-regulated and FOXO3 phosphorylation (T32) decreased, with a corresponding increase in p27^{Kip1} levels. Contrary to BT474 cells, which have high levels of endogenous HER2, naive MEFs showed very low levels of HER2. Upon lapatinib treatment, HER2 levels increased notably. Next, we assessed how long-term cell

viability of triple *foxo1/3/4* knock-out MEFs was affected by lapatinib treatment using clonogenic assays. FOXO Knock-out MEFs cells formed more robust colonies in the absence of the drug, probably as an indication of their increased transformation and survival capacity, that were less susceptible to lapatinib treatment in the 1-5 μM range (Figure 3.2C). Thus, these results clearly suggest that triple *Foxo1/3/4* knock-out MEFs are more resistant to lapatinib compared to naïve MEFs.

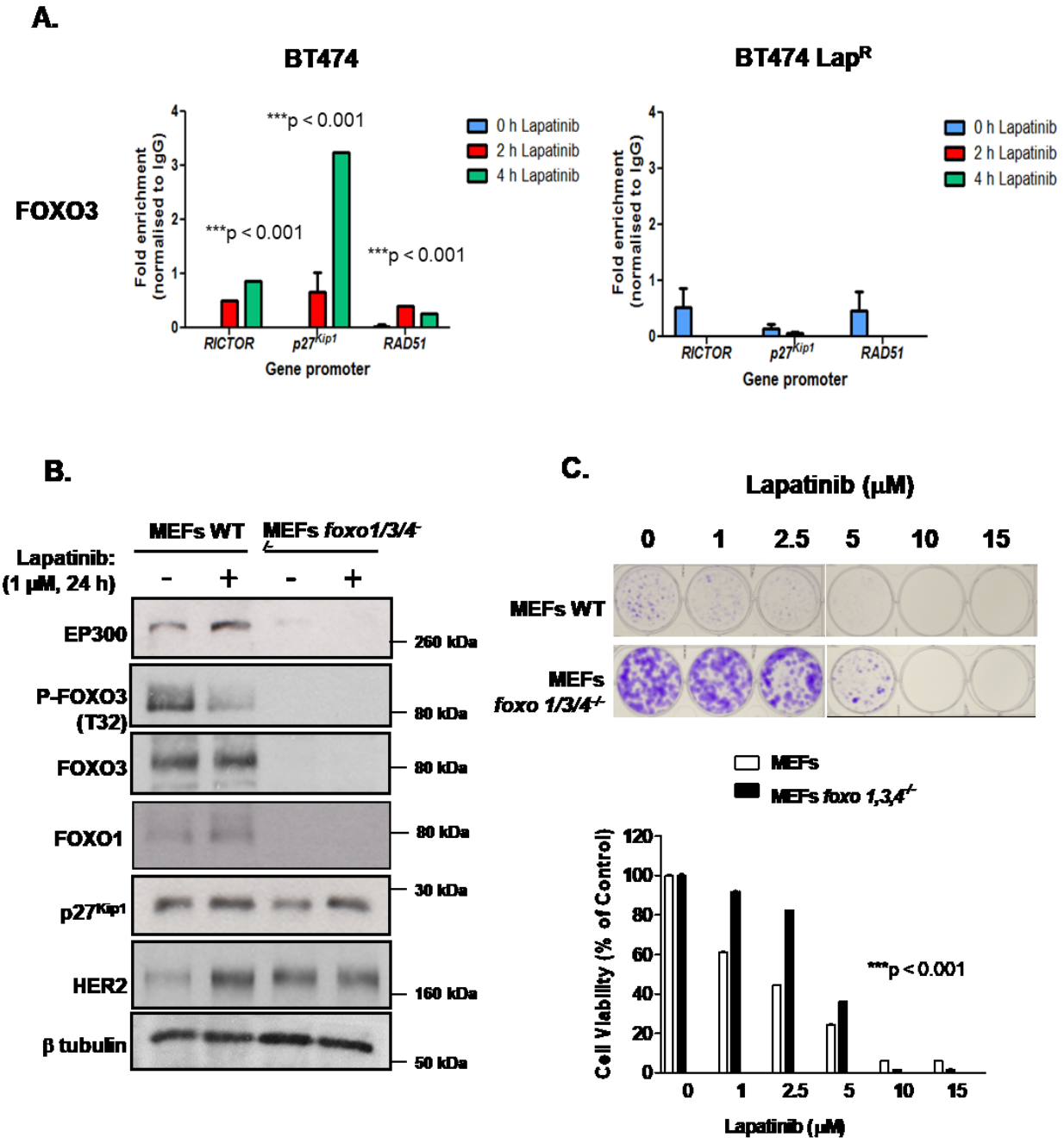


Figure 3.2 FOXO3 regulates lapatinib sensitivity in BT4T4 and MEFs A. Lapatinib induces FOXO3 recruitment to its target gene promoters in BT474 cells. Sensitive (WT) and drug resistant BT474 Lap^R cells were harvested following treatment with 1 μM lapatinib for 0, 2, or 4 hours. FOXO3 binding to the gene promoters of *RICTOR*, *p27^{Kip1}* and *RAD51* was then assessed by Chromatin

immunoprecipitation (ChIP) analysis using anti-FOXO3 antibody. After crosslink reversal, immunoprecipitated DNA was amplified by qPCR using primers for each gene promoter indicated. Data were analysed using the fold enrichment method and bars represent the means ± SEM of three independent experiments (n=3). The kinetics of FOXO3-binding were analyzed by two-way ANOVA and found to be significantly different between BT474 and BT474 Lap^R cells (***$p < 0.001$, for all genes, respectively). **B.** Western blot analysis was performed to analyse the protein levels of EP300, FOXO3, FOXM1 and others indicated in MEFs and *Foxo1,3,4*$^{-/-}$ MEFs. Representative western blots are shown. **C.** Wild-type MEFs and *Foxo1,3,4*$^{-/-}$ MEFs were treated with increasing doses of lapatinib and their sensitivity to lapatinib was assessed by clonogenic assay. Their clonogenicity in response to lapatinib was analyzed by two-way ANOVA and found to be significantly different (***$p < 0.001$) from one another.

3.2.4 FOXO3 plays a key role in regulating lapatinib sensitivity in BT474 Lap^R and triple *foxo1/3/4* knock-out MEFs

To further demonstrate that FOXO3 plays a key role in lapatinib response, we studied the effects of reintroduction of FOXO3 in the BT474-Lap^R (Figure 3.3) and the triple *foxo1/3/4* knock-out MEFs (Figure 3.4). Overexpression of wild-type (unphosphorylated) FOXO3 in these FOXO3-depleted cells had similar effects as treatment of the BT474 and WT MEFs with lapatinib, as FOXO3 is the target of lapatinib in the wild-type BT474 and MEFs. Specifically, overexpression of FOXO3 caused a loss of clonogenicity in both the BT474-Lap^R and the triple *foxo1/3/4* knock-out MEFs. Furthermore, increased lapatinib dosages caused additional decreases in clonogenicity, further supporting the idea that FOXO3 is a key target of lapatinib and downregulation of FOXO3 expression causes lapatinib resistance.

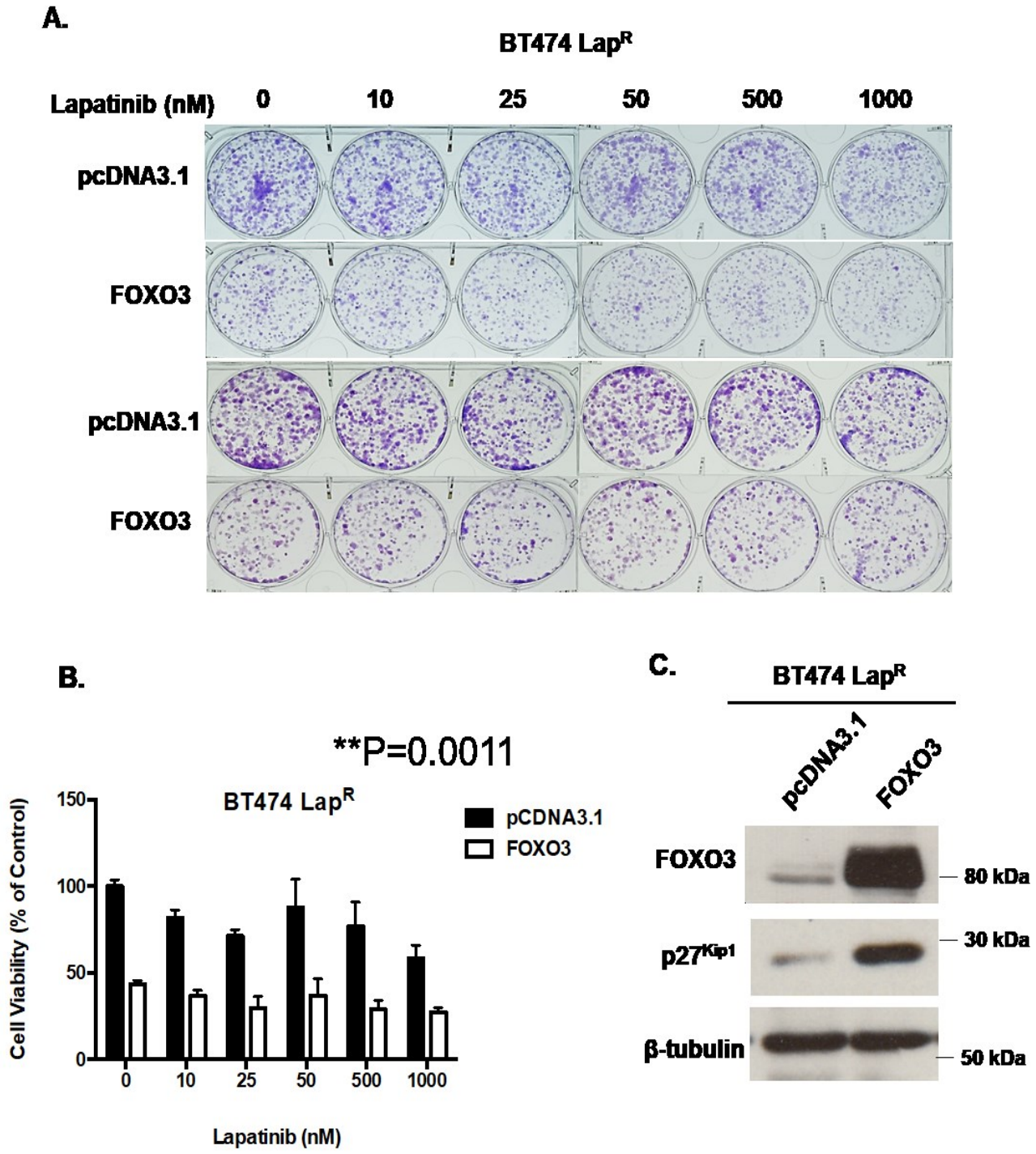


Figure 3.3 Overexpression of FOXO3 in BT474 Lap^R cells reduces cell viability. A. BT474 Lap^R cells were transiently transfected with the empty vector pcDNA3.1 and the plasmid encoding FOXO3. The transfected cells were then seeded in 6 well plates (1000 cells per well), allowed to grow overnight and then treated with the lapatinib concentrations indicated (0, 10, 25, 50, 500 and 1000 nM). Twenty-four hours following treatment the medium was changed and colony formation was allowed for 14 days. Cells were then fixed with 4% para formaldehyde and stained with crystal violet. **B**. The stain was solubilised with 33% acetic acid and absorbance obtained at 592 nm. Bars represent the mean ± SEM of three independent transfection experiments (n=3, R=3) and statistical analysis was performed using two-way ANOVA analysis (*p<0.05, **p<0.01, ***p<0.001). **C.** Western blot analysis demonstrated FOXO3 overexpression.

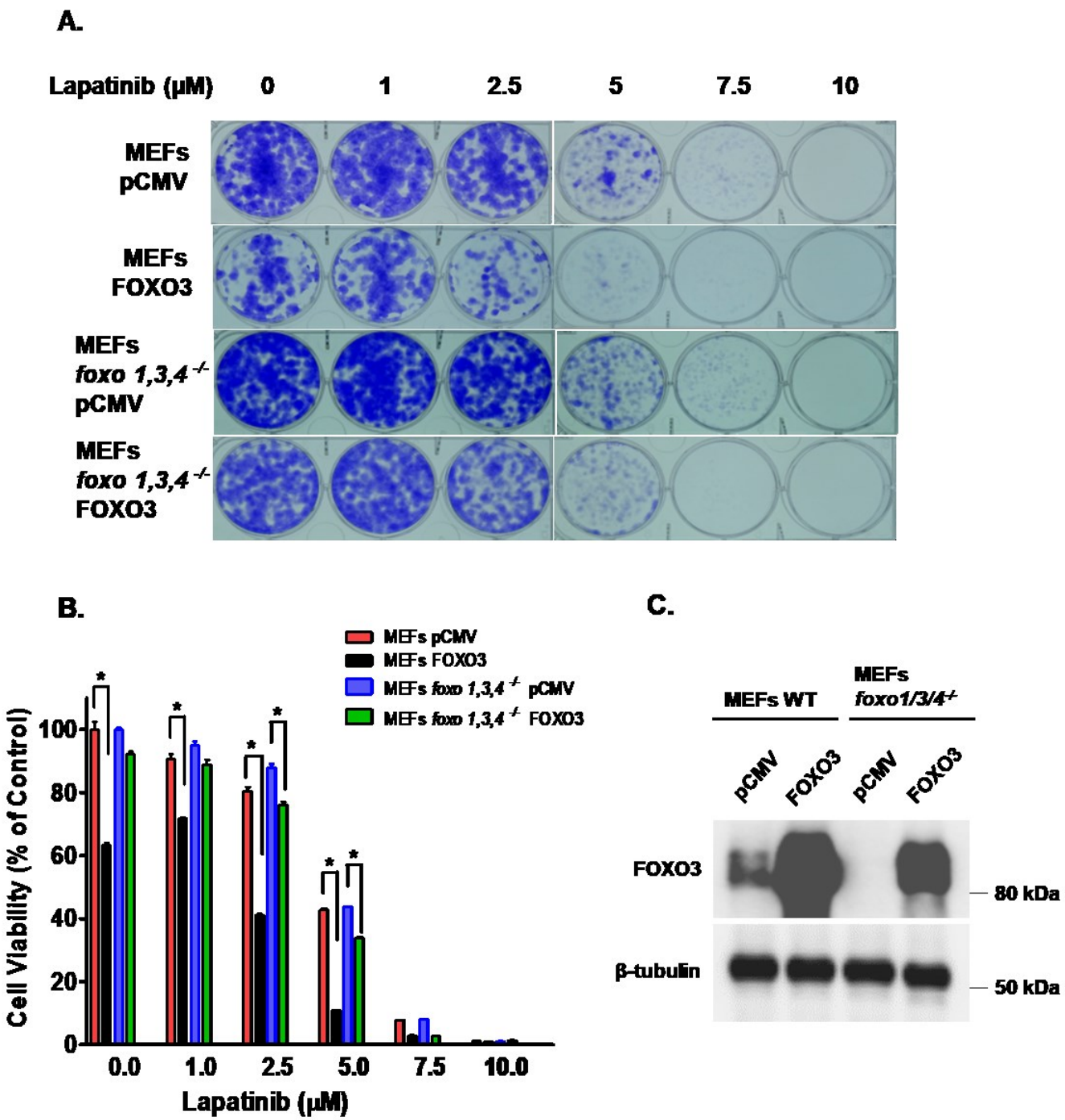


Figure 3.4. Overexpression of FOXO3 in MEFs cells inhibits cell growth. A. Wild-type MEFs and *Foxo1,3,4*$^{-/-}$ MEFs cells were transiently transfected with the empty vector pCMV and the plasmid encoding FOXO3. The transfected cells were then seeded in 6 well plates (1000 cells per well), allowed to grow overnight and then treated with the lapatinib concentrations indicated. Twenty-four hours following treatment the medium was changed and colony formation was allowed for 14 days. Cells were then fixed with 4% para formaldehyde and stained with crystal violet. **B.** The stain was solubilised with 33% acetic acid and absorbance obtained at 592 nm. Bars represent the mean ± SEM of three independent transfection experiments (n=3, R=3) and statistical analysis was performed using two-way ANOVA analysis (*p<0.05). **C.** Western blot analysis demonstrated FOXO3 overexpression.

3.2.5 EP300-FOXO3 interaction is induced by lapatinib treatment in BT474 cells

To investigate the interaction between FOXO3 and EP300, a duolink proximity ligation assay (PLA) was performed. Lapatinib treatment induced EP300-FOXO3 interaction in a time-dependent manner in BT474 cells as more red specks were observed, both in the nucleus and the perinuclear region, after 4h and more intensely at 8h treatment (Figure 3.5). On the other hand, no interaction was observed in BT474-Lap^R cells. This finding suggests that lapatinib treatment induces the interaction between FOXO3 and EP300 and provides a possible indication of enhanced FOXO3 acetylation in lapatinib sensitive BT474 cells.

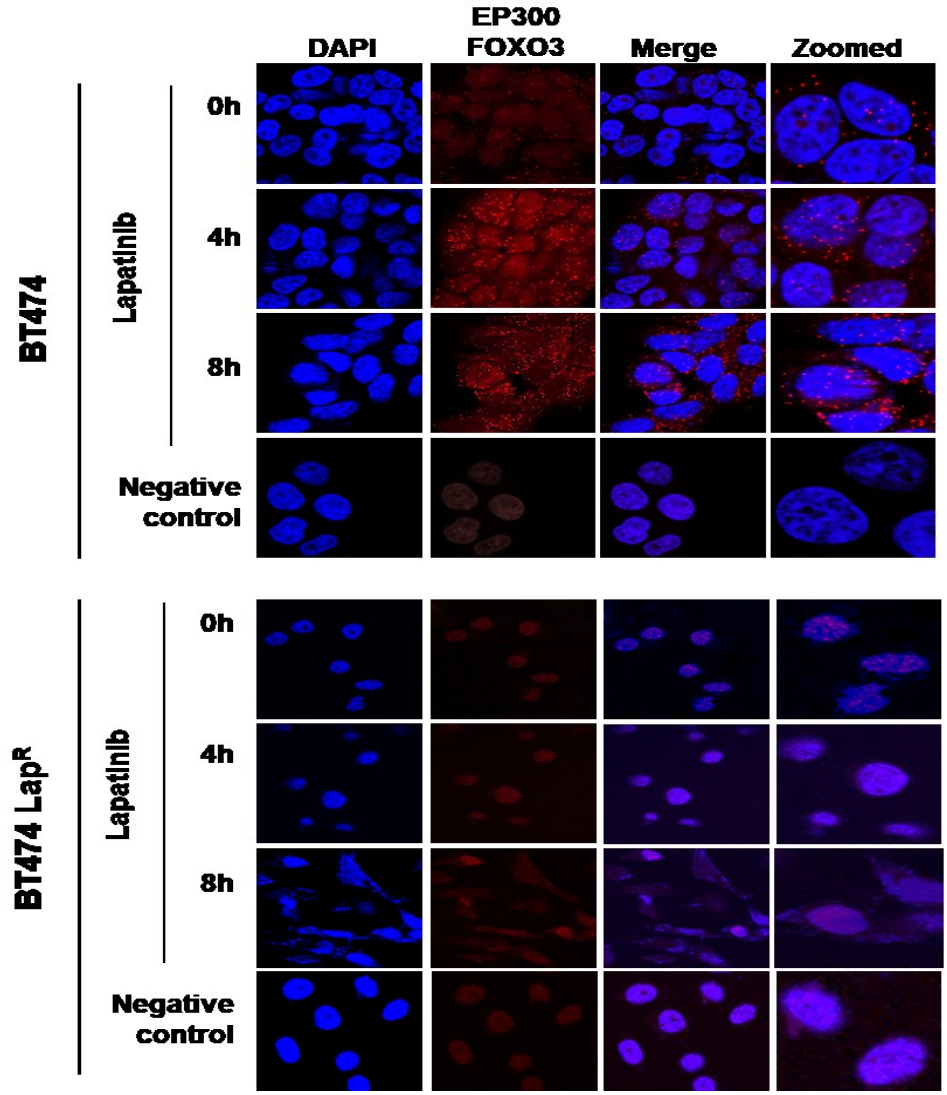


Figure 3.5 Duolink proximity ligation assay (PLA) for detecting the protein-protein interactions between EP300 and FOXO3 in BT474 and BT474 Lap^R cells. BT474 and BT474 Lap^R cells were treated with 1 μM lapatinib for 0, 4, and 8 hours. Cells without EP300 and FOXO3 antibodies were used as negative control. Cells were visualized with a Leica TCS SP5 confocal microscope equipped with a 63X oil immersion objective and LAS-AF software. Each red spot represents a single interaction and DNA was stained with 4, 6-diamidino-2-phenyl indole (DAPI) in blue. Representative confocal images are shown from three independent experiments.

3.2.6 EP300 acetylates FOXO3 and induces lapatinib sensitivity

To further investigate the role of EP300-mediated acetylation of FOXO3 upon lapatinib treatment, we used an acetyl-transferase-defective mutant (HAT mutation at H1415A, E1423A, Y1424A, L1428S, Y1430A, and H1434A) to transiently transfect BT474 and BT474-Lap^R cells. Western blot and RT qPCR analysis indicated that upon transfection of wild-type EP300 in BT474 cells there was an upregulation of FOXO3 expression, while the upregulation of FOXO3 was comparatively weaker upon transfection of the EP300 HAT mutant (Figure 3.6A, B). However, this EP300-dependent FOXO3 up-regulation did not occur in BT474-Lap^R cells suggesting the deregulation of EP300-FOXO3 cascade in resistant cells. As expected, acetylation of FOXO3 (K242/245) and histone 3 (K27) were induced upon wild-type EP300 transfection in BT474 cells, but this induction was comparatively weaker upon transfection of the HAT mutant. No changes in FOXO3 or histone 3 acetylation were observed in BT474-Lap^R cells. These data were further confirmed by co-immunoprecipitation experiments in BT474 cells (Figure 3.7A, C). The FOXO3-EP300 interaction that we had previously detected by PLA (Figure 3.5) was reconfirmed when pulling-down using either FOXO3 (Figure 3.7A) or EP300 (Figure 3.7B) antibodies, as the intensity of the EP300 and FOXO3 bands, respectively, upon transfection of wild-type EP300 were stronger than with the HAT mutant. As expected, FOXO3 acetylation (K242/245) increased upon transfection with the wild-type, but not with the EP300 HAT mutant (FOXO3 pull-down and acetylated FOXO3 detection; Figure 3.7A). Similarly, when reverse co-immunoprecipitation was used to pull-down proteins with acetylated lysines, acetylated FOXO3 (K242/245) was clearly detectable upon transfection with FOXO3 and wild-type EP300, but not with the EP300 HAT mutant (Figure 3.7C). Consistently, ectopic expression of wild-type EP300 induced the expression of downstream FOXO3 target genes Bim, p27^{Kip1}, p130 and p16^{INK4a} in BT474 but not in BT474-Lap^R cells (Figure 3.6A, B). Importantly, up-regulation of FOXO3 target genes did not occur upon transfection of the EP300 HAT mutant. This further confirms the positive regulatory role of EP300-mediated acetylation on FOXO3 transcriptional activity.

Since EP300 overexpression can induce FOXO3 activity and its downstream antiproliferative targets in parental, but not the BT474-Lap^R resistant cells, we next

performed sulphorhodamine B (SRB) assays to assess lapatinib sensitivity upon EP300 transfection. Over-expression of wild-type EP300, but not the acetyl-transferase deficient HAT EP300 mutant, increased lapatinib sensitivity in BT474 cells (Figure 3.7D, upper panel). Notably, ectopic expression of EP300 HAT mutant led to a slight but not significant increase in cell viability in sensitive BT474 cells upon lapatinib treatment, suggesting that the acetyl-transferase deficient EP300 mutant can titre the normal acetyl-transferase activity, as previously described for truncated mutants of EP300 [160]. On the contrary, EP300 over-expression in BT474-Lap^R cells did not result in any significant effect on lapatinib response until lapatinib reached 2 μM concentration (Figure 3.7D, lower panel; Appendix Figure A3.2) and this could be due to the high levels of deacetylases (e.g. SIRTs) expression in resistant cells. Almost similar results were also observed for the lapatinib sensitive and resistant SKBR3 and SKBR3-Lap^R breast cancer cell lines (Appendix Figure A3.4 and A3.5). In summary, these data further confirm EP300 mediated FOXO3 acetylation in lapatinib sensitive BT474 cells and that EP300 induced FOXO3 acetylation leads to an increase in lapatinib sensitivity.

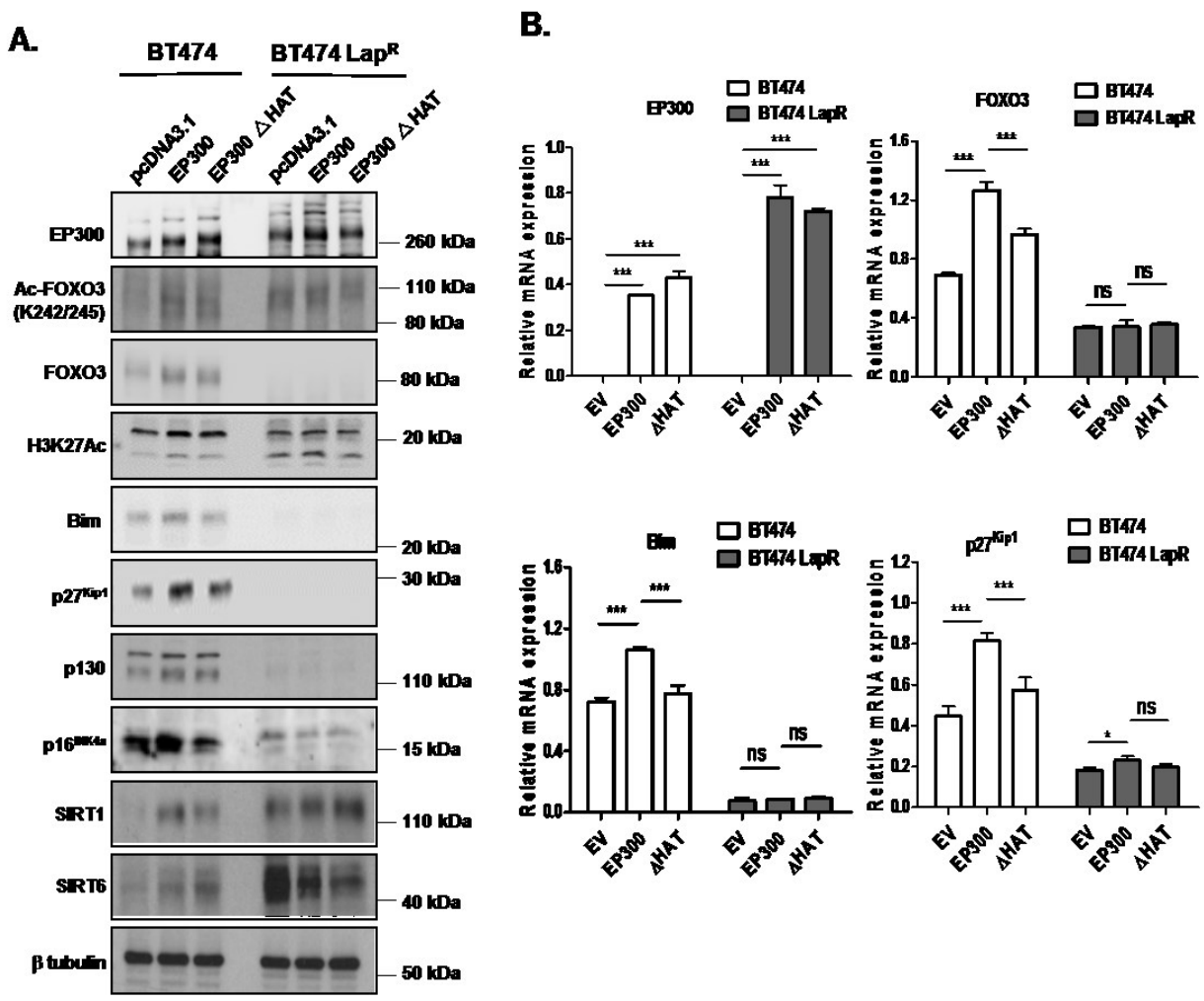


Figure 3.6 EP300 overexpression upregulates FOXO3 acetylation and its transcriptional activity. A. BT474 and BT474-Lap^R cells were transiently transfected with the empty vector pcDNA3.1, the plasmid encoding wild-type EP300, or the one encoding for its acetyl-transferase mutant derivative (EP300 △HAT). Proteins were obtained from whole cell extracts after 24 hours following transfection. Western blotting was performed using the protein lysates to assess the expression levels of EP300, FOXO3 and other indicated proteins. **B.** The mRNA levels of *EP300, FOXO3,* Bim and *p27^{kip1}* were assessed by real time RT qPCR. The kinetics of mRNA expressions were analyzed by one-way ANOVA. Data are representative of at least 3 independent experiments. Data represent means ± SEM (***p < 0.001, **p < 0.01, *p < 0.05, ns=non-significant).

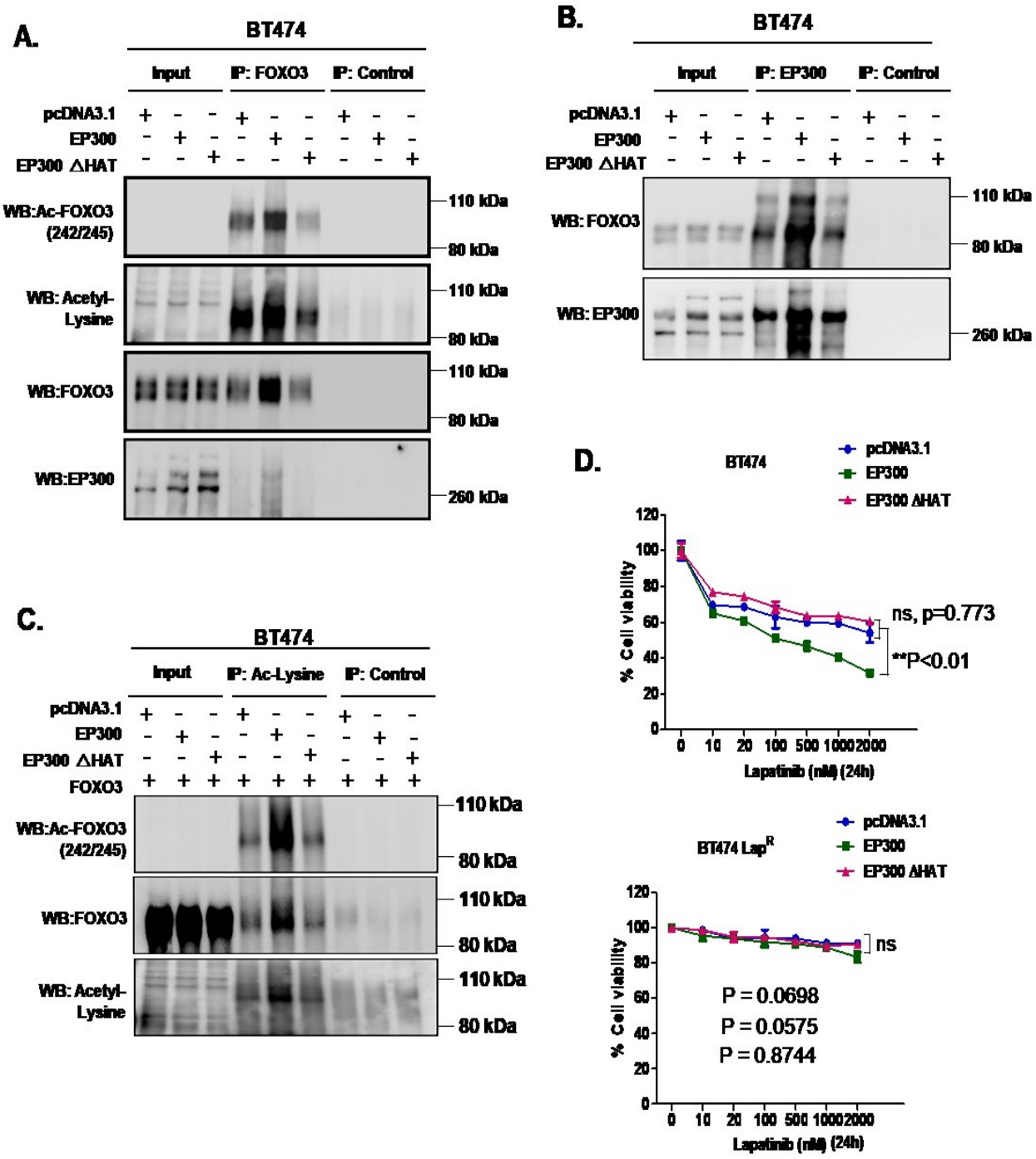


Figure 3.7 EP300 overexpression upregulates FOXO3 acetylation and increases lapatinib sensitivity. A, B. Protein lysates of BT474 cells transiently transfected with EP300 or EP300 △HAT obtained were assessed by Co-immunoprecipitation (Co-IP) with an anti-FOXO3 antibody (A) and anti-EP300 antibody (B). Subsequent immunoblotting was performed using antibodies against Ac-Lys, Ac-FOXO3 FOXO3 and EP300. The anti-IgG was used as a negative control. **C.** Reverse-Co-IP was performed with anti-Acetyl Lysine antibody using the protein lysates of BT474 cells transiently transfected with EP300 and FOXO3 or EP300 △HAT and FOXO3. Subsequent immunoblotting was performed using antibodies against Ac-Lys, Ac-FOXO3 and FOXO3. The anti-IgG was used as a negative control. **D.** Transiently transfected BT474 WT and Lap^R cells were seeded in 96-well plates and treated with lapatinib at a range of concentrations from 10 to 2000 nM. Twenty-four hours after treatment, cells were fixed and stained with the protein-binding dye SRB. Values obtained were normalized against the corresponding untreated controls and presented as percentages. Data represent means ± SEM (2-way ANOVA; non-significant, ns; significant, **P<0.01).

3.2.7 EP300 regulates long-term lapatinib sensitivity in wild-type BT474 but not in BT474-Lap^R cells

Changes in short-term drug sensitivity may lead to long-term proliferation properties important in cancer treatment. In order to ascertain whether the short-term data shown above had any effect on the long-term lapatinib viability of BT474 cells, we performed clonogenic assays 24 h after EP300 transfection. Indeed, EP300 overexpressing BT474 cells showed increased lapatinib sensitivity when compared with control cells transfected with the empty vector or the acetyl-transferase defective mutant (Figure 3.8A; upper panel and appendix figure A3.3). These results suggest that EP300-mediated acetylation has a role in lapatinib-mediated cytotoxicity in sensitive BT474 cells. It is also noteworthy that the resistant cells over-expressing EP300 had lower clonogenicity compared to the control cells, suggesting that EP300 is involved in long-term cell viability and self-renewal properties of resistant cancer cells, but does not affect drug sensitivity in BT474-Lap^R cell lines (Figure 3.8A; lower panel and appendix figure A3.3). To examine further the role of EP300 in lapatinib sensitivity, siRNA-mediated knockdown of EP300 was performed in BT474 cells. The results showed a significant elevation of long-term cell viability and clonogenic cell forming ability around 50 nM of lapatinib treatment after silencing EP300 (Figure 3.8B). Thus, both overexpression and knock-down approach followed by clonogenic assays suggest that acetylation of FOXO3 by EP300 leads to long-term sensitivity to lapatinib. The fact that overexpression of EP300 has no significant effect on FOXO3 acetylation and lapatinib-sensitivity of BT474-Lap^R cells also suggests that FOXO3 acetylation is modulated by other regulators, including the deacetylases, SIRTs (Sirtuins).

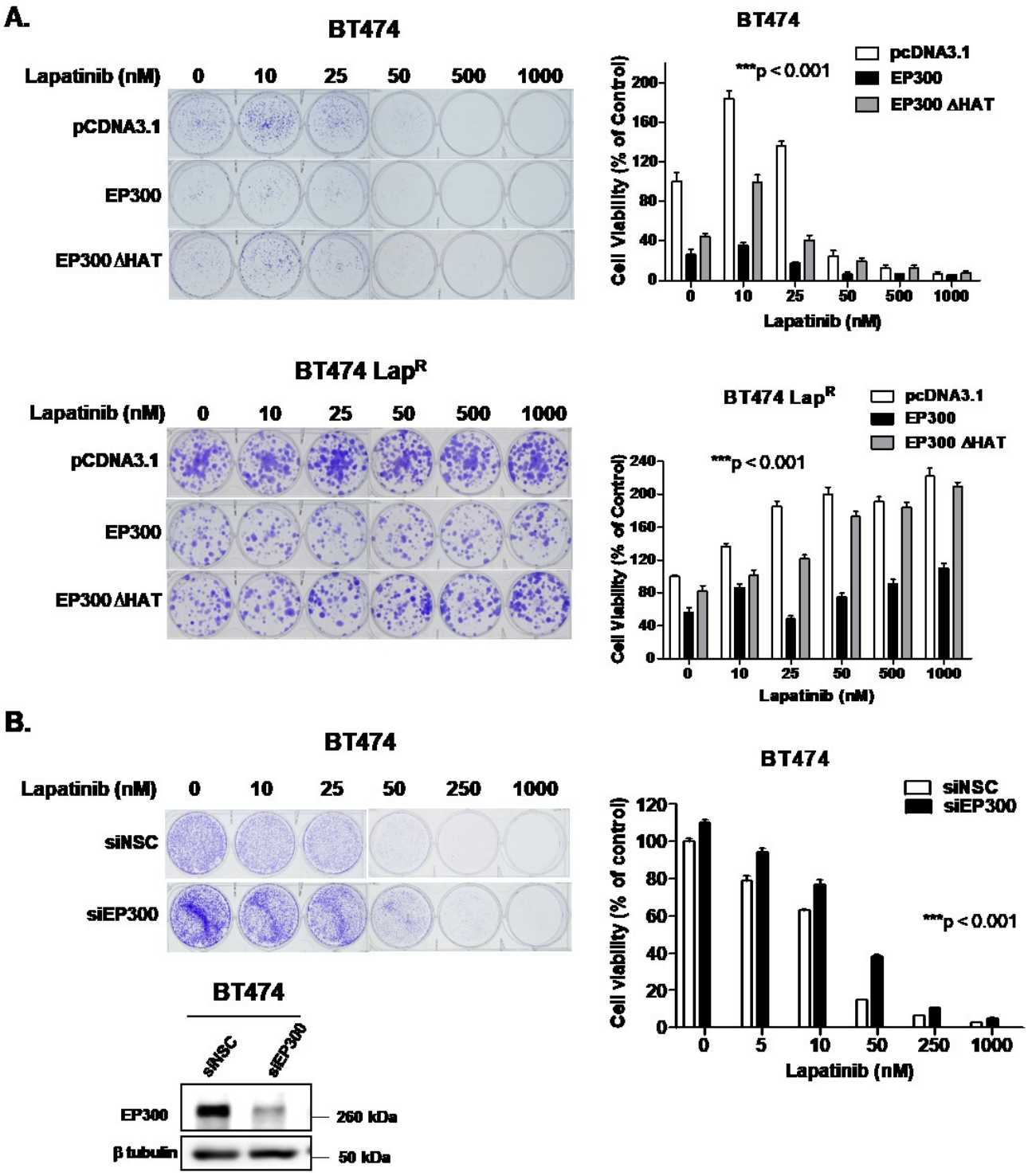


Figure 3.8. EP300 expression correlates with increased long-term lapatinib cytotoxicity in sensitive but not BT474 Lap^R cells. A. BT474 and lapatinib resistant BT474 Lap^R cells were seeded 2,000 and 1000 cells per well, respectively, in 6-well plates and transfected with the empty vector pcDNA3.1, wild-type EP300, or EP300 △HAT mutant expressing vector. The transfected cells were then allowed to grow overnight and then treated with the lapatinib concentrations indicated (0, 10, 25, 50, 500 and 1000 nM). Twenty-four hours following treatment the medium was changed and colony formation was allowed for 28 and 14 days in sensitive and resistant BT474 cells, respectively. Cells were then fixed with 4% para formaldehyde and stained with crystal violet. The stain was solubilised with 33% acetic acid and absorbance obtained at 592 nm. Data were normalised to the respective untreated empty-vector transfected cells. Bars represent the mean ± SEM of two independent transfection experiments and statistical analysis was performed using two-way ANOVA analysis

(***p<0.001) comparing the EP300, EP300 △HAT **B.** BT474 cells were seeded 2,000 cells per well and transfected with non-targeting control (siNSC) or EP300-targeting siRNA pools. The transfected cells were then allowed to grow overnight and then treated with the lapatinib concentrations indicated (0, 10, 25, 50, 250, and 1000 nM). Western blot analysis demonstrated EP300 depletion (lower panel). Twenty-four hours following treatment the medium was changed and colony formation was allowed for 14 days. Cells were then fixed with 4% para formaldehyde and stained with crystal violet. The stain was solubilised with 33% acetic acid and absorbance obtained at 592 nm. Data were normalised to the respective untreated siNSC transfected cells. Bars represent the mean ± SEM of three independent transfection experiments and statistical analysis was performed using two-way ANOVA analysis (***p<0.001)

3.2.8 SIRT1 and SIRT6 regulate the acetylation status, expression and activity of FOXO3 in MEFs

To investigate the mechanisms underlying FOXO3 acetylation and the associated role of SIRT1 and SIRT6, we first used wild type (WT) and knockout (SIRT1 and SIRT6) mouse embryonic fibroblasts (MEFs) cells. Whole cell extracts from MEFs were subjected to analysis by western blotting procedure. According to the results, acetylated FOXO3 levels increased in both SIRT1 and SIRT6 knockout MEFs compared to WT MEFs (Figure 3.9 A, B). Previously performed forward and reverse co-immunoprecipitation experiment from our lab (By Mattaka Khongkow) also confirmed the presence of high acetylation level of FOXO3 in *Sirt6*$^{-/-}$ MEFs (Figure 3.9C). The western blot data also shows that, phosphorylated FOXO3 level is negatively correlated with acetylated FOXO3 level in WT and knockout cells. Moreover, the elevated expression of FOXO3 found to reduce FOXM1 expression and also induce its downstream antiproliferative targets, p27^{Kip1} upon SIRT1 and SIRT6 depletion both at mRNA and protein levels (Figure 3.9 A, B, left and right panel) suggesting the effects of FOXO3 acetylation on its transcriptional activity. Collectively, these results suggest that SIRT1 and SIRT6 regulates FOXO3 expression and activity by modulating its acetylation status.

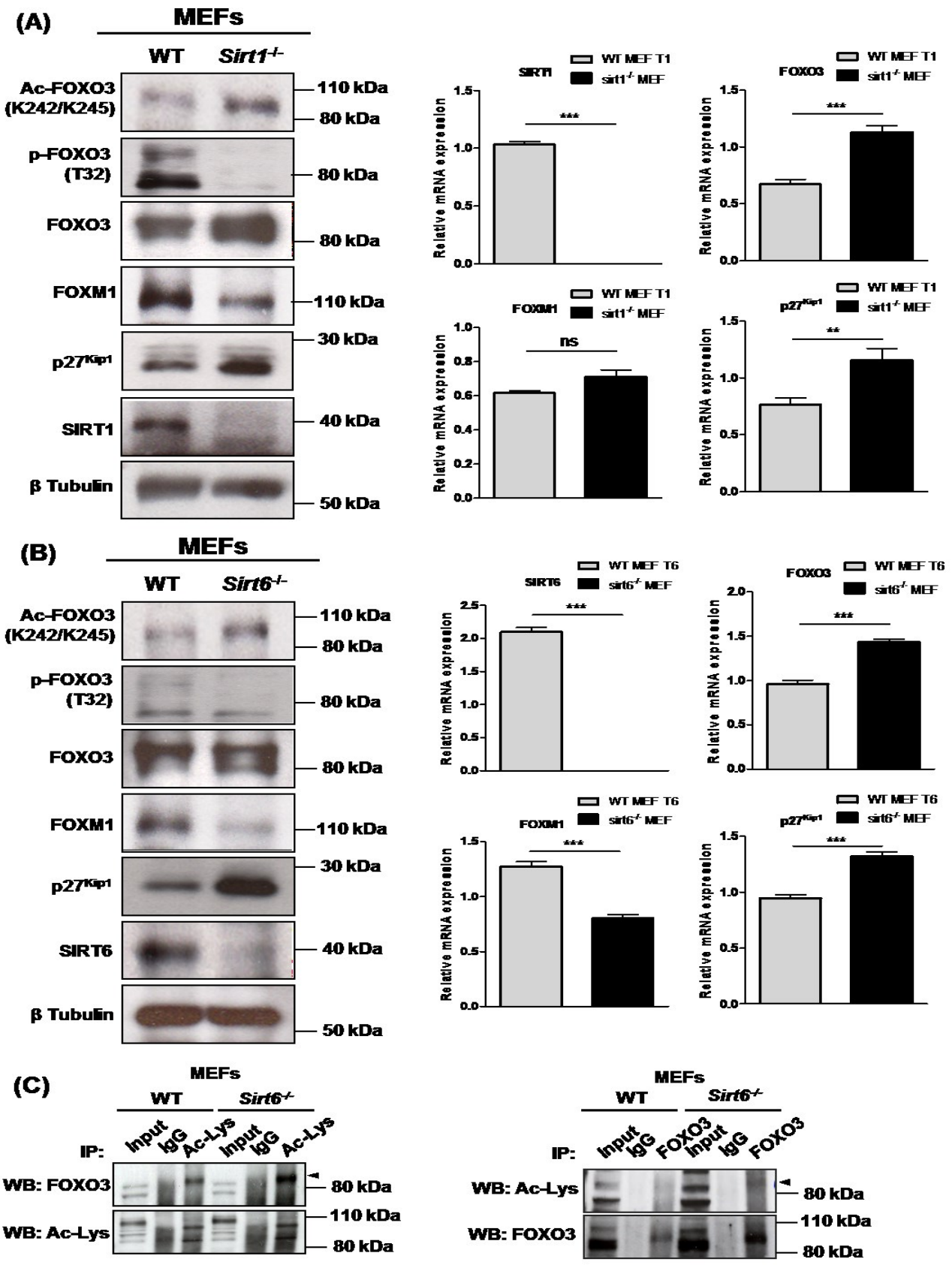


Figure 3.9 SIRT1 and SIRT6 regulate the acetylation status, expression levels and activity of FOXO3. A. Western blot analysis of Ac-FOXO3, FOXO3, FOXM1, SIRT1 and other indicated proteins in WT and Sirt1$^{-/-}$ MEFs (Left Panel). Tubulin was used as a control for protein loading. RT qPCR was

performed to check the mRNA levels of SIRT1, FOXO3, FOXM1 and $p27^{Kip1}$ (right panel). Statistical analysis was performed by student t-test and data represent Mean ± SEM from two independent experiments (***P<0.001, **P<0.01, *P<0.05, ns=nonsignificant). **B.** Western blot analysis of Ac-FOXO3, FOXO3, FOXM1, SIRT6 and other indicated proteins in WT and $Sirt6^{-/-}$ MEFs. RT qPCR was performed to check the mRNA levels of SIRT1, FOXO3, FOXM1 and $p27^{Kip1}$ (right panel). Statistical analysis was performed by student t-test and data represent Mean ± SEM from two independent experiments (***P<0.001, **P<0.01, *P<0.05, ns=nonsignificant). **C.** Protein lysates from WT and $Sirt6^{-/-}$ MEFs were subjected to co-immunoprecipitation with specific antibodies against acetylated lysine (Ac-Lys), FOXO3 or normal rabbit immunoglobulin G as a control (Performed by Mattaka Khongkow). The immunoprecipitates were then evaluated for the presence of the indicated proteins by western blot.

3.2.9 Lapatinib treatment increases acetylated FOXO3 levels as well as its activity in MEFs

In order to examine the effect of Lapatinib in the regulation of acetylation of FOXO3, both WT, *Sirt1* $^{-/-}$ MEFs and *Sirt6* $^{-/-}$ MEFs were treated with 1 μM Lapatinib and harvested at different time points of 0, 4, 8, 24, and 48 hours. As lapatinib acts as a tyrosine kinase inhibitor it was found that lapatinib is highly active at 48 hours of treatment in WT MEFs indicated by low level of P- AKT and P-FOXO3 levels (Figure 3.10A). However, lapatinib did not show its activity in knockout MEFs as almost consistent levels of P- AKT and P-FOXO3 were observed in *Sirt1* $^{-/-}$ MEFs (Figure 3.10A). On the other hand, for WT MEFs (T6) and *Sirt6* $^{-/-}$ MEFs lapatinib activity was observed in a time course manner from 4 hours to 48 hours of treatment as indicated by reduced level of P- AKT and P-FOXO3 in both WT and SIRT6 knockout MEFs (Figure 3.11A). Moreover, it was shown by western blotting that the time dependent Lapatinib treatment increases the acetylated FOXO3 level in both WT MEFs and SIRT1/SIRT6 knockout MEFs although the elevation of FOXO3 acetylation level upon lapatinib treatment is higher in SIRT1/SIRT6 knockout MEFs (Figure 3.10A, Figure 3.11A). In addition, higher FOXO3 acetylation was found to be positively correlated with higher FOXO3 expression both at protein and mRNA levels (Figure 3.10 A, B, Figure 3.11 A, B). Notably, acetylation of FOXO3 upon lapatinib treatment also induces its downstream transcriptional target genes Bim, $p27^{Kip1}$, $p16^{INK4a}$ and p130 both at mRNA and protein levels (Figure 3.10 A, B). The data also reveals that high level of acetylated FOXO3 is positively correlated with lapatinib induced increase of EP300 levels in WT and SIRT1/SIRT6 knockout cells. Therefore, all the results suggest that SIRT1 and SIRT6 play a key role in regulating EP300 mediated FOXO3 acetylation as well as its transcriptional activity upon lapatinib response in MEFs cells.

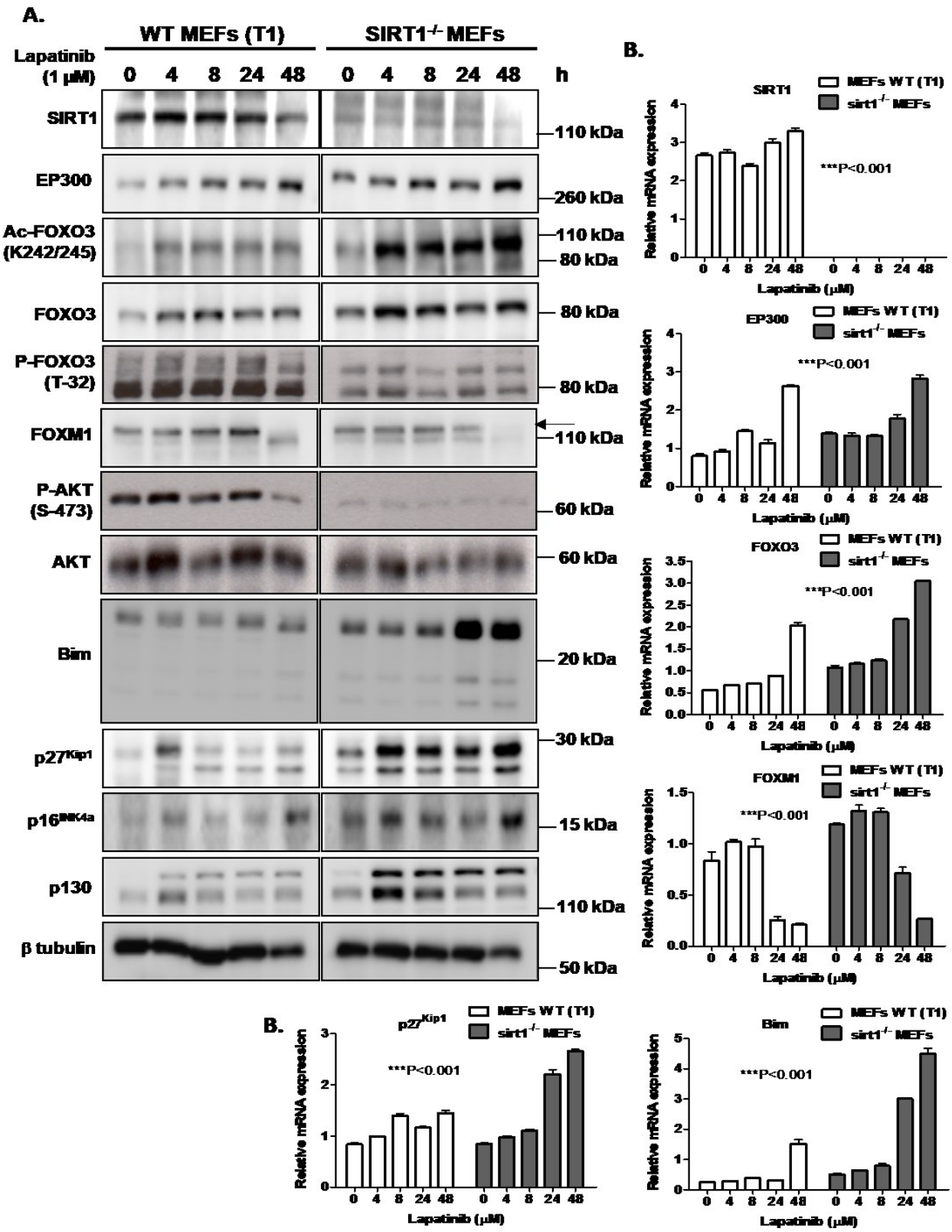


Figure 3.10 Assessment of the role of SIRT1 in regulating acetylation of FOXO3 upon lapatinib treatment. A. WT and Sirt1$^{-/-}$ MEFs were treated with 1 μM lapatinib for the times indicated and harvested for Western Blot analysis. Tubulin was used as a control for protein loading. **B.** RT qPCR was performed to check the mRNA levels of indicated genes. Statistical analysis was performed by two-way ANOVA and data represents Mean ± SEM from two independent experiments (***P<0.001, **P<0.01, *P<0.05, ns=nonsignificant).

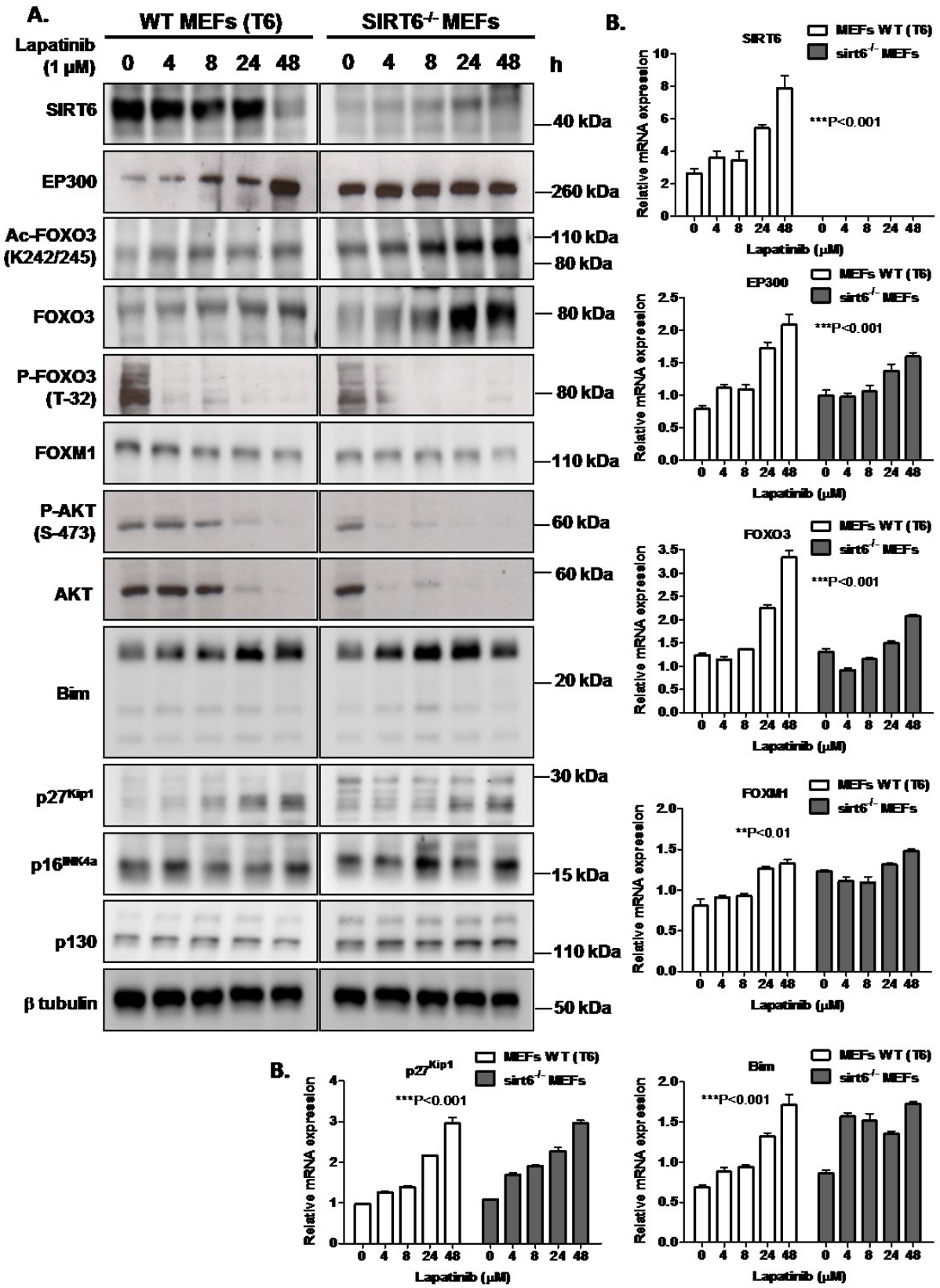


Figure 3.11 Assessment of the role of SIRT6 in regulating acetylation of FOXO3 upon lapatinib treatment. A. WT and Sirt6$^{-/-}$ MEFs were treated with 1 μM lapatinib for the times indicated and harvested for Western Blot analysis. Tubulin was used as a control for protein loading. **B.** RT qPCR was performed to check the mRNA levels of indicated genes. Statistical analysis was performed by two-way ANOVA and data represents Mean ± SEM from two independent experiments (***P<0.001, **P<0.01, *P<0.05, ns=nonsignificant).

3.2.10 Silencing of SIRT1 and SIRT6 correlates with increased FOXO3 acetylation and its transcriptional activity in HER2 overexpressed breast cancer

To further investigate the mechanisms regulating FOXO3 acetylation we determined how knocking-down deacetylases SIRT1 and SIRT6 affected FOXO3 activation following lapatinib treatment. The levels of acetylated FOXO3 increased after knocking down of SIRT1 and SIRT6, which in turn activated FOXO3 downstream anti-proliferative target gene expression such as $p27^{Kip1}$ and Bim both at mRNA and protein level in BT474 cells (Figure 3.12A, B, 3.13A, B). Moreover, the expression of FOXO3, $p27^{Kip1}$ and Bim were found to be also increased after lapatinib treatment upon sirtuin-depletion (Figure 3.12A, B, 3.13A, B). Notably, upregulation of FOXO3 was found to be positively correlated with p53 acetylation and tumour suppressive p53 (Tp53) expression (Figure 3.12A, B, 3.13A, B). In addition, western blotting and RT qPCR data revealed that EP300 expression was up-regulated upon SIRT1 or SIRT6 knock-down, which further increased in cells treated with 1 μM lapatinib for 8 h. The increased acetylation of FOXO3 upon lapatinib treatment and SIRT1 or SIRT6 knockdown was also confirmed by co-immunoprecipitation experiments as FOXO3 or acetyl-Lys antibodies pulled down more complexes, detected with both total FOXO3 and acetylated FOXO3 (K242/245) antibodies, upon sirtuin RNA interference (Figure 3.14A, B).

The acetylation status of FOXO3 after knocking down of SIRT1 and SIRT6 was further examined in a more sensitive and efficient way by Duolink PLA using antibodies for FOXO3 and to acetylated Lysine. Depletion of SIRT1 or SIRT6 induced the formation of red specks indicating FOXO3 acetylation in BT474 cells (Figure 3.14C). Collectively, all these results suggest that SIRT1 and SIRT6 regulate the expression and the activity of FOXO3 and may have a significant role in fine-tuning FOXO3 acetylation.

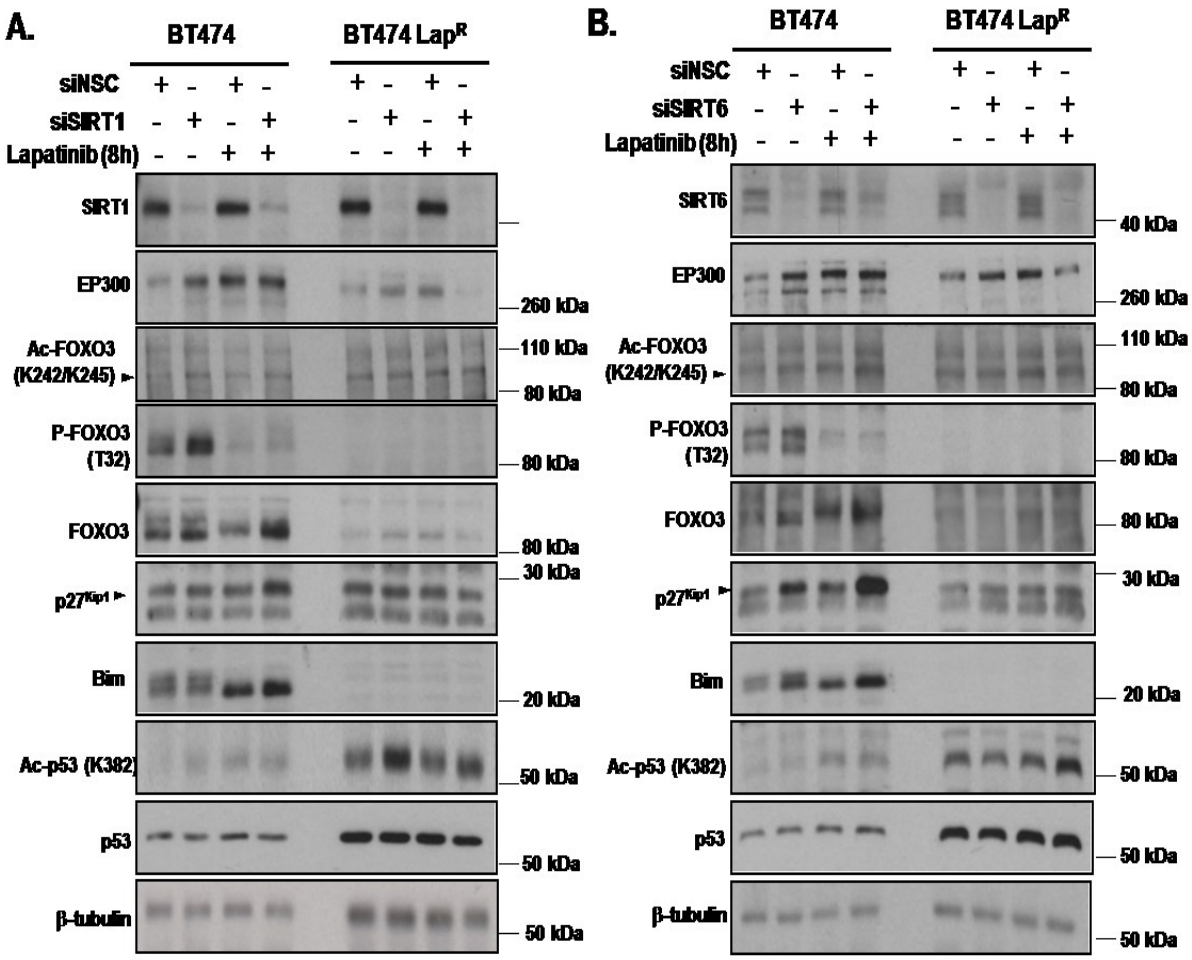


Figure 3.12 Silencing of SIRT1 and SIRT6 with or without Lapatinib treatment correlates with increased FOXO3 acetylation and its transcriptional activity. A, B. BT474 and BT474 Lap^R cells were transfected with Control (siNSC), siSIRT1 or siSIRT6 siRNAs and treated with or without 1 μM Lapatinib for 8 hours. After harvesting, protein lysates were obtained, and subsequent western blotting was performed to assess FOXO3 acetylation and its transcriptional activity using antibodies against Ac-FOXO3, FOXO3, p27^{Kip1}, Bim and others as indicated. The β-tubulin was used as a loading control.

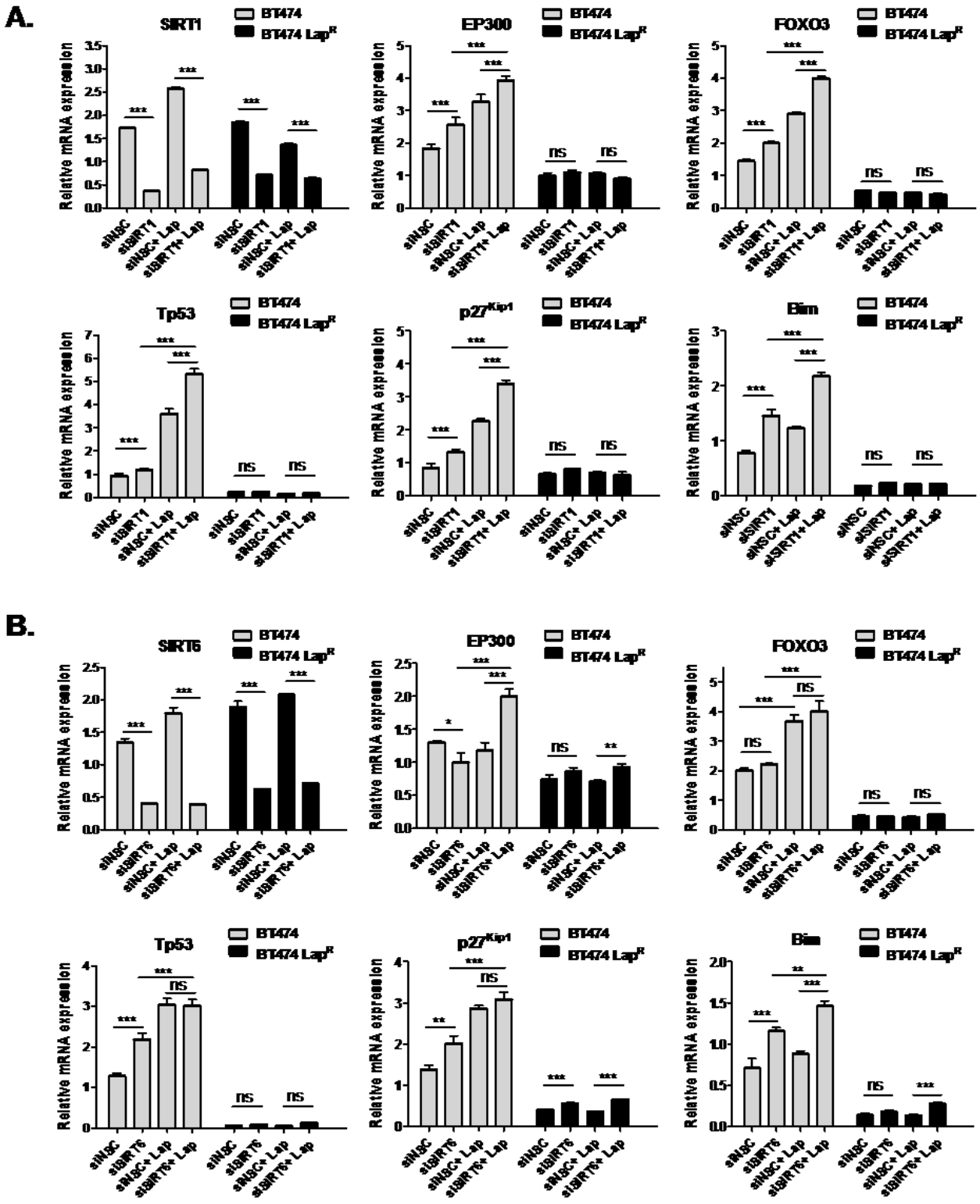


Figure 3.13 Silencing of SIRT1 and SIRT6 with or without Lapatinib treatment correlates with increased FOXO3 transcriptional activity. A, B. BT474 and BT474 Lap^R cells were transfected with Control (siNSC), siSIRT1 or siSIRT6 siRNAs and treated with or without 1 μM Lapatinib for 8 hours. After harvesting, mRNA extracted from the cell pellet and RT qPCR was performed to check the mRNA levels of SIRT1, SIRT6, EP300, FOXO3, TP53, p27^{Kip1} and Bim. Statistical analysis was performed by one-way ANOVA and data represents Mean ± SEM from three independent experiments (***P<0.001, **P<0.01, *P<0.05, ns=nonsignificant).

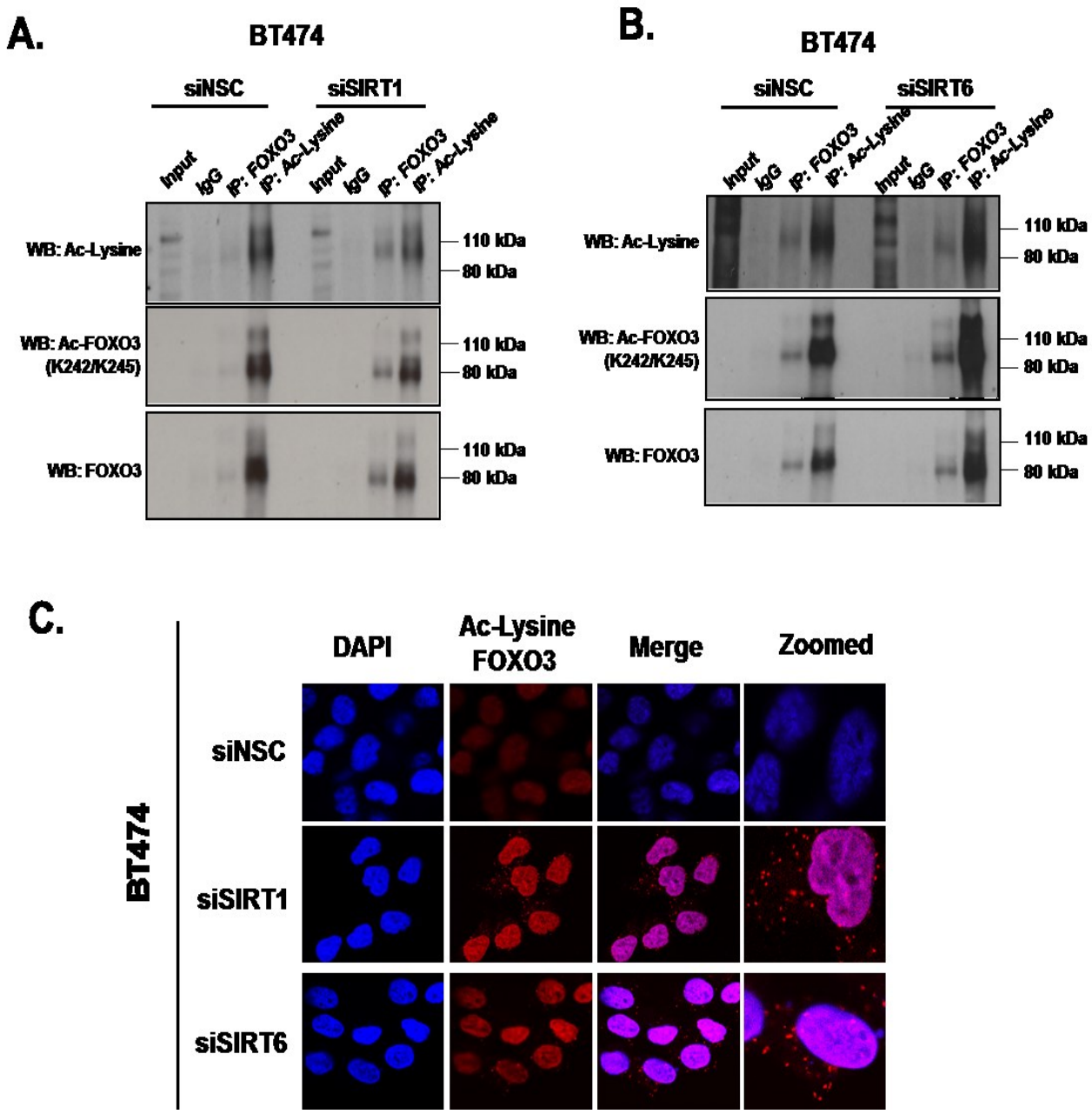


Figure 3.14 Silencing of SIRT1 and SIRT6 positively correlates with increased FOXO3 acetylation. A, B. BT474 cells were transfected with control (siNSC), siSIRT1 or siSIRT6 siRNAs. After harvesting, protein lysates were obtained, and subsequent co-immunoprecipitation (Co-IP) was performed with anti-FOXO3 and anti-acetylated lysine antibody. Subsequent immunoblotting was performed using antibodies against Ac-Lys, Ac-FOXO3 and FOXO3. The anti-IgG antibody was used as a negative control. **C.** BT474 cells were transfected with siNSC/siSIRT1/siSIRT6 siRNAs. After 24 hrs of transfection, cells were seeded in 8 chamber wells plate and Duolink PLA experiment was conducted using anti-Acetylated lysine antibody and anti-FOXO3 antibody. Representative confocal images are shown. Cells were visualized with a Leica TCS SP5 confocal microscope equipped with a 63X oil immersion objective and LAS-AF software. Each red spot represents for a single interaction and DNA was stained with 4, 6-diamidino-2-phenyl indole (DAPI) in blue.

3.2.11 Knockdown of SIRT6 increases lapatinib cytotoxicity in sensitive cells

To ascertain the role of SIRT1 and SIRT6 in long-term survival of cells upon lapatinib treatment, we performed clonogenic assays comparing the ability of BT474 and BT474-Lap^R cells to survive and form colonies upon RNA interference and in response to lapatinib treatment. Depletion of SIRT6 reduced cell proliferation in comparison with the siNSC control in the absence of lapatinib treatment (Figure 3.15A). Upon lapatinib treatment, SIRT6 knock-down BT474 cells showed greater sensitivity than siNSC control cells, especially at 50 nM or higher concentrations (Appendix Figure A3.6). These effects were not observed upon SIRT1 depletion in BT474 cells (Figure 3.15A). On the other hand, BT474-Lap^R cell lines did not show any significant changes in clonogenicity or lapatinib sensitivity upon SIRT-depletion (Figure 3.15B). Thus, depletion of SIRT6, but not SIRT1, increases lapatinib sensitivity in BT474 cells.

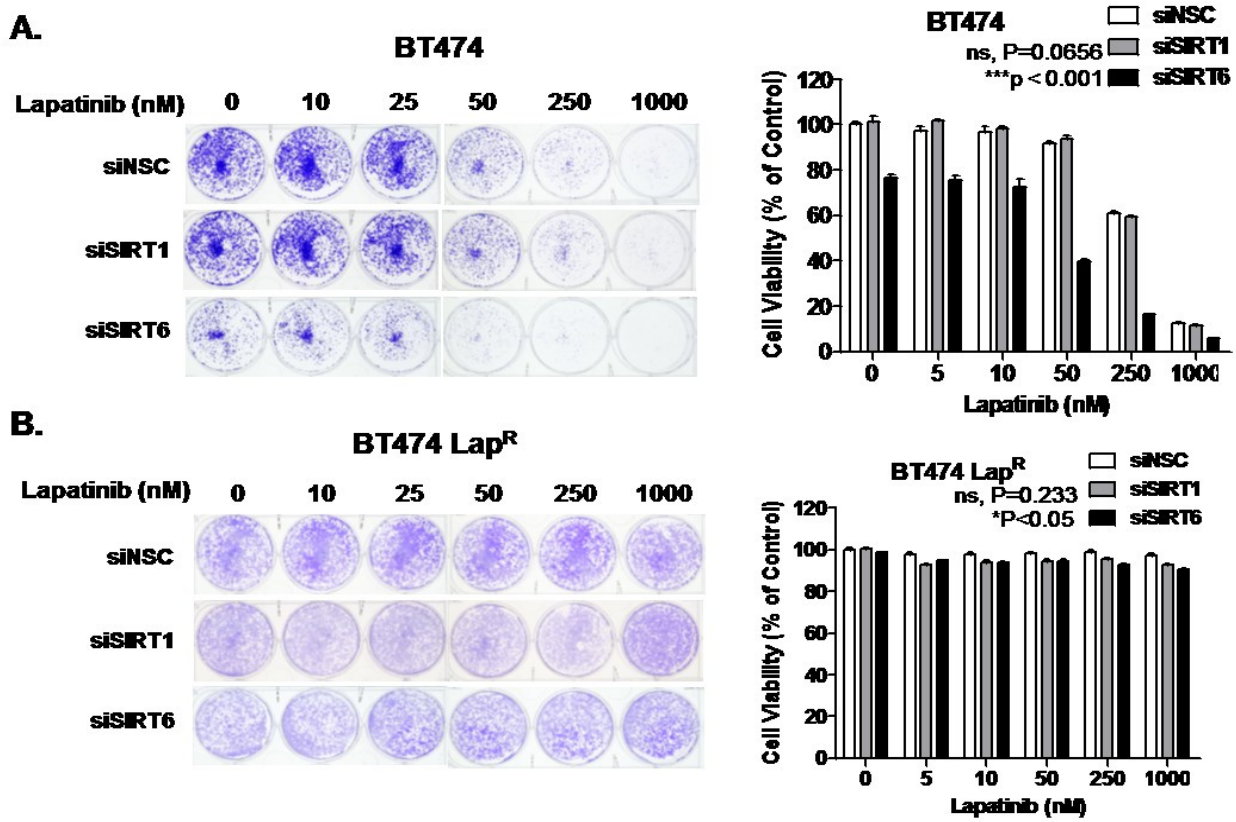


Figure 3.15 Silencing of SIRT6 increases long-term lapatinib cytotoxicity in BT474 cells. A, B. BT474 and BT474 Lap^R cells were transfected with siNSC, siSIRT1, or siSIRT6 siRNA smartpool. After 24 hours of transfection, 1000 cells were seeded per well, in 6-well plates. Cells were allowed to grow overnight and then treated with the lapatinib concentration indicated (0, 5, 10, 50, 250 and 1000 nM). Drug containing media was removed after 24 hours and cells were further grown for the colony formation for 14 days. At the end of this time period, cells were fixed with 4% para formaldehyde and stained with crystal violet. The stain was solubilised with 33% acetic acid and absorbance at 592 nm were obtained. Data represent the mean ± SEM of three independent transfection experiments (n=3, R=3) and statistical analysis was performed using two-ANOVA analysis (*p<0.05, **p<0.01, ***p<0.001, ns=nonsignificant) (right panel).

3.2.12 Inhibition of sirtuins by sirtinol induces FOXO3 acetylation and reduces cell proliferation

Due to the role of sirtuins in lapatinib response described above, we determined the effect of a sirtuin inhibitor, sirtinol, in both sensitive and resistant BT474 cell lines. EP300 protein levels increased upon sirtinol treatment up to 48 h in BT474 cells (Figure 3.16A). In addition, Ac-FOXO3 and Ac-p53 levels also increased, although with different kinetics. Ac-FOXO3 peaked after 24 h whereas Ac-p53 peaked after 8 h sirtinol treatment. Furthermore, sirtinol treatment increased total FOXO3 expression thus up-regulating its downstream target gene $p27^{Kip1}$ expression in BT474 cells (Figure 3.16A). To confirm the elevated acetylation status of FOXO3, we performed co-IP experiments. Subsequent western blotting result showed a significant increase of acetylation after sirtinol treatment for 24 h in BT474 cells (Figure 3.16B, upper panel) that was validated by reverse co-IP (Figure 3.16B, lower panel). Although there was also a slight increase in FOXO3 acetylation upon sirtinol treatment in lapatinib-resistant cells (Figure 3.16B, upper panel), this was not further confirmed in reverse co-IP experiments (Figure 3.16B, lower panel). Clonogenic assays confirmed that sirtinol inhibits proliferation at 20-50 μM in BT474 cells but not in lapatinib-resistant cells (Figure 3.16C). Collectively, these data indicate that sirtuins have an important role in FOXO3 acetylation, activation and cell proliferation in BT474 cells but not in BT474-Lap^R cells.

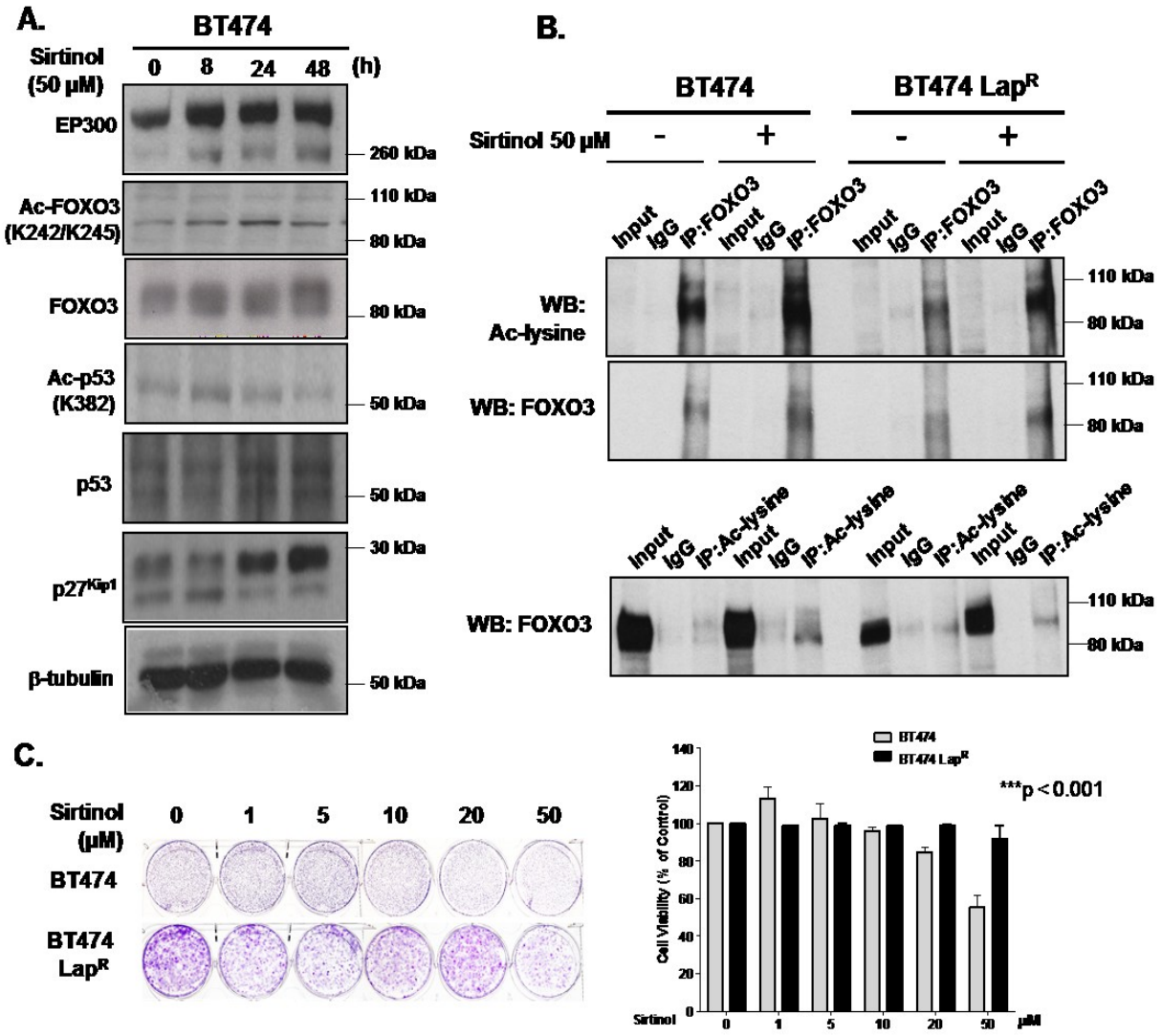
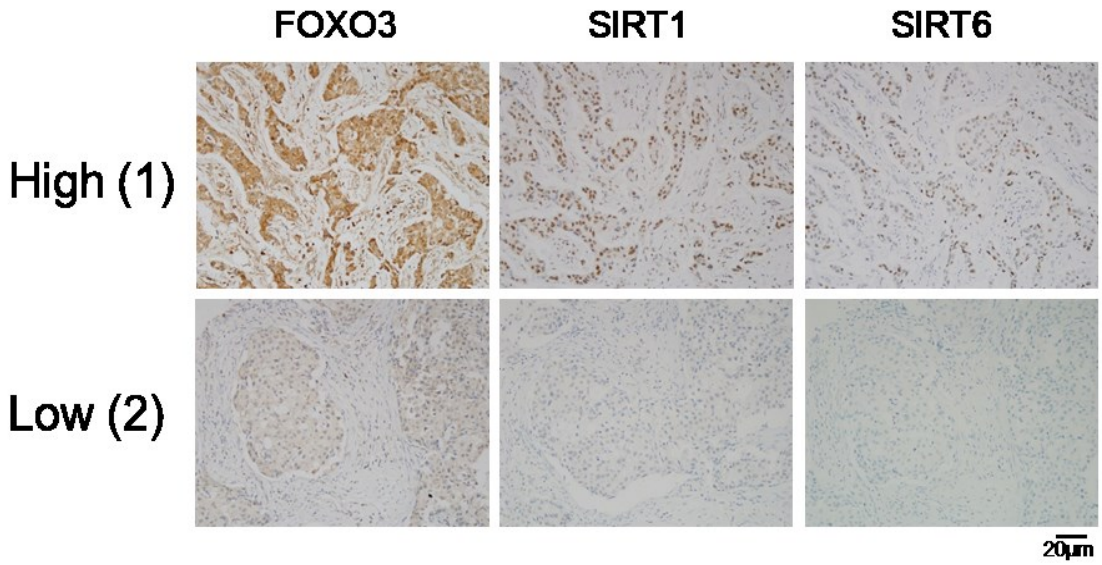


Figure 3.16. Sirtinol treatment increases FOXO3 acetylation and inhibits long-term cell growth in BT474 cells. A. Protein lysates of BT474 cells obtained following treatment with or without 50 μM sirtinol for different time-point and were assessed by western blotting to check the expression of Ac-FOXO3, $p27^{kip1}$ and for others indicated. **B.** Co-immunoprecipitation (Co-IP) was performed with an anti-FOXO3 antibody (upper panel). Subsequent immunoblotting was performed using antibodies against Ac-Lysine and FOXO3. A reverse Co-IP was performed with a pan acetylated lysine antibody and subsequent immunoblotting was done by using anti-FOXO3 antibody (lower panel). The anti-IgG antibody was used as a negative control. **C.** Clonogenic assay was employed after treating with different concentrations of sirtinol for 24 hour and stained with crystal violet after 2-3 weeks (left panel). The stain was solubilised with 33% acetic acid and absorbance at 592 nm were measured. Data represent the mean ± SEM of three independent transfection experiments (n=3, R=3) and statistical analysis was performed using two-ANOVA analysis (*p<0.05, **p<0.01, ***p<0.001, ns=nonsignificant) (right panel).

3.2.13 FOXO3 expression correlates with SIRT6 and SIRT1 levels in different breast cancer subtypes

Hitherto, our data showed that SIRT1 and SIRT6 directly inhibit FOXO3 acetylation and its activity. To investigate this finding further, we studied the relationships between FOXO3, SIRT1 and SIRT6 expression by immunohistochemistry in a cohort of patients of different breast cancer subtypes (Figure 3.17A). The staining results showed that both cytoplasmic and nuclear FOXO3 was positively correlated with the expression levels of SIRT6, (***$P < 0.001$) and SIRT1 (***$P < 0.001$) in ER+HER2- breast cancer patients and cytoplasmic FOXO3 with SIRT6 (*$P < 0.05$) in triple-negative breast cancer (TNBC) samples (Figure 3.17B). Interestingly, cytoplasmic FOXO3 was found to be positively correlated with the expression levels of SIRT6 ($P < 0.001$) but not SIRT1 in HER2+ (ER+ and ER-) breast cancer patients (Figure 3.17C). However, SIRT1 demonstrated a potential positive trend with the expression levels of cytoplasmic FOXO3 in HER2+ breast cancer subtypes with negative estrogen receptor status (ER-) (Figure 3.17C). We and others have previously shown that constitutive high FOXO3 expression, particularly in the nucleus, predicts FOXO3 deregulation/inactivation and poor prognosis in patients [30, 343]. Together these data provide further evidence that SIRT1 and SIRT6 cooperate to deregulate FOXO3 activity. As overexpression of the tumour suppressor FOXO3, specifically in the nucleus, can trigger cell cycle arrest and cell death, it is proposed that high levels of SIRT1/6 are expressed as an adaptive response to deacetylate FOXO3 and neutralise its potent anti-proliferative function.

A.



B.

ER+/HER2- breast cancer (n=373)

		FOXO3 (nuclear)	FOXO3 (cyto)	SIRT1	SIRT6
FOXO3 (nuclear)	rho		-.189**	.237**	.211**
	P-value		.000	.000	.000
FOXO3 (cyto)	rho	-.189**		.193**	.279**
	P-value	.000		.000	.000
SIRT1	rho	.237**	.193**		.302**
	P-value	.000	.000		.000
SIRT6	rho	.211**	.279**	.302**	
	P-value	.000	.000	.000	

**, very significant <.01.

TNBC breast cancer (n=190)

		FOXO3 (nuclear)	FOXO3 (cyto)	SIRT1	SIRT6
FOXO3 (nuclear)	rho		-.200**	.058	.182
	P-value		.006	.429	.012
FOXO3 (cyto)	rho	-.200**		.132	.087
	P-value	.006		.069	.233
SIRT1	rho	.058	.132		.282**
	P-value	.429	.069		.000
SIRT6	rho	.182	.087	.282**	
	P-value	.012	.233	.000	

**, very significant <.01; *, significant <.05.

C.

HER2+ breast cancer (n=125)

		FOXO3 (nuclear)	FOXO3 (cyto)	SIRT1	SIRT6
FOXO3 (nuclear)	rho		-.098	.023	.175
	P-value		.275	.800	.051
FOXO3 (cyto)	rho	-.098		.165	.225*
	P-value	.275		.065	.011
SIRT1	rho	.023	.165		.308**
	P-value	.800	.065		.000
SIRT6	rho	.175	.225*	.308**	
	P-value	.051	.011	.000	

**, very significant <.01; *, significant <.05.

ER-/HER2+ breast cancer (n=81)

		FOXO3 (nuclear)	FOXO3 (cyto)	SIRT1	SIRT6
FOXO3 (nuclear)	rho		-.068	.007	.185
	P-value		.545	.952	.099
FOXO3 (cyto)	rho	-.068		.217	.442**
	P-value	.545		.051	.000
SIRT1	rho	.007	.217		.300**
	P-value	.952	.051		.007
SIRT6	rho	.185	.442**	.300**	
	P-value	.099	.000	.007	

**, very significant <.01; *, significant <.05.

Figure 3.17. FOXO3 expression correlates with SIRT6 and SIRT1 levels in different breast cancer subtypes. A. Representative immunohistochemical staining images from two samples (patient 1 and 2) showing correlations between FOXO3, SIRT1, and SIRT6 expression. **B, C.** Staining results and Chi-square analysis. Chi-square statistical analysis was used to test the correlations between FOXO3, SIRT1, and SIRT6 expression in patients using SPSS 16.0. In statistical analysis, $P < 0.05$ was considered as significant (*$P < 0.05$, **$P < 0.01$). (Performed by Hee-jin Lee and Gyungyub Gong).

3.3 Discussion

HER2 gene is found to be overexpressed in ~20–25% of primary breast cancers, and is associated with poor clinical outcomes in cancer patients [344]. Monoclonal antibodies and tyrosine-kinase inhibitors are the two major targeted therapies for HER2-positive breast cancer, but these cancer cells often quickly develop adaptive responses to these HER2-targeted therapies becoming resistant to those drugs [345]. Previously, we and others have shown FOXO3 to be an important regulator in the antiproliferative potency of the tyrosine kinase inhibitors Gefitinib and lapatinib [75, 337-340]. BT474 cell lines express very high level of HER2, proving its candidacy as a tyrosine kinase inhibitor targets and thus we considered it as a very good model to study the lapatinib resistance of HER2 positive breast cancers. To investigate the role and regulation of FOXO3 in HER2-targeted therapies, a resistant derivative (BT474-Lap^{R}) of the lapatinib-sensitive BT474 breast cancer cell line has been established. Lapatinib treatment induces dephosphorylation of EGFR, HER2 and AKT, and subsequently promotes dephosphorylation and activation of FOXO3. Moreover, EP300, FOXO3 and p27^{Kip1} expression is increased upon lapatinib treatment in sensitive BT474 cells but not in resistant BT474-Lap^{R} cells, suggesting that EP300-mediated acetylation increases FOXO3 activity and expression in response to lapatinib in sensitive but not in the resistant BT474 cells. In addition, Duolink PLA assays and co-immunoprecepitation experiments confirm that lapatinib induces interactions between EP300 and FOXO3 and the associated FOXO3 acetylation. All together the results suggest that effective lapatinib response involves EP300 and FOXO3 interaction which results in FOXO3 acetylation and subsequent antiproliferative target gene expression in BT474 sensitive cells. Notably, this EP300-mediated FOXO3 acetylation requires the acetyl-transferase activity of EP300 as the acetyl-transferase deficient HAT mutant fails to induce FOXO3 acetylation in BT474 cells.

To evaluate the effect of FOXO3 acetylation more thoroughly, transient EP300 over-expression has been performed in both BT474 and BT474-Lap^{R} cells. The results show that EP300 overexpression induces FOXO3 expression and acetylation, which promotes the expression of the anti-proliferative target genes, including *p27^{Kip1}* and *Bim* in the sensitive BT474 cells. However, FOXO3 is deregulated and downstream

targets uncoupled from FOXO3 in the resistant cells. In agreement, overexpression of FOXO3 increases both short and long-term lapatinib sensitivity in BT474 but not in BT474-Lap^R cells. ChIP assays provide further evidence that the insensitivity of the resistant cells to lapatinib treatment could be due to the failure of FOXO3 to be recruited to its target genes. Together, these results suggest a significant role of EP300-mediated acetylation of FOXO3 in regulating HER2-positive breast cancer cell survival and their lapatinib sensitivity.

Notably, consistent low levels of EP300 and high levels of nuclear sirtuins (SIRT1 and SIRT6) are found in BT474-Lap^R cells. This suggests that the de-acetylation of FOXO3 by these nuclear SIRTs might also contribute to lapatinib resistance. Another sirtuin, SIRT2, which shuttles between the nucleus and cytoplasm, is also detected in both BT474 and the BT474-Lap^R cells. However, it is unlikely that SIRT2 plays a major role in lapatinib resistance as its levels are both constant and low in both cells. Therefore, FOXO3 acetylation, regulated co-ordinately by EP300 and sirtuins, is an important PTM which regulates FOXO3 expression and transcriptional activity to modulate lapatinib sensitivity in breast cancer. Consistently, sirtuin-mediated deacetylation of FOXO3 has been reported to restrict EP300-mediated transactivation of FOXO3 and promote stress resistance and longevity [184, 204]. Our data show that SIRT1 and SIRT6 knockdown in combination with lapatinib treatment causes an upregulation of FOXO3 expression and acetylation. Enhanced FOXO3 acetylation mediated by SIRT-depletion in BT474 cells also induces the expression of FOXO3 downstream target genes, such as *p27^{Kip1}* and *Bim*. It is noteworthy that the combination treatment of SIRT knockdown with lapatinib treatment stimulates FOXO3 activity compared to silencing of SIRT1/6 alone by increasing the expression of Bim and p27^{Kip1}. Moreover, knockdown of SIRT6 reduces the cell proliferation and enhances lapatinib sensitivity in BT474 cells, although depletion of SIRT1 does not result in any significant effects on drug sensitivity. This could be due to the fact that SIRT6 plays a more significant role in the inhibition of FOXO3 acetylation in these cells and/or that SIRT6 can functionally compensate for the loss of SIRT1. Since, the levels of SIRT1 and SIRT6 do not change in response to lapatinib treatment, they are unlikely to have a direct role in modulating lapatinib signalling but may instead play a part in fine-tuning FOXO3

acetylation and therefore lapatinib sensitivity by setting the baseline for the de-acetylation activity in both lapatinib sensitive and resistant cancer cells. In agreement, the pan-sirtuin inhibitor, sirtinol which can target both SIRT1 and SIRT6 increases $p27^{Kip1}$ expression in the BT474 cells. The finding that inhibition of SIRT1/6 by sirtinol does not increase lapatinib sensitivity in the resistant cells is likely due to the fact that EP300, which plays a critical part in FOXO3 acetylation, is not induced in the lapatinib resistant cells. This further suggests that SIRT1 and SIRT6 cooperate to set a threshold for FOXO3 acetylation in the cancer cells. Immunohistochemical (IHC) staining results also show that FOXO3 expression correlates positively with SIRT6/1 level in different breast cancer subtypes. As high FOXO3 expression, particularly in the nucleus, predicts FOXO3 deacetylation, deregulation/inactivation as well as poor prognosis in patients [30, 343], these IHC results provide further evidence that SIRT1 and SIRT6 cooperate to deregulate FOXO3 activity.

Collectively lapatinib treatment is correlated with EP300 expression, FOXO3 acetylation and dephosphorylation (T32) and an increase in FOXO3 expression as well as its downstream transcriptional activity in the sensitive BT474 cells. This suggests that lapatinib-induced FOXO3 acetylation via EP300 might drive FOXO3 dephosphorylation (T32), nuclear translocation and activation. Consistently, overexpression of wild-type EP300 alone can also induce FOXO3 acetylation, dephosphorylation (T32), and transcriptional activation in the sensitive BT474 cells. Interestingly, EP300 has previously been shown to mediate FOXO3 acetylation to antagonise its antiproliferative activity through restricting Bim expression [346]. In contrast, we show in here that EP300 promotes the antiproliferative function of FOXO3 through mediating its acetylation. In agreement with our findings, FOXO3 acetylation has been shown to mediate the antiproliferative functions of glucocorticoid in B acute lymphoblastic leukaemia (B-ALL) [347]. Notably, we found that both HER2 and P-AKT are downregulated while EGFR is upregulated in the Lapatinib resistant cells, and this is at odds with a previous study showing that both HER2 and P-AKT were upregulated in the Lapatinib resistant cells [2]. The reason for the discrepancy is unclear. However, the HER2-inhibitor resistant cells used in the other study were primarily generated by retrovirally transducing hotspot PIK3CA

mutations into HER2-amplified cells [348]. The transduced PIK3CA mutations would maintain the high HER2 expression and high P-AKT activities as the PIK3CA mutations function downstream of HER2 will directly activate AKT activity. We have previously found that FOXO3 can control AKT activity (P-AKT) in a negative feedback mechanism [349]. The Lapatinib resistant cells have low FOXO3 expression as an adaptive response during the development of lapatinib resistance and as a result AKT activity (P-AKT) is also lower in the resistant cells.

In summary, in this study I have identified a role of EP300-mediated FOXO3 acetylation in the regulation of lapatinib sensitivity in breast cancer. My findings also suggest that SIRT1 and SIRT6 play a coordinate role in fine-tuning FOXO3 acetylation and therefore lapatinib sensitivity by setting a threshold for the de-acetylation activity in both lapatinib sensitive and resistant cancer cells. My data suggest that FOXO3 acetylation by EP300 could be a potential marker for the identification of tumours that are likely to be sensitive to these drugs and indicate a novel therapeutic strategy to overcome lapatinib resistance in HER2-positive breast cancers. This will in turn enable the recognition of this modification as a biomarker for predicting treatment response in breast cancer patients. Once this is established, its manipulation for increasing anti-cancer drug efficacy in the future could be possible.

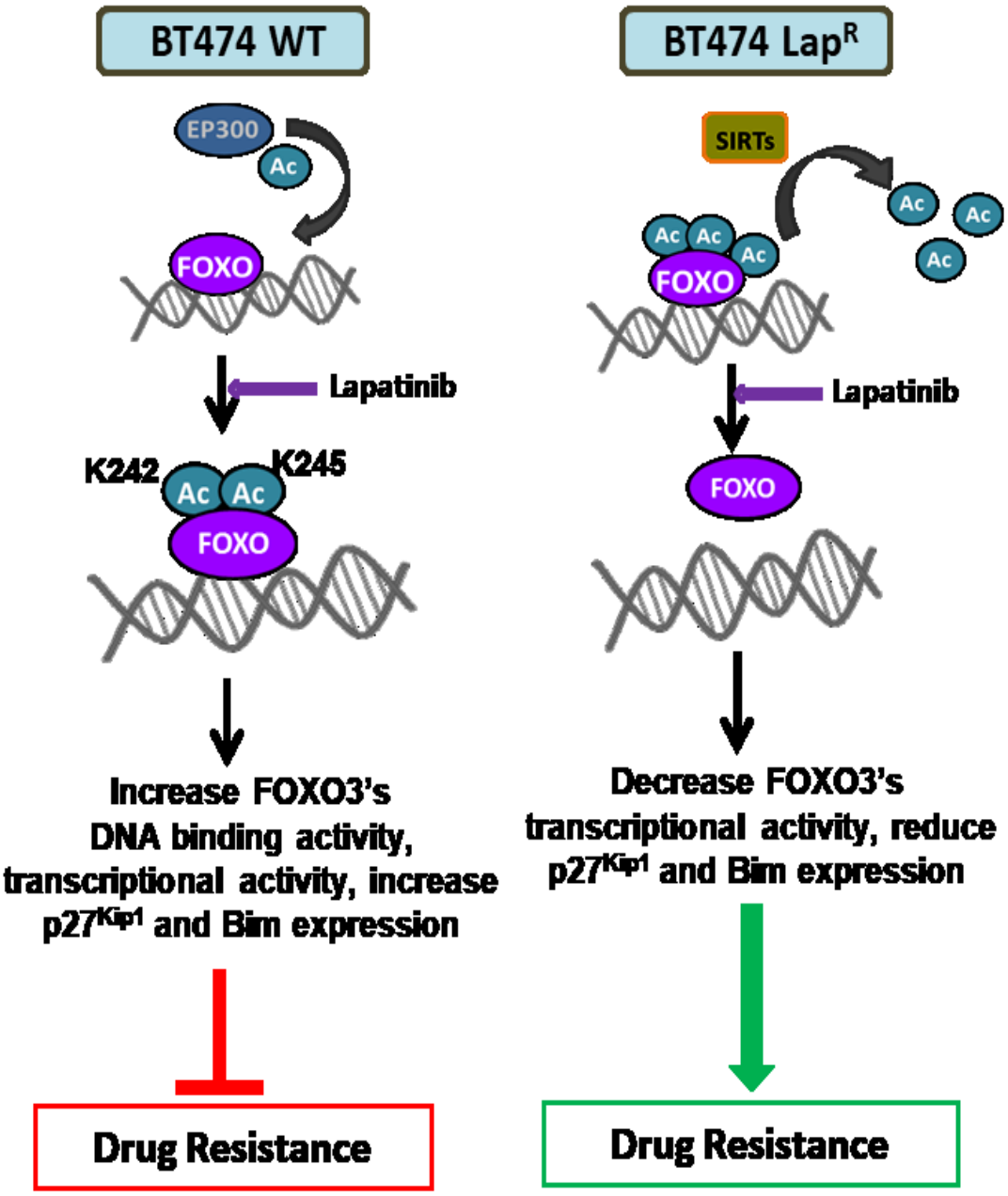


Figure 3.18. Schematic model showing the regulation of FOXO3 acetylation by EP300 and SIRT1/6 and its subsequent outcome on Lapatinib sensitivity and resistance in breast cancer cells.

CHAPTER 4

CBP mediated FOXO3 acetylation increases lapatinib sensitivity via inducing cell senescence and apoptotic cell death of breast cancer

4.1 Introduction

Several post-transcriptional modifications of FOXO transcription factors have been identified and among them phosphorylation is the highly studied mechanism. Although, acetylation of FOXO is less studied there are some significant findings that suggest FOXO3 acetylation as a key PTM to regulate cellular functions mediated by FOXOs. For example, acetylation has been shown to activate or inactivate FOXOs and modulate their biological functions. In some cases, acetylation of FOXO was found to attenuate FOXO transcriptional activity [184]. For example, three acetylation sites (K242, K245, and K262) of FOXO1 are located within the wing 2 (W2) region of the forkhead domain. In addition, the C-terminus region of FOXO1 accomodates the W2 region. As the C-terminus region directly involves in DNA recognition and binding, therefore, acetylation of these three positively charged lysine sites in W2 might attenuates FOXO ability to bind DNA sequences of its transcriptional target genes [350]. In contrast, the histone deacetylases SIRTs interacts with FOXO to promote its deacetylation and cytoplasmic sequestration, indicating that FOXO acetylation enhances its transcriptional activity [351]. Therefore, elucidation of the mechanisms of FOXO3 acetylation to regulate FOXO transcriptional activities is important to determine future therapeutic strategies in cancer prevention.

CREB binding protein (CBP) is a close paralog of EP300 which possesses histone acetyltransferase activity and modulates gene expression by catalysing targeted acetylation of the ϵ-amino group of lysine residues on histones and several nonhistone proteins. CBP proteins are also ubiquitously expressed global transcriptional coactivators that have critical roles in a myriad of biological processes including cell cycle control, differentiation, and apoptosis [352].

Although CBP and EP300 are highly related and share many cellular functions, there are evidences that these factors are not really interchangeable. Subtle differences in the expression of CBP and EP300 during development may explain why knockouts of the two coactivators in mice result in somewhat distinct phenotypes [353]. Distinct roles for CBP and EP300 have also been suggested in the differentiation of muscle and F9 teratocarcinoma cells [354, 355]. Apart from histone, CBP can also

acetylates several nonhistone proteins such as p53 and FOXOs with functional consequences. For example, CBP directly interacts with p53 and acetylates the tumour suppressor *in vivo* and *in vitro* to enhance its transcriptional activity as well as DNA repair [356]. However, the mechanism of CBP mediated FOXO acetylation and its functional consequences is still unclear. Therefore, I aimed to elucidate the mechanism underlying the CBP mediated acetylation of FOXO3 and how that acetylation affects FOXO3 transcriptional activity as well as lapatinib sensitivity.

In this study, I investigated the cellular functions and molecular mechanisms of CBP mediated FOXO3 acetylation involved in tumorigenesis and drug resistance of HER2 overexpressed breast cancer. More specifically, I examined and elucidated the interaction between CBP and FOXO3 acetylation and their synergistic regulation on lapatinib sensitivity of breast cancer via modulating cell senescence, apoptotic and/or autophagic cell deaths.

4.2 Results

4.2.1 Lapatinib treatment enhances CBP expression which in turn induces FOXO3 acetylation and transcriptional activity

It has been shown that CBP plays a key role in regulating non-histone protein acetylation and activity [357, 358]. Therefore, to identify the role of CBP in regulating FOXO3 and lapatinib response, I examined the effects of lapatinib on CBP expression as well as FOXO3 acetylation and activity in BT474 cells and its resistant derivative BT474 Lap^R cells. EP300 and FOXO3 expression were increased upon lapatinib exposure in a time dependent manner, an effect similarly observed in previously performed experiment mentioned in chapter 3 (Figure 4.1). However, we observed an induction of CBP as well from 2 to 8h of lapatinib treatment, indicating that CBP may play an important role in regulating FOXO3 acetylation. In addition, Ac-FOXO3 level was found to be increased upon lapatinib treatment and thus FOXO3 acetylation shows a positive correlation with CBP induction (Figure 4.1). As expected, there were no acetylation changes in BT474-Lap^R cells. Lower levels of EP300 and higher levels of the nuclear deacetylases, sirtuins (e.g. SIRT1 and SIRT6) were also detected in the BT474-Lap^R cells, which may contribute to the reduced FOXO3 activity in BT474-Lap^R cells, and therefore responsible for lapatinib resistance (Figure 4.1). However, another sirtuin SIRT2, which can shuttle between the cytoplasm and the nucleus, was found to be expressed but at low or similar levels in the lapatinib sensitive and resistant BT474 cells. Notably, high levels of CBP and acetylated FOXO3 after lapatinib treatment in BT474 cells positively correlated with the expression of its downstream transcriptional target p27^{Kip1} (Figure 4.1). Moreover, lapatinib treatment caused a time-dependent increase in the expression of autophagic markers [359] p62 and microtubule-associated protein 1A/1B-light chain 3 (LC3) (Figure 4.1). Thus, lapatinib induces CBP expression, FOXO3 acetylation and autophagy inducing protein expression in BT474 cells.

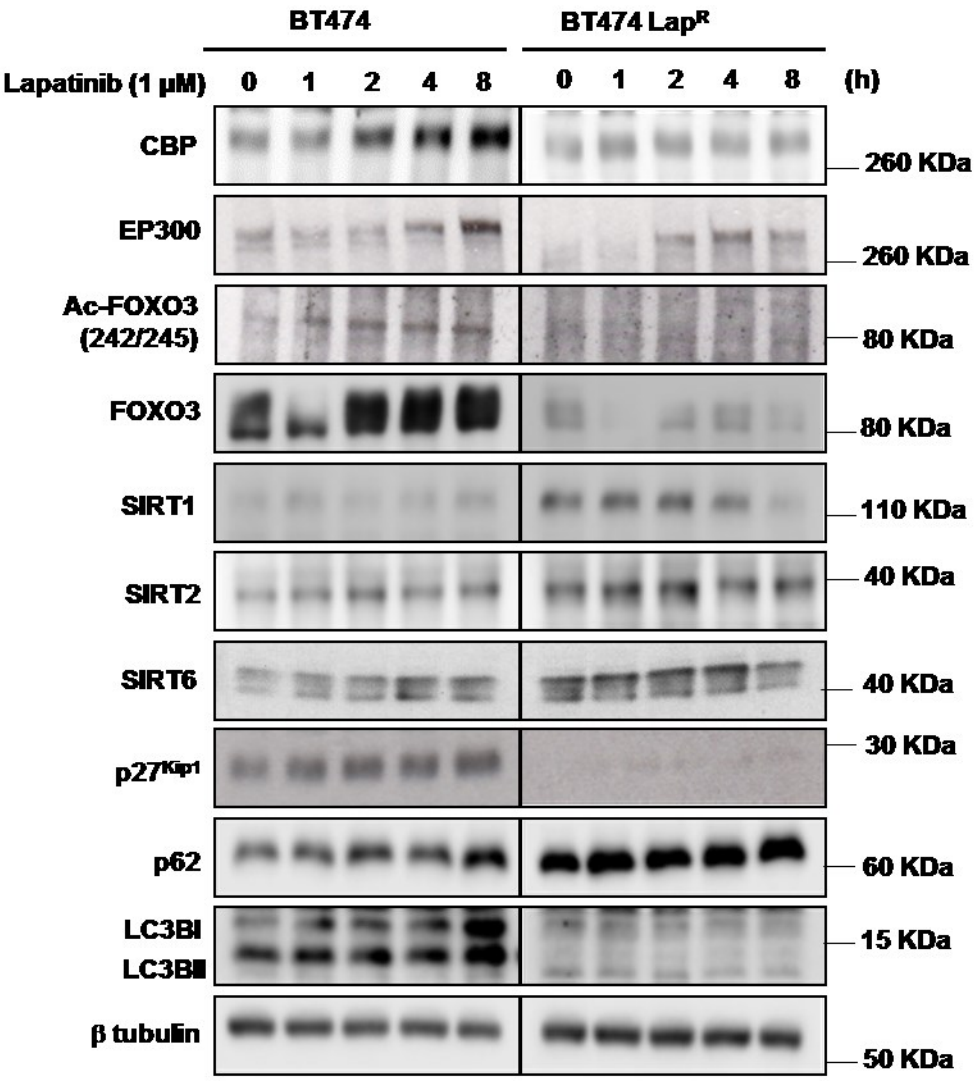


Figure 4.1. Lapatinib treatment enhances CBP expression which in turn induces FOXO3 acetylation. The sensitive (BT474) and lapatinib resistant BT474 Lap^R cells were either left untreated or treated with 1 μM lapatinib for the mentioned time points. Protein lysates from whole-cell extracts were then analysed by western blotting using the antibodies against the proteins indicated. Molecular weight markers are shown.

4.2.2 CBP overexpression caused an increase of FOXO3 acetylation which sequentially upregulates the expression of cell senescence, apoptotic and autophagic markers

To explore the role of CBP-mediated acetylation of FOXO3, I used an acetyl-transferase-defective mutant to stably transfect BT474 and BT474-Lap^R cells. From the western blot results, it was found that, upon transfection of wild-type CBP in BT474 cells there was an upregulation of Ac-FOXO3 (242/245) and total FOXO3 expression, while the upregulation of these proteins was comparatively weaker upon

transfection of the CBP HAT mutant (Figure 4.2). However, this CBP-dependent FOXO3 up-regulation occurred at low levels in BT474-Lap^{R} cells. Notably, FOXO3 expression induced by CBP showed similar trend at mRNA level (Figure 4.3). In addition, ectopic expression of wild-type CBP induced the expression of downstream FOXO3 target genes p130 and Bim in BT474 whereas a very low induction of these target genes was observed in BT474-Lap^{R} cells (Figure 4.2, 4.3). Importantly, up-regulation of FOXO3 target genes was found to be reduced upon transfection of the CBP HAT mutant compared to WT CBP. This further ensures the positive regulatory role of CBP-mediated acetylation on FOXO3 downstream transcriptional activity. Furthermore, CBP overexpression enhances the expression of cell senescence marker p27^{Kip1} and p16^{INK4a} [360], [361] at both mRNA and protein levels, while the overexpression of CBP HAT mutant reduces their expression (Figure 4.2, 4.3). Moreover, CBP also enhances the expression of autophagic markers such as p62 and LC3BII, whereas their expression was found at lower level upon overexpression of the HAT mutated CBP. Therefore, the acetyl-transferase activity of CBP and more importantly FOXO3 acetylation by CBP plays a significant role in inducing the expression of cell senescence and autophagic marker in BT474 cells.

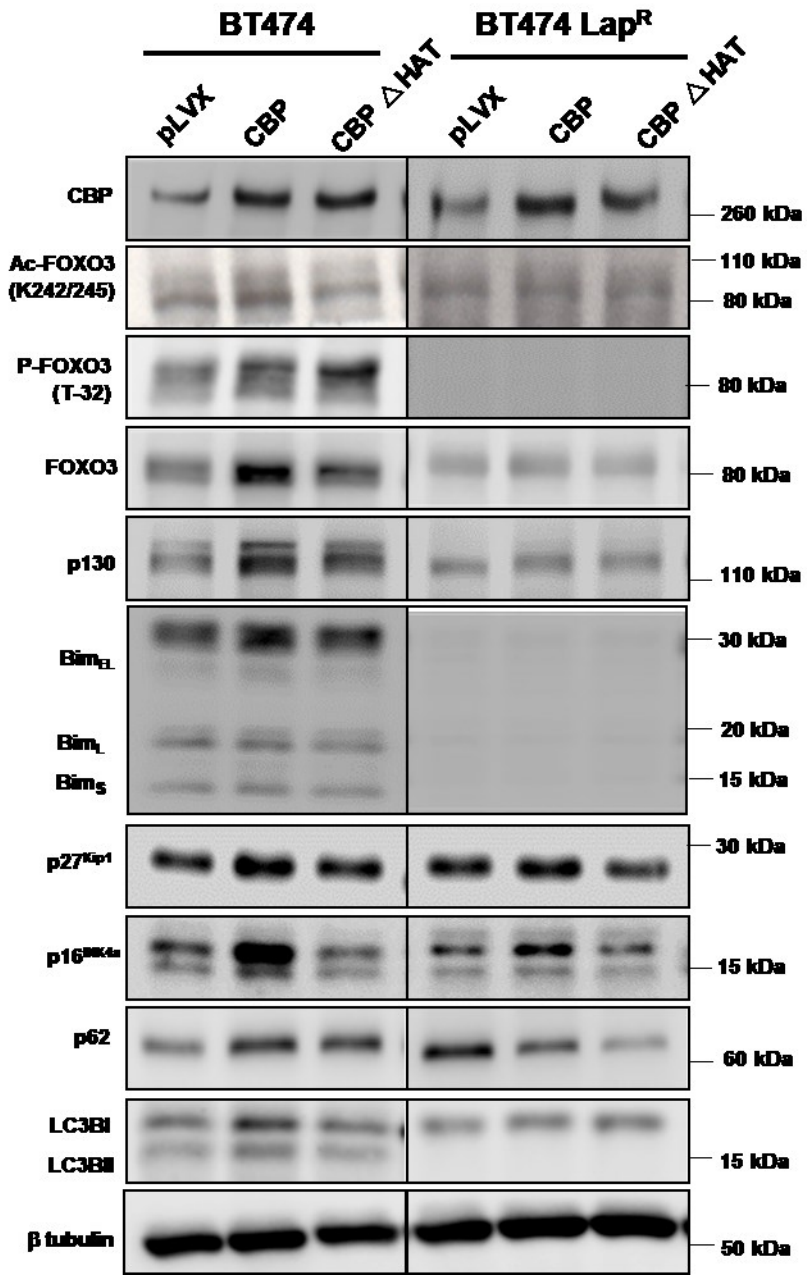


Figure 4.2. CBP overexpression upregulates FOXO3 acetylation and its downstream transcriptional activity. BT474 and BT474 Lap^R cells were stably transfected with the empty vector pLVX, the plasmid encoding wild-type CBP, or the one encoding for its acetyl-transferase mutant derivative (CBP △HAT). Proteins were obtained from whole cell extracts and western blotting was performed using the protein lysates to assess the expression levels of CBP, FOXO3 and other indicated proteins.

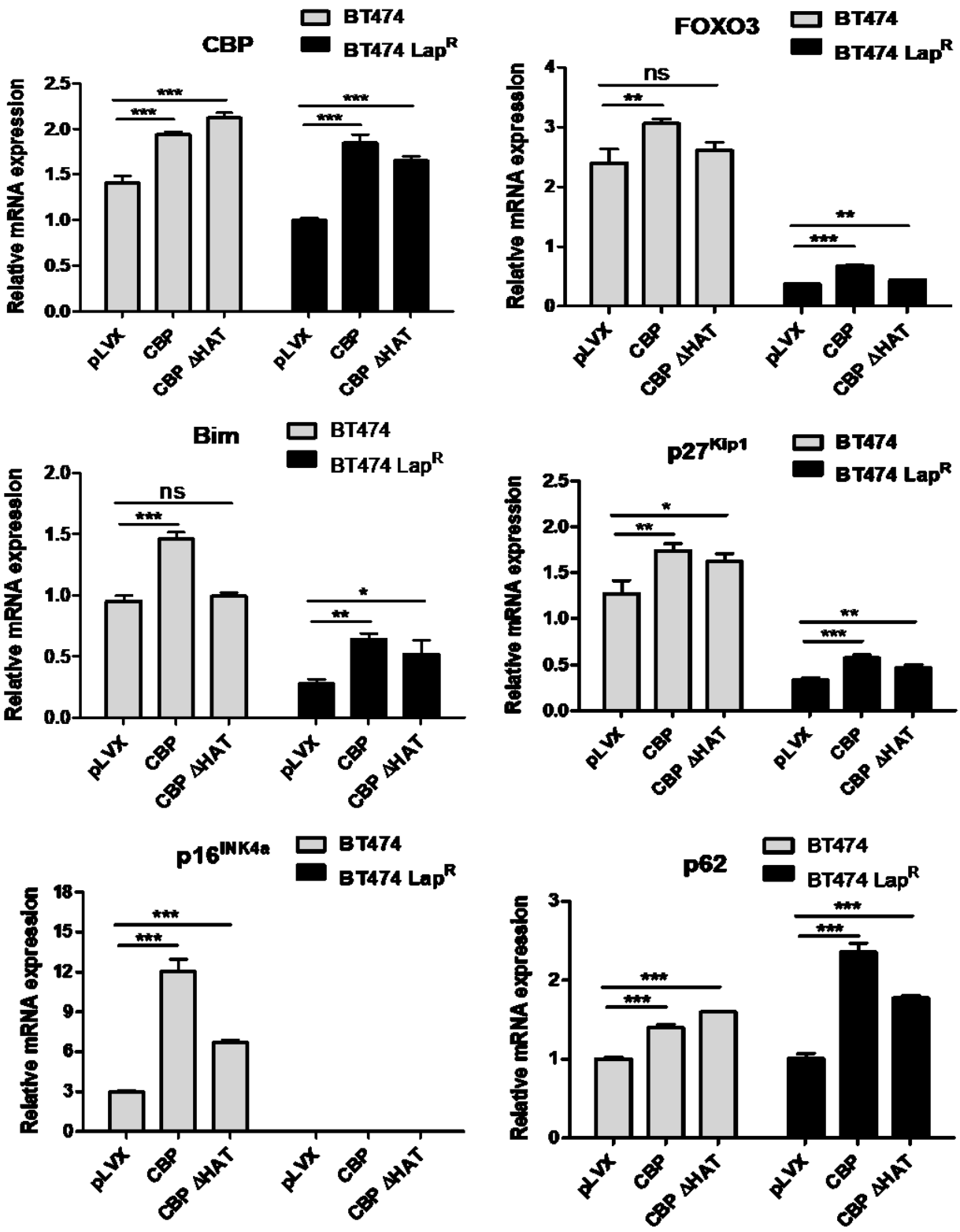


Figure 4.3 CBP overexpression upregulates FOXO3 acetylation and its downstream transcriptional activity. BT474 and BT474 Lap^R cells were stably transfected with the empty vector pLVX, the plasmid encoding wild-type CBP, or the one encoding for its acetyl-transferase mutant derivative (CBP △HAT). The mRNA levels of *CBP, FOXO3, Bim, p27^{kip1}, p16^{INK4a} and p62* were assessed by real time qPCR. The RPL19/RPS14 housekeeping gene was used as a control to normalise gene expression. Data represents means ± SEM from three independent experiments and analysed by one-way ANOVA (***P<0.001, **P<0.01, *P<0.05, ns=nonsignificant).

4.2.3 CBP downregulates breast cancer drug resistant genes ABCG2, ABCC1, ABCC4 and ABCC5 in BT474 Lap^R cells

ABC transporters belong to the largest superfamily of transporter group of proteins [362] and over 12 of these transporters have been found to overexpress and linked to multi-drug resistance (MDR) of cancer cell lines [363]. Therefore, to evaluate the role of CBP in regulating lapatinib resistance genes, I aimed to check the expression of ABC transporter genes in lapatinib resistant BT474 cells at mRNA level. RT qPCR results exhibited the upregulation of MDR resistance genes ABCG2, ABCC1 and ABCC4 in resistant cells suggesting their possible linkage to lapatinib resistance of BT474 cells (Figure 4.4). In addition, high level of sirtuins (SIRT1, 2, 6) expression in BT474 Lap^R cells suggest that deacetylation of FOXO3 may have possible role in the induction of the above mentioned MDR causing genes. Notably, overexpression of CBP in BT474 Lap^R cells reduces the mRNA level of ABCG2, ABCC1, ABCC2 and ABCC4 which suggests the possible role of CBP mediated FOXO3 acetylation to reduce lapatinib resistance (Figure 4.4). However, ABCC3 was found to be unchanged when compared between pLVX and CBP overexpressed resistant BT474 cells.

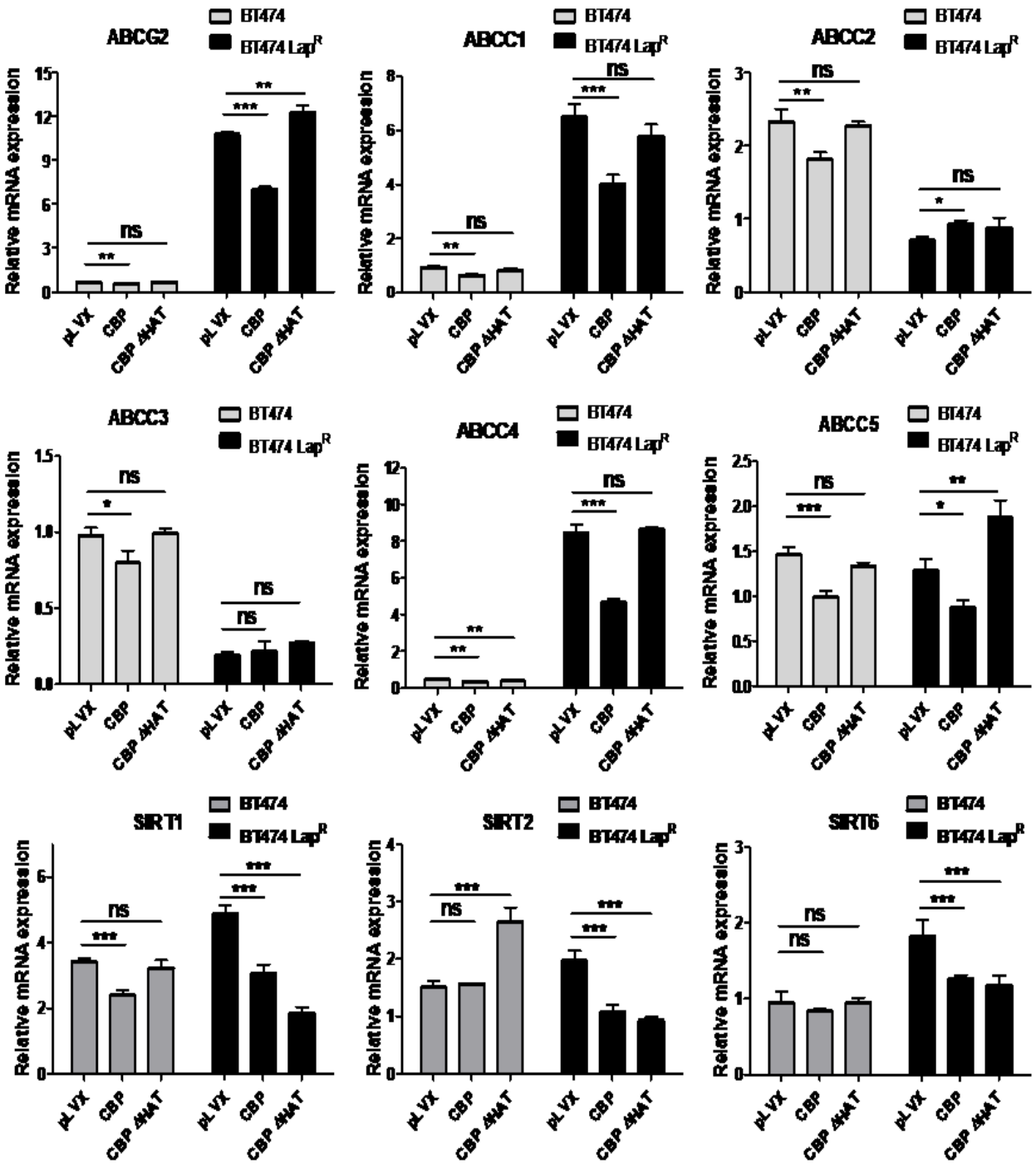


Figure 4.4. CBP downregulatesdrug resistant genes ABCG2, ABCC1, ABCC4 and ABCC5. BT474 and BT474-Lap^R cells were stably transfected with the empty vector pLVX, the plasmid encoding wild-type CBP, or the one encoding for its acetyl-transferase mutant derivative (CBP △HAT). The mRNA levels of ABC transporter genes were assessed by real time qPCR. The RPS14 housekeeping gene was used as a control to normalise gene expression. Data represents means ± SD from three independent experiments and analysed by one-way ANOVA (***P<0.001, **P<0.01, *P<0.05, ns=nonsignificant).

4.2.4 Co-immunoprecipitation assay confirms CBP mediated FOXO3 acetylation and shows the interaction between CBP and FOXO3

Substantial evidence pointed that CBP interacts with other non-histone proteins to acetylate and regulate their activity [364], [365]. To assess CBP mediated FOXO3 acetylation, I performed co-immunoprecipitation experiment in BT474 cells. As expected, FOXO3 acetylation (K242/245) increased upon transfection with the wild-type, but not with the CBP HAT mutant (pull down of FOXO3 and detection of Ac-FOXO3 (242/245); Figure 4.5A). However, we found that the variation in the acetylation level of FOXO3 between wild-type CBP and HAT mutant CBP transfected cells is higher in FOXO3 overexpressed cells in comparison with naïve cells (Figure 4.5B). In sequence, the FOXO3-CBP interaction was confirmed when pulling-down using either FOXO3 (Figure 4.5A,B) or CBP (Figure 4.6A,B) antibodies, as the intensity of the CBP and FOXO3 bands, respectively, upon transfection of wild-type CBP were stronger than with the HAT mutant CBP. Interestingly, CBP and FOXO3 interaction is weaker in naive cells whereas they interact more strongly in FOXO3 overexpressed BT474 cells (Figure 4.6B).

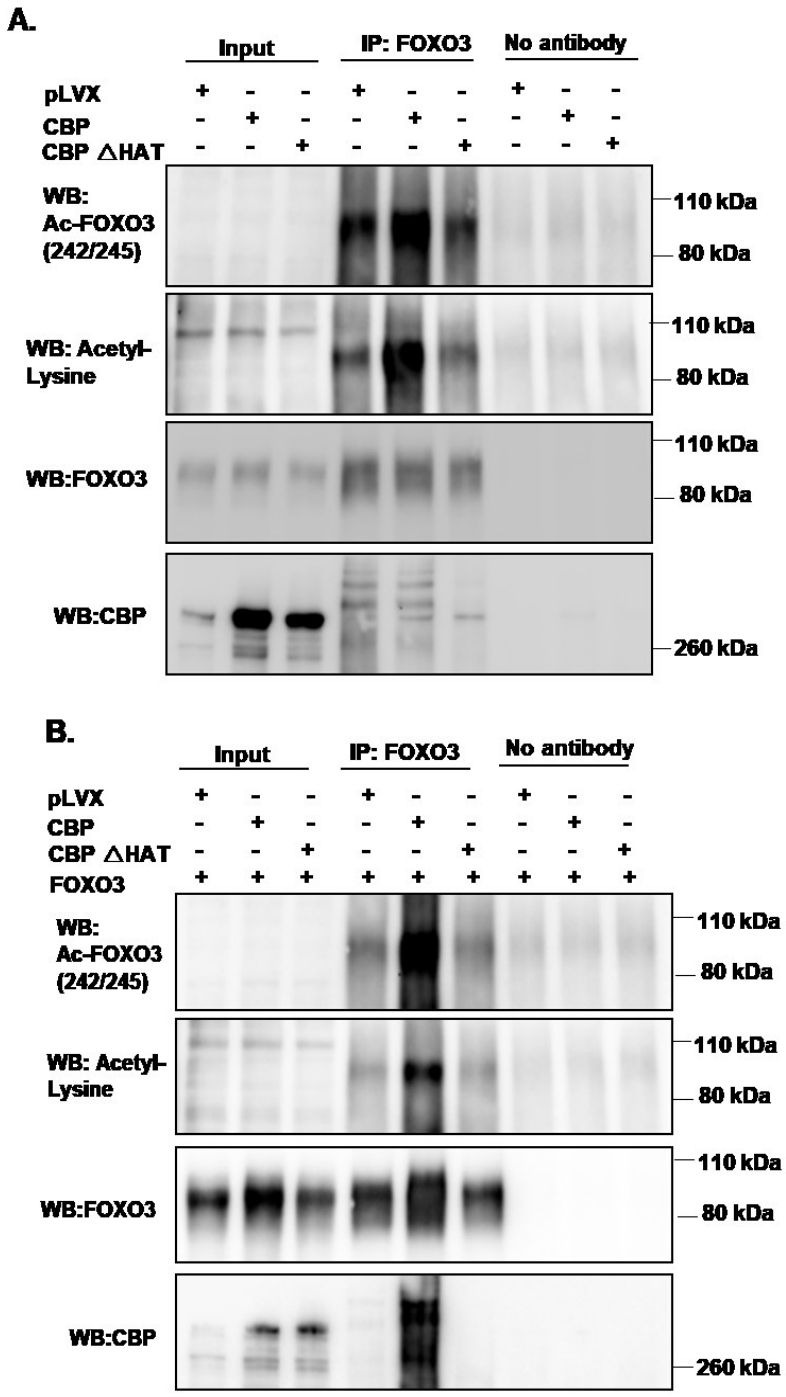


Figure 4.5 CBP acetylates FOXO3 in BT474 cells. A. BT474 cells were transiently transfected with the empty vector pLVX, the plasmid encoding wild-type CBP, or the one encoding for its acetyl-transferase mutant derivative (CBP △HAT). Proteins were obtained from whole cell extracts after 48 hours of transfection and co-immunoprecipitation (Co-IP) was performed with an anti-FOXO3 antibody. Subsequent immunoblotting was performed using antibodies against Ac-Lys, Ac-FOXO3, FOXO3 and CBP. The anti-IgG was used as a negative control. **B.** Co-IP was performed with anti-FOXO3 antibody using the protein lysates of BT474 cells transiently transfected with CBP and FOXO3 or CBP △HAT and FOXO3. Subsequent immunoblotting was performed using antibodies against Ac-Lys, Ac-FOXO3, FOXO3 and CBP. The anti-IgG was used as a negative control.

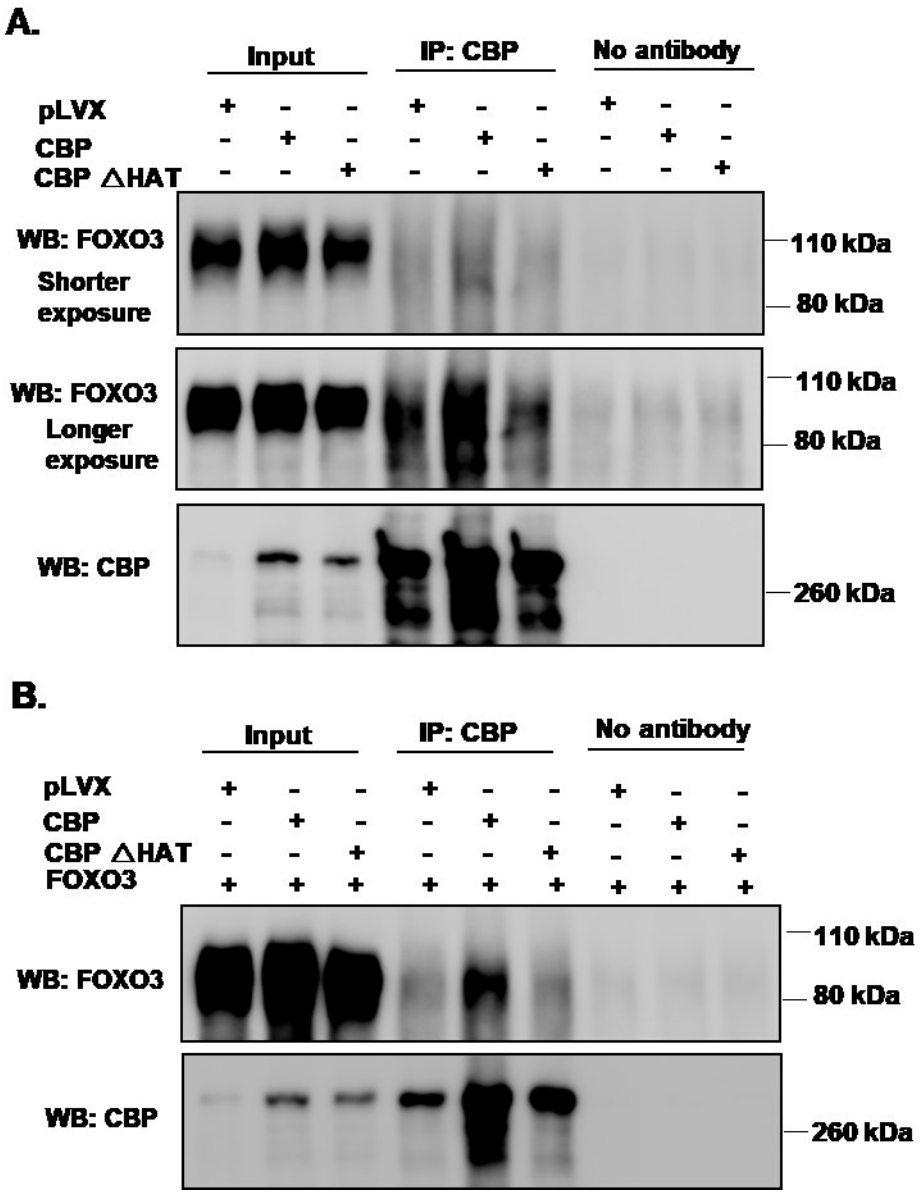


Figure 4.6. CBP interacts with FOXO3 in naïve and FOXO3 overexpressed cells. A. BT474 cells were transiently transfected with the empty vector pLVX, the plasmid encoding wild-type CBP, or the one encoding for its acetyl-transferase mutant derivative (CBP △HAT). Proteins were obtained from whole cell extracts after 48 hours of transfection and co-immunoprecipitation (Co-IP) was performed with an anti-CBP antibody. Subsequent immunoblotting was performed using antibodies against FOXO3 and CBP. The anti-IgG was used as a negative control. **B.** Co-IP was performed with anti-CBP antibody using the protein lysates of BT474 cells transiently transfected with CBP and FOXO3 or CBP △HAT and FOXO3. Subsequent immunoblotting was performed using antibodies against FOXO3 and CBP. The anti-IgG was used as a negative control.

4.2.5 Ectopic overexpression of CBP enhances short-term and long-term lapatinib sensitivity

Since, CBP overexpression can induce FOXO3 activity and its downstream antiproliferative targets in parental, but not the BT474-Lap^R resistant cells, I next performed sulphorhodamine B (SRB) assays to assess lapatinib sensitivity upon CBP transfection. Over-expression of wild-type CBP, but not the acetyl-transferase deficient HAT CBP mutant, increased lapatinib sensitivity in BT474 cells (Figure 4.7A, left panel). Notably, ectopic expression of CBP HAT mutant led to a slight but not significant decrease in cell viability in sensitive BT474 cells upon lapatinib treatment. On the contrary, CBP over-expression in BT474-Lap^R cells did not result in any significant effect on lapatinib response (Figure 4.7A, right panel) and this could be due to the high levels of deacetylases (e.g. SIRTs). Similar results were also observed for the lapatinib sensitive and resistant SKBR3 and SKBR3-Lap^R breast cancer cell lines (Appendix Figure A4.3).

In order to ascertain whether the short-term data shown above had any effect on the long-term lapatinib sensitivity of BT474 cells, we performed clonogenic assays. Truly, CBP overexpressing cells showed increased lapatinib sensitivity when compared with control cells transfected with the empty vector or the acetyl-transferase defective mutant (Figure 4.7B). These results suggest that CBP-mediated FOXO3 acetylation has a role in lapatinib-mediated cytotoxicity in sensitive BT474 cells. It is also noteworthy that the resistant cells over-expressing CBP had lower clonogenicity compared to the control cells, suggesting that CBP is involved in long-term cell viability and self-renewal, but does not affect drug sensitivity in BT474-Lap^R cell lines (Figure 4.7B). However, the fact that HAT mutant CBP overexpressing resistant cells show reduced cell proliferation (Figure 4.7) reveals a possible de-regulation of FOXO3 acetylation in resistant cells. Finally, these data confirm that CBP mediated FOXO3 acetylation leads to an increase in short and long-term lapatinib sensitivity.

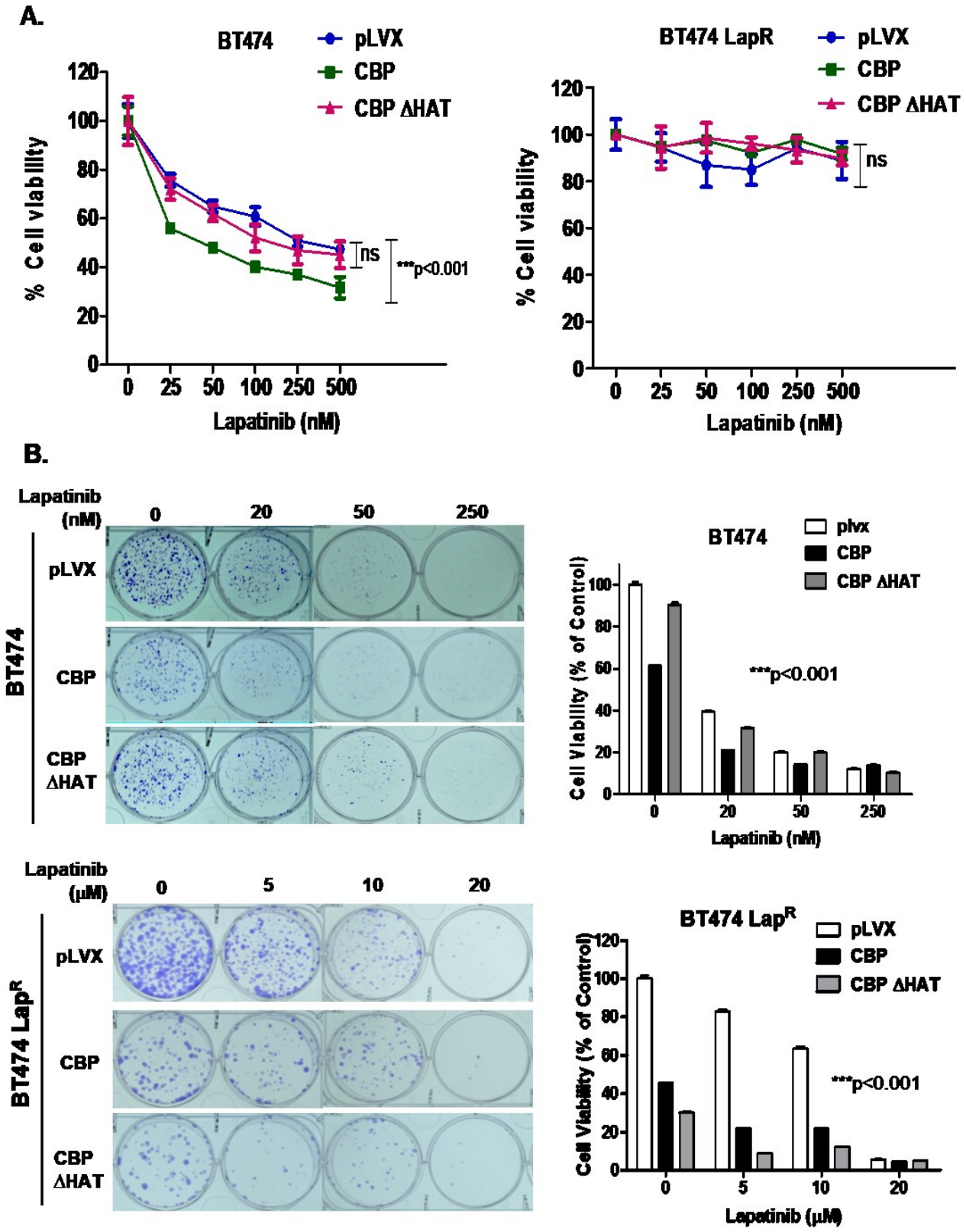


Figure 4.7. CBP overexpression increases short and long-term lapatinib sensitivity. A. BT474 and BT474-Lap^R cells were stably transfected with the empty vector pLVX, the plasmid encoding wild-type CBP, or the one encoding for its acetyl-transferase mutant derivative (CBP△HAT). Stably transfected BT474 and BT474 Lap^R cells were seeded in 96-well plates and treated with lapatinib (0 to 500 nM). Twenty-four hours after treatment, cells were fixed and stained with the protein-binding dye SRB. Values obtained were normalized against the corresponding untreated controls and

presented as percentages. Data represent means ± SEM (2-way ANOVA; non-significant, ns; significant, **P<0.001). **B.** Stably transfected cells were allowed to grow overnight and then treated with the lapatinib concentrations indicated (for BT474 0, 20, 50, 250 nM and for LapR 0, 5, 10, 20 μM). Twenty-four hours following treatment the medium was changed and colony formation was allowed for 28 and 14 days in sensitive and resistant BT474 cells, respectively. Cells were then fixed with 4% para formaldehyde and stained with crystal violet. The stain was solubilised with 33% acetic acid and absorbance obtained at 592 nm. Data were finally normalised to the respective untreated empty-vector transfected cells. Bars represent the mean ± SEM of three independent transfection experiments (n=3, R=3) and statistical analysis was performed using two-way ANOVA analysis (*p<0.05, **p<0.01, ***p<0.001).

4.2.6 Ectopic CBP overexpression reduces mammosphere forming capacity of BT474 and BT474 Lap^R cells

Acquisition of a stem cell-like phenotype is a well-known characteristics of drug resistant cancer cells [366]. In order to explore the role of CBP to affect CSC-like populations, the mammosphere formation assay was performed. Overexpression of CBP showed a remarkable reduction in the sphere formation capacity as compared to the control empty vector transfected cells (Figure 4.8A). Again, the loss of HAT domain was found to be associated with large mammosphere formation indicating the role of CBP acetyl-transferase activity in reducing sphere formation (Figure 4.8A). Moreover, similar result was observed in resistant cells where CBP also inhibit sphere formation capacity of resistant cells. I further checked the mRNA level of cancer stem cell regulating genes such as nanog, sox2 and pou5F1 in BT474 cells. As shown in figure 4.8B, there was a significant reduction of pluripotency markers upon CBP overexpression at mRNA level which also support the phenotypic observations.

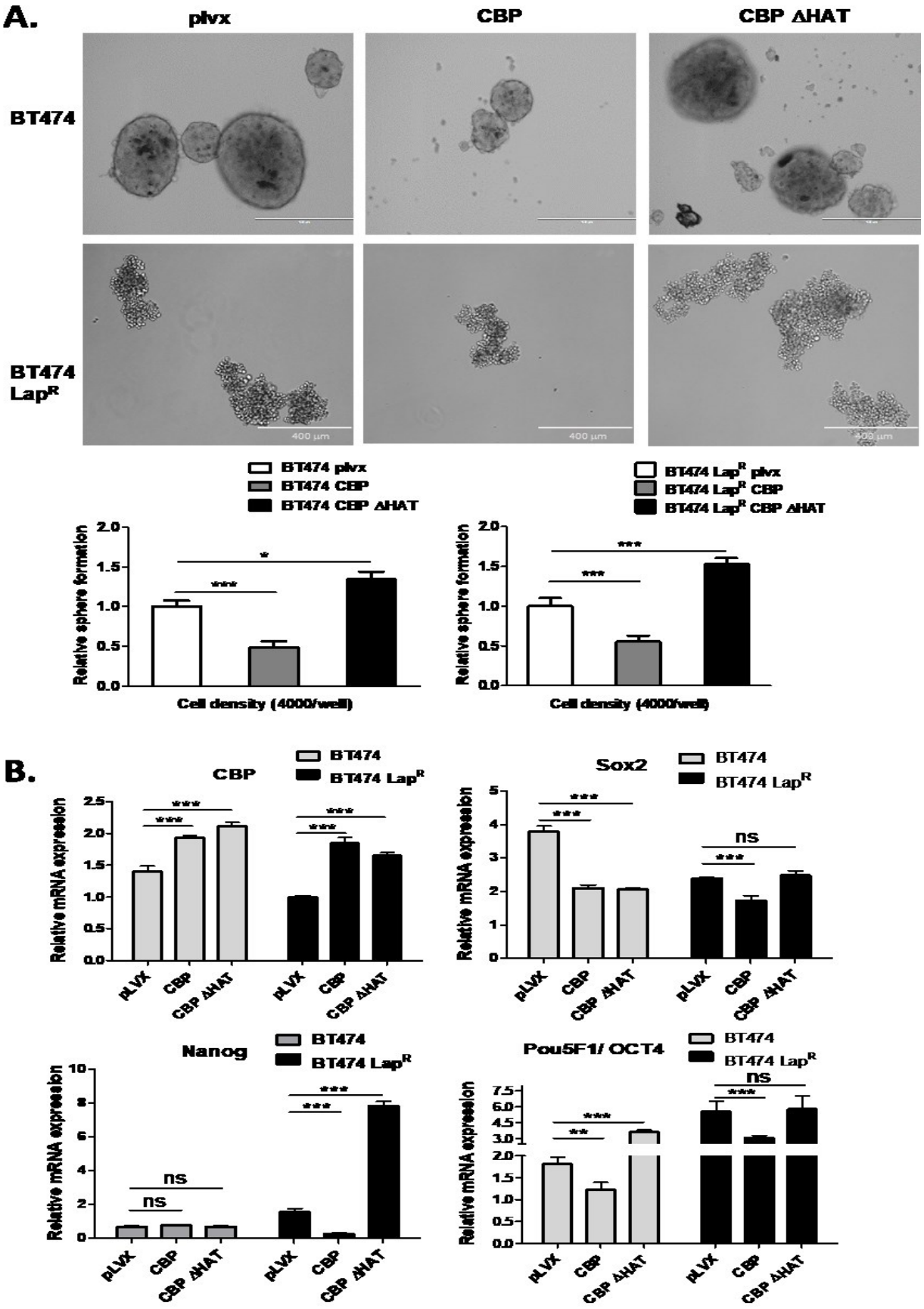


Figure 4.8 CBP regulates mammosphere forming capacity in both sensitive and resistant BT474 cells. A. BT474 and BT474 Lap^R cells were transfected with pLVX, CBP and CBP △HAT.

Then transfected cells were seeded in 6-well low attachment plate and left in growth factor (bFGF, EGF) containing media for 2 weeks. Then formed spheres were counted and representative mammospheres pictures are shown from three independent assay. The graph (bottom panel of A) represents the relative numbers mammospheres compared with control. Bars represent Mean ± SD. Statistical significance was determined by Students t-test (***$p \leq 0.001$ *versus* control). **B.** mRNA levels of CBP, sox2, nanog and pou5F1 were examined by RT-qPCR. Data were analysed by one-way ANOVA and presented as means ± SEM (***P<0.001, **P<0.01, *P<0.05, ns=nonsignificant).

4.2.7 Overexpression of CBP can be combined with lapatinib to promote FOXO3 acetylation and activity

To confirm whether CBP can modulate the ability of lapatinib to mediate FOXO3 acetylation and its downstream activity, I next determined if CBP overexpression in combination with lapatinib can enhance FOXO3 activity. Western blot results show that CBP overexpression can increase FOXO3 acetylation as shown previously, however, the acetylation level is higher upon treatment with 0.1 μM of lapatinib. This combination treatment can further upregulate FOXO3 activity as the protein levels of P-FOXO3 (T32) and FOXM1 were reduced significantly (Figure 4.9). Moreover, SIRT1 and SIRT6 expression were also found to be reduced upon combination of CBP overexpression and lapatinib treatment. In addition, I found that $p27^{Kip1}$ and $p16^{INK4a}$ expression levels were increased with or without lapatinib treatment whereas, lapatinib treatment cannot enhance Bim or Bax expression when combined with CBP overexpression suggesting that combination treatment turns BT474 cells to go for senescence. Thus, CBP overexpression combined with lapatinib treatment enhances FOXO3 acetylation and suggests its increased activity that turns cells to go for senescence.

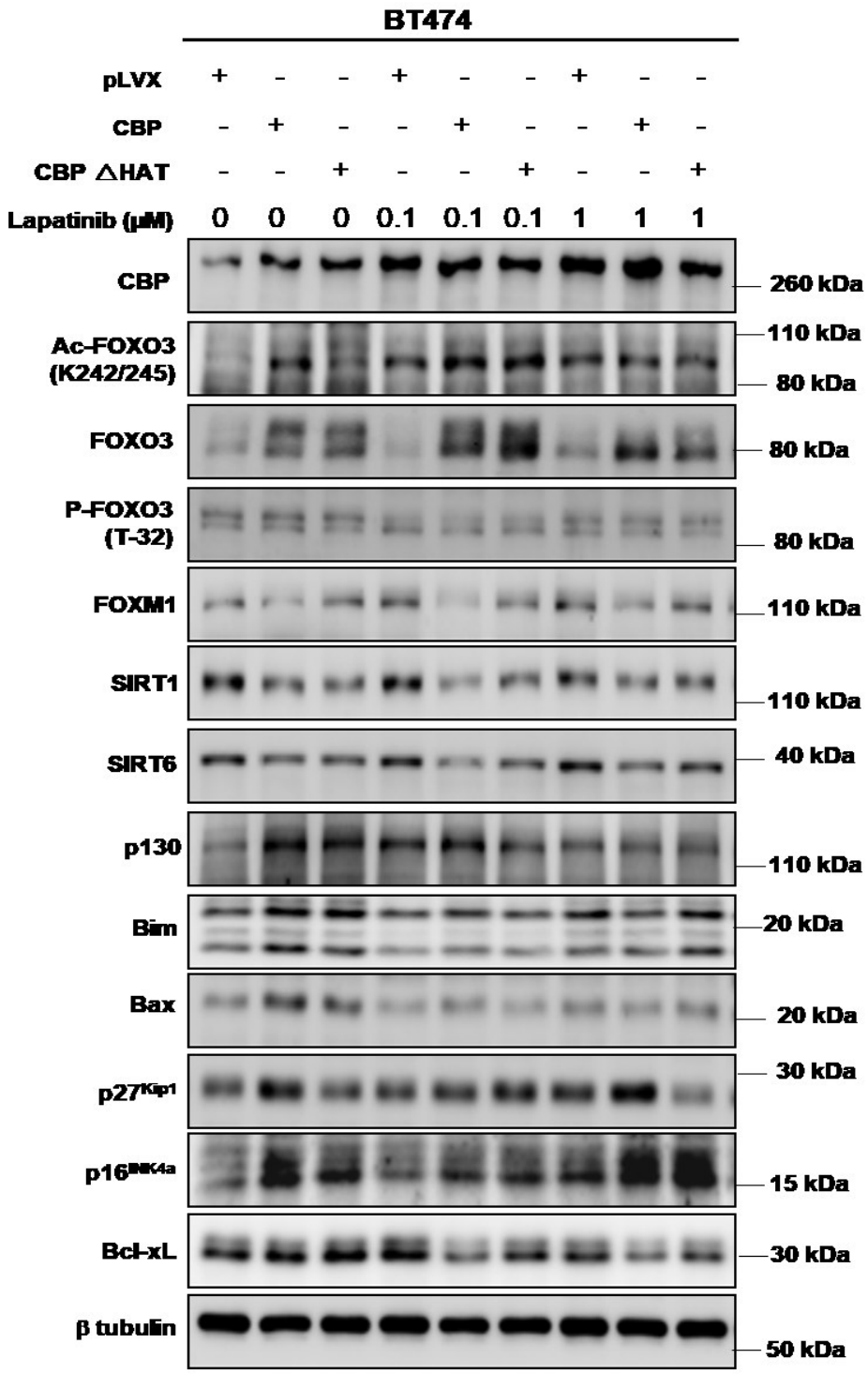


Figure 4.9. CBP overexpression combined with lapatinib upregulates FOXO3 acetylation and its activity. BT474 cells were stably transfected with the empty vector pLVX, the plasmid encoding wild-type CBP, or the one encoding for its acetyl-transferase mutant derivative (CBP △HAT). After 24 hours of seeding, cells were treated with 0, 0.1 and 1 μM lapatinib. Proteins were obtained from whole cell extracts after 24 hours following Lapatinib treatment. Western blotting was performed using the protein lysates to assess the expression levels of CBP, FOXO3 and other indicated proteins.

4.2.8 CBP overexpression augments senescent phenotype in both BT474 and SKBR3 upon lapatinib treatment

To test the role of CBP combined with lapatinib in mediating cell senescence, senescent associated phenotypes in BT474 were elucidated. Firstly, the grade of senescence was examined for the expression of β-galactosidase expression by SA-β-Gal assay. As shown in figure 4.10A, the level of senescence-associated β-galactosidase in the absence of lapatinib treatment was markedly higher in CBP overexpressed cells compared to empty vector transfected cells. In addition, higher numbers of senescent cells were also observed in CBP overexpressed cells upon lapatinib treatment (Figure 4.10A). Similar results were observed in SKBR3 (Figure 4.10B). These results finally suggest a role of CBP in inducing cellular senescence of BT474 as well as SKBR3 when treated alone or combined with lapatinib.

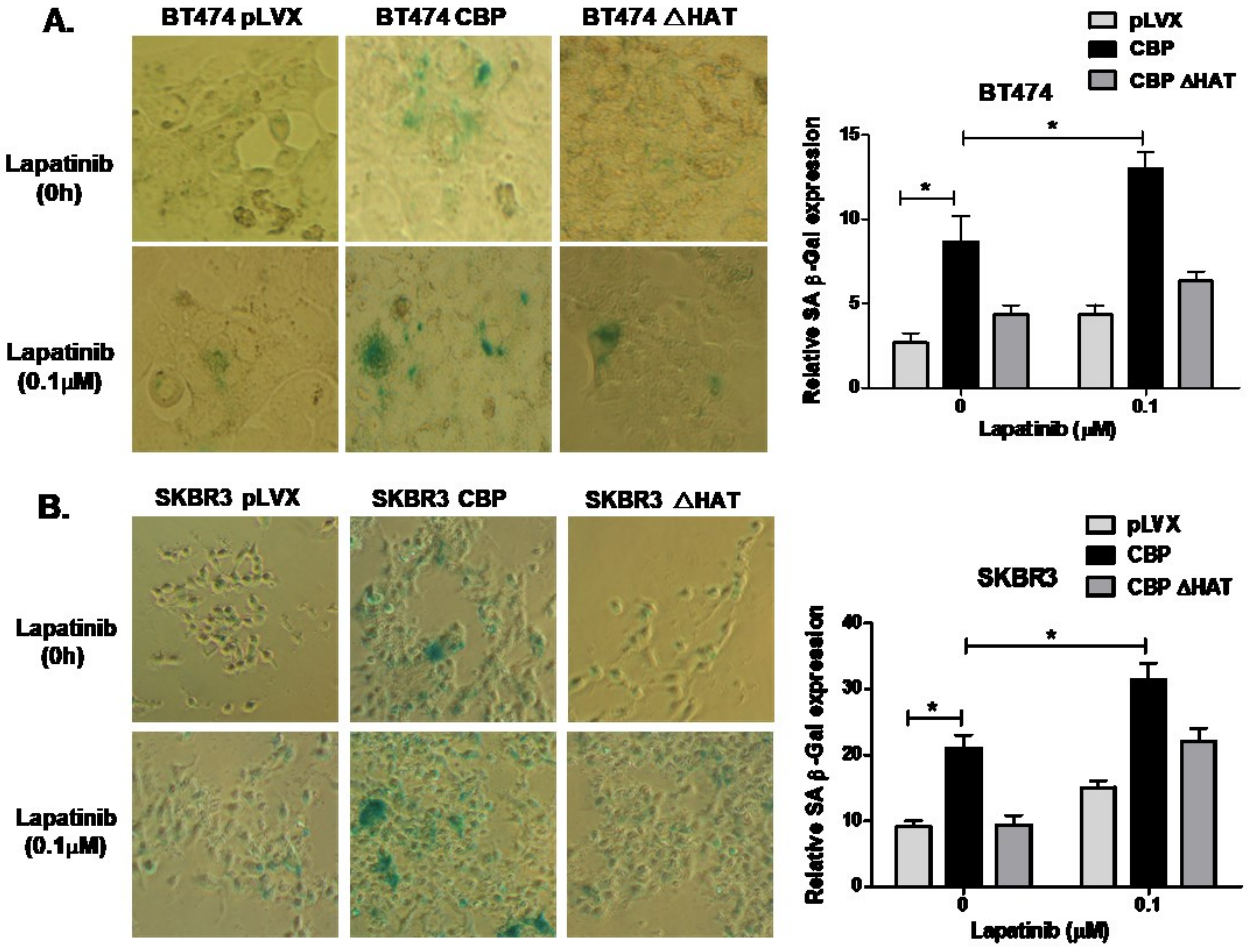


Figure 4.10 CBP overexpression with lapatinib treatment increases SA-β-Gal expression in BT474 and SKBR3 cells. BT474 (A) and SKBR3 (B) cells were transfected with pLVX, CBP and CBP △HAT. Then transfected cells were treated with 0.1 μM lapatinib for 24h. Representative pictures from SA-β-Gal assay are shown. The graph (right panel) represents the relative numbers of β-gal positive cells compared with control from 5 different fields. Bars represent Mean ± SD. Statistical significance was determined by Students t-test (*$p \leq 0.05$ *versus* control).

4.2.9 CBP overexpression facilitates caspase mediated apoptosis in BT474 cells

Apoptosis happens by either death receptor- or mitochondria mediated pathway where initiator caspases (-8 and -9) activate effector caspases 3 or 7 to do final execution [367]. Based on the findings from western blotting and RT qPCR that Bim is up-regulated in CBP overexpressed cells (Figure 4.3), it was asked whether presence of CBP can play any role in regulating the expression of caspase 3/7, -8 or -9. As depicted by caspase Glo assay in figure 4.11, overexpression of CBP in BT474 led to the activation of both caspase-3/7, caspase 8 and -9. Additionally, I found higher level of luminescence from caspase 3/7 or -9 in CBP overexpressing lapatinib treated cells (at 1 μm) (Figure 4.11). Thus, overexpression of CBP led to a significant upregulation ($P<0.05$) of the Caspase-3/7, -8 or -9 activity suggesting that CBP induces caspase mediated apoptosis in BT474 cells.

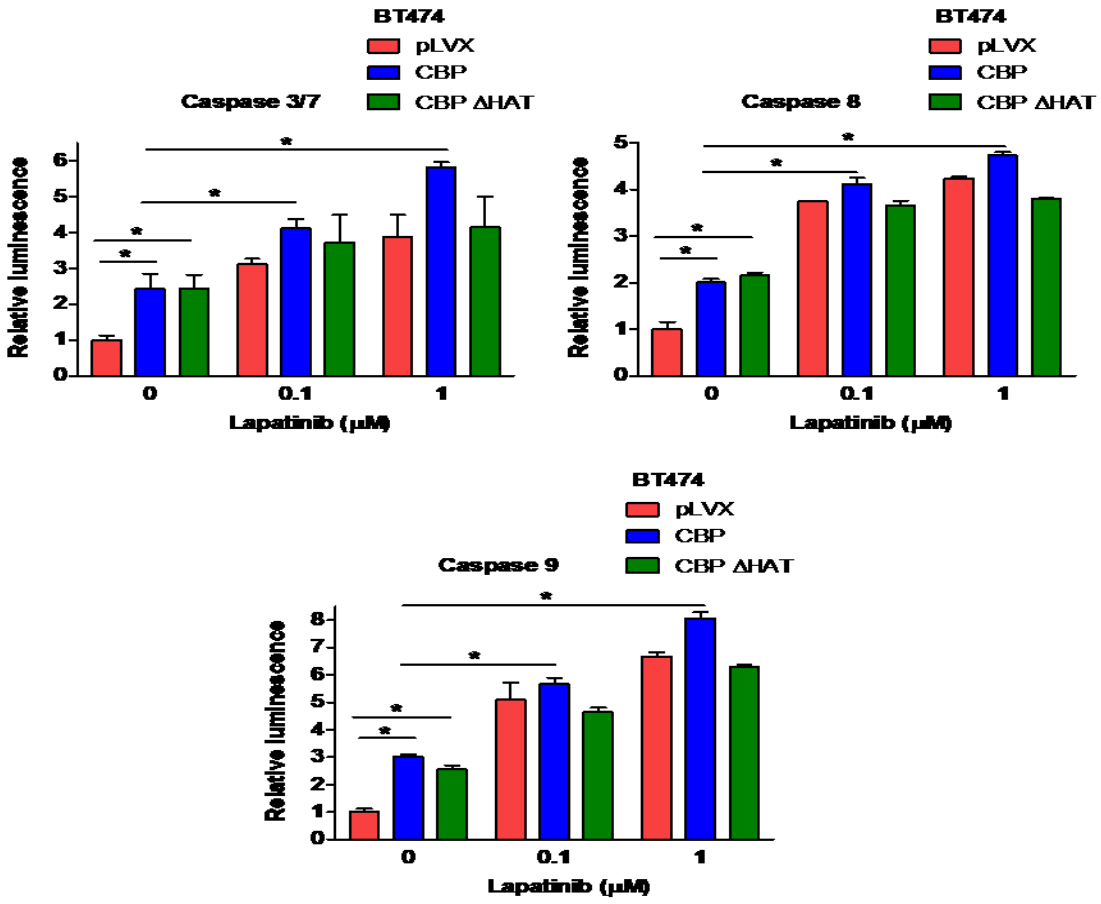


Figure 4.11 CBP overexpressed cells undergo apoptosis via caspase pathway. BT474 cells were stably transfected with, pLVX, CBP and CBP ΔHAT. After 24 hours of seeding, cells were seeded at a density of 10,000 cells/well in white 96-well plates and treated for 24 hours with lapatinib (0, 0.1 and 1 μM). After that, they were treated and incubated for 45 min to an hour with Caspase-Glo® -3/7, -8 and -9 (Promega) reagents and the luminescent signals were read using a luminometer. The values obtained were normalized from the empty vector controls and analyses were performed by student's *t*-test where * $p < 0.05$ was considered as statistically significant.

4.2.10 CBP overexpressing cells gain motility and invasion

In order to assess the functional significance of the CBP overexpression, I used scratch assay and trans-well migration/invasion assay to determine the capacity of cells to acquire motility and invasiveness. Indeed, the migration of CBP overexpressed BT474 cells decreased significantly with respect to control cells which was confirmed by both wound healing scratch assay and trans-well cell migration assay (Figure 4.12 and Figure 4.14). Similar results were also observed in BT474 Lap^R cells (Figure 4.13 and Figure 4.14). In addition, trans-well invasion assay revealed a significant reduction of both sensitive and resistant cell invasion upon CBP overexpression but not upon HAT mutant CBP overexpression (Figure 4.15). Finally, these data suggest CBP mediated inhibition of cell migration and invasion of lapatinib sensitive and resistant BT474 cells.

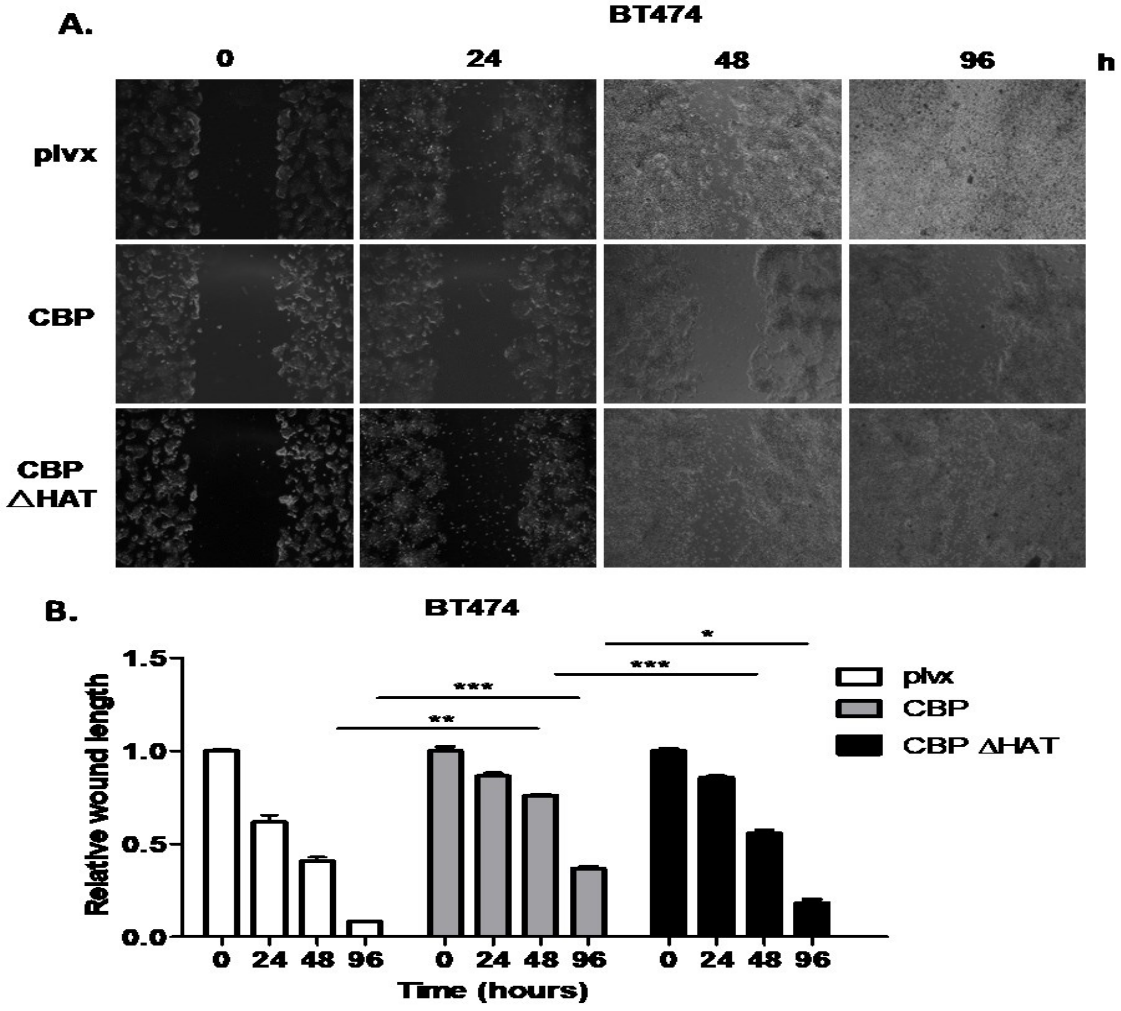


Figure 4.12 CBP impairs BT474 cell motility. (A) BT474 cells were transfected with plvx, CBP and CBP ΔHAT plasmid. Two days after seeding, confluent BT474 monolayer was scratched and monitored at 0, 24, 48, and 96 h. Representative images of wound closure at the beginning and till 96 hour of scratch experiment, 10× magnification. **(B)** Bar graphs showing the relative quantification of the distance between scratch edges. Data are represented as mean ± SD of three independent experiments each with three technical repeats. Statistical significance was determined using Student's *t*-test where * $p < 0.05$, ** $p < 0.01$, *** $p < 0.001$.

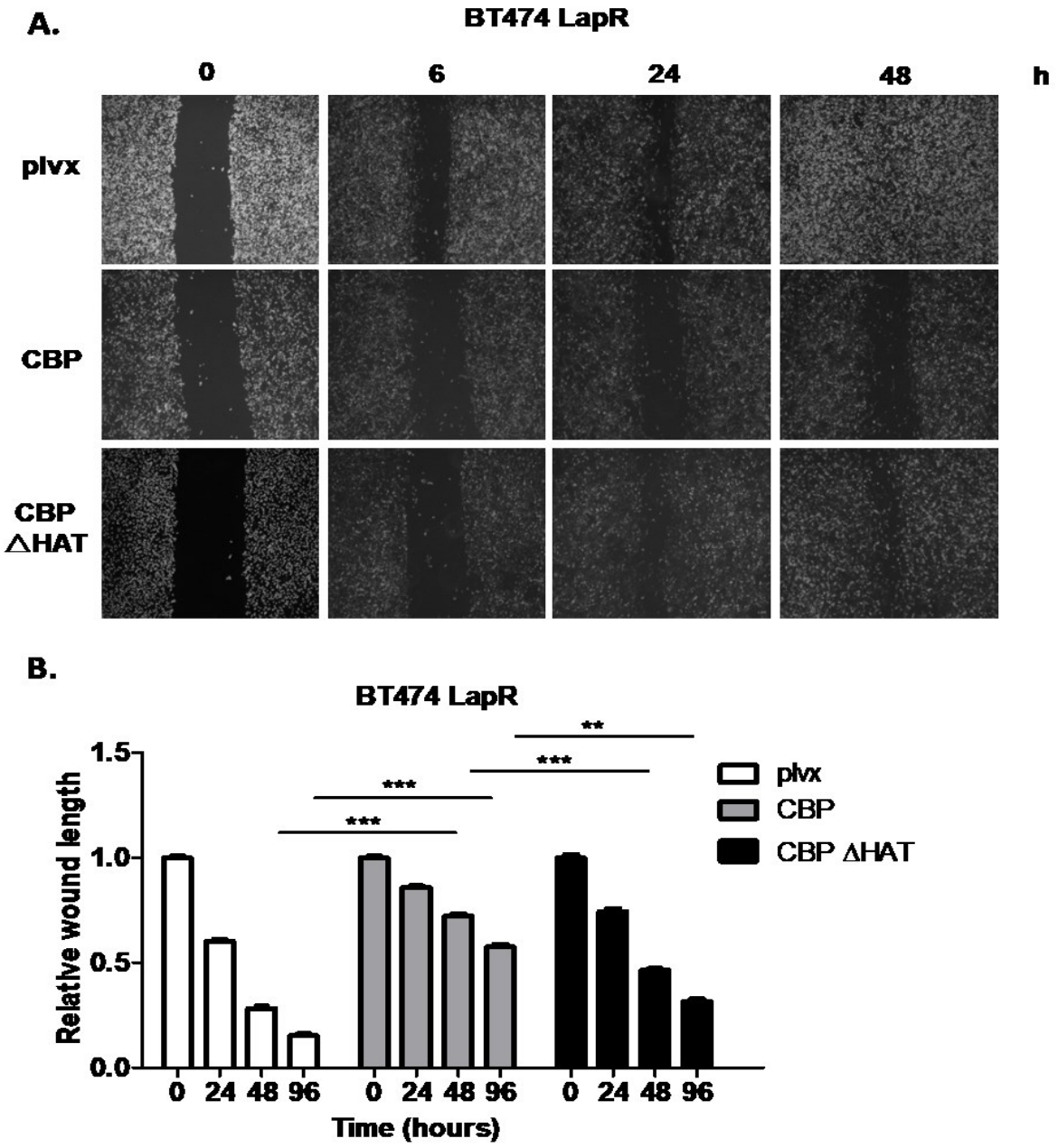


Figure 4.13 CBP impairs BT474 Lap^R cell motility. (A) BT474 Lap^R cells were transfected with plvx, CBP and CBP ΔHAT plasmid. Two days after seeding, confluent BT474 Lap^R monolayer was scratched and monitored at 0, 6, 24, and 48 h. Representative images of wound closure at the beginning and till 48 hour of scratch experiment, 10× magnification. **(B)** Bar graphs showing the relative quantification of the distance between scratch edges. Data are represented as mean ± SD of three independent experiments each with three technical repeats. Statistical significance was determined using Student's *t*-test where * $p < 0.05$, ** $p < 0.01$, *** $p < 0.001$.

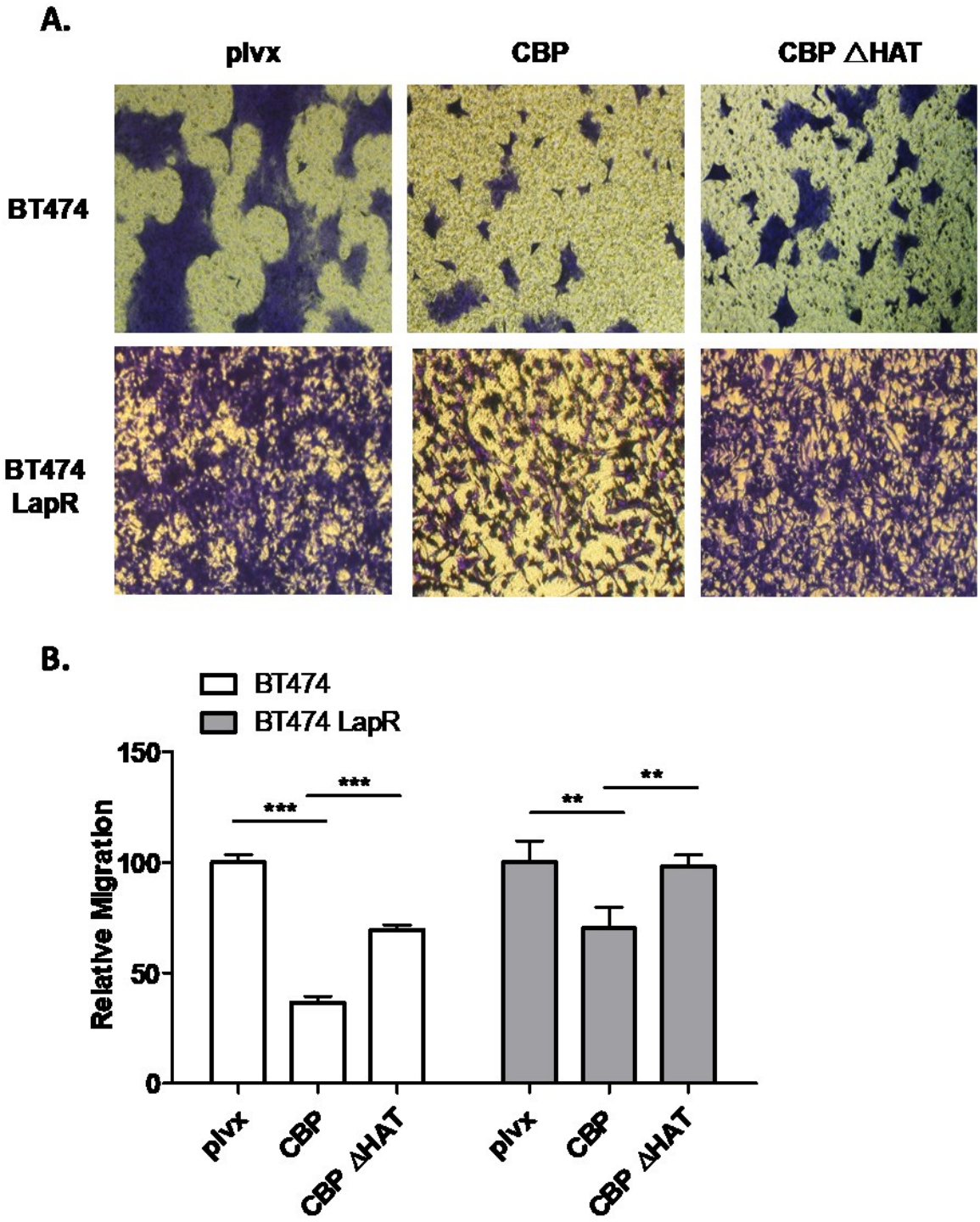


Figure 4.14 CBP overexpression reduces cell migration capabilities. A) For the migration assays through transwells, cells were stained with crystal violet. Representative images are shown. **B)** To obtain numerical data, migrated cells were quantified by ImageJ analysis and represented as mean ± SD of three independent experiments. Statistical significance was determined using Student's *t*-test where * $p < 0.05$, ** $p < 0.01$, *** $p < 0.001$.

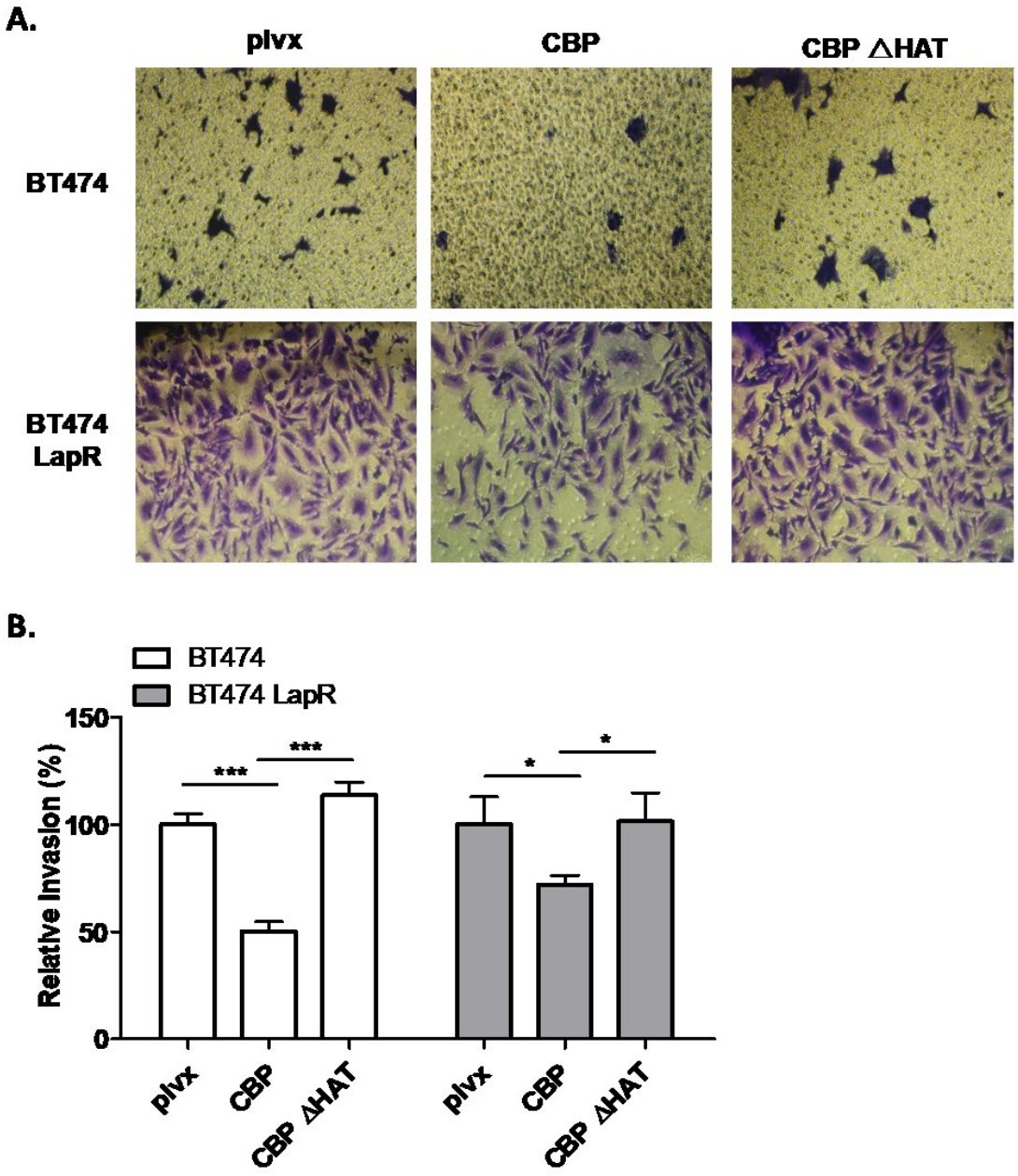


Figure 4.15 CBP overexpression reduces cell invasion capabilities. A) For the invasion assays through Matrigel coated transwells, cells were stained with crystal violet. Representative images are shown. **B)** To obtain numerical data invaded cells were quantified by imageJ analysis and represented as mean ± SD of three independent experiments. Statistical significance was determined using Student's *t*-test where * $p < 0.05$, ** $p < 0.01$, *** $p < 0.001$.

4.2.11 siRNA mediated knockdown of CBP suppresses the expression of Bim, $p27^{Kip1}$, $p16^{INK4a}$ and LC3BII

To examine further the role of CBP in FOXO3 acetylation and activity, siRNA-mediated knockdown of CBP was performed in BT474 and BT474 Lap^R cells. Western blot and RT qPCR analysis confirmed significant knockdown of CBP (Figure 4.16A, B) which in turn reduces FOXO3 acetylation at 242/245 sites. This effect results in a slight decrease of FOXO3 at protein level but significantly at mRNA levels. Sub-cellular fractionation confirms the nuclear localization of CBP and FOXO3 and exhibits a positive co-relation between CBP, FOXO3 and its target genes expression (Appendix Figure A4.1). Moreover, reduced FOXO3 acetylation further inhibits the expression of FOXO3 downstream targets Bim and $p27^{Kip1}$ (Figure 4.16A, B). In effect, de-acetylation of FOXO3 in CBP deficient cells show downregulation of $p16^{INK4a}$, p62 and LC3BII both at protein and mRNA levels (Figure 4.16A, B). Therefore, BT474 cells survive from senescence and autophagic stimulation which increase their growth potential in absence of CBP.

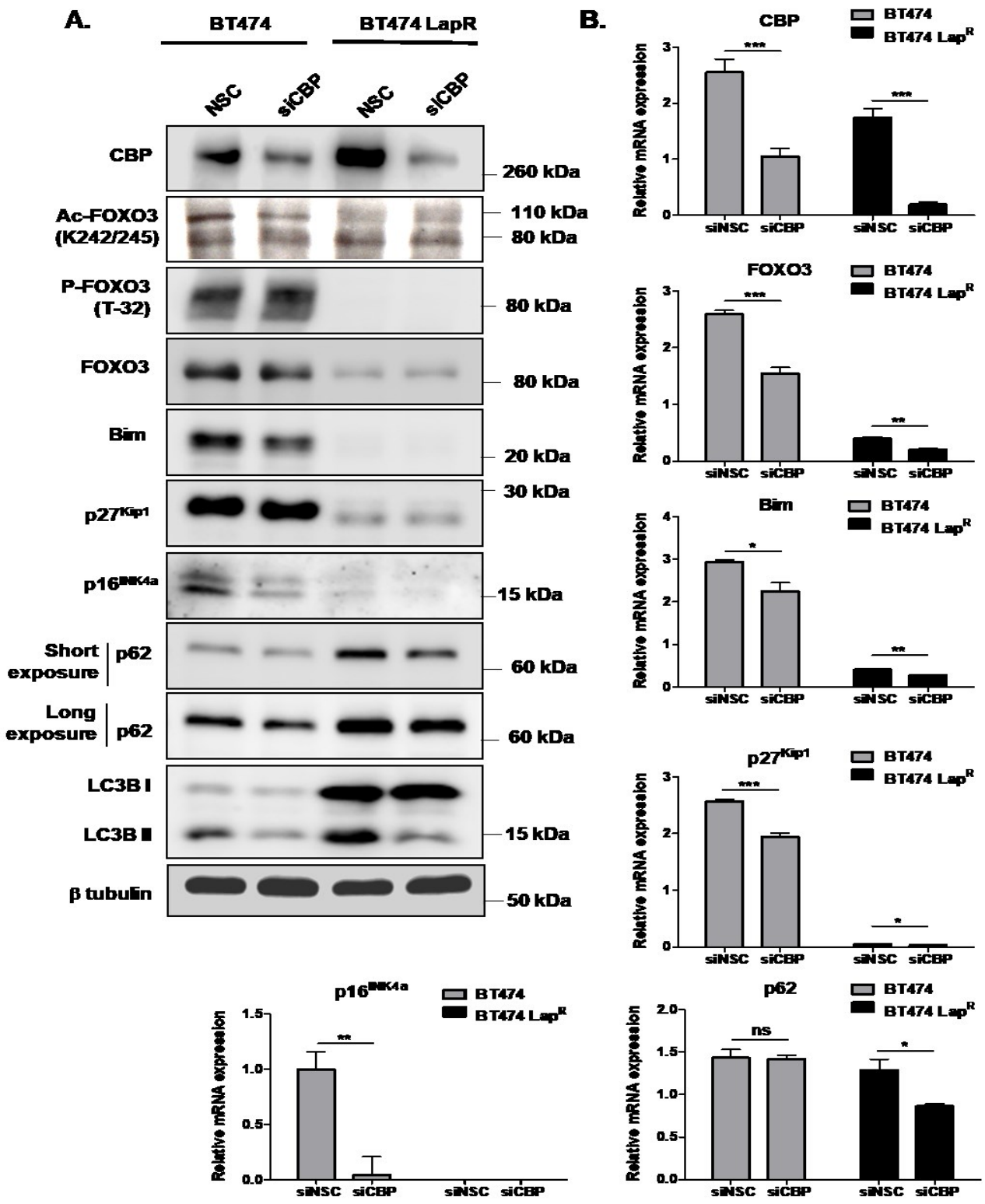


Figure 4.16. Knockdown of CBP inhibits FOXO3 acetylation and its transcriptional activity. A. BT474 and lapatinib resistant BT474 Lap^R cells were transiently transfected with non-targeting control (siNSC) or CBP-targeting siRNA pools. Proteins were isolated from whole cell extract after 48 hours of transfection. Western blot was performed from protein lysates using antibodies against CBP, Ac-FOXO3, FOXO3 and other mentioned. Tubulin used as a protein loading control. **(C)** The mRNA levels of *CBP, FOXO3, p27^{kip1}* and others mentioned genes were assessed by real time qPCR.The RPL19/RPS14 housekeeping gene was used as a control to normalise gene expression. Statistical significance was determined using Student's *t*-test where * $p < 0.05$, ** $p < 0.01$, *** $p < 0.001$.

4.2.12 CBP deficient BT474 cells are resistant to lapatinib

To further assess the role of CBP mediated FOXO3 acetylation in regulating lapatinib sensitivity, I first performed a short-term proliferation assay by using sulphorhodamine-B. Notably, silencing of CBP significantly reduce lapatinib sensitivity compared to its non-silenced counterpart (Figure 4.17A), suggesting that the acetyl-transferase CBP deficiency is responsible for lapatinib resistance. On the contrary, CBP knockdown in BT474-Lap^R cells did not result in any significant effect on lapatinib response and this could be due to the high levels of deacetylases (e.g. SIRTs) in Lap^R cells. Thus, deacetylated FOXO3 may leads to decrease in lapatinib sensitivity in BT474 cells. To elaborate and ascertain this hypothesis, I performed clonogenic assays 24h after siRNA transfection. Indeed, CBP deficient cells showed higher clone formation and reduced lapatinib sensitivity when compared with control cells (Figure 4.17B). However, CBP deficient BT474 Lap^R cells also showed higher clonogenicity which we did not observed in short term SRB assay (Figure 4.17A), suggesting that FOXO3 de-acetylation plays a role in regulating clonogenicity of resistant cells. It is also noteworthy that knocking down of CBP does not affect drug sensitivity in BT474-Lap^R cell lines (Figure 4.17A, B). In summary, all these data suggest that reduced level of FOXO3 acetylation upon CBP silencing results in lapatinib resistance which further enhances cell growth and clonogenicity.

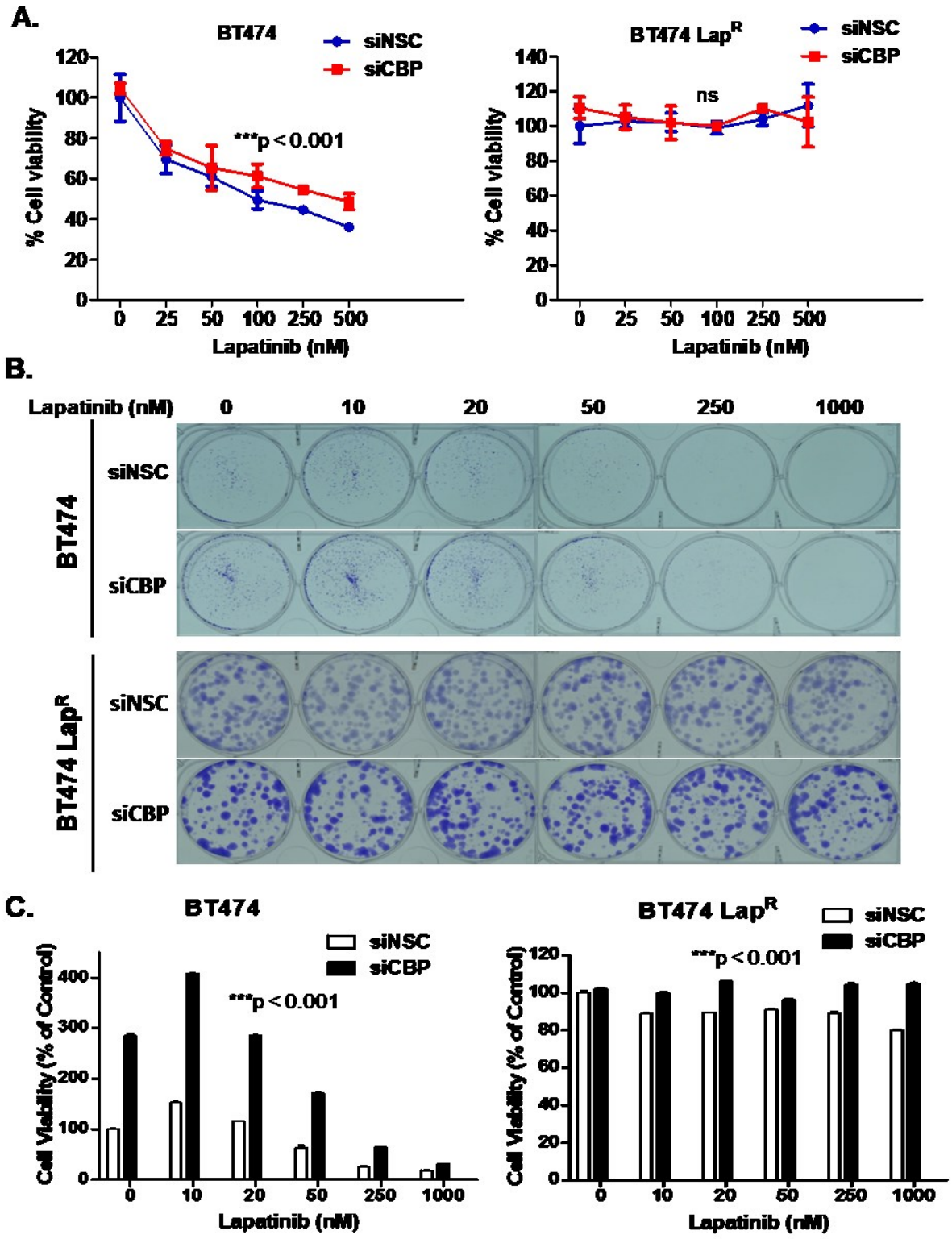


Figure 4.17. CBP deficient cells are resistant to lapatinib compared to non-silenced control.

A. BT474 WT and BT474-Lap^R cells were transiently transfected with siRNA for NSC and CBP. After 24 hours of transfection, cells were seeded in 96-well plates and treated with lapatinib (0 to 500 nM). Twenty-four hours after treatment, cells were fixed and stained with the protein-binding dye SRB. Values obtained were normalized against the corresponding untreated controls and presented as percentages. Data represent means ± SEM (two-way ANOVA; non-significant, ns; significant, ***P<0.001). **B.** Transiently transfected cells were seeded in 6 well plates and on the following day they were treated with the lapatinib concentrations indicated (0, 10, 20, 50, 250, 1000 nM). Twenty-

four hours following treatment the medium was changed and colony formation was allowed for 14 days. Cells were then fixed with 4% para formaldehyde and stained with crystal violet. **C**.The stain was solubilised with 33% acetic acid and absorbance obtained at 592 nm. Data represent the mean ± SEM of three independent transfection experiments and statistical analysis was performed using two-way ANOVA analysis (***p<0.001).

4.2.13 Knockdown of CBP enhances cell migration of both BT474 and BT474 Lap^R

To assess the effect of the silencing of CBP in regulating cell motility, I performed wound healing scratch assay. Figure 4.18 and 4.19 show that siRNA mediated CBP silencing accelerates cell migration capacity of both BT474 and BT474 Lap^R cell lines as the scratch closure was faster in CBP silenced cell lines.

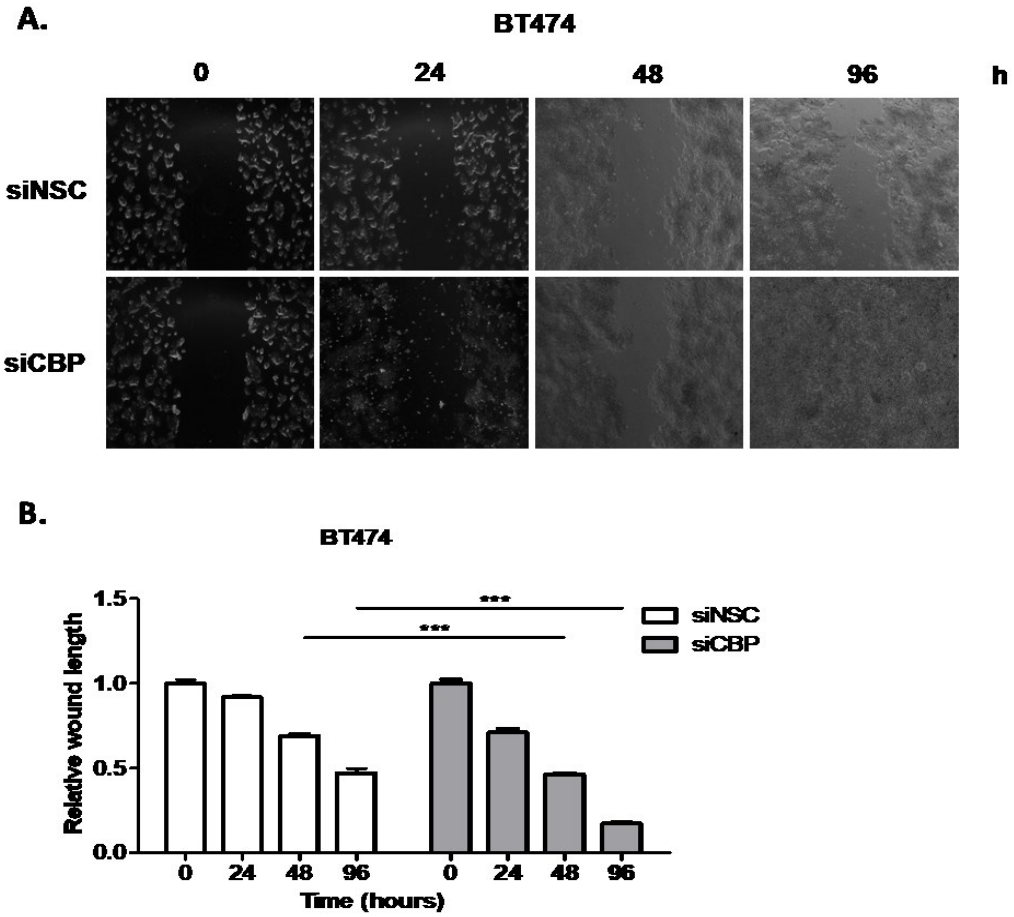


Figure 4.18 Knockdown of CBP enhances BT474 cell motility. (A) BT474 cells were transfected with siNSC and siCBP siRNAs. Two days after transfection, confluent BT474 monolayer was scratched and monitored at 0, 24, 48 and 96 h. Representative images of wound closure at the beginning and till 96 hour of scratch experiment, 10× magnification. **(B)** Bar graphs showing the relative quantification of the distance between scratch edges. Data are represented as mean ± SD of three independent experiments each with three technical repeats. Statistical significance was determined using Student's *t*-test where * $p < 0.05$, ** $p < 0.01$, *** $p < 0.001$.

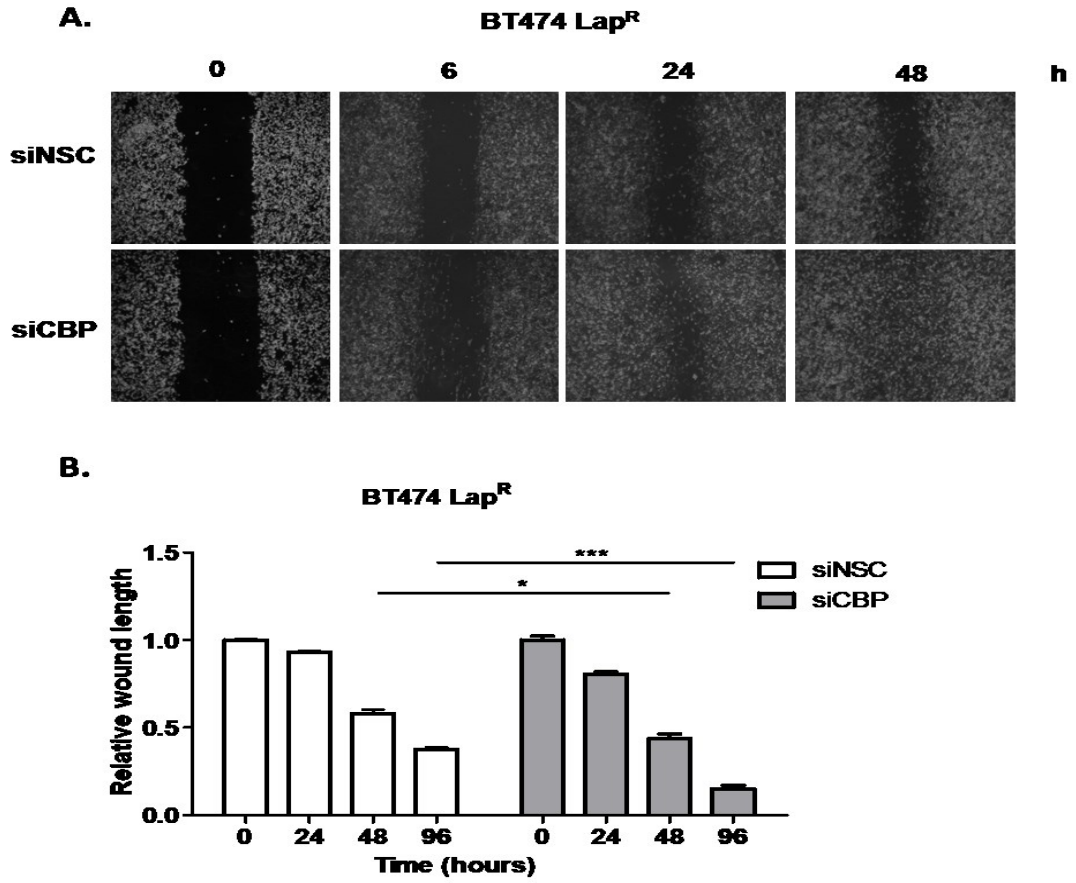


Figure 4.19 Knockdown of CBP enhances BT474 LapR cell motility. (A) BT474 Lap^R cells were transfected with siNSC and siCBP siRNAs. Two days after transfection, confluent BT474 Lap^R monolayer was scratched and monitored at 0, 6, 24, and 48h. Representative images of wound closure at the beginning and till 48 hour of scratch experiment, 10× magnification. **(B)** Bar graphs showing the relative quantification of the distance between scratch edges. Data are represented as mean ± SD of three independent experiments each with three technical repeats. Statistical significance was determined using Student's t-test where * $p < 0.05$, ** $p < 0.01$, *** $p < 0.001$.

4.2.14. Silencing of CBP favours mammosphere formation in BT474 and BT474 Lap^R cells

To further evaluate the role of CBP in regulating tumorigenesis, I conducted a mammosphere formation assay. According to the result shown in figure 4.20, knocking down of CBP helps to produce more or larger stem cell producing spheres formation of BT474 as compared to the non-silencing control (Figure 4.20A). Similar result observed in BT474 Lap^R cells suggesting that CBP also control tumorigenic potential of resistant cells. RT-qPCR result further supported our phenotypic observation as CSC producing genes nanog, sox2 and pou5F1 were found to be increased significantly upon the depletion of CBP especially in BT474 cells (Figure 4.20B). However, enhanced mRNA expression of nanog was observed in BT474

Lap^R cells upon CBP silencing. Thus, silencing of CBP suggestively facilitates sphere formation of both sensitive and resistant BT474 cells.

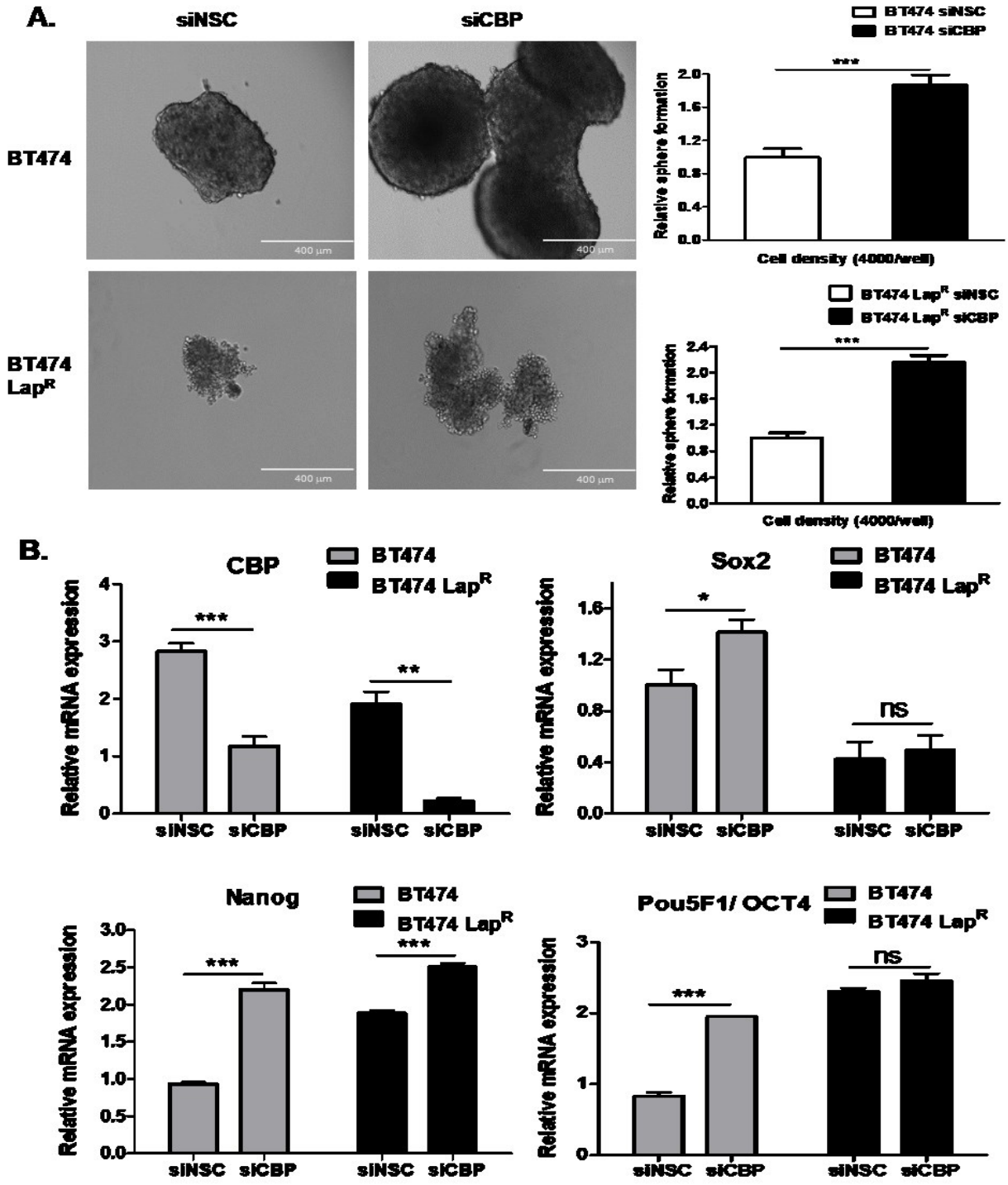


Figure 4.20 Silencing CBP increases sphere forming capacity A. BT474 andBT474 Lap^R cells were transfected with siRNA for NSC and CBP. Then transfected cells were seeded in 6-well low attachment plate and left in growth factor (bFGF, EGF) containing media for 2 weeks. Then formed spheres were counted and representative mammosphere pictures are shown from three independent assay. The graph (right panel of A) represents the relative numbers of mammospheres compared with control. Bars represent Mean ± SD. Statistical significance was determined by Students t-test (***$p \leq 0.001$ *versus* control). **B.** mRNA levels of CBP, sox2, nanog and pou5F1 were examined by RT-qPCR. Statistical significance was determined using Student's t-test where * $p < 0.05$, ** $p < 0.01$, *** $p < 0.001$.

4.2.15 CBP inhibitors C646 and PFCBP1 reduces FOXO3 acetylation and downstream transcriptional activity

In order to assess the role of CBP in drug resistance I used two inhibitors of CBP e.g. C646 and PFCBP1. C646 is a selective and competitive inhibitor of CBP/EP300 which target HAT domain of CBP/EP300 [368]. In contrast, PFCBP1 is a highly selective inhibitor of the CBP bromodomains that are involved in transcriptional regulation through the recognition of acetyl lysine modifications on histone or non-histone proteins [369]. I first performed a drug sensitivity assay using SRB and determined that C646 concentrations up to 10 μM were not highly toxic for BT474 cells and drug resistant derivatives whereas for PFCBP1 up to 20 μM was found to be non-toxic (Figure 4.21A). Then, I performed co-immunoprecipitation assay which confirms a significant reduction of FOXO3 acetylation upon C646 treatment (Figure 4.21B). In addition, western blot and RT-qPCR data reveals that C646 substantially reduces FOXO3 acetylation as well as its transcriptional activity depicted by reduced expression of Bim, $p27^{Kip1}$ and $p16^{INK4a}$ levels (Figure 4.22, 4.23). In contrast, PFCBP1 can reduce FOXO3 acetylation and activity at 10 μM treatment, however, higher (20 μM) PFCBP1 found to increase the expression level of FOXO3 targets may be because of the response to high drug treatment.

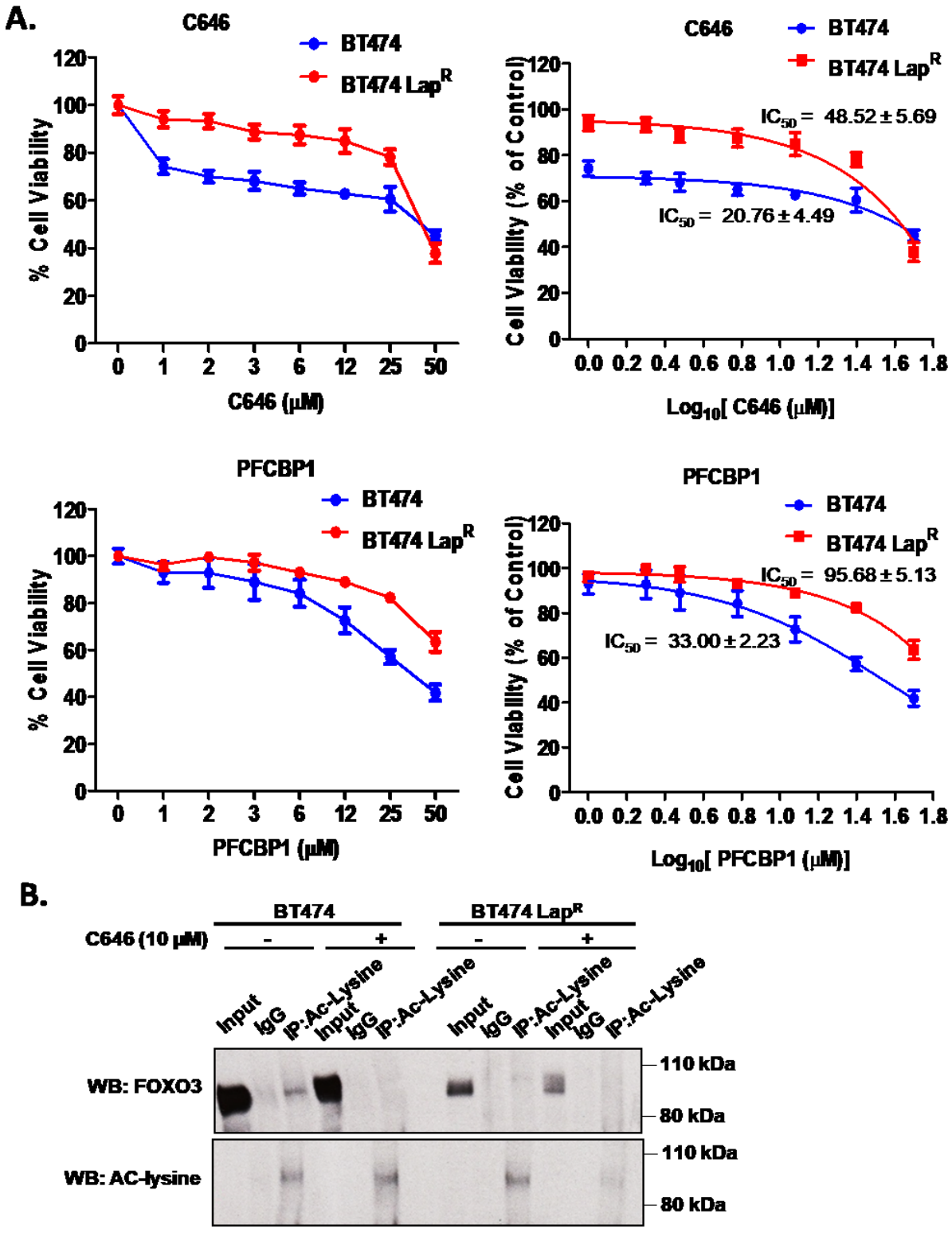


Figure 4.21 Determination of IC50 of C646 and PFCBP1 in BT474 and BT474 Lap^R cells. A. BT474 and BT474 Lap^R cells were seeded in 96 well plates and treated with different concentrations of C646 and PFCBP1 for 72 hours. After treatment cells were fixed with 40% TCA and stained with sulphorhodamine B. Absorbance was taken at 492 nm and data represents mean ± SD from three different experiment (Left panel). Best fit curves were generated to determine IC50 (right panel) **B.** Cells were collected after treatment with 10 µM C646 and co-immunoprecipitation experiment performed by pulling down of Ac-Lysine using antibody against Ac-Lysine. Subsequent western blotting was performed using antibody against FOXO3 and Ac-Lysine.

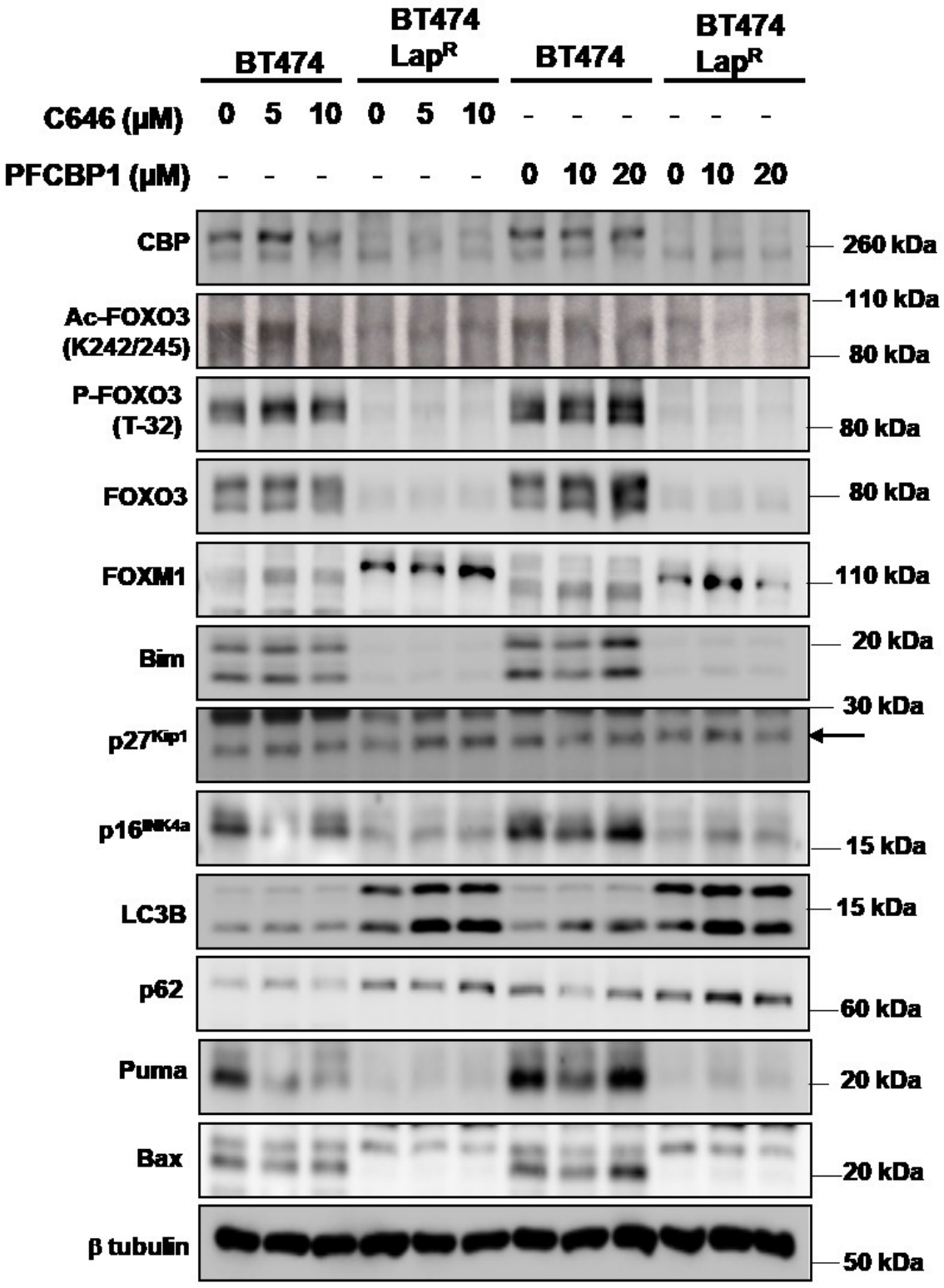


Figure 4.22 CBP inhibitors reduces FOXO3 acetylation and activity. A. BT474 and lapatinib resistant BT474 Lap^R cells were treated with 0, 5 and 10 μM of C646 and with 0, 10 and 20 μM of PFCBP1. Proteins were isolated from whole cell extract after 72 hours of treatment. Western blot was performed from protein lysates using antibodies against CBP, Ac-FOXO3, FOXO3 and other mentioned. Tubulin was used as a protein loading control.

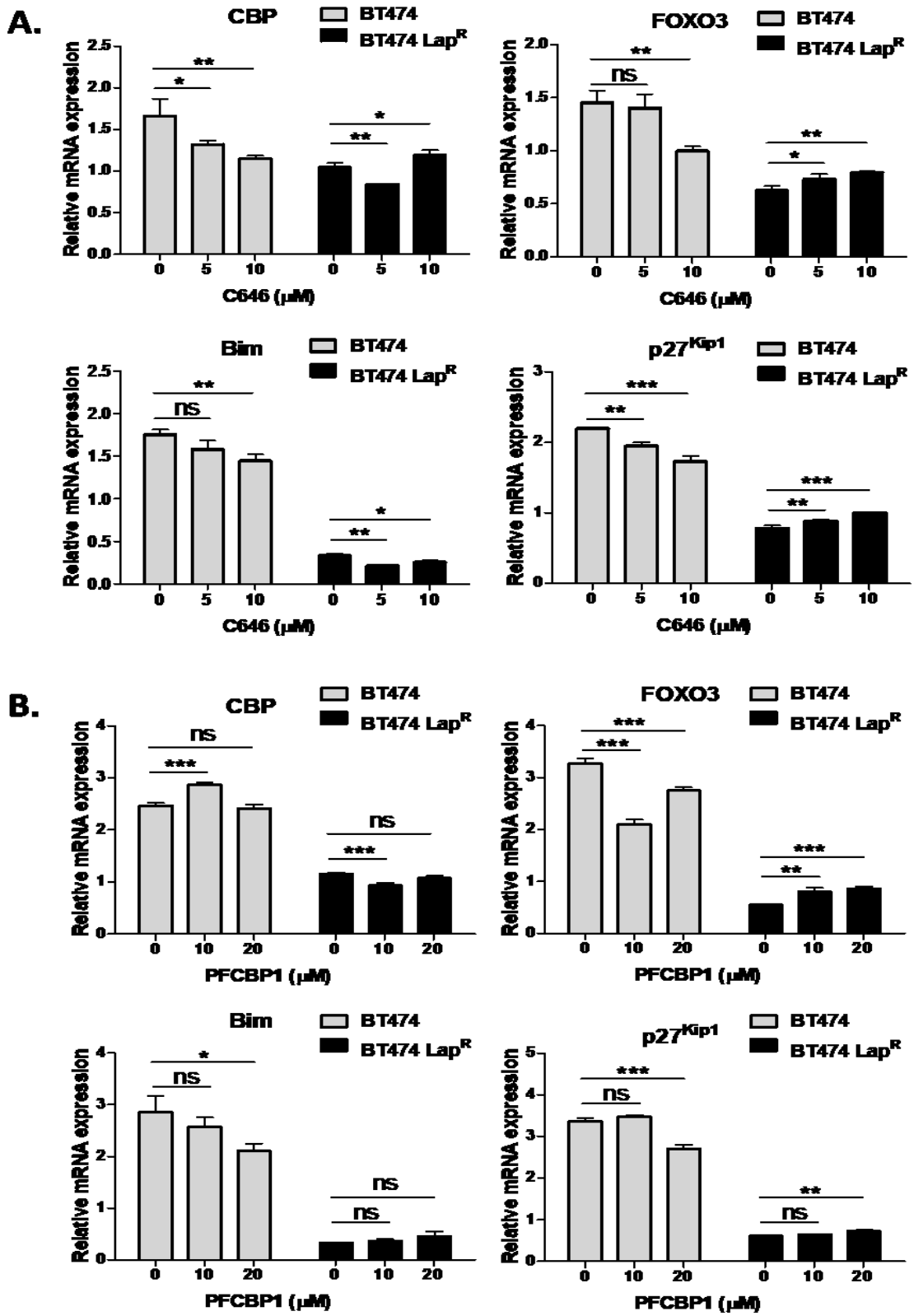


Figure 4.23 CBP inhibitors reduces FOXO3 expression and its transcriptional activity. BT474 and lapatinib resistant BT474 Lap^R cells were treated with 0, 5 and 10 μM of C646 **(A)** and with 0, 10 and 20 μM of PFCBP1 **(B)**. The mRNA levels of *CBP, FOXO3, p27^{kip1}* and *Bim* genes were assessed by real time qPCR. The RPL19/RPS14 housekeeping gene was used as a control to normalise gene expression. Data were analyzed by one-way ANOVA and presented as means ± SEM (***$p < 0.001$, **$p < 0.01$, *$p < 0.05$, ns=non-significant).

4.2.16 CBP inhibitors C646 and PFCB1 increases clonogenic potentiality of BT474 cells

In agreement with the inhibitor's experiments, I asked whether C646 or PFCBP1 could affect lapatinib sensitivity of WT and resistant BT474 cells. For this I performed long-term clonogenic assays to identify cells that survive and form clones after lapatinib treatment. When wild type BT474 cells were treated with both C646/PFCBP1 the generation of resistant clones increased significantly (approximately 2.4-fold in BT474 cells treated with 10 μM C646; and~1.90 fold in BT474 cells treated with 20 μM PFCBP1) (Figure 4.24). However, C646 or PFCBP1 did not induce any significant effect in the generation of clones from resistant BT474 Lap^R cells. Notably, CBP inhibition was not found to increase lapatinib sensitivity in BT474 cells. Thus, pharmacological inhibition of CBP enhances cell growth and colony formation efficiency of BT474 cells. To date, inhibition of CBP resulted in significant reduction of lapatinib resistance of BT474 Lap^R cells (Figure 4.25) suggesting a vulnerable role of CBP in resistant cells. This also suggest that CBP mediated FOXO3 acetylation is deregulated in lapatinib resistant cell lines.

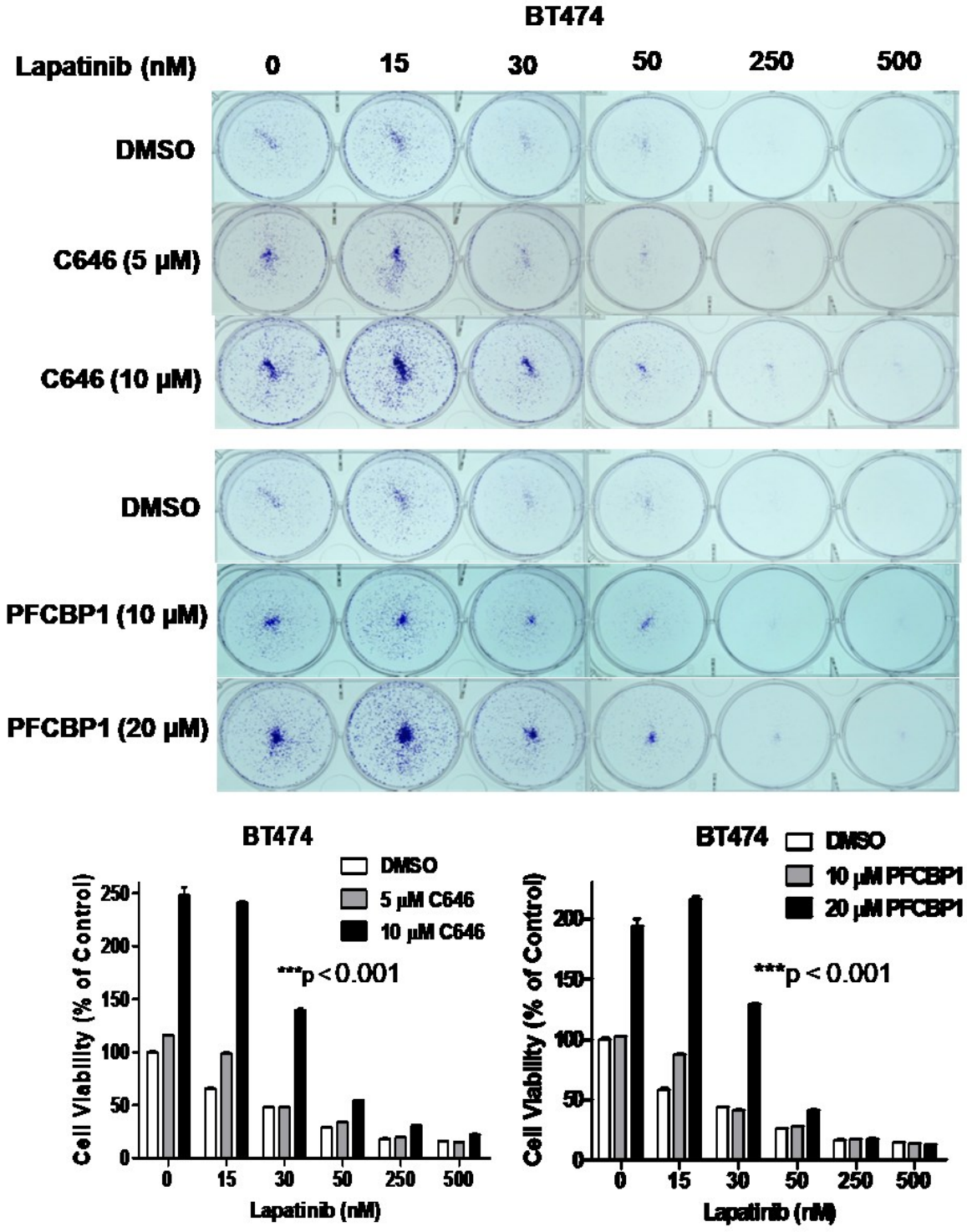


Figure 4.24. CBP inhibition increases clonogenic potential in BT474 cells. BT474 cells were seeded in 6-wells plate and on the following day they were treated with 0, 5 and 10 µM of C646 and with 0. 10 and 20 µM of PFCBP1. After 24 hours of drug treatment, cells were treated with lapatinib (0 to 500 nM). Twenty-four hours following lapatinib treatment the medium was changed, and colony formation was allowed for 21 days. Cells were then fixed with 4% para formaldehyde and stained with crystal violet. The stain was solubilised with 33% acetic acid and absorbance obtained at 592 nm. Data represent the mean ± SEM of three independent transfection experiments and statistical analysis was performed using two-way ANOVA analysis (***p<0.001).

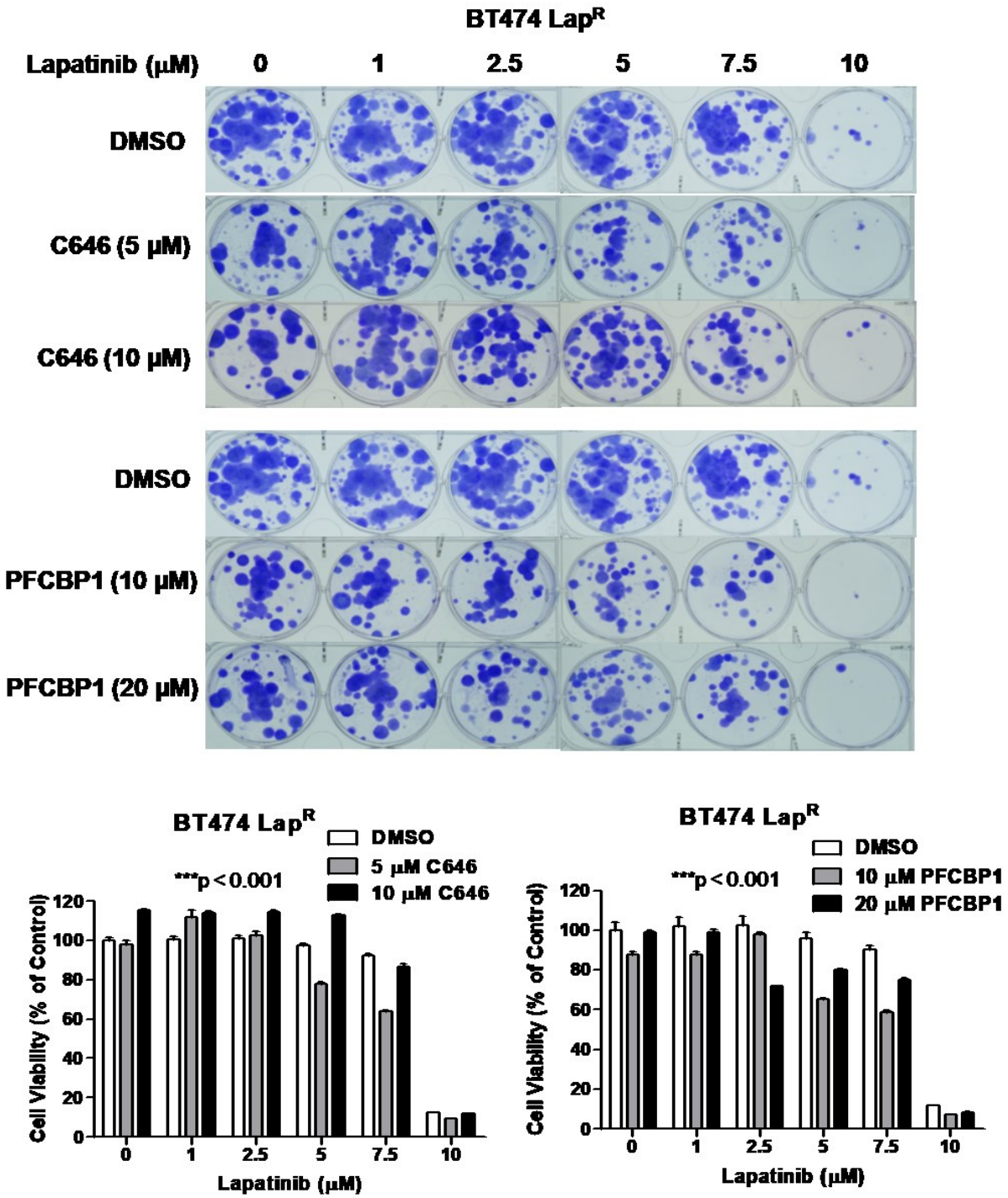


Figure 4.25. CBP inhibition reduces lapatinib resistance in BT474 Lap^R. BT474 Lap^R cells were seeded in 6-wells plate and on the following day they were treated with 0, 5 and 10 μM of C646 and with 0. 10 and 20 μM of PFCBP1. After 24 hours of drug treatment, cells were treated with lapatinib (0 to 10 μM). Twenty-four hours following lapatinib treatment the medium was changed, and colony formation was allowed for 14 days. Cells were then fixed with 4% para formaldehyde and stained with crystal violet. The stain was solubilised with 33% acetic acid and absorbance obtained at 592 nm. Data represent the mean ± SEM of three independent transfection experiments and statistical analysis was performed using two-way ANOVA analysis (***p<0.001).

4.3 Discussion

FOXO transcription factors play a significant in maintaining cellular homeostasis and their activity is tightly controlled by PTMs that are differentially induced according to the type of growth factor, oxidative stress and other environmental stimulus present [226]. FOXO PTMs often regulated by CBP acetyltransferases and play a vital role in defining the FOXO protein's function and activity in cancer initiation and progression. Of all PTMs, acetylation has been identified as a novel axis regulating FOXO3. However, it is still controversial as to whether FOXO3 acetylation enhances or reduces its DNA binding ability and consequent transcriptional activity [204, 252]. Therefore, I sought to better characterise the significance of CBP-mediated regulation and potential acetylation of FOXO3 and how this affects the anti-proliferative and pro-apoptotic functions of the tumour suppressor in drug sensitive and resistant BT474 cells.

To determine a potential linkage between FOXO3 acetylation and lapatinib resistance, FOXO3 and its modified form acetylated Ac-FOXO3 were evaluated in both sensitive and resistant BT474 cells. Interestingly, the level of FOXO3 and Ac-FOXO3 was found to be high in BT474 and low in resistant breast cancer cells BT474 Lap^R. Time-course treatment with 1 μM lapatinib appeared to enhance Ac-FOXO3 levels which is also positively correlated with increased CBP levels. On the other hand, CBP and Ac-FOXO3 remained relatively constant in BT474 Lap^R cells. This can be explained by increased FOXO3 de-acetylation as a result of high SIRTs expression in resistant BT474 cells. Furthermore, SIRT1 induced de-acetylation of FOXO3 has been reported to inhibit CBP/EP300-mediated transactivation of FOXO3 and promote stress resistance and longevity [184, 204]. In addition, upregulation of sirtuin has shown to suppress apoptosis in cancer cells which in turn leads to drug resistance [227, 251]. Therefore, higher SIRTs expression in resistant cells cpuld be responsible for the low levels of FOXO3 acetylation. We also found that lapatinib treatment upregulates CBP and EP300 protein levels as well as $p27^{Kip1}$ expression, suggesting that CBP mediated acetylation of FOXO3 activates its target gene expression involved in cell cycle arrest in sensitive cells. Moreover, concomitant increase of p62 and LC3B upon lapatinib treatment suggest that CBP mediated FOXO3 acetylation is involved in autophagy induction of sensitive BT474 cells.

These data thus far have suggested that the levels of FOXO3 and its acetylated form are involved in regulating lapatinib sensitivity of BT474 cells.

To evaluate the effect of CBP mediated FOXO3 acetylation more thoroughly, I performed stable over-expression of wild-type CBP as well as the acetyl-transferase mutant (ΔHAT) CBP in both sensitive and resistant BT474 cells. Protein levels of total FOXO3, as well as Ac-FOXO3 were found to be increased upon CBP over-expression in sensitive BT474 but not in Lap^R cells. The increased acetylation of FOXO3 further increased its transcriptional activity as revealed by the elevated expression of p130, Bim, $p27^{Kip1}$ and $p16^{INK4a}$ expression from both western blot and RT qPCR results (Figure 4.2 and 4.3). In fact, CBP has been shown to cause an increase of FOXO3 downstream transcriptional activity [370]. Moreover, RT-qPCR analysis revealed a significant role of CBP in suppressing the expression of ABC transporter genes such as ABCG2, ABCC1 and ABCC4.

Protein-protein interaction plays an important role to induce any modification of neighbour proteins. Previous report predicted possible interaction between CBP and FOXO3 [371]. For this reason, I performed co-immunoprecipitation assays in order to monitor the FOXO3-CBP interaction and how this impact on FOXO3 post-translational modifications. Co-IP results have shown that the FOXO3 acetylation increases upon CBP overexpression in lapatinib sensitive BT474 cells (Figure 4.6). Then, I checked the interaction of CBP and FOXO3 by co-immunoprecipitation assay. Expectedly I found higher interaction in CBP overexpressed cells compared to the empty vector and HAT mutant transfected BT474 cells. This result further confirmed that CBP mediated FOXO3 acetylation requires close proximity of CBP and FOXO3 and thus proving their protein-protein interaction.

To investigate the role of FOXO3 acetylation in drug response and its potential involvement in resistance, I subsequently employed short- and long-term drug sensitivity assays. Over-expression of CBP resulted to increased lapatinib cytotoxicity in sensitive BT474 cells, as indicated by the SRB and clonogenic assays (Figure 4.6A,B). On the contrary, ectopic expression of CBP in Lap^R cells did not seem to have any significant effect until 24 hours post-treatment, where cells were found to show decreased survival when compared to their respective negative

controls (Figure 4.6B). Using the SRB data I can suggest that Lap^R cells do not show an elevated drug response upon CBP over-expression, since percentage survival remains relatively constant in the presence and absence of lapatinib. However, CBP overexpression in resistant cells reduces cell proliferation and clonal survival. This suggests that an increased acetyl-transferase activity can induce apoptosis or inhibit cell cycle progression upon CBP over-expression in resistant cells [372, 373]. Furthermore, BT474 cells transfected with the acetyl-transferase mutant showed similar drug response at all timepoints as the pLVX transfected ones, thus raising the possibility that wild-type BT474 cells have a non-functional or mutated form of CBP that does not possess normal acetyl-transferase activity. Moreover, overexpression of CBP HAT mutant was found to restrict long-term clonal survival in resistant cells (Figure 4.6B), suggesting the presence of a CBP threshold level in BT474 Lap^R cells.

Overexpression of CBP in BT474 and Lap^R cells leads to a less aggressive phenotype, characterized by reduced mammosphere formation capacity confirmed by sphere formation assay. Moreover, the reduced expression of nanog, sox2 and pou5F1 upon CBP overexpression further supported the role of CBP in suppressing the expression of stem cell markers. This is accompanied by increases in cell migration and invasion. Thus, in BT474 sensitive and resistant cells, CBP has a traditional tumour suppressive, metastasis inhibiting role. I further asked whether CBP overexpression combined with lapatinib can increase FOXO3 acetylation and activity rather than CBP alone (Figure 4.9). I found that lapatinib treatment has additive effect along with CBP overexpression to induce FOXO3 acetylation and its transcriptional activity. For example, 0.1 μM lapatinib induces FOXO3 acetylation and its activity when combined with CBP overexpression rather than CBP overexpression only. Functionally, I found that CBP overexpression and combined 0.1 μM lapatinib treatment induces cellular senescence phenotype compared to CBP overexpressed cell without lapatinib. In SKBR3 cells I also found similar cell senescence phenotype. Furthermore, caspase Glo assay revealed that the apoptotic pathway is based on caspase mediated pathway where CBP and lapatinib treatment enhances caspase 3/7, caspase 8 and caspase 9 expression although the expression level is higher in combination treatment.

Next, I wanted to check the role of CBP by knocking down of CBP expression in both sensitive and resistant cells. To my observations, CBP knockdown reduces FOXO3 acetylation in BT474 cells whereas in Lap^R cells it is almost similar suggesting that depletion of CBP does not affect FOXO3 acetylation in resistant cells because of the lower level of FOXO3 in resistant cell lines. In addition, decreased acetylated FOXO3 further reduces FOXO3 transcriptional activity as revealed by low levels of Bim, $p16^{INK4a}$ and LC3B both at protein and mRNA levels. I also found that siRNA mediated CBP knockdown increases lapatinib resistance as proved by SRB assay. However, in terms of long term clonogenic assay, CBP knockdown found to increase cell viability but not affecting lapatinib sensitivity both in sensitive and resistant cells (Figure 4.17).

Furthermore, silencing of CBP was found to be responsible for favouring mammosphere formation which was also confirmed by the upregulation of stem cell markers including nanog, sox2 and pou5F1. Knocking down of CBP also enhances cell migration of both BT474 and Lap^R cells suggesting the role of CBP in regulating cell motility. To further elucidate the role of CBP, I used a pharmacological approach to inhibit CBP acetyl-transferase activity and to inhibit its bromodomain activity. C646 was used as a HAT inhibitor and PFCBP1 was used as bromodomain inhibitor. C646 reduces FOXO3 acetylation as confirmed by co-IP experiment which in turn reduces FOXO3 expression and activity as revealed by western blot data (Figure 4.22). PFCBP1 also reduces FOXO3 acetylation and its activity suggesting the involvement of CBP bromodomain in FOXO3 acetylation. Finally, drug resistance clonogenic assay revealed a significant role of CBP inhibitor to increase cell proliferation and lapatinib resistance suggesting that reduced FOXO3 acetylation upon inhibition of CBP may responsible for lapatinib resistance.

Taken together, in this study I have identified a role of CBP-mediated FOXO3 acetylation in the regulation of tumorigenesis and lapatinib sensitivity of breast cancer. My results have suggestively concluded that lapatinib responses are mediated by CBP induced FOXO3 acetylation and subsequent activation of its target genes, potentially through the induction of cell senescence and apoptosis.

CHAPTER 5

Elucidating the role of SIRT2 in regulating FOXO3 acetylation as well as lapatinib sensitivity of breast and nasopharyngeal cancer

5.1 Introduction

Sirtuins (silent information regulator 2–related proteins) belong to the histone deacetylase (HDAC) family of enzymes, which have been grouped into four major classes based on homology to proteins found in yeast [374] Class I, II and IV HDACs are Zn^{+2} dependent, whereas the sirtuins employ as NAD^{+} protein deacetylase [375]. Seven isoforms of the Sirtuins (SIRT1-7) have been identified in humans, which varies in terms of cellular localization, function and specificity. Sirtuin 1 (SIRT1) and sirtuin 2 (SIRT2) are the most studied proteins and can shuttle between the nucleus and the cytoplasm. Moreover, SIRT1 and SIRT2 have been shown to deacetylate a number of histone lysine residues, such as histone H3 lysine 9 (H3K9ac), H3K14ac, H3K16ac (by SIRT1) and H3K9ac (by SIRT2) [265-267]. In addition, these sirtuins act upon both histone and non–histone substrates, including chromatin–associated proteins (EP300, Suv39h1, EZH2), stress–related proteins (p53, NF-kB, c–Jun), DNA–repair proteins (Ku70, XPA, PARP1), and proteins involved in metabolism (ACS1/2, LXR, FXR, GDH), as well as numerous others (alpha–tubulin, CDH1, cyclophilin D) [376]. Therefore, sirtuins play a significant role in various biological processes such as ageing, inflammation, metabolism, autophagy, and DNA repair [377-380].

Since SIRT2 regulates the cell cycle during mitosis, it is expected that its deregulation has been linked to a variety of cancers [270-280]. However, the role of this protein in cancer is multifaceted and likely context specific. For example, a selective SIRT2 inhibitor has been recently shown to result in proteolytic degradation of c–Myc [281], suggesting SIRT inhibition to be a strategy to combat c-Myc driven cancers. Aside from cancer, deregulation of SIRT2 has been linked to type II diabetes [381-383], bacterial infections [384], cardiovascular diseases [385] and neurological disorders [386-389], assuring its potential therapeutic importance. Given the fact that there is still much to be learnt about the precise role of SIRT2 in human biology and diseases, the availability of well-characterised and selective inhibitors is of prime importance to assist with further validation of this promising target. A number of small molecule SIRT2 inhibitors have been reported, including the physiological sirtuin inhibitor nicotinamide and its derivatives [297-299], sirtinol and analogues [390], cambinol [300, 301], benzamide [391], and derivative [392], AGK2 [302] and bicyclic pyrazoles [393].

Nasopharyngeal carcinoma (NPC) is a malignancy of head and neck epithelial cells that originates from the nasopharyngeal cavity. NPC is an important health problem in Southern China and Southeast Asia [39], with about 86,500 NPC new cases recorded annually, and over 40,000 deaths from the disease every year in Asia alone [394]. The most common treatment for NPC is the combination of radiotherapy and chemotherapy. Radiotherapy is a mainstay for treatment for early NPC, while chemotherapy is frequently used for the advanced locoregionally NPC. It has been shown that the combination of chemotherapy and radiation enhances the survival rates [395]. However, advanced NPCs usually fail to respond to chemotherapy treatment because of the development of drug resistance that leads to metastasis and relapse, resulting in poor prognosis [396]. In consequence, there is an urgent need for the identification of novel therapeutic strategies as well as the mechanisms of chemotherapeutic resistance for NPC. To date, the mechanisms for the development of resistance to conventional therapeutics, such as CDDP, paclitaxel (PTX), 5-fluorouracil (5-FU), and vincristine (VCR) have been extensively studied [397-400]. These include overexpression of multidrug-resistant genes, enhanced DNA repair, deregulation of apoptosis, and/or modifications of drug targets [397-400].

Both the epidermal growth factor receptor (EGFR) and HER2 (human epidermal growth factor receptor 2; ERBB2) are commonly overexpressed in NPC [401, 402]. Moreover, activation of EGFR/HER2 pathway has also been shown to promote NPC progression and invasion [403]. Previous studies have demonstrated that the dual EGFR/HER2 tyrosine kinase inhibitor, lapatinib, can restrict cell proliferation and invasion, and promote anoikis in NPC cells [404, 405]. Despite its promising efficacy, lapatinib has a half maximal inhibitory concentration (IC_{50}) in the micromolar range in most cell lines [405], and strategies to sensitize NPC to lapatinib are currently under investigation.

FOXO3 and FOXM1 are members of the forkhead box transcription factor family which play opposite roles in tumorigenesis, drug resistance and cancer progression. FOXO3 is a key tumour suppressor which functions downstream of the PI3K/AKT (protein kinase B) signalling pathway. Conversely, FOXM1 is an important oncogene that promotes cell transformation, cancer progression and resistance to

chemotherapy. In addition, FOXM1 and FOXO3 negatively regulate the expression of one another and compete for same binding sites to promote or inhibit the transcription of target genes [406]. Furthermore, FOXO3 has also be shown to be regulated by post-translational modifications, such as phosphorylation, methylation, ubiquitination, glycosylation and acetylation. The reversible acetylation/deacetylation of FOXO3 is regulated by class I histone deacetylases (HDACs) as well as class III HDACs named sirtuins (SIRT 1-7) and histone acetyl transferases (HATs e.g. EP300/CBP) [407]. The function of SIRT proteins is to reverse the acetylation of FOXO3 to induce the cell cycle arrest, protection from oxidative stress and to repress the expression of apoptotic genes [408]. In NPC cells, FOXM1 is overexpressed and it is associated with cancer metastasis and chemoresistance [409, 410]. In NPC patients, low FOXO3 and high HIF-1 expression has been found to be correlated with poor prognosis [411]. However, the role and regulation of FOXO3 and FOXM1 in NPC have not been not fully investigated.

In this study, we investigated the role of SIRT2 in regulating FOXO3 deacetylation as well as in lapatinib response of HER2 positive breast cancers and metastatic NPC cells. We found that the deacetylation of FOXO3 by SIRT2 plays an important role in the regulation of lapatinib response and resistance of breast and nasopharyngeal cancers.

5.2 Results

5.2.1 Duolink proximity ligation assay indicates upregulation of acetylation of FOXO3 after silencing SIRT2

The acetylation status of FOXO3 after knocking down of SIRT2 was examined in a sensitive and efficient way by Duolink proximity ligation assay (PLA). The results showed that depletion of SIRT2 induces acetylation of FOXO3 compared to control NSC cells in sensitive BT474 cell lines. On the other hand, lower level of acetylated FOXO3 was found in resistant cells (Figure 5.1). This suggest the role of the SIRT2 in the increase of FOXO3 acetylation.

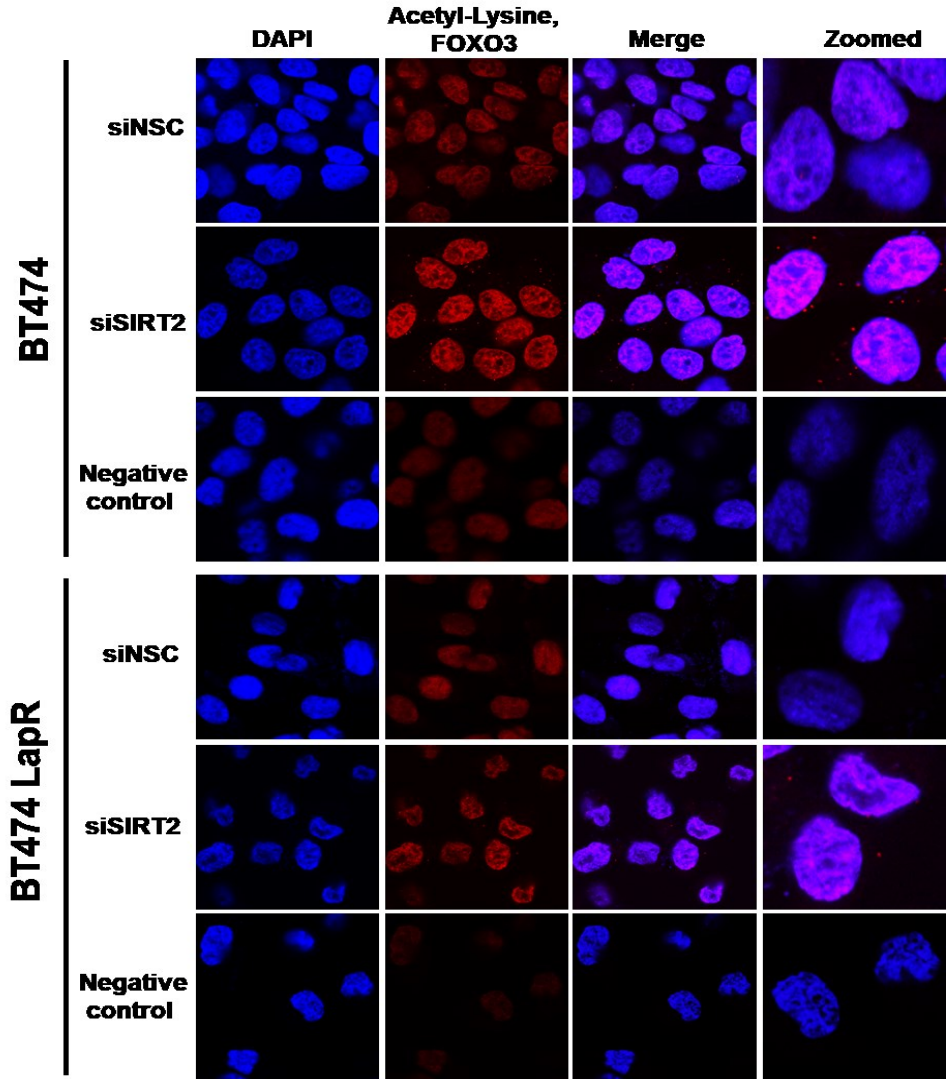


Figure 5.1 Duolink proximity ligation assay (PLA) for detecting the acetylation level of FOXO3 by silencing of SIRT2 in BT474 WT and BT474 Lap^R cell lines. BT474 and BT474 Lap^R cells were transfected with siNSC/siSIRT2 siRNAs for 48h. Cells without Ac-Lys and FOXO3 antibodies were used as negative control. Representative confocal images are shown. Cells were visualized with a Leica TCS SP5 confocal microscope equipped with a 63X oil immersion objective and LAS-AF software. Each red spot represents for a single interaction and DNA was stained with 4, 6-diamidino-2-phenyl indole (DAPI) in blue.

5.2.2 Silencing of SIRT2 combined with lapatinib treatment upregulates FOXO3 acetylation and its transcriptional activity

To determine whether SIRT2 can modulate the ability of lapatinib to mediate FOXO3 acetylation, I performed siRNA mediated knockdown of SIRT2 in BT474 and BT474 Lap^R. Western blot and co-immunoprecipitation experiments revealed that silencing of SIRT2 can increase FOXO3 acetylation in the absence or presence of lapatinib treatment (Figure 5.2A, B). Silencing of SIRT2 in combination with lapatinib treatment is more effective in inducing FOXO3 acetylation than SIRT2 siRNA alone probably because of lapatinib being more effective in inhibiting SIRT2 activity (Figure 5.2 and 5.4). Depletion of SIRT2 increased the expression of EP300 and CBP which in turn induce FOXO3 acetylation and expression (Figure 5.2A, 5.4). Furthermore, SIRT2 silenced cells showed higher levels of FOXO3 target genes such as Bim, $p27^{Kip1}$, p130 and $p16^{Ink4a}$ expression (Figure 5.2A). In addition, FOXO3 induced expression of Bim and Puma suggest that absence of SIRT2 promotes FOXO3 mediated apoptosis. To check the correct mechanism of apoptosis, I performed western blot for cleaved caspases and found that FOXO3 mediated apoptosis occurred by induction of initiator caspase9 and effector caspase7 as the cleaved caspases increased upon SIRT2 knockdown and/or with lapatinib treatment (Figure 5.3). Knocking down of SIRT2 also found to increase the expression of cleaved PARP although at a low level. Taken together, these results reveal that SIRT2 has a role in modulating FOXO3 acetylation and its downstream transcriptional activity.

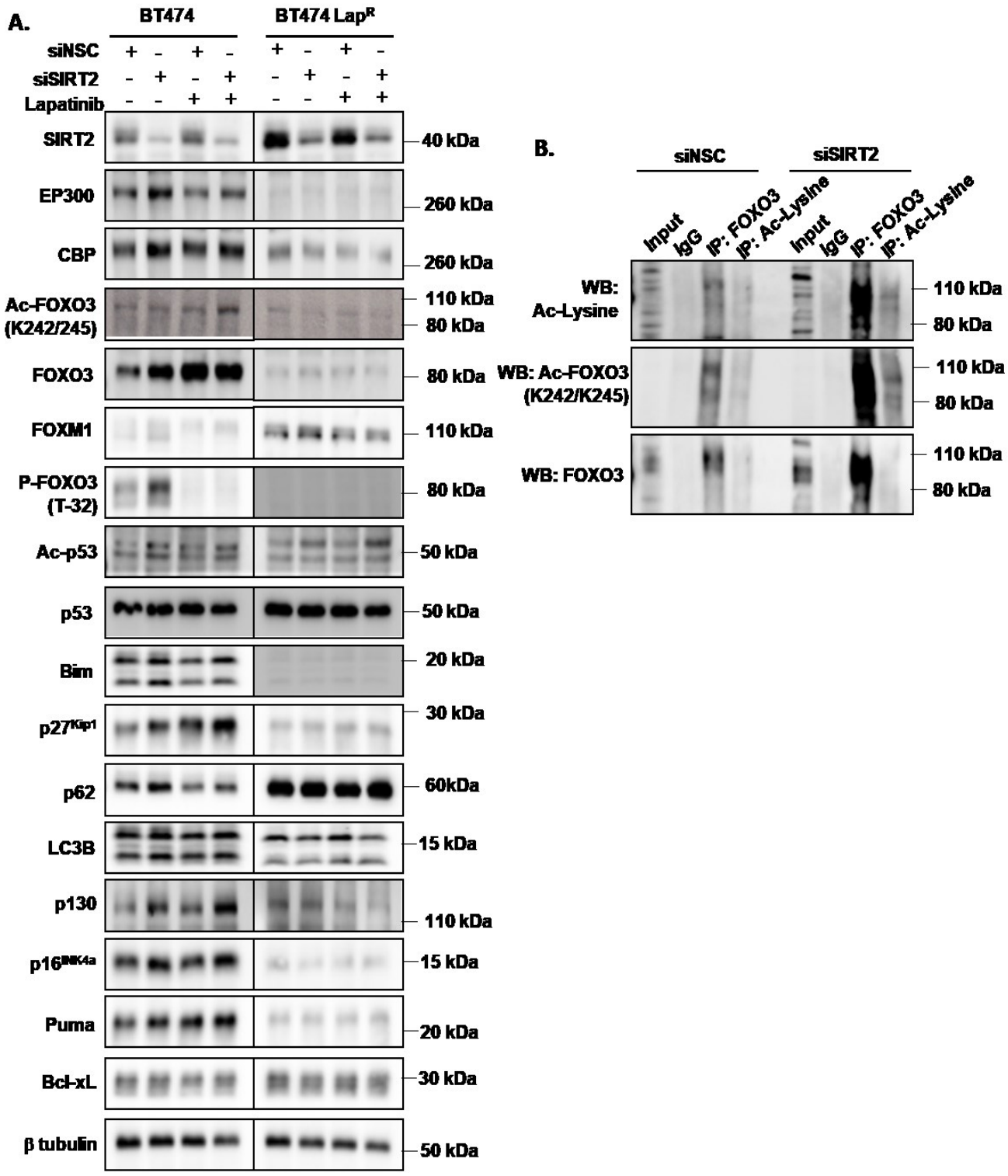


Figure 5.2 Silencing of SIRT2 with lapatinib treatment correlates with increased FOXO3 acetylation and its transcriptional activity. A. BT474 and BT474 Lap^R cells were transfected with control siNSC and siSIRT2 siRNAs and treated with or without 1 μM Lapatinib for 8 hours. After harvesting, protein lysates were obtained, and subsequent western blotting was performed to assess FOXO3 acetylation and its transcriptional activity using antibodies against Ac-FOXO3, FOXO3, p27^{Kip1}, Bim and others as indicated. The β-tubulin was used as a loading control. **B.** BT474 cells were transfected with Control (siNSC), and siSIRT2 siRNAs. After harvesting, protein lysates were obtained, and subsequent co-immunoprecipitation (Co-IP) was performed with anti-FOXO3 and anti-acetylated lysine antibody. Subsequent immunoblotting was performed using antibodies against Ac-Lys, Ac-FOXO3 and FOXO3. The anti-IgG antibody was used as a negative control.

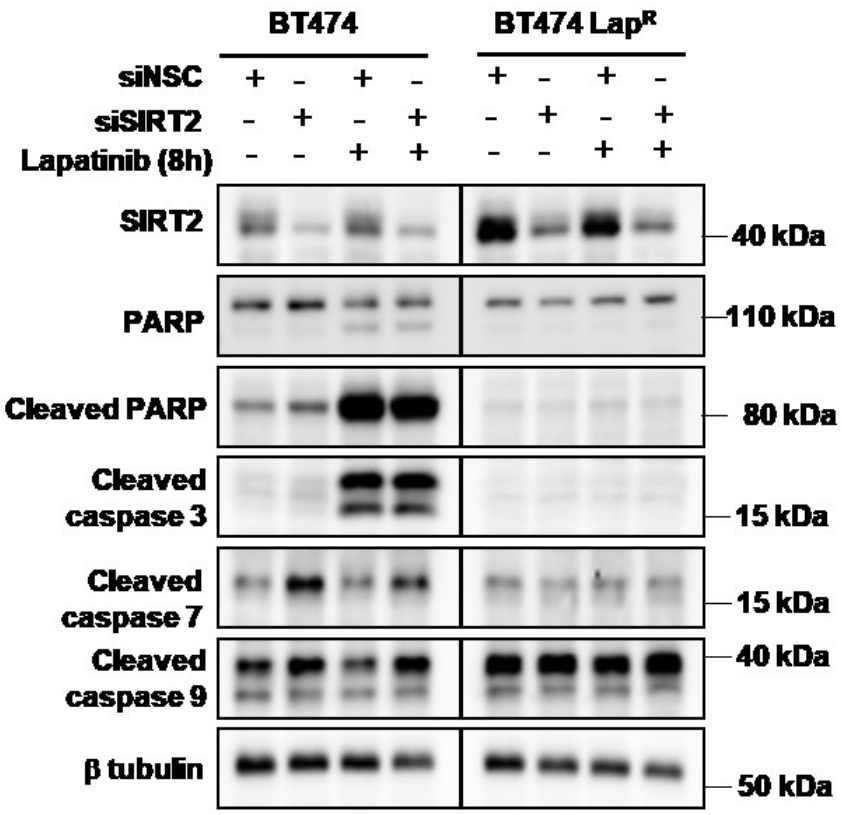


Figure 5.3 Silencing of SIRT2 with or without lapatinib induces caspase mediated apoptosis. BT474 and BT474 Lap^R cells were transfected with Control siNSC and siSIRT2 siRNAs and treated with or without 1 μM Lapatinib for 8 hours. After harvesting, protein lysates were obtained, and subsequent western blotting was performed to assess the expressions of cleaved PARP, caspase 3, 7and 9. The β-tubulin was used as a loading control.

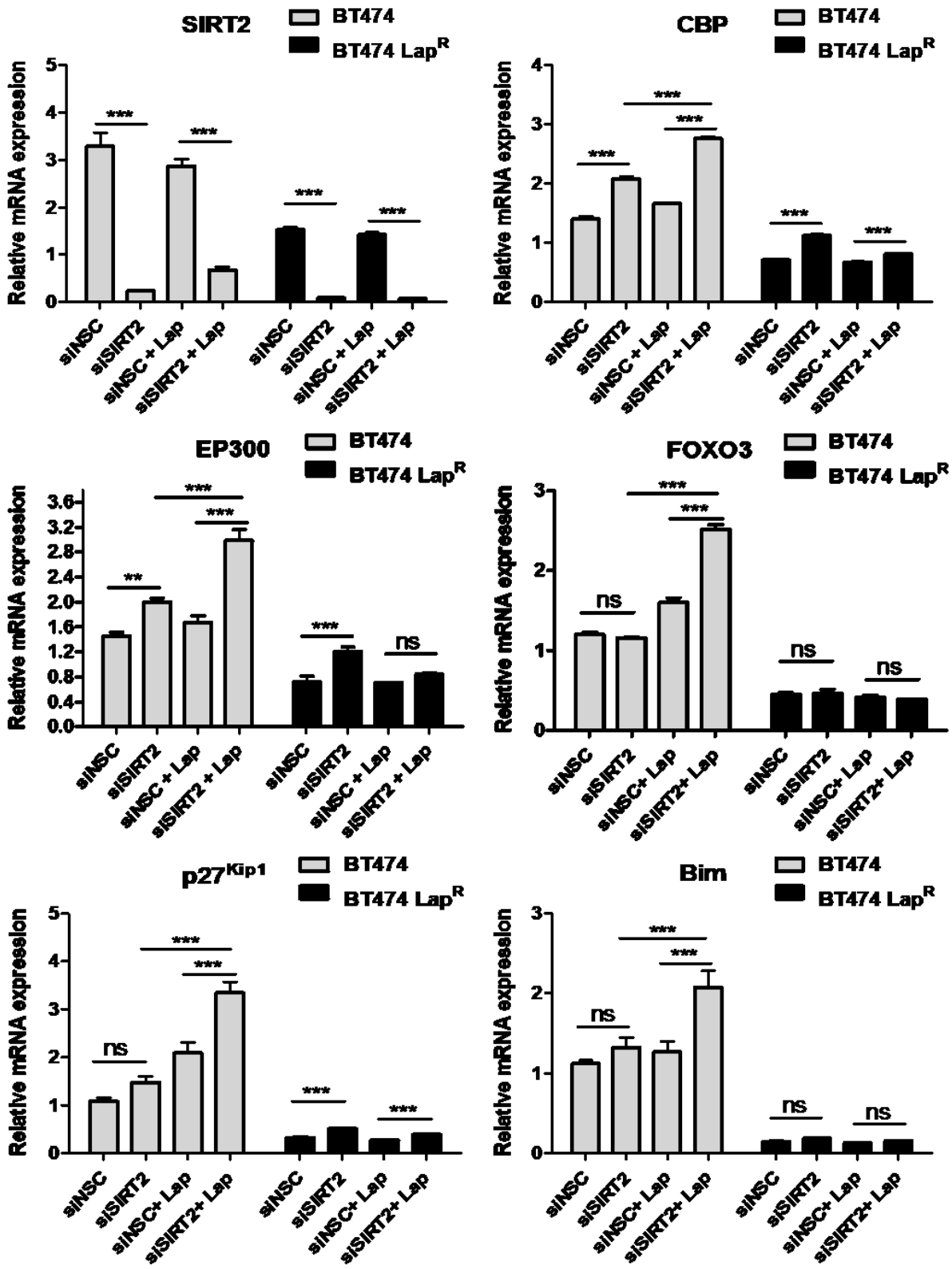


Figure 5.4. Knockdown of SIRT2 with lapatinib increases FOXO3 expression and activity at mRNA level. BT474 and BT474 Lap^R cells were transfected with control siNSC and siSIRT2 siRNAs and treated with or without 1 μM Lapatinib for 8 hours. The mRNA samples were analysed by real time RT qPCR to check the expression of mentioned genes. RPL19/RPS14 were used to normalise the expression level of mRNA. Statistical analyses were performed by one-way ANOVA (***$p < 0.001$, **$p < 0.01$, *$p < 0.05$, ns=non-significant).

5.2.3 Knockdown of SIRT2 increases lapatinib cytotoxicity in sensitive cells

To ascertain the role of SIRT2 in long-term survival of cells upon lapatinib treatment, I performed clonogenic assays comparing the ability of BT474 and BT474 Lap^R cells to survive and form colonies upon RNA interference and in response to lapatinib treatment. Depletion of SIRT2 suppressed and reduced cell proliferation in comparison with the siNSC control in the absence of lapatinib treatment (Figure 5.5). Upon lapatinib treatment, SIRT2 knock-down BT474 cells showed greater sensitivity than siNSC control cells, especially at 10 to 50 nM concentrations. Moreover, BT474 Lap^R cell lines also showed significant changes in clonogenicity or lapatinib sensitivity upon SIRT2 depletion (Figure 5.5). Thus, depletion of SIRT2 increases lapatinib sensitivity in BT474 cells but reduces cell proliferation of BT474 Lap^R cells.

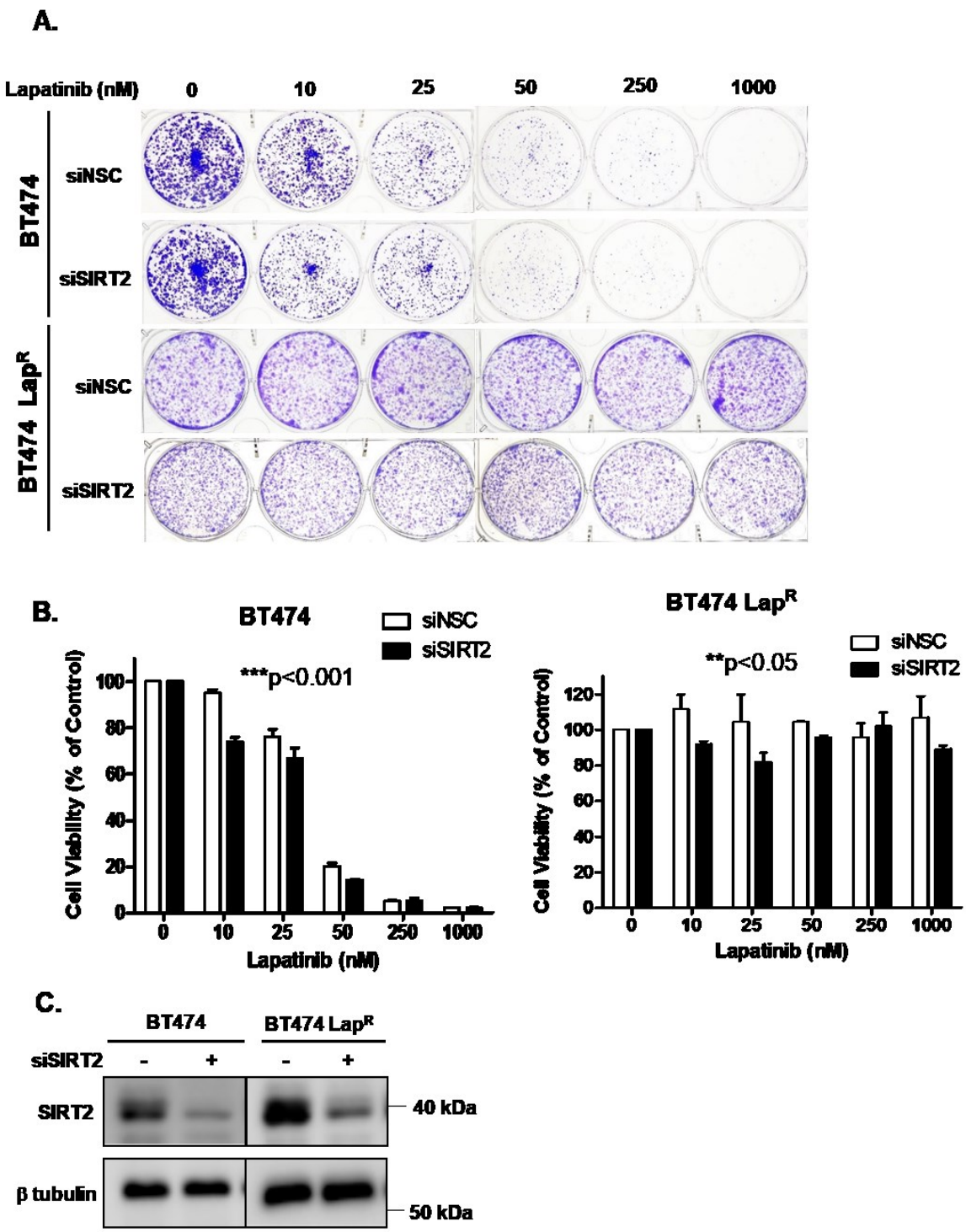


Figure 5.5 Knocking down of SIRT2 correlates with increased long-term lapatinib cytotoxicity in sensitive and resistant BT474 cells. A. BT474 and lapatinib resistant BT474 Lap^R cells were seeded 2,000 and 1000 cells per well, respectively, in 6-well plates and transfcted with non-targeting control (siNSC) and SIRT2-targeting siRNA pools. The transfected cells were then allowed to grow overnight and then treated with the lapatinib concentrations indicated (0, 10, 25, 50, 250 and 1000 nM). Twenty-four hours following treatment the medium was changed and colony formation was allowed for 28 and 14 days in sensitive and resistant BT474 cells, respectively. Cells were then fixed with 4% para formaldehyde and stained with crystal violet. **B.** The stain was solubilised with 33% acetic acid and absorbance obtained at 592 nm. Data were finally normalised to the respective untreated empty-vector transfected cells. Bars represent the mean ± SD of three independent transfection experiments (n=3, R=3) and statistical analysis was performed using two-way ANOVA analysis (***p<0.001, **p<0.05). **C.** Western blot analysis demonstrated SIRT2 depletion.

5.2.4 Newly designed SIRT2 inhibitor exhibited potential cellular activity by increasing acetylated tubulin levels

A thienopyrimidinone based SIRT2–selective inhibitor, ScA-B8A44, has been designed recently by Matthew J. Fuchter et al. [412]. To demonstrate the cellular activity of this novel SIRT2 inhibitor I studied the effect of active analogues to result in acetylation of *α*–tubulin, a well–known substrate for SIRT2 [413]. The MCF–7 breast epithelial cancer cell line was treated with different concentrations of ScA-B8A44. The previously published SIRT2 inhibitor DK-029 [414] and AGK2 [302] were used as positive controls. Additionally, analogue ScA-A13B7 lacking *in vitro* activity against SIRT2 was used as a negative control. To rule out the possibility of increased acetylation of α–tubulin due to histone deacetylase activity by metallo-HDACs (particularly HDAC6), Trichostatin A, [415] a pan HDAC inhibitor with no effect on SIRT2 activity, was employed in the experiments. Treatment of cells with ScA-B8A44 resulted in increased levels of α–tubulin acetylation in a dose dependent manner (Figure 5.6, 5.7). In contrast, no effect on tubulin acetylation levels was observed with ScA-A13B7 (Figure 5.6, 5.7) confirming that the enzymatic SIRT2 inhibition by ScA-B8A44 correlates to α–tubulin hyperacetylation even without TSA treatment. For other inhibitors DK-029 and AGK-2, tubulin hyperacetylation was only observed when treated in combination with TSA and at a treatment concentration of 10-20 μM or higher concentration (Figure 5.6). While this might be due to the slightly improved SIRT2 inhibitory potency of DK-029 (IC_{50} = 1.45 μM) vs ScA-B8A44 (IC_{50} = 0.58 μM). Clearly other physiochemical and stability differences between these two inhibitors are going to result in different in cell potency. In addition, acetylated tubulin levels found from western blot data were quantified and analysed by graphs generated by using ImageJ software (Figure 5.7). Comparative data of tubulin hyperacetylation upon the treatment of different SIRT2 inhibitor with or without TSA, were shown (Figure 5.7A-H).

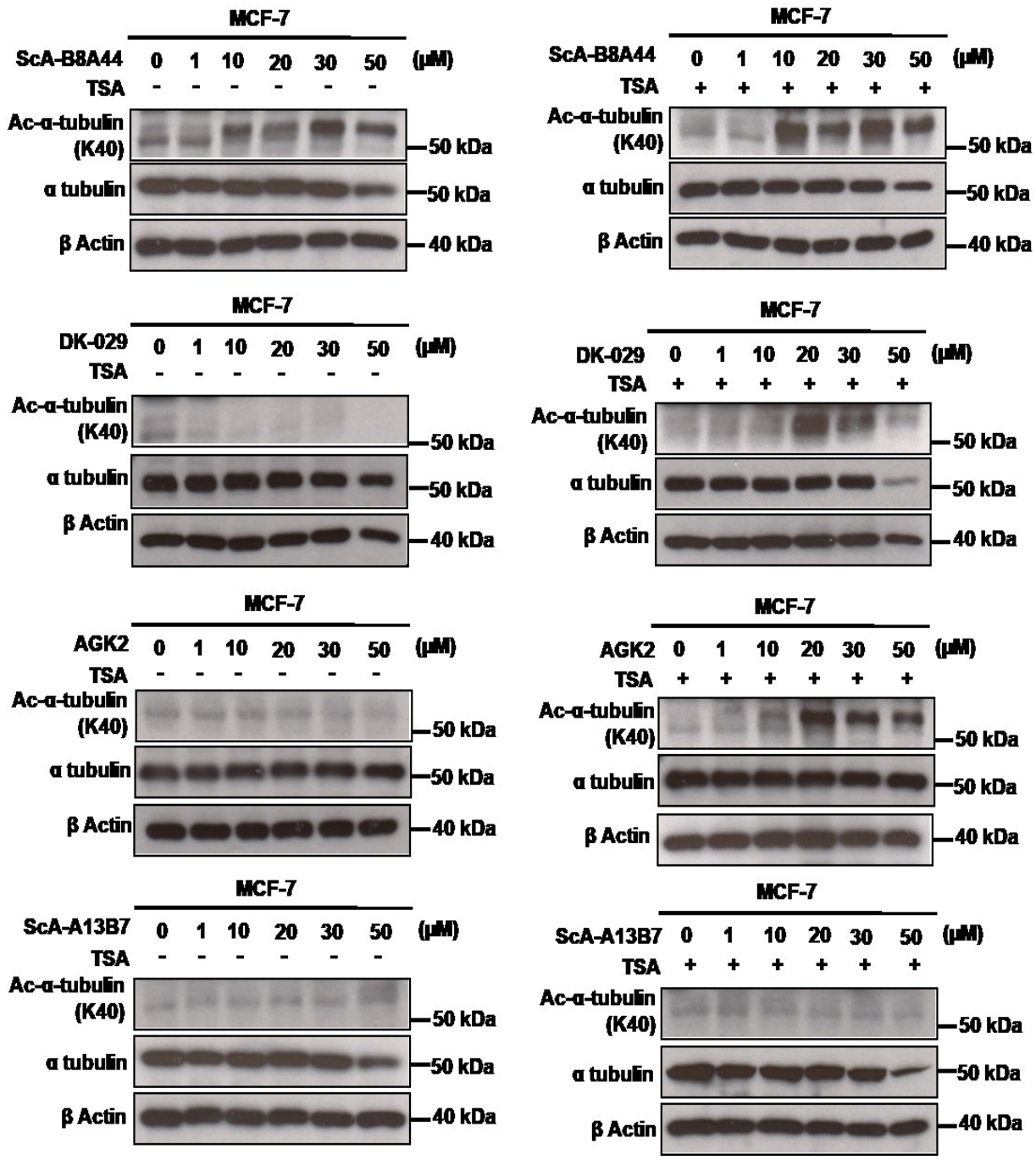


Figure 5.6 Effect of SIRT2 inhibitors on tubulin acetylation. MCF–7 cell lines were treated with different SIRT2 inhibitors at the doses stated for 24 hours with or without the presence of trichostatin A (TSA) (50 nM). TSA was added to ensure the inhibition of the non-sirtuin histone deacetylase activity. Protein samples were analysed by western blotting using antibodies against acetylated (Lysine-40) α-tubulin, total α-tubulin and β-actin. β-actin was probed as a control for protein loading.

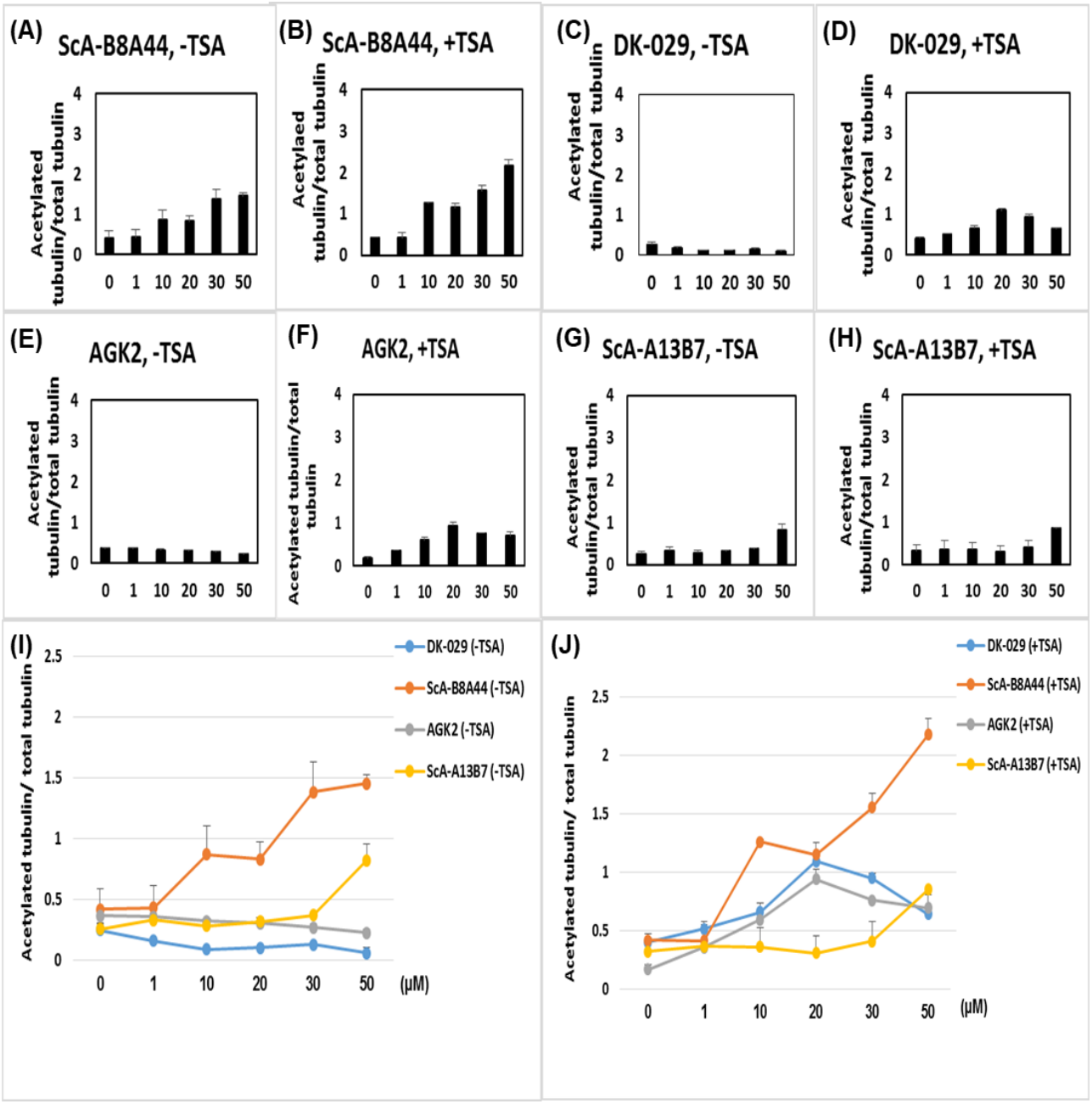


Figure 5.7 Protein quantification analysis by using ImageJ. Acetylated tubulin levels following the treatment of different SIRT2 inhibitor were quantified from western blot data and a comparative data analysis are shown from graphs generated using Microsoft excel. Quantified acetylated tubulin levels were normalized to total alpha tubulin. Quantification of protein expression was performed using ImageJ software.

5.2.5 SIRT2 inhibitors maintain FOXO3 levels but reduces FOXM1 and c-Myc expression in MCF-7 cells

In order to investigate the effect of novel SIRT2 inhibitors on FOXO3, FOXM1 expression I treated MCF-7 cells with varied concentrations (0, 1, 10, 20, 30 and 50 μM) of SIRT2 inhibitor compounds in combination with or without 50 nM trichostatin A (TSA) (T8552, Sigma-Aldrich, UK) for 24 hours. TSA was used to abolish the activity of non-sirtuin HDAC members. Following the treatment, whole cell extracts were used for protein isolation and subsequent western blotting was performed for the assessment of protein levels. Western blot analysis revealed a significant induction of FOXO3 acetylation in MCF-7 cells, when treated with 10 or 20 μM of ScA-B8A44 (Figure 5.8A). Unexpectedly, Ac-FOXO3 levels were found to be decreased upon high concentration of drug treatment. The SIRT2 inhibitor ScA-B8A44 also reduces EP300 level upon high doses of drug, which suggests an associated reduction of acetylated level of FOXO3. Surprisingly DK-029 and AGK2 did not induce FOXO3 acetylation although they reduced the expression of FOXM1, suggesting that their tumour suppressing activity may regulated by other mechanisms (Figure 5.8B, C). The negative control ScA-A13B7 showed a constant level of EP300 and Ac-FOXO3 (Figure 5.8D).

The fact that, deacetylation of FOXO3 by SIRT2 has been shown to result in Skp2-mediated ubiquitination and degradation of FOXO3, [268] suggesting inhibition of SIRT2 can increases FOXO3 stability. The western blot result for ScA-B8A44, Dk-029 and AGK-2 showed that, all SIRT2 inhibitors maintain a significant level of FOXO3 levels while they decrease the expression of oncogenic proteins, FOXM1 and c-Myc (Figure 5.8 A-C).To further assess FOXO3 stability and activity regulated by acetylation, expression of its downstream target genes, $p27^{Kip1}$, Bim, MnSOD expression at mRNA and protein level should be analysed. Moreover, since, there has been much interest in sirtuin inhibition as potential therapy for breast and lung cancers, [264, 296] the effects of compound ScA-B8A44 as well as other SIRT2 inhibitors on the proliferation of MCF-7 cells should be examined by proliferation assays.

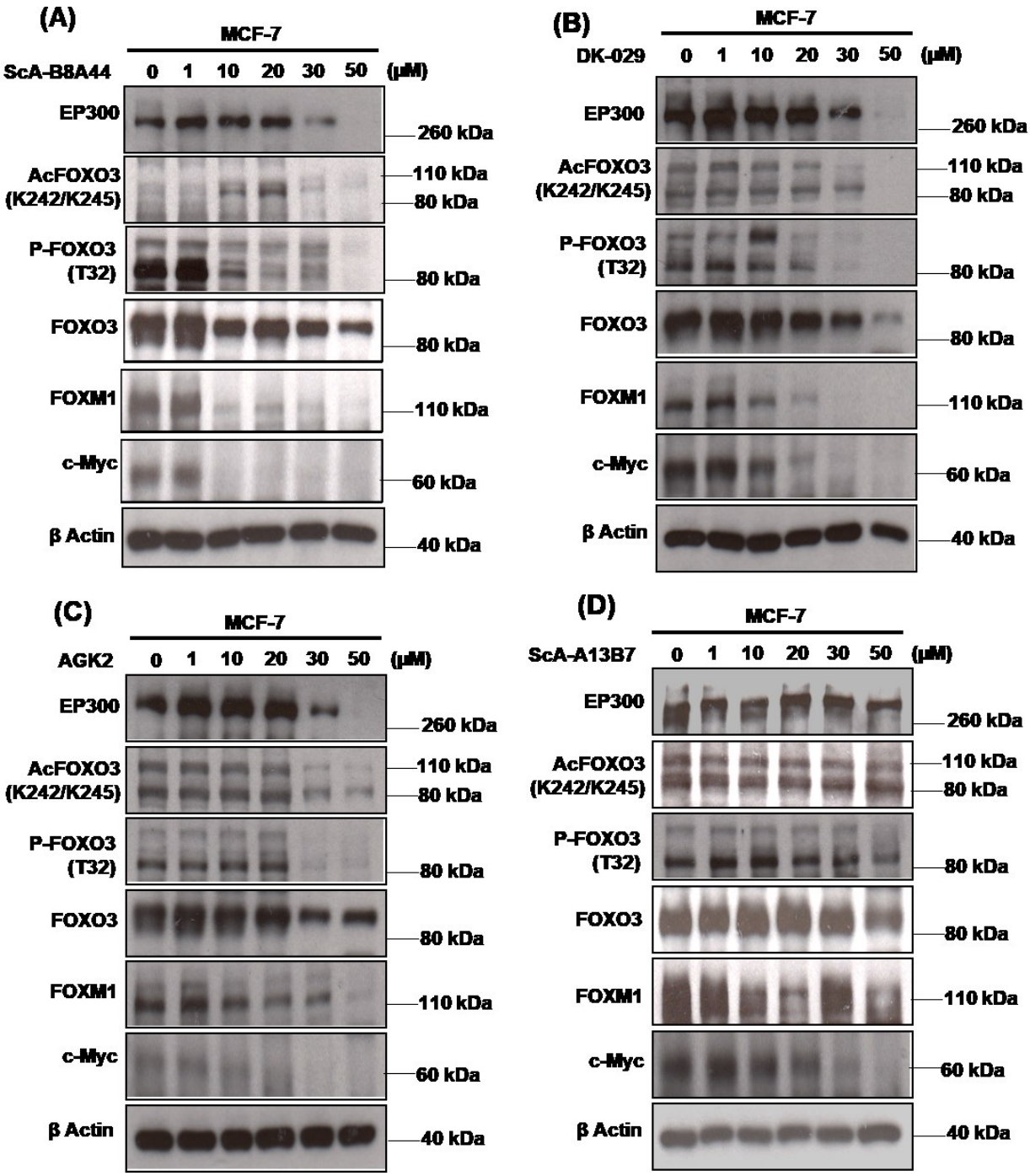


Figure 5.8 Effect of ScA-B8A44, DK-029, AGK2 and ScA-A13B7 in the regulation of expression of FOXO3, Ac-FOXO3 and FOXM1. MCF–7 cell lines were treated with ScA-B8A44, DK-029, AGK2 and ScA-A13B7 at the doses stated for 24 hours. Protein samples were analysed by western blotting using antibodies against EP300, Ac-FOXO3, FOXO3, FOXM1 and others indicated protein. β-actin was probed as a control for protein loading.

5.2.6 SIRT2 inhibitor scAB8A44 induces FOXO3 acetylation and its transcriptional activity in BT474 cells

To examine the role of scAB8A44, I performed western blotting experiment after treating BT474 and Lap^R cells with or without TSA. I found that the SIRT2 inhibitor increases the expression of CBP and EP300 both at protein and mRNA levels (Figure 5.9 and 5.10) which in turn induces FOXO3 acetylation. Importantly, TSA provided additive effect to promote CBP mediated FOXO3 acetylation. However, this effect of the inhibitor was found to be deregulated in the resistant cells may be because of higher FOXM1 expression (Figure 5.9). SIRT2 inhibition by scAB8A44 also found to upregulate the expression of FOXO3 target genes mainly Bim, Puma, $p16^{InK4a}$ and LC3B, suggesting that suppression of SIRT2 can induce apoptosis in BT474 cells (Figure 5.9 and 5.10). In agreement, I found the elevated expression of cleaved PARP and cleaved caspase 3, 9 indicating caspase mediated apoptosis. To further confirm this, caspase Glo assay was employed which showed increased caspase 8, 9 and caspase 3/7 expression upon treatment with SIRT2 inhibitor (Figure 5.11). Therefore, scAB8A44 induced FOXO3 acetylation increases FOXO3 activity and caspase mediated apoptosis in BT474 cells.

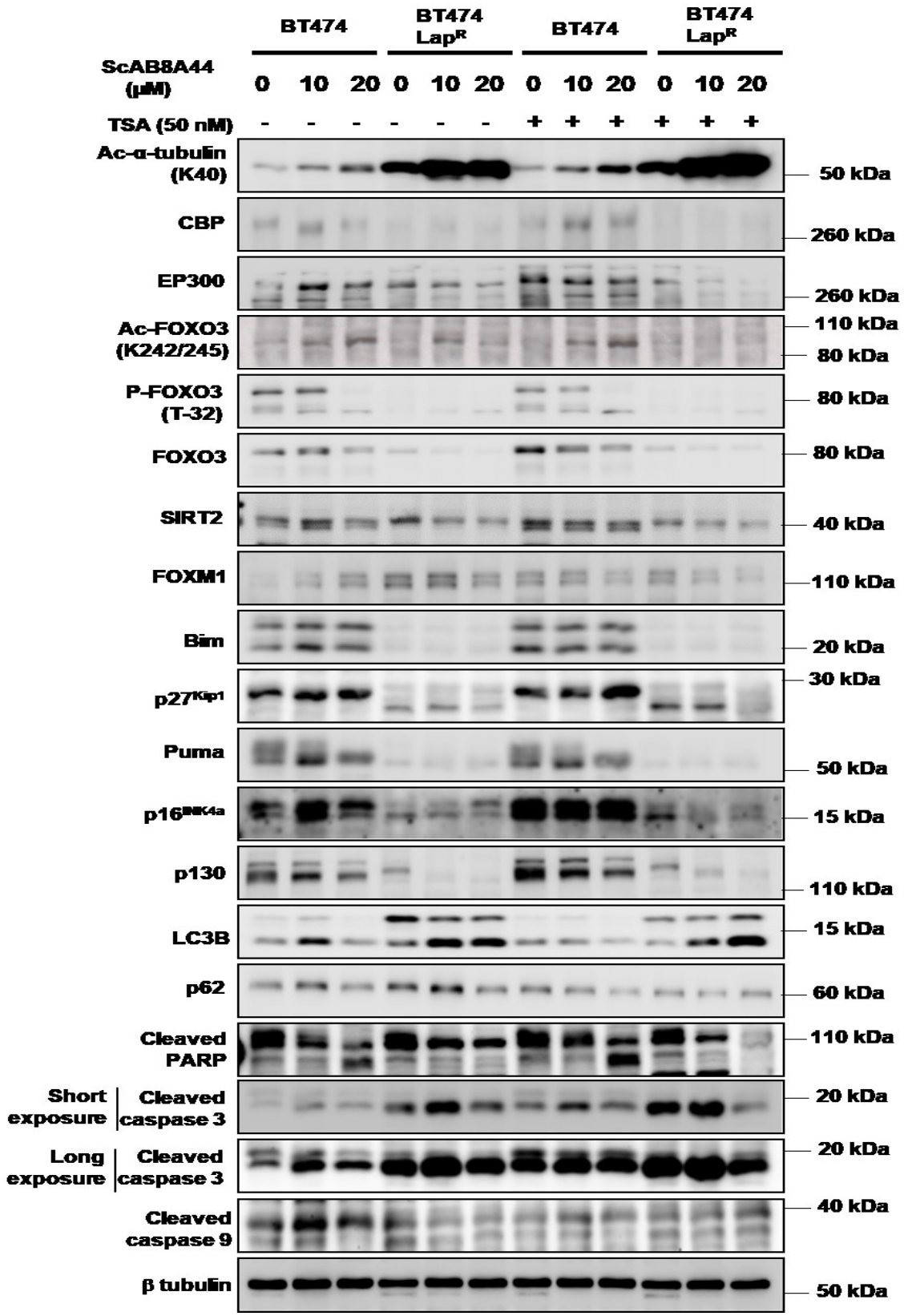


Figure 5.9 Effect of SIRT2 inhibitor ScAB8A44 on FOXO3 acetylation and activity in BT474. BT474 WT and Lap^R cell lines were treated with scAB8A44 at the doses stated for 24 hours with or without the presence of trichostatin A (TSA) (50 nM). TSA was added to ensure the inhibition of the non-sirtuin histone deacetylase activity. Protein samples were analysed by western blotting using antibodies against AcFOXO3, FOXO3 and others mentioned. β-tubulin was probed as a control for protein loading.

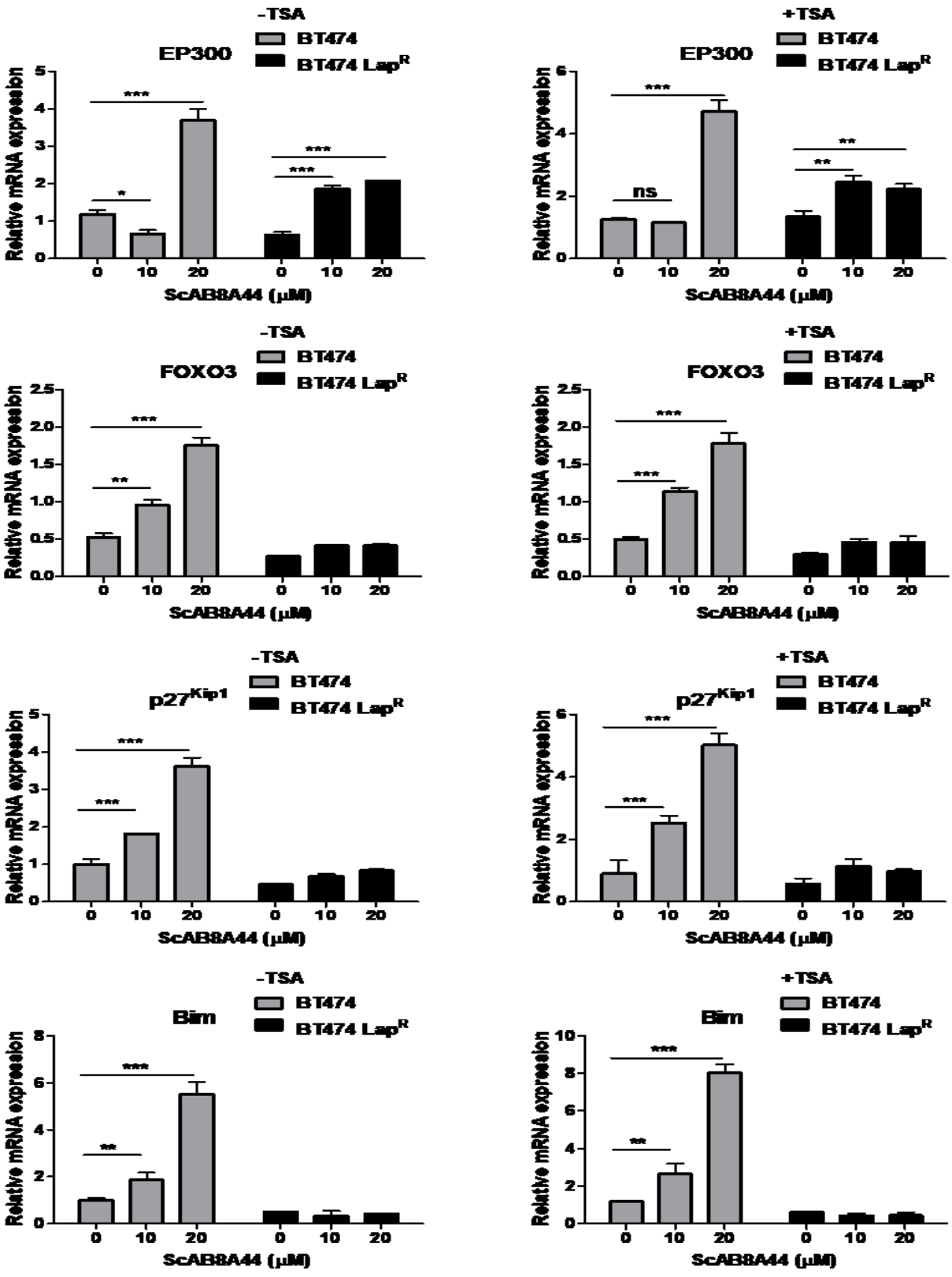


Figure 5.10 Effect of SIRT2 inhibitor ScAB8A44 on FOXO3 acetylation and activity in BT474. BT474 WT and Lap^R cell lines were treated with scAB8A44 at the doses stated for 24 hours with or without the presence of trichostatin A (TSA) (50 nM). TSA was added to ensure the inhibition of the non-sirtuin histone deacetylase activity. mRNA samples were analysed by real time RT qPCR to check the expression of mentioned genes. RPL19/RPS14 were used to normalise the expression level of mRNA. Statistical analyses were performed by one-way ANOVA (***$p < 0.001$, **$p < 0.01$, *$p < 0.05$, ns=non-significant).

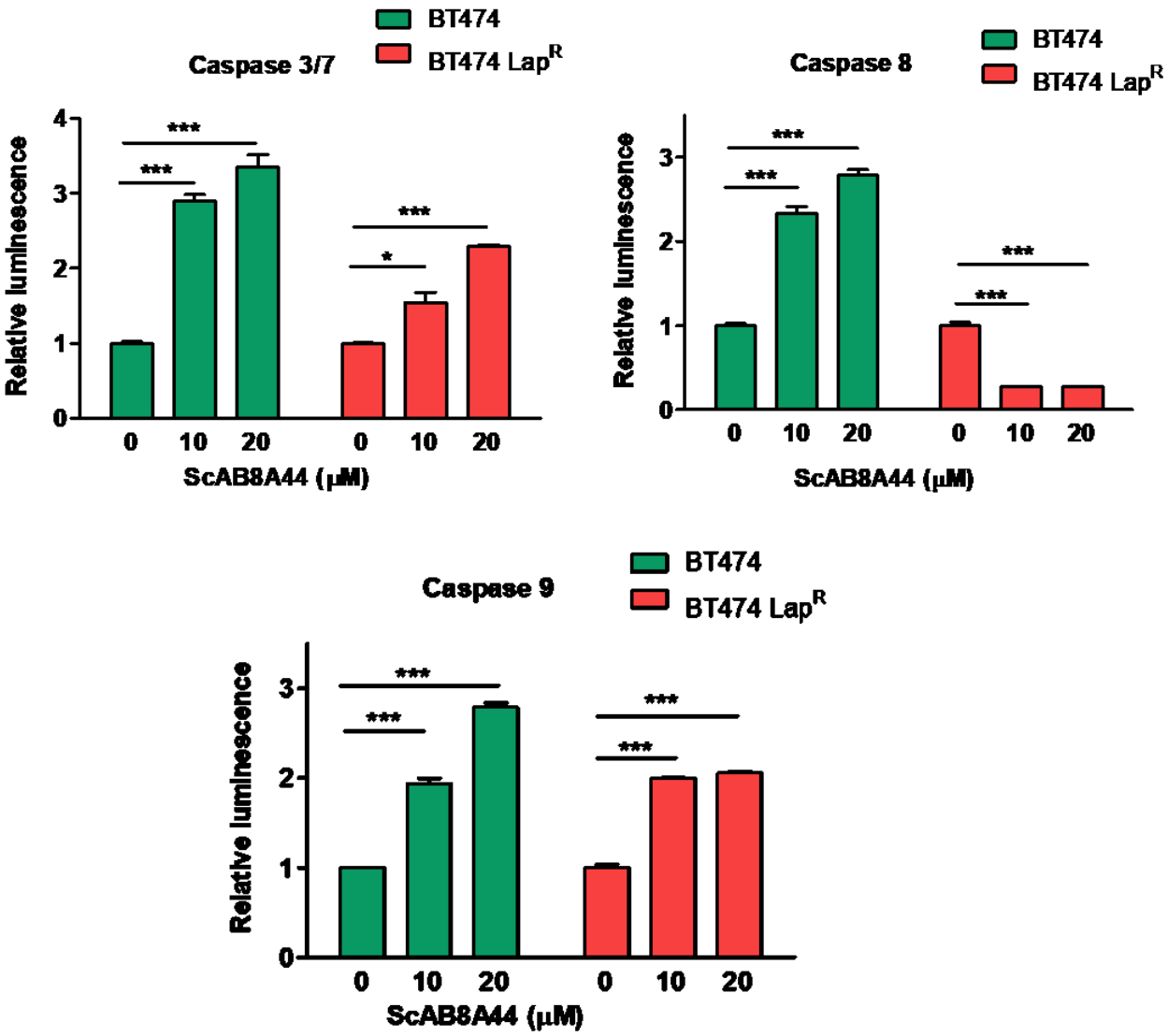


Figure 5.11 ScAB8A44 induces cell death via caspase activation pathway. BT474 WT and Lap^R cells were seeded at a density of 10,000 cells/well in white 96-well plates and treated for 24 hours with scAB8A44 (0, 10 and 20 µM) after which they were treated and incubated for 45 min to an hour with Caspase-Glo® -3/7, -8 and -9 (Promega) reagents and the luminescent signals were read using a luminometer. The values were compared with respect to the untreated controls. Statistical analyses were performed by one-way ANOVA (***$p < 0.001$, **$p < 0.01$, *$p < 0.05$, ns=non-significant).

5.2.7 Inhibition of SIRT2 facilitates FOXO3 acetylation which results in a reduced cell proliferation and increased lapatinib sensitivity of BT474 cells

To further assess the role of SIRT2 inhibitors on FOXO3 acetylation, I performed forward and reverse co-immunoprecipitation assay after treating BT474 WT and resistant cells with SIRT2 inhibitor scAB8A44 and AGK2 (Figure 5.12A and 5.13A). Significant level of increased Ac-FOXO3 was observed after scAB8A44 treatment in BT474 cells, however acetylation was reduced in BT474 Lap^R cells (Figure 5.12A). Moreover, upon AGK2 treatment, acetylation of FOXO3 was increased as depicted by forward co-IP, although reverse co-IP showed opposite result (Figure 5.13A). This is may be because of possible nonspecific pulling down of proteins by pan-acetyl antibody or any other experimental errors. I also analysed the cell viability of BT474 cells in presence of these inhibitors by clonogenic assays. The scAB8A44 does not induce growth inhibition, however it increases lapatinib sensitivity of BT474 cells at 10 μM concentration (Figure 5.12B,C). For the resistant cells, this inhibitor affects cell growth, reducing the proliferation of BT474 Lap^R cells but cannot induce drug sensitivity. On the other hand, AGK2 significantly inhibited cell proliferation in a dose-dependent manner. AGK2 significantly inhibited cell growth from low doses such as at 10 μM in both sensitive and resistant cell lines (Figure 5.13B,C).

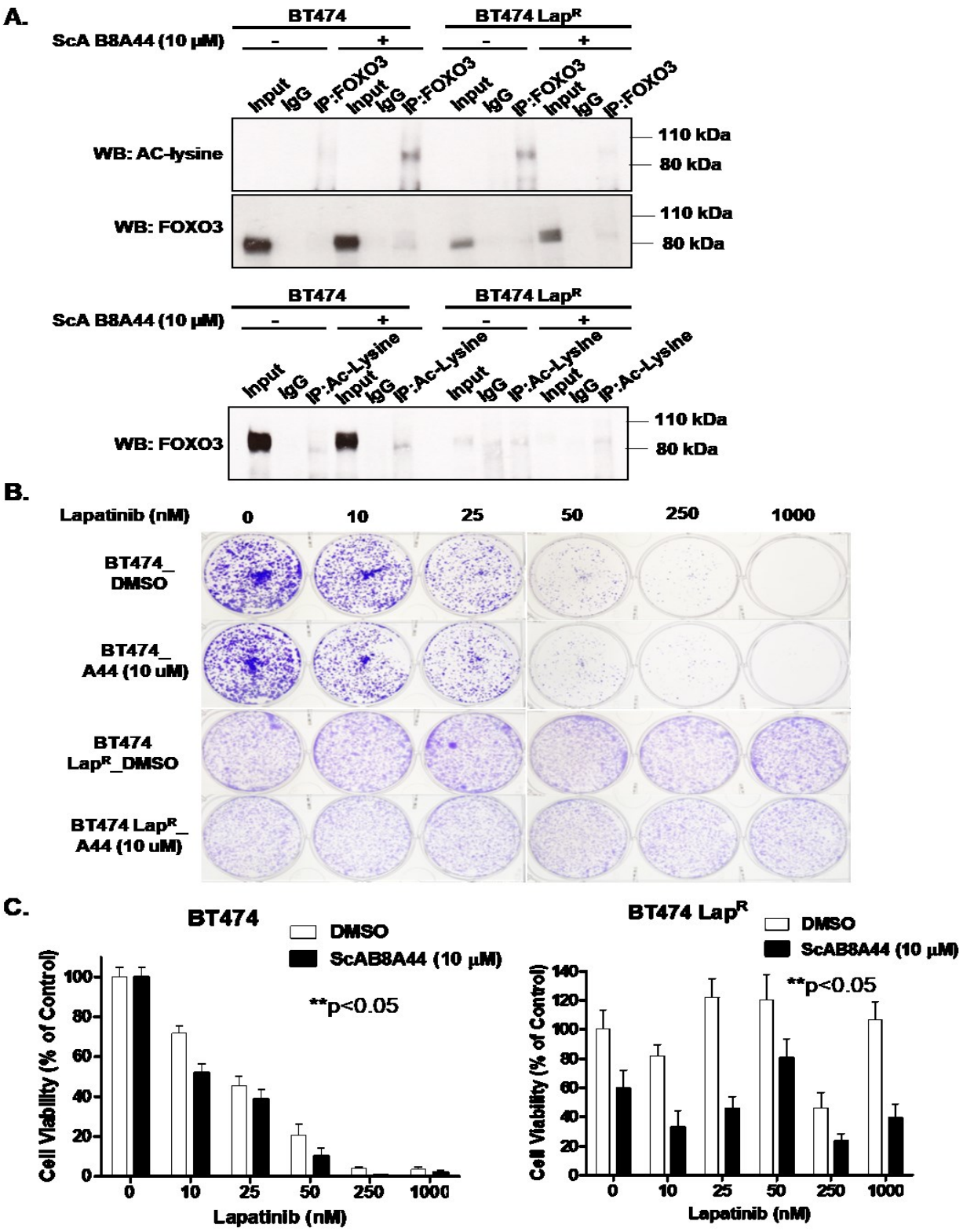


Figure 5.12 ScAB8A44 induced FOXO3 acetylation increases lapatinib sensitivity in BT474 cells. A. BT474 WT and Lap^R cells were seeded and treated for 24 hours with scAB8A44 (10 µM). Protein lysates of drug treated cells were assessed by forward and reverse co-immunoprecipitation (Co-IP) with anti-FOXO3 and anti-Ac-Lysine antibody. Subsequent immunoblotting was performed using antibodies against Ac-Lysine and FOXO3. The anti-IgG was used as a negative control. **B.** SIRT2 inhibitor treated cells were then allowed to grow overnight and then treated with the lapatinib concentrations indicated (0, 10, 25, 50, 250 and 1000 nM). Twenty-four hours following treatment the

medium was changed and colony formation was allowed for 28 and 14 days in sensitive and resistant BT474 cells, respectively. Cells were then fixed with 4% para formaldehyde and stained with crystal violet. The stain was solubilised with 33% acetic acid and absorbance obtained at 592 nm. Statistical analysis was performed using two-way ANOVA (**p<0.05).

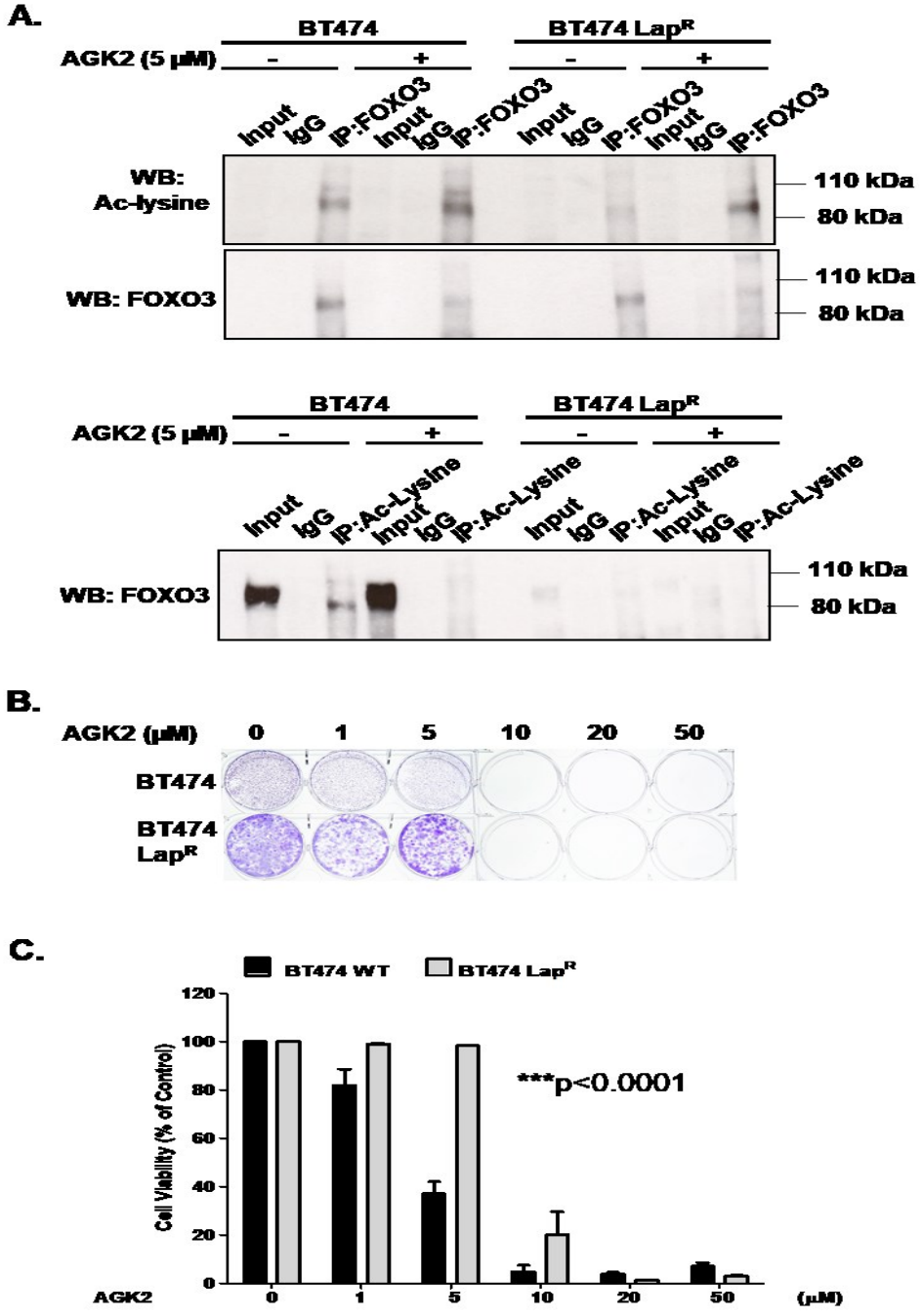
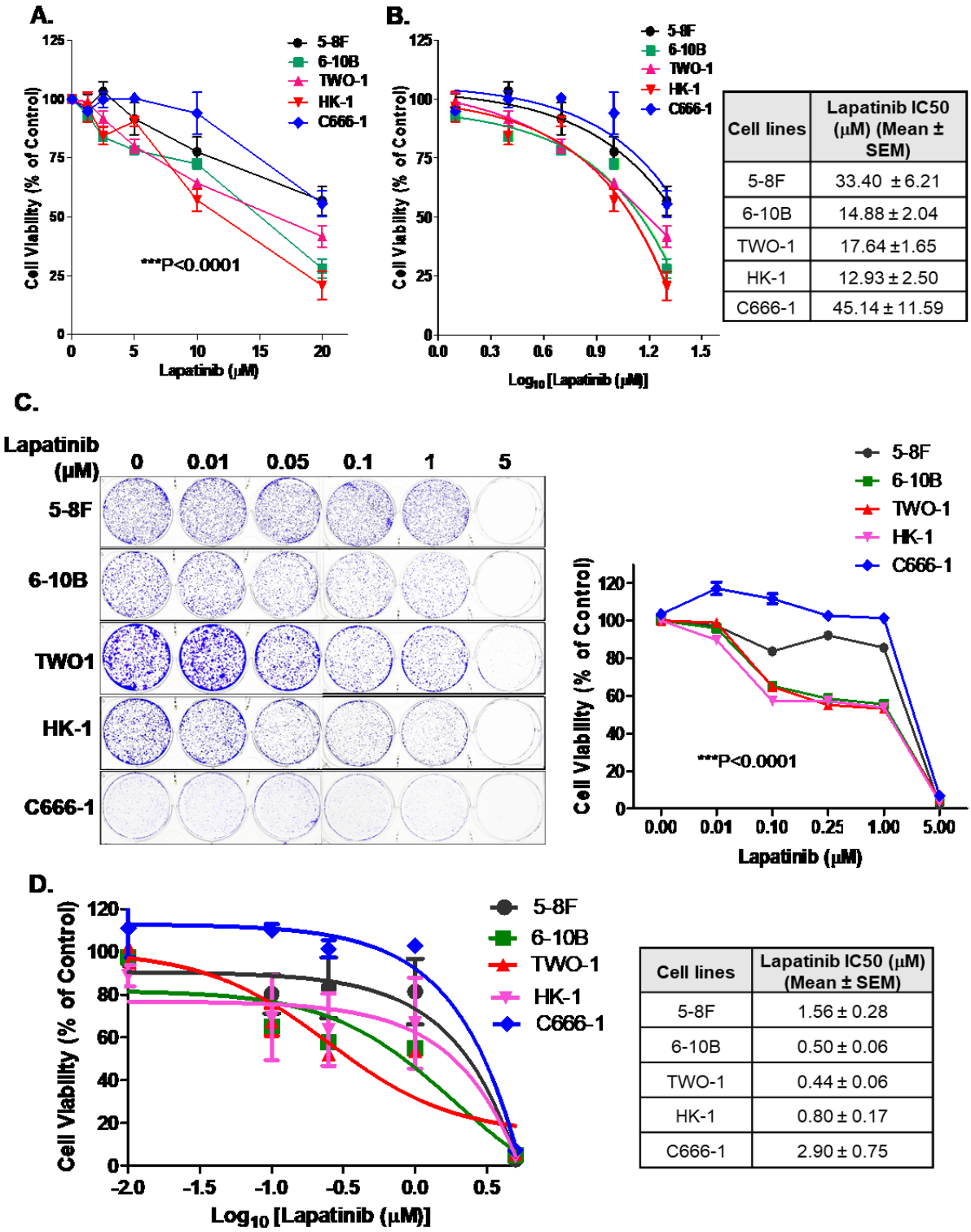


Figure 5.13 AGK2 induced FOXO3 acetylation inhibits cell proliferation. A. BT474 WT and Lap^R cells were seeded and treated for 24 hours with AGK2 (5 µM). Protein lysates of drug treated cells were assessed by forward and reverse co-immunoprecipitation (Co-IP) with anti-FOXO3 and anti-Ac-Lysine antibody. Subsequent immunoblotting was performed using antibodies against Ac-Lysine and FOXO3. The anti-IgG was used as a negative control. **B.** Cells were treated with different concentrations of AGK2 for 48 hours after treatment, the medium was changed, and colony formation was allowed for 28 and 14 days in sensitive and resistant BT474 cells, respectively. Cells were then fixed with 4% para formaldehyde and stained with crystal violet. The stain was solubilised with 33% acetic acid and absorbance obtained at 592 nm. Statistical analysis was performed using two-way ANOVA (***p<0.0001).

5.2.8 Effects of lapatinib on cell viability of different nasopharyngeal carcinoma (NPC) cell lines

Previous studies have demonstrated that the dual EGFR/HER2 tyrosine kinase inhibitor, lapatinib, can restrict cell proliferation and invasion, and promote anoikis in NPC cells [404, 405]. Therefore, we used nasopharyngeal carcinoma cell lines to better understand SIRT2 regulated lapatinib sensitivity.

In order to identify the cellular mechanisms which modulate lapatinib sensitivity, we first analysed its effect on the proliferation of NPC cell lines with distinct metastatic status. To this end, two highly metastatic (C666-1 and 5-8F) and three poorly metastatic (6-10B, TW01 and HK-1) NPC cell lines were treated with increasing concentrations of lapatinib (from 0 μM to 20 μM) for 48 h and their viability measured by the sulforhodamine B (SRB) assay. The results showed that lapatinib caused a dose-dependent reduction of cell proliferation in all NPC cells. The results also indicated that there were significant differences in lapatinib sensitivity between the NPC cell lines at 48 h (Figure5.14A) (2-way ANOVA, ****P<0.0001). Moreover, the highly metastatic (C666-1 and 5-8F) lines were significantly more resistant to lapatinib than the three poorly metastatic lines (6-10B, TW01 and HK-1) (Figure 5.14B). These results were further confirmed by clonogenic assays, in which the surviving cells were allowed to further proliferate and form clones. The highly metastatic C666-1 and 5-8F lines were also significantly more resistant to lapatinib than the three poorly metastatic lines (6-10B, TW01 and HK-1) in longer term assays (Figure 5.14C, 5.14D).



Cell lines	Lapatinib IC50 (μM) (Mean ± SEM)
5-8F	33.40 ± 6.21
6-10B	14.88 ± 2.04
TWO-1	17.64 ± 1.65
HK-1	12.93 ± 2.50
C666-1	45.14 ± 11.59

Cell lines	Lapatinib IC50 (μM) (Mean ± SEM)
5-8F	1.56 ± 0.28
6-10B	0.50 ± 0.06
TWO-1	0.44 ± 0.06
HK-1	0.80 ± 0.17
C666-1	2.90 ± 0.75

Figure 5.14 Effect of Lapatinib on cell growth and proliferation of NPC cells. A) Lapatinib sensitivity curves in NPC cells was determined by Sulforhodamine B staining. Cells ($3x10^3$ / well) were seeded in 96-well plates and treated with increasing concentrations of lapatinib for 72h before staining and measurement of optical density at 492 nm. **B)** Best-fit curves were generated to determine IC_{50} for each NPC cells against Lapatinib. **C)** NPC cells were seeded into 6-well plates ($1x10^3$ cells / well) and treated with Lapatinib for 72h. Colony formation was monitored after 15 days, stained with crystal violet (representative pictures are shown) and absorbance at 592 nm determined (*right panel*). **D)** Best-fit curves were generated to determine IC_{50} for each NPC cells against Lapatinib in terms of clonogenic assay. Numerical data represent the average ± SEM of three different experiments (*** *P*<0.0001**).** [This experiment was performed in collaboration with Sathid Aimjongjun]

5.2.9 Effects of lapatinib on the expression and activity of proteins involved in EGFR/ERBB2 signalling in the 5-8F and 6-10B NPC cells

In order to identify the potential mechanisms involved in modulating lapatinib sensitivity, we analysed by western blotting the effects of lapatinib on the expression of molecules implicated in lapatinib signalling and sensitivity. To this end, the two NPC cell lines, SUNE 5-8F (highly metastatic) and 6-10B (poorly metastatic) with differential lapatinib sensitivity (low and high, respectively) were treated with 5 μM lapatinib for 0 to 48 h (Figure 5.15). Western blot results showed a reduction in P-ERBB1 and P-ERBB2 upon lapatinib treatment (Figure 5.15), indicating the drug is effective in inhibiting ERBB1/ERBB2 activity in both NPC lines. Notably, both total ERBB1 and ERBB2, but not ERBB3, were expressed at high levels in both NPC lines and their expression remained at high levels after lapatinib treatment. FOXO3 has previously been shown to mediate the cytotoxic function of lapatinib through repressing FOXM1 expression. The p38 and Jun N-terminal kinase (JNK) MAPKs have also been demonstrated to phosphorylate and activate FOXO3 in response to lapatinib, while AKT has been reported to be repressed by lapatinib, leading to FOXO3 dephosphorylation (T32) and derepression. In agreement, western blot analysis showed that FOXO3 became dephoshorylated (T32) and activated upon lapatinib treatment in the sensitive 6-10B but remained phosphorylated (T32) and inactivated in the resistant 5-8F cells. The FOXO3 dephosphorylation was also correlated with downregulation of FOXM1 expression in the 6-10B and not the 5-8F cells, further confirming the role of FOXO3 in mediating lapatinib action. Interestingly, the induction of p38 and JNK phosphorylation was not observed in the sensitive 6-10B cells upon lapatinib treatment, suggesting p38 and JNK are unlikely to be instrumental in activating FOXO3 in response to lapatinib. FOXO3 activity can also be enhanced by acetylation, which have been shown to be promoted by EP300 and repressed by the nuclear sirtuins, SIRT1, -2 and -6. Western blot analysis showed EP300 was at low levels in the resistant, metastatic 5-8F cells but was induced upon lapatinib treatment, whereas EP300 was expressed at high levels in 6-10B and was downregulated in response to lapatinib. The results also showed SIRT1 and -6 were expressed at comparable levels in both 5-8F and 6-10B cells, and their expression

was not substantially affected by lapatinib treatment. The observed expression patterns of EP300, SIRT1 and SIRT6 suggested that they are unlikely to be responsible for FOXO3 activation by lapatinib, even though EP300, SIRT1 and SIRT6 could still modulate FOXO3 acetylation and activity in these NPC cells. By contrast, upon lapatinib treatment the expression levels of SIRT2 remained constitutively high in the resistant 5-8F cells but were downregulated by lapatinib in the sensitive 6-10B cells, suggesting that SIRT2 can potentially mediate lapatinib response through modulating FOXO3 acetylation and activity in these NPC cells. These results suggest that highly metastatic and EBV positive cell lines are more resistant to lapatinib, probably due to their high levels of FOXM1 and P-FOXO3 expression, suggesting that SIRT2 induces lapatinib resistance through FOXO3 deacetylation which in turn led to reduction in FOXO3 activity.

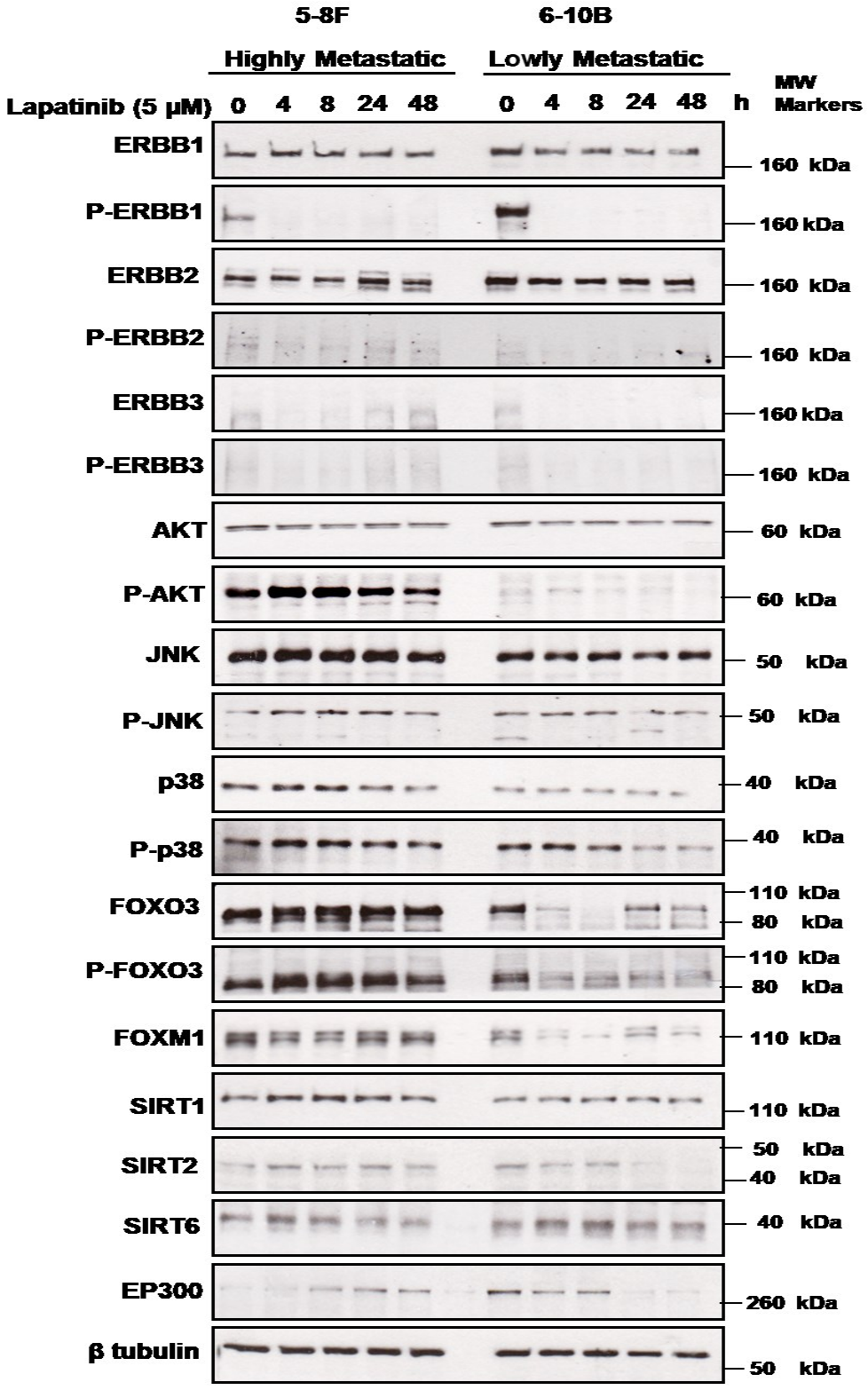


Figure 5.15 Effect of lapatinib on the expression and activation of proteins involved in ERBB1 and ERBB2 signaling pathways in high and low metastatic NPC cell lines. The high and low metastatic NPC cells were either left untreated or treated with 5 μM lapatinib for 4, 8, 24, 48 h. Protein lysates from whole-cell extracts were collected and then analysed by western blotting using the antibodies against ERBB1, P-ERBB1, ERBB2, P-ERBB2, ERBB3, P-ERBB3, AKT, P-AKT and others indicated. Molecular markers are shown on the right panel of each blot. Data are representative of at least three independent experiments. [This experiment was performed in collaboration with Sathid Aimjongjun]

5.2.10 FOXOs mediate the cytotoxic function of lapatinib

FOXO proteins have previously been shown to be functionally redundant and can compensate for one another [416]. To verify the role of FOXO3 in mediating the cytotoxic response of lapatinib, the effects of lapatinib treatment were investigated in wild-type (WT) and *foxo1/3/4* $^{-/-}$ MEFs. Western blot and RT-qPCR analyses confirmed the Foxo1/3/4 knockout in the *foxo1/3/4* $^{-/-}$ MEFs and demonstrated EGFR/HER2 overexpression in both wild-type (WT) and *foxo1/3/4* $^{-/-}$ MEFs (Figure 5.16A,B), implying that they are potentially sensitive to lapatinib inhibition. Clonogenic assays showed that both wild-type (WT) and *foxo1/3/4* $^{-/-}$ MEFs are indeed sensitive to the antiproliferative functions of lapatinib (Figure 5.16C). Clonogenic assays also revealed that *foxo1/3/4*-deficient MEFs displayed higher self-renewal ability and was significantly less sensitive to the antiproliferative effects of lapatinib compared with the WT MEFs (2-way ANOVA, ****P<0.0001) (Figure 5.16C and 5.16D), confirming the key role of FOXOs in mediating the cytotoxic functions of lapatinib.

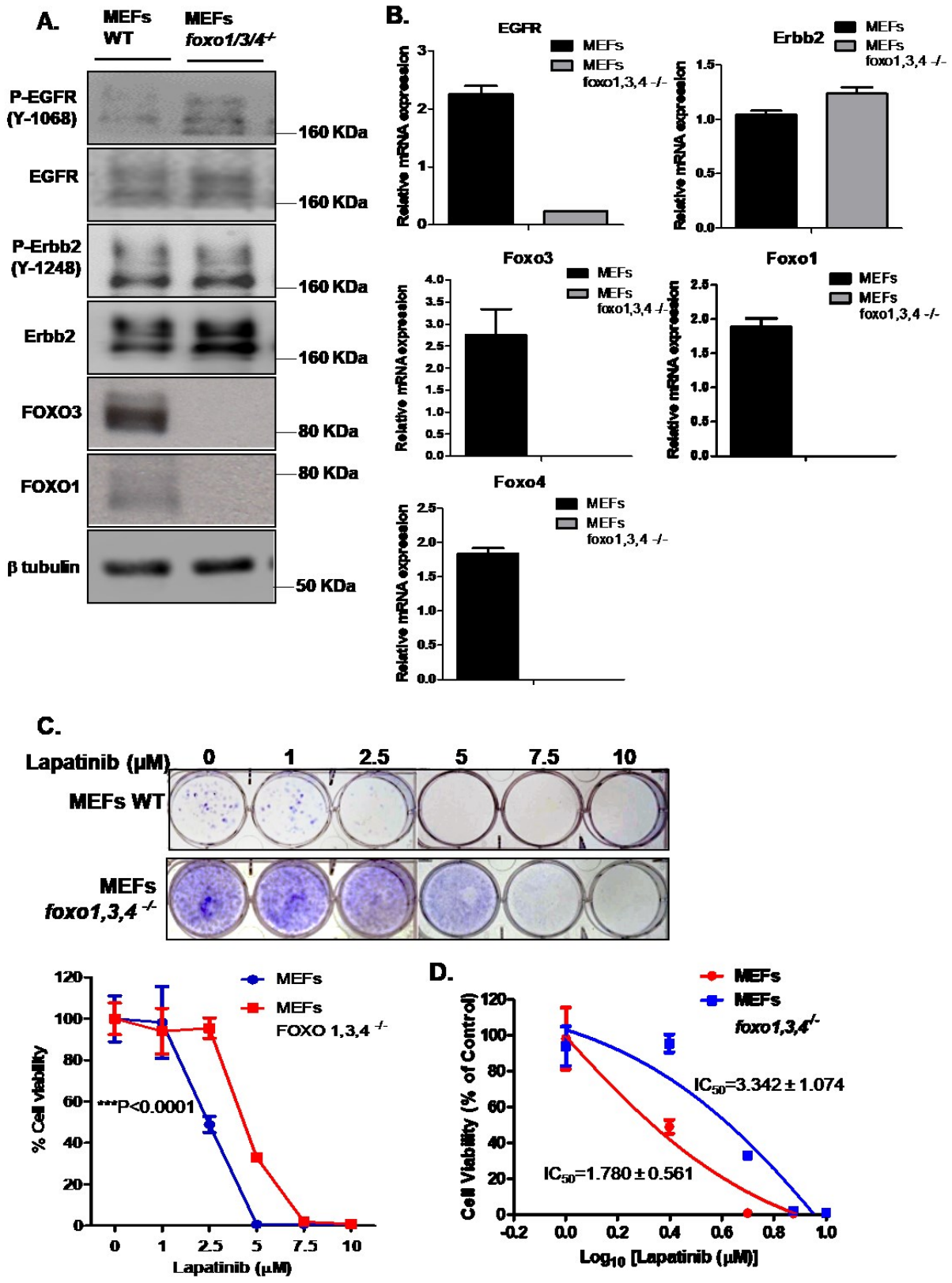
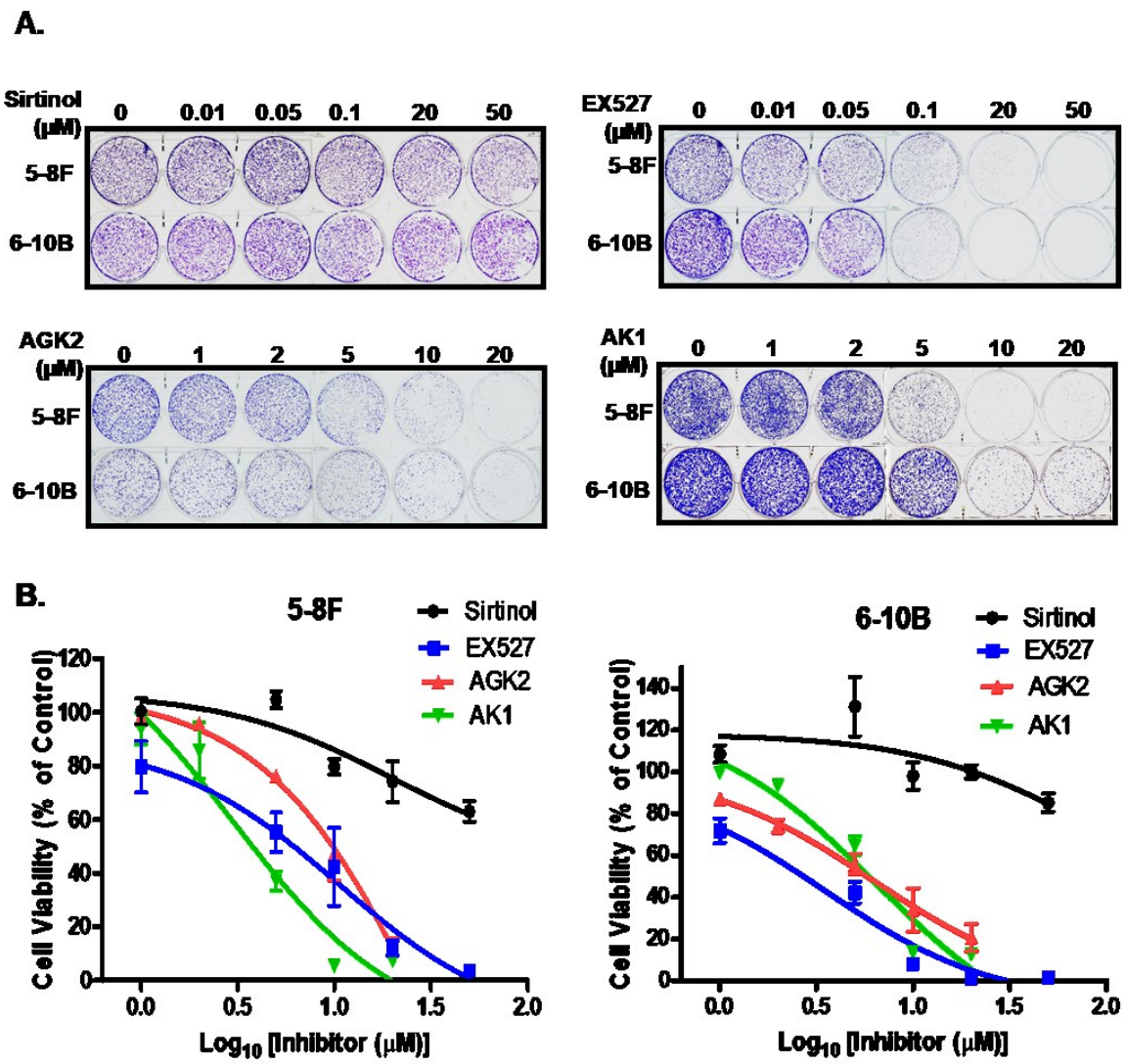


Figure 5.16 FOXO3 regulates EGFR and ERBB2 expression and increases lapatinib sensitivity in mouse embryonic fibroblast cells. **A.** Western blot analysis was performed to analyse the protein levels of P-EGFR, EGFR, P-ERBB2, ERBB2, FOXO3, FOXO1 in MEFs and *Foxo1,3,4*$^{-/-}$ MEFs. Representative western blot results are shown. Tubulin was used as a protein loading control. **B.** The mRNA levels of *EGFR, ERBB2, FOXO3, FOXO,* and *FOXO4* were assessed by real time RT qPCR.

The RPL19 housekeeping gene was used as a control to normalise gene expression. **C.** Wild-type MEFs and *Foxo1,3,4*$^{-/-}$ MEFs were treated with increasing concentration of Lapatinib for 3 days and colony formation was observed for 1 week. Cells were then stained with crystal violet and absorbance was taken at 592 nm (right panel). The colony formation capacity was analysed by two-way ANOVA and found to be significantly different (***$p < 0.0001$) from one another. **D.** Best-fit curves were generated to determine IC_{50} for each cell against Lapatinib in terms of clonogenic assay.

5.2.11. The clonogenic survival of NPC cells is sensitive to chemical inhibitors of SIRTs

The anti-proliferative activity of FOXO3 is promoted by acetylation which can be attenuated by nuclear SIRTs. In order to investigate if the viability of the NPC cells is also modulated by SIRTs, we subjected both the lapatinib resistant 5-8F and sensitive 6-10B NPC cells to treatment with the SIRT1-specific (e.g. EX527), SIRT2-specific (e.g. AK1 and AGK2) and pan-SIRT (e.g. Sirtinol) inhibitors individually for 72 h and their subsequent long-term survival examined by clonogenic assays (Figure 5.17A and 5.17B). The results showed that all four SIRT-inhibitors decreased the clonogenic survival of both NPC cell lines, with EX527, AK1 and AGK2 being more effective compared to Sirtinol, suggesting that the activity of SIRT1 and -2 might have a role in modulating the long-term viability of NPC cells.



Inhibitor	IC_{50} in 5-8F	IC_{50} in 6-10B
Sirtinol	73.02 ± 13.14	505.50 ± 613.01
EX527	5.34 ± 1.07	2.33 ± 0.37
AGK2	9.65 ± 1.85	5.72 ± 0.68
AK1	3.78 ± 0.90	6.06 ± 1.35

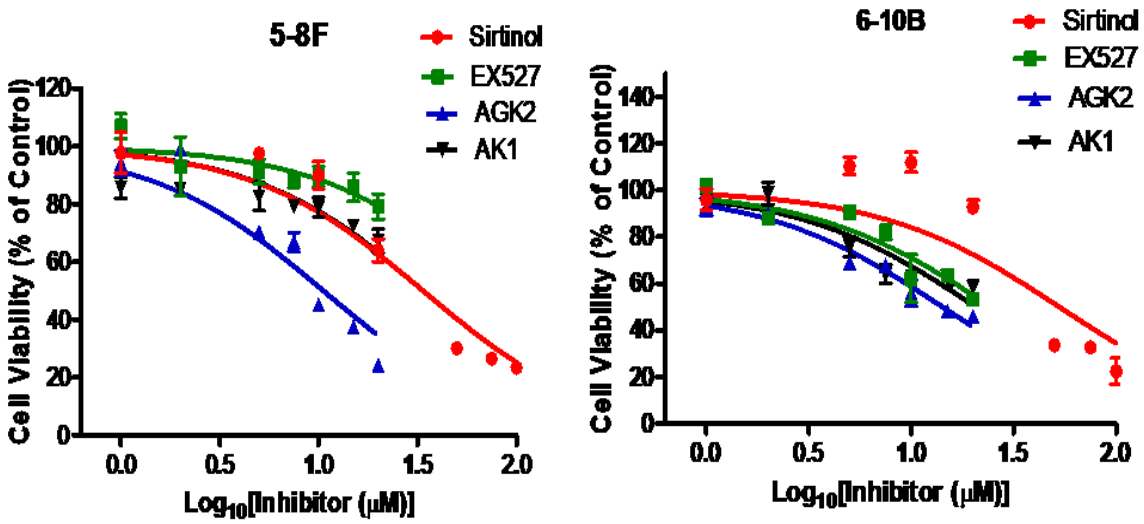
Figure 5.17 Inhibition of SIRT2 by AGK2, AK1 and EX527 inhibits long-term cell growth and colony formation of high and low metastatic NPC cells. A) 5-8F and 6-10B cells were seeded in 6-well and treated with the drug concentration indicated for 72h. Then, cell culture media was removed, and colony formation observed for 15 days. At the end of this time period, cells were fixed with 4% para formaldehyde and stained with crystal violet. Representative pictures from triplicate experiments are shown. **B)** The stain was solubilised with 33% acetic acid and absorbance at 592 nm were obtained. Best fit-curves were generated to determine the IC50 of each drug for 5-8F and 6-10B cells.

5.2.12 SIRT2 inhibitors AK1 and AGK2 function cooperatively with lapatinib in NPC cells

Next, we tested if the SIRT inhibitors can act cooperatively with lapatinib and enhance its antiproliferative functions. To this end, the resistant 5-8F and sensitive 6-10B NPC cells were cultured with sub-optimal levels of SIRT inhibitors (Figure 5.18) or vehicle controls in the presence of increasing doses of lapatinib and their cell viability examined by SRB assays (Figure 5.19). Surprisingly, combining the pan-SIRT inhibitor Sirtinol with lapatinib significantly increased the overall viability of both NPC cell lines compared to lapatinib treatment alone (2-way ANOVA, ****P<0.0001). Similarly, EX527 increased the viability of the lapatinib-treated 6-10B cells (2 way-ANOVA, **P=0.0011) but had no significant effects on the viability of the lapatinib-treated 5-8F cells (2 way-ANOVA, non-significant; P=0.3667). By contrast, the SIRT2 inhibitor AGK2 demonstrated additive effects on the cytotoxicity of lapatinib (2 way-ANOVA, ****P<0.0001, respectively) in both the sensitive 6-10B (IC_{50}: 5.94 ± 0.86 to 1.02 ± 0.27 μM) and the resistant 5-8F (10.55 ± 1.52 to 1.88 ± 0.26 μM) NPC lines (Figure 5.19 and 5.20). Similarly, the SIRT2-inhibitor AK1 also functioned additively with lapatinib in the 5-8F cells (2 way-ANOVA, *P=0.0331; IC_{50}: 11.77 ± 2.43 to 2.88 ± 0.57 μM) but had no significant positive effects on lapatinib in the sensitive 6-10F cells (2-way ANOVA, non-significant P=0.3667; IC_{50}: 5.80 ± 1.15 to = 6.50 ± 0.66 μM). AK1 did not demonstrate any additive effects with lapatinib in 6-10B cells, probably because of the predominant anti-proliferative function of lapatinib in the lapatinib-sensitive cells. Moreover, lapatinib also functions to downregulate SIRT2 expression in 6-10B, and therefore, AK1 might be redundant in inhibiting SIRT2 after the downregulation of SIRT2 in these cells by lapatinib. However, overall the SIRT2 inhibitors AGK2 and AK1, but not the SIRT1 and pan-SIRT inhibitors, demonstrated additive antiproliferative effects on lapatinib in SRB cell proliferative assays, suggesting that SIRT2 plays a specific role in limiting lapatinib cytotoxicity and in promoting lapatinib resistance in NPC cells.

To ascertain further the role of SIRT2 in enhancing lapatinib resistance in NPC cells, we performed clonogenic survival assays on the two NPC cell lines to study the long-term antiproliferative effects of the two SIRT2 inhibitors AGK2 and AK1 on lapatinib (Figure 5.21). In clonogenic assays, both SIRT2-inhibitors displayed additive effects

on lapatinib in NPC cell lines (2-way ANOVA, ****P<0.0001, for all except **P<0.0033 for AK1 in 6-10B), further reducing the overall clonogenic survival of lapatinib-treated cells (Figure 5.21B). When combined with lapatinib, AGK2 showed additive effects on the anti-proliferative functions of lapatinib in both the lapatinib resistant 5-8F (IC_{50}: 2.31 ± 1.06 to 0.21 ± 0.07 μM) and sensitive 6-10B (IC_{50}: 0.66 ± 0.08 to 0.21 ± 0.02 μM) NPC cells (Figure 5.21C). The SIRT2-inhibitor AK1 also functioned additively with lapatinib in both the resistant 5-8F and (IC_{50}: 1.07 ± 0.15 to 0.28 ± 0.03 μM) and sensitive 6-10B (IC_{50}: 0.66 ± 0.10 to 0.28 ± 0.05 μM) cells (Figure5.21C).



Inhibitor	IC_{50} in 5-8F	IC_{50} in 6-10B
Sirtinol	33.76 ± 3.744	52.8 ± 11.596
EX527	76.61 ± 15.062	24.48 ± 2.576
AGK2	10.56 ± 1.013	14.21 ± 0.824
AK1	34.55 ± 3.859	20.71 ± 2.034

Figure 5.18 Determination of IC50 of SIRT inhibitors from SRB assay. Cells ($3x10^3$/well) were seeded in 96-well plates and treated with increasing concentrations of SIRT inhibitors for 48h before staining and measurement of optical density at 492 nm. Data were analysed by generating curves using graph-pad prism. Best-fit curves were generated to determine the IC_{50} of inhibitors for each NPC cells.

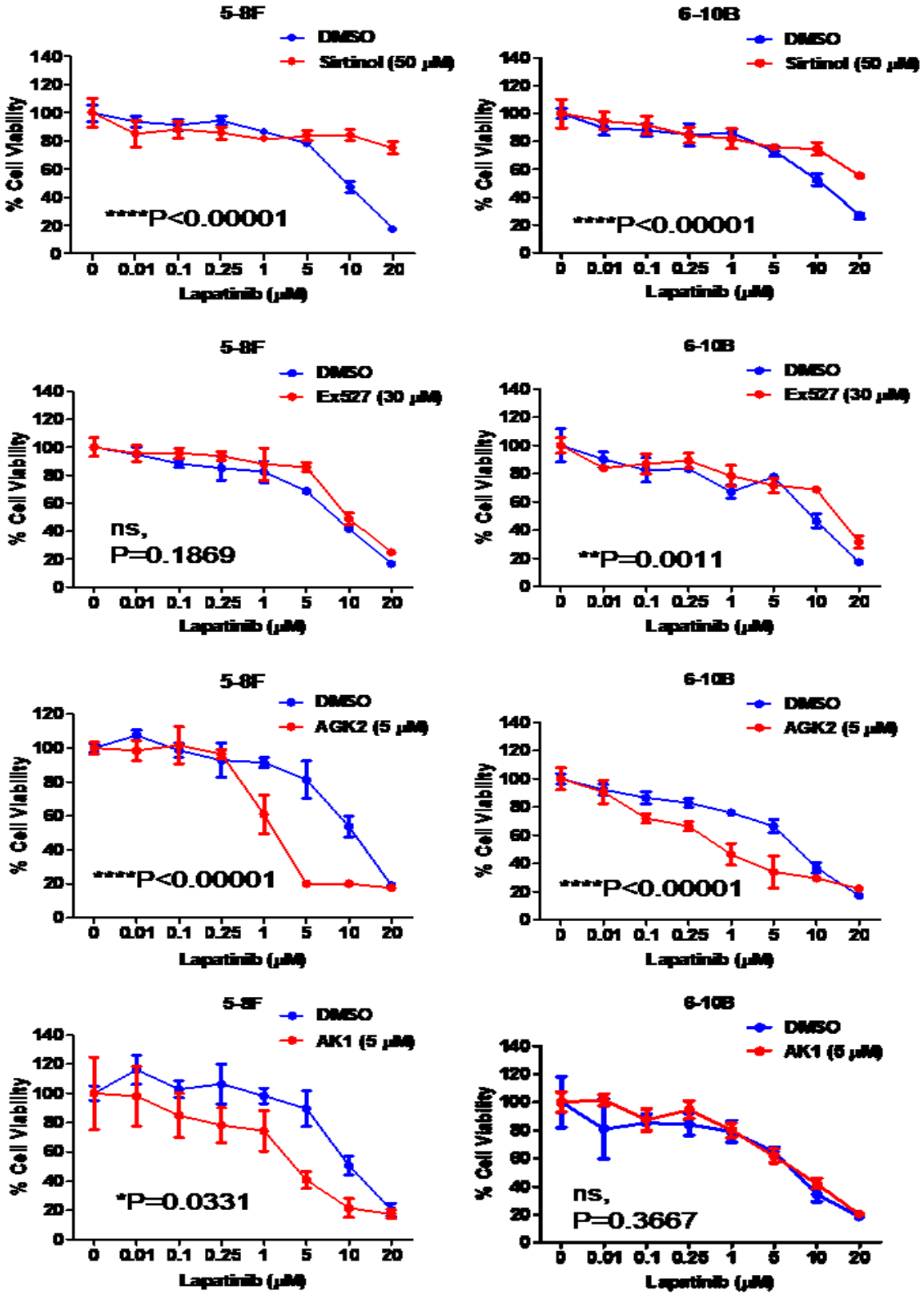


Figure 5.19 High and low metastatic NPC cells show increased Lapatinib sensitivity upon combination treatment with AGK2 and AK1 but not with Sirtinol or EX527. Cells ($3x10^3$ / well) were seeded in 96-well plates and treated with increasing concentrations of lapatinib for 48h before staining and measurement of optical density at 492 nm. Data were analysed by generating curves using graph-pad prism. Numerical data represent the average ± SEM of three different experiments (**** *P*<0.0001, ns= non-significant).

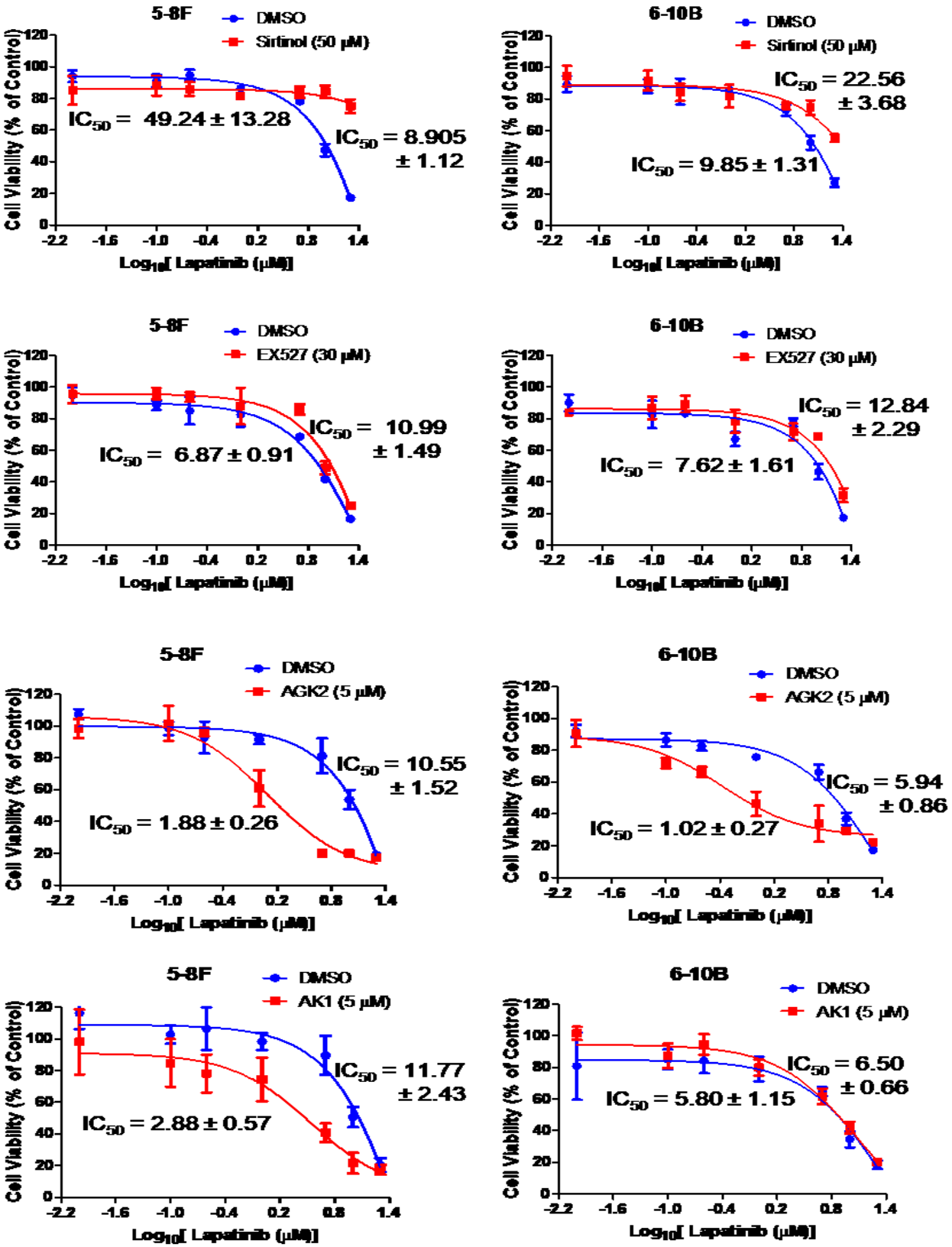


Figure 5.20 High and low metastatic NPC cells show increased Lapatinib sensitivity upon combination treatment with AGK2 and AK1 but not with Sirtinol or EX527. Cells ($3x10^3$/well) were seeded in 96-well plates and treated with increasing concentrations of lapatinib for 48h before staining and measurement of optical density at 492 nm. Best-fit curves were generated by graph pad prism to determine the effect of AGK2 or AK1 on reducing the IC_{50} of Lapatinib for each NPC cells.

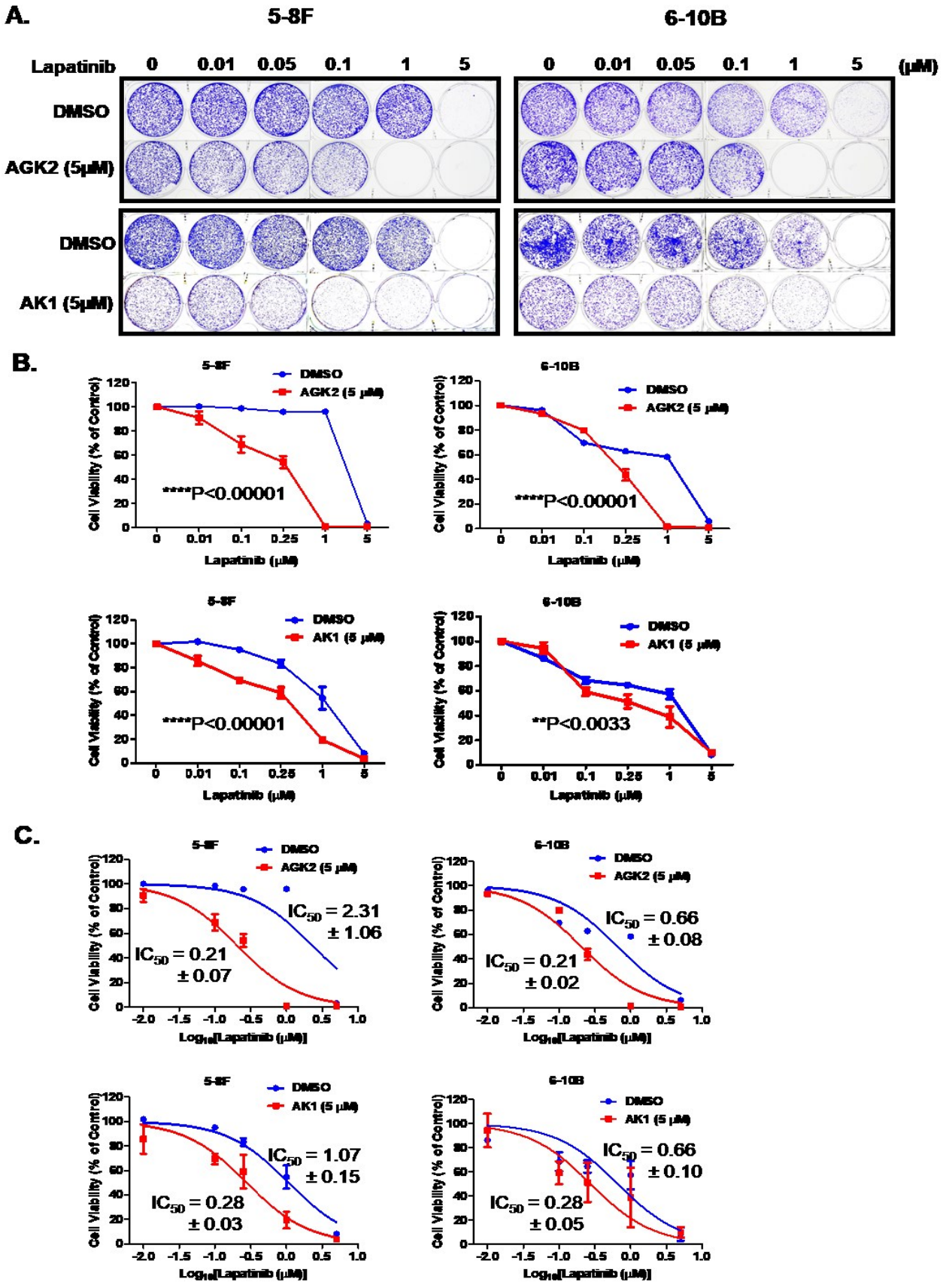


Figure 5.21 Lapatinib in combination with AGK2/AK1 increase long term cell sensitivity compared to lapatinib alone. A) 5-8F and 6-10B cells were seeded in 6-well and treated with the Lapatinib concentration indicated for 72h. 5 μM AGK2 and AK1 was used for combination treatment.

Then, cell culture media was removed, and colony formation observed for 15 days. At the end of this time, cells were fixed with 4% para formaldehyde and stained with crystal violet. Representative pictures from triplicate experiments are shown. **B)** The stain was solubilised with 33% acetic acid and absorbance at 592 nm were obtained. Graphs were generated to show the effect of combination treatment. Numerical data represent the average ± SEM of three different experiments (**** *P*<0.0001, ns= non-significant). **C)** Best fit-curves were generated to determine the effect of AGK2/AK1 to reduce the IC_{50} of lapatinib in 5-8F and 6-10B cells.

5.2.13 Silencing of SIRT2 enhances lapatinib sensitivity of NPC cells

To confirm further the role of SIRT2 in promoting lapatinib resistance, we next examined if siRNA-depletion of SIRT2 can enhance the antiproliferative effects of lapatinib in the 5-8F and 6-10B NPC cells using clonogenic assays. Knock-down of SIRT2 was confirmed by western blotting analysis before the NPC cells were subjected to clonogenic assays (Figure 5.22A). The results showed that despite the subtle effects, depleting SIRT2 has additive effects on lapatinib when compared with the non-silencing siRNA controls in both the NPC cell lines (2-way ANOVA, ****P<0.0001, respectively) (Figure 5.22B). Significantly, the SIRT2-siRNA enhanced the anti-proliferative functions of lapatinib in both the resistant 5-8F and (IC_{50}: 4.64 ± 0.38 to 2.85 ± 0.41 μM) and sensitive 6-10B (IC_{50}: 1.12 ± 0.10 to 0.90 ± 0.10 μM) cells (Figure 5.22C). In consequence, the results suggest that SIRT2 knockdown can significantly enhance the cytotoxic and cytostatic functions of lapatinib in both the sensitive and resistant NPC cells, consistent with the findings from the SIRT2 pharmaceutical inhibitors, AK1 and AGK2. Collectively, these results demonstrated that selective inhibition of SIRT2 can promote lapatinib sensitivity, indicating SIRT2 is a potential target for overcoming lapatinib resistance in NPCs.

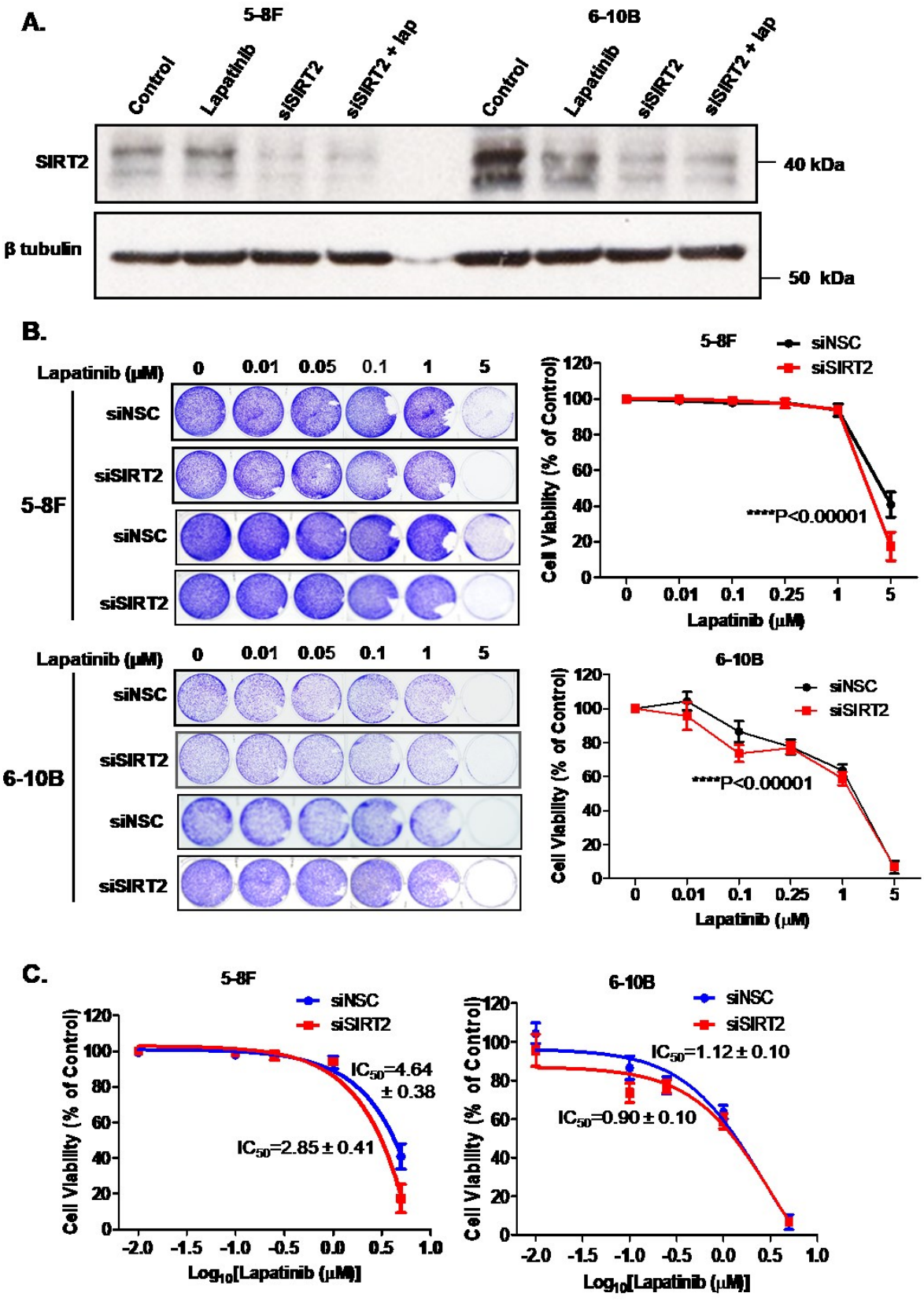


Figure 5.22 Silencing of SIRT2 increases long-term lapatinib cytotoxicity in NPC cells. A) NPC cells were transfected with siNSC and siSIRT2 smartpool. After 24h both siNSC and siSIRT2 cells were treated with DMSO or 5 uM Lapatinib for another 24h. After 48h from transfection, cells were harvested and SIRT2 protein knockdown was confirmed by western blot analysis. **B)** After 48 hours of

transfection, 1000 cells were seeded per well, in 6-well plates and then treated with the lapatinib concentration indicated (0, 0.01, 0.05, 0.1, 1, 5 μM) for 72h and colony formation observed for 15 days. At the end of this time period, cells were fixed with 4% para formaldehyde and stained with crystal violet. The stain was solubilised with 33% acetic acid and absorbance at 592 nm were obtained. Graphs were generated to show the effect of silencing SIRT2 on Lapatinib sensitivity. **C)** Best fit-curves were generated to determine the effect of Knocking down of SIRT2 to reduce the IC_{50} of lapatinib in 5-8F and 6-10B cells. Numerical data represent the average ± SEM of three different experiments (**** P<0.0001).

5.2.14 Inhibition and silencing of SIRT2 can combine with lapatinib to promote FOXO3 acetylation

To confirm that SIRT2 can modulate the ability of lapatinib to mediate FOXO3 acetylation, we next determined if chemical inhibition or silencing of SIRT2 can affect FOXO3 acetylation in the absence or presence of lapatinib treatment using co-immunoprecipitation (IP) assays (Figure 5.23). Relative FOXO3 acetylation levels were then determined by comparing the ratio of acetylated to total FOXO3 co-precipitated. The computed results showed that SIRT2-depletion by siRNA or inhibition by AGK2 can induce FOXO3 acetylation in both the lapatinib resistant 5-8F and the sensitive 6-10B cell lines (Figure 5.23A, B). The chemical inhibitor AGK2 is more effective in inducing FOXO3 acetylation than SIRT2 siRNA probably because it is more effective in inhibiting SIRT2 activity. Importantly, both chemical inhibition and siRNA-depletion of SIRT2 enhanced the FOXO3 acetylation induced by lapatinib in both the lapatinib resistant 5-8F and sensitive 6-10B cell lines, except for the 6-10B cells treated with SIRT2 siRNA. The low levels of acetylated FOXO3 precipitated from the sensitive 6-10B following combined lapatinib and SIRT2-siRNA treatment is likely to be due to the high levels of global protein degradation as a result of cell death caused by the combination of SIRT2-depletion and lapatinib treatment. Moreover, lapatinib also downregulates SIRT2 in the sensitive 6-10B cell line, rendering the effects of SIRT2-siRNA redundant. Overall, these IP results suggest that SIRT2 restricts the lapatinib-mediated FOXO3 acetylation in NPCs. In summary, our collective results reveal that SIRT2 has a role in modulating FOXO3 acetylation and lapatinib response in NPCs and that targeting SIRT2 can enhance the sensitivity of NPCs to lapatinib and to overcome lapatinib resistance in NPC.

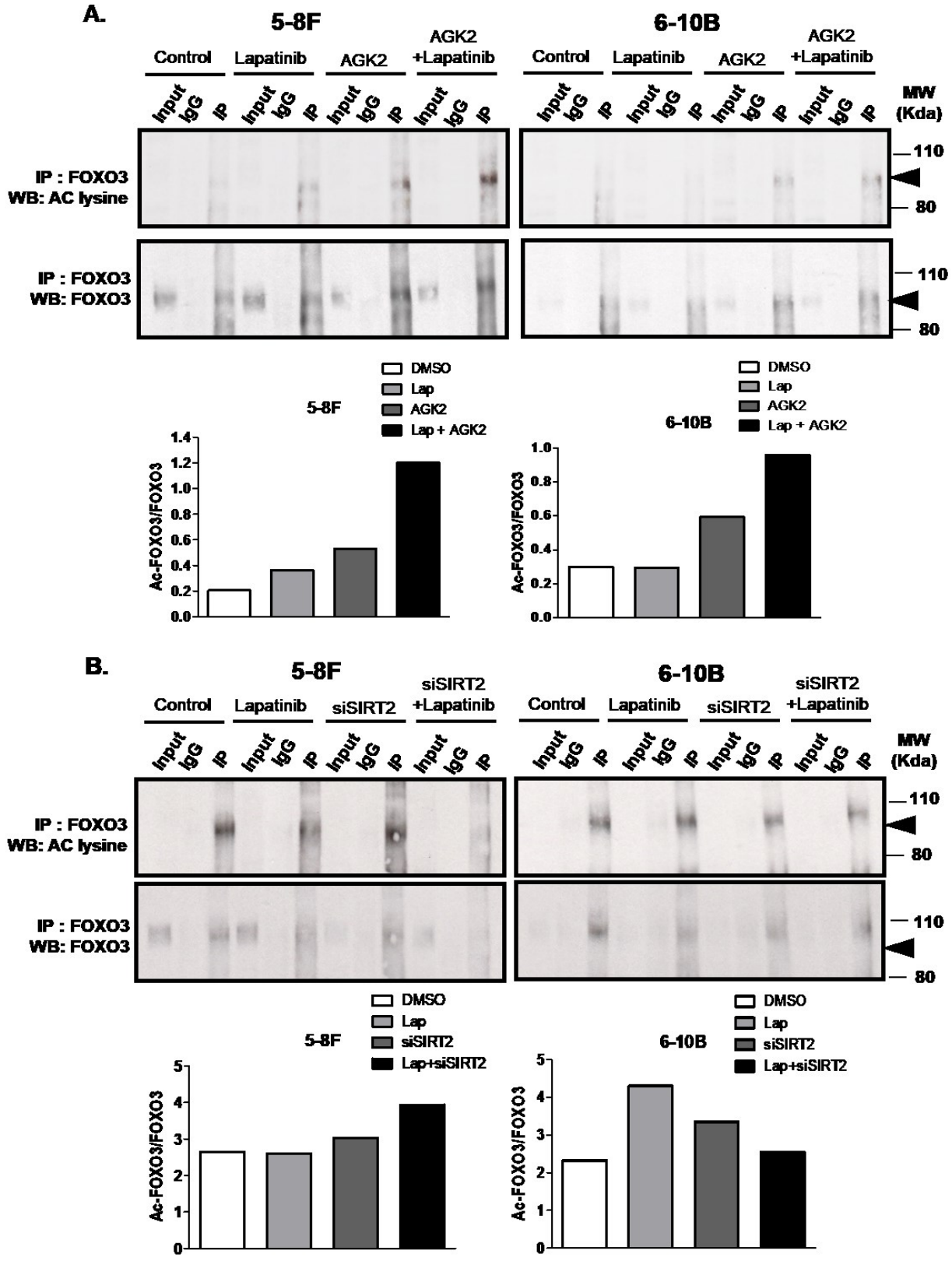


Figure 5.23 Inhibition of SIRT2 by AGK2 as well as silencing of SIRT2 in combination with Lapatinib upregulates acetylated FOXO3 levels in 5-8F and 6-10B cells. A) NPC were treated with AGK2 alone or in combination with Lapatinib for 48h. Proteins were obtained from whole cell extracts and assessed by Co-immunoprecipitation (Co-IP) with an anti-FOXO3 antibody. Subsequent immunoblotting was performed using antibodies against Ac-Lys and FOXO3. The anti-IgG was used as a negative control. Acetylated FOXO3 levels were determined by using ImageJ analysis and

representative bar diagram are shown (bottom panel after the blot) **B)** NPC cells were transiently transfected with siNSC and siSIRT2 and treated with 5 μM lapatinib for 24h. Proteins were obtained from whole cell extracts and assessed by Co-immunoprecipitation (Co-IP) with an anti-FOXO3 antibody. Subsequent immunoblotting was performed using antibodies against Ac-Lys and FOXO3. Acetylated FOXO3 levels were determined by using ImageJ analysis and representative bar diagram are shown (bottom panel).

5.3 Discussion

SIRT2 primarily act as deacetylases and their catalytic action occurs on histone substrates, with variable specificity [267], and on a large number of nonhistone proteins [376]. Thus, as a consequence, SIRT2 play a significant role in various biological processes as well as cancer metastasis. Notably, SIRT2 is highly expressed in various types of human cancer, and inhibition of SIRT2 generally exhibits anti-tumourigenic effects [417]. Here, we have elucidated the role of SIRT2 as a critical mediator of FOXO3 deacetylation and a modulator of lapatinib sensitivity in breast and nasopharyngeal cancers.

To elucidate the role of SIRT2 in mediating FOXO3 acetylation, I performed duolink proximity assay upon silencing SIRT2 in BT474 WT and Lap^R cell lines. Depletion of SIRT2 found to enhance significant level of FOXO3 acetylation in sensitive BT474 cells (Figure 5.1). Western blot analysis revealed that knockdown of SIRT2 increases EP300 and CBP expression which in turn induces FOXO3 expression. However, I did not observe significant increase of FOXO3 acetylation upon SIRT2 silencing although increased acetylation was observed in duolink PLA assay as mentioned. Therefore, I attempted combination treatment of lapatinib upon silencing SIRT2 and found that FOXO3 acetylation increased significantly. Since, combination treatment offers higher acetylation level compared to lapatinib alone, therefore silencing SIRT2 has additive effect to induce FOXO3 acetylation. Moreover, silencing SIRT2 alone and combination treatment both were found to enhance acetylation of p53. Notably, the induced FOXO3 acetylation further increases its downstream gene expression e.g. Bim, $p27^{Kip1}$, p130, and $p16^{INK4a}$. In addition, elevated expression of cleaved PARP and cleaved caspases were observed upon SIRT2 silencing suggesting that silencing of SIRT2 enhances FOXO3 acetylation and its activity. Furthermore, silencing of SIRT2 was found to increase lapatinib

cytotoxicity of BT474, however, it can not affect cell growth of BT474 Lap^R cells (Figure 5.5).

To further assess the role of SIRT2, I used a newly designed SIRT2 inhibitor scAB8A44. This novel inhibitor increases FOXO3 acetylation when treated both MCF7 cells and BT474 cells (Figure 5.8 and 5.9). The activity in inducing acetylation is higher when compared with other SIRT2 inhibitors e.g. DK-029 or AGK2. Moreover, scAB8A44 found to enhance EP300 mediated FOXO3 acetylation, expression and also enhances its transcriptional activity. Furthermore, scAB8A44 sensitizes BT474 to lapatinib compared to untreated cells. However, in BT474 Lap^R cells the inhibitor only affects cell proliferation but not the lapatinib sensitivity (Figure 5.12). Taken together, these data suggest an important role of SIRT2 in deacetylating FOXO3 and regulating lapatinib resistance of HER2 positive breast cancer BT474.

Metastasis and drug resistance are the characteristics of aggressive cancers and the major causes for poor survival in nasopharyngeal carcinoma (NPC) [418, 419]. An understanding of the mechanisms involved in the development of NPC metastasis and drug resistance will aid the development of early diagnostic biomarkers and the identification of potential therapeutic targets. Previous studies have reported lapatinib could effectively induce cell death and autophagy in NPC cells [404, 405]. Clinical studies also suggest that lapatinib alone or combined with standard chemotherapies are well-tolerated and promote patient survival in metastatic/recurrent head and neck squamous cell carcinoma [420]; however, not all patients benefit from lapatinib-based treatments [421, 422]. In the present study, we found that the highly metastatic (C666-1 and 5-8F) NPC lines are significantly more lapatinib resistant compared to poorly metastatic lines (6-10B, TW01 and HK-1), suggesting that the molecular mechanisms involved in metastasis in NPC may overlap with those responsible for the development of lapatinib resistance.

FOXO3 is a tumour suppressive transcription factor and an important modulator of sensitivity to chemotherapy [196, 230]. FOXO3 inhibits cell growth by driving the

transcription of genes, such as Bim, FasL, $p27^{Kip1}$, p130 (RB2), essential for cell proliferative arrest, cell death and differentiation [196, 230]. Conversely, inactivation of FOXO3 is a crucial step for oncogenic transformation and the development of cytotoxic drug resistance [196, 230]. Previous work has also suggested that FOXO3 mediates the cytotoxicity of lapatinib in breast cancer [75, 76]. Herein, we have shown definitively using foxo1/3/4-deficient fibroblasts that FOXO3 along with FOXO1 and -4 are involved in mediating the cytotoxic functions of lapatinib. Consistent with this, recent evidence has showed that natural products, such as curcumin, inhibits the growth and induces apoptosis in NPC cell by increasing FOXO3 expression [423]. In addition, the G-quadruplex ligand SYUIQ-5 also induces NPC autophagy by down-regulating AKT phosphorylation and promoting FOXO3 nuclear translocation [424].

The activity, expression and subcellular localization of FOXO3 are regulated by a diverse range of post-translational modifications [179]. Phosphorylation of FOXO3 by kinases, particularly AKT (also called PKB), ERK, IKB kinase (IKK) and serum and glucocorticoid-regulated kinase (SGK) can enhance FOXO3 nuclear to cytoplasmic shuttling and its degradation [179, 230]. Conversely, other kinases, such as p38 MAPK [238], stress activated c-Jun-NH2-kinase (JNK) [425] have also been demonstrated to promote FOXO3 activity and expression. Consistent with previous studies with EGFR1/HER2 (ERBB2)-targeted tyrosine kinase inhibitors (TKIs) [76, 338], we found that lapatinib can cause FOXO3-dephosphorylation (T32) and the downregulation of its target FOXM1 in lapatinib-sensitive NPC cells. However, although EGFR1/HER2 inhibitors have previously been shown to modulate p38 and JNK activity [426, 427], we did not observe any substantial changes in p38 and JNK phosphorylation/activity in NPC cells in response to lapatinib treatment, suggesting it is unlikely that lapatinib modulates FOXO3 activity via p38 and JNK in these NPC cells. FOXM1 is a potent oncogene negatively regulated by FOXO3 [230] and contributes to cancer drug resistance through controlling many genes involved in cell proliferation, survival, DNA repair, and tubulin destabilization [230, 428, 429]. Consistent with a role for FOXO3 in lapatinib action in NPC cells, we found that FOXM1 expression is repressed by lapatinib in the sensitive cells but remains constitutively high in the resistant NPC cells, suggesting a role of FOXM1 in NPC lapatinib resistance. In agreement, FOXM1 has been shown to be able to mediate

paclitaxel resistance by regulating the gene transcription of the ABCC5 drug efflux transporter in NPC [410]. In addition, overexpression of FOXM1 is directly associated with metastasis in NPC, and targeting FOXM1 with inhibitors or siRNA knockdown can effectively restrict the cell proliferation, migration, angiogenesis and survival of NPC cells [421, 430].

Besides phosphorylation, FOXO3 is also regulated by other post-translational modifications such as acetylation, methylation, ubiquitination and glycosylation. The nuclear sirtuins SIRT1, SIRT2 and SIRT6 have been shown to negatively regulate FOXO3 acetylation and its activity [194, 431, 432]. In the present study, we found that SIRT2 specifically modulates the cytotoxicity of lapatinib and is linked to lapatinib resistance using specific chemical inhibitors and SIRT2 siRNAs. Although our findings show that all four SIRT inhibitors (i.e. sirtinol, EX527, AGK2 and AK1) can limit NPC cell proliferation, only the SIRT2 specific inhibitors AGK2 and AK1 function cooperatively with lapatinib, supporting the idea that SIRT2 specifically modulates lapatinib response and resistance. Nevertheless, all four SIRT inhibitors can restrict normal NPC cell viability and clonogenicity, and this suggests that the nuclear sirtuins SIRT1, -2 and -6 detected in NPC are all potential oncogenes. In agreement, SIRT1 upregulation has been shown to be associated with tumour progression and metastasis in NPC biopsies [433]. The pan-SIRT inhibitor sirtinol has previously been shown to induce p53 acetylation and cell death through targeting both SIRT1 and SIRT2 [264]. However, like EX527, the sirtinol concentrations employed here preferentially inhibit SIRT1 and have limited activities towards SIRT2 [264]. Therefore, these observations support further the notion that SIRT2 specifically moderates the cytotoxic action of lapatinib and mediates lapatinib resistance, independently of SIRT1. The reason for the finding that both the SIRT inhibitors sirtinol and EX527 oppose the cytotoxic functions of lapatinib is unclear. However, a context dependent tumour suppressive role for SIRT1 has previously been proposed [434]. In concordance, SIRT1-deficient cells have been shown to be defective in the ability to normally upregulate the p19 (ARF) senescence mediator and its potent downstream tumour suppressor p53 [434], and this might account for the ability of sirtinol and EX527 to attenuate the antiproliferative function of lapatinib. Inhibition of SIRT2 by chemical inhibitor or silencing significantly enhances the cytotoxicity of lapatinib not only in the sensitive but also in the resistant NPC cells, suggesting that

SIRT2 not only modulates the cytotoxic functions of lapatinib in the sensitive NPC cells, but it also mediates lapatinib resistance. This implies that targeting SIRT2 can enhance the cytotoxicity of lapatinib and may represent a novel strategy for overcoming lapatinib resistance in NPC. This role of SIRT2 in modulating lapatinib response and sensitivity is confirmed by SIRT2 depletion experiments showing silencing SIRT2 can enhance the cytotoxicity in both lapatinib sensitive and resistant NPC cells. Although the siRNA depletion approach has less off-target effects, it also relies on high delivery efficiencies; the incomplete SIRT2 depletion might account for the small additional effects on lapatinib. In agreement, overexpression of SIRT2 has been shown to essentially lengthen the M phase and defer mitotic exit [407]. Moreover, SIRT2 can induce the cell proliferation of leukaemia and resistance to apoptosis [435]. Conversely, decreased SIRT2 activity can reduce glioma cell survival by induced both necrosis and apoptosis [436] and limit melanoma cell growth and clonogenicity [437]. Furthermore, overexpression of SIRT1 and SIRT2 can also confer resistance to chemotherapy such as paclitaxel [438].

Furthermore, our co-IP experiments also show that the lapatinib induces FOXO3 acetylation and that inhibition of SIRT2 by chemical inhibitor or silencing also promotes FOXO3 acetylation in NPC cells. Importantly, SIRT2 inhibition or silencing can combine with lapatinib to cause further enhancement of FOXO3 acetylation than lapatinib treatment alone in both sensitive and resistant NPC cells, suggesting that SIRT2 can moderate the cytotoxic functions of lapatinib and promote resistance through limiting FOXO3 acetylation. In agreement, FOXO3 deacetylation by SIRT2 has previously been reported to enhance FOXO3 ubiquitination and proteasomal degradation [439].

Collectively, these data suggest that the cytotoxic functions of lapatinib are mediated through the acetylation and activation of FOXO3, and that SIRT2 can specifically antagonise the cytotoxicity of lapatinib through mediating FOXO3 deacetylation in both sensitive and resistant BT474 and NPC cells. The present findings also suggest that SIRT2 can be an important biomarker for metastatic and lapatinib resistant NPC and that targeting the SIRT2-FOXO3 axis may provide a means to treat NPC and to overcome NPC chemoresistance.

Chapter 6

Oncogenic EP300 can be targeted with inhibitors of aldo-keto reductases (AKR1C) in triple negative breast cancer Hs578T

6.1 Introduction

E-cadherin is an important transmembrane glycoprotein that mediates epithelial cell-cell adhesion [98]. Use of E-cadherin expression as a biomarker for breast cancer diagnosis [440], becomes low or absent in some types of breast cancer such as metaplastic breast carcinoma, especially in the spindle subtype which shows characteristics of epithelial-to-mesenchymal transition (EMT) [441, 442]. Unlike invasive lobular carcinoma (ILC), primary invasive, or infiltrating, ductal carcinoma (IDC) shows good immunoreactivity for E-cadherin if lymph nodes have not been invaded, but the staining is very weak when metastases have occurred [443]. In addition, E-cadherin has a tumour suppressor role as its down-regulation triggers EMT, acquisition of stem cell-like properties and drug resistance [444, 445].

Regulation of E-cadherin gene (*CDH1*) expression occurs at multiple levels and the mechanisms leading to its repression are well studied. Promoter hypermethylation as well as inactivating mutations spreading along the extracellular domain have all been reported in different cancers [334, 446]. Negative regulation by transcription factors such as Snail, Slug, Twist and ZEB1/2, resulting in EMT is also well understood [447]. However, the role of activators of E-cadherin expression (such as EP300, RUNX1 and FOXA1 [448, 449]) during EMT is less studied.

Previously our lab described a novel E-cadherin regulatory axis controlled by the miR-106b~25 cluster which down-regulates the E-cadherin transcriptional activator EP300 [315, 450]. Silencing of EP300 in breast epithelial cancer cells down-regulates E-cadherin, triggers an EMT as well as an increase in cancer stem cell-like cells (CSCs) and drug resistance. Conversely, ectopic overexpression of EP300 in basal-like triple negative breast cancer cells rescues the mesenchymal-like phenotype, coupled with an increase in epithelial-like properties [170]. Similar results have also been reported in pancreatic [451] and colorectal cancer [156]. Moreover, Kaplan-Meier plots using a large cohort (>4,000) of breast cancer patients, suggest that both EP300 and E-cadherin are good prognostic indicators [452]. However, other reports support an oncogenic role for EP300 in prostate [453], hepatocellular [454] or nasopharyngeal cancer [455].

Recently, we have demonstrated a strong down-regulation of both EP300 and E-cadherin in metaplastic breast carcinoma, a rare, but aggressive form of invasive breast cancer which has a poor clinical outcome [170]. Previously we showed a strong positive correlation between EP300 and E-cadherin expression by immunohistochemistry (IHC) in IDC and ILC, although some clinical samples were EP300^{high}/E-cadherin^{low} and find that both markers taken together were better predictors of lymph node metastasis than E-cadherin alone. However, EP300 can act as an oncogene in a cell model with hypermethylation of the *CDH1* promoter, leading to an increase in EMT and CSC markers, migration, invasion, anchorage independence and drug resistance.

The major aim of this chapter was to elucidate the oncogenic role of EP300 in Hs578T cells independent of FOXO3 acetylation. Moreover, the role of EP300 in regulating EMT inducing transcription factors, cancer stem cell markers as well as drug resistance was thoroughly studied. Finally, I attempted to use a pharmacological inhibitor to target the oncogenic functions of EP300 in Hs578T.

6.2 Preliminary Results

6.2.1 Correlation of EP300 and E-cadherin in breast tissue

Work performed in our lab prior to my incorporation indicated that in non-malignant breast tissues, both EP300 and E-cadherin staining showed, as expected, intense signals. E-cadherin consistently showed membrane staining scoring 3 and EP300 showed a strong / intermediate nuclear signal in 18 out of 20 samples. The remaining two samples showed scores of 0 and 1 in the nucleus, but with intermediate staining (score 2) in the cytoplasm, and thus all cases were considered EP300^{high}/E-cadherin^{high}. When IDC cases were analysed, their IHC score varied from 1 to 3, indicating low to high expression for both EP300 and E-cadherin. Most cases were either EP300^{high}/E-cadherin^{high} or EP300^{low}/E-cadherin^{low}, 10 and 6, respectively, out of 20 (Figure6.1). Of the 21 ILCs, 6 cases were EP300^{high}/E-cadherin^{high}, 7 EP300^{low}/E-cadherin^{low} and, more importantly, 7 EP300^{high}/E-cadherin^{low}. Only 2 cases scored 3 for both E-cadherin and EP300, the remaining of the high cases with intermediate levels of expression (score 2) for both proteins (Figure6.1 and Table 6.1).

As EP300 is a transcriptional activator of E-cadherin expression, our lab hypothesized that IHC signals of both proteins would vary in parallel. Normal and non-malignant breast tissues showed, as expected, a consistent strong expression for both EP300 and E-cadherin. Importantly, a positive correlation was found in 80% (49 out of 61) of all samples analyzed with strongly significant concordance between EP300 and E-cadherin (P <0.0001, Chi-square test; Table 6.1). When only cancer samples were considered, the concordance between EP300 and E-cadherin was maintained (P = 0.0046, Chi-square test; Table 6.1). These data with a relatively small cohort are strongly supported by the previous literature [448] and our laboratory studies demonstrating a positive E-cadherin control by EP300 [170, 315, 450]. However, some cancer cases with a negative correlation, either EP300^{high}/E-cadherin^{low} (9 out of 41, 22%) or EP300^{low}/E-cadherin^{high} (3 out of 41, 7.3%; Table 6.1) were also found, indicating that in malignant tissues other factors may play a role in E-cadherin expression.

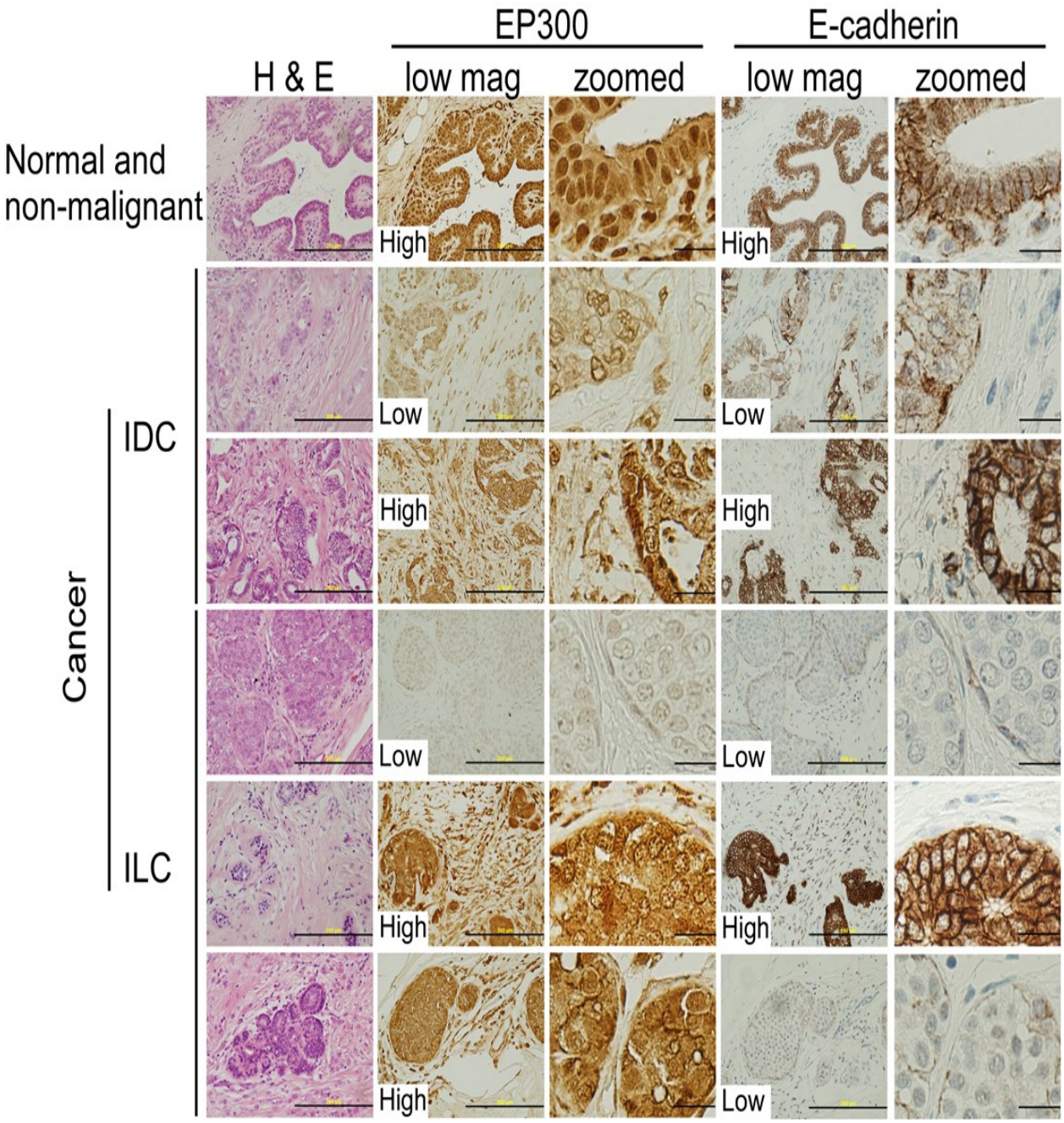


Figure 6.1. EP300 and E-cadherin expression in breast tissue.
Representative immunohistochemical images after staining for EP300 and E-cadherin. *IDC,* invasive ductal carcinoma; *ILC,* invasive lobular carcinoma. Scores have been included in the low magnification pictures. Most of the IDC cases were either EP300^{low}/E-cadherin^{low} or EP300^{high}/E-cadherin^{high} whereas in ILC the distribution of cases between EP300^{low}/E-cadherin^{low} EP300^{high}/E-cadherin^{high} and EP300^{high}/E-cadherin^{low} was similar (Table 1). *H&E,* haematoxylin and eosin staining. Scale bar represents 200 μm in the low magnification pictures and 20 μm in the zoomed images.

Table 6.1. Expression of E-cadherin correlates with that of its transcriptional activator EP300 in both non-malignant and breast cancer

	EP300 and E-cadherin expression				
	Positive correlation		Negative correlation		
Tissue	$EP300^{high}$/E-$cadherin^{high}$	$EP300^{low}$/E-$cadherin^{low}$	$EP300^{high}$/E-$cadherin^{low}$	$EP300^{low}$/E-$cadherin^{high}$	
Non-malignant	20	0	0	0	$n = 20$
IDC[a]	10	6	2	2	$n = 20$
ILC[b]	6	7	7	1	$n = 21$
Total	36	13	9	3	$P < 0.0001$[c]
Cancer total	16	13	9	3	$P = 0.0046$[c]

[a]invasive ductal breast carcinoma
[b]invasive lobular breast carcinoma
[c]Chi-square test

6.2.2 Loss of EP300 and E-cadherin expression correlates with metastatic lymph node invasion in breast cancer

As EP300 transcriptionally activates E-cadherin expression and E-cadherin is a key molecule in metastatic reprogramming [456], my lab analyzed the expression of these two markers in relation to the invasion of lymph nodes in breast cancer patients. In both IDC and ILC the group with a positive correlation between both markers, lymph node metastasis was less frequent (3 versus 13, 18.7%) in the $EP300^{high}$/E-$cadherin^{high}$ patients. Conversely, an $EP300^{low}$/E-$cadherin^{low}$ phenotype led to a high frequency of lymph node metastasis (10 versus 3, 76.9%; $P = 0.006$, Chi-square test; Table 6.2). Importantly, both markers when applied together were better predictors of lymph node metastasis than E-cadherin alone ($P = 0.006$ vs. $P = 0.025$, respectively). Overall, these data support an anti-metastatic role for EP300 via its activation of the tumour suppressor E-cadherin.

Table 6.2. Correlation between EP300 and E-cadherin expression is a good predictor of lymph node metastasis

	EP300 and E-cadherin markers				Single E-cadherin marker		
	Positive correlation		Negative correlation				
Lymph node metastasis	EP300^{high}/E-cadherin^{high}	EP300^{low}/E-cadherin^{low}	EP300^{high}/E-cadherin^{low}	EP300^{low}/E-cadherin^{high}	E-cadherin^{high}	E-cadherin^{low}	
Y[a]	**3**	**10**	**5**	**1**	**4**	**15**	n =19
N	**13**	**3**	**4**	**2**	**15**	**7**	n =22
	P = 0.006[b]		P = 0.505[b]		P = 0.025[b]		

[a]at least one lymph node invaded with cancer cells
[b]Chi-square test of above 2x2 table highlighted in bold

6.3 Results

6.3.1 A cell model to study EP300 function independently of E-cadherin

In order to gain an insight into the potential dual role of EP300 as oncogene or tumour suppressor, I reasoned it would be necessary to differentiate it from its role in activating E-cadherin expression. Histone acetyl transferases help to relax chromatin thus enabling gene expression, although this only occurs in less methylated loci [457]. *CDH1* (encoding E-cadherin) promoter has been found to be methylated in a proportion of breast cancer patients, where it may contribute to the repression of the locus [458]. I asked whether EP300^{high}/E-cadherin^{low} and EP300^{high}/E-cadherin^{high} patient's tumours had a different methylation profile at the *CDH1* proximal promoter. For this we analyzed the methylation status of 21 CpGs by bisulphite conversion and pyrosequencing. As expected, methylation in EP300^{high}/E-cadherin^{high} samples was low and no CpG showed values above 6%. Conversely, EP300^{high}/E-cadherin^{low} samples showed a greater variation in the methylation percentage, with some CpGs as high as 33% (Figure 6.2A). Taking all the CpGs analyzed, the overall percentage of methylation at the *CDH1* locus in EP300^{high}/E-cadherin^{low} was twice that found in EP300^{high}/E-cadherin^{high} samples (Figure 6.2B). Thus, methylation of the E-cadherin promoter may explain, at least in part, the lack of E-cadherin expression in EP300^{high}/E-cadherin^{low} tumours.

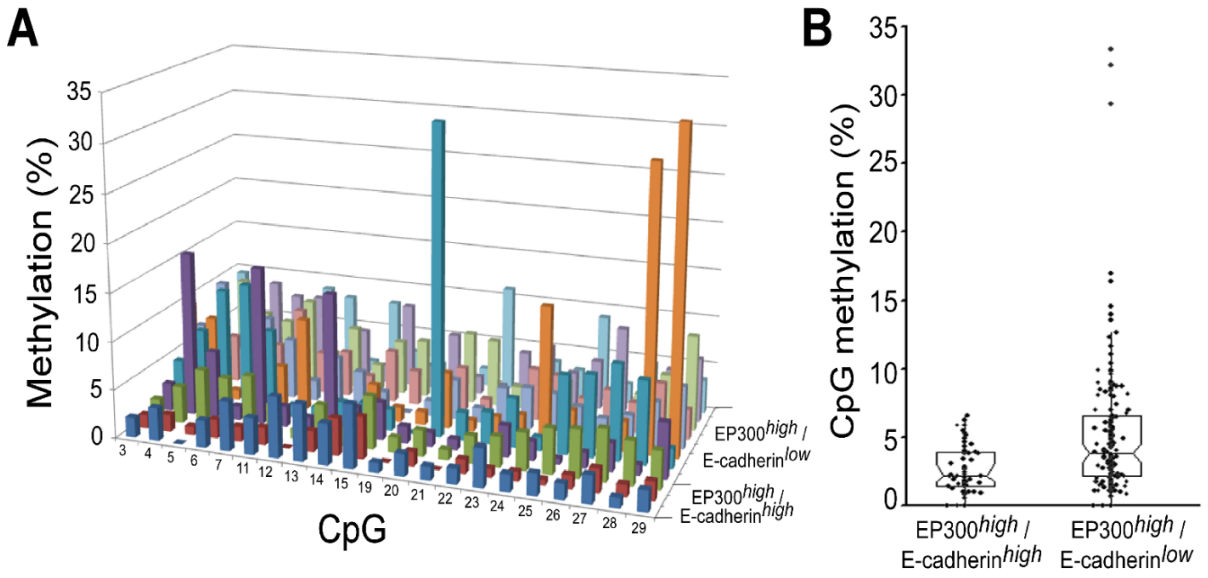


Figure 6.2. E-cadherin promoter is methylated in EP300^{high}/E-cadherin^{low} tumours. Methylation at 21 CpGs in the proximal *CDH1* (E-cadherin) promoter was determined after bisulphite conversion and pyrosequencing in DNA isolated from EP300^{high}/E-cadherin^{high} (n = 3) and EP300^{high}/E-cadherin^{low} (n = 8) FFPE tissue samples. **A)** Individual methylation values in 21 CpGs. CpG numbering corresponds to that previously described [334]. **B)** Box plot representation of the methylation percentage in 21 CpGs in all patients analyzed. Box plot indicates the mean within the box at 95% confidence interval. Data were analyzed using the Mann-Whitney test (p<0.0001).

E-cadherin promoter methylation is well characterized in some breast cancer cell lines and, in particular, Hs578T cells which show an average of 47% methylation across 29 CpG sites with no, or minimal, E-cadherin expression [334]. Thus, I decided to use derivatives of this cell line previously established in our lab by stably overexpressing EP300 that could be used as a cell model for EP300^{high}/E-cadherin^{low} breast cancer, allowing us to test the role of EP300 in an E-cadherin-null background.

6.3.2 EP300 overexpression upregulates the expression of epithelial to mesenchymal transition (EMT) markers in Hs578T cells

The three derivatives of the triple-negative breast cancer cell line Hs578T, Hs578T-EV, Hs578T-EP300 and Hs578T-CDH1, were previously generated in our lab by stable transfection of EP300 or E-cadherin expressing plasmids. Hs578T-EV cells were transfected with empty pcDNA 3.1 and served as negative control.

EMT is the first step in the metastatic cascade and cells undergoing EMT present a set of characteristic markers accompanying the acquisition of mesenchymal-like phenotype [459]. Hs-EP300 cells showed increased expression levels of N-cadherin

(an adhesion molecule expressed in mesenchymal cells and neural tissues), vimentin (a mesenchymal intermediate filament), as well as the E-cadherin transcriptional repressors Snail, Slug and Zeb1 (Figure 6.3A). Although control Hs-EV cells expressed these molecules due to the triple-negative, basal-like, nature of Hs578T cells, EP300 overexpression increased further both their RNA and protein levels. Snail and Zeb1 are two EMT-inducing transcription factors known for their E-cadherin repressing activity [460]. EMT markers were found to be highest in the EP300 overexpressed cell lines. Moreover, EP300 overexpression did not induce E-cadherin expression, either at mRNA or protein level, in contradiction to previously reported data in some other triple negative breast cancer cell lines [170]. High level of N-cadherin and Vimentin expression in EP300 overexpressed cells were confirmed by assessing the level of mRNA using RT qPCR (Figure 6.3B). Furthermore, immunofluorescence experiment was performed to validate the expression of E-cadherin and Vimentin in EP300 overexpressed cells (Figure 6.4A, B). I also used E-cadherin (CDH1) overexpressed Hs578T cells as a positive control and found that overexpression of E-cadherin can downregulate the expression of EMT markers such as vimentin, snail, slug and zeb1.

On the other hand, Ac-FOXO3 and sirtuin expression were assessed by immunoblotting to determine any involvement of FOXO3 acetylation in EMT induction in EP300 overexpressed cells (Figure 6.3C). Phosphorylated form of FOXO3 (T32) was found to be highly expressed compared to Ac-FOXO3 expression which indicates inactivation of FOXO3. Moreover, it has been shown that SIRT1 and FOXM1 plays very important role to induce EMT in cancer cells [461], [462], [463]. Supporting these previous results, we found that upregulation of FOXM1 and sirtuins (SIRT1, SIRT2, SIRT6) expression (Figure 6.3C) occurred upon EP300 overexpression in Hs578T cells which also suggest deregulation of FOXO3 acetylation as well as its inactivation in Hs578T cells. Therefore, all these results suggest that overexpression of EP300 in the E-cadherin-null background of Hs578T cells increases EMT markers through activation of EP300/FOXM1/SIRT1 cascade and inactivation of EP300/FOXO3 axis.

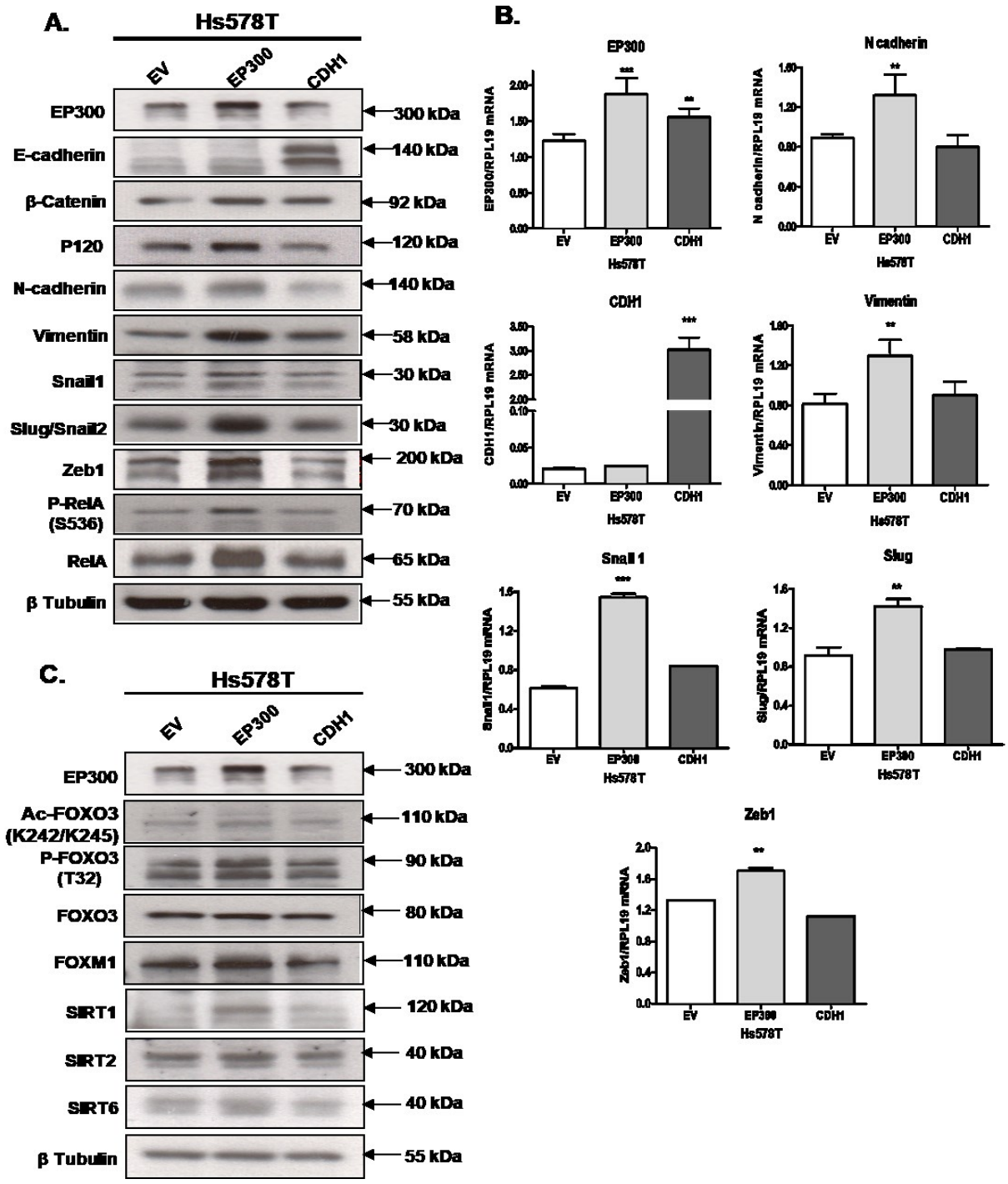


Figure 6.3 EP300 overexpression upregulates expression of epithelial to mesenchymal transition (EMT) markers in Hs578T cells. (A) and (C). Protein lysates obtained from Hs578T cells transfected with plasmid carrying the pcDNA3.1 empty vector, EP300 and CDH1 were subjected to western blotting to examine the expression of EMT markers such as E-cadherin, N-cadherin, snail, slug, zeb1 and others indicated. **(B)** The mRNA levels of E-cadherin, EP300, N-cadherin, and Vimentin were assessed by real time qPCR. Here, bars represent the mean ± SD (standard deviation) of three independent experiments. The RPL19 housekeeping gene was used as a control to normalise gene expression. The mRNA amount in each cell was analysed against cells transfected with empty vector (EV) via Student's t-test analysis to determine significance with $P < 0.05$ *, $P < 0.005$ **, $P < 0.001$ ***.

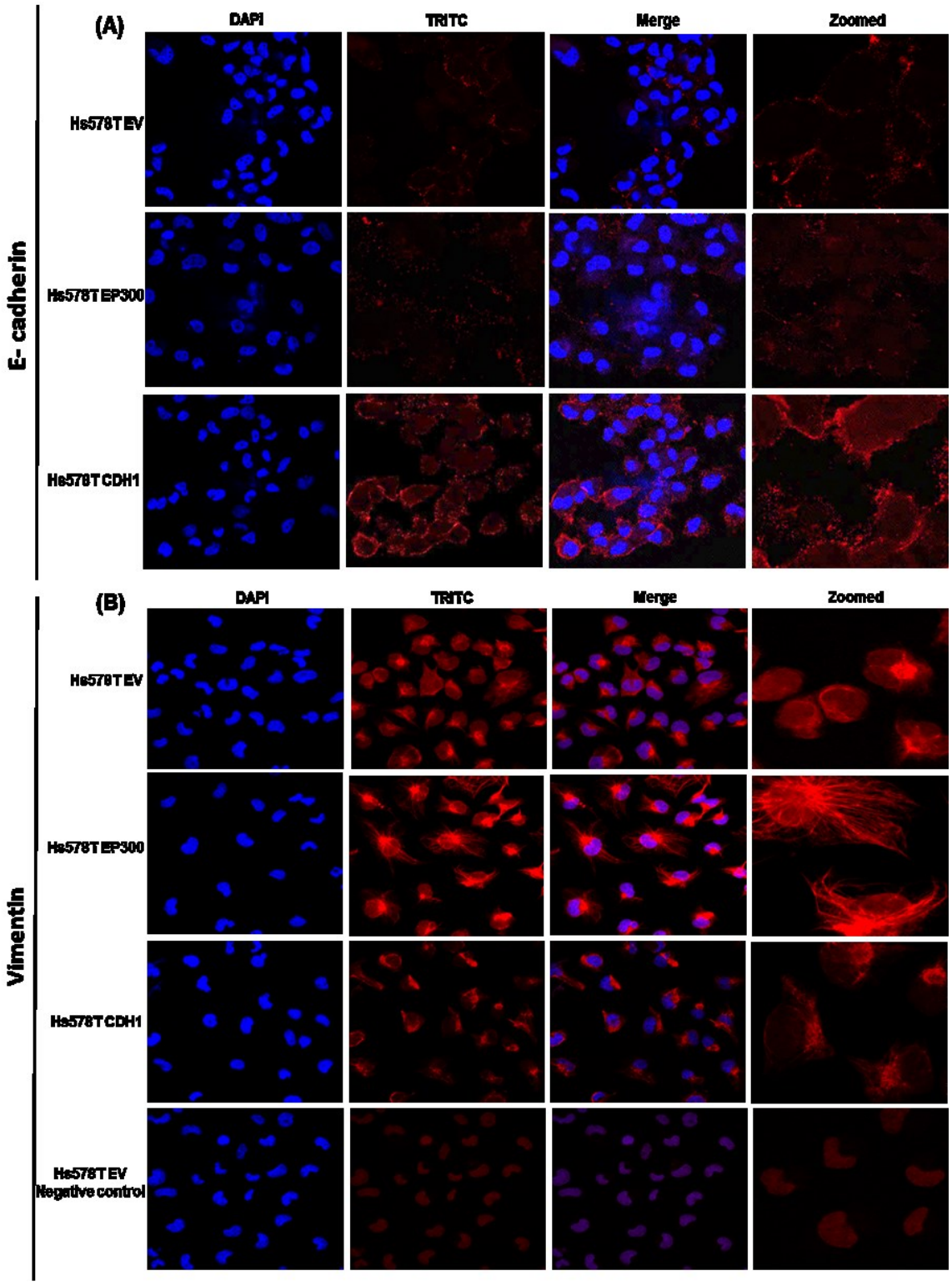


Figure 6.4. Immunofluorescence experiment confirms EP300 mediated EMT induction (^{low}E-cadherin/^{High}Vimentin). Immunofluorescence assay was performed to assess E-cadherin and vimentin expression in EP300 and CDH1 overexpressed Hs578T cells. Cells were treated with respective primary antibody and Alexa fluoro anti-rabbit immunoglobulin G secondary antibody conjugates (red). Cells were visualized with a Leica TCS SP5 confocal microscope equipped with a 63X oil immersion objective and LAS-AF software. Cell nucleus was stained with 4,6-diamidino-2-phenyl indole (DAPI) in blue. Scale bar: 50 µm. Representative confocal images are shown.

6.3.3 EP300 cannot induce FOXO3 acetylation but acetylates snail and zeb1 in Hs578T cells

To further explore the western blot result whether EP300 induce FOXO3 acetylation or not, I performed a co-IP experiment by pulling down of all acetylated protein using pan-acetyl antibody. Subsequent immunoblotting with anti FOXO3 antibody showed that EP300 overexpressed Hs578T cells showed almost same level of acetylation compared to empty vector transfected Hs578T cells (Figure 6.5). This further suggests that acetylation of FOXO3 does not have significant role in terms of oncogenic signature or in the EMT induction upon EP300 overexpression. Moreover, some reports showed that acetylation can contribute in the activation and nuclear localisation of EMT inducing transcription factors [464-466]. Therefore, we tested the acetylation level of snail and zeb1 by using co-IP experiment. Overexpression of EP300 induces acetylation of EMT transcription factor snail and zeb1 (Figure 6.5B and 6.5C), suggesting the role of acetylation in activating EMT transcription factors.

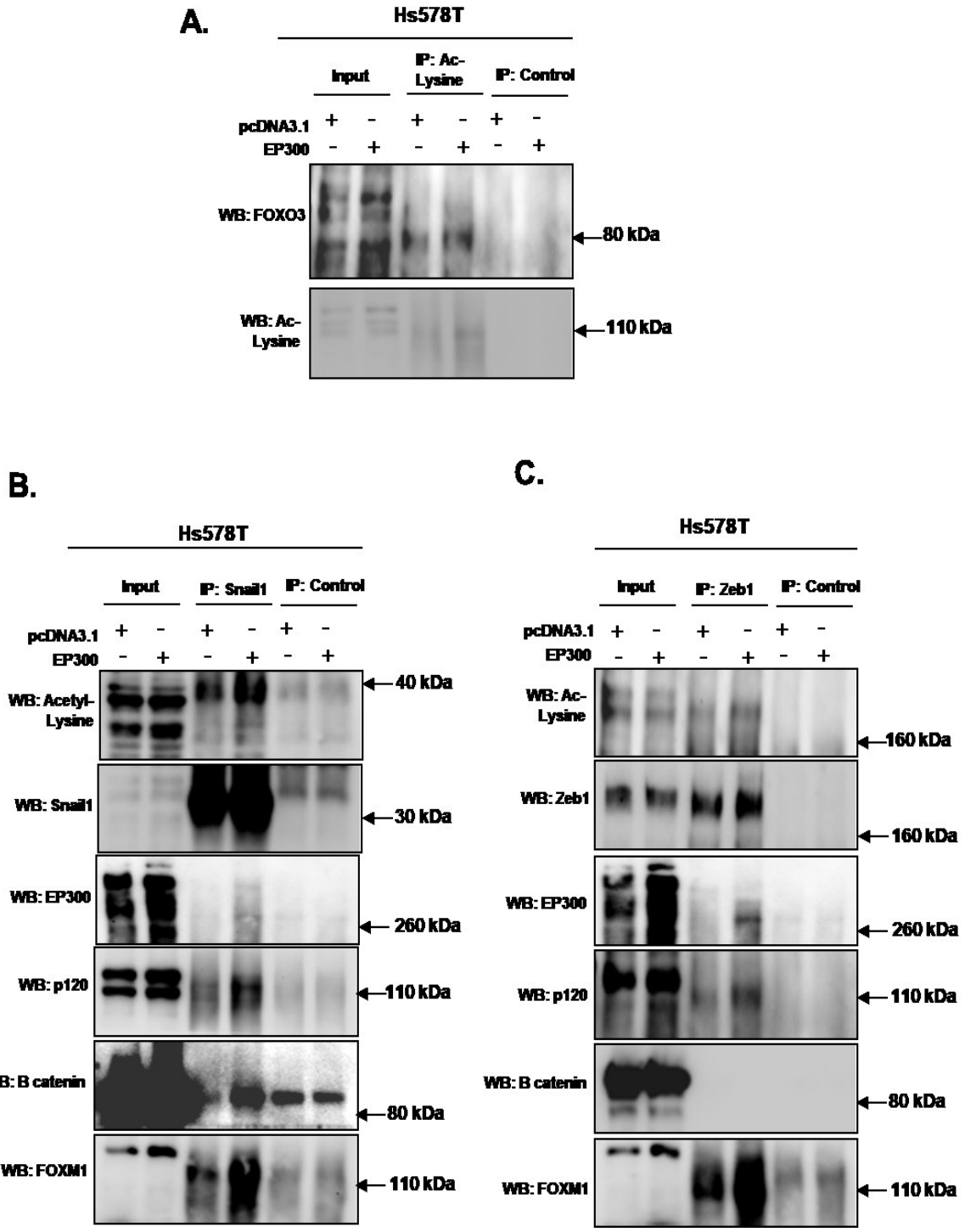


Figure 6.5 EP300 cannot increase acetylation of FOXO3 but induces acetylation of snail and zeb1 in Hs578T cells. A. Proteins were obtained from Hs-EP300 whole cell extracts after 48 hours of seeding and co-immunoprecipitation (Co-IP) was performed with an anti-acetyl lysine antibody. Subsequent immunoblotting was performed using antibodies against FOXO3 and Ac-Lys antibody. The anti-IgG was used as a negative control. **B, C.** Co-IP was performed with anti-snail and anti-zeb1 antibody respectively using the protein lysates of Hs578T cells stably transfected with EP300. Subsequent immunoblotting was performed using antibodies against Ac-Lys, snail, zeb1, EP300, p120, beta caetnin and FOXM1. The anti-IgG was used as a negative control.

6.3.4 Subcellular fractionation confirmed nuclear localisation of EMT inducing transcription factors

In order to gain more insights into the effect of EP300 in the expression of EMT inducing transcription factors, I assessed the sub-cellular distribution of these transcription factors in EP300 over-expressing Hs578T cells. EP300 was primarily localised in nucleus, whereas β-catenin was found to be distributed both in cytoplasm and nucleus in Hs578T-EP300 cells (Figure 6.6). Moreover, high level of snail, slug and zeb1 in nucleus was found in EP300 overexpressing cells, indicating the role of nuclear EP300 in the induction of the expression of EMT inducing transcription factors (Figure 6.6).

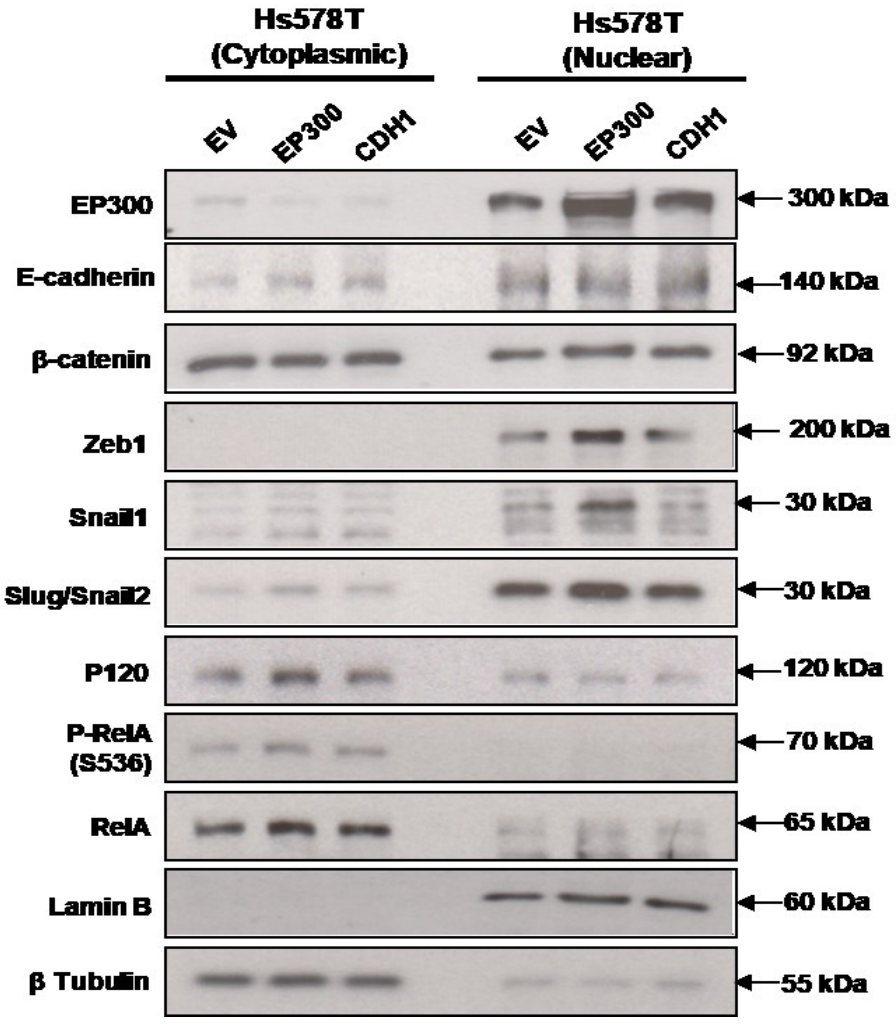


Figure 6.6 Subcellular fractionation confirms nuclear localization of EMT inducing transcription factors. Cytoplasmic and nuclear extracts were isolated from three different types of Hs578T cells. Western Blotting was subsequently used to monitor the sub-cellular distribution of EP300, snail, slug and zeb1. Beta-tubulin and Lamin B were used as loading controls for cytoplasmic and nuclear extracts, respectively. Data presented are representative of two independent biological repeats.

6.3.5 5-Aza-dC treatment restores E-cadherin expression in EP300 overexpressed Hs578T cells

From all the above results we hypothesized that EP300 could not transcriptionally activate the *CDH1* gene in Hs578T and instead might acts on other down-stream pathways/activators/repressors to establish an oncogenic environment to induce EMT phenotype. It is well established that a high level of E-cadherin promoter methylation is found in various breast cancer cell lines including Hs578T [467]. Therefore, in an attempt to reduce E-cadherin promoter methylation, I treated Hs578T cells with different amounts of 5-aza-dC (0, 0.1 and 1 μM) for 96 hours, and E-cadherin, N-cadherin, Vimentin expression levels examined by both western blotting and RT–qPCR (Figure 6.7A, B). In Hs578T-EP300 cells, E-cadherin mRNA and protein expression was significantly induced after treatment with 1 μM of 5'-aza-dC for 96 hours (Figure 6.7A, B). In agreement, the EP300 expression was also increased after 5'-aza-dC treatment in both Hs578T-EV and Hs578T-EP300 cells which might be responsible for the increase of N-cadherin and Vimentin expression after Aza-C treatment. Importantly, E-cadherin expression was higher in Hs-EP300 than in control cells (Figure6.7A, B), indicating that EP300 is functional and could transcriptionally activate the demethylated *CDH1* locus. It is also noteworthy that Aza-C treatment does not have significant effect on the phosphorylated NF-KB or total NF-KB expression.

Collectively, these data suggest that demethylation by 5'-aza-dC treatment can restore E-cadherin level in EP300 overexpressed cells. This further confirms that, we have generated a cell model in which EP300 is overexpressed and functionally active but does not activate expression from the *CDH1* locus.

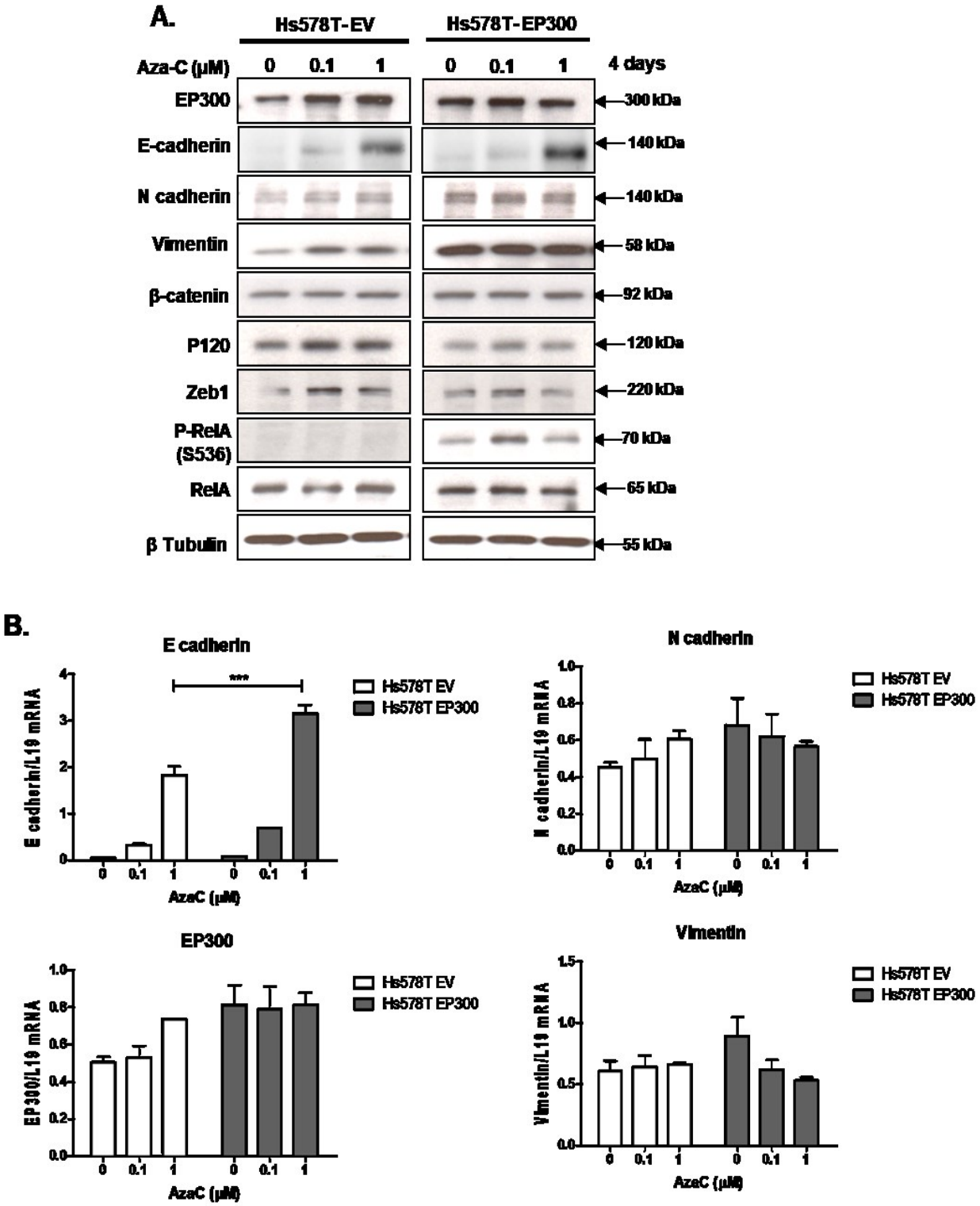


Figure 6.7 5´-Aza-dC treatment restores E-cadherin expression in EP300 overexpressed Hs578T cells. (A) Hs578T-EV and Hs578T-EP300 cells were treated with 0, 0.1 and 1 μM 5-azacytidine for 4 days and subsequent immunoblot analysis was carried out to see the expression of E-cadherin and EMT related proteins. **(B)** The mRNA levels of E-cadherin, EP300, N-cadherin, and Vimentin were assessed by real time qPCR. Here, bars represent the mean ± SD (standard deviation) of three independent experiments. The RPL19 housekeeping gene was used as a control to normalise gene expression. The mRNA amount in each cell was analysed against the respective concentration of AzaC treatment in empty vector transfected cells via Student's t-test analysis to determine significance with $P < 0.05$ *, $P < 0.005$ **, $P < 0.001$ ***.

6.3.6 High level of ALDH activity identifies involvement of EP300 in producing cancer stem cells

A very well-known strategy for identifying cells with a stem cell phenotype is the measurement of ALDH activity [468]. FACS analysis revealed that approximately 8% of Hs-EV control cells were $ALDH^+$, which increased to approximately 16% in Hs-EP300 cells (Figure 6.8). However, overexpression of CDH1 was found to express reduced level of ALDH suggesting its role in suppressing CSC like properties. Therefore, EP300 is associated with a stem cell type phenotype in this breast cancer cell line.

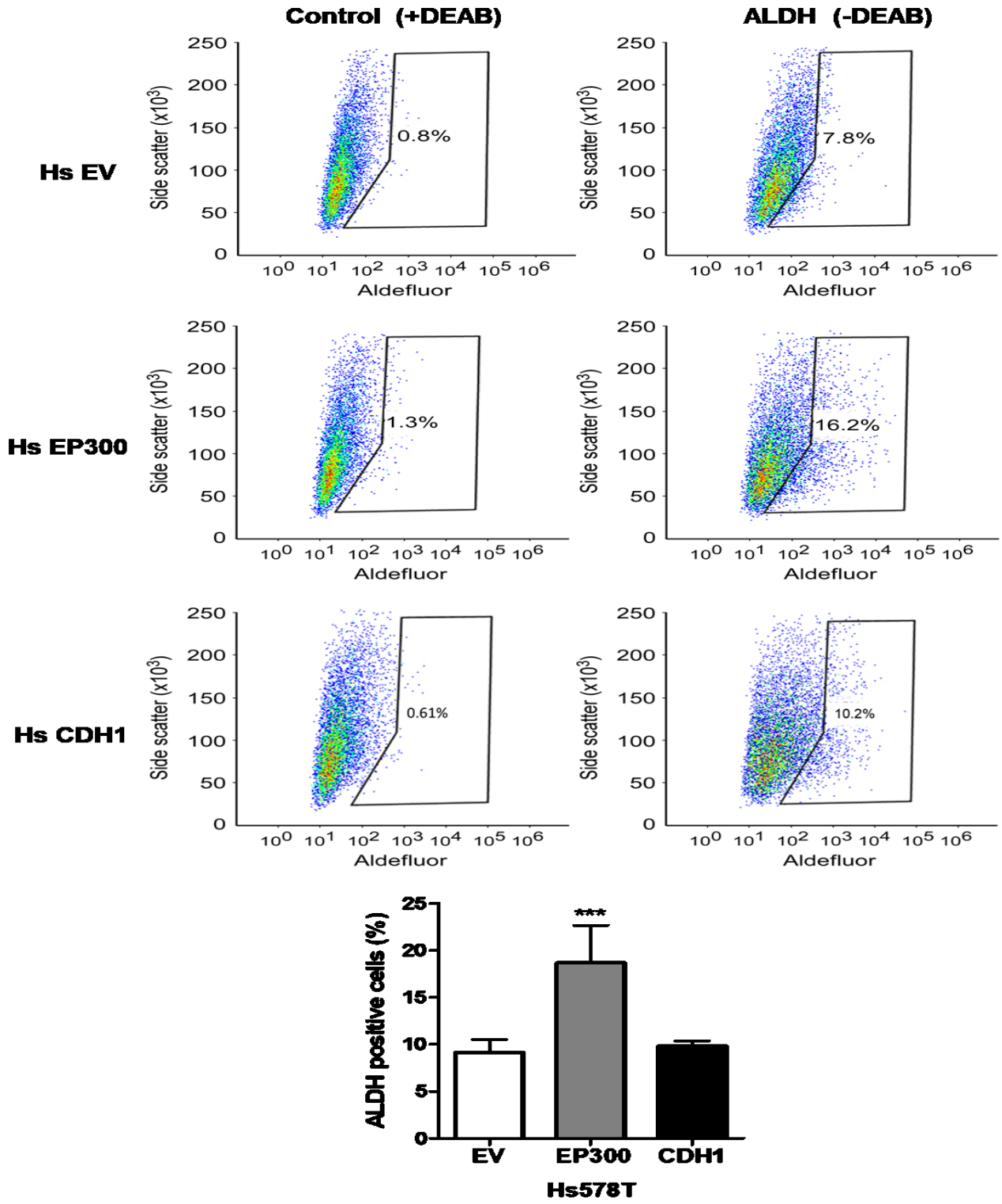


Figure 6.8. High level of aldehyde dehydrogenase (ALDH) activity identifies involvement of EP300 in producing cancer stem cells. Hs578T-EV, Hs578T-EP300 and Hs578T-CDH1 cells were examined for ALDH activity with ALDEFLUOR® assay kit (StemCell Technologies) as per the manufacturer's guidelines. As a negative control for all experiments, an aliquot of ALDEFLUOR®-stained cells was immediately quenched with 1.5-mM diethylaminobenzaldehyde (DEAB), a specific ALDH inhibitor. Cells were analysed by flow cytometry and with flowjo software. In the top panels, cells which fell within the circled regions were considered to represent subpopulations of cells with enhanced ALDH activity relative to the rest of the cell population. The bottom panel show representative comparison of ALDH positive cells through bar diagram where $P < 0.05$ *** considered as significant.

6.3.7 EP300 overexpressing Hs578T cells are enriched in a $CD44^{high}CD24^{low}$ cell sub-populations

It is well-documented that CSC-like populations in breast cancers express a $CD44^{high}CD24^{low}$ phenotype [469]. As EMT generates cells with properties of stem cells [6], we asked whether Hs-EP300 cells would show an increase in CSC markers. Therefore, flow cytometry was performed to characterise the EP300 overexpressed Hs578T cells in terms of CD44 and CD24 expression. Notably, upregulation of EP300 resulted in a significant enrichment of the $CD44^{high}CD24^{low}$ sub-populations (Figure 6.9). However, the E-cadherin overexpressed cell lines showed almost similar levels of the sub-population in comparison with the Hs578T-EV control. Thus, overexpression of EP300 positively correlates with the enrichment of $CD44^{high}CD24^{low}$ CSC population in Hs578T cells. Breast CSCs are typically represented by a $CD44^{high}/CD24^{low}$ subpopulation that increased from 45% in Hs-EV cells to 60% in Hs-EP300 cells (Figure 6.9). These results indicate that overexpression of EP300 in the E-cadherin-null background of Hs578T cells increases CSC markers.

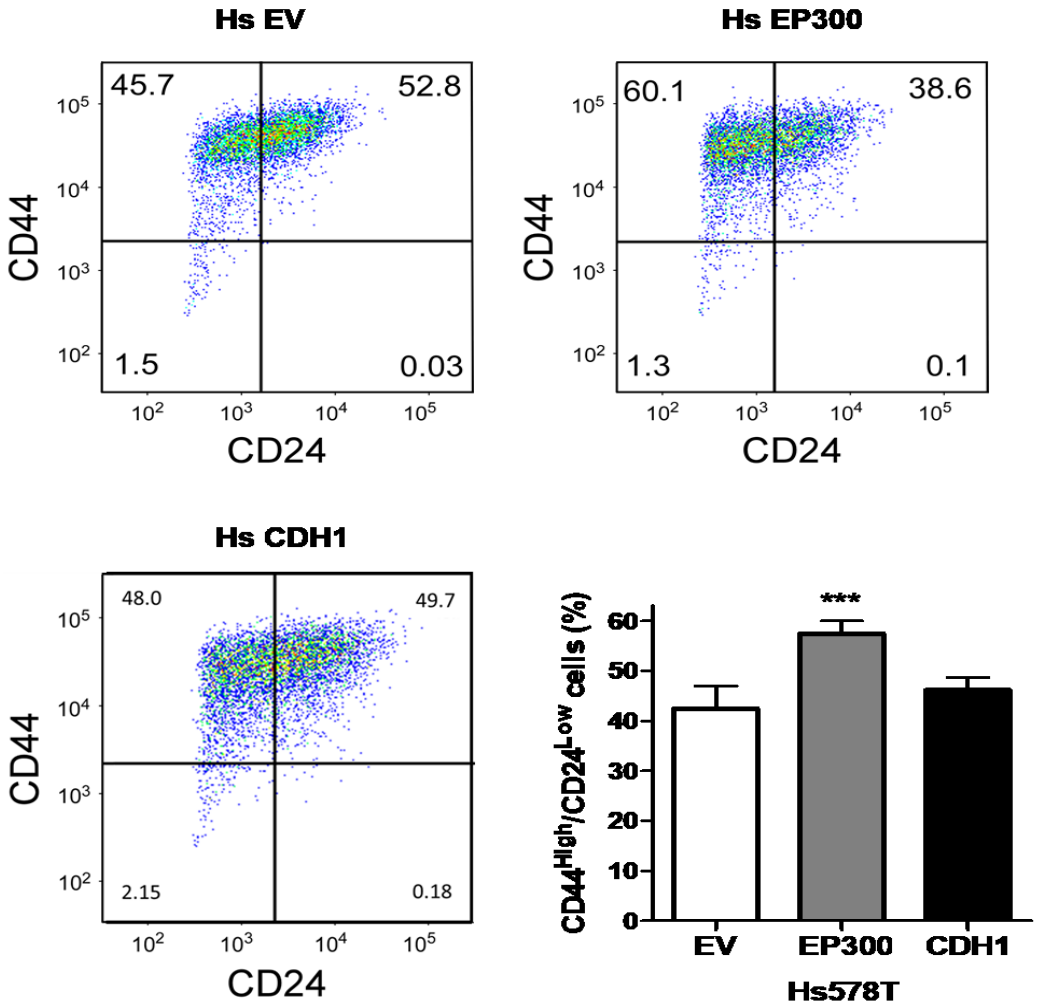


Figure 6.9. EP300 overexpressed cells are enriched in $CD44^{high}CD24^{low}$ cell population. Representative flow cytometry plot for Hs578T cells stably transfected with EV, EP300 or CDH1. Cells were assessed for CD44 and CD24 expression by flow cytometry using allophycocyanin (APC) - and phycoerytrin (PE) -conjugated specific antibodies. The bottom-right figure shows representative comparison of $CD44^{high}CD24^{low}$ cells through bar diagram where $P < 0.05$ *** considered as significant.

6.3.8 EP300 overexpressing Hs578T cells gain migration and invasion capacity

In order to assess the functional significance of the increase in EMT markers, we used trans-wells to determine the capacity of cells to migrate through in the presence or absence of Matrigel. Indeed, the motility of Hs-EP300 cells increased approximately 6-fold with respect to control cells, whereas the capacity to invade through Matrigel increased approximately 3-fold (Figure 6.10A, B). Cancer cell metastasis is responsible for as much as 90% of cancer-associated mortality, yet it remains very poorly understood [470]. Since both cell migration and invasion are critical properties for the spreading of cancer cells and metastases, I further

investigated the cell motility and invasiveness using *in vitro* migration and invasion assays. The migration assay using uncoated transwell chambers is a common method to examine the *in vitro* migration ability of tumor cells. Cells that migrated to the bottom of the transwell were fixed, stained and counted. In comparison with the control group (Hs578T-EV), EP300 overexpression showed an increase of the number of migrated cells (Figure 6.10A). Additionally, Matrigel coated transwell chambers were used to investigate the invasive capacities of breast cancer cells. Consistent with the finding in migration assay, EP300 overexpressing cells showed a significant increase in their invasion ability in comparison with the control (Figure 6.10B). It is also noteworthy that CDH1 overexpressed cells showed similar pattern in terms of migration or invasion like Hs578T-EV cells although a slight increase of cell motility was observed. Taken together, these results indicate that overexpression of EP300 increases the motility and invasive properties of Hs578T breast cancer cells.

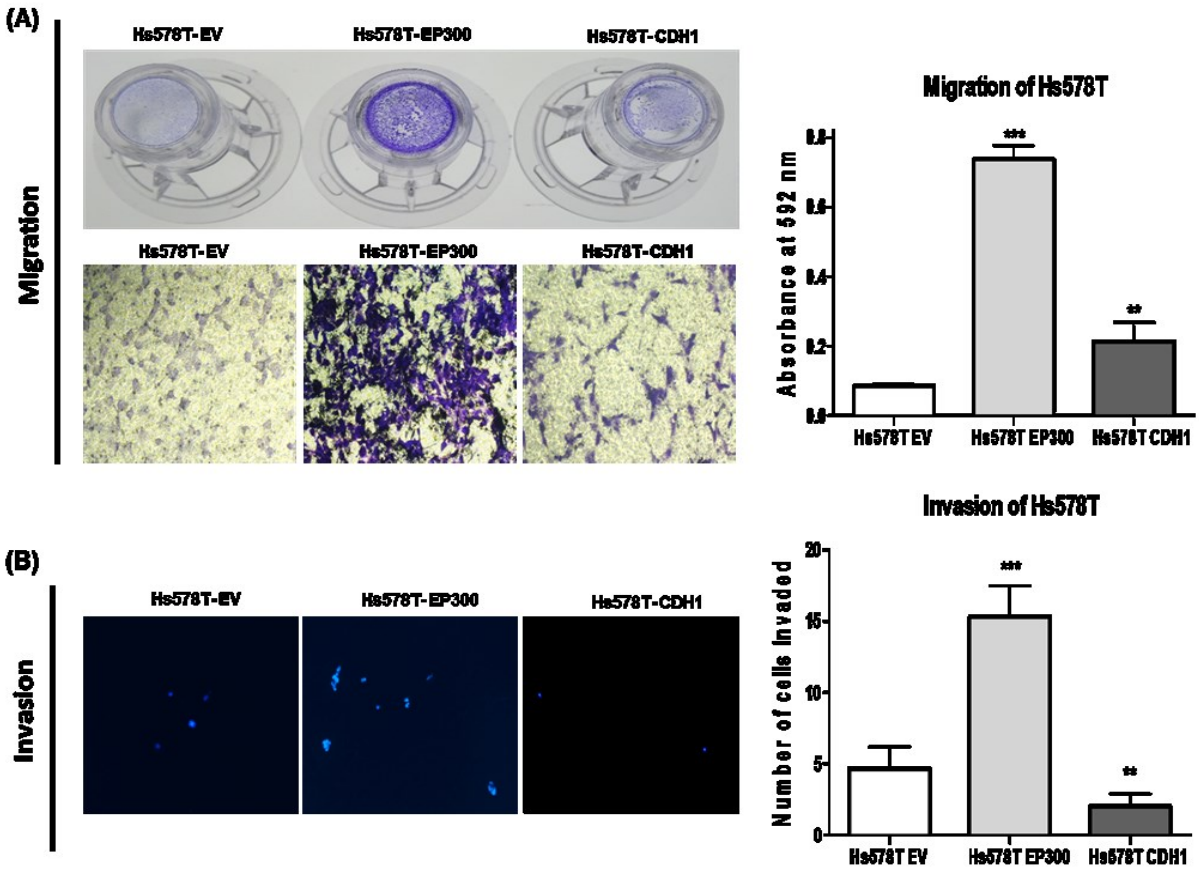


Figure 6.10 EP300 overexpression correlates with increased cell migration and invasion of Hs578T. (A) Cell migration was determined using Boyden transwell chambers. Hs578T cells stably transfected with EV, EP300 or CDH1 were suspended in serum-free medium and seeded on 24-well

transwell plates. DMEM media with 10% FCS was incubated in the lower chamber as the chemoattractant. Cells migrated though pores to the bottom surface of the transwell were fixed with 4% para-formaldehyde, washed with PBS and stained with 0.5% crystal violet and counted. Six random microscopic fields were counted for each group. **(B)** Cell invasion was assayed in transwell coated with Matrigel. Cells crossed the Matrigel-coated filter were fixed, stained with DAPI and counted. Representative pictures of the bottom surface are shown. Six random microscopic fields were counted for each group. The results presented are an average of six random microscopic fields from three independent experiments with three technical repeats. Significant increase of migration and invasion was observed after overexpression of EP300 in Hs578T cells. ***P < 0.001.

6.3.9 EP300 overexpression enhances mammosphere forming efficiency and anchorage independent soft agar cell growth of Hs578T cells

CSCs are considered the tumour initiating sub-population [444] and thus its increase would lead to a higher number of tumours. In order to functionally test this *in vitro*, I used two methods to assess cell transformation and anchorage independence. Growth in soft agar showed that overexpression of EP300 led to an increase of approximately 1.5-fold in the number of clones (Figure 6.11). Equally, growth in low-attachment plates indicated an increase in the number of mammospheres (~ 2.2-fold) in Hs-EP300 cells (Figure 6.12). I further checked the mRNA level of cancer stem cell markers such as nanog, oct4 and sox2 in EP300 and CDH1 transfected Hs578T cells. As shown in figure 6.12B, there was a significant enhancement of pluripotency markers upon EP300 overexpression at mRNA level which also support the phenotypic observations. Thus, EP300 activates an EMT programme characterized by acquisition of CSC properties in an E-cadherin non-permissive background.

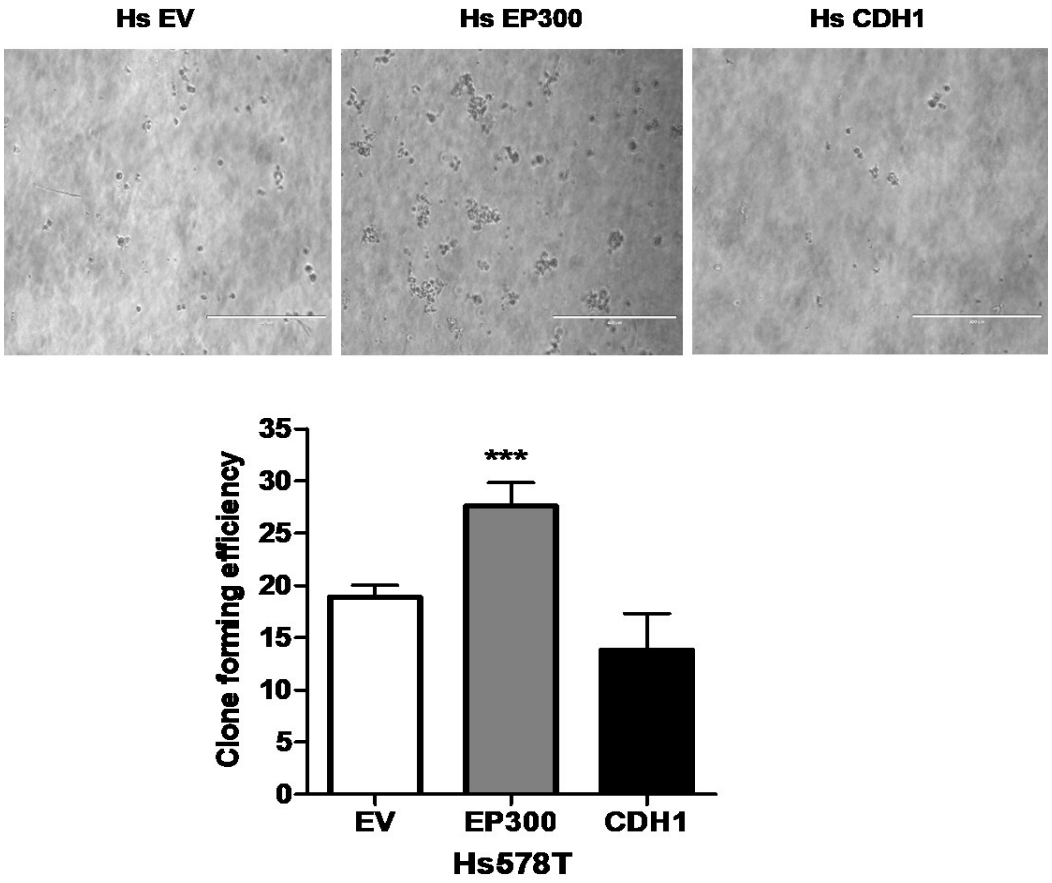


Figure 6.11 EP300 enhances anchorage independent growth of Hs578T
Cells ($5x10^4$ / well) were seeded in 6-well dishes with medium containing soft agar and the formation of colonies determined after 8 weeks of culture. Clone forming efficiency calculated relative to the total number of plated cells x100. Pictorial data show representatives of at least three independent experiments. Numerical data represent the average ± SD of three different experiments (* P<0.05). Bar represents 400 µm.

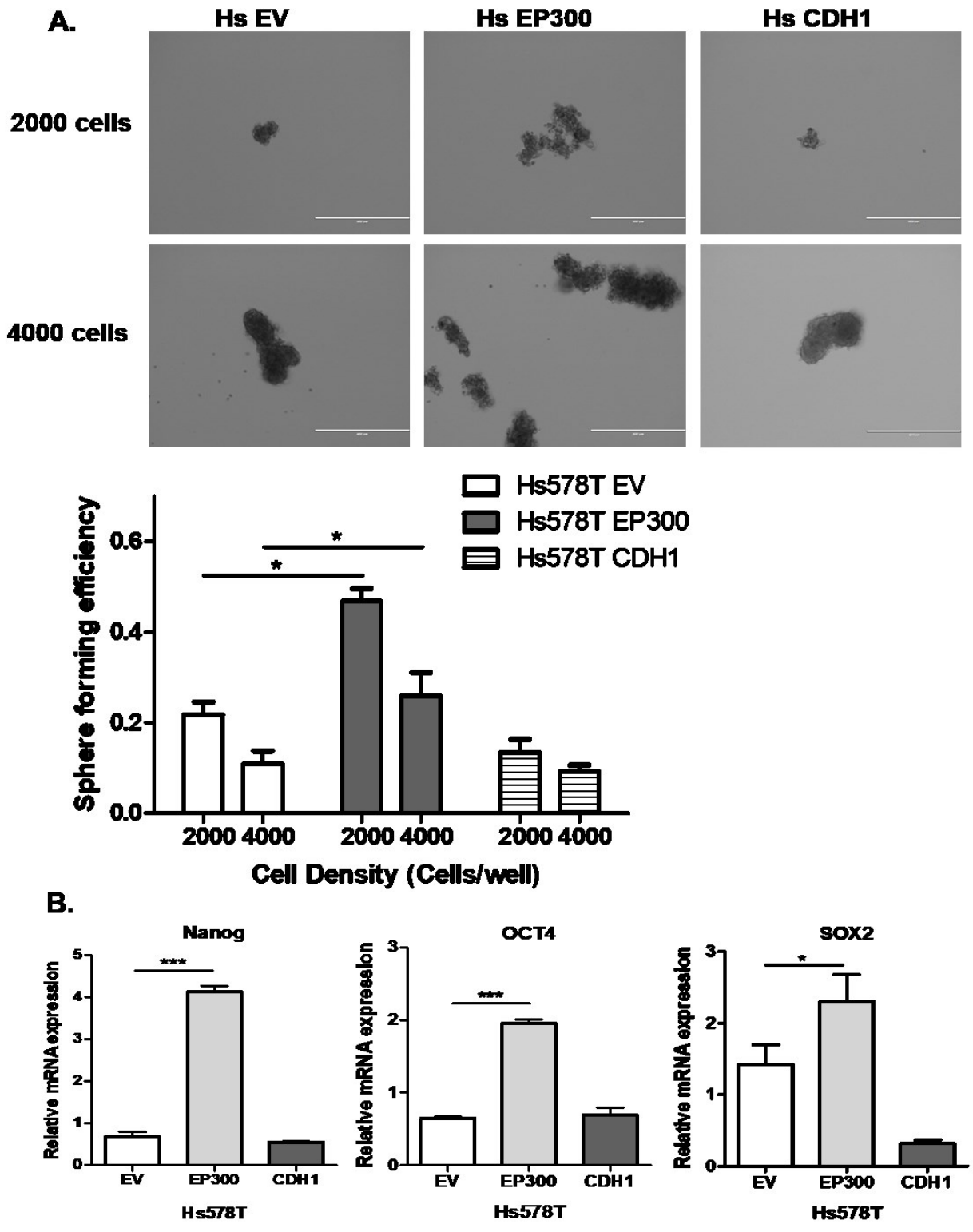


Figure 6.12 EP300 enhances mammosphere formation efficiency of Hs578T
A. Cells ($2x10^3$ and$4x10^3$ / well) were grown in 6-well low attachment plates for two weeks and the number of spheres counted. Sphere forming efficiency calculated relative to the total number of plated cells x100. Pictorial data show representatives of at least three independent experiments. Numerical data represent the average ± SD of three different experiments (* *P*<0.05). Bar represents 400 µm. **B.** RT qPCR data to determine the mRNA expression of CSC markers. Numerical data represent the average ± SD of three different experiments (***P<0.001, **P<0.01, *P<0.05).

6.3.10 EP300 increases long-term doxorubicin and paclitaxel resistance in Hs578T cells

EMT and CSCs are two phenomena tightly interlinked with drug resistance [471]. I therefore asked whether the increase in EMT and CSC characteristics gained after EP300 overexpression was also accompanied by an increase in drug resistance. To test this, we treated both Hs-EV and Hs-EP300 cells with paclitaxel or doxorubicin and monitored the generation of surviving drug resistant clones. Indeed, 28 days after drug treatment Hs-EP300 cells produced approximately four times more doxorubicin- and five times more paclitaxel-resistant clones than control Hs-EV cells (Figure 6.13, 6.14 respectively).

Loss of E-cadherin expression has been known to drive EMT and contribute to the emergence of drug resistant cancer cells [472]. Therefore, I tested whether overexpression of the EP300, would reduce long term resistance to doxorubicin and paclitaxel in Hs578T breast cancer cell lines. Clonogenic assays showed a level of increased doxorubicin resistance at 25 nM and 50 nM treatment compared with the control cells (Figure 6.13A, B) ($p<0.001$). Analysis of paclitaxel resistance in EP300 overexpressing cells using the same method showed similar pattern of resistance (Figure 6.14C, D). Moreover, E-cadherin overexpression showed a decreased level of long-term doxorubicin and paclitaxel resistance and thus behaves similarly as empty vector transfected Hs578T cells. Thus, EP300 overexpressing hs578T cells become drug resistant in an E-cadherin non-permissive background.

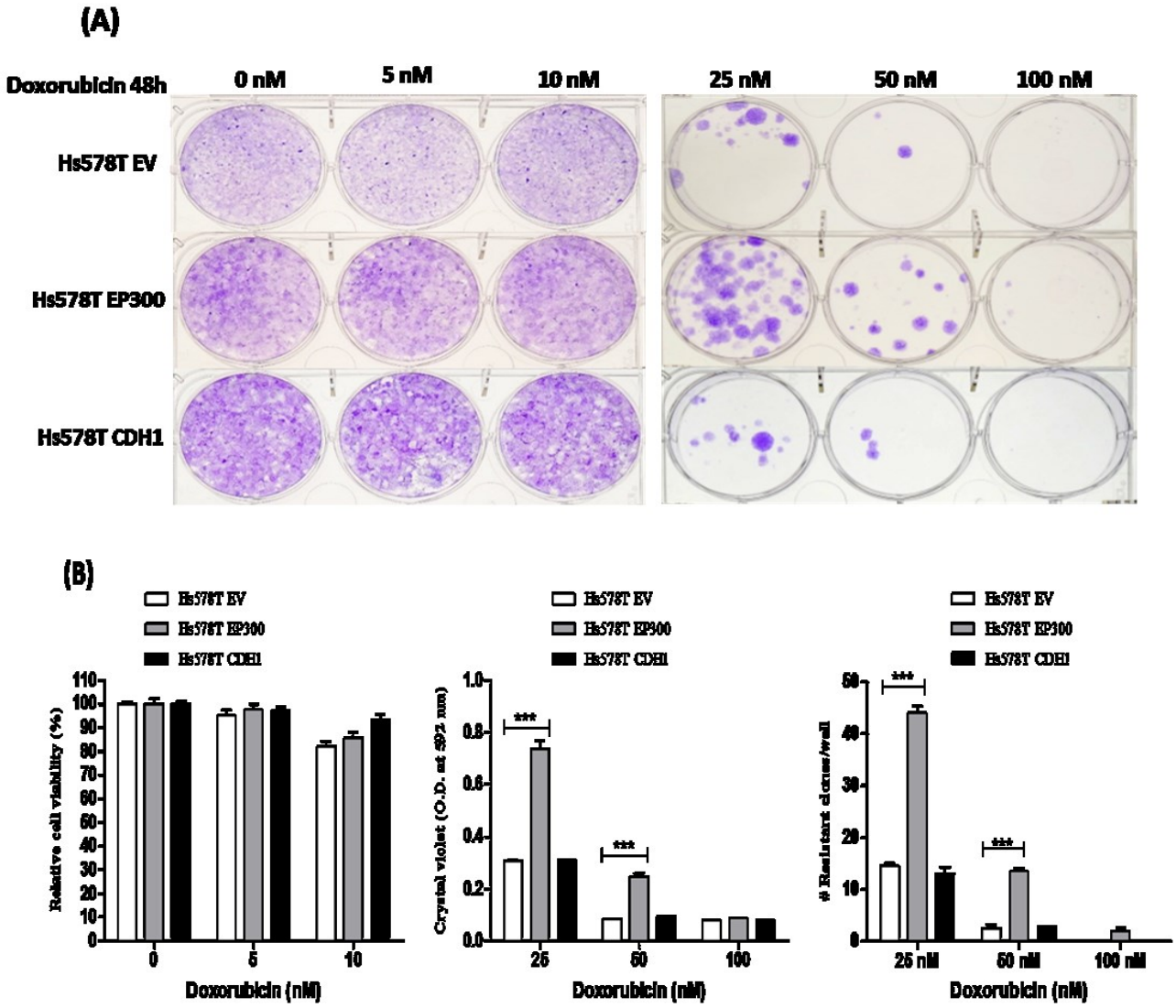


Figure 6.13 Overexpressing EP300 increases long-term doxorubicin and paclitaxel resistance in Hs578T cells. (A, B) Hs578T cells stably transfected with EV, EP300 or CDH1 were seeded 2,000 cells per well in 6-well plates. Cells were allowed to grow overnight and then treated with the doxorubucin concentration indicated (5, 10, 25, 50 and 100 nM). Forty-eight hours following treatment the medium was changed and colony formation was allowed for 14 (for 5, 10 nM) and 28 days (for 25,50 and 100 nM). At the end of this time period, cells were fixed with 4% para formaldehyde and stained with crystal violet. Pictures were taken, the stain was solubilised with 33% acetic acid and absorbance taken at 592 nm. Bars represent the mean ± SD of three independent transfection experiments and statistical analysis was performed using a paired t-test and compared with the control (empty vector). (***p≤0.001).

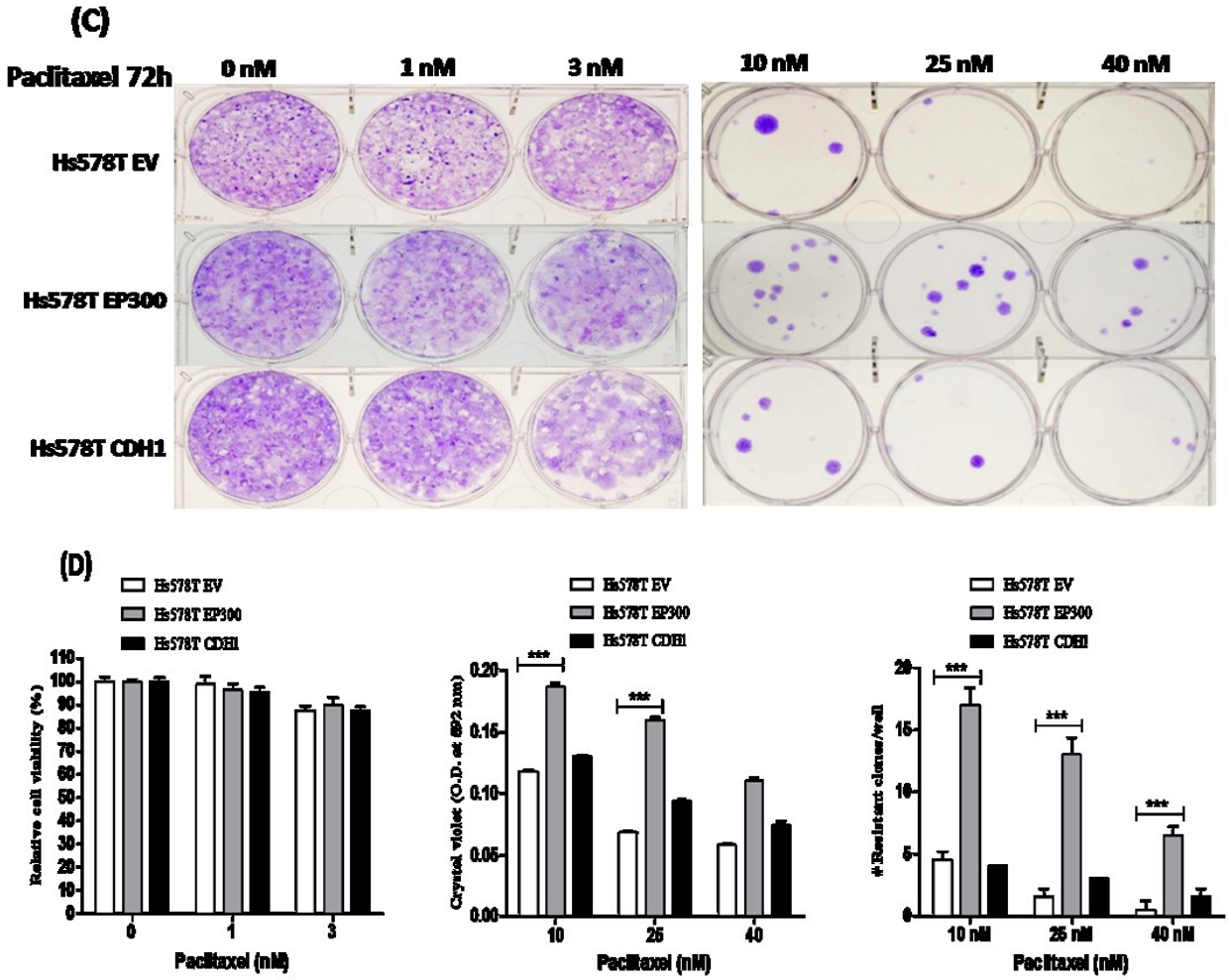


Figure 6.14 Overexpressing EP300 increases long-term doxorubicin and paclitaxel resistance in Hs578T cells. (C, D) Hs578T cells stably transfected with EV, EP300 or CDH1 were seeded 2,000 cells per well in 6-well plates. Cells were allowed to grow overnight and then treated with the paclitaxel concentration indicated (1, 3, 10, 25 and 40 nM). Seventy-two hours following treatment the medium was changed and colony formation was allowed for 14 (for 1, 3 nM) and 28 days (for 10, 25 and 40 nM). At the end of this time period, cells were fixed with 4% para formaldehyde and stained with crystal violet. Pictures were taken, the stain was solubilised with 33% acetic acid and absorbance taken at 592 nm. Bars represent the mean ± SD of three independent transfection experiments and statistical analysis was performed using a paired t-test and compared with the control (empty vector). (***p≤0.001).

6.3.11 Molecular signature of oncogenic EP300 indicates a major role of aldo-keto reductases

In order to gain insights into the molecular mechanisms underlying EP300 oncogenic function, we performed genome-wide transcriptome analysis of Hs-EP300 cells. A total of 950 transcripts were differentially regulated between Hs-EP300 and Hs-EV control cells (GEO accession number **GSE116370**; a list of the most differentially regulated genes is shown in Table 6.3). *AKR1C1* (encoding Aldo-keto Reductase

Family 1, Member C1) was the most up-regulated gene (5.5-fold), although members C2 and C3 (*AKR1C2* and *AKR1C3*) were also up-regulated by 3.5- and 3.0-fold, respectively. Aldo-keto reductases are a major superfamily of NAD(P)H-dependent oxidoreductases and family C members AKR1C1–AKR1C4, sharing a high percentage of amino-acid sequence identity (from 84 to 98%), are involved in progesterone, testosterone, prostaglandin, and xenobiotic ketones metabolism [473, 474]. In addition, AKR1C members have been found to be up-regulated in many cancers [475] and be associated with therapy response [476].

Table 6.3. Selection of most up-and down-regulated genes in Hs-EP300 cells.

Gene	Description	Fold change[a]	*P*
AKR1C1	Aldo-keto reductase family 1, member C1	5.53	0.00002
ELF1	E74 Like ETS (E26 transformation-specific related) Transcription Factor	5.03	0.00450
MEF2C	Myocyte enhancer factor 2C	3.68	0.00020
UGT1	UDP glucuronosyltransferase 1 family, polypeptides A1, A6, A4, A10, A8, A7, A5, A3, A9	3.61	0.00002
KRT81	Keratin 81	3.61	0.00003
AKR1C2	Aldo-keto reductase family 1, member C2	3.50	0.00030
ALDH1A1	Aldehyde dehydrogenase 1 family, member A1	3.39	0.00360
AKR1C3	Aldo-keto reductase family 1, member C3	2.99	0.00010
CDH6	Cadherin 6	2.94	0.00010
NUDT6	Nudix hydrolase 6	2.85	0.01770
GORAB	Golgin, RAB6-interacting	2.69	0.04680
ARL4A	ADP-ribosylation factor like GTPase 4A	2.66	0.00350
ATP6V1C1	ATPase, H+ transporting, lysosomal 42kDa, V1 subunit C1	2.60	0.00110
AVEN	Apoptosis and caspase activation inhibitor	2.41	0.00080
ALDH1A2	Aldehyde dehydrogenase 1 family, member A2	2.27	0.00240
TP53INP1	Tumor protein p53 inducible nuclear protein 1	-2.26	0.00210
BIN3	Bridging integrator 3	-2.48	0.02100
IGFBP3	Insulin like growth factor binding protein 3	-2.54	0.00020
MXI1	MAX interactor 1, dimerization protein	-2.59	0.00020
BGN	Biglycan	-2.62	0.00030
TAGLN	Transgelin	-2.65	0.00040
KCTD11	Potassium channel tetramerization domain containing 11	-2.67	0.00010
POTEM; POTEG	POTE ankyrin domain family, members M and G	-2.72	0.00460
TUFT1	Tuftelin 1	-3.57	0.00100

[a]Positive expression values denote up-regulation and negative expression values denote down-regulation respect to Hs-EV control cells

6.3.12 Validation of up/down-regulated genes by RT qPCR

RT-qPCR data indicated that *AKR1C1, AKR1C2* and *AKR1C3* were up-regulated by approximately 2.5-, 3.5- and 2-fold, respectively, upon EP300 overexpression in Hs578T cells (Figure 6.15). In addition, we confirmed the up-regulation of MEF2C, ALDH1, CDH6, ATP6, ELF1 and AVEN (Figure 6.15). We also investigated and confirmed the downregulated genes such as TP53, KCTD11, IGFBP3 and MXI, however, BIN3 did not show significant downregulation as shown in microarray results (Figure 6.16). Finally, although quantitatively different to the fold values obtained with microarrays, as these methods use completely different technologies, these data validate the up-regulation of *AKR1C1, AKR1C2* and *AKR1C3* in Hs-EP300 cells.

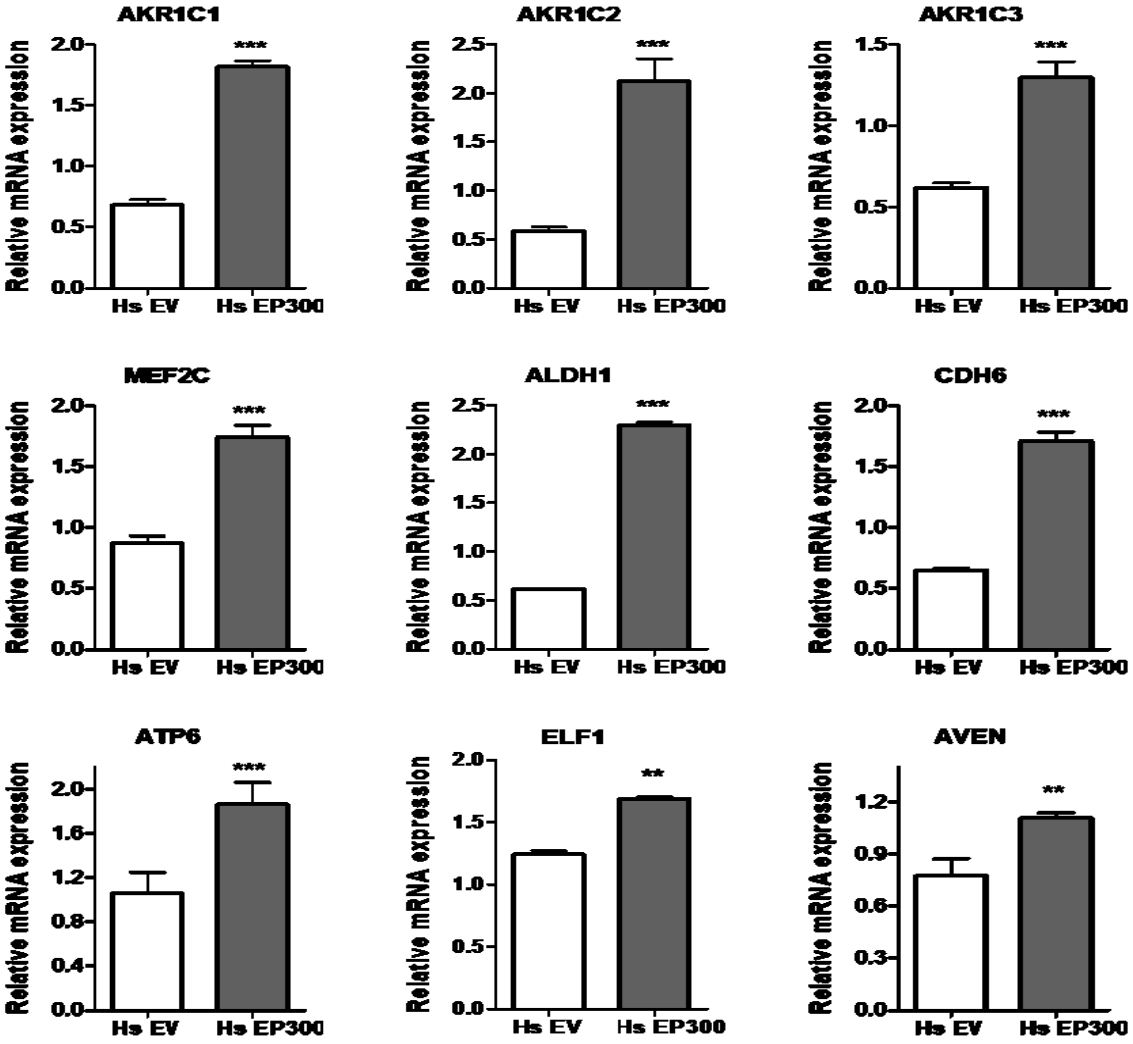


Figure 6.15 Validation of up-regulated genes from micro-array analysis.
Genes that were up-regulated in transcriptome analysis was further confirmed by RT qPCR. mRNA levels in Hs EP300 and control Hs EV cells were examined by real-time PCR and normalized to the expression of *RPL19* mRNA. Statistical analysis was performed using students t test where ***P<0.001, **P<0.01, *P<0.05.

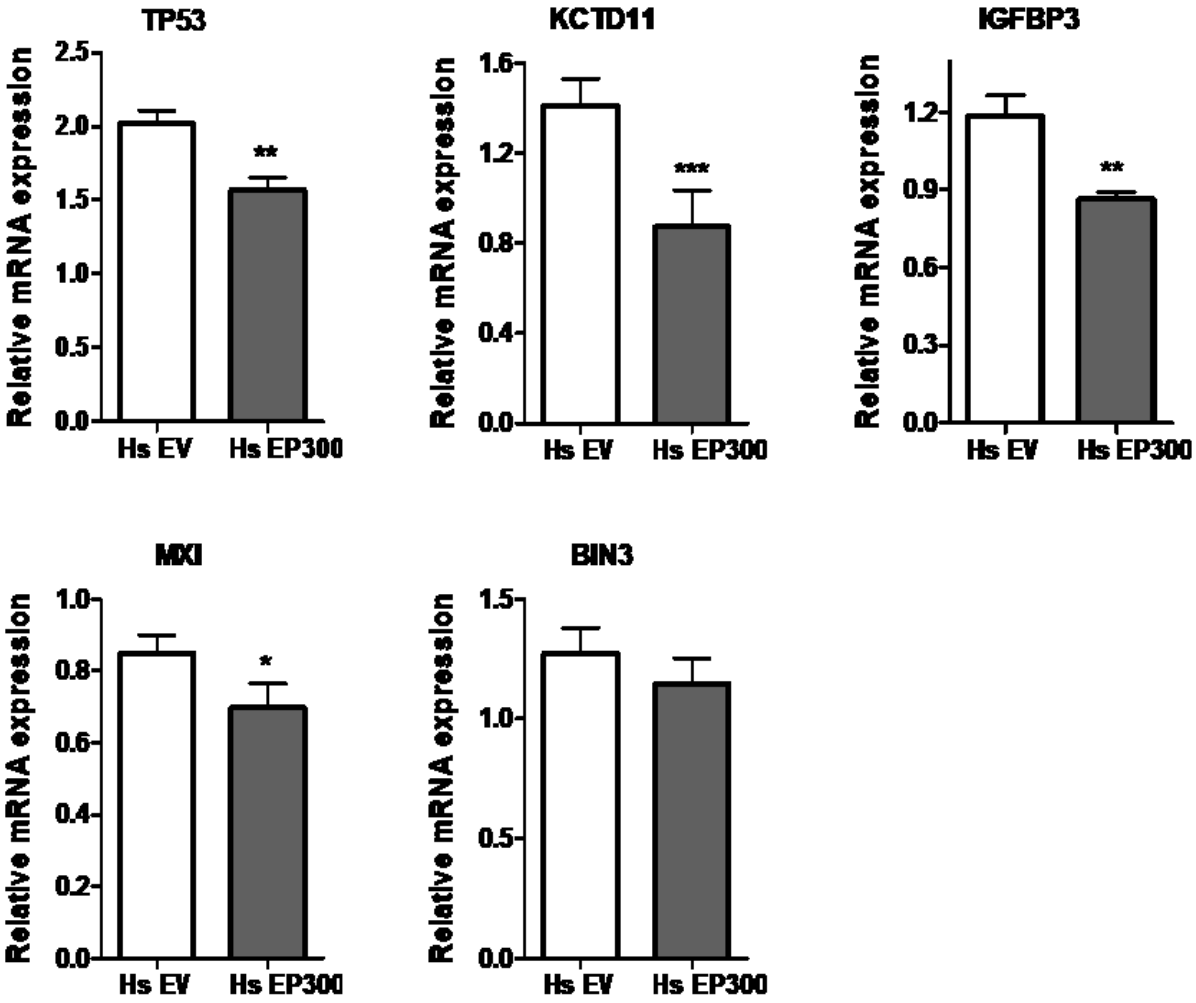


Figure 6.16 Validation of down--regulated genes from micro-array analysis.
Genes that were down-regulated in transcriptome analysis was further confirmed by RT qPCR. mRNA levels in Hs EP300 and control Hs EV cells were examined by real-time PCR and normalized to the expression of *RPL19* mRNA. Statistical analysis was performed using students t-test where ***P<0.001, **P<0.01, *P<0.05.

6.3.13 Drug resistant Hs578T cells show upregulated AKR1C as well as EMT markers

At first, to validate the resistance of Hs578T cells to doxorubicin and paclitaxel we performed SRB experiments using the drug resistant derivatives of Hs578T, Hs DOX and Hs TAX cell lines (generated by Dr. Ernesto Yagüe). The best-fit curve analysis and IC_{50} values revealed approximately 5-fold doxorubicin resistance in Hs DOX cells and approximately 8-fold paclitaxel resistance in Hs TAX cells when compared with drug sensitive Hs578T cells (Figure 6.17A) (replicate data of SRB experiments is shown which was performed together with Mr. Uttom Kumar). Western blot analysis indicated that EP300 was upregulated in both resistant cells (Figure 6.17B). To date, drug resistant Hs578T cells acquired increased expression of EMT markers such as, N-cadherin, vimentin and elevated level of EMT inducing transcription factor snail, zeb1. Enhanced level of MDR1 was observed in paclitaxel resistance but not in doxorubicin resistant cells (Figure 6.17B). Reassuringly, aldo-keto reductases expression was also up-regulated in both resistant cells, although *AKR1C2* and *AKR1C3* were the most up-regulated (between 4- and 10-fold, respectively; (Figure 6.17C).

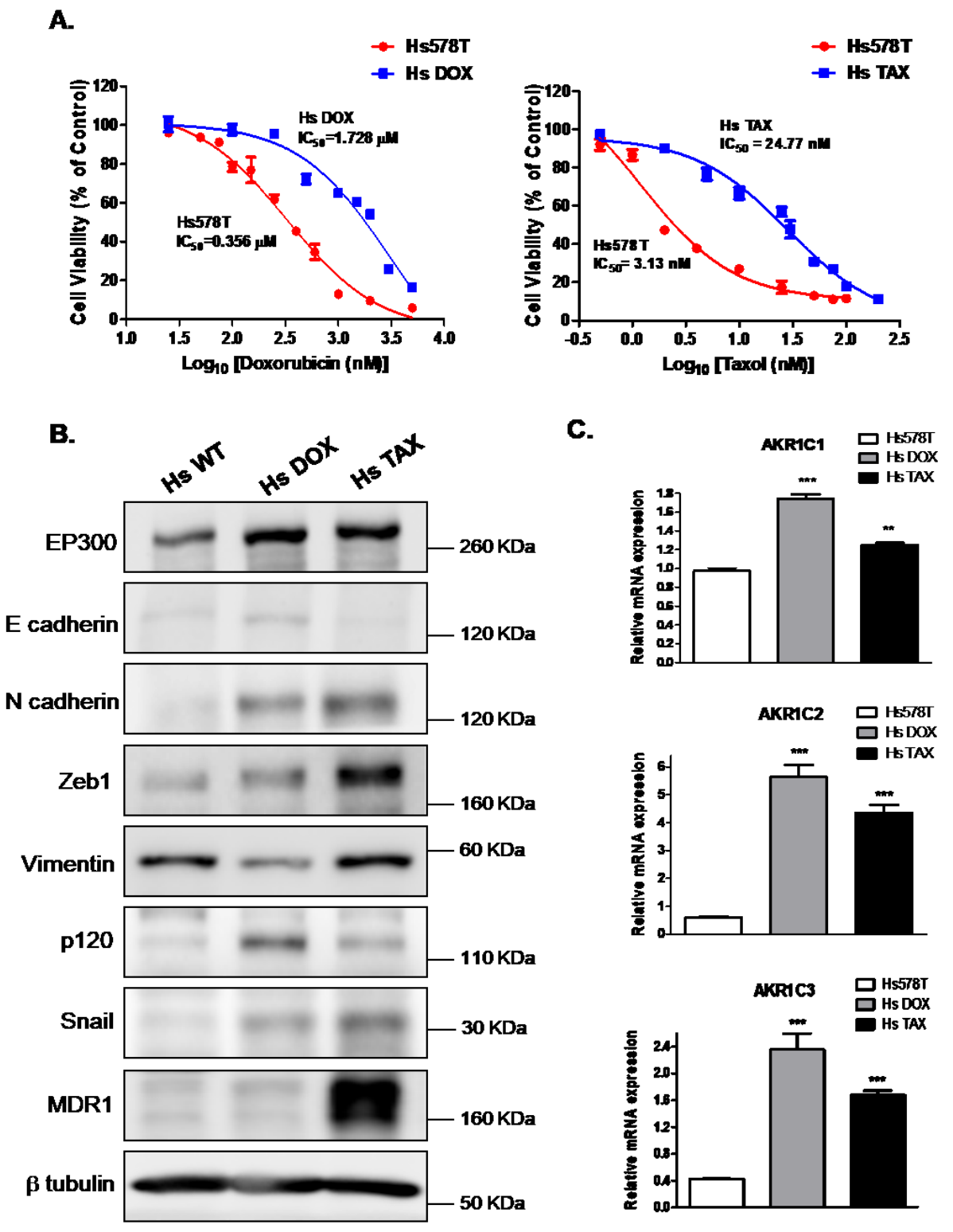


Figure 6.17 Up-regulation of aldo-keto reductases and EMT markers in Hs578T drug resistant cells. **A)** HS578T cells were used to generate doxorubicin (Hs-DOX) and paclitaxel (Hs-TAX) resistant derivatives. Drug sensitivity best-fit curves determined by sulphorhodamine B assays (Performed together with Uttom Kumar). **B)** EP300 expression and other indicated EMT markers determined by western blot analysis in drug naive and resistant cells. **C)** Determination of aldo-keto reductases mRNA levels in drug naive and resistant cells HS578T cells by real-time PCR normalized to the expression of *RPL19* mRNA. Numerical data represent the average ± SD of three different experiments (*** $P<0.05$).

6.3.14 Bioinformatic analyses of ChIP-seq data indicates the binding of EP300 to AKR1C genes promoter

Bioinformatic analyses of chromatin immunoprecipitation-sequencing data from The Encyclopedia of DNA Elements (ENCODE) [477] indicated that EP300 binds to *AKR1C1, AKR1C2* and *AKR1C3* promoters in A549, HeLa-S3, HepG2, MCF-7 and T47-D cells (Figure 6.18). Thus, it is likely that during the generation of drug resistance, EP300 expression is activated, leading to up-regulation of *AKR1C1, AKR1C2* and *AKR1C3*.

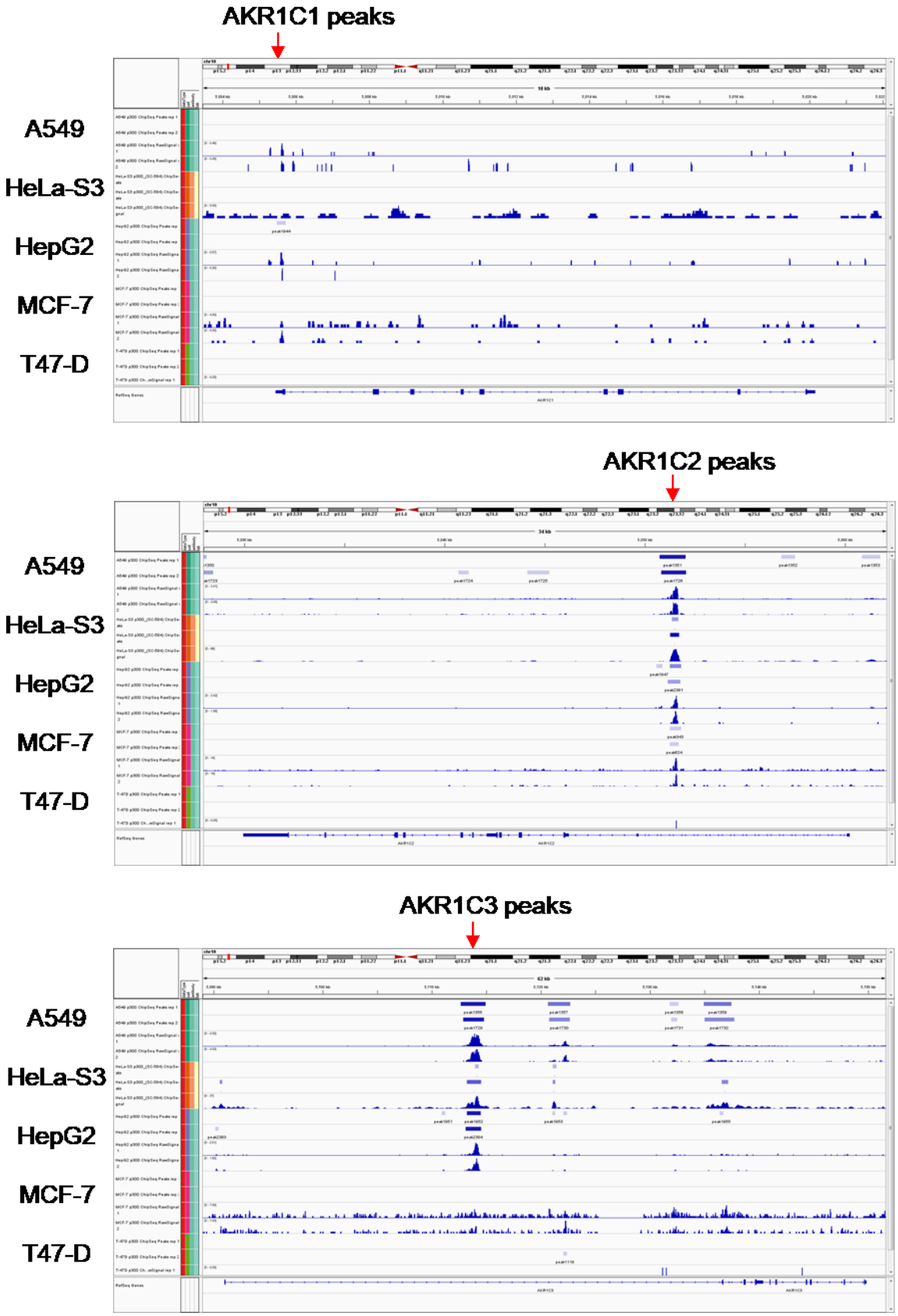


Figure 6.18 Bioinformatic analyses of chromatin immunoprecipitation-sequencing (ChIP-seq) data from The Encyclopedia of DNA Elements (ENCODE).

6.3.15 Oncogenic EP300 can be targeted with FFA

In order to assess the role of *AKR1C1, AKR1C2* and *AKR1C3* in drug resistance we used a pharmacological approach. Flufenamic acid (FFA) is a non-steroidal anti-inflammatory pan-AKR1C1-4 inhibitor [473] clinically used for a variety of rheumatic disorders [478]. For this I first performed drug sensitivity assays and determined that FFA concentrations up to 50 μM were not highly toxic for Hs578T cells and drug resistant derivatives (Figure 6.19A). Then, I asked whether FFA could resensitize drug resistant Hs578T cells. For this we performed long-term clonogenic assays to identify cells that survive and proliferate after doxorubicin/paclitaxel treatment. Reassuringly, FFA did not produce any significant effect in the generation of clones from resistant cells in the absence of doxorubicin or paclitaxel. However, when drug resistant cells were treated with both FFA and chemotherapeutic drug (either doxorubicin or paclitaxel) the generation of resistant clones diminished dramatically (from ~45% in Hs DOX cells treated with 50 nM doxorubicin to ~10% when treated with 50 nM doxorubicin and 50 μM FFA; and from ~70% in Hs TAX cells treated with 20 nM paclitaxel to ~30% when treated with 20 nM paclitaxel and 40 μM FFA; Figure 6.19B,C). Thus, pharmacological inhibition of aldo-keto reductases resensitizes Hs578T drug resistant cells.

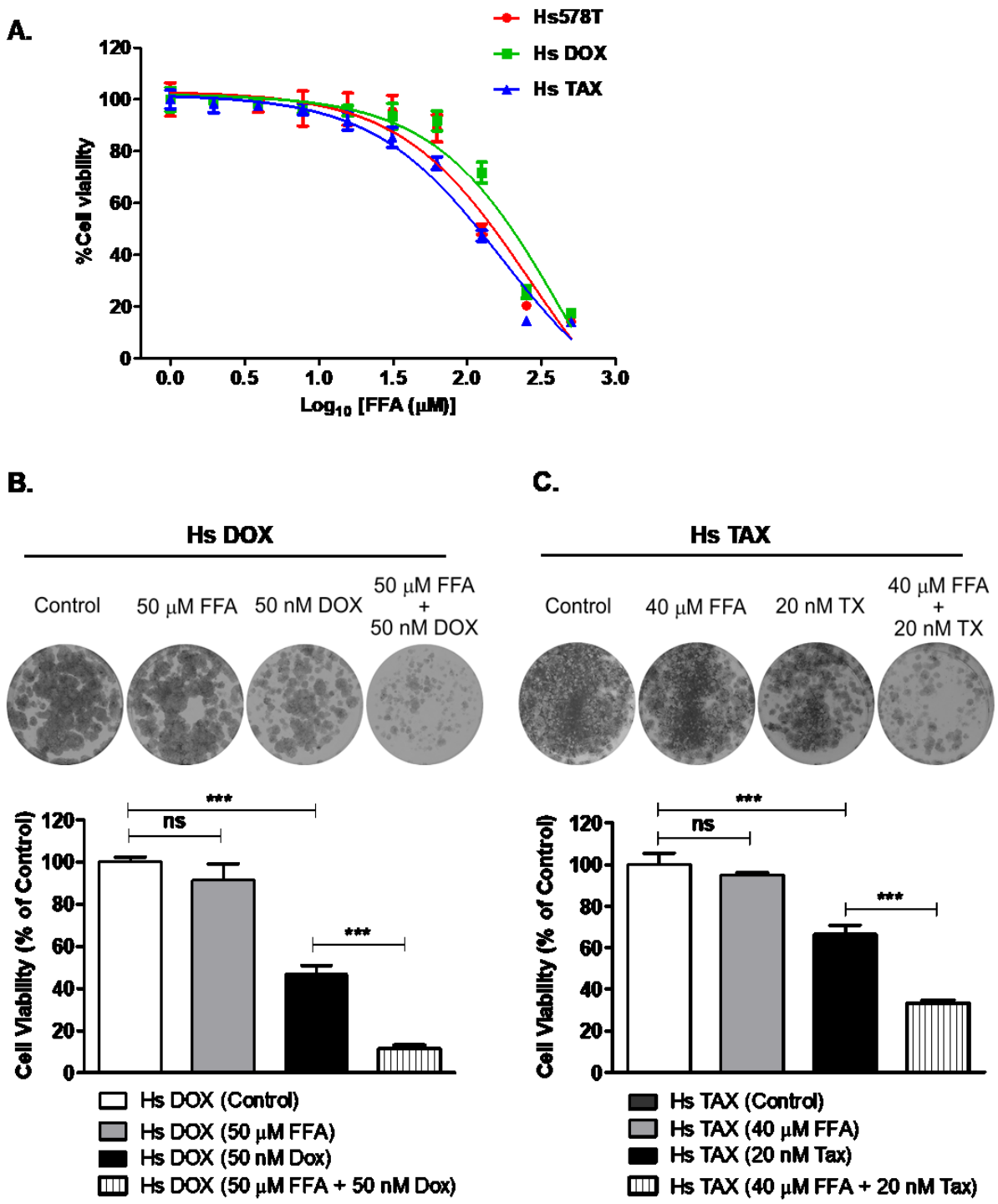


Figure 6.19. Pharmacological inhibition of aldo-keto reductases reverts drug resistance
(A) FFA toxicity best-fit curves in drug naive HS578T and doxorubicin (Hs DOX) and paclitaxel (Hs TAX) resistant cells determined by sulforhodamine B staining. Cells ($3x10^3$ / well) were seeded in 96-well dishes and treated with increasing concentrations of FFA for 3 days before staining and measurement of optical density at 492 nm. Doxorubicin resistant Hs DOX cells **(B)** or paclitaxel resistant Hs TAX cells **(C)** were seeded into 6-well plates ($1x10^3$ cells / well) and treated with FFA, doxorubicin (DOX) or paclitaxel (TX/TAX), or a combination of both drugs for 3 days. Clone growth was monitored after 15 days, stained with crystal violet (representative pictures on top) and absorbance at 592 nm determined (bottom histograms). Numerical data represent the average ± SD of three different experiments (*** P<0.001).

6.3.16 FFA reduces the expression of some EMT markers and AKR1Cs in drug resistant Hs578T cells

Using the drug resistant cells generated in this study I performed an experiment to test the effect of FFA on EMT markers. As can be seen in figure 6.20A, FFA had a clear effect on N-cadherin, twist and MDR1 expression that was less evident for vimentin and repressors Slug and Snail. However, these changes were not associated with significant increase of E-cadherin, and necessary to claim a full reversion to an epithelial phenotype. This could be explained by the lack of effect of FFA to demethylate the CDH1 promoter. In addition, RT-qPCR analysis revealed that FFA reduces the expression of AKR1C1, 2, and 3 at mRNA level (Figure 6.20B). Thus, although FFA changed the expression of some EMT markers, these changes were not enough to revert EMT because of E-cadherin promoter methylation in these cells and this need to be further explored.

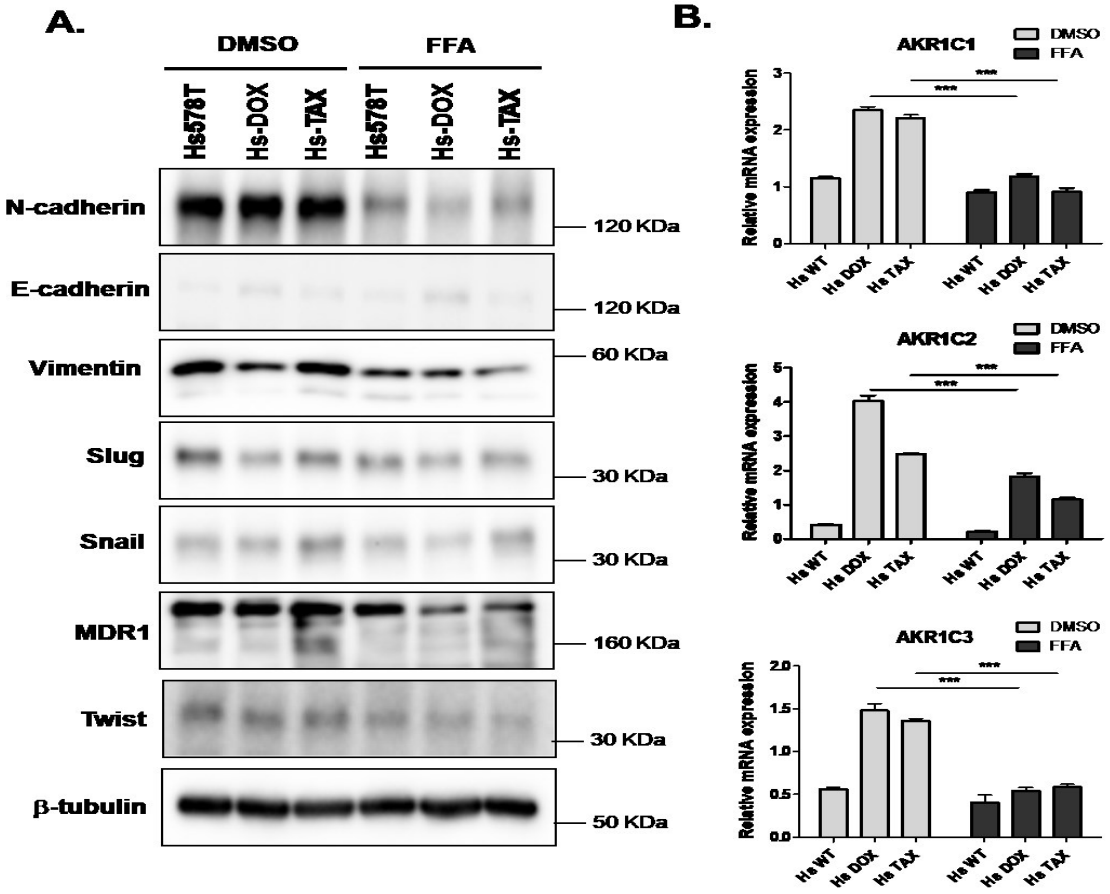


Figure 6.20 FFA reduces the expression of some EMT markers and AKR1Cs. **A**. Effect of FFA (50 μM) on EP300 expression and other indicated EMT markers was determined by western blot analysis in drug naive and resistant cells. **B.** mRNA expression of AKR1Cs was analysed by RT qPCR. Statistical analysis was performed using one-way ANOVA where ***P<0.001, **P<0.01, *P<0.05.

6.3.17 FFA inhibits sphere forming efficiency of both EP300 overexpressed and drug resistant Hs578T cells

As aldo-keto reductases, and particularly AKR1C3, reduce prostaglandins generating proliferating signals that may lead to breast cancer development [479], I asked whether their pharmacological inhibition with FFA might affect *in vitro* tumour initiation properties. Indeed, when Hs-EP300 cells, which overexpress AKR1C1, AKR1C2 and AKR1C3, were treated with 50 μM FFA for 12 days, their mammosphere formation was reduced by 60%, whereas the reduction in control Hs-EV cells was just 45%. Equally, there was a reduction in mammosphere volume upon FFA treatment of ~25% in Hs-EV control cells that increased to ~70% in Hs-EP300 cells (Figure 6.21). Furthermore, reduced mammosphere formation was also observed upon treatment with FFA in doxorubicin and paclitaxel resistant Hs578T cells (Figure 6.22).

Thus, the oncogenic, metastatic and drug resistance capacity of EP300 in a non-permissive E-cadherin background are due, at least in part, to the activation of aldo-keto reductases.

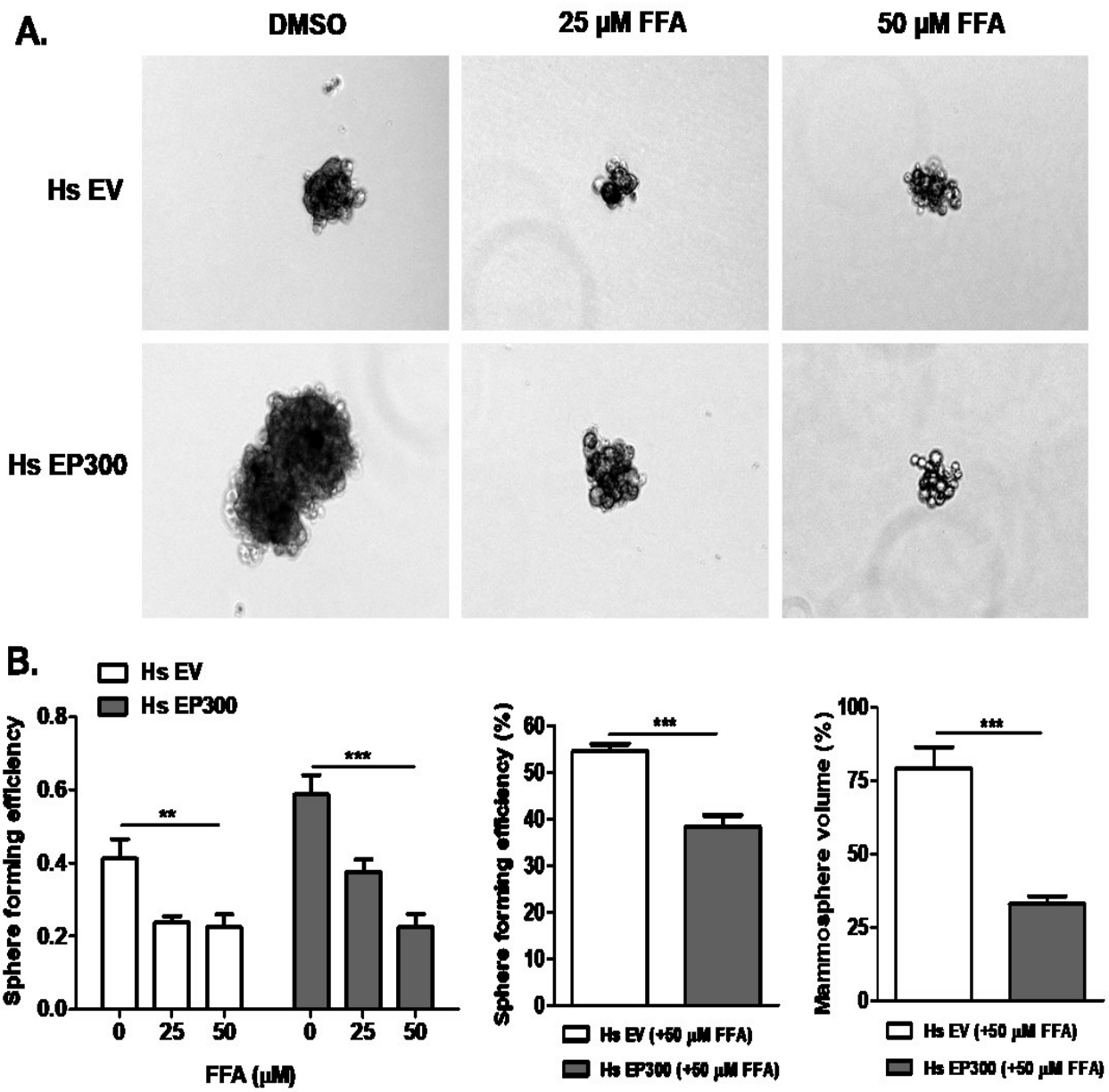


Figure 6.21 FFA reduces anchorage independent growth.
Anchorage independence was monitored in Hs EP300 and control Hs EV cells by sphere formation in liquid medium using low attachment plates. Cells were seeded in 6 well plates ($4x10^3$ cells / well) and treated with 25 µM, 50 µM FFA or vehicle control. **A.** Pictorial data show representatives of at least three independent experiments. Scale bar = 100 µm. **B.** Mammospheres were counted after 12 days (left and middle histogram) and their volume calculated (right histogram indicates relative volume of each cell line to the corresponding vehicle control). Statistical analysis was performed using students t test where ***P<0.001, **P<0.01, *P<0.05.

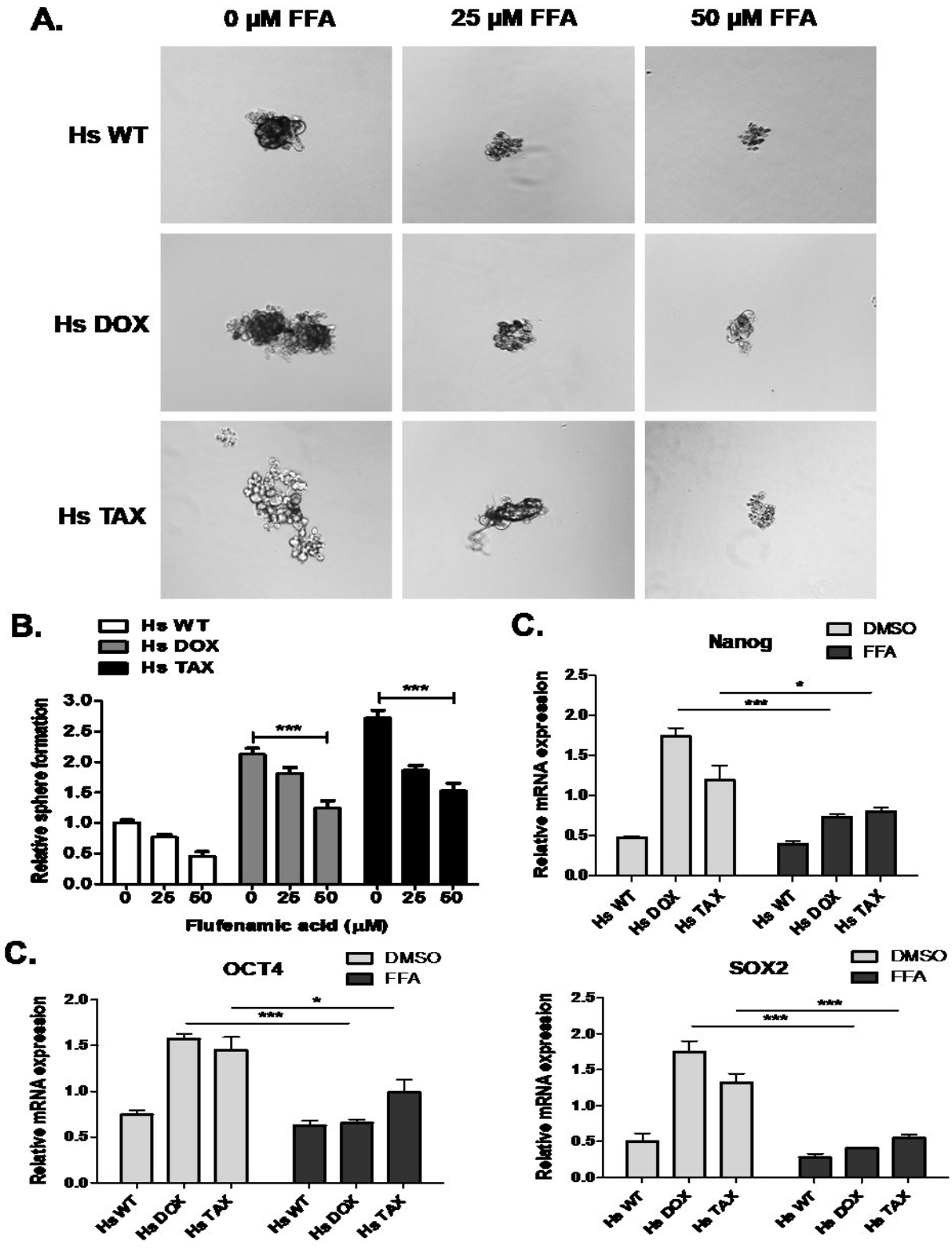


Figure 6.22 FFA reduces mammosphere formation of drug resistant Hs578T cells
Mammosphere formation was monitored in Hs DOX, Hs TAX and control Hs WT cells in liquid medium using low attachment plates. Cells were seeded in 6 well plates (4x103 cells / well) and treated either with 25 µM, 50 µM FFA or vehicle control. **A, B.** After 14 days of seeding, microscopic images were captured (scale bar = 400 µm), mammospheres were counted (left histogram) and compared with control Hs WT cells. Pictorial data show representatives of at least two independent experiments. **C.** RT qPCR data was performed to determine the mRNA expression of CSC markers. Numerical data represent the average ± SD of three different experiments (*** P<0.001, *P<0.05).

6.4 Discussion

Transcription factors such as snail, slug, twist, zeb1 and zeb2 usually repress E-cadherin expression which is well established. However, studies of E-cadherin transcriptional activators, such as EP300, are yet to be established and in some cases with contradictory findings [451, 455]. It has been revealed that both EP300 and E-cadherin are down-regulated in metaplastic breast carcinoma [170], as EP300 acts as a positive modulator of E-cadherin. In this chapter at first, we demonstrated a positive correlation between the expression of these two markers, using two types of breast cancer, preselected to cover both E-cadherin^{low} and E-cadherin^{high} cases, reassuring an EP300 positive regulatory role on the expression of E-cadherin. Importantly, using both markers together might be better at predicting lymph node metastasis than E-cadherin or EP300 alone. These data also support the well-established anti-tumourigenic role of EP300 in various types of cancers, including breast cancer reported by Dr. Ernesto Yagüe [170] and others [156, 451, 452].

Preliminary data from our lab depicted that out of the 41 breast cancer cases analyzed, 9 showed E-cadherin low or null expression despite showing high EP300 level. This offers a complex and contradictory scenario in the regulation of E-cadherin expression by EP300. In addition, *CDH1* locus possesses some truncating mutations which have been defined in a few ILC cases [480] [481], although these mutations responsible for only a minority of cases of E-cadherin dysfunction in cancer [482]. Reduced or null expression of E-cadherin can also be explained due to promoter hypermethylation, which has been demonstrated in ILC [483], acting as a dominant phenotype, as well as loss of heterozygosity, also high in ILC [484]. Again, E-cadherin promoter region shows a relatively higher percentage of methylation in EP300^{high}/E-cadherin^{low} than in EP300^{high}/E-cadherin^{high} patient samples. However, this does not rule out a role of transcriptional repressors, potential *CDH1* mutations or loss of heterozygosity that might contribute to suppression of E-cadherin expression. Nonetheless, this prompted us to ask whether EP300 might have an oncogenic role, independent of its activity on *CDH1* that could shed light on EP300 function to resolve conflicting published reports. For this, we decided to experimentally over-express EP300 in Hs578T cells, a breast cancer cell line with hypermethylation of the *CDH1* locus, as EP300 is unable to transcriptionally activate

its promoter. Our lab also previously presented a clear up-regulation of E-cadherin expression upon EP300 over-expression in E-cadherin-null MDA-MB-231 cells [170]. Pyrosequencing experiment showed that the average percentage of methylation in 29 CpG sites at the proximal *CDH1* promoter in MDA-MB-231 cells is just 13%, less than the 21% found in MCF-7 cells which are epithelial-like and high E-cadherin expressing cells. In contrast, the *CDH1* promoter in Hs578T cells is methylated by 47% [334]. This clarifies the differential ability of EP300 activating the *CDH1* promoter in both cell lines and, confirms the suitability of this cell model to study EP300 oncogenic effects in an E-cadherin-independent manner.

Ectopic over-expression of EP300 in Hs578T cells caused an increased expression of the EMT markers which support its positive correlation in inducing EMT. Moreover, immunofluorescence assay confirmed the higher expression of ^{low}E-cadherin/^{high}vimentin which is an important marker of mesenchymal phenotype. Subsequent subcellular fractionation also supports EP300 mediated nuclear expression and localisation of snail, slug, and zeb1. To validate our hypothesis of E-cadherin promoter hypermethylation, I treated naïve and EP300 overexpressed Hs578T cells with 5'-Aza dC. The results confirmed that upon demethylation due to 5'-Aza dC, EP300 could in fact allow the transcription from the CDH1 gene, although the nature of these short-term expression did not allow for enough accumulation of E-cadherin protein to reverse or reduce mesenchymal phenotype. Furthermore, zeb1 is already known for switching to an activator protein upon binding to EP300 via its N-terminus. Co-immunoprecipitation studies suggest a direct protein-protein contact between EP300 and zeb1 or snail1 and EP300 mediated acetylation of these EMT activator proteins.

The increasingly recognized link between EMT, chemotherapeutic drug resistance and cancer stem cells (CSC) [444, 472, 485] prompted us to assess the role of EP300 in inducing CSC characteristics of Hs578T. FACS experiment revealed an enhanced activity of ALDH in EP300 overexpressed Hs578T cells. Moreover, breast cancer stem cell populations CD44^{high}CD24^{low} were also up-regulated by EP300. This is accompanied by increases in cell motility, invasion and anchorage independence. Thus, in Hs578T, EP300 possesses a traditional oncogenic, metastasis promoting role. In PC3 prostate cancer cells, which have high expression

of N-cadherin and low/null levels of E-cadherin [486], with only 15% methylation of *CDH1* promoter [334], experimental knock-down of EP300 leads to apoptotic cell death and decline in motility and invasion [487]. Thus, oncogenic EP300 in PC3 cells may reflect more its inability to induce *CDH1* transcription and outcompete transcriptional repressors rather than the methylation status of *CDH1* promoter. EP300 also found to act as an oncogene in hepatocellular and nasopharyngeal carcinoma, as high levels positively correlate with aggressive metastatic features and patient poor prognosis [488, 489]. In some hepatocellular and nasopharyngeal carcinoma cell lines, experimental down-regulation of EP300 paradoxically leads to increased expression of E-cadherin and suppression of EMT [454, 455]. However, whether this is a direct repression of the *CDH1* locus by EP300 [490], or an indirect effect, remains unknown. Therefore, the oncogenic or tumour suppressive role of EP300 is clearly cancer /context dependent and can have both activation and repression roles on E-cadherin expression, controlling EMT, drug resistance, and metastasis positively or negatively.

Furthermore, EP300 overexpressed Hs578T cells show enhanced expression of AKR1Cs when analysed by RT-qPCR. Thus, the oncogenic signature of EP300 in Hs578T cells indicates its regulation of AKR1C1, AKR1C2 and AKR1C3, probably by direct transcriptional activation. AKR1C members have been found to be up-regulated in many cancers, although in breast cancer this seems to be limited to AKR1C3 [475]. Aldo-keto reductases can catalyse detoxification reactions of anthracyclines, and AKR1C3 reduces doxorubicin to the corresponding C13 alcohol metabolite, doxorubicinol, which has less toxicity and DNA binding capacity [475, 491]. This explains the doxorubicin resistant phenotype upon EP300 overexpresssion in Hs578T cells. It is still unclear whether paclitaxel is a substrate for aldo-keto reductases, although AKR1C1 confers resistance to a non-substrate, such as cisplatin, in gastric carcinoma cells, probably via indirect mechanisms [492]. Importantly, tumour initiation capacity is also dependent on aldo-keto reductase activity, as it decreases upon treatment with FFA. AKR1C3 is up-regulated in invasive ductal breast carcinoma and correlates with a worst prognosis [493]. AKR1C3 is involved in several metabolic reactions that may lead to the development of breast cancer by increasing estrogenic signals. However, in triple negative breast cancer, the reduction of prostaglandins has a more important role as it generates

hormone-independent proliferative signals by increase in MAPK signaling, NFkB activity and decrease of PPARγ activity [479]. Although the development of novel aldo-keto reductase inhibitors specific for each isoform [475] would be a strategy to consider in cancer therapy, some caution must be exerted as aldo-keto reductases help relieve cardiac toxic effects of anthracyclins [494] and inhibitors might increase chemotherapy side effects. Whether aldo-keto reductases contribute also to the oncogenic effects of EP300 in different cancers and cell models, remains to be established.

In summary, EP300 acts as a tumour suppressor when able to activate transcription of E-cadherin by inducing drug sensitivity, suppression of EMT and reduction of cancer stemness. However, if E-cadherin expression is blocked because of hypermethylated CDH1 promoter, EP300 acts as an oncogene via up-regulation of aldo-keto reductases which can be treated by using AKR1Cs inhibitor.

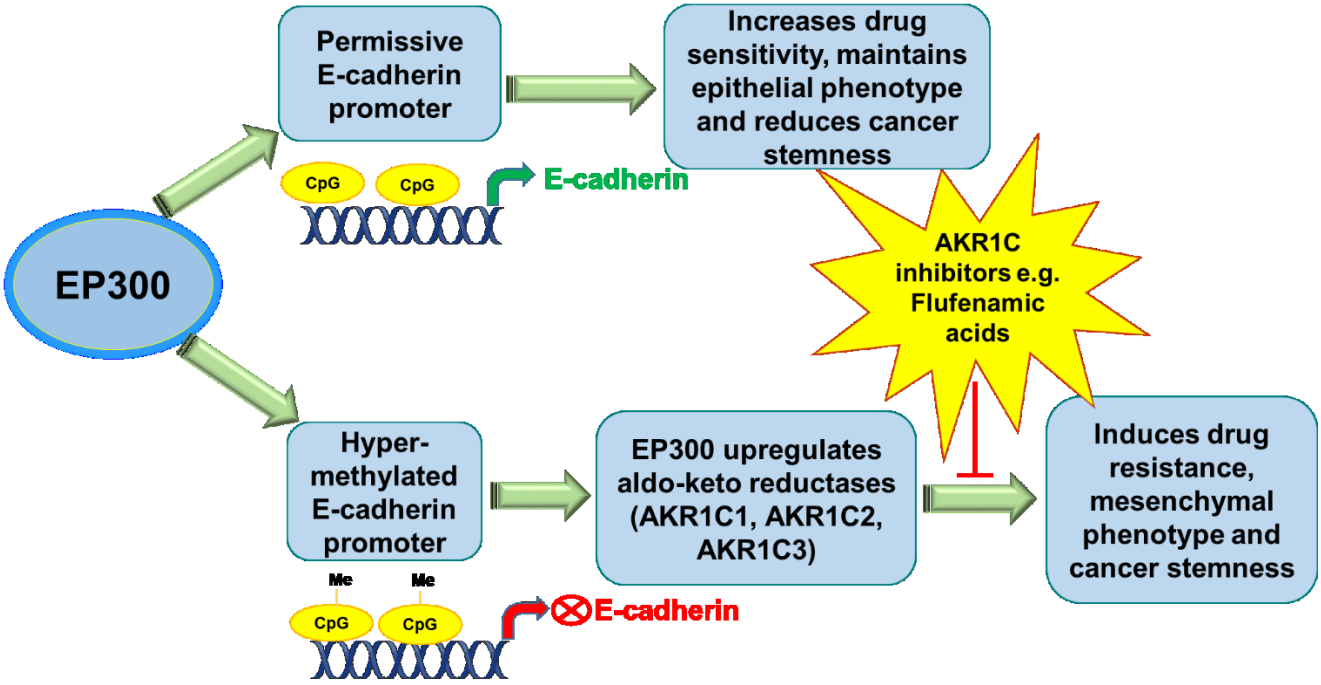


Figure 6.23 Schematic model representing the oncogenic role of EP300 that can be targeted with inhibitor of AKR1C

CHAPTER 7

Final discussions

7.1 EP300 and SIRT1/6 co-regulate lapatinib sensitivity via modulating FOXO3 acetylation

EP300 and CBP are the two most-studied transcriptional co-activators possessing histone acetyltransferase activity and thus involve in the regulation of chromatin structure. These co-activators modulate multitude of cellular programs, including cell cycle progression, differentiation, cell proliferation, apoptosis and many other biological processes. Importantly, a wide range of intracellular transcription factors co-operate with EP300 and CBP. For example, FOXO transcription factors play their regulatory roles in various signalling pathways that are initiated due to DNA damage response, metabolic stress and/or other environmental stimuli [313]. Moreover, FOXO activity is firmly modulated by multiple PTMs that are differentially activated and induced depending on the stimulus present [226]. Specially, FOXO3 acetylation has been found to be regulated at post-translational level by the acetyl-transferase activity of EP300/CBP. However, their dual role and contradictory findings from scientific studies prompted us to elucidate and determine the regulation of FOXO3 acetylation and its subsequent effect on cancer drug sensitivity and resistance.

Firstly, to elucidate the function of FOXO3 in HER2 positive breast cancer, I performed western blotting using the lysates collected from BT474 and BT474 Lap^R and observed that treatment with lapatinib enhances dephosphorylation of EGFR, HER2, AKT, and FOXO3. In addition, elevated levels of Ac-FOXO3 and EP300 were found when a time-course experiment was conducted using lapatinib. BT474 cells also showed a gradual increase of FOXO3 as well as its target proteins $p27^{Kip1}$ and Bim upon treatment with lapatinib.

To evaluate the functional outcome of FOXO3 acetylation, transient overexpression of EP300 was performed in both lapatinib sensitive and resistant BT474 cells. In addition, I also performed transient over-expression of the acetyl-transferase mutant (HAT-) derivative of EP300 which was used to clarify that any changes witnessed are attributable to the acetyl-transferase activity of EP300. Overexpression of EP300 enhances FOXO3 expression and acetylation, which in turn promote the expression of its target genes, including *$p27^{Kip1}$* and *Bim* in the BT474 cells. However, FOXO3 is deregulated and downstream targets uncoupled from FOXO3 in the resistant cells. In BT474 cells, induction of acetylation of FOXO3 upon EP300 overexpression causes

higher mRNA and protein levels of $p27^{Kip1}$ and Bim expression, which propose that EP300-mediated FOXO3 acetylation leads to the preferential induction of cell cycle arrest and pro-apoptotic genes.

In order to explore the significant role of FOXO3 acetylation in lapatinib response, short- and long-term drug sensitivity assays were employed. Over-expression of EP300 caused an elevated lapatinib sensitivity in BT474 cells, as indicated by the SRB and clonogenic assays (Figures 3.7D and 3.8A). On the contrary, up-regulation of EP300 in BT474 Lap^R cells did not seem to have enough effect on lapatinib sensitivity, however, it has been found to show reduction in clonal survival when compared with the empty vector transfected control cells (Figure 3.8A). Moreover, SRB experiment revealed that EP300 overexpressed BT474 Lap^R cells do not show an enhanced lapatinib response. To date, HAT mutant transfected cells appear to have similar lapatinib response as the empty-vector transfected ones, suggesting the possibility of having a non-functional or truncated or mutated form of EP300 due to the absence of HAT activity in BT474 Lap^R cells. In agreement, these results suggest a significant role of EP300-mediated acetylation of FOXO3 in regulating HER2-positive breast cancer cell survival, proliferation and their lapatinib sensitivity.

Since EP300 over-expression correlates with enhanced drug sensitivity in BT474 cells, I wanted to examine the intrinsic mechanism behind this significant finding. For this, I performed co-immunoprecipitation assays and duolink proximity ligation assays in order to monitor the FOXO3-EP300 interaction and how this impact on FOXO3 acetylation. Co-IP results have shown that the FOXO3-EP300 interaction as well as FOXO3 acetylation increases upon EP300 overexpression in sensitive cells. From duolink PLA, Ac-FOXO3 levels were found to be upregulated in BT474 cells that have been treated with lapatinib for 4 and 8 hours, indicating that an increased HAT activity is positively associated with increased Ac-FOXO3 levels in BT474 cells. Thus, lapatinib sensitivity depends on the accumulation of Ac-FOXO3 in sensitive BT474 cells. However, whether the elevated acetylated FOXO3 stimulate downstream activation of target genes, depends on the ability of FOXO3 to bind and recruit EP300 to target gene promoter sequences. This was explained and verified by the data obtained from ChIP analysis (Figure 3.2). For instance, an increased binding of FOXO3 on its target gene promoter sequences e.g. *Rictor, $p27^{Kip1}$, Rad51*,

was observed in BT474 cells, whereas, very weak or no binding was found in BT474 Lap^R cells.

Furthermore, sirtuin-mediated deacetylation of FOXO3 has been reported to restrict EP300-mediated transactivation of FOXO3 [184, 204]. Ectopic over-expression of sirtuin has also been reported to reduce apoptosis in cancer cells which in turn lead to acquired drug resistance [251, 495]. Therefore, I attempted the siRNA mediated gene knockdown of sirtuins and the use of sirtuin inhibitors e.g. sirtinol to dissect the role of FOXO3 acetylation. Gene silencing of SIRT1 and SIRT6 in combination with lapatinib treatment induces an upregulation of FOXO3 acetylation and thus increases the expression of $p27^{Kip1}$ and *Bim*. Moreover, depletion of SIRT6 restricts the cell growth, proliferation and increases lapatinib sensitivity in BT474 cells, although depletion of SIRT1 does not show significant effects on lapatinib sensitivity. In addition, sirtinol induced inhibition of SIRT1/6 does not affect cell proliferation and clonal survival in the resistant cells is possibly due to the fact that EP300 expression is null or very low in the lapatinib resistant cells. This further suggests that SIRT1 and SIRT6 cooperate to set a threshold level for FOXO3 acetylation in the cancer cells. In agreement, immunohistochemical (IHC) staining results also show that FOXO3 expression correlates positively with SIRT6/1 level in different breast cancer subtypes. As high FOXO3 expression, particularly in the nucleus, predicts FOXO3 deregulation/inactivation and poor prognosis in patients [30, 343], these IHC results provide further evidence that SIRT1 and SIRT6 cooperate to deregulate FOXO3 activity by inducing its deactylation.

Although the above results provide substantial evidence that FOXO3 acetylation positively regulates lapatinib sensitivity in HER2 positive breast cancer, nevertheless, some future works must be needed to improve our findings that are mentioned below.

- It has been reported that EP300 can increase FOXO3-dependent transcription of *Bim* in human embryonic kidney cells [496]. To validate the binding of FOXO3 on its target genes promoter, a luciferase reporter assay should be performed. To do this, the promoters of target genes need to be cloned upstream of the luciferase gene and transfected into naïve BT474 cells, cells over-expressing EP300 as well as in cells over-expressing the acetylation

defective FOXO3 mutant. Measurement of the luciferase activity will confirm the role of acetylation in inucing FOXO3-dependent gene transcription.

- Although I found the increased interaction between EP300 and FOXO3 upon lapatinib exposure from both duolink PLA assay and co-IP assays (Figure 3.5 and 3.7B), however, sequential ChIP (Re-ChIP) should be also performed to ensure the interaction of FOXO3 and EP300 on a particular gene promoter sequence. Moreover, duolink PLA should also be performed in EP300 overexpressed BT474 to further confirm FOXO3 acetylation.

- Silencing of FOXO3 followed by treatment with lapatinib would be required in EP300 overexpressed cells to validate the role of EP300 in regulating FOXO3 expression at transcriptional and translational levels.

- Whether acetylating FOXO3 increases the localisation and stability of FOXO3 in BT474 cells, should be confirmed by cycloheximide treatment in a time-course manner. Subsequent assessment of the expression of FOXO3 and Ac-FOXO3 levels by western blotting would be required to examine the stability of FOXO3 and its acetylated form.

- As high level of SIRT1 and SIRT6 was observed in BT474 Lap^R cells which induces FOXO3 deacetylation as well as their proteosomal degradation, therefore, use of lapatinib and the proteosomal inhibitors in combination would be required to suggest possible treatment strategy to combat lapatinib resistant breast cancer.

Finally, my results have suggestively concluded that lapatinib sensitivity in BT474 cells is modulated by the binding of FOXO3 on its target genes promoter and the subsequent transcriptional activation of target genes, especially through recruitment and interaction of the co-activator EP300. In contrast, in BT474 Lap^R cells the recruitment and binding of FOXO3 and EP300 are usually inhibited possibly by other mechanisms which may be responsiblke for lapatinib resistance. Thus, elucidating the role of EP300 mediated FOXO3 acetylation on its functional activity is critical for our ability to determine the role of this tumour suppressor in lapatinib sensitivity and

resistance of breast cancer. My findings also suggest that SIRT1 and SIRT6 play a coordinate role in fine-tuning FOXO3 acetylation and therefore lapatinib sensitivity by setting a threshold for the de-acetylation activity in both lapatinib sensitive and resistant cancer cells. Therefore, my data suggest that FOXO3 acetylation by EP300 could be a potential biomarker for the identification of tumours that are likely to be sensitive to these drugs and indicate a novel therapeutic strategy to overcome lapatinib resistance in HER2-positive breast cancers.

7.2 CBP mediated FOXO3 acetylation suppresses cell proliferation via inducing cellular senescence and apoptosis

The functional roles and regulation of CBP in cancer progression and metastasis is largly focused on its gene mutation or chromosomal translocation [497, 498] . Although some researchers reported the anti-oncogenic effects of CBP inhibition by suppressing its HAT activity or playing as a transcriptional co-activator protein [499, 500], however, the mechanism is still unclear. Nevertheless, the genuine functional roles and mechanisms by which CBP acetyl-transferases regulate FOXO3 acetylation and how it is involved in tumor growth and metastasis have still been largely unknown. Therefore, to evaluate the functional significance of FOXO3 acetylation more thoroughly, I aimed to assess the role of acetyl-transferases activity of CBP on FOXO3 acetylation and its downstream effect on drug resistance of cancer. As, lapatinib treatment showed a time dependent increase of FOXO3 expression in BT474 cells but not significantly in resistant cells (Figure 4.1), I overexpressed CBP in both BT474 and Lap^R cell lines. CBP overexpression upregulates AcFOXO3 levels and thus enhances expression of cell cycle arrest genes as well as the autophagic markers specifically p62 and LC3BII suggesting the involvement of CBP in regulating cell cycle arrest and autophagy. Furthermore, CBP is thought to elevate gene expression through recruitment and binding of basal transcriptional machinery to the promoter sequence by interacting with other transcriptional factors [501, 502]. Therefore, I aimed to perform a co-IP experiment which suggests the positive interaction between CBP and FOXO3 upon CBP overexpression and this interaction was found to induce FOXO3 acetylation as mediated by CBP HAT domain (Figure 4.5 and 4.6). Expectedly, HAT mutant CBP overexpression showed reduced level of Ac-FOXO3 expression. Moreover, Ectopic

CBP overexpression was found to increase short-term lapatinib sensitivity and inhibit long-term cell proliferation of BT474 cells (Figure 4.7). Functional assays revealed that CBP reduces mammosphere formation and induces cellular senescence as well as caspase mediated apoptosis (Figure 4.8, 4.10 and 4.11). Wound healing scratch assay depicted a significant reduction of cell migration and invasion upon CBP overexpression which was also supported by transwell cell migration assay (Figure 4.12 to Figure 4.15). Thus, acetylation of FOXO3 by CBP induces lapatinib sensitivity as like as EP300, however the mechanism of induction may vary that EP300 doing it via regulating cell cycle arrest and/or apoptotic induction whereas CBP doing it predominantly via regulating cellular senescence, apoptosis and/or autophagic cell death.

To further support aforementioned data, I performed siRNA mediated knockdown of CBP in both sensitive and resistant BT474 cells (Figure 4.16). CBP silencing suppresses the expression of cell senescence markers such as $p27^{Kip1}$ and $p16^{INK4a}$ and also the autophagic marker LC3BII, again suggesting that CBP regulates FOXO3 acetylation by modulating cell senescence and autophagic markers (Figure 4.16). Importantly, knockdown of CBP reduces lapatinib sensitivity in SRB assay, however, depletion of CBP increases cell proliferation when long-term clonogenic assay was performed both in sensitive and resistant BT474 cells (Figure 4.17). Functional assays such as wound healing scratch assay and mammosphere assay upon CBP knockdown conclusively showed that in the absence of CBP, BT474 cells gain motility and acquire mammosphere forming capacity (Figure 4.18 to Figure 4.20). These data further supported by the use of CBP inhibitor such as C646 where C646 was found to induce the inhibition of CBP function, causing a reduction of Ac-FOXO3 level and thus enhancing cell growth (Figure 4.22 to Figure 4.24). Similar results were observed by the use of a bromodomain inhibitor e.g. PFCBP1, supporting the idea that bromodomain has a positive effect on HAT activities (Figure 4.22 to Figure 4.24) [503]. Finally, all these data suggest that CBP mediated FOXO3 acetylation positively regulates lapatinib sensitivity in HER2 positive breast cancer cells.

In conclusion, determining the functional role of PTMs, and more specifically acetylation of FOXO3 on its functional activities is crucial for our ability to better

understand the role of CBP in lapatinib sensitivity and resistance of breast cancer. Characterisation of FOXO3 acetylation and its association with enhanced lapatinib sensitivity will enable the recognition of this modification as a biomarker for HER2 positive breast cancer. Therefore, in future, its application for increasing anti-cancer drug efficacy would be possible. Hence, elucidating the role of CBP-mediated acetylation of FOXO3 will enable a more promising and cautious approach in the choice and combination of drugs used for treating patients with HER2 over-expressing breast cancers. However, for the purpose of practical implications, future supporting experiments still need to be performed which are summerised below.

- FOXO3 is known to target so many other genes such as GADD45, MnSOD, FasL etc. which are involve in the regulation of multiple cellular and biological processes. Therefore, the recruitment and binding of FOXO3 on these target genes should be confirmed to elucidate the functional role of FOXO3 acetylation in CBP overexpressed BT474 cells. Subsequently duolink PLA and subcellular fractionation experiment should be performed to confirm the expression and localisation of FOXO3 and Ac-FOXO3. Moreover, ceycloheximide treatment would further allow us to assess the stablility of FOXO3 and its acetylated form.

- To further validate the role of CBP in inducing apoptosis, we should perform BrdU assay and annexinV staining assay in CBP overexpressed BT474 as well as in HAT mutant BT474 cells. BrdU assay confirms any effect on cell proliferation, whereas annexin-V assay is needed to confirm the CBP mediated apoptotic inductions.

- CBP mediated FOXO3 acetylation and their downstream effects should be confirmed in other breast cancer subtypes, in in-vivo animal models as well as in different cohorts of clinical samples. This could represent a starting point for the development of targeted therapies using FOXO3 acetylation as a biomarker for cancers that have a higher expression of HER2 and may ultimately help prolong breast cancer patient's survival.

7.3 SIRT2 mediated FOXO3 deacetylation modulates lapatinib sensitivity both in BT474 and nasopharyngeal carcinoma

As mentioned before, FOXO3 regulation is mediated by post-translational modifications such as acetylation, methylation, ubiquitination and glycosylation. Lysine acetyl-transferases EP300/CBP has been shown to regulate FOXO3 acetylation, however, the nuclear sirtuins SIRT1, SIRT2 and SIRT6 also have been shown to regulate FOXO3 acetylation and its activity [194, 431, 432]. In chapter 3, I explored the role of SIRT1 and SIRT6 in FOXO3 acetylation, but then I observed that depletion of SIRT2 by siSIRT2 also increases FOXO3 acetylation suggesting the role of SIRT2 in FOXO3 deacetylation (Figure 5.1). Notably, enhanced FOXO3 acetylation was observed in duolink proximity ligation assay upon SIRT2 knockdown (Figure 5.1). To date, SIRT2 knockdown was found to induce the expression of FOXO3 downstream target genes such as, $p27^{Kip1}$, p130, and $p16^{INK4a}$. Moreover, deficiency of SIRT2 also found to increase the expression of cleaved PARP and cleaved caspase suggesting that knocking down of SIRT2 induces caspase mediated apoptosis that has been identified in recent study (Figure 5.3) [504]. Long-term clonogenic assay reassuringly suggests our hypothesis that SIRT2 mediated FOXO3 deacetylation positively regulates lapatinib sensitivity in HER2 positive cancer cells (Figure 5.5).

To further confirm the role of SIRT2, we tested a recently synthesized novel SIRT2 inhibitor [412] and other commercial inhibitors in order to suppress SIRT2 mediated deacetylase activity. Interestingly, the newly designed SIRT2 inhibitor showed higher credibility to inhibit deacetylase activity compared to other inhibitors in deacetylating a well-established SIRT2 target named alpha tubulin (Figure 5.2). The inhibitor ScA-B8A44 also found to increase Ac-FOXO3 levels significantly at 20 μM concentration alone, although addition of TSA further increases acetylation of FOXO3 suggesting that SIRT2 inhibition is enough to increase significant level of FOXO3 acetylation (Figure 5.8 and 5.9). Importantly, this induced FOXO3 acetylation upon inhibiting SIRT2 found to increase FOXO3 target genes expression as well as cleaved PARP and caspases to enhance FOXO3 mediated cell cycle arrest and/or apoptosis (Figure 5.9 and 5.11). Furthermore, pharmacological inhibition of SIRT2 by ScAB8A44 and AGK2 significantly upregulates FOXO3 acetylation which in turn induces lapatinib sensitivity of BT474 cells (Figure 5.12 and 5.13). Therefore, inhibition of SIRT2

suggestively contributes to cell mediated apoptosis as well as the enhancement of lapatinib sensitivity in BT474 cells via induction of FOXO3 acetylation.

To elaborate our SIRT2 study, we used NPC cell line as some recent findings explored the role of SIRT2 to regulate lapatinib sensitivity in NPC, although the mechanism remains unclear. By using four SIRT inhibitors (i.e. sirtinol, EX527, AGK2 and AK1) we found that these inhibitors can limit NPC cell proliferation. However, only the SIRT2 specific inhibitors AGK2 and AK1 function cooperatively with lapatinib (Figure 5.14). This result supports the idea that SIRT2 specifically modulates lapatinib response and resistance. As all four SIRT inhibitors can restrict normal NPC cell viability and clonogenicity, and thus suggests that the nuclear sirtuins SIRT1, -2 and -6 detected in NPC are all potential oncogenes. The pan-SIRT inhibitor sirtinol has previously been shown to induce p53 acetylation and cell death through targeting both SIRT1 and SIRT2 [264]. However, like EX527, the sirtinol concentrations employed here preferentially inhibit SIRT1 and have limited activities towards SIRT2 [264]. Therefore, these observations support further the notion that SIRT2 specifically moderates the cytotoxic action of lapatinib and mediates lapatinib resistance, independently of SIRT1. In addition, inhibition of SIRT2 by chemical inhibitor or silencing significantly enhances the cytotoxicity of lapatinib not only in the sensitive but also in the resistant NPC cells, suggesting that SIRT2 not only modulates the cytotoxic functions of lapatinib in the sensitive NPC cells, but it also mediates lapatinib resistance. This implies that targeting SIRT2 can enhance the cytotoxicity of lapatinib and may represent a novel strategy for overcoming lapatinib resistance in NPC. This role of SIRT2 in modulating lapatinib response and sensitivity is confirmed by SIRT2 depletion experiments showing silencing SIRT2 can enhance the cytotoxicity in both lapatinib sensitive and resistant NPC cells (Figure 5.22). Furthermore, co-IP experiments also show that the lapatinib induces FOXO3 acetylation and that inhibition of SIRT2 by chemical inhibitor or silencing also promotes FOXO3 acetylation in NPC cells (Figure 5.23). Importantly, SIRT2 inhibition or silencing can combine with lapatinib to cause further enhancement of FOXO3 acetylation than lapatinib treatment alone in both sensitive and resistant NPC cells, suggesting that SIRT2 can moderate the cytotoxic functions of lapatinib and promote resistance through limiting FOXO3 acetylation. In agreement, FOXO3 deacetylation

by SIRT2 has previously been reported to enhance FOXO3 ubiquitination and proteasomal degradation [439].

Collectively, these data suggest that SIRT2 modulate the cytotoxic functions of lapatinib that is mediated through the acetylation of FOXO3. Our results also suggest that SIRT2 can be an important biomarker for metastatic and lapatinib resistant BT474 as well as for NPC and that targeting the SIRT2-FOXO3 axis may provide a pathway to treat and overcome chemoresistance of HER2 positive breast cancer and NPC cancers. However, it would be important to conduct following works for the future implications of our findings.

- To validate the role of novel SIRT2 inhibitor scAB8A44 in inducing apoptosis, we should conduct BrdU assay and annexinV staining assay upon treatment with this inhibitor in BT474 as well as in NPC cells. BrdU assay will confirm any effect of SIRT2 inhibitor on cell growth and proliferation, whereas annexin-V assay will suggest any apoptotic induction.

- The major experiments conducted in this chapter should be performed on other related HER2 positive breast cancer cell lines such as SKBR3, T47D and also in other NPC cell lines such as C666-1, TW01 and HK-1 to validate the role of SIRT2 in regulating FOXO3 acetylation.

- It would also be very important to examine the expression of SIRT2 and FOXO3 (both total and acetylated form) in in-vivo animal models and in real tumour tissue samples collected from primary and metastatic cancer patients.

7.4 Oncogenic EP300 can be targeted with inhibitors of AKR1Cs

EMT is exclusively a developmental process which is increasingly recognised for contributing cancer progression, metastasis and more inmportantly for inducing cancer stem cell (CSC) phenotypes [472]. Biologically, it is defined by the loss of epithelial protein markers, mainly E-cadherin, and the simultaneous acquisition of mesenchymal protein markers such as N-cadherin, vimentin and fibronectin [505]. Recently, the loss of EP300 has been found to be linked with EMT and drug

resistance in breast and colon cancers and thus supported its tumour suppressing activity [170, 315, 450]. However, there is evidence that EP300 could play a role as an oncoprotein in breast cancer, although little is known about the exact mechanism behind its oncogenic properties [506, 507]. Therefore, in this chapter, I sought to investigate the role of EP300 in EMT, drug resistance and acquisition of stem cell characteristics in the metaplastic triple negative breast cancer cell line Hs578T.

To characterise the involvement of EP300 in EMT, western blotting was performed using three different types of Hs578T cells which were transfected with plasmid encoding EP300 and E-cadherin (CDH1) or empty vector pcDNA3.1. After confirming the over-expression of EP300 and CDH1 at both the mRNA and protein levels (Figure 6.3A, B), I tested the levels of E-cadherin in EP300-transfected cells. Unexpectedly, I observed no significant changes in the expression of E-cadherin both at mRNA and protein level in the EP300 overexpressed cells. Therefore, the result did not support our preliminary hypothesis for a positive correlation between EP300 and E-cadherin expression in breast cancer. Interestingly, it has been shown that Hs578T cell line has highly methylated CDH1 promoter [467]. So, it was hypothesized that EP300 could not transcriptionally activate CDH1 gene in Hs578T and then acts on other down-stream pathways/activators /repressors to establish an oncogenic environment. This in turn also highlights the non-histone protein acetyl-transferase activity of EP300 and/or its contribution in cellular processes other than histone acetylation and E-cadherin up-regulation [156, 372].

Apparently, EP300 overexpression caused an increased expression of the EMT markers which supports its positive correlation in inducing EMT in Hs578T cells (Figure 6.3). Moreover, immunofluorescence assay confirmed the presence of ^{low}E-cadherin / ^{high}vimentin which is an important biomarker of mesenchymal phenotype (Figure 6.4). Subsequent subcellular fractionation also supports EP300 mediated nuclear expression and localisation of snail, slug, and zeb1 (Figure 6.6). Furthermore, to validate my hypothesis of E-cadherin promoter hypermethylation, I performed 5'-Aza dC experiment which confirmed that upon demethylation EP300 could in fact allow for transcription from the CDH1 gene, although the nature of these short-term expression did not allow for enough accumulation of E-cadherin protein to reverse or reduce mesenchymal phenotype (Figure 6.7A, B). Furthermore, upon

binding to EP300 via its N-terminus region, zeb1 usually converts to an activator protein [508]. From the co-IP experiments, I found a direct protein-protein interaction between EP300 and zeb1 or snail1 (Figure 6.5). Moreover, there was unchanged level of FOXO3 acetylation as observed from co-IP experiment upon EP300 overexpression in Hs578T cells suggesting that FOXO3 acetylation does not have a significant role in EMT induction (Figure 6.5A).

Since a link between EMT, drug resistance and CSCs is increasingly recognised [444, 472, 485], I aimed to assess the role of EP300 in inducing CSC characteristics of Hs578T. FACS analysis revealed an elevated activity of ALDH in EP300 overexpressed cells. Moreover, breast cancer stem cell populations $CD44^{high}CD24^{low}$ were also up-regulated by EP300 as shown in figure 6.9. Cell migration and invasion experiment further supported the EP300 induced cell invasiveness and metastasis of Hs578T cells (Figure 6.10). Finally, since EP300 over-expression seemed to up-regulate EMT characteristics, I also wanted to assess if it can affect doxorubicin and paclitaxel sensitivity and resistance in Hs578T. Remarkably, cells over-expressing EP300 were found to be more resistant to paclitaxel and doxorubicin, drugs that used for the treatment of triple negative metastatic breast cancers (Figure 6.13 and 6.14).

Therefore, my hypothesis was that in epithelial models (E-cadherin positive) or basal with not massive hypermethylation of CDH1 promoter, EP300 acts as a tumour suppressor. However, in cells like Hs578T in which the E-cadherin promoter is hypermethylated, expression of EP300 cannot overcome this chromatin shut-down and then it is free to act on other down-stream pathways (e.g. NF-kB) and lead to an oncogenic phenotype. Overall, my data support the hypothesis that EP300 positively regulates the related characteristics of EMT, drug resistance, and CSC populations, in part through its role in activating other EMT pathways rather than activating E-cadherin. We also found promoter hypermethylation in the patient sample with EP300-high but E-cadherin-low samples (Figure 6.2). In addition, using drug resistant Hs578T cells I observed that high level of EP300 and AKR1C expression correlates with drug resistance of these cells (Figure 6.17). Furthermore, use of AKR1C inhibitor FFA found to reduce clonal survival of cells and increase drug sensitivity (Figure 6.19). Importantly, decreased mammosphere formation upon

treatment with FFA was also observed in both EP300 overexpressed Hs578T and in drug resistant Hs578T cells that are shown in figure 6.21 and figure 6.22 respectively. Taken together, my results suggest that targeting AKR1C to inhibit oncogenic EP300 may provide effective treatment strategy for triple negative breast cancers. However, for future implications, some important works should be performed which are mentioned below.

- The interaction between EP300 and the transcriptional repressor proteins that bind to the promoter of their target genes would be checked by ChIP assays. This would further suggest possible EP300 mediated acetylation level of these proteins and also their target gene expression at transcriptional level, which can be examined by subsequent co-IP or duolink PLA. Treatment of cells using the histone de-acetylase (HDAC) inhibitor, TSA, will also enable us to further assess the relevance of histone acetylation in the expression of the EMT-inducing genes.

- It has also been reported that many of the transcription factor protein's activities are HAT-independent [509]. Therefore, it needs to perform a transfection experiments with EP300 mutated within its HAT domain, in order to establish whether the oncogenic activity of EP300 is HAT dependent or independent.

- Overexpression of EP300 and concomitant knockown of AKR1Cs in drug resistant cell lines Hs-DOX and Hs-TAX should be conducted to check the expression of EMT markers and related drug resistances. Moreover, knockdown of AKR1Cs in Hs-EP300 cells will further confirm the coordinated regulation between these two proteins and EMT markers.

- Since, prostaglandins are the direct metabolite of AKR1C enzymes, therefore, the use of Aspirin to inhibit AKR1Cs activities should be examined to check whether this inhibition would revert EMT and rug resistance in Hs-DOX and Hs-TAX cells.

- Verification of the expression of AKR1Cs in the 9 patient samples with $EP300^{high}$/$E\text{-}caherin^{low}$ is required to validate the direct role of AKR1Cs in these tissue samples.

- Since, DNA methyltransferase inhibitors are currently being pursued as cancer treatments, a better understanding of hypermethylation induced oncogenic activity of EP300 would allow more effective development and application of these treatments. In addition, an extensive study should be performed in other triple negative cancer cell lines, in vivo animal models and also in patients with metastatic cancers to further establish the oncogenic role of EP300.

In conclusion, the implication that EP300 mediated EMT regulation is influenced by E-cadherin promoter hypermethylation, as well as the association of EP300's in other interactions and cellular processes both need further exploration to determine the role of this multi-faceted protein. Finally, according to the above accumulated evidence it can be summarized that the oncogenic role of EP300 and targeting EP300 by AKR1C inhibitors offer the rationale of using these inhibitors in the current treatment strategies and will enable us to develop new cancer therapeutics in treating EP300 mediated metastatic triple negative breast cancers.

REFERENCES

1. Bray, F., et al., *Global cancer statistics 2018: GLOBOCAN estimates of incidence and mortality worldwide for 36 cancers in 185 countries.* CA Cancer J Clin, 2018. **68**(6): p. 394-424.
2. Ferlay, J., et al., *Cancer incidence and mortality worldwide: sources, methods and major patterns in GLOBOCAN 2012.* Int J Cancer, 2015. **136**(5): p. E359-86.
3. Larsen, M.J., et al., *Hereditary breast cancer: clinical, pathological and molecular characteristics.* Breast Cancer (Auckl), 2014. **8**: p. 145-55.
4. Wiseman, M., *The second World Cancer Research Fund/American Institute for Cancer Research expert report. Food, nutrition, physical activity, and the prevention of cancer: a global perspective.* Proc Nutr Soc, 2008. **67**(3): p. 253-6.
5. Honrado, E., J. Benitez, and J. Palacios, *The molecular pathology of hereditary breast cancer: genetic testing and therapeutic implications.* Mod Pathol, 2005. **18**(10): p. 1305-20.
6. Hayashi, S.I., et al., *The expression and function of estrogen receptor alpha and beta in human breast cancer and its clinical application.* Endocr Relat Cancer, 2003. **10**(2): p. 193-202.
7. Rimawi, M.F., R. Schiff, and C.K. Osborne, *Targeting HER2 for the treatment of breast cancer.* Annu Rev Med, 2015. **66**: p. 111-28.
8. Perou, C.M., *Molecular Stratification of Triple-Negative Breast Cancers.* Oncologist, 2010. **15**: p. 39-48.
9. Sorlie, T., et al., *Repeated observation of breast tumor subtypes in independent gene expression data sets.* Proc Natl Acad Sci U S A, 2003. **100**(14): p. 8418-23.
10. Sorlie, T., et al., *Gene expression patterns of breast carcinomas distinguish tumor subclasses with clinical implications.* Proc Natl Acad Sci U S A, 2001. **98**(19): p. 10869-74.
11. Malhotra, G.K., et al., *Histological, molecular and functional subtypes of breast cancers.* Cancer Biol Ther, 2010. **10**(10): p. 955-60.
12. Menard, S., et al., *Biologic and therapeutic role of HER2 in cancer.* Oncogene, 2003. **22**(42): p. 6570-8.
13. Riese, D.J. and D.F. Stern, *Specificity within the EGF family ErbB receptor family signaling network.* Bioessays, 1998. **20**(1): p. 41-48.
14. Brandt-Rauf, P.W., M.R. Pincus, and W.P. Carney, *The c-erbB-2 protein in oncogenesis: molecular structure to molecular epidemiology.* Crit Rev Oncog, 1994. **5**(2-3): p. 313-29.
15. Brennan, P.J., et al., *HER2/neu: mechanisms of dimerization/oligomerization.* Oncogene, 2000. **19**(53): p. 6093-101.
16. Vandergeer, P., T. Hunter, and R.A. Lindberg, *Receptor Protein-Tyrosine Kinases and Their Signal-Transduction Pathways.* Annual Review of Cell Biology, 1994. **10**: p. 251-337.
17. Moasser, M.M., *The oncogene HER2: its signaling and transforming functions and its role in human cancer pathogenesis.* Oncogene, 2007. **26**(45): p. 6469-87.
18. Nahta, R., et al., *Insulin-like growth factor-I receptor/human epidermal growth factor receptor 2 heterodimerization contributes to trastuzumab resistance of breast cancer cells.* Cancer Res, 2005. **65**(23): p. 11118-28.
19. Ursini-Siegel, J., et al., *Insights from transgenic mouse models of ERBB2-induced breast cancer.* Nat Rev Cancer, 2007. **7**(5): p. 389-97.

20. Baselga, J. and S.M. Swain, *Novel anticancer targets: revisiting ERBB2 and discovering ERBB3.* Nat Rev Cancer, 2009. **9**(7): p. 463-75.
21. Ellis, M.J., et al., *Estrogen-independent proliferation is present in estrogen-receptor HER2-positive primary breast cancer after neoadjuvant letrozole.* J Clin Oncol, 2006. **24**(19): p. 3019-25.
22. De Laurentiis, M., et al., *A meta-analysis on the interaction between HER-2 expression and response to endocrine treatment in advanced breast cancer.* Clin Cancer Res, 2005. **11**(13): p. 4741-8.
23. Slamon, D.J., et al., *Human breast cancer: correlation of relapse and survival with amplification of the HER-2/neu oncogene.* Science, 1987. **235**(4785): p. 177-82.
24. Pollock, N.I. and J.R. Grandis, *HER2 as a Therapeutic Target in Head and Neck Squamous Cell Carcinoma.* Clinical Cancer Research, 2015. **21**(3): p. 526-533.
25. Piccart, M., *The role of taxanes in the adjuvant treatment of early stage breast cancer.* Breast Cancer Research and Treatment, 2003. **79**: p. S25-S34.
26. Wu, J., et al., *Response and prognosis of taxanes and anthracyclines neoadjuvant chemotherapy in patients with triple-negative breast cancer.* J Cancer Res Clin Oncol, 2011. **137**(10): p. 1505-10.
27. Froelich-Ammon, S.J. and N. Osheroff, *Topoisomerase poisons: harnessing the dark side of enzyme mechanism.* J Biol Chem, 1995. **270**(37): p. 21429-32.
28. Minotti, G., et al., *Anthracyclines: molecular advances and pharmacologic developments in antitumor activity and cardiotoxicity.* Pharmacol Rev, 2004. **56**(2): p. 185-229.
29. Zhou, B.B. and S.J. Elledge, *The DNA damage response: putting checkpoints in perspective.* Nature, 2000. **408**(6811): p. 433-9.
30. Chen, J., et al., *Constitutively nuclear FOXO3a localization predicts poor survival and promotes Akt phosphorylation in breast cancer.* PLoS One, 2010. **5**(8): p. e12293.
31. Hudis, C.A., *Drug therapy: Trastuzumab - Mechanism of action and use in clinical practice.* New England Journal of Medicine, 2007. **357**(1): p. 39-51.
32. Pohlmann, P.R., I.A. Mayer, and R. Mernaugh, *Resistance to Trastuzumab in Breast Cancer.* Clinical Cancer Research, 2009. **15**(24): p. 7479-7491.
33. Medina, P.J. and S. Goodin, *Lapatinib: a dual inhibitor of human epidermal growth factor receptor tyrosine kinases.* Clin Ther, 2008. **30**(8): p. 1426-47.
34. Burris, H.A., 3rd, et al., *Phase I safety, pharmacokinetics, and clinical activity study of lapatinib (GW572016), a reversible dual inhibitor of epidermal growth factor receptor tyrosine kinases, in heavily pretreated patients with metastatic carcinomas.* J Clin Oncol, 2005. **23**(23): p. 5305-13.
35. Liu, Y. and N.S. Gray, *Rational design of inhibitors that bind to inactive kinase conformations.* Nature Chemical Biology, 2006. **2**(7): p. 358-364.
36. Zhou, H. and S. Huang, *mTOR signaling in cancer cell motility and tumor metastasis.* Crit Rev Eukaryot Gene Expr, 2010. **20**(1): p. 1-16.
37. Blackwell, K.L., et al., *Randomized study of Lapatinib alone or in combination with trastuzumab in women with ErbB2-positive, trastuzumab-refractory metastatic breast cancer.* J Clin Oncol, 2010. **28**(7): p. 1124-30.
38. Gayle, S.S., et al., *MEK inhibition increases lapatinib sensitivity via modulation of FOXM1.* Curr Med Chem, 2013. **20**(19): p. 2486-99.
39. Wei, W.I. and J.S.T. Sham, *Nasopharyngeal carcinoma.* The Lancet, 2005. **365**(9476): p. 2041-2054.
40. Raab-Traub, N., *Epstein–Barr virus in the pathogenesis of NPC.* Seminars in Cancer Biology, 2002. **12**(6): p. 431-441.

41. Lee, V.H., et al., *Prognostication of serial post-intensity-modulated radiation therapy undetectable plasma EBV DNA for nasopharyngeal carcinoma.* Oncotarget, 2017. **8**(3): p. 5292-5308.
42. Peng, H., et al., *Survival analysis of patients with advanced-stage nasopharyngeal carcinoma according to the Epstein-Barr virus status.* Oncotarget, 2016. **7**(17): p. 24208-16.
43. Zhang, P., et al., *p53, MDM2, eIF4E and EGFR expression in nasopharyngeal carcinoma and their correlation with clinicopathological characteristics and prognosis: A retrospective study.* Oncology Letters, 2015. **9**(1): p. 113-118.
44. Zhang, L., et al., *Phase II clinical study of gemcitabine in the treatment of patients with advanced nasopharyngeal carcinoma after the failure of platinum-based chemotherapy.* Cancer Chemotherapy and Pharmacology, 2008. **61**(1): p. 33-38.
45. Rubio, L., et al., *Morphometric study of tumor angiogenesis as a new prognostic factor in nasopharyngeal carcinoma patients.* Pathology & Oncology Research, 2000. **6**(3): p. 210-216.
46. You, B., et al., *A Phase II Trial of Erlotinib as Maintenance Treatment After Gemcitabine Plus Platinum-based Chemotherapy in Patients With Recurrent and/or Metastatic Nasopharyngeal Carcinoma.* American Journal of Clinical Oncology, 2012. **35**(3): p. 255-260.
47. Chia, M.C., et al., *A Conditionally Replicating Adenovirus for Nasopharyngeal Carcinoma Gene Therapy.* Mol Ther, 2004. **9**(6): p. 804-817.
48. Liu, R.-y., et al., *Adenovirus-mediated delivery of interferon-γ gene inhibits the growth of nasopharyngeal carcinoma.* Journal of Translational Medicine, 2012. **10**: p. 256-256.
49. Ye, M., et al., *FM807, a curcumin analogue, shows potent antitumor effects in nasopharyngeal carcinoma cells by heat shock protein 90 inhibition.* Oncotarget, 2017. **8**(9): p. 15364-15376.
50. Chan, K.C., et al., *A novel Hsp90 inhibitor AT13387 induces senescence in EBV-positive nasopharyngeal carcinoma cells and suppresses tumor formation.* Molecular Cancer, 2013. **12**.
51. Liu, Y., et al., *Cancer drug resistance: redox resetting renders a way.* Oncotarget, 2016. **7**(27): p. 42740-42761.
52. Gottesman, M.M., T. Fojo, and S.E. Bates, *Multidrug resistance in cancer: role of ATP-dependent transporters.* Nat Rev Cancer, 2002. **2**(1): p. 48-58.
53. Triller, N., et al., *Multidrug resistance in small cell lung cancer: expression of P-glycoprotein, multidrug resistance protein 1 and lung resistance protein in chemo-naive patients and in relapsed disease.* Lung Cancer, 2006. **54**(2): p. 235-40.
54. Nooter, K., et al., *The prognostic significance of expression of the multidrug resistance-associated protein (MRP) in primary breast cancer.* Br J Cancer, 1997. **76**(4): p. 486-93.
55. Zalcberg, J., et al., *MRP1 not MDR1 gene expression is the predominant mechanism of acquired multidrug resistance in two prostate carcinoma cell lines.* Prostate Cancer and Prostatic Diseases, 2000. **3**(2): p. 66-75.
56. Doyle, L.A., et al., *A multidrug resistance transporter from human MCF-7 breast cancer cells.* Proc Natl Acad Sci U S A, 1998. **95**(26): p. 15665-70.
57. Robey, R.W., et al., *Inhibition of ABCG2-mediated transport by protein kinase inhibitors with a bisindolylmaleimide or indolocarbazole structure.* Mol Cancer Ther, 2007. **6**(6): p. 1877-85.

58. Shukla, S., Z.S. Chen, and S.V. Ambudkar, *Tyrosine kinase inhibitors as modulators of ABC transporter-mediated drug resistance.* Drug Resistance Updates, 2012. **15**(1-2): p. 70-80.
59. Bhatavdekar, J.M., et al., *Overexpression of CD44: a useful independent predictor of prognosis in patients with colorectal carcinomas.* Ann Surg Oncol, 1998. **5**(6): p. 495-501.
60. Shervington, A. and C. Lu, *Expression of multidrug resistance genes in normal and cancer stem cells.* Cancer Invest, 2008. **26**(5): p. 535-42.
61. Laurentiis, M.D., et al., *Taxane-Based Combinations As Adjuvant Chemotherapy of Early Breast Cancer: A Meta-Analysis of Randomized Trials.* Journal of Clinical Oncology, 2008. **26**(1): p. 44-53.
62. Jordan, N.J., et al., *Increased constitutive activity of PKB/Akt in tamoxifen resistant breast cancer MCF-7 cells.* Breast Cancer Research and Treatment, 2004. **87**(2): p. 167-180.
63. Martin, L.A., et al., *Enhanced estrogen receptor (ER) alpha, ERBB2, and MAPK signal transduction pathways operate during the adaptation of MCF-7 cells to long term estrogen deprivation.* J Biol Chem, 2003. **278**(33): p. 30458-68.
64. Gee, J.M., et al., *The antiepidermal growth factor receptor agent gefitinib (ZD1839/Iressa) improves antihormone response and prevents development of resistance in breast cancer in vitro.* Endocrinology, 2003. **144**(11): p. 5105-17.
65. Noguchi, S., *Predictive factors for response to docetaxel in human breast cancers.* Cancer Sci, 2006. **97**(9): p. 813-20.
66. Rouzier, R., et al., *Microtubule-associated protein tau: a marker of paclitaxel sensitivity in breast cancer.* Proc Natl Acad Sci U S A, 2005. **102**(23): p. 8315-20.
67. Zhou, W., et al., *NEK2 Induces Drug Resistance Mainly through Activation of Efflux Drug Pumps and Is Associated with Poor Prognosis in Myeloma and Other Cancers.* Cancer Cell, 2013. **23**(1): p. 48-62.
68. Thomas, H. and H.M. Coley, *Overcoming multidrug resistance in cancer: an update on the clinical strategy of inhibiting p-glycoprotein.* Cancer Control, 2003. **10**(2): p. 159-65.
69. Faneyte, I.F., et al., *Expression of the Breast Cancer Resistance Protein in Breast Cancer.* Clinical Cancer Research, 2002. **8**(4): p. 1068-1074.
70. Bugg, B.Y., et al., *Expression of a mutant DNA topoisomerase II in CCRF-CEM human leukemic cells selected for resistance to teniposide.* Proc Natl Acad Sci U S A, 1991. **88**(17): p. 7654-8.
71. Farmer, H., et al., *Targeting the DNA repair defect in BRCA mutant cells as a therapeutic strategy.* Nature, 2005. **434**(7035): p. 917-921.
72. Berns, K., et al., *A functional genetic approach identifies the PI3K pathway as a major determinant of trastuzumab resistance in breast cancer.* Cancer Cell, 2007. **12**(4): p. 395-402.
73. Nagata, Y., et al., *PTEN activation contributes to tumor inhibition by trastuzumab, and loss of PTEN predicts trastuzumab resistance in patients.* Cancer Cell, 2004. **6**(2): p. 117-27.
74. Scaltriti, M., et al., *Expression of p95HER2, a truncated form of the HER2 receptor, and response to anti-HER2 therapies in breast cancer.* J Natl Cancer Inst, 2007. **99**(8): p. 628-38.
75. Xia, W., et al., *A model of acquired autoresistance to a potent ErbB2 tyrosine kinase inhibitor and a therapeutic strategy to prevent its onset in breast cancer.* Proc Natl Acad Sci U S A, 2006. **103**(20): p. 7795-800.

76. Karadedou, C.T., et al., *FOXO3a represses VEGF expression through FOXM1-dependent and -independent mechanisms in breast cancer.* Oncogene, 2012. **31**(14): p. 1845-58.
77. Zeng, C.M., et al., *Aldo-Keto Reductase AKR1C1-AKR1C4: Functions, Regulation, and Intervention for Anti-cancer Therapy.* Front Pharmacol, 2017. **8**: p. 119.
78. Tian, H., et al., *High expression of AKR1C1 is associated with proliferation and migration of small-cell lung cancer cells.* Lung Cancer-Targets and Therapy, 2016. **7**: p. 53-61.
79. Wenners, A., et al., *Stromal markers AKR1C1 and AKR1C2 are prognostic factors in primary human breast cancer.* Int J Clin Oncol, 2016. **21**(3): p. 548-56.
80. Sinreih, M., et al., *Important roles of the AKR1C2 and SRD5A1 enzymes in progesterone metabolism in endometrial cancer model cell lines.* Chem Biol Interact, 2015. **234**: p. 297-308.
81. Wsol, V., et al., *Aldo-keto reductases (AKR) from the AKR1C subfamily catalyze the carbonyl reduction of the novel anticancer drug oracin in man.* Toxicology, 2007. **238**(2-3): p. 111-8.
82. Zhong, T., et al., *Aldo-keto reductase 1C3 (AKR1C3) is associated with the doxorubicin resistance in human breast cancer via PTEN Loss.* Biomedicine & Pharmacotherapy, 2015. **69**: p. 317-325.
83. Hofman, J., et al., *Anthracycline resistance mediated by reductive metabolism in cancer cells: the role of aldo-keto reductase 1C3.* Toxicol Appl Pharmacol, 2014. **278**(3): p. 238-48.
84. Matsunaga, T., et al., *Induction of aldo-keto reductases (AKR1C1 and AKR1C3) abolishes the efficacy of daunorubicin chemotherapy for leukemic U937 cells.* Anticancer Drugs, 2014. **25**(8): p. 868-77.
85. Kalluri, R. and E.G. Neilson, *Epithelial-mesenchymal transition and its implications for fibrosis.* J Clin Invest, 2003. **112**(12): p. 1776-84.
86. Lee, J.M., et al., *The epithelial-mesenchymal transition: new insights in signaling, development, and disease.* J Cell Biol, 2006. **172**(7): p. 973-81.
87. Thiery, J.P., *Epithelial-mesenchymal transitions in tumour progression.* Nat Rev Cancer, 2002. **2**(6): p. 442-54.
88. Kong, D., et al., *Cancer Stem Cells and Epithelial-to-Mesenchymal Transition (EMT)-Phenotypic Cells: Are They Cousins or Twins?* Cancers, 2011. **3**(1): p. 716-729.
89. Nilendu, P., et al., *Breast cancer stem cells as last soldiers eluding therapeutic burn: A hard nut to crack.* International Journal of Cancer, 2018. **142**(1): p. 7-17.
90. Massague, J., *TGF beta in cancer.* Cell, 2008. **134**(2): p. 215-230.
91. Polyak, K. and R.A. Weinberg, *Transitions between epithelial and mesenchymal states: acquisition of malignant and stem cell traits.* Nature Reviews Cancer, 2009. **9**(4): p. 265-273.
92. De Leeuw, W.J., et al., *Simultaneous loss of E-cadherin and catenins in invasive lobular breast cancer and lobular carcinoma in situ.* J Pathol, 1997. **183**(4): p. 404-11.
93. Lombaerts, M., et al., *E-cadherin transcriptional downregulation by promoter methylation but not mutation is related to epithelial-to-mesenchymal transition in breast cancer cell lines.* British Journal of Cancer, 2006. **94**(5): p. 661-671.
94. Tomono, T., K. Yano, and T. Ogihara, *Snail-Induced Epithelial-to-Mesenchymal Transition Enhances P-gp-Mediated Multidrug Resistance in HCC827 Cells.* J Pharm Sci, 2017. **106**(9): p. 2642-2649.

95. Page-McCaw, A., A.J. Ewald, and Z. Werb, *Matrix metalloproteinases and the regulation of tissue remodelling.* Nat Rev Mol Cell Biol, 2007. **8**(3): p. 221-33.
96. Nawrocki-Raby, B., et al., *E-Cadherin mediates MMP down-regulation in highly invasive bronchial tumor cells.* Am J Pathol, 2003. **163**(2): p. 653-61.
97. Brabletz, T., et al., *Variable beta-catenin expression in colorectal cancers indicates tumor progression driven by the tumor environment.* Proc Natl Acad Sci U S A, 2001. **98**(18): p. 10356-61.
98. Hanahan, D. and R.A. Weinberg, *Hallmarks of cancer: the next generation.* Cell, 2011. **144**(5): p. 646-74.
99. Grant, C.M. and N. Kyprianou, *Epithelial mesenchymal transition (EMT) in prostate growth and tumor progression.* Transl Androl Urol, 2013. **2**(3): p. 202-211.
100. Serrano-Gomez, S.J., M. Maziveyi, and S.K. Alahari, *Regulation of epithelial-mesenchymal transition through epigenetic and post-translational modifications.* Molecular Cancer, 2016. **15**.
101. Kotiyal, S. and S. Bhattacharya, *Epithelial Mesenchymal Transition and Vascular Mimicry in Breast Cancer Stem Cells.* Crit Rev Eukaryot Gene Expr, 2015. **25**(3): p. 269-80.
102. Taube, J.H., et al., *Core epithelial-to-mesenchymal transition interactome gene-expression signature is associated with claudin-low and metaplastic breast cancer subtypes.* Proceedings of the National Academy of Sciences of the United States of America, 2010. **107**(35): p. 15449-15454.
103. Dongre, A. and R.A. Weinberg, *New insights into the mechanisms of epithelial-mesenchymal transition and implications for cancer.* Nature Reviews Molecular Cell Biology, 2019. **20**(2): p. 69-84.
104. Berx, G., et al., *E-cadherin is inactivated in a majority of invasive human lobular breast cancers by truncation mutations throughout its extracellular domain.* Oncogene, 1996. **13**(9): p. 1919-1925.
105. Grady, W.M., et al., *Methylation of the CDH1 promoter as the second genetic hit in hereditary diffuse gastric cancer.* Nature Genetics, 2000. **26**(1): p. 16-17.
106. Kaurah, P., et al., *Founder and recurrent CDH1 mutations in families with hereditary diffuse gastric cancer.* JAMA, 2007. **297**(21): p. 2360-72.
107. Berx, G. and F. Van Roy, *The E-cadherin/catenin complex: an important gatekeeper in breast cancer tumorigenesis and malignant progression.* Breast Cancer Res, 2001. **3**(5): p. 289-93.
108. Berx, G., et al., *Mutations of the human E-cadherin (CDH1) gene.* Hum Mutat, 1998. **12**(4): p. 226-37.
109. Schrader, K.A., et al., *Hereditary diffuse gastric cancer: association with lobular breast cancer.* Fam Cancer, 2008. **7**(1): p. 73-82.
110. Onder, T.T., et al., *Loss of E-cadherin promotes metastasis via multiple downstream transcriptional pathways.* Cancer Res, 2008. **68**(10): p. 3645-54.
111. Das, V., et al., *The basics of epithelial-mesenchymal transition (EMT): A study from a structure, dynamics, and functional perspective.* J Cell Physiol, 2019.
112. Wu, Y. and B.P. Zhou, *TNF-α/NF-κB/Snail pathway in cancer cell migration and invasion.* British Journal Of Cancer, 2010. **102**: p. 639.
113. Alves, C.C., et al., *Role of the epithelial-mesenchymal transition regulator Slug in primary human cancers.* Front Biosci (Landmark Ed), 2009. **14**: p. 3035-50.
114. Hartwell, K.A., et al., *The Spemann organizer gene, Goosecoid, promotes tumor metastasis.* Proc Natl Acad Sci U S A, 2006. **103**(50): p. 18969-74.
115. Oh, J.H., et al., *RAE1 mediated ZEB1 expression promotes epithelial–mesenchymal transition in breast cancer.* Scientific Reports, 2019. **9**(1): p. 2977.

116. Burks, H.E., et al., *Abstract 1034: ZEB2 promotes cell motility and metastasis in ER+ breast cancer cells.* Cancer Research, 2014. **74**(19 Supplement): p. 1034-1034.
117. Yang, M.-H., et al., *Direct regulation of TWIST by HIF-1α promotes metastasis.* Nature Cell Biology, 2008. **10**: p. 295.
118. Du, C., et al., *Protein Kinase D1 Suppresses Epithelial-to-Mesenchymal Transition through Phosphorylation of Snail.* Cancer Research, 2010. **70**(20): p. 7810-7819.
119. Mani, S.A., et al., *Mesenchyme Forkhead 1 (FOXC2) plays a key role in metastasis and is associated with aggressive basal-like breast cancers.* Proceedings of the National Academy of Sciences, 2007. **104**(24): p. 10069-10074.
120. Gravgaard, K.H., et al., *The miRNA-200 family and miRNA-9 exhibit differential expression in primary versus corresponding metastatic tissue in breast cancer.* Breast Cancer Research and Treatment, 2012. **134**(1): p. 207-217.
121. Vogt, M., et al., *Frequent concomitant inactivation of miR-34a and miR-34b/c by CpG methylation in colorectal, pancreatic, mammary, ovarian, urothelial, and renal cell carcinomas and soft tissue sarcomas.* Virchows Archiv, 2011. **458**(3): p. 313-322.
122. Turner, N. and R. Grose, *Fibroblast growth factor signalling: from development to cancer.* Nat Rev Cancer, 2010. **10**(2): p. 116-29.
123. Mehner, C., et al., *Tumor cell expression of MMP3 as a prognostic factor for poor survival in pancreatic, pulmonary, and mammary carcinoma.* Genes Cancer, 2015. **6**(11-12): p. 480-9.
124. Fenizia, C., et al., *SMYD3 promotes the epithelial–mesenchymal transition in breast cancer.* Nucleic Acids Research, 2018. **47**(3): p. 1278-1293.
125. Goto, M., et al., *FAD104, a regulator of adipogenesis, is a novel suppressor of TGF-β–mediated EMT in cervical cancer cells.* Scientific Reports, 2017. **7**(1): p. 16365.
126. Kornberg, R.D. and Y. Lorch, *Twenty-five years of the nucleosome, fundamental particle of the eukaryote chromosome.* Cell, 1999. **98**(3): p. 285-94.
127. Goll, M.G. and T.H. Bestor, *Histone modification and replacement in chromatin activation.* Genes Dev, 2002. **16**(14): p. 1739-42.
128. Ediriweera, M.K., K.H. Tennekoon, and S.R. Samarakoon, *Emerging role of histone deacetylase inhibitors as anti-breast-cancer agents.* Drug Discovery Today, 2019. **24**(3): p. 685-702.
129. Brownell, J.E., et al., *Tetrahymena histone acetyltransferase A: a homolog to yeast Gcn5p linking histone acetylation to gene activation.* Cell, 1996. **84**(6): p. 843-51.
130. Lee, K.K. and J.L. Workman, *Histone acetyltransferase complexes: one size doesn't fit all.* Nature Reviews Molecular Cell Biology, 2007. **8**: p. 284.
131. Li, Y. and E. Seto, *HDACs and HDAC Inhibitors in Cancer Development and Therapy.* Cold Spring Harb Perspect Med, 2016. **6**(10).
132. Bertrand, P., *Inside HDAC with HDAC inhibitors.* Eur J Med Chem, 2010. **45**(6): p. 2095-116.
133. Fraga, M.F., et al., *Loss of acetylation at Lys16 and trimethylation at Lys20 of histone H4 is a common hallmark of human cancer.* Nat Genet, 2005. **37**(4): p. 391-400.
134. Suzuki, J., et al., *Protein acetylation and histone deacetylase expression associated with malignant breast cancer progression.* Clin Cancer Res, 2009. **15**(9): p. 3163-71.
135. Krusche, C.A., et al., *Histone deacetylase-1 and -3 protein expression in human breast cancer: a tissue microarray analysis.* Breast Cancer Res Treat, 2005. **90**(1): p. 15-23.
136. Rey, M., et al., *HDAC6 is required for invadopodia activity and invasion by breast tumor cells.* European Journal of Cell Biology, 2011. **90**(2-3): p. 128-135.

137. Ververis, K. and T.C. Karagiannis, *An atlas of histone deacetylase expression in breast cancer: fluorescence methodology for comparative semi-quantitative analysis.* Am J Transl Res, 2012. **4**(1): p. 24-43.
138. Weichert, W., *HDAC expression and clinical prognosis in human malignancies.* Cancer Lett, 2009. **280**(2): p. 168-76.
139. Wu, M.-Y. and R.-C. Wu, *A Sensitive and Flexible Assay for Determining Histone Deacetylase 1 (HDAC1) Activity*, in *Histone Deacetylases: Methods and Protocols*, S. Sarkar, Editor. 2016, Springer New York: New York, NY. p. 3-13.
140. Bedford, D.C., et al., *Target gene context influences the transcriptional requirement for the KAT3 family of CBP and p300 histone acetyltransferases.* Epigenetics, 2010. **5**(1): p. 9-15.
141. Kasper, L.H., et al., *CBP/p300 double null cells reveal effect of coactivator level and diversity on CREB transactivation.* EMBO J, 2010. **29**(21): p. 3660-72.
142. Creyghton, M.P., et al., *Histone H3K27ac separates active from poised enhancers and predicts developmental state.* Proc Natl Acad Sci U S A, 2010. **107**(50): p. 21931-6.
143. Jin, Q., et al., *Distinct roles of GCN5/PCAF-mediated H3K9ac and CBP/p300-mediated H3K18/27ac in nuclear receptor transactivation.* EMBO J, 2011. **30**(2): p. 249-62.
144. Ito, A., et al., *p300/CBP-mediated p53 acetylation is commonly induced by p53-activating agents and inhibited by MDM2.* Embo Journal, 2001. **20**(6): p. 1331-1340.
145. Bereshchenko, O.R., W. Gu, and R. Dalla-Favera, *Acetylation inactivates the transcriptional repressor BCL6.* Nat Genet, 2002. **32**(4): p. 606-13.
146. Chan, H.M. and N.B. La Thangue, *p300/CBP proteins: HATs for transcriptional bridges and scaffolds.* J Cell Sci, 2001. **114**(Pt 13): p. 2363-73.
147. Park, S., et al., *The CH2 domain of CBP/p300 is a novel zinc finger.* Febs Letters, 2013. **587**(16): p. 2506-2511.
148. Delvecchio, M., et al., *Structure of the p300 catalytic core and implications for chromatin targeting and HAT regulation.* Nat Struct Mol Biol, 2013. **20**(9): p. 1040-6.
149. Kraus, W.L., E.T. Manning, and J.T. Kadonaga, *Biochemical analysis of distinct activation functions in p300 that enhance transcription initiation with chromatin templates.* Molecular and Cellular Biology, 1999. **19**(12): p. 8123-8135.
150. Rack, J.G.M., et al., *The PHD finger of p300 influences its ability to acetylate histone and non-histone targets.* J Mol Biol, 2014. **426**(24): p. 3960-3972.
151. Thompson, P.R., et al., *Regulation of the p300 HAT domain via a novel activation loop.* Nat Struct Mol Biol, 2004. **11**(4): p. 308-15.
152. Henry, R.A., Y.M. Kuo, and A.J. Andrews, *Differences in Specificity and Selectivity Between CBP and p300 Acetylation of Histone H3 and H3/H4.* Biochemistry, 2013. **52**(34): p. 5746-5759.
153. McManus, K.J. and M.J. Hendzel, *Quantitative analysis of CBP- and P300-induced histone acetylations in vivo using native chromatin.* Molecular and Cellular Biology, 2003. **23**(21): p. 7611-7627.
154. Park, S., et al., *Role of the CBP catalytic core in intramolecular SUMOylation and control of histone H3 acetylation.* Proc Natl Acad Sci U S A, 2017. **114**(27): p. E5335-E5342.
155. Dancy, B.M. and P.A. Cole, *Protein lysine acetylation by p300/CBP.* Chem Rev, 2015. **115**(6): p. 2419-52.
156. Krubasik, D., et al., *Absence of p300 induces cellular phenotypic changes characteristic of epithelial to mesenchyme transition.* Br J Cancer, 2006. **94**(9): p. 1326-32.

157. Tang, Z., et al., *CREB-binding protein regulates lung cancer growth by targeting MAPK and CPSF4 signaling pathway.* Mol Oncol, 2016. **10**(2): p. 317-29.
158. Attar, N. and S.K. Kurdistani, *Exploitation of EP300 and CREBBP Lysine Acetyltransferases by Cancer.* Cold Spring Harb Perspect Med, 2017. **7**(3).
159. Miller, R.W. and J.H. Rubinstein, *Tumors in Rubinstein-Taybi syndrome.* Am J Med Genet, 1995. **56**(1): p. 112-5.
160. Gayther, S.A., et al., *Mutations truncating the EP300 acetylase in human cancers.* Nat Genet, 2000. **24**(3): p. 300-3.
161. Nishihara, A., et al., *Role of p300, a transcriptional coactivator, in signalling of TGF-beta.* Genes Cells, 1998. **3**(9): p. 613-23.
162. Pao, G.M., et al., *CBP/p300 interact with and function as transcriptional coactivators of BRCA1.* Proceedings of the National Academy of Sciences of the United States of America, 2000. **97**(3): p. 1020-1025.
163. Grossman, S.R., et al., *p300/MDM2 complexes participate in MDM2-mediated p53 degradation.* Mol Cell, 1998. **2**(4): p. 405-15.
164. Monteiro, A.N., A. August, and H. Hanafusa, *Evidence for a transcriptional activation function of BRCA1 C-terminal region.* Proc Natl Acad Sci U S A, 1996. **93**(24): p. 13595-9.
165. Mullan, P.B., J.E. Quinn, and D.P. Harkin, *The role of BRCA1 in transcriptional regulation and cell cycle control.* Oncogene, 2006. **25**(43): p. 5854-63.
166. Wu, J., L.Y. Lu, and X. Yu, *The role of BRCA1 in DNA damage response.* Protein Cell, 2010. **1**(2): p. 117-23.
167. Derynck, R., R.J. Akhurst, and A. Balmain, *TGF-beta signaling in tumor suppression and cancer progression.* Nat Genet, 2001. **29**(2): p. 117-29.
168. Feng, X.H., et al., *The tumor suppressor Smad4/DPC4 and transcriptional adaptor CBP/p300 are coactivators for smad3 in TGF-beta-induced transcriptional activation.* Genes Dev, 1998. **12**(14): p. 2153-63.
169. Sen, P., et al., *Histone Acetyltransferase p300 Induces De Novo Super-Enhancers to Drive Cellular Senescence.* Molecular Cell, 2019. **73**(4): p. 684-+.
170. Asaduzzaman, M., et al., *Tumour suppressor EP300, a modulator of paclitaxel resistance and stemness, is downregulated in metaplastic breast cancer.* Breast Cancer Research and Treatment, 2017. **163**(3): p. 461-474.
171. Kalkhoven, E., *CBP and p300: HATs for different occasions.* Biochem Pharmacol, 2004. **68**(6): p. 1145-55.
172. Pasqualucci, L., et al., *Inactivating mutations of acetyltransferase genes in B-cell lymphoma.* Nature, 2011. **471**(7337): p. 189-95.
173. Ringel, A.E. and C. Wolberger, *A New RING Tossed into an Old HAT.* Structure, 2013. **21**(9): p. 1479-1481.
174. Forbes, S.A., et al., *COSMIC: exploring the world's knowledge of somatic mutations in human cancer.* Nucleic Acids Research, 2015. **43**(D1): p. D805-D811.
175. Li, Q., et al., *Acetylation of histone H3 lysine 56 regulates replication-coupled nucleosome assembly.* Cell, 2008. **134**(2): p. 244-55.
176. Yuan, Z.M., et al., *Role for p300 in stabilization of p53 in the response to DNA damage.* J Biol Chem, 1999. **274**(4): p. 1883-6.
177. Vempati, R.K., et al., *p300-mediated acetylation of histone H3 lysine 56 functions in DNA damage response in mammals.* J Biol Chem, 2010. **285**(37): p. 28553-64.
178. Das, C., et al., *CBP/p300-mediated acetylation of histone H3 on lysine 56.* Nature, 2009. **459**(7243): p. 113-7.
179. Lam, E.W., et al., *Forkhead box proteins: tuning forks for transcriptional harmony.* Nat Rev Cancer, 2013. **13**(7): p. 482-95.

180. Lam, E.W. and A.R. Gomes, *Forkhead box transcription factors in cancer initiation, progression and chemotherapeutic drug response.* Front Oncol, 2014. **4**: p. 305.
181. van der Horst, A., et al., *FOXO4 is acetylated upon peroxide stress and deacetylated by the longevity protein hSir2(SIRT1).* J Biol Chem, 2004. **279**(28): p. 28873-9.
182. Kaestner, K.H., W. Knochel, and D.E. Martinez, *Unified nomenclature for the winged helix/forkhead transcription factors.* Genes Dev, 2000. **14**(2): p. 142-6.
183. Fu, Z. and D.J. Tindall, *FOXOs, cancer and regulation of apoptosis.* Oncogene, 2008. **27**(16): p. 2312-9.
184. Daitoku, H., J. Sakamaki, and A. Fukamizu, *Regulation of FoxO transcription factors by acetylation and protein-protein interactions.* Biochim Biophys Acta, 2011. **1813**(11): p. 1954-60.
185. Lam, E.W., R.E. Francis, and M. Petkovic, *FOXO transcription factors: key regulators of cell fate.* Biochem Soc Trans, 2006. **34**(Pt 5): p. 722-6.
186. Weigel, D. and H. Jackle, *The fork head domain: a novel DNA binding motif of eukaryotic transcription factors?* Cell, 1990. **63**(3): p. 455-6.
187. Tsai, K.L., et al., *Crystal structure of the human FOXO3a-DBD/DNA complex suggests the effects of post-translational modification.* Nucleic Acids Res, 2007. **35**(20): p. 6984-94.
188. Furuyama, T., et al., *Identification of the differential distribution patterns of mRNAs and consensus binding sequences for mouse DAF-16 homologues.* Biochem J, 2000. **349**(Pt 2): p. 629-34.
189. Brent, M.M., R. Anand, and R. Marmorstein, *Structural basis for DNA recognition by FoxO1 and its regulation by posttranslational modification.* Structure, 2008. **16**(9): p. 1407-16.
190. Wang, F., et al., *Biochemical and structural characterization of an intramolecular interaction in FOXO3a and its binding with p53.* J Mol Biol, 2008. **384**(3): p. 590-603.
191. Obsil, T. and V. Obsilova, *Structure/function relationships underlying regulation of FOXO transcription factors.* Oncogene, 2008. **27**(16): p. 2263-75.
192. Bella, L., et al., *FOXM1: A key oncofoetal transcription factor in health and disease.* Semin Cancer Biol, 2014. **29**: p. 32-9.
193. van der Vos, K.E. and P.J. Coffer, *The extending network of FOXO transcriptional target genes.* Antioxid Redox Signal, 2011. **14**(4): p. 579-92.
194. Khongkow, M., et al., *SIRT6 modulates paclitaxel and epirubicin resistance and survival in breast cancer.* Carcinogenesis, 2013. **34**(7): p. 1476-86.
195. Hornsveld, M., et al., *Re-evaluating the role of FOXOs in cancer.* Semin Cancer Biol, 2018. **50**: p. 90-100.
196. Yao, S., L.Y. Fan, and E.W. Lam, *The FOXO3-FOXM1 axis: A key cancer drug target and a modulator of cancer drug resistance.* Semin Cancer Biol, 2018. **50**: p. 77-89.
197. Myatt, S.S., J.J. Brosens, and E.W. Lam, *Sense and sensitivity: FOXO and ROS in cancer development and treatment.* Antioxid Redox Signal, 2011. **14**(4): p. 675-87.
198. Ho, K.K., S.S. Myatt, and E.W. Lam, *Many forks in the path: cycling with FoxO.* Oncogene, 2008. **27**(16): p. 2300-11.
199. Cox, J., et al., *Nuclear to Cytoplasmic Translocation of FOXO3 Determines the Sensitivity of Human Hepatocellular Carcinoma to Doxorubicin.* Hepatology, 2014. **60**: p. 880a-880a.
200. Collado, M., et al., *Inhibition of the phosphoinositide 3-kinase pathway induces a senescence-like arrest mediated by p27Kip1.* J Biol Chem, 2000. **275**(29): p. 21960-8.

201. Wang, K. and P.F. Li, *Foxo3a regulates apoptosis by negatively targeting miR-21.* J Biol Chem, 2010. **285**(22): p. 16958-66.
202. Sunters, A., et al., *FoxO3a transcriptional regulation of Bim controls apoptosis in paclitaxel-treated breast cancer cell lines.* J Biol Chem, 2003. **278**(50): p. 49795-805.
203. Hui, R.C., et al., *Doxorubicin activates FOXO3a to induce the expression of multidrug resistance gene ABCB1 (MDR1) in K562 leukemic cells.* Mol Cancer Ther, 2008. **7**(3): p. 670-8.
204. Brunet, A., et al., *Stress-dependent regulation of FOXO transcription factors by the SIRT1 deacetylase.* Science, 2004. **303**(5666): p. 2011-5.
205. Sunayama, J., et al., *FoxO3a Functions as a Key Integrator of Cellular Signals That Control Glioblastoma Stem-like Cell Differentiation and Tumorigenicity.* Stem Cells, 2011. **29**(9): p. 1327-1337.
206. Santamaria, C.M., et al., *High FOXO3a expression is associated with a poorer prognosis in AML with normal cytogenetics.* Leukemia Research, 2009. **33**(12): p. 1706-1709.
207. Naka, K., et al., *TGF-beta-FOXO signalling maintains leukaemia-initiating cells in chronic myeloid leukaemia.* Nature, 2010. **463**(7281): p. 676-80.
208. Zhou, Y., et al., *Salinomycin decreases doxorubicin resistance in hepatocellular carcinoma cells by inhibiting the beta-catenin/TCF complex association via FOXO3a activation.* Oncotarget, 2015. **6**(12): p. 10350-10365.
209. Kops, G.J.P.L., et al., *Forkhead transcription factor FOXO3a protects quiescent cells from oxidative stress.* Nature, 2002. **419**(6904): p. 316-321.
210. Mammucari, C., et al., *FoxO3 controls autophagy in skeletal muscle in vivo.* Cell Metab, 2007. **6**(6): p. 458-71.
211. Zhao, J., et al., *FoxO3 coordinately activates protein degradation by the Autophagic/Lysosomal and proteasomal pathways in atrophying muscle cells.* Cell Metabolism, 2007. **6**(6): p. 472-483.
212. Medema, R.H., et al., *AFX-like Forkhead transcription factors mediate cell-cycle regulation by Ras and PKB through p27kip1.* Nature, 2000. **404**(6779): p. 782-787.
213. de Keizer, P.L., et al., *Activation of forkhead box O transcription factors by oncogenic BRAF promotes p21cip1-dependent senescence.* Cancer Res, 2010. **70**(21): p. 8526-36.
214. Courtois-Cox, S., et al., *A negative feedback signaling network underlies oncogene-induced senescence.* Cancer Cell, 2006. **10**(6): p. 459-72.
215. Cayrol, C., M. Knibiehler, and B. Ducommun, *p21 binding to PCNA causes G1 and G2 cell cycle arrest in p53-deficient cells.* Oncogene, 1998. **16**(3): p. 311-20.
216. Gomez-Puerto, M.C., et al., *Activation of autophagy by FOXO3 regulates redox homeostasis during osteogenic differentiation.* Autophagy, 2016. **12**(10): p. 1804-1816.
217. Qiu, G.L., et al., *SIRT1 is a regulator of autophagy: Implications in gastric cancer progression and treatment.* Febs Letters, 2015. **589**(16): p. 2034-2042.
218. Hariharan, N., et al., *Deacetylation of FoxO by Sirt1 Plays an Essential Role in Mediating Starvation-Induced Autophagy in Cardiac Myocytes.* Circ Res, 2010. **107**(12): p. 1470-82.
219. Giannakou, M.E. and L. Partridge, *The interaction between FOXO and SIRT1: tipping the balance towards survival.* Trends in Cell Biology, 2004. **14**(8): p. 408-412.
220. Fullgrabe, J., D.J. Klionsky, and B. Joseph, *Histone post-translational modifications regulate autophagy flux and outcome.* Autophagy, 2013. **9**(10): p. 1621-3.
221. Yeung, F., et al., *Modulation of NF-kappaB-dependent transcription and cell survival by the SIRT1 deacetylase.* EMBO J, 2004. **23**(12): p. 2369-80.

222. Lee, I.H., et al., *A role for the NAD-dependent deacetylase Sirt1 in the regulation of autophagy.* Proc Natl Acad Sci U S A, 2008. **105**(9): p. 3374-9.
223. Zhao, Y., et al., *Cytosolic FoxO1 is essential for the induction of autophagy and tumour suppressor activity.* Nature Cell Biology, 2010. **12**(7): p. 665-U88.
224. Zhao, J., et al., *FoxO3 coordinately activates protein degradation by the autophagic/lysosomal and proteasomal pathways in atrophying muscle cells.* Cell Metab, 2007. **6**(6): p. 472-83.
225. Zhou, J., et al., *FOXO3 induces FOXO1-dependent autophagy by activating the AKT1 signaling pathway.* Autophagy, 2012. **8**(12): p. 1712-23.
226. Calnan, D.R. and A. Brunet, *The FoxO code.* Oncogene, 2008. **27**(16): p. 2276-88.
227. de Moraes, G.N., et al., *Insights into a Critical Role of the FOXO3a-FOXM1 Axis in DNA Damage Response and Genotoxic Drug Resistance.* Current Drug Targets, 2016. **17**(2): p. 164-177.
228. van der Heide, L.P. and M.P. Smidt, *Regulation of FoxO activity by CBP/p300-mediated acetylation.* Trends Biochem Sci, 2005. **30**(2): p. 81-6.
229. Paradis, S. and G. Ruvkun, *Caenorhabditis elegans Akt/PKB transduces insulin receptor-like signals from AGE-1 PI3 kinase to the DAF-16 transcription factor.* Genes Dev, 1998. **12**(16): p. 2488-98.
230. Myatt, S.S. and E.W. Lam, *The emerging roles of forkhead box (Fox) proteins in cancer.* Nat Rev Cancer, 2007. **7**(11): p. 847-59.
231. Brunet, A., et al., *Protein kinase SGK mediates survival signals by phosphorylating the forkhead transcription factor FKHRL1 (FOXO3a).* Mol Cell Biol, 2001. **21**(3): p. 952-65.
232. Corrado, P., et al., *Acetylation of FOXO3a transcription factor in response to imatinib of chronic myeloid leukemia.* Leukemia, 2009. **23**(2): p. 405-6.
233. Greer, E.L. and A. Brunet, *FOXO transcription factors at the interface between longevity and tumor suppression.* Oncogene, 2005. **24**(50): p. 7410-7425.
234. Biggs, W.H., 3rd, et al., *Protein kinase B/Akt-mediated phosphorylation promotes nuclear exclusion of the winged helix transcription factor FKHR1.* Proc Natl Acad Sci U S A, 1999. **96**(13): p. 7421-6.
235. Hu, M.C., et al., *IkappaB kinase promotes tumorigenesis through inhibition of forkhead FOXO3a.* Cell, 2004. **117**(2): p. 225-37.
236. Serra, V., et al., *PI3K inhibition results in enhanced HER signaling and acquired ERK dependency in HER2-overexpressing breast cancer.* Oncogene, 2011. **30**(22): p. 2547-57.
237. Hui, R.C., et al., *The forkhead transcription factor FOXO3a increases phosphoinositide-3 kinase/Akt activity in drug-resistant leukemic cells through induction of PIK3CA expression.* Mol Cell Biol, 2008. **28**(19): p. 5886-98.
238. Ho, K.K., et al., *Phosphorylation of FOXO3a on Ser-7 by p38 promotes its nuclear localization in response to doxorubicin.* J Biol Chem, 2012. **287**(2): p. 1545-55.
239. Deavall, D.G., et al., *Drug-induced oxidative stress and toxicity.* J Toxicol, 2012. **2012**: p. 645460.
240. Wang, X., W.R. Chen, and D. Xing, *A pathway from JNK through decreased ERK and Akt activities for FOXO3a nuclear translocation in response to UV irradiation.* J Cell Physiol, 2012. **227**(3): p. 1168-78.
241. Yang, J.Y., et al., *ERK promotes tumorigenesis by inhibiting FOXO3a via MDM2-mediated degradation.* Nat Cell Biol, 2008. **10**(2): p. 138-48.
242. Greer, E.L., et al., *The energy sensor AMP-activated protein kinase directly regulates the mammalian FOXO3 transcription factor.* J Biol Chem, 2007. **282**(41): p. 30107-19.

243. Klotz, L.O., et al., *Redox regulation of FoxO transcription factors.* Redox Biol, 2015. **6**: p. 51-72.
244. Cruickshanks, N., et al., *Lapatinib and obatoclax kill breast cancer cells through reactive oxygen species-dependent endoplasmic reticulum stress.* Mol Pharmacol, 2012. **82**(6): p. 1217-29.
245. Moy, B. and P.E. Goss, *Lapatinib: current status and future directions in breast cancer.* Oncologist, 2006. **11**(10): p. 1047-57.
246. Brown, A.K. and A.E. Webb, *Regulation of FOXO Factors in Mammalian Cells.* Curr Top Dev Biol, 2018. **127**: p. 165-192.
247. Birkenkamp, K.U. and P.J. Coffer, *Regulation of cell survival and proliferation by the FOXO (Forkhead box, class O) subfamily of Forkhead transcription factors.* Biochem Soc Trans, 2003. **31**(Pt 1): p. 292-7.
248. Fukuoka, M., et al., *Negative regulation of forkhead transcription factor AFX (Foxo4) by CBP-induced acetylation.* Int J Mol Med, 2003. **12**(4): p. 503-8.
249. Motta, M.C., et al., *Mammalian SIRT1 represses forkhead transcription factors.* Cell, 2004. **116**(4): p. 551-63.
250. Daitoku, H., et al., *Silent information regulator 2 potentiates Foxo1-mediated transcription through its deacetylase activity.* Proc Natl Acad Sci U S A, 2004. **101**(27): p. 10042-7.
251. Saunders, L.R. and E. Verdin, *Sirtuins: critical regulators at the crossroads between cancer and aging.* Oncogene, 2007. **26**(37): p. 5489-504.
252. Shiota, M., et al., *Foxo3a expression and acetylation regulate cancer cell growth and sensitivity to cisplatin.* Cancer Sci, 2010. **101**(5): p. 1177-85.
253. Mahmud, D.L., et al., *Phosphorylation of forkhead transcription factors by erythropoietin and stem cell factor prevents acetylation and their interaction with coactivator p300 in erythroid progenitor cells.* Oncogene, 2002. **21**(10): p. 1556-62.
254. Horio, Y., et al., *Cellular and molecular effects of sirtuins in health and disease.* Clin Sci (Lond), 2011. **121**(5): p. 191-203.
255. Jing, E., S. Gesta, and C.R. Kahn, *SIRT2 regulates adipocyte differentiation through FoxO1 acetylation/deacetylation.* Cell Metab, 2007. **6**(2): p. 105-14.
256. Michishita, E., et al., *Evolutionarily conserved and nonconserved cellular localizations and functions of human SIRT proteins.* Mol Biol Cell, 2005. **16**(10): p. 4623-35.
257. Schwer, B., et al., *The human silent information regulator (Sir)2 homologue hSIRT3 is a mitochondrial nicotinamide adenine dinucleotide-dependent deacetylase.* J Cell Biol, 2002. **158**(4): p. 647-57.
258. Olmos, Y., J.J. Brosens, and E.W.F. Lam, *Interplay between SIRT proteins and tumour suppressor transcription factors in chemotherapeutic resistance of cancer.* Drug Resistance Updates, 2011. **14**(1): p. 35-44.
259. Chu, F., et al., *Control of multidrug resistance gene mdr1 and cancer resistance to chemotherapy by the longevity gene sirt1.* Cancer Res, 2005. **65**(22): p. 10183-7.
260. Kojima, K., et al., *A role for SIRT1 in cell growth and chemoresistance in prostate cancer PC3 and DU145 cells.* Biochem Biophys Res Commun, 2008. **373**(3): p. 423-8.
261. Kobayashi, Y., et al., *SIRT1 is critical regulator of FOXO-mediated transcription in response to oxidative stress.* International Journal of Molecular Medicine, 2005. **16**(2): p. 237-243.
262. Olmos, Y., et al., *SirT1 regulation of antioxidant genes is dependent on the formation of a FoxO3a/PGC-1alpha complex.* Antioxid Redox Signal, 2013. **19**(13): p. 1507-21.

263. North, B.J. and E. Verdin, *Mitotic regulation of SIRT2 by cyclin-dependent kinase 1-dependent phosphorylation.* J Biol Chem, 2007. **282**(27): p. 19546-55.
264. Peck, B., et al., *SIRT inhibitors induce cell death and p53 acetylation through targeting both SIRT1 and SIRT2.* Mol Cancer Ther, 2010. **9**(4): p. 844-55.
265. Vaquero, A., et al., *SirT2 is a histone deacetylase with preference for histone H4 Lys 16 during mitosis.* Genes Dev, 2006. **20**(10): p. 1256-61.
266. Jing, H. and H. Lin, *Sirtuins in epigenetic regulation.* Chem Rev, 2015. **115**(6): p. 2350-75.
267. Imai, S., et al., *Transcriptional silencing and longevity protein Sir2 is an NAD-dependent histone deacetylase.* Nature, 2000. **403**(6771): p. 795-800.
268. Wang, F., et al., *Deacetylation of FOXO3 by SIRT1 or SIRT2 leads to Skp2-mediated FOXO3 ubiquitination and degradation.* Oncogene, 2012. **31**(12): p. 1546-57.
269. Jing, E.X., S. Gesta, and C.R. Kahn, *SIRT2 regulates adipocyte differentiation through FoxO1 acetylation/deacetylation.* Cell Metabolism, 2007. **6**(2): p. 105-114.
270. Kim, H.S., et al., *SIRT2 maintains genome integrity and suppresses tumorigenesis through regulating APC/C activity.* Cancer Cell, 2011. **20**(4): p. 487-99.
271. Serrano, L., et al., *The tumor suppressor SirT2 regulates cell cycle progression and genome stability by modulating the mitotic deposition of H4K20 methylation.* Genes Dev, 2013. **27**(6): p. 639-53.
272. Oberdoerffer, P., et al., *SIRT1 redistribution on chromatin promotes genomic stability but alters gene expression during aging.* Cell, 2008. **135**(5): p. 907-18.
273. Wang, R.H., et al., *Impaired DNA damage response, genome instability, and tumorigenesis in SIRT1 mutant mice.* Cancer Cell, 2008. **14**(4): p. 312-23.
274. Chalkiadaki, A. and L. Guarente, *The multifaceted functions of sirtuins in cancer.* Nat Rev Cancer, 2015. **15**(10): p. 608-24.
275. Voelter-Mahlknecht, S. and U. Mahlknecht, *The sirtuins in the pathogenesis of cancer.* Clin Epigenetics, 2010. **1**(3-4): p. 71-83.
276. Sebastian, C. and R. Mostoslavsky, *The role of mammalian sirtuins in cancer metabolism.* Semin Cell Dev Biol, 2015. **43**: p. 33-42.
277. Soung, Y.H., K. Pruitt, and J. Chung, *Epigenetic silencing of ARRDC3 expression in basal-like breast cancer cells.* Scientific Reports, 2014. **4**: p. 3846.
278. Zhao, D., et al., *Lysine-5 Acetylation Negatively Regulates Lactate Dehydrogenase A and Is Decreased in Pancreatic Cancer.* Cancer Cell, 2013. **23**(4): p. 464-476.
279. Zhao, D., et al., *NOTCH-induced aldehyde dehydrogenase 1A1 deacetylation promotes breast cancer stem cells.* The Journal of Clinical Investigation. **124**(12): p. 5453-5465.
280. Li, Z., et al., *SIRT2 inhibits non-small cell lung cancer cell growth through impairing Skp2-mediated p27 degradation.* Oncotarget, 2016.
281. Jing, H., et al., *A SIRT2-Selective Inhibitor Promotes c-Myc Oncoprotein Degradation and Exhibits Broad Anticancer Activity.* Cancer Cell, 2016. **29**(3): p. 297-310.
282. Li, Y.Z., et al., *SIRT2 down-regulation in HeLa can induce p53 accumulation via p38 MAPK activation-dependent p300 decrease, eventually leading to apoptosis.* Genes to Cells, 2011. **16**(1): p. 34-45.
283. Rothgiesser, K.M., et al., *SIRT2 regulates NF-kappaB dependent gene expression through deacetylation of p65 Lys310.* J Cell Sci, 2010. **123**(Pt 24): p. 4251-8.
284. McGlynn, L.M., et al., *SIRT2: tumour suppressor or tumour promoter in operable breast cancer?* Eur J Cancer, 2014. **50**(2): p. 290-301.
285. Mostoslavsky, R., et al., *Genomic instability and aging-like phenotype in the absence of mammalian SIRT6.* Cell, 2006. **124**(2): p. 315-329.

286. Mao, Z., et al., *SIRT6 promotes DNA repair under stress by activating PARP1.* Science, 2011. **332**(6036): p. 1443-6.
287. Kaidi, A., et al., *Human SIRT6 Promotes DNA End Resection Through CtIP Deacetylation.* Science, 2010. **329**(5997): p. 1348-1353.
288. McCord, R.A., et al., *SIRT6 stabilizes DNA-dependent protein kinase at chromatin for DNA double-strand break repair.* Aging-Us, 2009. **1**(1): p. 109-121.
289. Kawahara, T.L., et al., *SIRT6 links histone H3 lysine 9 deacetylation to NF-kappaB-dependent gene expression and organismal life span.* Cell, 2009. **136**(1): p. 62-74.
290. Scher, M.B., A. Vaquero, and D. Reinberg, *SirT3 is a nuclear NAD(+)-dependent histone deacetylase that translocates to the mitochondria upon cellular stress.* Genes & Development, 2007. **21**(8): p. 920-928.
291. Sundaresan, N.R., et al., *SIRT3 is a stress-responsive deacetylase in cardiomyocytes that protects cells from stress-mediated cell death by deacetylation of Ku70.* Molecular and Cellular Biology, 2008. **28**(20): p. 6384-6401.
292. Vakhrusheva, O., et al., *Sirt7 increases stress resistance of cardiomyocytes and prevents apoptosis and inflammatory cardiomyopathy in mice.* Circ Res, 2008. **102**(6): p. 703-10.
293. Wang, Y.J., et al., *An overview of Sirtuins as potential therapeutic target: Structure, function and modulators.* European Journal of Medicinal Chemistry, 2019. **161**: p. 48-77.
294. Napper, A.D., et al., *Discovery of indoles as potent and selective inhibitors of the deacetylase SIRT1.* J Med Chem, 2005. **48**(25): p. 8045-54.
295. Grozinger, C.M., et al., *Identification of a class of small molecule inhibitors of the sirtuin family of NAD-dependent deacetylases by phenotypic screening.* J Biol Chem, 2001. **276**(42): p. 38837-43.
296. Lara, E., et al., *Salermide, a Sirtuin inhibitor with a strong cancer-specific proapoptotic effect.* Oncogene, 2009. **28**(6): p. 781-91.
297. Avalos, J.L., K.M. Bever, and C. Wolberger, *Mechanism of Sirtuin Inhibition by Nicotinamide: Altering the NAD+ Cosubstrate Specificity of a Sir2 Enzyme.* Molecular Cell, 2005. **17**(6): p. 855-868.
298. Cui, H., et al., *Discovery of potent and selective sirtuin 2 (SIRT2) inhibitors using a fragment-based approach.* J Med Chem, 2014. **57**(20): p. 8340-57.
299. Ai, T., et al., *5-((3-Amidobenzyl)oxy)nicotinamides as Sirtuin 2 Inhibitors.* J Med Chem, 2016. **DOI: 10.1021/acs.jmedchem.5b01376**.
300. Heltweg, B., et al., *Antitumor activity of a small-molecule inhibitor of human silent information regulator 2 enzymes.* Cancer Res, 2006. **66**(8): p. 4368-77.
301. Mahajan, S.S., et al., *Development of pyrazolone and isoxazol-5-one cambinol analogues as sirtuin inhibitors.* J Med Chem, 2014. **57**(8): p. 3283-94.
302. Outeiro, T.F., et al., *Sirtuin 2 inhibitors rescue alpha-synuclein-mediated toxicity in models of Parkinson's disease.* Science, 2007. **317**(5837): p. 516-9.
303. Tervo, A.J., et al., *An in silico approach to discovering novel inhibitors of human sirtuin type 2.* J Med Chem, 2004. **47**(25): p. 6292-8.
304. Audrito, V., et al., *Nicotinamide blocks proliferation and induces apoptosis of chronic lymphocytic leukemia cells through activation of the p53/miR-34a/SIRT1 tumor suppressor network.* Cancer Res, 2011. **71**(13): p. 4473-83.
305. Ota, H., et al., *Sirt1 inhibitor, Sirtinol, induces senescence-like growth arrest with attenuated Ras-MAPK signaling in human cancer cells.* Oncogene, 2006. **25**(2): p. 176-85.
306. Jin, K.L., et al., *The effect of combined treatment with cisplatin and histone deacetylase inhibitors on HeLa cells.* J Gynecol Oncol, 2010. **21**(4): p. 262-8.

307. Liu, P.Y., et al., *The histone deacetylase SIRT2 stabilizes Myc oncoproteins.* Cell Death Differ, 2013. **20**(3): p. 503-14.
308. Solomon, J.M., et al., *Inhibition of SIRT1 catalytic activity increases p53 acetylation but does not alter cell survival following DNA damage.* Mol Cell Biol, 2006. **26**(1): p. 28-38.
309. Matsushita, N., et al., *Role of NAD-dependent deacetylases SIRT1 and SIRT2 in radiation and cisplatin-induced cell death in vertebrate cells.* Genes Cells, 2005. **10**(4): p. 321-32.
310. Kalle, A.M., et al., *Inhibition of SIRT1 by a small molecule induces apoptosis in breast cancer cells.* Biochem Biophys Res Commun, 2010. **401**(1): p. 13-9.
311. Oh, W.K., et al., *Amurensin G, a potent natural SIRT1 inhibitor, rescues doxorubicin responsiveness via down-regulation of multidrug resistance 1.* Mol Pharmacol, 2010. **78**(5): p. 855-64.
312. Tan, Y.J., et al., *BZD9L1 sirtuin inhibitor as a potential adjuvant for sensitization of colorectal cancer cells to 5-fluorouracil.* Ther Adv Med Oncol, 2019. **11**: p. 1758835919878977.
313. Taylor, S., et al., *Evaluating the evidence for targeting FOXO3a in breast cancer: a systematic review.* Cancer Cell Int, 2015. **15**(1): p. 1.
314. Vogt, P.K., H. Jiang, and M. Aoki, *Triple layer control: phosphorylation, acetylation and ubiquitination of FOXO proteins.* Cell Cycle, 2005. **4**(7): p. 908-13.
315. Zhou, Y., et al., *The miR-106b~25 cluster promotes bypass of doxorubicin-induced senescence and increase in motility and invasion by targeting the E-cadherin transcriptional activator EP300.* Cell Death Differ, 2014. **21**(3): p. 462-74.
316. May, C.D., et al., *Epithelial-mesenchymal transition and cancer stem cells: a dangerously dynamic duo in breast cancer progression.* Breast Cancer Res, 2011. **13**(1): p. 202.
317. Korpal, M., et al., *The miR-200 family inhibits epithelial-mesenchymal transition and cancer cell migration by direct targeting of E-cadherin transcriptional repressors ZEB1 and ZEB2.* J Biol Chem, 2008. **283**(22): p. 14910-4.
318. van der Vos, K.E., et al., *Modulation of glutamine metabolism by the PI(3)K-PKB-FOXO network regulates autophagy.* Nat Cell Biol, 2012. **14**(8): p. 829-37.
319. Shu, C.H., et al., *Cell cycle G2/M arrest and activation of cyclin-dependent kinases associated with low-dose paclitaxel-induced sub-G1 apoptosis.* Apoptosis, 1997. **2**(5): p. 463-70.
320. Song, L.B., et al., *[Molecular mechanisms of tumorgenesis and metastasis in nasopharyngeal carcinoma cell sublines].* Ai Zheng, 2002. **21**(2): p. 158-62.
321. Huang, P.Y., et al., *C-KIT overexpression and mutation in nasopharyngeal carcinoma cell lines and reactivity of Imatinib on these cell lines.* Chin J Cancer, 2010. **29**(2): p. 131-5.
322. Huang, D.P., et al., *Establishment of a cell line (NPC/HK1) from a differentiated squamous carcinoma of the nasopharynx.* Int J Cancer, 1980. **26**(2): p. 127-32.
323. Cheung, S.T., et al., *Nasopharyngeal carcinoma cell line (C666-1) consistently harbouring Epstein-Barr virus.* Int J Cancer, 1999. **83**(1): p. 121-6.
324. Tandon, N., et al., *Generation of Stable Expression Mammalian Cell Lines Using Lentivirus.* Bio-protocol, 2018. **8**(21): p. e3073.
325. Chen, L.F., Y. Mu, and W.C. Greene, *Acetylation of RelA at discrete sites regulates distinct nuclear functions of NF-kappaB.* Embo J, 2002. **21**(23): p. 6539-48.
326. Soderberg, O., et al., *Characterizing proteins and their interactions in cells and tissues using the in situ proximity ligation assay.* Methods, 2008. **45**(3): p. 227-32.

327. Tanabe, M., Y. Ishino, and H. Nishida, *From Structure-Function Analyses to Protein Engineering for Practical Applications of DNA Ligase.* Archaea, 2015. **2015**: p. 267570.
328. Nestal de Moraes, G., et al., *SUMOylation modulates FOXK2-mediated paclitaxel sensitivity in breast cancer cells.* Oncogenesis, 2018. **7**(3): p. 29.
329. Lee, J.J., et al., *Expression of FOXM1 and related proteins in breast cancer molecular subtypes.* Int J Exp Pathol, 2016. **97**(2): p. 170-7.
330. Wolff, A.C., et al., *Reply to E.A. Rakha et al.* J Clin Oncol, 2015. **33**(11): p. 1302-4.
331. Mahmud, Z., et al., *Oncogenic EP300 can be targeted with inhibitors of aldo-keto reductases.* Biochemical Pharmacology, 2019. **163**: p. 391-403.
332. Hu, Y.H., et al., *Sorcin silencing inhibits epithelial-to-mesenchymal transition and suppresses breast cancer metastasis in vivo.* Breast Cancer Research and Treatment, 2014. **143**(2): p. 287-299.
333. Lombardo, Y., et al., *Nicastrin regulates breast cancer stem cell properties and tumor growth in vitro and in vivo.* Proc Natl Acad Sci U S A, 2012. **109**(41): p. 16558-63.
334. Reinhold, W.C., et al., *Detailed DNA methylation profiles of the E-cadherin promoter in the NCI-60 cancer cells.* Molecular Cancer Therapeutics, 2007. **6**(2): p. 391-403.
335. Raguz, S., et al., *Loss of O(6)-methylguanine-DNA methyltransferase confers collateral sensitivity to carmustine in topoisomerase II-mediated doxorubicin resistant triple negative breast cancer cells.* Biochem Pharmacol, 2013. **85**(2): p. 186-96.
336. Liu, L., et al., *p53 sites acetylated in vitro by PCAF and p300 are acetylated in vivo in response to DNA damage.* Molecular and Cellular Biology, 1999. **19**(2): p. 1202-1209.
337. Francis, R.E., et al., *FoxM1 is a downstream target and marker of HER2 overexpression in breast cancer.* Int J Oncol, 2009. **35**(1): p. 57-68.
338. McGovern, U.B., et al., *Gefitinib (Iressa) represses FOXM1 expression via FOXO3a in breast cancer.* Mol Cancer Ther, 2009. **8**(3): p. 582-91.
339. Krol, J., et al., *The transcription factor FOXO3a is a crucial cellular target of gefitinib (Iressa) in breast cancer cells.* Mol Cancer Ther, 2007. **6**(12 Pt 1): p. 3169-79.
340. Hegde, P.S., et al., *Delineation of molecular mechanisms of sensitivity to lapatinib in breast cancer cell lines using global gene expression profiles.* Mol Cancer Ther, 2007. **6**(5): p. 1629-40.
341. Eijkelenboom, A., et al., *Genome-wide analysis of FOXO3 mediated transcription regulation through RNA polymerase II profiling.* Mol Syst Biol, 2013. **9**: p. 638.
342. Paik, J.H., et al., *FoxOs are lineage-restricted redundant tumor suppressors and regulate endothelial cell homeostasis.* Cell, 2007. **128**(2): p. 309-323.
343. Qian, Z., et al., *Overexpression of FoxO3a is associated with glioblastoma progression and predicts poor patient prognosis.* Int J Cancer, 2017. **140**(12): p. 2792-2804.
344. Slamon, D.J., et al., *Studies of the HER-2/neu proto-oncogene in human breast and ovarian cancer.* Science, 1989. **244**(4905): p. 707-12.
345. Singla, H., et al., *Recent Updates on the Therapeutic Potential of HER2 Tyrosine Kinase Inhibitors for the Treatment of Breast Cancer.* Curr Cancer Drug Targets, 2018. **18**(4): p. 306-327.
346. Jeung, Y.J., et al., *Shikonin induces apoptosis of lung cancer cells via activation of FOXO3a/EGR1/SIRT1 signaling antagonized by p300.* Biochim Biophys Acta, 2016. **1863**(11): p. 2584-2593.

347. Consolaro, F., et al., *FOXO3a and Posttranslational Modifications Mediate Glucocorticoid Sensitivity in B-ALL.* Mol Cancer Res, 2015. **13**(12): p. 1578-90.
348. Rexer, B.N., et al., *Direct inhibition of PI3K in combination with dual HER2 inhibitors is required for optimal antitumor activity in HER2+breast cancer cells.* Breast Cancer Research, 2014. **16**(1).
349. Hui, R.C.Y., et al., *The forkhead transcription factor FOXO3a increases phosphoinositide-3 kinase/Akt activity in drug-resistant leukemic cells through induction of PIK3CA expression.* Molecular and Cellular Biology, 2008. **28**(19): p. 5886-5898.
350. Lai, E., et al., *Hepatocyte nuclear factor 3/fork head or "winged helix" proteins: a family of transcription factors of diverse biologic function.* Proceedings of the National Academy of Sciences, 1993. **90**(22): p. 10421-10423.
351. Zhang, P., et al., *Tumor suppressor p53 cooperates with SIRT6 to regulate gluconeogenesis by promoting FoxO1 nuclear exclusion.* Proc Natl Acad Sci U S A, 2014. **111**(29): p. 10684-9.
352. Giordano, A. and M.L. Avantaggiati, *p300 and CBP: partners for life and death.* J Cell Physiol, 1999. **181**(2): p. 218-30.
353. Partanen, M., J. Motoyama, and C.C. Hui, *Developmentally regulated expression of the transcriptional cofactors/histone acetyltransferases CBP and p300 during mouse embryogenesis.* International Journal of Developmental Biology, 1999. **43**(6): p. 487-494.
354. Ugai, H., et al., *The coactivators p300 and CBP have different functions during the differentiation of F9 cells.* J Mol Med (Berl), 1999. **77**(6): p. 481-94.
355. Puri, P.L., et al., *Differential roles of p300 and PCAF acetyltransferases in muscle differentiation.* Molecular Cell, 1997. **1**(1): p. 35-45.
356. Brooks, C.L. and W. Gu, *Ubiquitination, phosphorylation and acetylation: the molecular basis for p53 regulation.* Curr Opin Cell Biol, 2003. **15**(2): p. 164-71.
357. Yang, X.J., *The diverse superfamily of lysine acetyltransferases and their roles in leukemia and other diseases.* Nucleic Acids Research, 2004. **32**(3): p. 959-976.
358. Brooks, C.L. and W. Gu, *Ubiquitination, phosphorylation and acetylation: the molecular basis for p53 regulation.* Current Opinion in Cell Biology, 2003. **15**(2): p. 164-171.
359. Schlafli, A.M., et al., *Prognostic value of the autophagy markers LC3 and p62/SQSTM1 in early-stage non-small cell lung cancer.* Oncotarget, 2016. **7**(26): p. 39544-39555.
360. Alexander, K. and P.W. Hinds, *Requirement for p27^{KIP1} in Retinoblastoma Protein-Mediated Senescence.* Molecular and Cellular Biology, 2001. **21**(11): p. 3616-3631.
361. McConnell, B.B., et al., *Inhibitors of cyclin-dependent kinases induce features of replicative senescence in early passage human diploid fibroblasts.* Current Biology, 1998. **8**(6): p. 351-354.
362. Gottesman, M.M. and S.V. Ambudkar, *Overview: ABC transporters and human disease.* Journal of Bioenergetics and Biomembranes, 2001. **33**(6): p. 453-458.
363. Szakacs, G., et al., *Targeting multidrug resistance in cancer.* Nat Rev Drug Discov, 2006. **5**(3): p. 219-34.
364. Gu, W. and R.G. Roeder, *Activation of p53 sequence-specific DNA binding by acetylation of the p53 C-terminal domain.* Cell, 1997. **90**(4): p. 595-606.
365. Sakaguchi, K., et al., *DNA damage activates p53 through a phosphorylation-acetylation cascade.* Genes & Development, 1998. **12**(18): p. 2831-2841.

366. Voulgari, A. and A. Pintzas, *Epithelial-mesenchymal transition in cancer metastasis: mechanisms, markers and strategies to overcome drug resistance in the clinic.* Biochim Biophys Acta, 2009. **1796**(2): p. 75-90.
367. Adams, J.M., *Ways of dying: multiple pathways to apoptosis.* Genes Dev, 2003. **17**(20): p. 2481-95.
368. Gu, M.L., et al., *An inhibitor of the acetyltransferases CBP/p300 exerts antineoplastic effects on gastrointestinal stromal tumor cells.* Oncology Reports, 2016. **36**(5): p. 2763-2770.
369. Chekler, E.L.P., et al., *Transcriptional Profiling of a Selective CREB Binding Protein Bromodomain Inhibitor Highlights Therapeutic Opportunities.* Chemistry & Biology, 2015. **22**(12): p. 1588-1596.
370. Wang, X., S. Hu, and L. Liu, *Phosphorylation and acetylation modifications of FOXO3a: Independently or synergistically?* Oncol Lett, 2017. **13**(5): p. 2867-2872.
371. Wang, F., et al., *Structures of KIX domain of CBP in complex with two FOXO3a transactivation domains reveal promiscuity and plasticity in coactivator recruitment.* Proc Natl Acad Sci U S A, 2012. **109**(16): p. 6078-83.
372. Iyer, N.G., H. Ozdag, and C. Caldas, *p300/CBP and cancer.* Oncogene, 2004. **23**(24): p. 4225-31.
373. Iyer, N.G., et al., *p300 is required for orderly G1/S transition in human cancer cells.* Oncogene, 2007. **26**(1): p. 21-29.
374. Frye, R.A., *Phylogenetic classification of prokaryotic and eukaryotic Sir2-like proteins.* Biochem Biophys Res Commun, 2000. **273**(2): p. 793-8.
375. Sauve, A.A., *Sirtuin chemical mechanisms.* Biochim Biophys Acta, 2010. **1804**(8): p. 1591-603.
376. Martínez-Redondo, P. and A. Vaquero, *The Diversity of Histone Versus Nonhistone Sirtuin Substrates.* Genes & Cancer, 2013. **4**(3-4): p. 148-163.
377. Choi, J.E. and R. Mostoslavsky, *Sirtuins, metabolism, and DNA repair.* Curr Opin Genet Dev, 2014. **26**: p. 24-32.
378. Lombard, D.B., *Sirtuins at the breaking point: SIRT6 in DNA repair.* Aging (Albany NY), 2009. **1**(1): p. 12-6.
379. Rice, C.M., et al., *Mitochondrial sirtuins--a new therapeutic target for repair and protection in multiple sclerosis.* Eur J Neurosci, 2012. **35**(12): p. 1887-93.
380. Anderson, E.N., et al., *C. elegans lifespan extension by osmotic stress requires FUdR, base excision repair, FOXO, and sirtuins.* Mech Ageing Dev, 2016. **154**: p. 30-42.
381. Turkmen, K., A. Karagoz, and A. Kucuk, *Sirtuins as novel players in the pathogenesis of diabetes mellitus.* World J Diabetes, 2014. **5**(6): p. 894-900.
382. Kitada, M., et al., *Sirtuins as possible drug targets in type 2 diabetes.* Curr Drug Targets, 2013. **14**(6): p. 622-36.
383. Huynh, F.K., K.A. Hershberger, and M.D. Hirschey, *Targeting sirtuins for the treatment of diabetes.* Diabetes Manag (Lond), 2013. **3**(3): p. 245-257.
384. Eskandarian, H.A., et al., *A role for SIRT2-dependent histone H3K18 deacetylation in bacterial infection.* Science, 2013. **341**(6145): p. 1238858.
385. Matsushima, S. and J. Sadoshima, *The role of sirtuins in cardiac disease.* Am J Physiol Heart Circ Physiol, 2015. **309**(9): p. H1375-89.
386. de Oliveira, R.M., T.F. Pais, and T.F. Outeiro, *Sirtuins: common targets in aging and in neurodegeneration.* Curr Drug Targets, 2010. **11**(10): p. 1270-80.
387. Outeiro, T.F., O. Marques, and A. Kazantsev, *Therapeutic role of sirtuins in neurodegenerative disease.* Biochim Biophys Acta, 2008. **1782**(6): p. 363-9.
388. Gan, L. and L. Mucke, *Paths of convergence: sirtuins in aging and neurodegeneration.* Neuron, 2008. **58**(1): p. 10-4.

389. Anekonda, T.S. and P.H. Reddy, *Neuronal protection by sirtuins in Alzheimer's disease.* J Neurochem, 2006. **96**(2): p. 305-13.
390. Grozinger, C.M., et al., *Identification of a Class of Small Molecule Inhibitors of the Sirtuin Family of NAD-dependent Deacetylases by Phenotypic Screening.* Journal of Biological Chemistry, 2001. **276**(42): p. 38837-38843.
391. Sakai, T., et al., *Design, synthesis and structure-activity relationship studies of novel sirtuin 2 (SIRT2) inhibitors with a benzamide skeleton.* Bioorg Med Chem, 2015. **23**(2): p. 328-39.
392. Khanfar, M.A., et al., *Design and Evaluation of 3-(Benzylthio)benzamide Derivatives as Potent and Selective SIRT2 Inhibitors.* ACS Med Chem Lett, 2015. **6**(5): p. 607-11.
393. Therrien, E., et al., *Discovery of bicyclic pyrazoles as class III histone deacetylase SIRT1 and SIRT2 inhibitors.* Bioorg Med Chem Lett, 2015. **25**(12): p. 2514-8.
394. Mahdavifar, N., et al., *Epidemiology and Inequality in the Incidence and Mortality of Nasopharynx Cancer in Asia.* Osong Public Health and Research Perspectives, 2016. **7**(6): p. 360-372.
395. Ma, B.B.Y. and A.T.C. Chan, *Recent perspectives in the role of chemotherapy in the management of advanced nasopharyngeal carcinoma.* Cancer, 2005. **103**(1): p. 22-31.
396. Hsu, C.H., et al., *Prognostic Value of Multidrug Resistance 1, Glutathione-S-Transferase-π and p53 in Advanced Nasopharyngeal Carcinoma Treated with Systemic Chemotherapy.* Oncology, 2002. **62**(4): p. 305-312.
397. Jiang, R.-D., et al., *Establishment of a human nasopharyngeal carcinoma drug-resistant cell line CNE2/DDP and screening of drug-resistant genes*. Vol. 22. 2003. 337-45.
398. Cheung, H.W., et al., *Mitotic Arrest Deficient 2 Expression Induces Chemosensitization to a DNA-Damaging Agent, Cisplatin, in Nasopharyngeal Carcinoma Cells.* Cancer Research, 2005. **65**(4): p. 1450.
399. Wang, J., et al., *Down-regulation of P-glycoprotein is associated with resistance to cisplatin and VP-16 in human lung cancer cell lines.* Anticancer Res, 2010. **30**(9): p. 3593-8.
400. Pan, Y., et al., *Stat3 Inhibitor Stattic Exhibits Potent Antitumor Activity and Induces Chemo- and Radio-Sensitivity in Nasopharyngeal Carcinoma.* PLoS ONE, 2013. **8**(1): p. e54565.
401. Ma, B.B., et al., *Prognostic significance of tumor angiogenesis, Ki 67, p53 oncoprotein, epidermal growth factor receptor and HER2 receptor protein expression in undifferentiated nasopharyngeal carcinoma--a prospective study.* Head Neck, 2003. **25**(10): p. 864-72.
402. Jin, O., et al., *[Expression of CerbB-2 and EGFR mRNA in human nasopharyngeal carcinomas and pericarcinomatous tissues].* Hunan Yi Ke Da Xue Xue Bao, 1997. **22**(6): p. 487-90.
403. Ma, B.B., et al., *Preclinical activity of gefitinib in non-keratinizing nasopharyngeal carcinoma cell lines and biomarkers of response.* Invest New Drugs, 2010. **28**(3): p. 326-33.
404. Liu, L., et al., *Inhibition of eEF-2 kinase sensitizes human nasopharyngeal carcinoma cells to lapatinib-induced apoptosis through the Src and Erk pathways.* BMC Cancer, 2016. **16**: p. 813.
405. Lui, V.W.Y., et al., *Anti-invasion, anti-proliferation and anoikis-sensitization activities of lapatinib in nasopharyngeal carcinoma cells.* Investigational New Drugs, 2011. **29**(6): p. 1241-1252.

406. S.C. Wilson, M., et al., *FOXO and FOXM1 in Cancer: The FOXO-FOXM1 Axis Shapes the Outcome of Cancer Chemotherapy.* Current Drug Targets, 2011. **12**(9): p. 1256-1266.
407. Olmos, Y., J.J. Brosens, and E.W. Lam, *Interplay between SIRT proteins and tumour suppressor transcription factors in chemotherapeutic resistance of cancer.* Drug Resist Updat, 2011. **14**(1): p. 35-44.
408. Daitoku, H., J.-i. Sakamaki, and A. Fukamizu, *Regulation of FoxO transcription factors by acetylation and protein–protein interactions.* Biochimica et Biophysica Acta (BBA) - Molecular Cell Research, 2011. **1813**(11): p. 1954-1960.
409. Jiang, L., P. Wang, and H. Chen, *Overexpression of FOXM1 is associated with metastases of nasopharyngeal carcinoma.* Upsala Journal of Medical Sciences, 2014. **119**(4): p. 324-332.
410. Hou, Y., et al., *The FOXM1–ABCC5 axis contributes to paclitaxel resistance in nasopharyngeal carcinoma cells.* Cell Death & Disease, 2017. **8**(3): p. e2659.
411. Shou, Z., et al., *Expression and prognosis of FOXO3a and HIF-1α in nasopharyngeal carcinoma.* Journal of Cancer Research and Clinical Oncology, 2012. **138**(4): p. 585-593.
412. Sundriyal, S., et al., *Thienopyrimidinone Based Sirtuin-2 (SIRT2)-Selective Inhibitors Bind in the Ligand Induced Selectivity Pocket.* J Med Chem, 2017. **60**(5): p. 1928-1945.
413. North, B.J., et al., *The human Sir2 ortholog, SIRT2, is an NAD+-dependent tubulin deacetylase.* Mol Cell, 2003. **11**(2): p. 437-44.
414. Di Fruscia, P., et al., *The discovery of a highly selective 5,6,7,8-tetrahydrobenzo[4,5]thieno[2,3-d]pyrimidin-4(3H)-one SIRT2 inhibitor that is neuroprotective in an in vitro Parkinson's disease model.* ChemMedChem, 2015. **10**(1): p. 69-82.
415. Yoshida, M., et al., *Potent and specific inhibition of mammalian histone deacetylase both in vivo and in vitro by trichostatin A.* J Biol Chem, 1990. **265**(28): p. 17174-9.
416. Paik, J.H., et al., *FoxOs are lineage-restricted redundant tumor suppressors and regulate endothelial cell homeostasis.* Cell, 2007. **128**(2): p. 309-23.
417. Zhang, Y., et al., *Identification of a small molecule SIRT2 inhibitor with selective tumor cytotoxicity.* Biochem Biophys Res Commun, 2009. **386**(4): p. 729-33.
418. Hsu, C.H., et al., *Prognostic value of multidrug resistance 1, glutathione-S-transferase-pi and p53 in advanced nasopharyngeal carcinoma treated with systemic chemotherapy.* Oncology, 2002. **62**(4): p. 305-12.
419. Ting, Y., et al., *Prognostic significance of cystic lymph nodal metastasis in nasopharyngeal carcinoma.* Head Neck, 2017. **39**(9): p. 1832-1839.
420. Weiss, J.M., et al., *Capecitabine and lapatinib for the first-line treatment of metastatic/recurrent head and neck squamous cell carcinoma.* Cancer, 2016. **122**(15): p. 2350-2355.
421. Machiels, J.-P.H., et al., *Afatinib versus methotrexate as second-line treatment in patients with recurrent or metastatic squamous-cell carcinoma of the head and neck progressing on or after platinum-based therapy (LUX-Head & Neck 1): an open-label, randomised phase 3 trial.* The Lancet Oncology, 2015. **16**(5): p. 583-594.
422. Harrington, K.J., et al., *Final analysis: A randomized, blinded, placebo (P)-controlled phase III study of adjuvant postoperative lapatinib (L) with concurrent chemotherapy and radiation therapy (CH-RT) in high-risk patients with squamous cell carcinoma of the head and neck (SCCHN).* Journal of Clinical Oncology, 2014. **32**(15_suppl): p. 6005-6005.

423. Wu, J., et al., *Extracellular signal-regulated kinase signaling-mediated induction and interaction of FOXO3a and p53 contribute to the inhibition of nasopharyngeal carcinoma cell growth by curcumin.* International Journal of Oncology, 2014. **45**(1): p. 95-103.
424. Zhou, W.-J., et al., *A G-quadruplex ligand SYUIQ-5 induces autophagy by inhibiting the Akt-FOXO3a pathway in nasopharyngeal cancer cells*. Vol. 28. 2009. 1049-53.
425. Sunters, A., et al., *Paclitaxel-induced nuclear translocation of FOXO3a in breast cancer cells is mediated by c-Jun NH2-terminal kinase and Akt.* Cancer Res, 2006. **66**(1): p. 212-20.
426. Mora Vidal, R., et al., *Epidermal Growth Factor Receptor Family Inhibition Identifies P38 Mitogen-activated Protein Kinase as a Potential Therapeutic Target in Bladder Cancer.* Urology, 2018. **112**: p. 225 e1-225 e7.
427. Gschwantler-Kaulich, D., et al., *HER Specific TKIs Exert Their Antineoplastic Effects on Breast Cancer Cell Lines through the Involvement of STAT5 and JNK.* PLoS One, 2016. **11**(1): p. e0146311.
428. Carr, J.R., et al., *FoxM1 Mediates Resistance to Herceptin and Paclitaxel.* Cancer research, 2010. **70**(12): p. 5054-5063.
429. Miranda, S.C.W., et al., *FOXO and FOXM1 in Cancer: The FOXO-FOXM1 Axis Shapes the Outcome of Cancer Chemotherapy.* Current Drug Targets, 2011. **12**(9): p. 1256-1266.
430. Jiang, L., et al., *Down-regulation of FoxM1 by thiostrepton or small interfering RNA inhibits proliferation, transformation ability and angiogenesis, and induces apoptosis of nasopharyngeal carcinoma cells.* International Journal of Clinical and Experimental Pathology, 2014. **7**(9): p. 5450-5460.
431. Wang, F., et al., *SIRT2 deacetylates FOXO3a in response to oxidative stress and caloric restriction.* Aging Cell, 2007. **6**(4): p. 505-514.
432. Brunet, A., et al., *Stress-Dependent Regulation of FOXO Transcription Factors by the SIRT1 Deacetylase.* Science, 2004. **303**(5666): p. 2011.
433. Hu, C., et al., *A Global View of the Oncogenic Landscape in Nasopharyngeal Carcinoma: An Integrated Analysis at the Genetic and Expression Levels.* PLOS ONE, 2012. **7**(7): p. e41055.
434. Chua, K.F., et al., *Mammalian SIRT1 limits replicative life span in response to chronic genotoxic stress.* Cell Metab, 2005. **2**(1): p. 67-76.
435. Dan, L., et al., *The role of sirtuin 2 activation by nicotinamide phosphoribosyltransferase in the aberrant proliferation and survival of myeloid leukemia cells.* Haematologica, 2012. **97**(4): p. 551-559.
436. He, X., et al., *SIRT2 activity is required for the survival of C6 glioma cells.* Biochemical and Biophysical Research Communications, 2012. **417**(1): p. 468-472.
437. Wilking-Busch, M.J., et al., *RNA interference-mediated knockdown of SIRT1 and/or SIRT2 in melanoma: Identification of downstream targets by large-scale proteomics analysis.* Journal of Proteomics, 2018. **170**: p. 99-109.
438. Matsushita, N., et al., *Role of NAD-dependent deacetylases SIRT1 and SIRT2 in radiation and cisplatin-induced cell death in vertebrate cells.* Genes to Cells, 2005. **10**(4): p. 321-332.
439. Wang, F., et al., *Deacetylation of FOXO3 by SIRT1 or SIRT2 leads to Skp2-mediated FOXO3 ubiquitination and degradation.* Oncogene, 2011. **31**: p. 1546.
440. Singhai, R., et al., *E-Cadherin as a diagnostic biomarker in breast cancer.* N Am J Med Sci, 2011. **3**(5): p. 227-33.

441. Zhang, Y., K.A. Toy, and C.G. Kleer, *Metaplastic breast carcinomas are enriched in markers of tumor-initiating cells and epithelial to mesenchymal transition.* Mod Pathol, 2012. **25**(2): p. 178-84.
442. Weigelt, B., et al., *Metaplastic breast carcinoma: more than a special type.* Nat Rev Cancer, 2014. **14**(3): p. 147-8.
443. Jeschke, U., et al., *Expression of E-cadherin in human ductal breast cancer carcinoma in situ, invasive carcinomas, their lymph node metastases, their distant metastases, carcinomas with recurrence and in recurrence.* Anticancer Research, 2007. **27**(4A): p. 1969-1974.
444. Mani, S.A., et al., *The epithelial-mesenchymal transition generates cells with properties of stem cells.* Cell, 2008. **133**(4): p. 704-15.
445. Onder, T.T., et al., *Loss of E-Cadherin Promotes Metastasis via Multiple Downstream Transcriptional Pathways.* Cancer Research, 2008. **68**(10): p. 3645-3654.
446. Berx, G., et al., *Mutations of the human E-cadherin (CDH1) gene.* Human Mutation, 1998. **12**(4): p. 226-237.
447. Yang, J., et al., *Twist, a master regulator of morphogenesis, plays an essential role in tumor metastasis.* Cell, 2004. **117**(7): p. 927-39.
448. Liu, Y.N., et al., *Regulatory mechanisms controlling human E-cadherin gene expression.* Oncogene, 2005. **24**(56): p. 8277-90.
449. van Roy, F. and G. Berx, *The cell-cell adhesion molecule E-cadherin.* Cell Mol Life Sci, 2008. **65**(23): p. 3756-88.
450. Hu, Y., et al., *miR-106b~25 cluster regulates multidrug resistance in an ABC transporter-independent manner via downregulation of EP300.* Oncol Rep, 2016. **35**: p. 1170-1178.
451. Mees, S.T., et al., *EP300--a miRNA-regulated metastasis suppressor gene in ductal adenocarcinomas of the pancreas.* Int J Cancer, 2010. **126**(1): p. 114-24.
452. Gyorffy, B., et al., *An online survival analysis tool to rapidly assess the effect of 22,277 genes on breast cancer prognosis using microarray data of 1,809 patients.* Breast Cancer Research and Treatment, 2010. **123**(3): p. 725-731.
453. Santer, F.R., et al., *Inhibition of the acetyltransferase p300 as a novel pro-apoptotic and anti-invasion approach for treatment of prostate cancer.* Cancer Research, 2011. **71**.
454. Yokomizo, C., et al., *High expression of p300 in HCC predicts shortened overall survival in association with enhanced epithelial mesenchymal transition of HCC cells.* Cancer Letters, 2011. **310**(2): p. 140-147.
455. Liao, Z.W., et al., *P300 promotes migration, invasion and epithelial-mesenchymal transition in a nasopharyngeal carcinoma cell line.* Oncology Letters, 2017. **13**(2): p. 763-769.
456. Pecina-Slaus, N., *Tumor suppressor gene E-cadherin and its role in normal and malignant cells.* Cancer Cell Int, 2003. **3**(1): p. 17.
457. Allis, C.D. and T. Jenuwein, *The molecular hallmarks of epigenetic control.* Nature Reviews Genetics, 2016. **17**(8): p. 487-500.
458. Esteller, M., et al., *A gene hypermethylation profile of human cancer.* Cancer Research, 2001. **61**(8): p. 3225-3229.
459. Lambert, A.W., D.R. Pattabiraman, and R.A. Weinberg, *Emerging Biological Principles of Metastasis.* Cell, 2017. **168**(4): p. 670-691.
460. Peinado, H., D. Olmeda, and A. Cano, *Snail, Zeb and bHLH factors in tumour progression: an alliance against the epithelial phenotype?* Nat Rev Cancer, 2007. **7**(6): p. 415-28.

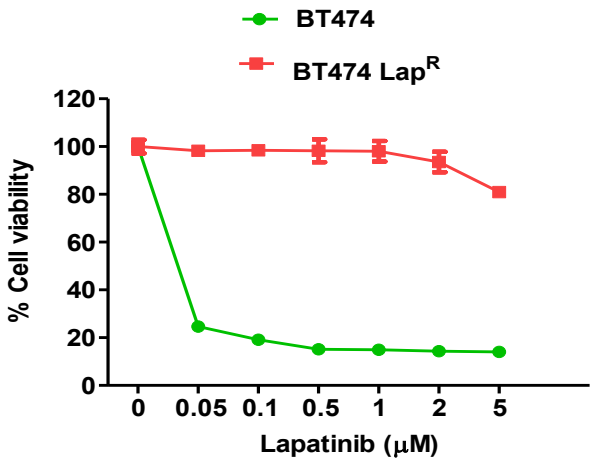
461. Byles, V., et al., *SIRT1 induces EMT by cooperating with EMT transcription factors and enhances prostate cancer cell migration and metastasis.* Oncogene, 2012. **31**(43): p. 4619-29.
462. Choupani, J., et al., *Narrower insight to SIRT1 role in cancer: A potential therapeutic target to control epithelial-mesenchymal transition in cancer cells.* J Cell Physiol, 2018. **233**(6): p. 4443-4457.
463. Meng, F.D., et al., *FoxM1 overexpression promotes epithelial-mesenchymal transition and metastasis of hepatocellular carcinoma.* World J Gastroenterol, 2015. **21**(1): p. 196-213.
464. Postigo, A.A., et al., *Regulation of Smad signaling through a differential recruitment of coactivators and corepressors by ZEB proteins.* The EMBO Journal, 2003. **22**(10): p. 2453-2462.
465. Feng, J., et al., *Histone deacetylase inhibitor valproic acid (VPA) promotes the epithelial mesenchymal transition of colorectal cancer cells via up regulation of Snail.* Cell Adh Migr, 2015. **9**(6): p. 495-501.
466. Chang, R., et al., *Snail acetylation by histone acetyltransferase p300 in lung cancer.* Thorac Cancer, 2017. **8**(3): p. 131-137.
467. Lombaerts, M., et al., *E-cadherin transcriptional downregulation by promoter methylation but not mutation is related to epithelial-to-mesenchymal transition in breast cancer cell lines.* Br J Cancer, 2006. **94**(5): p. 661-671.
468. Storms, R.W., et al., *Isolation of primitive human hematopoietic progenitors on the basis of aldehyde dehydrogenase activity.* Proc Natl Acad Sci U S A, 1999. **96**(16): p. 9118-23.
469. Jaggupilli, A. and E. Elkord, *Significance of CD44 and CD24 as cancer stem cell markers: an enduring ambiguity.* Clin Dev Immunol, 2012. **2012**: p. 708036.
470. Chaffer, C.L. and R.A. Weinberg, *A perspective on cancer cell metastasis.* Science, 2011. **331**(6024): p. 1559-64.
471. Wang, Z., et al., *Targeting miRNAs involved in cancer stem cell and EMT regulation: An emerging concept in overcoming drug resistance.* Drug Resist Updat, 2010. **13**(4-5): p. 109-18.
472. Singh, A. and J. Settleman, *EMT, cancer stem cells and drug resistance: an emerging axis of evil in the war on cancer.* Oncogene, 2010. **29**(34): p. 4741-51.
473. Li, C.Z., et al., *Stereospecific reduction of a potent kinesin spindle protein (KSP) inhibitor in human tissues.* Biochemical Pharmacology, 2010. **79**(10): p. 1526-1533.
474. Penning, T.M., *The aldo-keto reductases (AKRs): Overview.* Chemico-Biological Interactions, 2015. **234**: p. 236-246.
475. Zeng, C.M., et al., *Aldo-Keto Reductase AKR1C1-AKR1C4: Functions, Regulation, and Intervention for Anti-cancer Therapy.* Frontiers in Pharmacology, 2017. **8**.
476. Bortolozzi, R., et al., *AKR1C enzymes sustain therapy resistance in paediatric T-ALL.* British Journal of Cancer, 2018. **118**(7): p. 985-994.
477. Dunham, I., et al., *An integrated encyclopedia of DNA elements in the human genome.* Nature, 2012. **489**: p. 57.
478. Asif, M., *Study of Anthranylic Acid Derivatives: Mefenamic Acid and Its Various Analogues.* American Journal of Medicine Studies, 2014. **2**(1): p. 24-30.
479. Byrns, M.C. and T.M. Penning, *Type 5 17 beta-hydroxysteroid dehydrogenase/prostaglandin F synthase (AKR1C3): Role in breast cancer and inhibition by non-steroidal anti-inflammatory drug analogs.* Chemico-Biological Interactions, 2009. **178**(1-3): p. 221-227.
480. Berx, G., et al., *E-cadherin is a tumour invasion suppressor gene mutated in human lobular breast cancers.* Embo Journal, 1995. **14**(24): p. 6107-6115.

481. Droufakou, S., et al., *Multiple ways of silencing E-cadherin gene expression in lobular carcinoma of the breast.* International Journal of Cancer, 2001. **92**(3): p. 404-408.
482. Wong, S.H.M., et al., *E-cadherin: Its dysregulation in carcinogenesis and clinical implications.* Critical Reviews in Oncology Hematology, 2018. **121**: p. 11-22.
483. Sarrio, D., et al., *Epigenetic and genetic alterations of APC and CDH1 genes in lobular breast cancer: Relationships with abnormal E-cadherin and catenin expression and microsatellite instability.* International Journal of Cancer, 2003. **106**(2): p. 208-215.
484. Cleton-Jansen, A.M., *E-cadherin and loss of heterozygosity at chromosome 16 in breast carcinogenesis: different genetic pathways in ductal and lobular breast cancer?* Breast Cancer Research, 2002. **4**(1): p. 5-8.
485. Lamouille, S., J. Xu, and R. Derynck, *Molecular mechanisms of epithelial-mesenchymal transition.* Nat Rev Mol Cell Biol, 2014. **15**(3): p. 178-96.
486. Mishra, A., et al., *Hypoxia Stabilizes GAS6/Axl Signaling in Metastatic Prostate Cancer.* Molecular Cancer Research, 2012. **10**(6): p. 703-712.
487. Santer, F.R., et al., *Inhibition of the Acetyltransferases p300 and CBP Reveals a Targetable Function for p300 in the Survival and Invasion Pathways of Prostate Cancer Cell Lines.* Molecular Cancer Therapeutics, 2011. **10**(9): p. 1644-1655.
488. Li, M., et al., *High expression of transcriptional coactivator p300 correlates with aggressive features and poor prognosis of hepatocellular carcinoma.* Journal of Translational Medicine, 2011. **9**.
489. Liao, Z.W., et al., *High expression of p300 is linked to aggressive features and poor prognosis of Nasopharyngeal Carcinoma.* Journal of Translational Medicine, 2012. **10**.
490. Girdwood, D., et al., *P300 transcriptional repression is mediated by SUMO modification.* Mol Cell, 2003. **11**(4): p. 1043-54.
491. Hofman, J., et al., *Anthracycline resistance mediated by reductive metabolism in cancer cells: The role of aldo-keto reductase 1C3.* Toxicology and Applied Pharmacology, 2014. **278**(3): p. 238-248.
492. Chen, C.C., et al., *Gene expression profiling for analysis acquired oxaliplatin resistant factors in human gastric carcinoma TSGH-S3 cells: The role of IL-6 signaling and Nrf2/AKR1C axis identification.* Biochemical Pharmacology, 2013. **86**(7): p. 872-887.
493. Oduwole, O.O., et al., *17 beta-hydroxysteroid dehydrogenase type 1 is an independent prognostic marker in breast cancer.* Cancer Research, 2004. **64**(20): p. 7604-7609.
494. Minotti, G., et al., *Anthracyclines: Molecular advances and pharmacologic developments in antitumor activity and cardiotoxicity.* Pharmacological Reviews, 2004. **56**(2): p. 185-229.
495. Nestal de Moraes, G., et al., *Insights into a Critical Role of the FOXO3a-FOXM1 Axis in DNA Damage Response and Genotoxic Drug Resistance.* Curr Drug Targets, 2016. **17**(2): p. 164-77.
496. Senf, S.M., et al., *p300 Acetyltransferase activity differentially regulates the localization and activity of the FOXO homologues in skeletal muscle.* Am J Physiol Cell Physiol, 2011. **300**(6): p. C1490-501.
497. Lin, Z., et al., *Nuclear translocation of CBP/p300-interacting protein CITED1 induced by parathyroid hormone requires serine phosphorylation at position 79 in its 63–84 domain.* Cellular Signalling, 2014. **26**(11): p. 2436-2445.

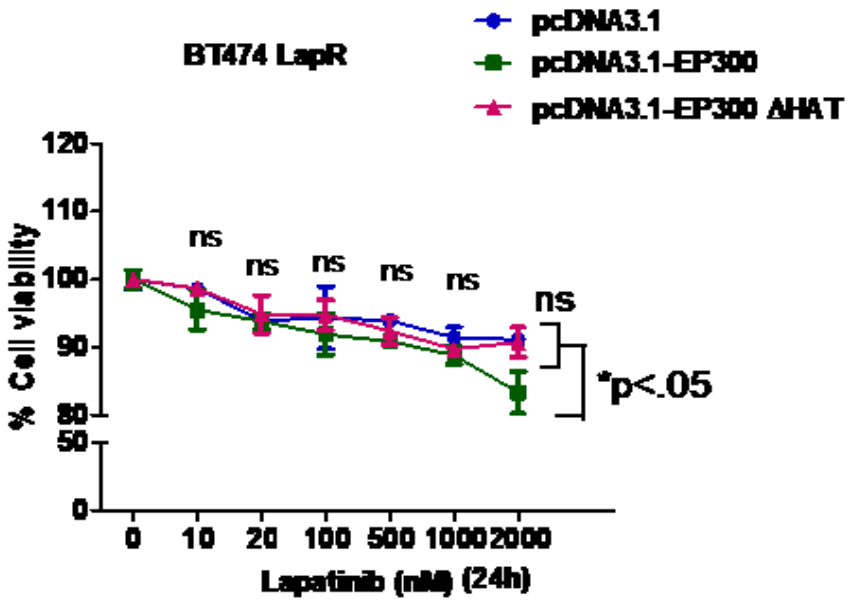
498. Mullighan, C.G., et al., *CREBBP mutations in relapsed acute lymphoblastic leukaemia.* Nature, 2011. **471**(7337): p. 235-239.
499. Arensman, M.D., et al., *The CREB-Binding Protein Inhibitor ICG-001 Suppresses Pancreatic Cancer Growth.* Molecular Cancer Therapeutics, 2014. **13**(10): p. 2303-2314.
500. Gajer, J.M., et al., *Histone acetyltransferase inhibitors block neuroblastoma cell growth in vivo.* Oncogenesis, 2015. **4**(2): p. e137-e137.
501. Jia, Y., et al., *Thymine DNA glycosylase promotes transactivation of β-catenin/TCFs by cooperating with CBP.* Journal of Molecular Cell Biology, 2014. **6**(3): p. 231-239.
502. Jansma, A.L., et al., *The High-Risk HPV16 E7 Oncoprotein Mediates Interaction between the Transcriptional Coactivator CBP and the Retinoblastoma Protein pRb.* Journal of Molecular Biology, 2014. **426**(24): p. 4030-4048.
503. Ebrahimi, A., et al., *Bromodomain inhibition of the coactivators CBP/EP300 facilitate cellular reprogramming.* Nat Chem Biol, 2019. **15**(5): p. 519-528.
504. Sun, F., et al., *Vincristine ablation of Sirt2 induces cell apoptosis and mitophagy via Hsp70 acetylation in MDA-MB-231 cells.* Biochem Pharmacol, 2019. **162**: p. 142-153.
505. Scheel, C. and R.A. Weinberg, *Cancer stem cells and epithelial-mesenchymal transition: concepts and molecular links.* Semin Cancer Biol, 2012. **22**(5-6): p. 396-403.
506. Fermento, M.E., et al., *Inhibition of p300 suppresses growth of breast cancer. Role of p300 subcellular localization.* Exp Mol Pathol, 2014. **97**(3): p. 411-24.
507. He, H., et al., *Transcriptional factors p300 and MRTF-A synergistically enhance the expression of migration-related genes in MCF-7 breast cancer cells.* Biochem Biophys Res Commun, 2015. **467**(4): p. 813-20.
508. Peña, C., et al., *The expression levels of the transcriptional regulators p300 and CtBP modulate the correlations between SNAIL, ZEB1, E-cadherin and vitamin D receptor in human colon carcinomas.* International Journal of Cancer, 2006. **119**(9): p. 2098-2104.
509. Baluchamy, S., et al., *Repression of c-Myc and inhibition of G1 exit in cells conditionally overexpressing p300 that is not dependent on its histone acetyltransferase activity.* Proc Natl Acad Sci U S A, 2003. **100**(16): p. 9524-9.

Appendices

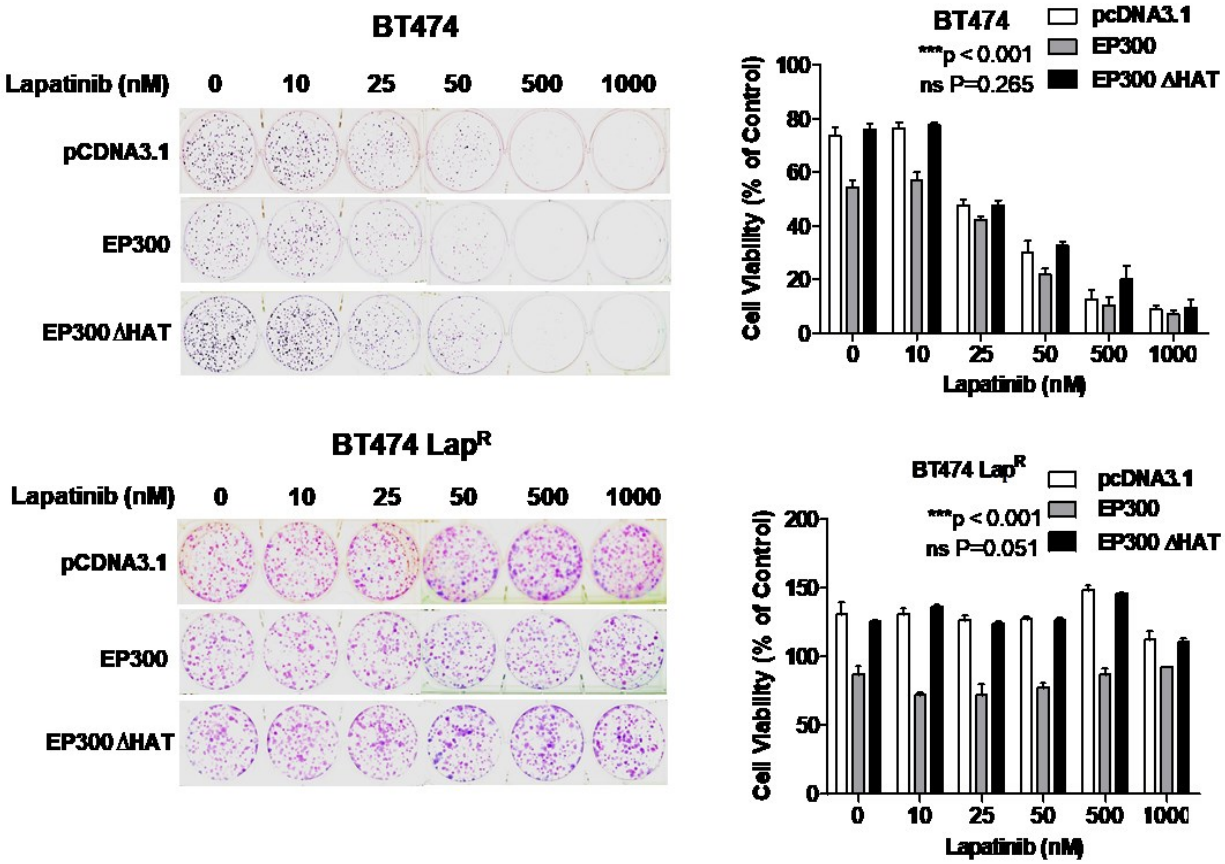
Appendix 1 (For chapter 3)



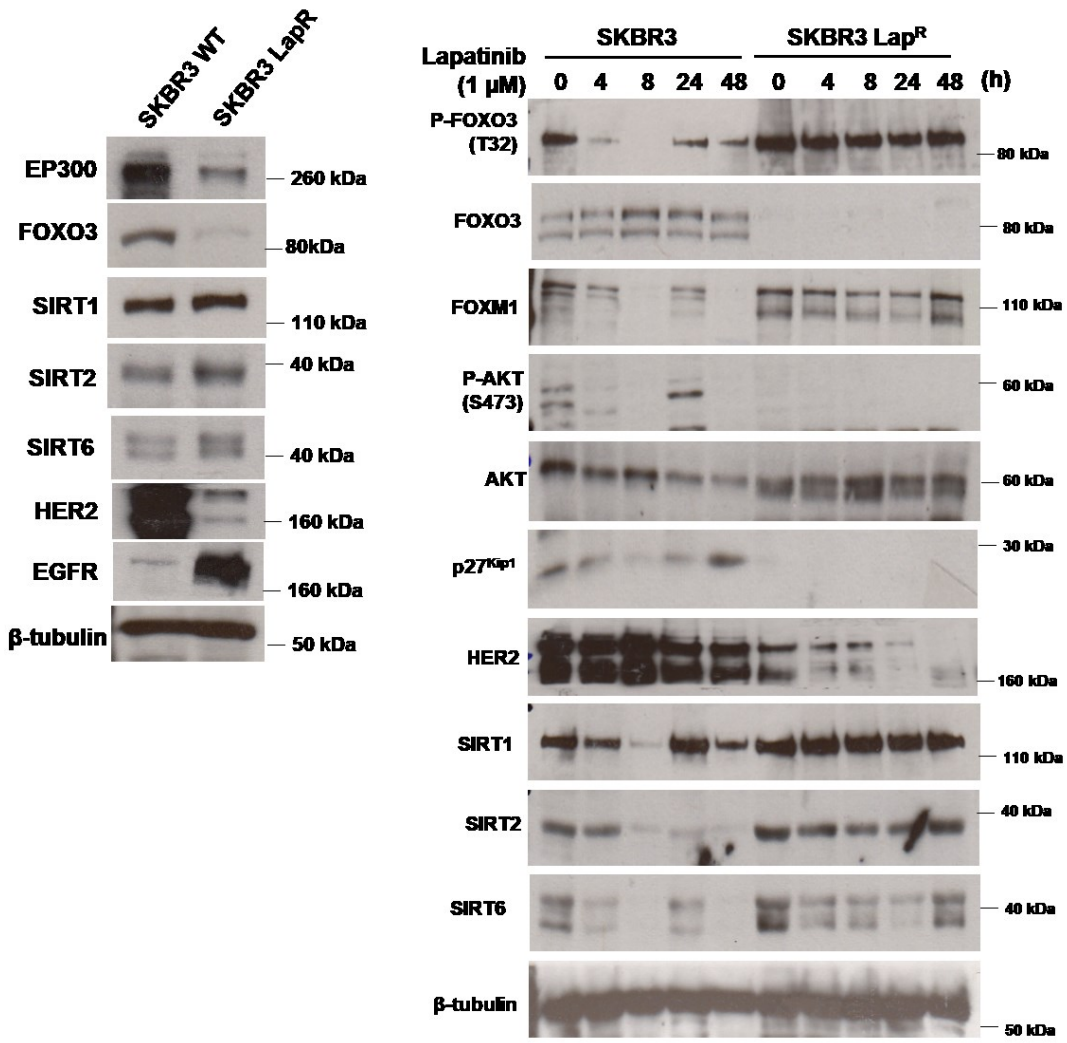
Appendix figure A3.1. Validation of Lapatinib resistance in BT474 Lap^R cells
BT474 and BT474 Lap^{R}cells were seeded in 96-well plates and treated with lapatinib at a range of concentration from 0.05 to 5 μM. Twenty-four hours after treatment, cells were fixed and stained with the protein-binding dye SRB. Values obtained were normalised against the corresponding untreated controls and presented as percentages (The cell survival value was normalized to 100% both untreated cells).



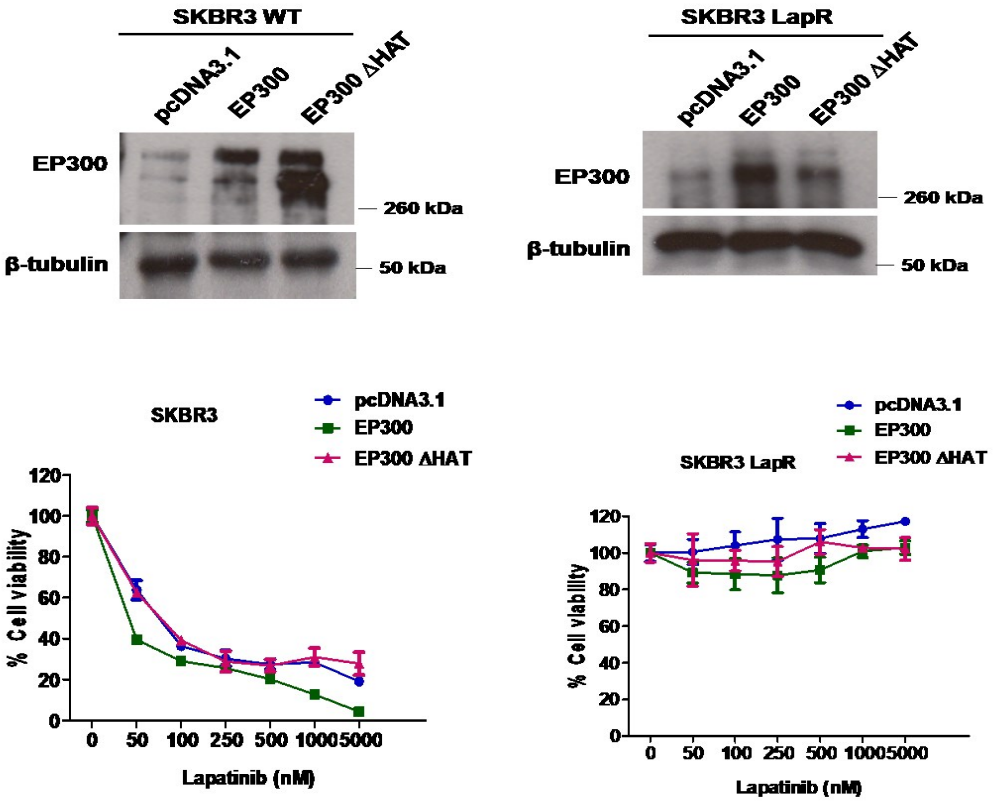
Appendix figure A3.2. Overexpression of EP300 or EP300 ΔHAT does not affect Lapatinib resistance in BT474 cells. BT474 Lap^{R}cells transfected with EP300 or EP300 ΔHAT was seeded in 96-well plates and treated with lapatinib at a range of concentration from 10 to 2000 nM. 24 hours after treatment, cells were fixed and stained with the protein-binding dye SRB. Values obtained were normalised against the corresponding untreated controls and presented as percentages.



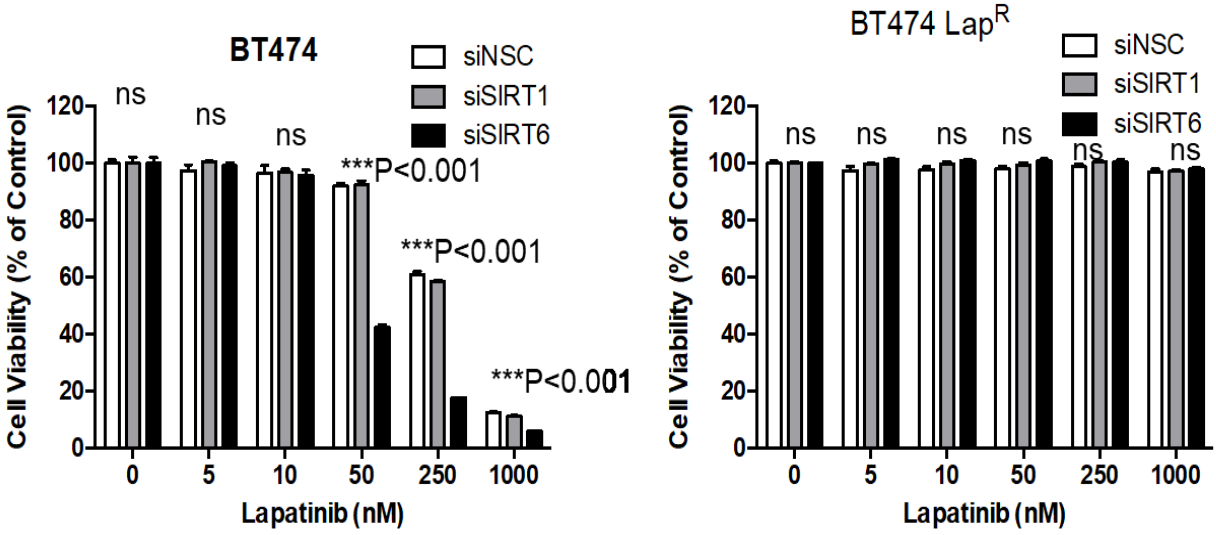
Appendix figure A3.3. Overxpression of EP300 in BT474 and Lap^R (Experiment performed by Ana Rita Gomes). Transiently transfected BT474 and BT474 Lap^R cells were allowed to grow overnight and then treated with the lapatinib concentrations indicated. After clone formation, cells were fixed with 4% para formaldehyde and stained with crystal violet. The stain was solubilised with 33% acetic acid and absorbance obtained at 592 nm. Data represent the mean ± SEM of three independent experiments and statistical analysis was performed using two-way ANOVA analysis (***p<0.001).



Appendix figure A3.4. Lapatinib treatment in SKBR3 cells.
The sensitive (SKBR3) and lapatinib resistant SKBR3 Lap^R cells were either left untreated or treated with 1 μM Lapatinib for the mentioned time points. Protein lysates from whole-cell extracts were then analysed by western blotting using the antibodies against the proteins indicated. Molecular weight markers are shown.

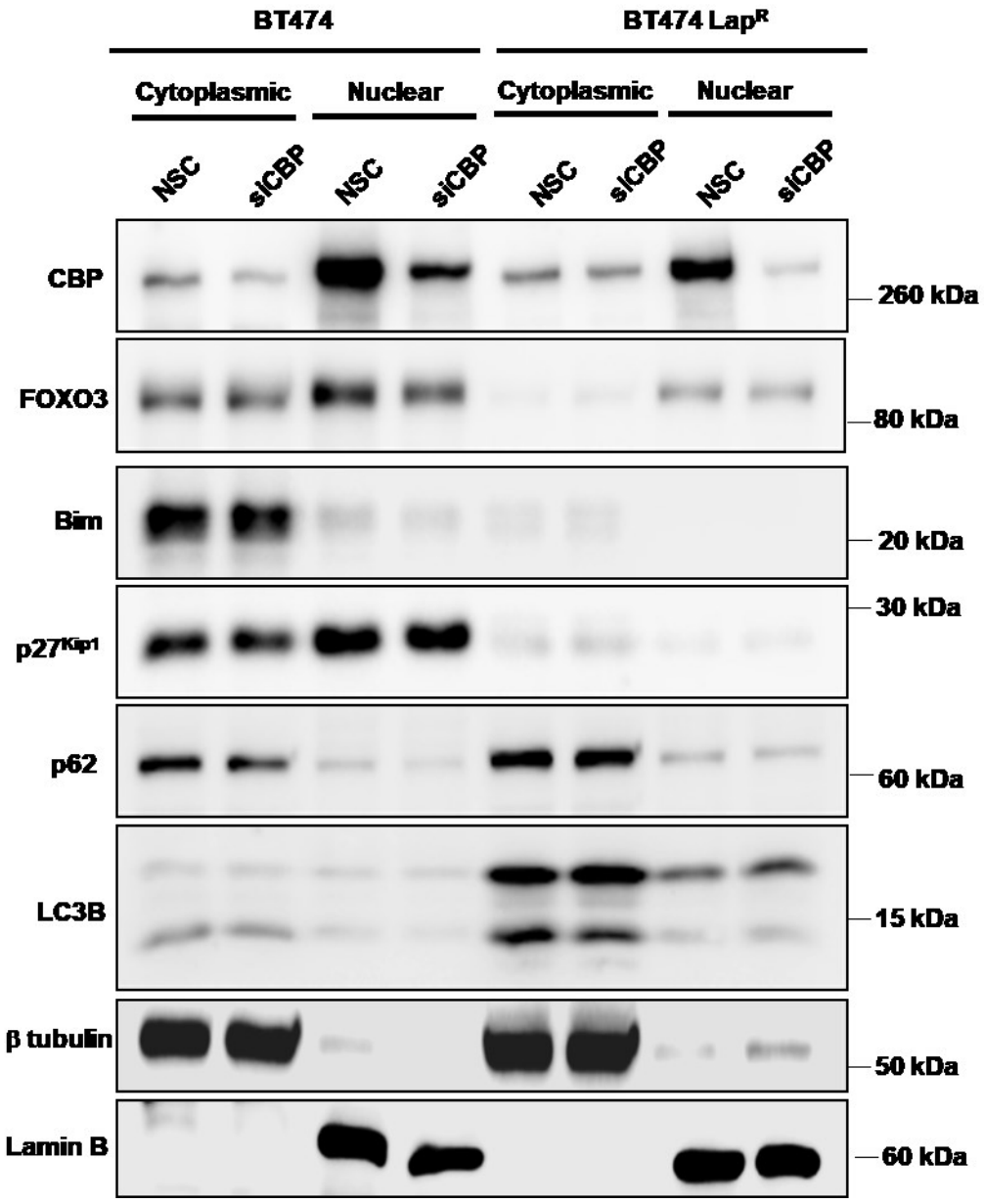


Appendix figure A3.5. Overexpression of EP300 in SKBR3 cells
SKBR3 and SKBR3 Lap^R cells were transiently transfected with the empty vector pcDNA3.1, the plasmid encoding wild-type EP300, or the one encoding for its acetyl-transferase mutant derivative (EP300 △HAT). Transiently transfected SKBR3 WT and LapR cells were seeded in 96-well plates and treated with lapatinib at a range of concentrations from 50 to 5000 nM. Twenty-four hours after treatment, cells were fixed and stained with the protein-binding dye SRB. Values obtained were normalized against the corresponding untreated controls and presented as percentages. Data represent means ± SEM (2-way ANOVA; non-significant, ns; significant, **P<0.01). Moreover, proteins were obtained from whole cell extracts after 24 hours following transfection. Western blotting was performed using the protein lysates to assess the expression levels of EP300.

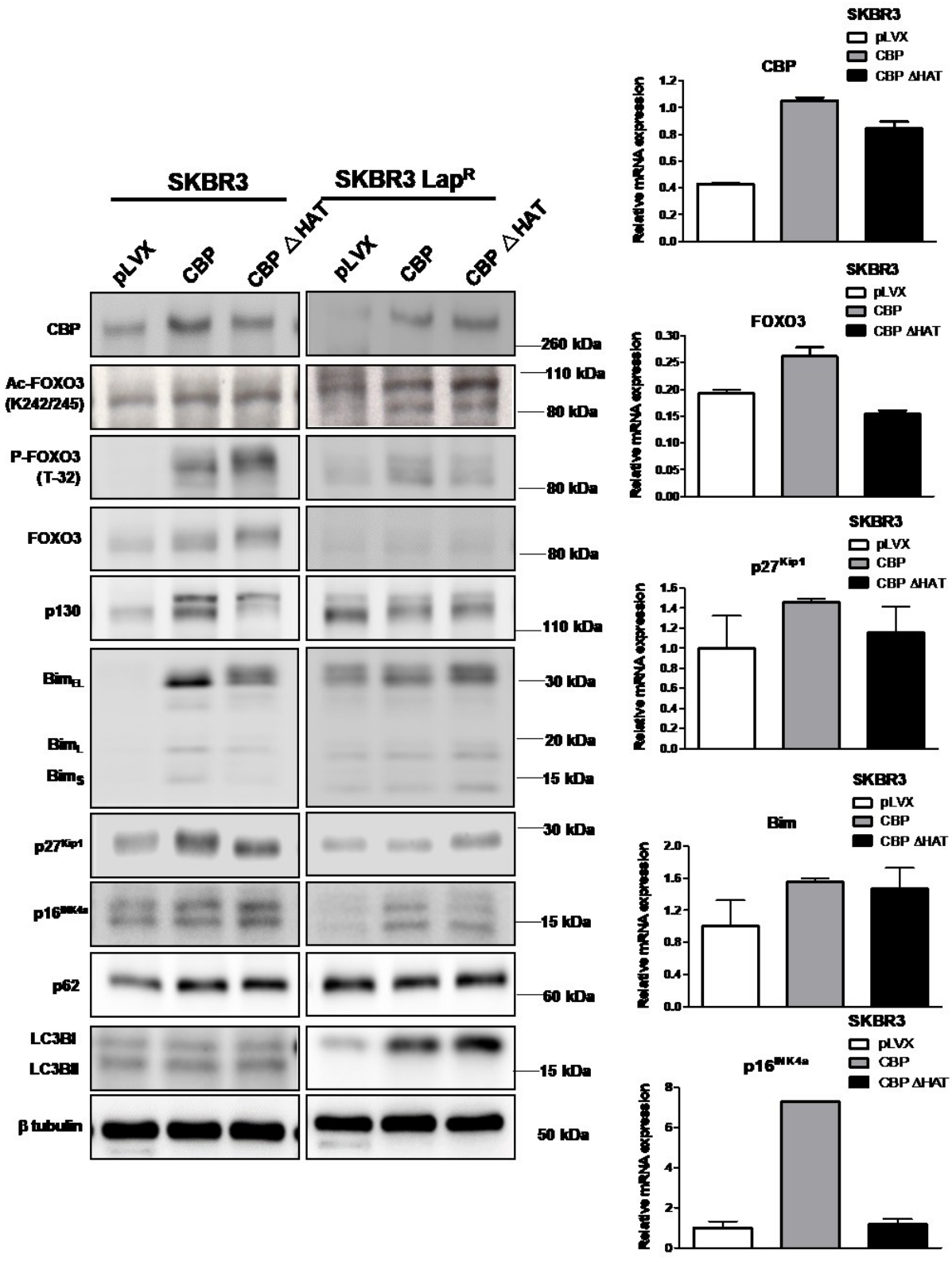


Appendix figure A3.6. Knockdown of SIRT6 increases lapatinib cytotoxicity in sensitive BT474 cells but not in resistant cells. Data represent the mean ± SEM of three independent experiments and statistical analysis was performed using two-way ANOVA analysis (***p<0.001).

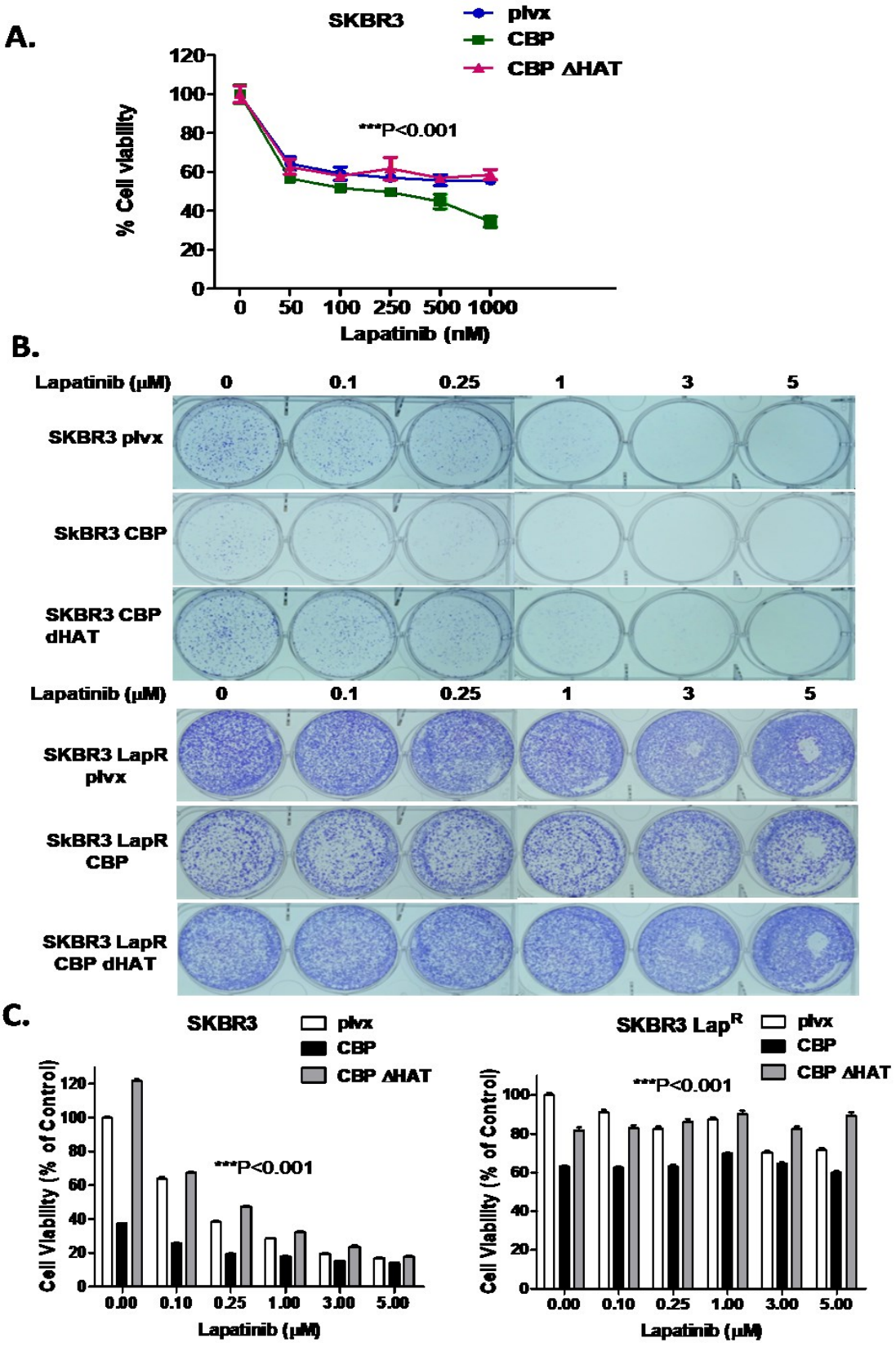
Appendix 2 (For chapter 4)



Appendix figure A4.1. Subcellular fractionation confirms nuclear localization of CBP and FOXO3. Cytoplasmic and nuclear extracts were isolated from control and CBP silenced BT474 and LapR cells. Western Blotting was subsequently used to monitor the sub-cellular distribution of CBP, FOXO3, Bim and other mentioned proteins. The β Tubulin and Lamin B were used as loading controls for cytoplasmic and nuclear extracts, respectively.



Appendix figure A4.2 Overexpression of CBP increases FOXO3 acetylation and its transcriptipnal activity in SKBR3 cells. A. SKBR3 and lapatinib resistant SKBR3 Lap^R cells were transfected with pLVX, CBP and CBP ΔHAT. Proteins were isolated from whole cell extract after 48 hours of transfection. Western blot was performed from protein lysates using antibodies against CBP, Ac-FOXO3, FOXO3 and other mentioned. Tubulin used as a protein loading control. **B.** The mRNA levels of CBP, FOXO3, p27^{kip1} and others mentioned genes were assessed by real time qPCR. The RPL19/RPS14 housekeeping gene was used as a control to normalise gene expression.



Appendix figure A4.3. CBP overexpressed SKBR3 cells are sensitive to lapatinib compared to control and HAT mutant. A. SKBR3 cells were stably transfected with pLVX, CBP and CBP ΔHAT. After 24 hours of seeding, cells were seeded in 96-well plates and treated with lapatinib (0 to 1000

nM). Twenty-four hours after treatment, cells were fixed and stained with the protein-binding dye SRB. Values obtained were normalized against the corresponding untreated controls and presented as percentages. Data represent means ± SEM (two-way ANOVA; non-significant, ns; significant, ***P<0.001). **B.** Stably transfected SKBR3 and SKBR3 Lap^R cells were allowed to grow overnight and then treated with the lapatinib concentrations indicated (0 to 5 μM). Twenty-four hours following treatment the medium was changed and colony formation was allowed for 14 days. Cells were then fixed with 4% para formaldehyde and stained with crystal violet. **C**.The stain was solubilised with 33% acetic acid and absorbance obtained at 592 nm. Data represent the mean ± SEM of three independent experiments and statistical analysis was performed using two-way ANOVA analysis (***p<0.001).